PROCEEDINGS: MECHANICS AND MITIGATION OF VIOLENT FAILURE IN COAL AND HARD-ROCK MINES

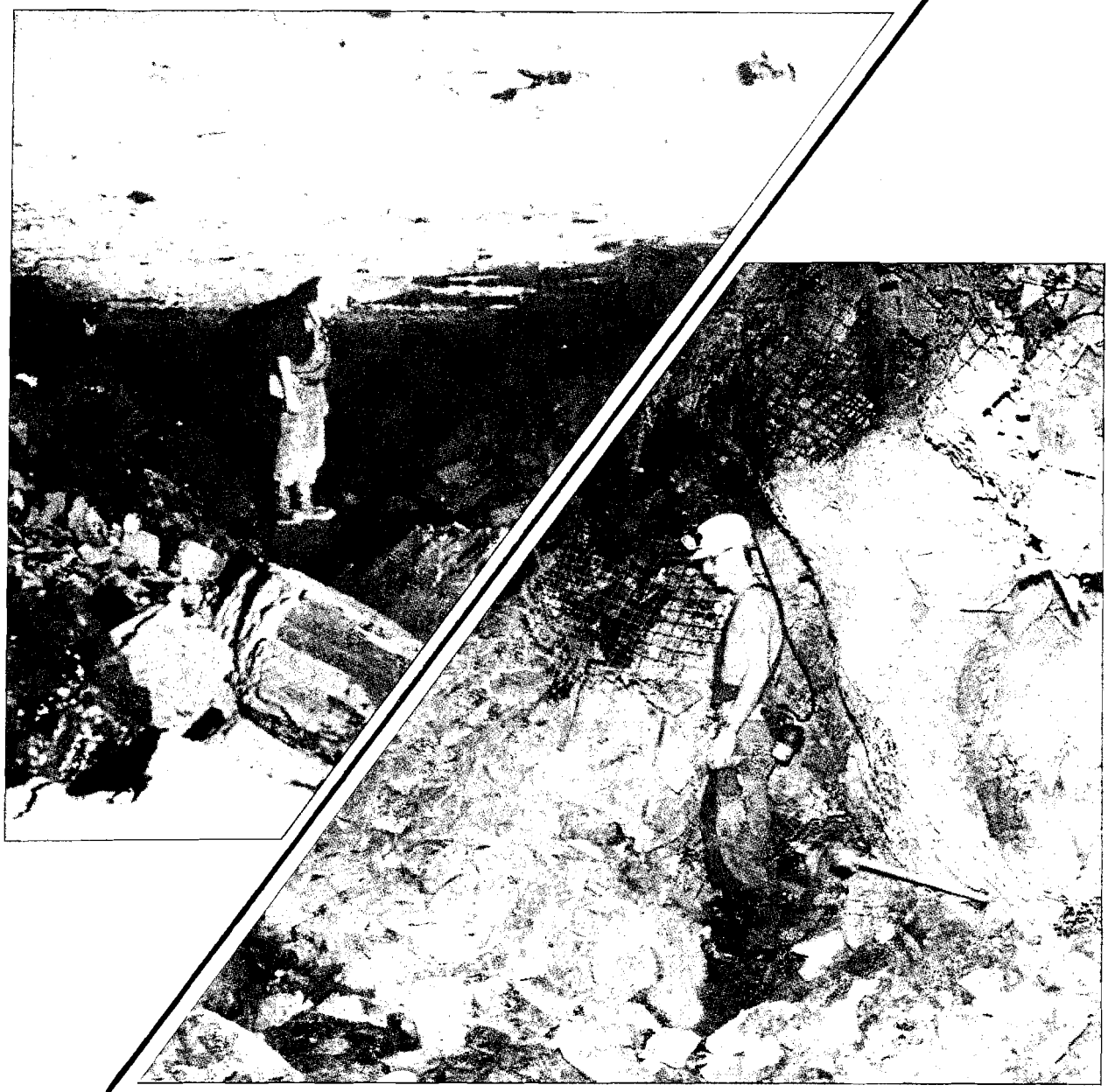

SPECIAL PUBLICATION 01-95

U.S. DEPARTMENT OF THE INTERIOR, BUREAU OF MINES

Special Publication 01-95

Proceedings: Mechanics and Mitigation of Violent Failure in Coal and Hard-Rock Mines

Edited by Hamid Maleki, Priscilla F. Wopat, Richard C. Repsher, and Robert J. Tuchman

UNITED STATES DEPARTMENT OF THE INTERIOR
Bruce Babbitt, Secretary

BUREAU OF MINES
Rhea L. Graham, Director

Library of Congress Cataloging in Publication Data:

Maleki, Hamid N.

Proceedings : mechanics and mitigation of violet failure in coal and hard-rock mines / edited by Hamid Maleki ... [et al.].

p. cm. — (USBM special publication; 01-95)

Includes bibliographical references.

Supt. of Docs. no.:I 29.151 : 01-95.

1. Rock bursts—Congresses. 2. Mine roof control—Congresses. 3. Coal mines and mining—Safety measures—Congresses. 4. Mines and mineral resources—Safety measures—Congresses. I. Title. II. Series: Special publication (United States. Bureau of Mines); SP 01-95.

TN317.M35 1995 622'.28—dc20 95-7138 CIP

PREFACE

During May 1995, the U.S. Bureau of Mines held technology transfer seminars at Coeur d'Alene, ID, Price, UT, and Norton, VA, on the subject of violent failure in coal and hard-rock mines. The papers presented at those seminars are contained in this proceedings.

A good deal of time and effort goes into preparing for meetings such as these. The editors would like to thank the organizing committee: Anthony Iannacchione, Pittsburgh Research Center, and Khamis Haramy and Bernard Steblay, Denver Research Center. Brian White, Spokane Research Center, deserves thanks for coordinating the underground visit to the Lucky Friday Mine for participants at the Coeur d'Alene seminar. In addition, the following persons should be recognized for assisting with the logistics of the conferences: Linda Noel, Nadine Hawley, and Kenneth Strunk, Spokane Research Center; Joseph Zelanko, Pittsburgh Research Center; and Angela Abruzzino, Pittsburgh Research Center.

DISCLAIMER OF LIABILITY

CONTENTS

UNIT OF MEASURE ABBREVIATIONS USED IN THIS REPORT

Metric Units

cm	centimeter	Mbyte	megabyte
cm/cm	centimeter per centimeter	m/d	meter per day
dB	decibel	MHz	megahertz
dB/m	decibel per meter	min	minute
deg	degree	m/km	meter per kilometer
Gbyte	gigabyte	mm	millimeter
GJ	gigajoule	m/m	meter per meter
GPa	gagapascal	m/ms	meter per millisecond
h	hour	MPa	megapascal
Hz	hertz	ms	millisecond
J	joule	m/s	meter per second
kbaud	kilobaud	N	newton
kbyte	kilobyte	N•m	newton-meter
kg	kilogram	pct	percent
kHz	kilohertz	s	second
kJ	kilojoule	s/cycle	second per cycle
km	kilometer	s/Mbyte	second per megabyte
km/s	kilometer per second	t	metric ton
kPa	kilopascal	V	volt
L	liter	W	watt
m	meter	μs	microsecond
m^2	square meter	°	degree
m^3	cubic meter		

U.S. Customary Units

ft	foot	lbf	pound of force
ft^2	square foot	mi	mile
ft/d	foot per day	mi^2	square mile
ft/mi	foot per mile	mi/h	mile per hour
gal	gallon	psi	pound per square inch
in	inch	st	short ton
in/in	inch per inch	yd	yard
lb	pound		

Reference to specific products does not imply endorsement by the U.S. Bureau of Mines.

PROCEEDINGS: MECHANICS AND MITIGATION OF VIOLENT FAILURE IN COAL AND HARD-ROCK MINES

Edited by Hamid Maleki,[1] Priscilla F. Wopat,[2] Richard C. Repsher,[3] and Robert J. Tuchman[4]

ABSTRACT

Papers presented at a U.S. Bureau of Mines (USBM) technology transfer seminar describe the causes of violent material failure in U.S. mines, measurement techniques for monitoring events that result in violent failure, and mitigation techniques for controlling failure. Specific factors contributing to violent failure are identified on the basis of geotechnical monitoring in 16 U.S. hard-rock and coal mines and on statistical analyses of 172 coal bump events. New monitoring and analysis techniques developed as tools for assessing violent failure; geotomographic methods that provide new capabilities for the study of material failure and stress changes over large areas; and seismic methods for determining source locations, calculating energy release, and determining source mechanisms are described. Fair correlations have been established among seismic parameters, elastic stresses, face support load, and violent events. USBM studies have identified the advantages using both yielding and stable pillars for coal bump control. A computer program has been developed as an aid for selecting room-and-pillar layouts. The practical aspects of implementing a destressing program is outlined for coal mines, while the importance of mine orientation and timely support installation in controlling buckling-type failure is identified for hard-rock mines.

[1]Mining engineer, Spokane Research Center, U.S. Bureau of Mines, Spokane, WA.
[2]Technical publications editor, Spokane Research Center.
[3]Staff engineer, Division of Health, Safety, and Mining Technology, U.S. Bureau of Mines, Washington, DC.
[4]Writer-editor, Pittsburgh Research Center, U.S. Bureau of Mines, Pittsburgh, PA.

INTRODUCTION

By Hamid Maleki

As part of its mission to improve safety, the U.S. Bureau of Mines (USBM) has long been involved in the study and development of techniques for control of both violent and nonviolent material failure in U.S. mines. Sudden, violent failures, generally known as rock bursts and coal bumps, are defined as failures that occur near mine entries and that are of such a magnitude that they expel large amounts of rock or coal into an excavation, restricting safe and efficient access to the working area. Such failures are also common in other countries, including Canada, Chile, Poland, Germany, England, France, China, India, and South Africa. Nonviolent failure, sometimes referred to as gradual or progressive failure, has less impact on mining continuity and safety and is generally controlled by timely scaling, cleaning, and bolting.

Although there is no distinct boundary between violent and nonviolent failure, the goal of this USBM technology transfer seminar is to focus on causes, measurement, and mitigation of violent failure in U.S. mines. These events are of deep concern because there are approximately 14 fatalities per decade in coal mines and 7 fatalities per decade in hard-rock mines that can be attributed to coal bumps and rock bursts. By including papers from both hard-rock and coal mine studies, it is hoped that information can be effectively transferred from coal mines to hard-rock mines and vice versa.

In fact, the geomechanics of conditions leading to violent failure are similar in both hard-rock mines and in coal mines, i.e., stresses exceed the strength of the rock mass near the mining excavation or at a geologic discontinuity. Mining takes place in near-horizontal seams under near-vertical maximum principal stress fields in most bump-prone U.S. coal mines; geologic discontinuities are primarily horizontal supplemented by near-vertical cleats and joints. Burst-prone U.S. hard-rock mines have a similar setting in which maximum principal stresses are horizontal and excavations are in near-vertical veins. Geologic discontinuities are also near vertical, i.e., a 90° rotation in comparison with coal mine settings. In addition, stress distortion by geologic structures has been quantified for both hard-rock mines and coal mines (Maleki and others, 1994)[1] and related to both violent and nonviolent material failure. Thus, a great benefit should be obtained by integrating research results from both hard-rock and coal mines.

Progress in a number of USBM research projects dealing with violent failure are described in this publication. New information is given on the causes of violent failure, new measurement and analytical techniques are provided for identifying the potential for violent failure, mining methods are reviewed, and excavation sequences and support systems used to minimize the potential for violent failure are discussed, as well as specific destressing techniques used to control bumps.

The papers have been divided into two groups: One deals with coal and the other with hard-rock mining. The following overview describes the highlights of each paper.

COAL MINES

The papers by Maleki, Iannacchione, and DeMarco provide analyses of the causes of violent failure based on 14 case studies in both Eastern and Western U.S. coal fields and a historical evaluation of 172 coal bumps. These case studies emphasize the influence of several factors on coal bumps, including rapid changes in stress over a short distance and time, the stiffness and yieldability of near-seam strata, and the dynamic effects associated with failure of surrounding rocks.

Maleki proposes a methodology for assessing coal bump potential based on stress analyses, in situ strength data, and energy release calculations resulting from the failure of surrounding rocks. Sames proposes a geologic criterion to assess bump-proneness based on an examination of overburden and lithologic information from two bump-prone mines. Campoli provides a computer program for assessing bump proneness in different room-and-pillar layouts.

Wilson, Westman, and Cox describe new monitoring and data analysis techniques to be used as tools for assessing the likelihood of violent failure. Wilson maps the location and intensity of microseismic events in four mines as part of long-term case studies and identifies interesting patterns at each site. In one study, it was reported that coal bumps were preceded by a high rate of microseismic activity that decreased dramatically immediately before the coal bumped. Westman presents studies of tomographic imaging in three mines and identifies areas of high velocity and stress within coal pillars and at the longwall face. Cox emphasizes the usefulness of real-time monitoring of hydraulic support (shield) loads and identifies a preliminary relationship among anomalous pillar stress changes, support loading, and sudden floor failures.

DeMarco, Zelanko, Iannacchione, and Campoli review the evolution of gate road and panel layout design in longwall mines and room-and-pillar panels. DeMarco

[1]Maleki, H., R. W. McKibbin, and F. M. Jones. Stress Variations and Stability in a Western U.S. Coal Mine. Presented at SME Ann. Meet., Albuquerque, NM, Feb. 14-17, 1994. SME preprint 94-249, 7 pp.

emphasizes the use of yield pillars and the importance of avoiding certain critical width-to-height ratios in pillars. Zelanko catalogs the use of stable "abutment" pillars in two Appalachian mines for the control of coal bumps. Campoli provides a new method in which a computer program is used to design room-and-pillar panels where pillar extraction is involved.

Practical implementation of destressing techniques are described by Haramy; when all design efforts fail to control coal bumps, destressing techniques and/or the practice of leaving large blocks of coal in place might be considered. The destressing techniques consist of volley firing, hydraulic fracturing, water infusion, auger drilling, and induced caving.

HARD-ROCK MINES

Studies in hard-rock mines and in coal mines complement research and emphasize the role of preexisting geologic structures on violent failure in hard-rock mines. White reports that rock bursts are influenced by these preexisting structures and the orientation of mine openings with respect to these structures, and the need for timely allocation of support to control strata buckling. Whyatt emphasizes that in situ stresses may be distorted by structures, such as faults and folds, that may influence the spatial distribution of mining-induced seismicity and rockburst hazards.

Further evidence of the interaction between mining-induced seismicity and preexisting structures is discussed by Swanson. He hypothesizes that mining-induced deformation was mobilized along a 1.5-km length of a geologic trend that lay subparallel to a major, locally steeply dipping fault system.

Williams and Estey describe monitoring systems used in the study of rock bursts in the Coeur d'Alene Mining District and show how these systems complement each other in tracing mining-induced seismicity and rock bursts.

Maleki and Scott describe the application of newly developed geotomographic methods for the study of rock failure and stress changes in two Western U.S. mines. They provide new insights into the mechanism of time-dependent failure and excavation-induced rock damage for sedimentary rocks and produce three-dimensional velocity and stress images for mine pillars in hard-rock mines. Girard and Filigenzi provide detailed guidelines for choosing a low-cost, PC-based data acquisition system to monitor mining-induced seismicity and, using finite-element techniques, establish a relationship between seismicity and elastic stresses.

Poad describes the logic and benefits gained by switching to an underhand cut-and-fill method to control seismicity at the Lucky Friday Mine. From a stability point of view, the method is advantageous because a block is mined from top to bottom, always toward virgin ground, which eliminates the formation of highly stressed sill pillars.

AN ANALYSIS OF VIOLENT FAILURE IN U.S. COAL MINES—CASE STUDIES

By H. Maleki[1]

ABSTRACT

A U.S. Bureau of Mines (USBM) researcher analyzed the causes of violent failure using data from 12 U.S. coal mines as part of the USBM's mission to improve mine safety. It was shown that coal bumps are influenced by stress, stiffness, and yieldability of surrounding rocks, and the dynamic effects associated with failure of surrounding strata. In all bump-prone mines studied, calculated seam stresses exceeded unstable strength levels by at least 20 to 30 pct. In addition, bumps occurred in parts of the mines where there had been rapid stress changes over a short period of time and/or distance. The dynamic effects associated with the failure of surrounding strata triggered bumps in these marginally stable seam structures.

While it was not possible to evaluate the influence of mine stiffness directly, it was shown that coal bumps generally occurred in mines with uniaxial compressive strength and Young's modulus ratios (roof to coal) exceeding 3 to 5. In addition, bump-prone coal exhibited the potential for storing high horizontal stresses. Yielding of the immediate roof and floor reduced horizontal stresses and enhanced gradual failure of coal. A method is proposed to assess coal bumps in which stress analyses, in situ strength data, stiffness and strength ratios of roof to coal, and expected wave magnitude resulting from strata failure and mining experience are incorporated.

INTRODUCTION

Sudden, violent failures of the rock around mine openings have compromised safety, ventilation, and access to mine workings in both hard-rock and coal mines in many countries, including the United States, Canada, Chile, Poland, Germany, England, France, China, India, and South Africa. Because of the catastrophic nature of these sudden failures, understanding the cause of failure and developing mine design and mitigation techniques for controlling failure have been the objective of many studies. The U.S. Bureau of Mines (USBM) has long been involved in such studies as part of its mission to improve mine safety.

Conditions leading to violent failure are similar in both hard-rock mines and in coal mines; i.e., stresses exceed the strength of the rock mass near the mining excavation or at a geologic discontinuity. In hard-rock mines, both strengths and stresses are higher than those at coal mines and failure is, in general, brittle. In coal mines, violent failure takes place at lower stresses from both brittle and semiductile strata deformation. Failure is generally influenced by local stress concentrations around mining excavations (which are influenced by the strength and stiffness of rocks), and the interaction of mining with regional tectonic structures. Tectonic structures, perhaps, play a bigger role in mining seismicity and rock-burst damage in some U.S. and Canadian hard-rock mines than in coal mines because hard-rock mines are located in proximity to these structures (Williams and others, 1993). Tectonic-related seismic events, however, have not been cataloged in detail for U.S. coal mines because there are no local monitoring systems. Mining-induced stress changes have

[1]Mining engineer, Spokane Research Center, U.S. Bureau of Mines, Spokane, WA.

been reported as triggering movements along faults 2 to 3 km (1 to 2 miles) below U.S. coal mines and have contributed occasionally to tremors having Richter magnitudes of 3.5 (Wong and others, 1989).

There is no consistent terminology for these sudden, violent failures. Hard-rock mines, with extensive seismic monitoring systems, have defined mine tremors better than have coal mines. Table 1 provides some definitions based on experience in hard-rock mines (Chavan and others, 1993); the severity of damage increases with wave amplitude. Ortlepp (1992) and other researchers, however, used peak particle velocity for assessment of damage and for design of support systems using the kinematics of ejected blocks.

Table 1.—Proposed definitions of seismic events and associated damage

Wave amplitude, mm	Definition
15-50	Minor burst
50-100	Medium burst
Greater than 100	Major burst

In view of the lack of a universal definition of coal failures, in this paper, coal bumps are defined as sudden, violent failures that occur near coal mine entries and that are of such a magnitude that they expel large amounts of coal and rock into an excavation, restricting safe and efficient access to the working area. Other terms, such as rock bursts, crump, mountain shot, mountain bump, pillow burst, pressure burst, quake and bounce, and outburst are often used interchangeably in coal mining. Outburst is a term generally defined as a coal bump assisted by gas pressure.

After a review of seismic events and damage in hard-rock mines, the author will attempt to describe simpler causes for coal bumps, excluding the more complex mathematical treatments by authors such as Lippmann (1990) and Kleczek and Zorychta (1993). Then the paper will focus on an analysis of the causes of coal bumps through a brief review of available monitoring data from 12 U.S. coal mines. Five case studies will be examined in more detail to identify specific factors that contributed to the occurrence of bumps or their absence. A preliminary methodology will be proposed for assessing coal bump potential, including the most important factors identified from these case studies.

CAUSES OF VIOLENT FAILURE

ROCK BURSTS

Rock bursts in hard-rock mines have been extensively studied through underground observations, static measurements, and seismic records; these studies revealed a correlation between mining activity and seismic events (Dubinski, 1990). Seismic events are apparently generated as mining activities change the stress field and often result in either rock crushing or movement along geological discontinuities. McGarr (1984) studied these events, proposed formulas for estimating their energy content, and showed that many events did not cause any damage in one property unless the local wave magnitude exceeded 2.5 on the Richter scale. Ryder (1988) proposed the criterion of excess shear stress, which is the difference between the prevailing shear stress prior to slip at a geologic discontinuity minus the dynamic strength of the contact plane, as a means of assessing the potential for slip along a geological discontinuity.

It is important to understand the cause of failure in order to find solutions to failure. Ortlepp (1992) (figure 1) has proposed a simplified concept for defining rockburst source mechanisms and their relationship with measured wave amplitudes as expressed in Richter magnitudes. The first three categories (strain, buckling, and pillar crushing) are influenced by stress concentrations near entries, while the last two categories (shear rupture and fault slip), which are generally the most violent, represent an ideal situation of shear failure along a plane or a preexisting geologic discontinuity. This simplified relationship (figure 1) is generic, and work by other investigators (Gibowicz, 1990) indicates that large events may not necessarily cause any damage, while small events may cause considerable damage.

Violent ejections of rock fragments and slabs from the surfaces of excavations are termed strain bursting and buckling, respectively. These events are caused by high stress concentrations near mine openings that exceed the strength of the rock. Pillar bursts are larger events resulting from complete failure of pillar(s) where pillar stresses exceed pillar strength. Recent USBM work (White and others, 1995) at the Lucky Friday Mines has identified the influence of preexisting joints on formation of slabs and subsequent ejection of these slabs in the form of buckling and pillar failure (figure 1). Pillar failure may not only affect local conditions, but can also result in a dynamic shock wave that can reach other critically loaded pillars long distances away, triggering spalling and rock bursts at these sites (Pritchard and Hedley, 1993).

Slip along a preexisting fault may result from decreased normal stresses and/or increase of shear stresses caused by nearby mining activities. As faults slip, a large amount of energy is released, and a portion of this energy is transmitted through the rock mass in the form of a seismic

Figure 1
Simplified Relationship Between Wave Magnitude and Rock Burst Source Mechanism.

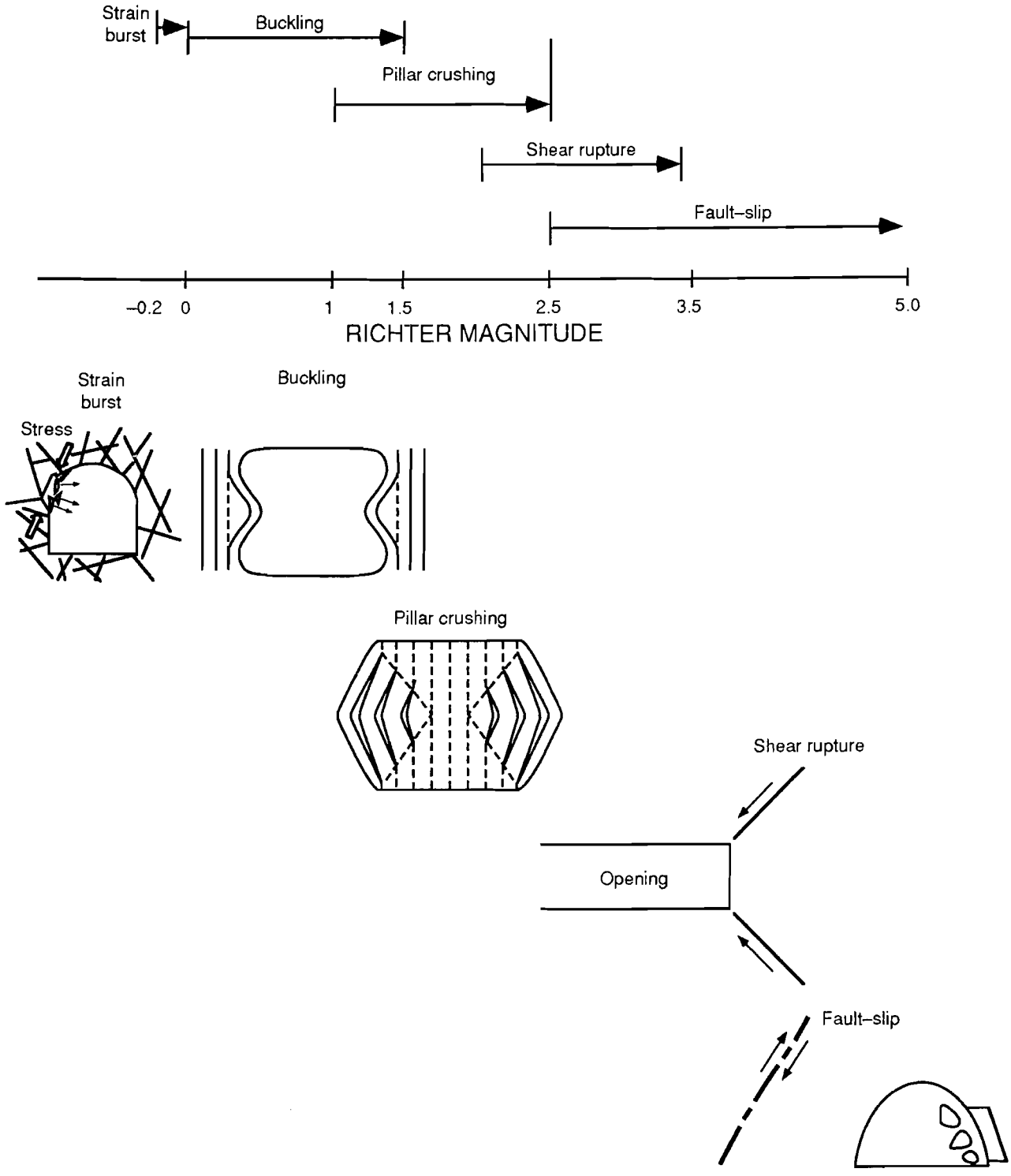

(Modified after Ortlepp, 1992.)

pulse, which reflects off the walls of an excavation and causes damage. Wave amplitude and frequency influence the type and location of damage to an opening (one rib or both ribs) (Yi and Kaiser, 1993).

COAL BUMPS

Rice (1935) categorized coal mine bumps into two general groups: (1) pressure (stress) bumps are influenced by static loading and failure of the seam material (figure 2*A*), and (2) shock (dynamic) bumps are triggered by failure of generally massive strata surrounding a seam (figure 2*B*). In spite of significant research since 1935, researchers have not been able to clearly identify source mechanisms for bumps in U.S. coal mines. To determine source mechanisms, there is a need for three-dimensional, seismic monitoring systems in proximity to underground mines. Also, there are difficulties in obtaining direct stress measurements within coal-measure rocks. Thus a clear understanding of material behavior and stress bumps has not been achieved.

Nonetheless, many laboratory, field, and theoretical investigations have provided some insight into the causes of coal bumps. Laboratory tests have given evidence regarding the influence of confining stresses (Babcock and Bickel, 1984) and postfailure characteristics of coal pillars in producing violent failure. Field studies have emphasized the influence of geology, the presence of stiff or competent noncaving roof and floor strata (Haramy and McDonnell, 1988), and mining layout and excavation sequences that subject coal to rapid stress increases over a short distance (Maleki and others, 1987) (figure 2*C* and 2*D*). Recent theoretical treatments (Lippmann, 1990; Kleczek and Zorychta, 1993) have provided better characterizations of the mechanics of coal bumps.

Some of these investigations into the causes of coal bumps and proposed criteria for assessing coal bump potential are reviewed here. Babcock and Bickel (1984) used a segmented platen and an acrylic sheet (figure 3*A*) to monitor and control confinement at the coal pillar-testing machine contact. The segmented platen constrained the top of the coal sample, while the acrylic sheet expanded laterally at the same rate as the coal. When the vertical stresses on the sample exceeded the unconfined compressive strength of the sample, the stability of the sample depended on the additional strength provided by the

Figure 2
Typical Coal Bumps.

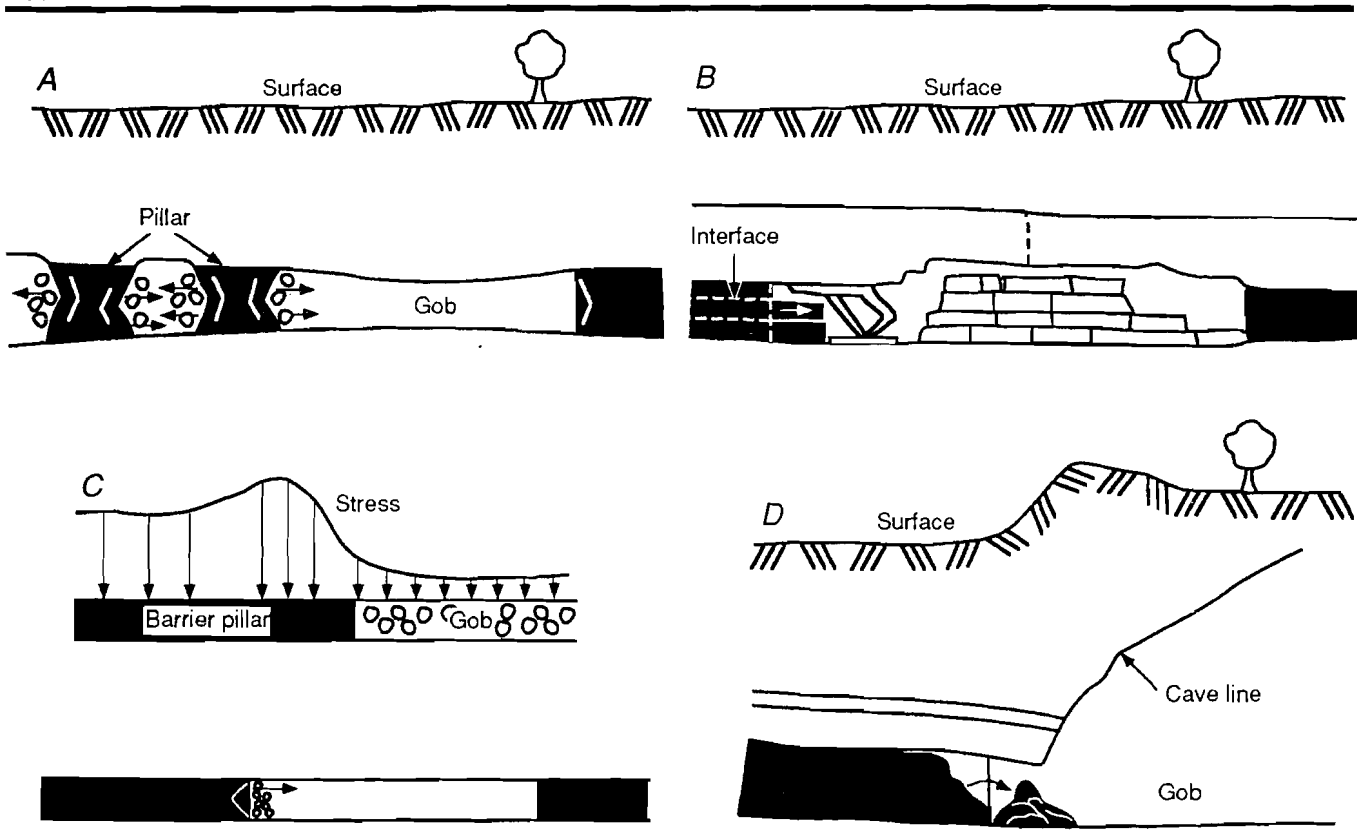

A, Stress bump; *B*, bump aided by breakage of near-seam strata; *C*, bump influenced by multiple seam workings; *D*, bump influenced by rapid increase in overburden.

constraint. When the constraint was lost as a result of slippage (measured at the acrylic sheet contact), the sample failed violently. Figure 3*A* demonstrates this effect using a Mohr-Columb failure criterion; sudden loss of confinement shifts the Mohr circle to the left and results in the failure of the sample coal pillar.

Babcock and Bickel (1984) used sample pillars with a width-to-height ratio of 8.5:1 from 15 mines and 11 seams. They concluded that stress can produce bumps in many coal seams if confinement is suddenly lost because of slippage at the interface. This finding is important because the frictional properties of contact planes at coal-roof-floor or coal-inseam partings are known to be variable (Maleki and others, 1988; Maleki, 1992).

Figure 3
Laboratory Concepts Relating to Stress Bumps.

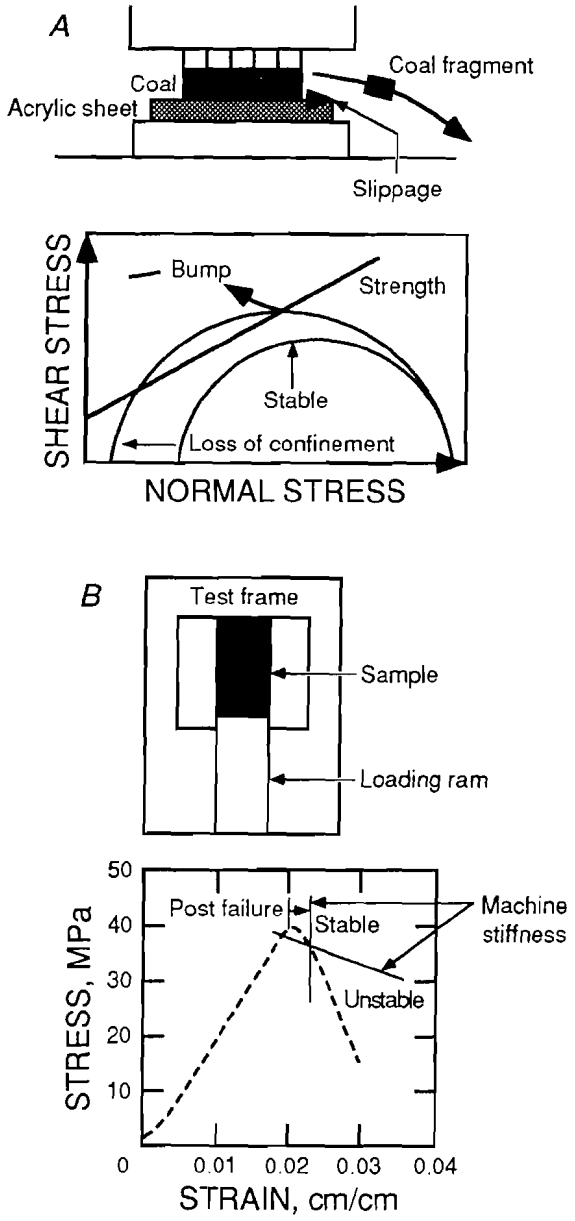

A, Segmented steel platen and loss of confinement; *B*, loading frame stiffness.

Cook and Hojem (1966) and Wawersik and Fairhurst (1970) emphasized the importance of testing machine stiffness in obtaining full-load deformation characteristics of coal pillars. A series of stiff testing machines were then introduced that did not store too much energy in the testing frame, driving the sample toward violent failure at peak pillar stresses. Starfield and Wawersik (1972) and Salamon (1970) introduced the concept of local mine stiffness and criteria for distinguishing between stable and unstable pillar failure. They suggested that stable failure occurs when the stiffness of the mine roof and floor exceeds the postfailure slope of coal pillars (figure 3*B*). Unstable failure occurs when local mine stiffness is less steep than the pillar postfailure slope.

Zipf (1992) implemented the local mine stiffness concept in a displacement-discontinuity code and established a linear relationship between local mine stiffness and Young's modulus for roof and floor rocks. Pen and Barron (1994) modified the local mine stiffness concept based on average pillar response and found a better correspondence between location of observed pillar bumps and sudden changes in local mine stiffness. The practical application of these boundary-element methods for coal bump prediction requires input about in situ material properties for coal seams, rock masses, and the gob, as well as caving geometry and the frictional properties of coal and rock at their contacts. Recently, Maleki (1992) produced in situ strength curves for selected U.S. coal seams, identifying stress levels beyond which roof, floor, and pillar stability problems occur. He provided some preliminary guidelines for estimating in situ postfailure behavior of two seams. This development refines the application of the concept of local mine stiffness to actual field conditions.

Numerous field investigators have identified unfavorable geologic and geometric factors that cause localized high stress concentrations on mine structures. Early South African research established a correlation between the rate of energy release and the frequency of rock bursts. To avoid rock-burst damage, it was then proposed to schedule mining activities so that mining could continue under more uniform stress, avoiding large amounts of potential energy release during single mining steps. Figure 4 is a schematic showing the application of this concept to scheduling panel mining sequences. Maleki and others (1987) applied this method to scheduling pillar pulling activities so that a uniform energy release rate was maintained for bump control. They also identified the importance of overall panel and barrier pillar design to avoid mining in areas where stresses had increased rapidly over a short distance. Zipf

and Heasley (1990) used this concept to examine different excavation sequences as well.

Campoli and others (1990), and DeMarco and others (1995) have discussed the importance of gate pillar design for coal-bump control. Experience with different gate pillar layouts at the Pocohantas No. 3 Seam indicates that it is important to have a large (stable) abutment pillar to control coal bumps, while DeMarco and others (1995) cataloged the use of yield pillars in several Western U.S. mines for coal-bump control.

Many field studies also have related coal bumps to the presence of competent, stiff, noncaving strata near the seam. Lippmann (1990) suggested that coal bumps occur only when rock in the roof and floor adjacent to the seam are about 10 times stiffer and stronger than the coal. Haramy and McDonnell (1988) used a Schmidt hammer in a rebound test to assess bump-proneness for different coal seams. Noncaving strata are thought to concentrate stress and accumulate large strain energy both in the rock and in the seam. Wu and Karfakis (1994) examined this energy accumulation for different strata and loading conditions in an attempt to identify bump-prone conditions. As strata fail, a portion of this energy is transferred to the coal seam in a dynamic pulse and may trigger slabbing, reduce static friction to sliding friction at geologic interfaces (Lippmann, 1990), and possibly contribute to loss of confinement (Iannachione and Zelanko, 1994). Wu and Karfakis (1994) used a relationship between this energy release and local wave magnitude and proposed that there will be coal-bump damage if wave magnitudes exceed 2.0 on the Richter scale.

EVALUATION OF BUMP CRITERIA

Several investigators have proposed specific criteria for assessing bump-prone conditions, but a comprehensive methodology is missing. These criteria use (1) laboratory stiffness and strength of mine roof rock, (2) local mine stiffness, (3) energy release rate, and (4) strain energy accumulation and local wave magnitude. Geotechnical data, numerical models, and in situ pillar strength data from seven bump-prone mines and five mines with nonviolent pillar failure were used to validate the effectiveness of some of the coal-bump prediction criteria (items 1, 2, and 3).

Figure 5 shows that using only ratios of roof or floor strength-to-coal strength and Young's modulus to assess bump-proneness, as implied by Lippmann (1990), is inadequate based on uniaxial data from 12 mines. Although most coal bumps have occurred in mines where the Young's modulus ratio (roof- or floor-to-coal) was greater than 8 and the strength ratio (roof- or floor-to-coal) was greater than 4, severe bumps occurred at two room-and-pillar operations where Young's modulus and strength ratios were as low as 5 and 3, respectively. The Young's modulus is shown to be linearly related to roof and floor stiffness (Zipf, 1992) and thus is used in this comparison.

To test the usefulness of the concept of local mine stiffness to the prediction of coal bumps, in situ pillar strength data from two mines showing violent and nonviolent pillar failure were used. The full load deformation of these pillars was characterized through geotechnical monitoring in which in situ pillar behavior for typical U.S. coal seams was identified (Maleki, 1992). Local mine stiffness was estimated using average pillar stiffness (Pen and Barron, 1994) (figure 6). The steeper line indicates slightly higher local mine stiffness for a sandstone roof in a bump-prone mine. Since local mine stiffness was steeper than the slope of pillar postfailure for both mines, pillar failure was predicted to be stable in both mines. Thus, these

Figure 4
Simplified Presentation of Mining Under Uniform Stress.

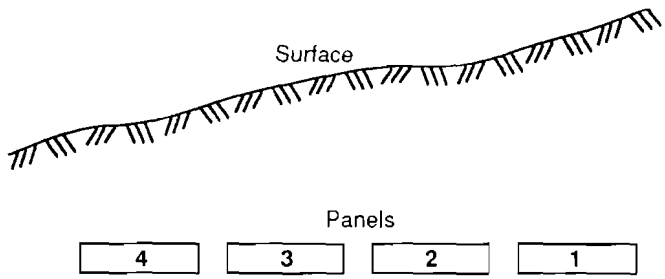

A panel mining sequence as numbered from right to left is advantageous because this sequence subjects each panel to similar levels of stress. Mining from left to right, however, can induce higher stresses on subsequent panels because of variations in cover (see Maleki, 1988).

Figure 5
Strength Ratio Versus Young's Modulus Ratio for Roof and Coal.

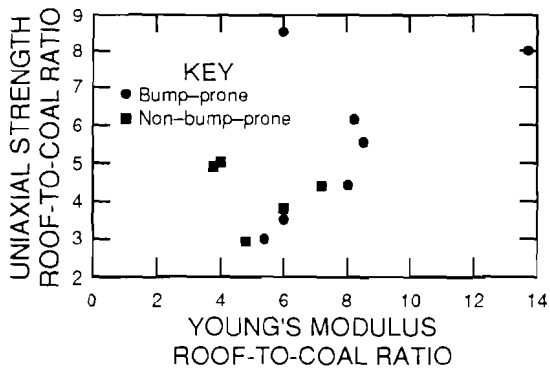

examples show that the local mine stiffness concept cannot consistently be used for predicting violent failures and is possibly more appropriate for distinguishing between stable and unstable "progressive" pillar failure as originally intended by Salamon (1970) and discussed by Zipf (1992). These example calculations are also influenced by (1) limitations of boundary-element methods in modeling the actual three-dimensional nature of coal mine excavations, (2) statistically insufficient data regarding the full load-deformation behavior of pillars across the example mines, (3) lack of scaling laws to adjust Young's modulus for rock masses based on joint spacing and other features, and (4) inadequate representation of local geologic factors, such as interfaces, cleats, and nonlinear deformation of immediate roof and floor strata.

Zipf and Heasley (1990) identified similar problems with the effectiveness of using energy release rate for coal-bump prediction. As shown in figure 5, many coal bumps occur in mines with stiff, competent roof and floor and not in seams surrounded by incompetent rocks, such as shales. Since the energy release rate is inversely proportional to roof and floor Young's modulus, a higher energy release rate and a less stable situation will be projected for mines with shalely roofs (assuming that shales are generally softer than sandstones). This is quite contrary to the experience in U.S. mines where many bumps have occurred when mining under sandstone roof.

In view of a lack of coherent criteria for coal bump occurrence, the author has examined several bump-prone mines. This leads to an additional preliminary methodology for assessing coal bump potential.

Figure 6
Pillar Stress-Strain Relationship and Local Mine Stiffness.

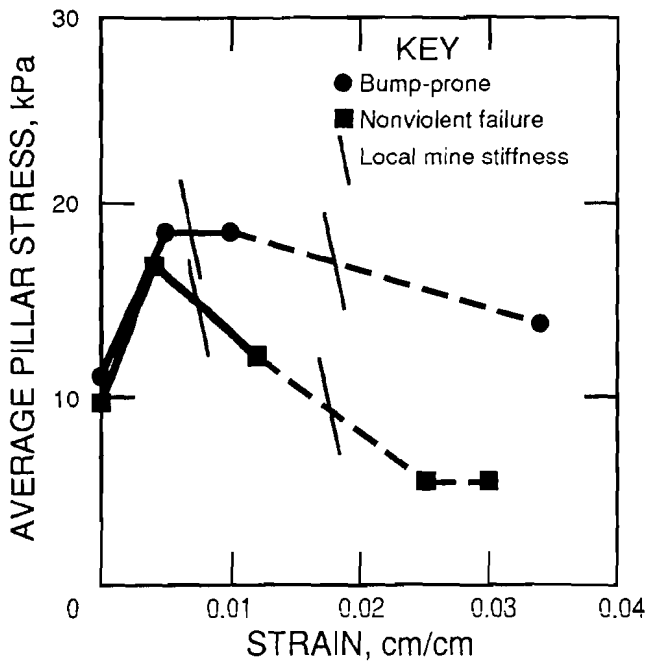

Dashed lines indicate estimated behavior.

ANALYSIS OF CASE STUDIES

Long-term measurements, underground observations, and numerical modeling results from studies of five coal mines were integrated to investigate the factors that influence violent failure. These mines represent typical conditions in Western and Appalachian coal fields where room-and-pillar and/or longwall methods are used in mining single and multiple seams. Four of the mines have experienced coal bumps. Geotechnical data from one mine with no significant coal bumps are also presented for comparative purposes. At the four bump-prone mines, four factors seem particularly relevant: (1) induced horizontal stresses, (2) rapid changes in stress gradient, (3) upper strata failure, and (4) lack of yielding.

CASE STUDY 1—INDUCED HORIZONTAL STRESSES

Site 1 is located in the Wasatch Plateau of central Utah in the Hiawatha and upper Blind Canyon coal seams. The immediate roof and floor are similar for both seams and consist of mudstones, siltstones, and sandstones (figure 7). The rock quality designation (RQD) ranges from 50 to 100, uniaxial compressive strength varies from 69 to 100 MPa (10,000 to 14,500 psi), and Young's modulus falls into a range between 19.3 and 39.3 GPa (2.8 and 5.7 $\times$ 10^6 psi). There are a number of thick-bedded, competent, and stiff units in the roof that resist regular caving and transfer loads to the face during retreat operations. The coal seams have similar laboratory mechanical properties (Maleki and others, 1987), but in situ pillar behavior and frequency of coal bumps are different.

Historically, the mine has experienced severe coal bumps in both the room-and-pillar workings and in the two-seam longwall workings. Geologic and geometric factors influencing major coal bumps in room-and-pillar panels were analyzed by Maleki and others (1987), and the importance of prudent mine layout design in avoiding coal bumps was identified. Two-seam longwall panels were initially associated with coal bumps when mining under remnant barrier pillars of the Blind Canyon Seam. These experiences led to the sole current use of full-extraction longwall mining methods with yielding gate pillars to avoid

Figure 7
Typical Lithology, RQD, and Strength Properties, Site 1.

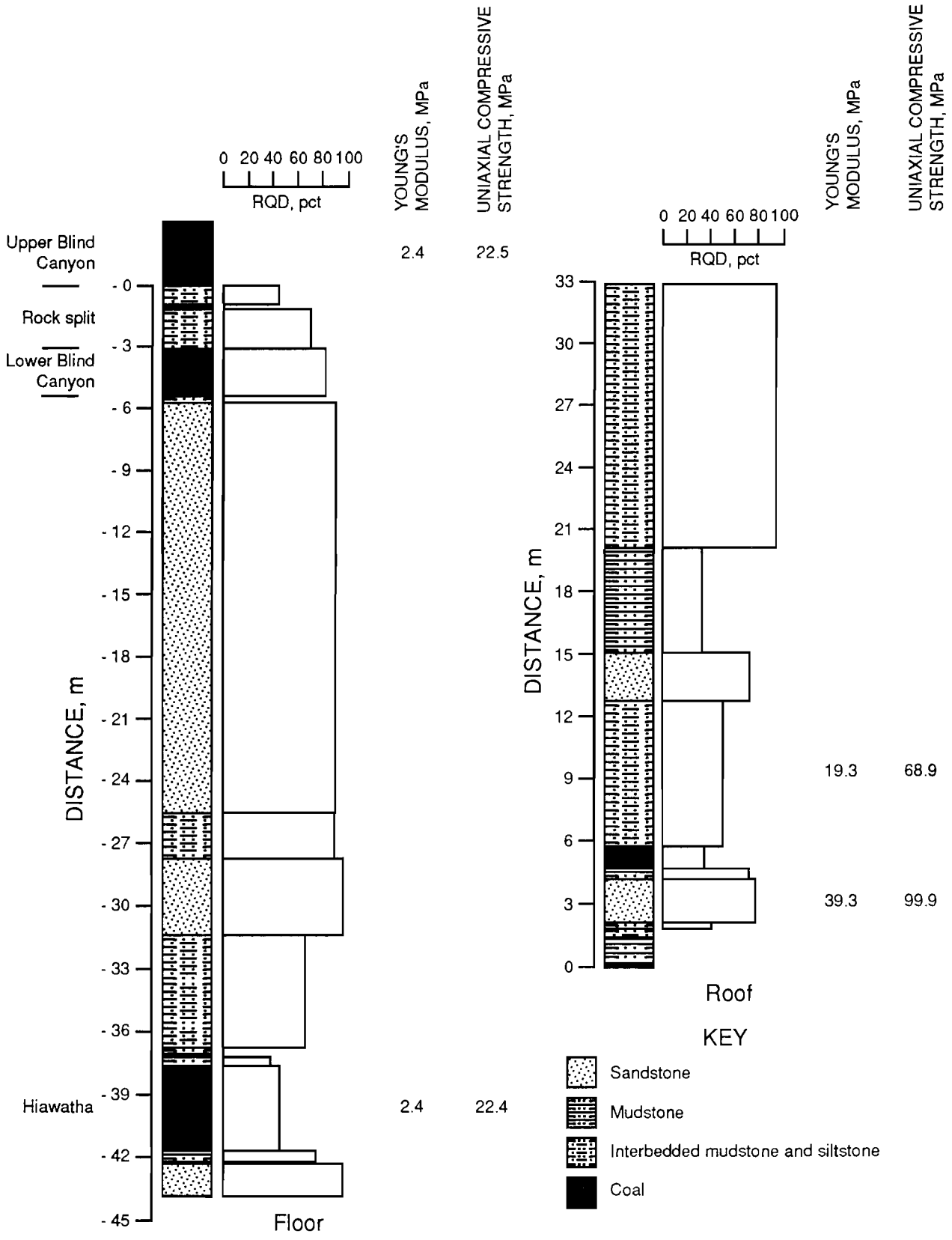

load transfer and coal bumps in the Hiawatha Seam. Excluding those bumps related to two-seam mining, the Blind Canyon Seam is known to be more bump prone than the Hiawatha Seam.

A field study was initiated by the mining company to compare the in situ behavior of the 9-m-wide by 25-m-long (30-ft-wide by 80-ft-long) "yielding" pillars in the upper Blind Canyon and Hiawatha gateroads (Maleki and others, 1988). The pillar in the upper Blind Canyon Seam exhibited higher strength and resistance to yielding than the pillar in the Hiawatha Seam. In fact, if not for the yielding of the mine floor, the Blind Canyon pillars could have experienced minor bumps. Mining depth was 610 and 190 m (2,000 and 620 ft) for the test sites in the Blind Canyon and Hiawatha seams, respectively. Premining horizontal stress fields were measured and shown to be small in comparison to the vertical stresses.

Pillar strength was measured as 27 MPa (4,000 psi) in the Blind Canyon Seam; this in situ strength was higher than the uniaxial compressive strength of coal [22 MPa (3,200 psi)], indicating pillar strengthening because of the confining horizontal stresses. Figure 8*A* demonstrates the buildup of horizontal stresses within the pillars as vertical stresses increased during the retreat of the longwall face toward the instruments (Poisson's ratio effect). In this figure, vertical and horizontal stresses are calculated on the basis of borehole pressure cell data oriented both horizontally and vertically and the procedures developed by Babcock (1986).

The confining horizontal stresses generally increased until the face passed the instruments by about 20 m (65 ft). Vertical stresses dropped, but quickly rebounded; at this time, there were numerous bounces (shocks) in the area that were possibly related to failure of the surrounding strata. Nevertheless, the confining stresses were significantly high in the pillar, helping to maintain gradual pillar unloading until the face passed the instruments at a distance of 250 m (800 ft).

Figure 8*B* illustrates pillar dilation history, confirming development of yield zones within the pillar as the face approached the instruments; pillar dilation was calculated by placing several anchors within the pillar and measuring the changes in the distance between these anchors and a reference point on the opposite side (solid block).

Roof-floor convergence measurements (Maleki and others, 1988) had a similar trend as shown in figure 8*B*; convergence increased significantly in the entries as the face approached the instrumented pillar. A total convergence of 0.5 m (1.6 ft) was measured; floor heave accounted for 97 pct of the total movement. Because the maximum deformation always occurred in the floor, it was inferred that the failure process was initiated in the mine floor as a result of pillar penetration. Failure and yielding of floor material were associated with rock dilation toward the entries; this reduced horizontal confining stresses gradually at the base and within the pillar, contributing to nonviolent failure (Maleki and others, 1993).

This case study is important because (1) it provides field evidence of buildup and loss of horizontal stresses in a pillar that reached the postfailure loading stage in a rather stable manner in spite of the presence of thick-bedded competent roof beams and (2) the gradual yielding of the immediate floor was an important natural barrier, reducing the potential for violent failure. Yielding of the floor material directly below the pillar was associated with rock dilation and a reduction in horizontal stresses.

Figure 8
Stress and Movement Profile for Selected Pillar Instruments.

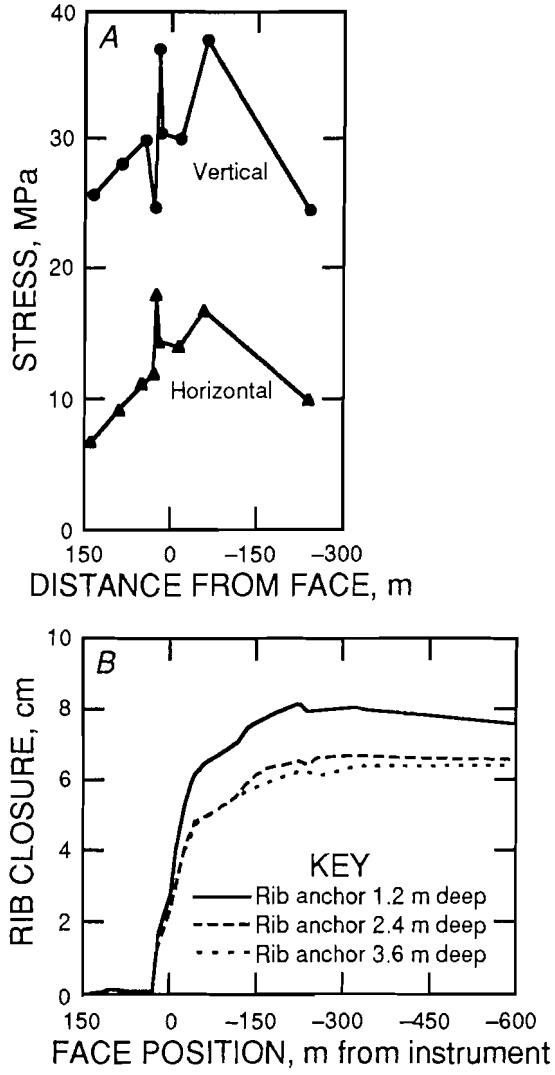

***A*, Calculated stresses from several pressure cells; *B*, pillar dilation history.**

CASE STUDY 2—RAPID CHANGES IN STRESS

This site is located in southeastern Kentucky. Room-and-pillar mining with occasional pillar pulling has been used in the overlying seam while longwall mining has been practiced in the lower seam, some 36 m (120 ft) below. The topography of the surface is rugged and mountainous.

The lower seam consists of four distinct coal beds, designated 180, 182, 184, and 186, separated with partings or splays (figure 9). The thickness and frictional properties of the splays vary over the deposit, influencing pillar behavior (Maleki, 1992). In a portion of the reserve, the splays change laterally into a sandstone channel approximately 7.6 m (25 ft) thick. With the exception of one coal bump thought to be related to sudden changes in topographic relief, coal bumps all have occurred within the zone of influence of this channel system and/or at locations influenced by the overlying room-and-pillar geometry.

The immediate roof generally consists of a series of shales, sandstones, and siltstones. The immediate floor consists of a meter of shale underlain by sandstone. As shown in figure 9, most roof and floor rocks are strong, stiff, and contain nonpersistent joints. The sandstone channel is not stronger than other roof strata, but it is more massive and lacks the bedding planes that enhance caving.

Coal bumps have generally caused displacement of large amounts of coal into openings, damaging equipment and occasionally injuring personnel; the bumps are believed to have been influenced by in-seam partings and seam-rock interfaces, as "red dust" has been consistently observed at these contact planes, indicating movement. These bumps have registered up to 3.8 on the Richter scale and have occurred either in the tailgate or at the face near the tailgate.

Among all events, there are two coal bumps that can be related to mining in areas where stresses and/or strength changed rapidly over a short distance and time. The first event registered 3.8 on the Richter scale and was associated with failure of an abutment pillar and a solid coal block at the tailgate position. The geology in this area was rather uniform, and thick sandstone channels were absent, but mining height was locally greater, which reduced pillar strength. In addition, mining had approached a topographic high where cover reached 670 m (2,200 ft). The 46- by 46-m (150- by 150-ft) abutment pillar was reported to have bumped, scattering coal around.[2]

As cover increases, abutment loads, which are transferred to the gate pillars, increase at a significant rate. [Mark (1990) assumes an increase proportional to the square of cover.] A rapid change in cover thickness thus increases stresses over a short distance and contributes to sudden failure of the abutment pillar. Preliminary elastic analyses have indicated that abutment pillar loads exceeded strength levels that caused stability problems (Maleki, 1992) by at least 30 pct during tailgate loading. Another local factor contributing to reduced pillar stability was an increase in mining height as a result of thinning of the partings at this location; pillar strength is inversely related to the mining height.

Figure 10 is a schematic that presents the two-seam mining geometry that contributed to the second coal bump. This bump occurred at the face during tailgate loading (second panel mining); a 7.5-m (25-ft) thick sandstone channel was present in this roof, but the topography was uniform [cover 610 m (2,000 ft)]. During the retreat of longwall 1, abutment stresses were transferred to the sides of the panel; these stresses caused crushing of the pillars in the upper seam (A, B) and transferred stresses farther toward panel 2. Because of caving in panel 1 and the proximity of the abutment loads in the upper seam, these stresses could not be fully redistributed over the gate pillars and were concentrated along the face of panel 2. In other words, pillar crushing in the upper seam made the gate pillar system in the lower seam very ineffective in limiting load transfer toward panel 2. Upon the retreat of panel 2, additional forward abutment stresses were transferred to the face area. Crushing in the C and D pillars in the upper seam further increased stress over a short time within the abutment zone and contributed to the face bumps.

In summary, this case study identified both two-seam and topographical geometries that locally increased stress over both short distances and periods of time and contributed to the violent failure of marginally stable gate pillars and/or longwall faces. In addition, a reduction in pillar strength because of variations in local geology further reduced pillar stability, which increased the potential for coal bumps. It is not always required to have a noncaving immediate roof and floor to generate coal bumps.

CASE STUDY 3—UPPER STRATA FAILURE

The mine studied for case 3 is located within the Book Cliffs Coal Field east of Price, UT; this field lies on the gentle northeastern flank of the San Rafael Swell. Continuous miner equipment has traditionally been used to mine coal from the Rock Canyon and Sunnyside seams.

In this area, coal-measure rocks are generally strong, stiff, and contain one to three sets of joints (figure 11). There are two regionally massive sandstones (upper and lower Sunnyside tongues) above the Rock Canyon Seam; these sandstones are approximately 12 m (40 ft) thick, have a uniaxial compressive strength of 103 MPa (15,000 psi), and an RQD of 100 pct. The Castle Gate Sandstone lies 110 m (330 ft) above the coal beds and is 60 to 90 m (200 to 300 ft) thick.

[2]Personal communication from J. Holloe, manager of Geology and Exploration, 1994.

Figure 9
Typical Core Hole Lithology, Uniaxial Compressive Strength, and Elastic Properties, Case Study 2.

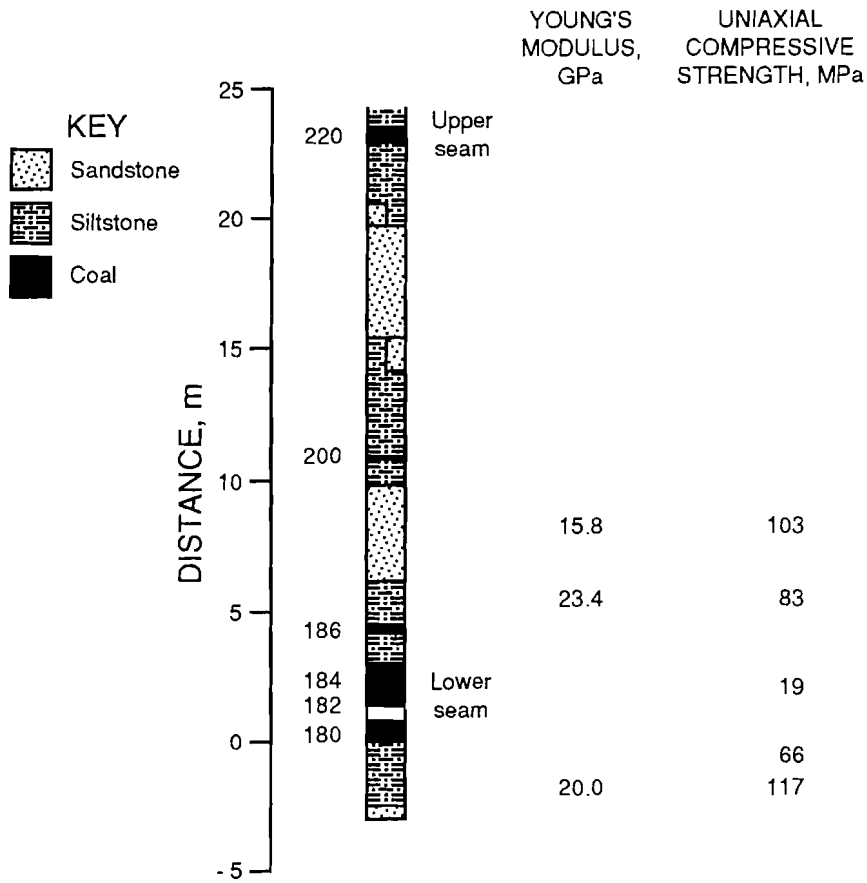

Figure 10
Load Transfer for Two-Seam Mining Geometry.

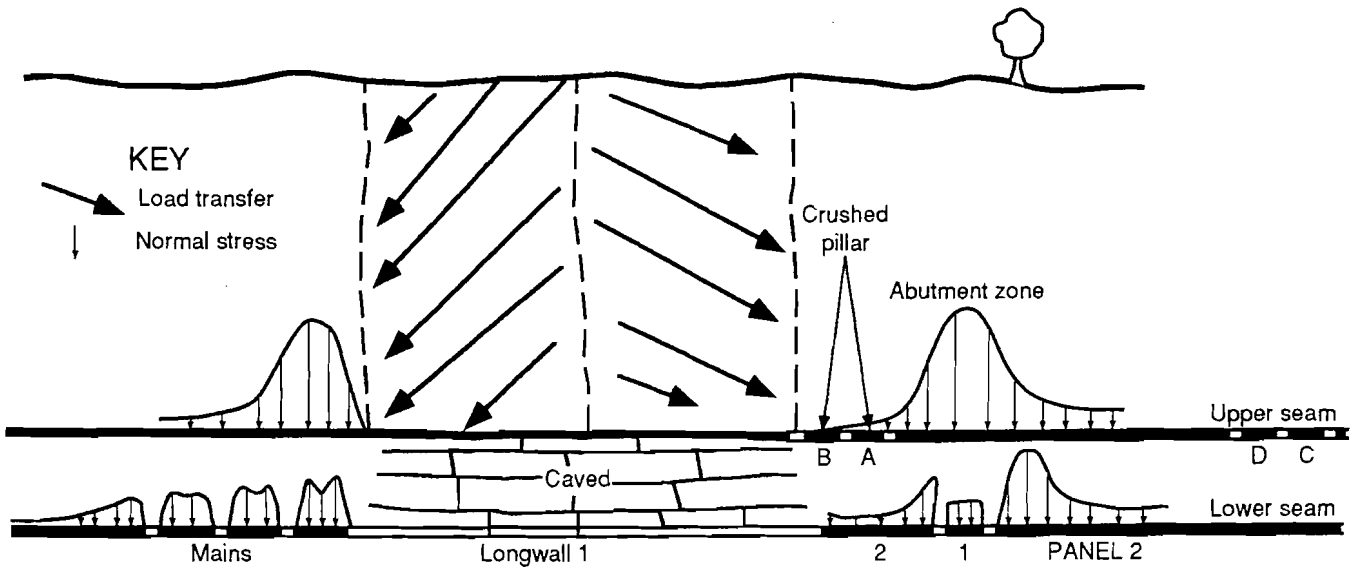

Figure 11
Typical Cross Section Lithology, Strength, and Modulus Log, Case Study 3.

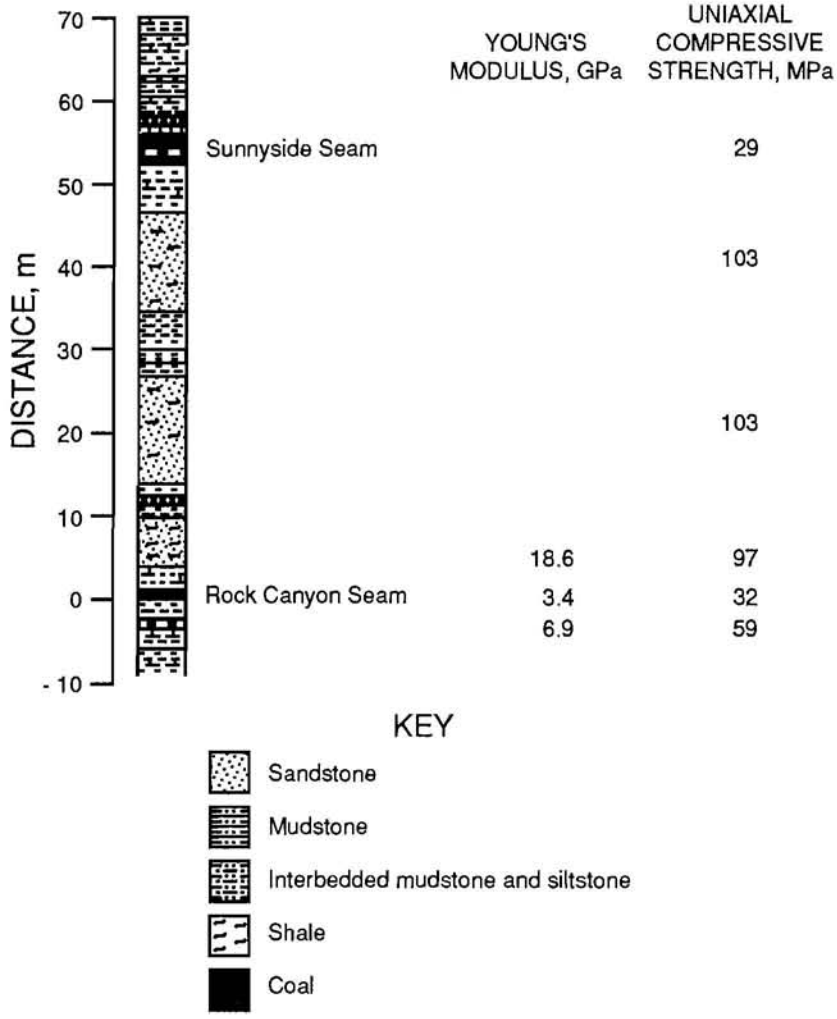

Recently, several coal bumps, one a 3.6-Richter-magnitude bump, occurred in an area of the Rock Canyon Seam, where cover ranged between 460 and 610 m (1,500 to 2,000 ft) thick (figure 12). These bumps took place where 18-m² (60-ft²) pillars and 6-m (20-ft) spans were being used. The time lag between panel development and pillar pulling was maximum (5 years) for panel A and minimum (1 year) for panels C and D. Underground observations indicated that the immediate roof (including the lower Sunnyside tongue) caved favorably in these sections.[3]

Following are some geometric and mining factors that contributed to bumping in panels B, C, and D (figure 12). Calculated elastic pillar stresses for these panel geometries were similar, exceeding the strength levels that were shown to cause roof, floor, and pillar stability problems (Maleki, 1992) by a minimum of 25 pct. Other factors contributing to such high pillar stresses were panel width and barrier pillar width, discussed elsewhere (Maleki and others, 1987; Zipf, 1993).

Many coal bumps occurred as the retreat line reached a distance equal to panel width (a square extraction). The cyclic nature of loading related to caving of upper strata that is associated with these square geometries has been identified by Maleki (1981) using direct pressure measurements in the gob (Maleki and others, 1984). The failure of upper strata was interpreted as a dynamic pulse that

[3]Personal communication from D. Spillman, mining engineer, 1994.

Figure 12
Panel Geometry and Bump Locations.

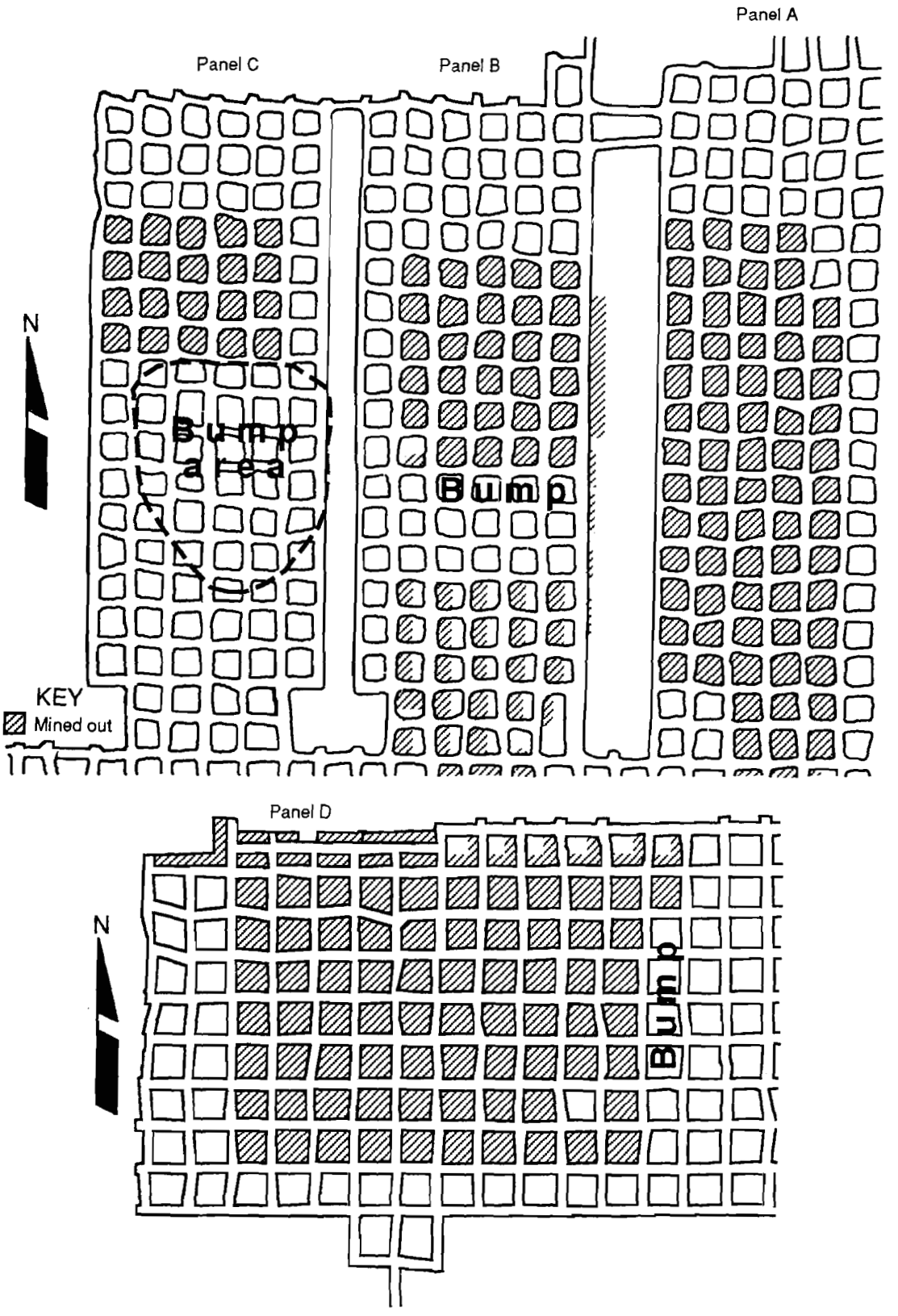

triggered violent failure of critically loaded pillars at the face.

Considering the size of the extracted areas and depth of cover, and using numerical models of caving progress (Maleki, 1981), it is suspected that the coal bumps in the B, C, and D panels were triggered by failure in the upper Sunnyside and Castle Gate sandstones, respectively. Seismic analysis of strain energy release for panel C[3] also pointed out that an additional source of energy beyond pillar strain energy was needed to balance the energy calculations; two possibilities were identified as supplying this additional energy, both relating to movement and collapse of roof strata.

In summary, this case study provides evidence of coal bumps triggered by failure of upper strata as much as 100 m (300 ft) above the coal seam. Coal pillars were critically loaded prior to caving by thick cover and panel geometries.

CASE STUDY 4—LACK OF YIELDING

This case study is similar to case study 1, except that there was no yielding in the mine floor, and thus coal bumps occurred frequently regardless of which alternative gate pillar layout was used. Yielding of the floor materials was associated with rock dilation, which reduced horizontal stresses in the pillar and enhanced gradual pillar failure.

The mine is located near Helper, UT. The longwall mining method has been used for the extraction of the D and Sub-3 seams (figure 13), which are some 130 m (430 ft) apart (Barron and others, 1994). Mining in the D Seam has been associated with the least number of coal bumps, while severe coal bumps in the Sub-3 coal seam have frequently interrupted mining.

The Sub-3 coal seam rests directly on the Star Point Sandstone, a thick, competent stratigraphic unit common in many mines in Utah. The seam contains a hard siltstone parting at midheight and two sets of cleats. The immediate roof is generally a thinly laminated siltstone underlain by 15 cm (6 in) of carbonaceous shale and intersected by sandstone channels (Bunnel and Taylor, 1986). Laboratory tests of mechanical properties of the immediate [6 m (19 ft)] roof and floor indicate that the materials are generally strong and stiff. No faults are present in the mining block and horizontal stress approximates vertical premining stress (Barron and others, 1994).

[3]Boler, F. M., S. Billington, and R. K. Zipf. Estimates of Radiated Energy and Strain Energy Release for a Magnitude 3.6 Coal Mine Event. Paper presented at the 1994 Seismological Society of America meeting, Apr. 4-7, 1994.

Longwall mining in the sub-3 Seam was conducted in areas with 300 to 610 m (1,000 to 2,000 ft) of cover and a high topographic relief. Both two- and three-gate entry systems using pillars 9, 15, 26, and 38 m (30, 50, 85, and 120 ft) in width were used to mitigate tailgate and face bump problems. None of these gate pillar layouts proved to be effective in controlling coal bumps as the second panel retreated.

Borehole pressure cell data indicated buildup of high horizontal stresses within the coal pillars, as illustrated in figure 14*B*. In this case, the pillars were 36 by 36 m (120 by 120 ft), a geometry that concentrated high stresses, particularly near the gob line (figure 14*A*). Coal bumps, however, persisted in this mine, irrespective of the gate pillar layout; nonyielding of the seam and floor contributed to the buildup of high stresses and sudden release of strain energy in the form of coal bumps.

CASE STUDY 5—NO BUMPS

The mine is located on the east margin of the Wasatch Plateau in Utah. The longwall mining method has been used to extract two-seam reserves within the Wattis and Third-Bed seams, which are 11 to 17 m (35 to 55 ft) apart. The cover varies over the longwall area from 300 to 350 m (1,000 to 1,160 ft). Cover materials are persistently jointed by three to four sets of joints. Horizontal stresses are directional and less than vertical stresses.

Figure 15 presents the lithology, RQD, and mechanical properties for the roof, floor, and Wattis Seam. This coal seam has a well-developed cleat system. The immediate roof and floor exhibit large strength variations but are generally weak. Sandstone channels have frequently replaced the siltstones in the mine roof. These channels are, however, well jointed and have caving characteristics similar to the siltstones and shales (Maleki, 1988).

During development and retreat of a 7-longwall block, no significant coal bumps occurred at this site. Underground measurements revealed that the 9- by 24-m (30- by 80-ft) gate pillars experienced rib yielding during development mining, transferring stresses to the pillar core. The pillar core lost confinement and crushed nonviolently as the face approached the instrumented site; this was shown by the vertical and horizontal borehole pressure cells positioned toward the middle of the pillar (figure 16).

In comparison to case study 1, pillar confining stresses were much less, pillar strength was significantly lower (38 pct), and the postfailure slope was higher for the gate pillars. The cleated nature of the coal, the yielding of the immediate floor, and the sharp contact between the roof

Figure 13
Stratigraphic Column, Case Study 4.

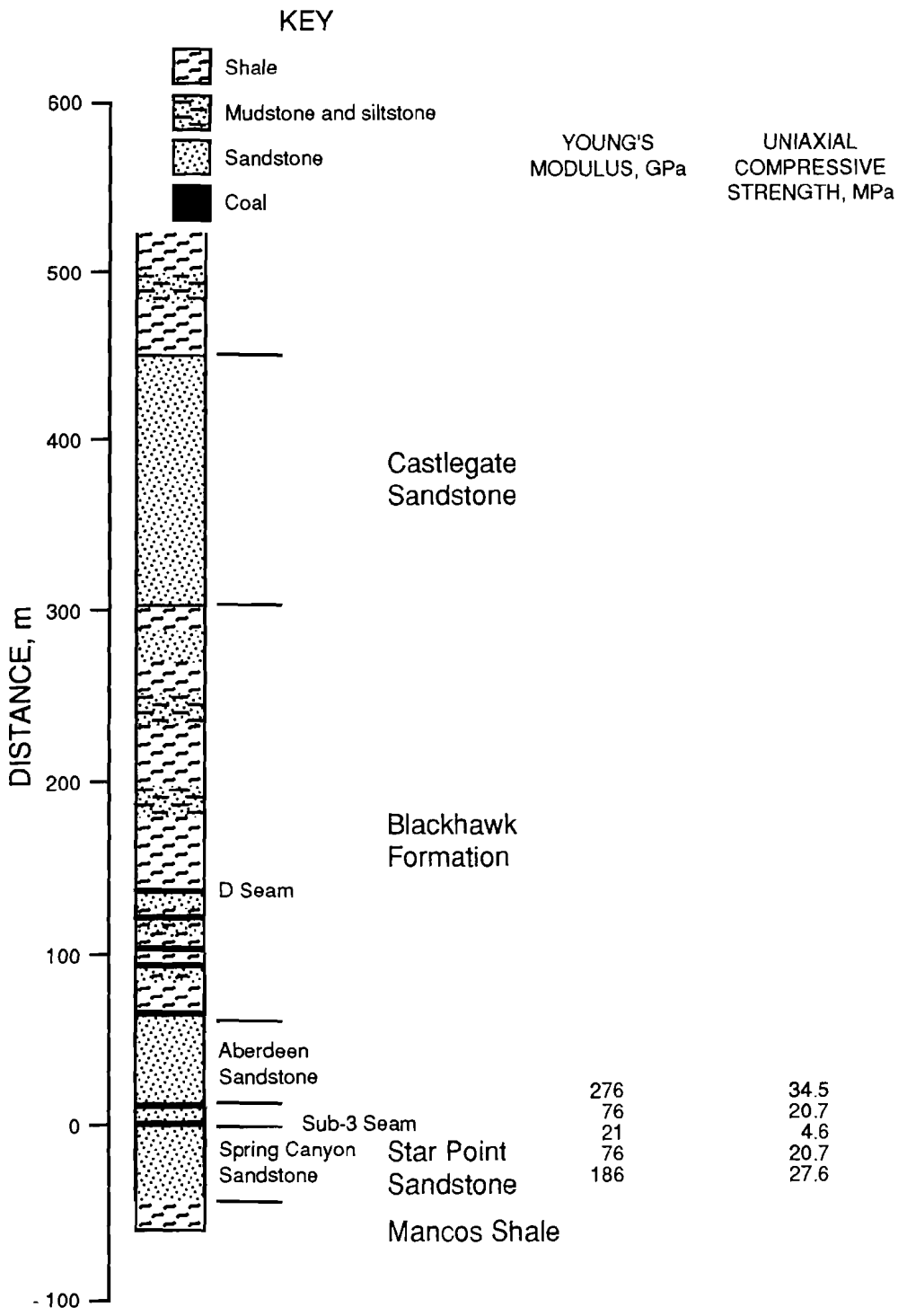

Figure 14
Borehole Pressure Cell Pressure Changes Versus Face Position, Case Study 4.

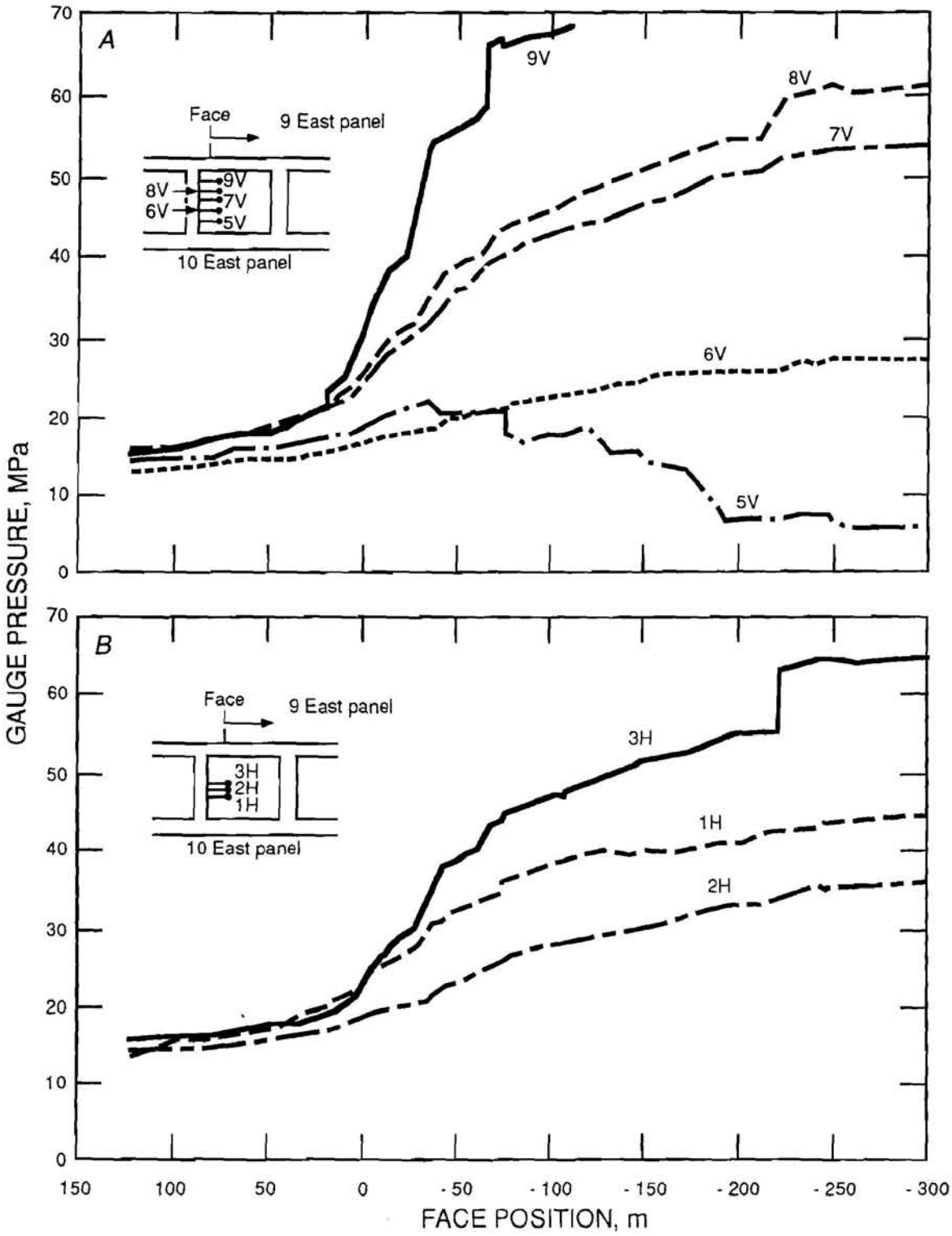

A, Vertical cells; *B*, horizontal cells.

Figure 15
Typical Near-Seam Rock Structure and Strength Properties, Case Study 5.

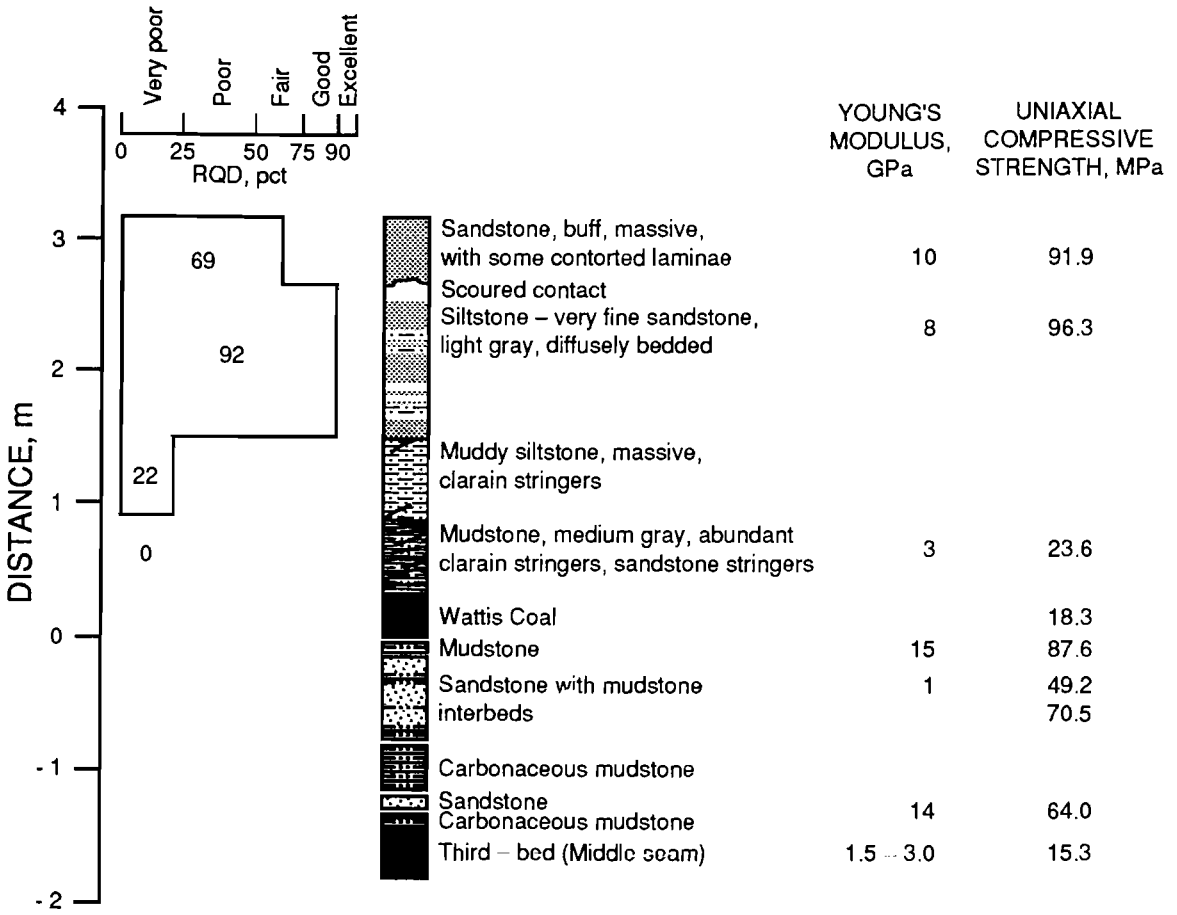

and the coal promoted gradual loss of confinement and nonviolent pillar behavior. Maleki (1988) and DeMarco and others (1995) have cataloged the benefits of such yield pillar systems for control of coal bumps.

In summary, pillar behavior in this mine is controlled by structural features consisting of cleats and sharp contact planes, as well as yielding floor strata. These factors reduced pillar strength and strain energy accumulation, leading to nonviolent failure. The well-jointed nature of the mine roof enhanced regular caving and noncyclic pillar loading.

SUMMARY

All case studies indicated that the calculated elastic pillar stresses exceeded by 20 to 30 pct the strength levels associated with roof, floor, and pillar stability problems (Maleki 1992). In addition, mining took place in areas where there was a rapid change in stress over a short distance and/or time, variations in topography, and pillar failure in an adjacent seam. Thus, a first step in minimizing coal bump potential is through development of mine layout and extraction sequences that would minimize activity in areas with high stress gradients.

Analysis of data from both bump-prone and nonbump-prone mines indicates that, in general, coal bump potential increases as the uniaxial compressive strength and Young's modulus ratios exceed 3 to 5. The role of mine stiffness could not be validated directly through the use of local stiffness in determining coal bump potential because there is not enough data regarding postfailure behavior of coal seams and the mechanical properties of large-scale rock masses.

Figure 16
Calculated Stresses From Two Pressure Cells.

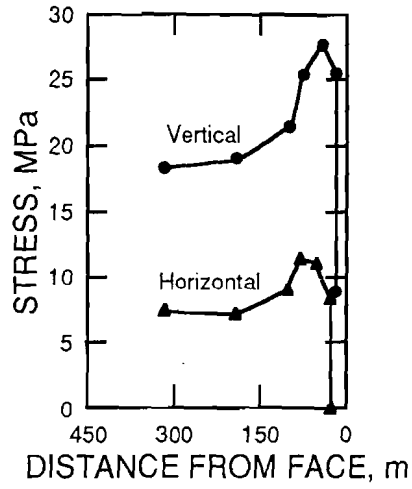

Striking differences in coal behavior exist in neighboring bump-prone and nonbump-prone mines, even when both mines have similar laboratory-determined mechanical properties. In bump-prone mines, high horizontal stresses formed within the coal and eventually dissipated while the immediate floor yielded. In the nonbump-prone mine, horizontal stress buildup was moderate and loss of stress occurred over a short time but in a very stable manner. The strength and behavior of this structurally controlled coal seam was influenced by persistent cleats, sharp contact between the roof and the seam, and the presence of readily yielding floor material. Yielding in the roof or floor was associated with dilation and a reduction in horizontal stresses, enhancing gradual pillar failure.

COAL BUMP ASSESSMENT METHODOLOGY

Through analyses of case studies and an evaluation of existing criteria, it is apparent that violent failures are influenced by the state of stress, stiffness of surrounding strata, dynamic effects associated with failure of surrounding strata, and near-seam depositional and structural features. It is apparent that existing criteria are generally too simplistic and address only either static or dynamic effects. A methodology is proposed here as a tool for assessing coal bump potential; this approach is useful during preliminary mine design to determine the potential for coal bump problems at an early stage in mine planning. If calculations reveal a high potential for coal bumps, additional geotechnical data may need to be collected during development of the property to increase confidence in predictions. Such calculations may include in situ strength of the coal seam, Young's modulus and uniaxial compressive strength ratios (roof- and/or floor-to-coal), beam thickness, overhang distances in the gob, and other factors.

This approach (figure 17) is initiated by thoroughly examining experience in mines with the same or other seams with similar geologic, strength, and loading conditions. If conditions are similar to the bump-prone seams, then additional considerations are highly recommended.

The first step in minimizing coal bump potential is through development of mine layout and extraction sequences that minimize activities in areas with high stress gradients. Specific designs may be evaluated by calculating the average strength and stress and ensuring that the ratio of the two (factor of safety) is greater than 1. Excluding yield pillar applications, all analyzed coal bumps occurred

Figure 17
Flow Chart for Assessing Coal Bump Potential.

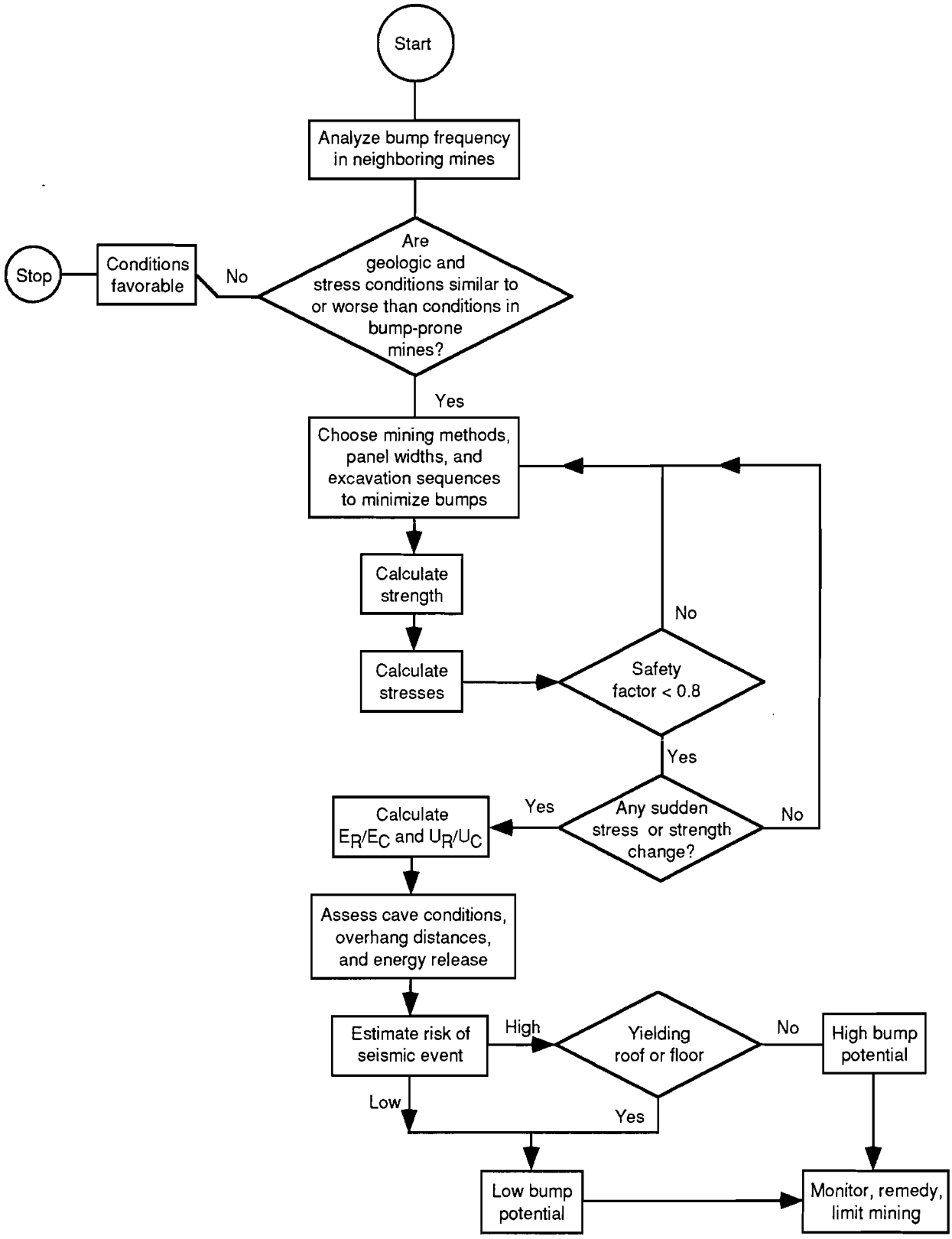

E_R/E_C = Young's modulus. U_R/U_C = Uniaxial compressive strength ratio.

when the stresses exceeded the strength levels associated with stability problems by a minimum of 20 pct (factor of safety 0.8).

Additional considerations should be given to any sudden changes in stresses caused by variations in topography and multiple-seam geometries. Localized changes in strength resulting from variations in geology and/or mining height should also be considered.

The Young's modulus ratio E_R/E_C (roof to coal) and uniaxial compressive strength ratio (U_R/U_C) should be calculated if safety factors are unfavorable. Modulus and strength ratios exceeding 5 to 3, respectively, and the absence of joints favor formation of large overhangs in the gob. Failure of these strata releases strain energy and contributes to coal bump incidence by providing a triggering mechanism for these marginally stable structures.

The damage potential of the seismic event may be estimated on the basis of expected local wave magnitude resulting from failure of surrounding strata. In general, wave magnitudes exceeding 2.5 on the Richter scale have been associated with high risks of damage.

Experience, numerical modeling, and engineering judgment may be used to assess the extent of yielding in mine roofs and floors; such controlled yielding may help reduce horizontal stresses and lead to less violent failures. Lack of yielding within the roof, coal, and seam promotes high bump potential where there is a high risk of a seismic event and a low factor of safety.

Mining conditions that are calculated to create a bump potential need special considerations to avoid production delays, damage to equipment, and danger to miners. Mining under such conditions should be conducted in conjunction with geotechnical monitoring and should be flexible in terms of remedial actions, including leaving blocks of coal in place. Seismic monitoring, tomographic surveys, and face support (shield) pressure recording can aid in detecting those anomalous geologic and stress conditions that contribute to coal bumps.

CONCLUSIONS

Geotechnical data, mining experience, and long-term underground observations were analyzed in an effort to better understand causes of violent failure in U.S. coal mines. It was shown that coal bumps are influenced by the interaction of geologic and stress conditions that govern postfailure behavior of coal-measure rocks. Case studies provided new insight into buildup and loss of horizontal stresses, geometric factors that cause zones with high stress gradients, contrasts in stiffness and the mechanical properties of rock and seam, and failure of upper strata.

Because geotechnical factors that influence coal bumps are multiple, existing criteria are inadequate to assess coal bumps. A preliminary methodology was developed based on experience in U.S. mines for assessing bump potential. In this approach, mining experience, stiffness and strength ratios, safety factors in coal structures, yieldability of roof and floor, sudden changes in stress gradient, and failure of roof strata are taken into consideration to assess coal bump potential.

REFERENCES

Babcock, C. O. Equation for the Analysis of Borehole Pressure Cell Data. Paper in Rock Mechanics: Key to Energy Production. 27th U.S. Symposium on Rock Mechanics (Univ. of AL, Tuscaloosa, AL, June 23-25, 1986). Soc. Min. Eng., 1986, pp. 233-240.

Babcock, C. O., and D. L. Bickel. Constraint — The Missing Variable in the Coal Burst Problem. Paper in Rock Mechanics in Productivity and Protection. Proceedings, 25th Symposium on Rock Mechanics, ed. by C. H. Dowding and M. M. Singh (Northwestern Univ., Evanston, IL, June 25-27, 1984). Soc. Min. Eng., 1984, pp. 639-647.

Barron, L. R., M. J. DeMarco, and R. O. Kneisky. Longwall Gateroad Stability in Four Deep Western U.S. Mines. USBM RI 9406, 1994, 84 pp.

Bunnel, M. D., and T. W. Taylor. Roof Lithology and Coal Seam Characteristics of the No. 3 Mine, Carbon County, Utah. Paper in Contributions to Economic Geology in Utah. Spec. Study 69, UT Geol. and Miner. Surv., 1986, pp. 1-29.

Campoli, A. A., T. M. Barton, F. C. Van Dyke, and M. Gauna. Mitigating Destructive Longwall Bumps Through Conventional Gate Entry Design. USBM RI 9325, 1990, 38 pp.

Chavan, A. S., N. M. Raju, and S. B. Srivastra. Rock Burst Prediction — An Empirical Approach. Paper in Rockbursts and Seismicity in Mines. Proceedings of the 3rd International Symposium on Rockbursts and Seismicity in Mines, ed. by R. P. Young (Kingston, ON, Aug. 16-18, 1993). Balkema, 1993, pp. 163-168.

Cook, N. G. W., and J. P. M. Hojem. A Rigid 50-Ton Compression and Tension Testing Machine. J. S. Afr. Inst. Mech. Eng., v. 1, 1966, pp. 89-92.

DeMarco, M. J., J. B. Koehler, and H. Maleki. Panel and Gateroad Design Considerations for the Mitigation of Coal Bumps in Western U.S. Longwall Operations. Paper in Proceedings: Mechanics and Mitigation of Violent Failure in Coal and Hard-Rock Mines. USBM Spec. Publ. 01-95, 1995, pp. 141-165.

Dubinski, J. Characteristics of Seismicity Induced by Mining Operations in the Upper Silesian Coal Field. Paper in Proceedings of the 18th Czechoslovakia-Poland Conference on Geophysics. 1990, v. 83. pp. 115-127.

Gibowicz, S. J. Keynote Lecture: The Mechanism of Seismic Events Induced by Mining. Paper in Rockbursts and Seismicity in Mines,

Proceedings of the 2nd International Symposium on Rockbursts and Seismicity in Mines, ed. by C. Fairhurst (Univ. of MN, Minneapolis, MN, June 8-10, 1988). Balkema, 1990, pp. 3-27.

Haramy, K. H., and J. P. McDonnell. Causes and Control of Coal Mine Bumps. USBM RI 9225, 1988, 35 pp.

Iannachione, T., and J. C. Zelanko. Pillar Mechanics of Coal Mine Bursts: A Control–Strategy. Paper in Proceedings of the 16th World Mining Congress, (Sofia, Bulgaria, Sept. 12-16, 1994). Bulgarian Nat. Organ. Comm., v. 5, 1994, pp. 15-23.

Kleczek, Z., and A. Zorychta. Coal Bumps Induced by Mining Tremors. Paper in Rockbursts and Seismicity in Mines 93. Proceedings of the 3rd International Symposium on Rockbursts and Seismicity in Mines, ed. by R. P. Young (Kingston, ON, Aug. 16-18, 1993). Balkema, 1993, pp. 87-90.

Lippmann, H. Mechanical Considerations of Bumps in Coal Mines: Keynote Lecture. Paper in Rockbursts and Seismicity in Mines, Proceedings of the 2nd International Symposium on Rockbursts and Seismicity in Mines, ed. by C. Fairhurst (Univ. of MN, Minneapolis, MN, June 8-10, 1988). Balkema, 1990, pp. 279-284.

Maleki, H. Coal Mine Ground Control. Ph.D. thesis, CO Sch. Mines, Golden, CO, 1981, 432 pp.

Maleki, H. Ground Response to Longwall Mining. CO Sch. Mines Q., v. 83, No. 3, 1988, 52 pp.

Maleki, H. In Situ Pillar Strength and Failure Mechanisms for U.S. Coal Seams. Paper in Proceedings of the Workshop on Coal Pillar Mechanics and Design, comp. by A. T. Iannacchione, C. Mark, R. C. Repsher, R. J. Tuchman, and C. C. Jones (Santa Fe, NM, June 7, 1992). USBM IC 9315, 1992, pp. 73-77.

Maleki, H., J. R. Aggson, F. Miller, and J. F. T. Agapito. Mine Design Layout for Coal Bump Control. Paper in 6th International Conference on Ground Control in Mining: Proceedings, ed. by S. S. Peng (WV Univ., Morgantown, WV, June 9-11, 1987). Dept. of Min. Eng., WV Univ., Morgantown, WV, 1987, pp. 32-46.

Maleki, H., W. Hustrulid, and D. Johnson. Pressure Measurements in the Gob. Paper in Rock Mechanics in Productivity and Protection. Proceedings, 25th Symposium on Rock Mechanics, ed. by C. H. Dowding and M. M. Singh (Northwestern Univ., Evanston, IL, June 25-27, 1984). Soc. Min. Eng., 1984, pp. 533-545.

Maleki, H., Y. Jung, and K. Hollberg. Case Study of Monitoring Changes in Roof Stability. Int. J. Rock Mech. Min. Sci. & Geomech. Abstr., v. 30, No. 7, 1993, pp. 1395-1401.

Maleki, H., M. Moon, and J. F. T. Agapito. In Situ Pillar Strength Determination for Two-Entry Longwall Gates. Paper in 7th International Conference on Ground Control in Mining: Proceedings, ed. by S. S. Peng (WV Univ., Morgantown, WV, Aug. 3-5, 1988). Dept. of Min. Eng., WV Univ., Morgantown, WV, 1988, pp. 10-19.

Mark, C. Pillar Design Methods for Longwall Mining. USBM IC 9247, 1990, 52 pp.

McGarr, A. Some Applications of Seismic Source Mechanism Studies to Assessing Underground Hazard. Paper in Rockbursts and Seismicity in Mines, ed. by N. C. Gay and E. H. Wainwright (Proc. of Symp. on Seismicity in Mines, Johannesburg, S. Afr., 1982). S. Afr. Inst. Min. Metall., Symp. Series 6, 1984, pp. 199-208.

Ortlepp, W. D. The Design of Support for the Containment of Rockburst Damage in Tunnels–An Engineering Approach: Invited Lecture. Paper in Rock Support in Mining and Underground Construction. Proceedings of the International Symposium on Rock Support, ed. by P. K. Kaiser and D. R. McCreath (Sudbury, ON, June 16-19, 1992). Balkema, 1992, pp. 593-609.

Pen, Y., and K. Barron. The Role of Local Mine Stiffness in Pillar Bump Prediction. Paper in Rock Mechanics Models and Measurements Challenges from the Industry. Proceedings of the 1st North American Rock Mechanics Symposium, ed. by P. P. Nelson and S. E. Laubach (Univ. of TX at Austin, TX, June 1-3, 1994). Balkema, 1994, pp. 1017-1024.

Pritchard, C. J., and D. G. F. Hedley. Progressive Pillar Failure and Rockbursting at Denison Mine. Paper in Rockbursts and Seismicity in Mines 93. Proceedings of the 3rd International Symposium on Rockbursts and Seismicity in Mines, ed. by R. P. Young (Kingston, ON, Aug. 16-18, 1993). Balkema, 1993, pp. 111-116.

Rice, G. S. Bumps in Coal Mines of the Cumberland Field, Kentucky and Virginia–Causes and Remedy. USBM RI 3267, 1935, 36 pp.

Ryder, J. A. Excess Shear Stress in the Assessment of Geologically Hazardous Situations. J. S. Afr. Inst. Min. Metall., v. 88, 1988, pp. 27-39.

Salamon, M. D. G. Stability, Instability, and Design of Pillar Workings. Int. J. Rock Mech. Min. Sci., v. 7, No. 6, 1970, pp. 613-631.

Starfield, A. M., and W. R. Wawersik. Pillars as Structural Components in Room-and-Pillar Mine Design. Paper in Basic and Applied Rock Mechanics. Proceedings, 10th Symposium on Rock Mechanics, ed. by K. E. Gray (Univ. TX at Austin, May 20-22, 1968). Soc. Min. Eng., 1972, pp. 793-809.

Wawersik, W. R., and C. Fairhurst. A Study of Brittle Rock Fracture in Laboratory Compression Experiments. Int. J. Rock Mech. Min. Sci., v. 7, No. 5, 1970, pp. 561-575.

White, B. G., J. K. Whyatt, and D. F. Scott. Geologic Factors in Rock Bursts in the Coeur d'Alene Mining District: Structure. Paper in Proceedings: Mechanics and Mitigation of Violent Failure in Coal and Hard-Rock Mines. USBM Spec. Publ. 01-95, 1995, pp. 243-264.

Williams, T. J., J. M. Girard, and C. J. Wideman. Investigation of a 3.5 M_L Rockburst. Paper in Rockbursts and Seismicity in Mines 93. Proceedings of the 3rd International Symposium on Rockbursts and Seismicity in Mines, ed. by R. P. Young (Kingston, ON, Aug. 16-18, 1993). Balkema, 1993, pp. 267-271.

Wong, I. G., J. R. Humphrey, J. A. Adams, and W. J. Silva. Observations of Mine Seismicity in the Eastern Wasatch Plateau, Utah, U.S.A.: A Possible Case of Implosional Failure. PAGEOPH, v. 129, 1989, pp. 369-405.

Wu, X., and M. G. Karfakis. An Analysis of Strain Energy Accumulation Around Longwall Panels Under Strong Roofs. Paper in Proceedings, 5th Conference on Ground Control for Midwestern U.S. Coal Mines, ed. by Y. P. Chugh and G. A. Beasley (Collinsville, IL, June 1994). 1994, pp. 230-253.

Yi, X., and P. K. Kaiser. Mechanisms of Rockmass Failure and Prevention Strategies in Rockburst Conditions. Paper in Rockbursts and Seismicity in Mines. Proceedings of the 3rd International Symposium on Rockbursts and Seismicity in Mines, ed. by R. P. Young (Kingston, ON, Aug. 16-18, 1993). Balkema, 1993, pp. 141-148.

Zipf, R. K., Jr. Analysis of Stable and Unstable Pillar Failure Using Local Mine Stiffness Method. Paper in Proceedings of the Workshop on Coal Pillar Mechanics and Design, comp. by A. T. Iannacchione, C. Mark, R. C. Repsher, R. J. Tuchman, and C. C. Jones (Santa Fe, NM, June 7, 1992). USBM IC 9315, 1992, pp. 128-143.

Zipf, R. K., Jr. Stress Analysis in Coal Mines With MULSIM/NL. Paper in Proceedings of the 89th Meeting of the Rocky Mountain Coal Mining Institute (Beaver Creek, CO, 1993). Rocky Mt. Coal Min. Instit., Lakewood, CO, 1993, pp. 38-43.

Zipf, R. K., Jr., and K. A. Heasley. Decreasing Coal Bump Risk Through Optimal Cut Sequencing With a Non-Linear Boundary Element Program. Paper in Rock Mechanics Contributions and Challenges: Proceedings of the 31st U.S. Symposium, ed. by W. A. Hustrulid and G. A. Johnson (CO Sch. of Mines, Golden, CO, June 18-20, 1990). Balkema, 1990, pp. 947-954.

OCCURRENCE AND REMEDIATION OF COAL MINE BUMPS: A HISTORICAL REVIEW

By Anthony T. Iannacchione[1] and Joseph C. Zelanko[2]

ABSTRACT

One of the most difficult, longstanding engineering problems associated with coal mining is the catastrophic failure of coal mine structures known as *bumps*. For more than 70 years, researchers and practitioners have assembled a wealth of technical information on coal bumps in an attempt to understand and control them. However, many technical issues raised long ago are still being debated today. This paper examines past experiences and recognizes achievements in the realm of coal bumps. U.S. Bureau of Mines (USBM) researchers collected and analyzed 172 coal bump incident reports and compiled the pertinent statistics into a database. Actual field studies are also discussed. Examination of past experience has shown that there is no one set of defining characteristics that is responsible for coal bumps. In all cases, bumps occur when complex arrangements of geology, stress, and mining conditions interact to interfere with the orderly dissipation of stress. However, it is evident from the database that a tremendous reservoir of knowledge has been established from past experience that has unquestionably limited the severity of coal mine bumps in the United States.

INTRODUCTION

Coal mine bumps have presented serious mining problems in the United States throughout the 20th century. Fatalities and injuries have resulted when these destructive events occurred at the working face of the mine. Persistent bump problems have caused the abandonment of large coal reserves and have led to premature mine closure.

Through the years, a variety of techniques were proposed and implemented to mitigate bumps. Mining history is rich with examples of innovative proposals that, at best, temporarily alleviated this complex problem. From the 1930's to the present, the U.S. Bureau of Mines (USBM) has conducted fundamental research on the geologic environments and failure mechanisms responsible for coal mine bumps and on methods to control them. This work supports the USBM's mission to improve safety for miners by eliminating their exposure to hazardous underground conditions.

During the 1930's, USBM research indicated that both geology and mining practice (geometry and sequence) play key functions in bump occurrence. Strong, stiff roof and floor strata not prone to failing or heaving were cited as contributing factors when combined with deep overburden. Various poor mining practices that tended to concentrate stresses near the working face were identified and discouraged. Although such qualitative geologic descriptions and design rules-of-thumb have persisted through the years, the need to better quantify bump-prone conditions remains.

Mine operators find little comfort in generalities when they have experienced a bump and must determine if another is imminent. Specific questions about the influence of individual factors and the interaction among factors arise but are often difficult to answer owing to the limited experience at a given mine site. Often, many

[1]Supervisory civil engineer.
[2]Mining engineer.
Pittsburgh Research Center, U.S. Bureau of Mines, Pittsburgh, PA.

parameters change simultaneously (for example, strength and stiffness of roof and floor, proximity of strong lithologic units to a coalbed, depth of overburden, mine geometry, and mining rate).

To better establish the range of circumstances under which bumps take place, the USBM compiled the Coal Bump Database, which contains information about bumps that have occurred in the United States since 1936. More than 172 coal mine bumps have been identified from various documents, including U.S. Mine Safety and Health Administration (MSHA) Reports of Investigation (Fatal and Nonfatal), USBM reports, mining conference proceedings, and mining company reports and memoranda. Information pertinent to mine design and geologic characterization of bump-prone ground has been extracted from the documents and assembled in a spreadsheet. It is the mining community's charge to rethink its understanding of bump phenomena while exploring innovative techniques to mitigate occurrences. Presentation of historical information in this format facilitates a reevaluation of the broad range of geologic and operational conditions under which bumps have been encountered and will help preserve knowledge acquired through experience.

BACKGROUND

The earliest U.S. coal mine bump included in the USBM Coal Bump Database dates back to 1936. However, several reports indicate that bumps had constituted a serious problem even earlier. For example, Watts (*30*)[3] reported bumps at the Sunnyside No. 1 Mine in Utah, and Rice (*27*) documented several bumps in the Cumberland Coalfield in eastern Kentucky. Bryson (*3*) indicates that bumps occurred in the Cumberland Coalfield as early as 1923 and became very troublesome from 1930 to 1934. In most cases, specific information on the events as described by these experts is not available, and thus these events have not been included in the database. However, the descriptions of various causes and attempted remedies for bumps provide valuable anecdotal information.

Notable among the early work on coal mine bumps are reports by Rice (*27*) and Holland and Thomas (*14*). Rice classifies bumps into two general types: *pressure bumps* and *shock bumps*. According to Rice, pressure bumps are caused when pillar stress exceeds bearing strength. Shock bumps are induced by breaking of thick, massive strata at a considerable distance above the coalbed, which causes the immediate mine roof to transmit a shock wave to the coal. Rice indicates several conditions favoring bumps, including thick overburden, strong overlying strata, and a strong floor not prone to heaving. Holland and Thomas define a similar range of conditions based on their examination of more than 117 instances of bumps in West Virginia, Kentucky, Utah, and Virginia. Their investigation also demonstrated that most bumps had been caused by improper mining methods and practices.

Reports from the 1950's document technical advances for mining in bump-prone ground. For example, Talman and Schroder (*29*) describe a novel barrier-splitting technique called the thin-pillar mining method. In thin-pillar mining, the barriers are segmented into a series of yield pillars too small to maintain significant stress levels or stored strain energy. Efforts in both Eastern and Western U.S. coalfields were also directed to maintaining low stress levels through planned destressing activities, such as large-hole auger drilling (*28*) and volley firing (*25*).

Despite technical advances in the 1950's, analyses of bump records from 1959 to 1984 (*12*) indicate that bumps still occurred at an alarming rate. Current information shows that bump-related accidents resulted in 42 fatalities since 1960 (table 1), 14 in the Eastern United States and 28 in the Western United States. Continuing bump problems probably stemmed in part from the same unfavorable mining conditions and practices discussed by Holland and Thomas.

Table 1.—Chronological distribution of bump events included in USBM Coal Bump Database

Time period	Number of bumps	Fatalities	Injuries
1930-39	1	1	0
1940-49	9	7	18
1950-59	38	28	43
1960-69	27	13	36
1970-79	30	10	21
1980-89	52	19	32
1990-present	9	0	8

The advent of the continuous mining machine resulted in different problems requiring new control solutions. The mobility and versatility of the continuous miner led to the development of novel pillar splitting and extraction sequencing designs for bump control.

With the widespread utilization of the longwall mining method over the last 15 years in the United States, bump problems have continued to threaten the safe mining of coal. One fatality on an advancing longwall face, several

[3]Italic numbers in parentheses refer to items in the list of references at the end of this paper.

injuries on retreating longwall faces, and at least one mine closure have been attributed to bumps (*18*). However, ingenuity and experience have prevailed, and several innovative designs for controlling bumps in longwall mines have been developed. Two designs focus on altering the size and shape of gate entry pillars. The conventional pillar design approach relies on increasing the gate pillar dimensions so that the pillars will prevent abutment load ride-over onto the active longwall face (*32*). The yield pillar approach effectively reduces gate pillar dimensions so that the pillars will yield in a controlled fashion, thereby eliminating tailgate pillar bumps and aiding in the controlled fracturing of the main roof (*7, 21*). A third approach, the advancing longwall method, eliminates the need for developing gate road pillar systems; advancing longwalls were first used in the United States at Mid-Continent Resource's coal mines in the 1970's (*19, 26*). All of these methods have some drawbacks, but they generally represent innovative design philosophies for controlling bumps.

U.S. coal bumps have been associated with a variety of conditions. Perhaps the most general conditions conducive to bumps are stiff, massive strata and high stresses. In some instances, these conditions are pervasive; in others, they are altered locally by geology or mining. For example, geologic structures such as faults or sandstone channels have, in some cases, affected the occurrence of bumps. Similarly, extraction sequences and mine layouts (e.g., multiple-seam mining scenarios) influence the way stresses are concentrated around mine openings and thus play a role in bump occurrence. Holland and Thomas (*14*, p. 34) state that the relationship between factors and circumstances causing bumps "actually is very complex, especially in a quantitative sense." Unique combinations of geology and mining systems have required many site-specific bump-control designs. Such designs must continually evolve as new geologic and mining scenarios are encountered. Solutions to new design challenges can result from evaluating past experiences.

OVERVIEW OF USBM COAL BUMP DATABASE

The USBM Coal Bump Database includes 172 specific bump events that occurred in four Eastern States and three Western States (figure 1). The database was constructed from USBM and MSHA coal bump accident and incident reports written between October 12, 1936, and January 21, 1993. A total of 87 fatalities and 163 injuries were identified. The 1980's witnessed the greatest outbreak of bumps, accounting for 31 pct of the total, while the second largest percentage occurred during the 1950's (23 pct). West Virginia recorded the greatest number of documented bumps (53), followed by Virginia (40), Colorado (30), Utah (26), and Kentucky (19). Alabama and Washington each had one reported bump event.

Analysis of information in the Coal Bump Database indicates that bumps have occurred in a variety of mining systems and operations. For example, pillar retreat mining accounted for 35 pct of the bumps, barrier-splitting for 26 pct, longwall mining for 25 pct, and development mining for 14 pct. Of the longwall incidents, 33 pct affected the longwall face, 19 pct the tailgate entries, 36 pct both the longwall face and the tailgate entries, and 6 pct the headgate entries. Generating 67 pct of the total, the act of excavating was associated with the greatest number of incidents. The coal-loading operation at the face accounted for another 22 pct of the total. Other, less-frequent bump incidents occurred during shot firing (5 pct) and installation of support (6 pct). Additionally, 22 pct of the bumps took place during nonproduction shifts. One event reportedly occurred in an abandoned section.

The database includes reports on individual bump events from more than 50 mines. As table 2 indicates, some mines account for a single bump record, whereas 20 or more events have been documented at two sites. With such high numbers of bumps at individual mines, it is not surprising that an impressive list of bump-control efforts has been developed. Unique mine designs have been employed to redistribute excessive stress conditions, for example, the thin-pillar method at the Gary No. 2 Mine and pillar-splitting methods at the Olga, Beatrice, and Cottonwood Mines. Innovative support strategies have been documented, ranging from yielding leg arches used at the Sunnyside Mines to material-filled cribs employed at several eastern Kentucky drift mines. The virtues and shortcomings of destressing techniques, including shot firing, auger drilling, and water infusion, have been identified. For example, extensive use of auger techniques with hole diameters ranging from 9 to 49 cm was attempted in the Gary district until a major bump during drilling resulted in fatalities in the early 1950's.

Information pertinent to mine design and geologic characterization of bump-prone ground was extracted from source documents for each mine and assembled into a computer spreadsheet. The spreadsheet format facilitates the identification of common conditions contributing to bumps and provides a means of readily evaluating the broad range of experiences. Moreover, the range of documented experiences shows that bumps manifest themselves in different ways with varying effects.

Table 2.—U.S. coal mines included in USBM Coal Bump Database

Mine	Company	City	County	State	Coalbed	No. of bumps
Bartley No. 3	Island Creek Corp.	Bartley	McDowell	WV	NA	1
Beatrice	Beatrice Pocahontas Co.	Keen Mountain	Buchanan	VA	Pocahontas No. 3	24
Belina No. 1	Valley Camp of Utah, Inc.	Clear Creek	Carbon	UT	Upper O'Connor	1
Braztah No. 3	Braztah Corp.	Helper	Carbon	UT	Subseam No. 3	2
Brookside	Kentucky Jellico Coal Co.	Brookside	Harlan	KY	Harlan	3
Buchanan No. 1	Consolidation Coal Co.	Mavisdale	Buchanan	VA	Pocahontas No. 3	2
C-2	Harlan Cumberland Coal Co.	Dione	Harlan	KY	Creech	1
Castle Gate	Castle Gate Coal Co.	Helper	Carbon	UT	Subseam No. 3	2
Castle Gate No. 2	Carbon Fuel Coal Co.	Helper	Carbon	UT	NA	1
Cottonwood	Energy West Mining Co.	Huntington	Emery	UT	Hiawatha	1
Deer Creek	Energy West Mining Co.	Huntington	Emery	UT	Blind Canyon	2
Dehue	Youngstown Mines Corp.	Dehue	Logan	WV	Eagle	2
Dutch Creek No. 1	Mid-Continent Resources, Inc.	Redstone	Pitkin	CO	B	16
Federal No. 1	Federal Mining Corp.	Elkhorn City	Pike	KY	Elswick	1
Gary No. 2	U.S. Steel Mining Co., Inc.	Gary	McDowell	WV	Pocahontas No. 4	20
Gary No. 6	U.S. Steel Mining Co., Inc.	Gary	McDowell	WV	Pocahontas No. 4	6
Glen Rogers No. 2	Raleigh Wyoming Mining Co.	Glen Rogers	Wyoming	WV	Beckley	2
H-2	Harlan Cumberland Coal Co.	Louellen	Harlan	KY	Harlan	1
Harewood	Allied Chemical Corp.	Longacre	Fayette	WV	Eagle	1
Holden	Howe Sound Co.	Holden	Chelan	WA	NA	1
Kenilworth	Carbon Fuel Coal Co.	Kenilworth	Carbon	UT	Castlegate D	2
L. S. Wood	Mid-Continent Resources, Inc.	Redstone	Pitkin	CO	B	10
Lynch No. 37	Arch of Kentucky, Inc.	Cumberland	Harlan	KY	Harlan	5
Maple Meadow	Maple Meadow Mining Co.	Fairdale	Raleigh	WV	Beckley	1
Marathon No. 1	Harlan Wallins Coal Co., Inc.	Verdo	Harlan	KY	Darby	1
Mary Helen No. 2	Mary Helen Coal Corp.	Coalgood	Harlan	KY	Harlan	1
Mary Helen No. 3	Mary Helen Coal Corp.	Coalgood	Harlan	KY	Harlan	1
Milburn No. 4	Milburn Colliery Co.	Milburn	Fayette	WV	No. 2 Gas	1
Mine No. 10	Wisconsin Steel Coal Mines	Benham	Harlan	KY	Harlan	1
Moss No. 2	Clinchfield Coal Co.	Clinchfield	Russell	VA	Tiller	5
Moss No. 3	Clinchfield Coal Co.	Duty	Dickenson	VA	Thick Tiller	1
No. D-1	Wisconsin Steel Coal Mines	Benham	Harlan	KY	D above Kellioka	1
No. 1	Turtle Creek Coal Co.	Coalgood	Harlan	KY	Harlan	1
No. 2	Chafin Coal Co.	Rita	Logan	WV	Upper Cedar Grove	2
No. 2	Clinchfield Coal Corp.	Dante	Russell	VA	Upper Banner	3
No. 4	Jim Walter Resources, Inc.	Brookwood	Tuscaloosa	AL	Blue Creek	1
No. 9	Jewell Eagle Coal Co.	Melville	Logan	WV	Eagle	2
No. 17	Island Creek Corp.	Red Jacket	Mingo	WV	Cedar Grove	1
No. 21	W-P Coal Co.	Stirrat	Logan	WV	Chilton	1
No. 27	Island Creek Corp.	Ragland	Mingo	WV	NA	1
No. 31	Peabody Coal Co.	Kenvir	Lee	VA	Darby	1
Olga	Olga Coal Co.	Coalwood	McDowell	WV	Pocahontas No. 4	12
Price River No. 3	Price River Coal Co.	Helper	Carbon	UT	Castlegate sub 3	1
Soldier Canyon	Soldier Creek Coal Co.	Wellington	Carbon	UT	Rock Canyon	1
Somerset	U.S. Steel	Somerset	Gunnison	CO	C above Kellioka	2
Sunnyside No. 1	Kaiser Steel Corp.	Sunnyside	Carbon	UT	Lower Sunnyside	7
Sunnyside No. 2	Kaiser Steel Corp.	Sunnyside	Carbon	UT	Upper Sunnyside	3
Trail Mountain No. 9	Beaver Creek Coal Co.	Orangeville	Emery	UT	Hiawatha	1
VP No. 3	Virginia Pocahontas Co.	Vansant	Buchanan	VA	Pocahontas No. 3	3
VP No. 6	Island Creek Corp.	Mavisdale	Buchanan	VA	Pocahontas No. 3	1
Wilberg	Emery Mining Corp.	Orangeville	Emery	UT	Hiawatha	3
NA	NA	NA	NA	CO	B	1
NA	NA	NA	NA	KY	NA	1
NA	NA	NA	NA	KY	NA	1
NA	NA	NA	NA	CO	Middle B	1

NA Not available.

Figure 1
Major U.S. Coal Basins Where Coal Mine Bumps Have Historically Been a Problem.

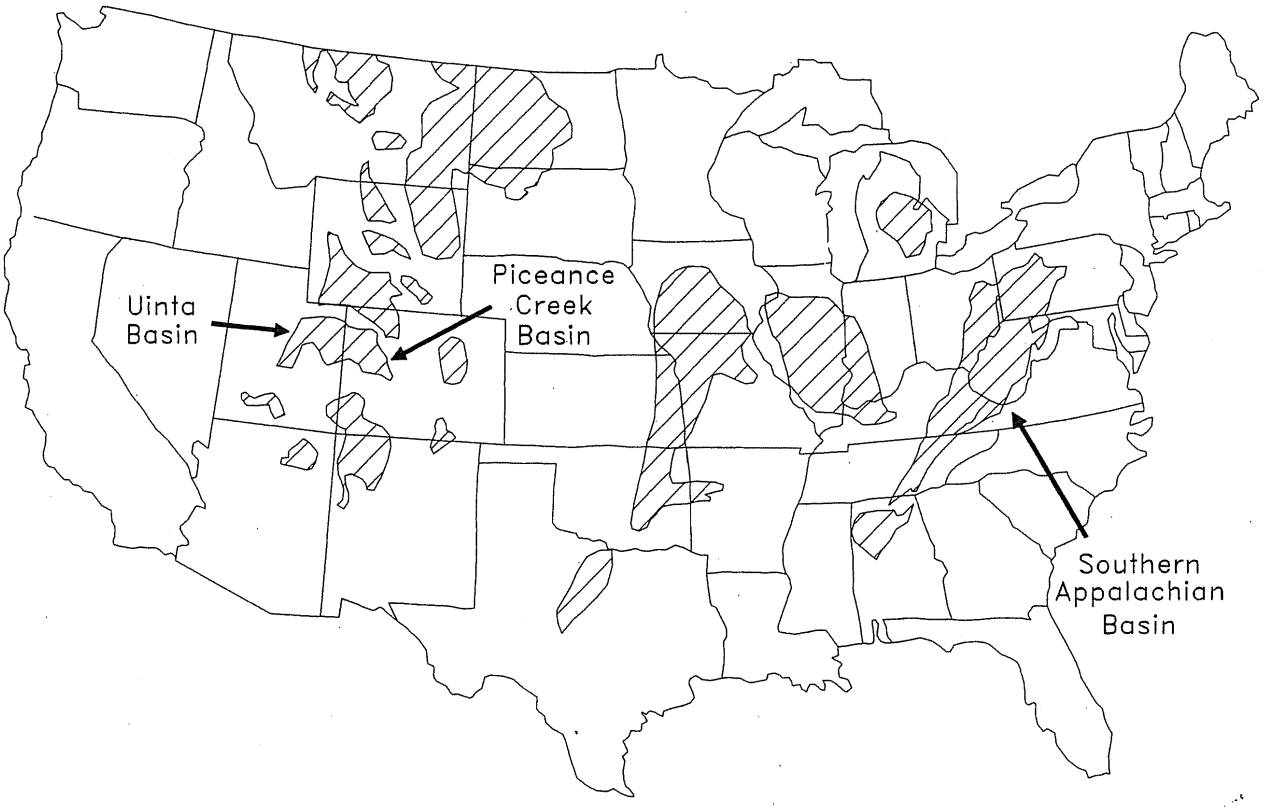

FACTORS CONDUCIVE TO BUMPS

Although specific mechanisms that trigger coal mine bumps are not well established, it is generally recognized that high stresses play a key role in bumps. Retreat mining and barrier-splitting often intensify the stresses. Abutment loading on pillar retreat lines and longwall gate roads can be extreme, especially when mining is conducted between stiff subjacent and superjacent strata. By design, barriers are intended to carry abutment loads in various situations, and thus barrier-splitting operations often involve high-stress environments. In development mining, stress redistribution generally affects areas near the openings. In areas of thick overburden (for example, >600 m), the redistribution of stresses caused by development mining alone may generate coal mine bumps.

High-stress conditions conducive to generating coal mine bumps are associated with a variety of factors. Caving characteristics of main roof units may have a significant impact on stress levels at a room-and-pillar retreat line or retreating longwall face. Geologic structures such as displacement faults, massive sandstone paleochannels, and rolls are important because of their ability to concentrate stress and control the caving and heaving characteristics of strata. Unfavorable mining practices or configurations (for example, multiple-seam interactions) can concentrate stresses in specific locations. Undoubtedly, these factors play a role in many of the bumps included in the USBM Coal Bump Database. Nevertheless, the simplest indicator of bump potential appears to be the presence of thick overburden. Overburden information is included in the database for more than 50 mines that have experienced bumps. Overburden thickness at these sites ranges from 143 to 760 m, but at most of the sites, overburden ranges from 400 to 550 m. Only 10 mines experienced bumps where overburden thickness was less than 300 m, while 9 were operating under more than 600 m when bumps occurred.

As indicated earlier, a variety of geologic factors have influenced the occurrence of bumps. In describing natural conditions conducive to coal bumps, a common factor in both U.S. and foreign mines is the proximity of the bump-prone coalbed to strong, thick, rigid strata (*2*). Of the 172 events comprising the USBM Coal Bump Database,

lithologic descriptions of the mine roof are included for 95 bump sites. In 86 instances, reference is made to the presence of *sandstone* immediately above to within a few meters of the coalbed. Terms such as "strong," "firm," "massive," and "thick" are used to describe the sandstone units. In 30 instances, a shale, sandy shale, siltstone, or mudstone unit of varying thickness was found to occur between the coalbed and the overlying sandstone units. Geologic descriptions of the mine floor are included for more than 80 sites. *Shale* is the predominant floor lithology in the database; the presence of sandstone in the floor is noted in only 25 pct of the site descriptions. Terms such as "hard" and "dense" are common descriptions of floor lithologies.

The implications of multiple-seam mining interactions in generating strata control problems are well documented (*5-6*). These problems can be the result of both stress concentration or strata displacement and can be experienced when the interburden is as thick as a few hundred meters. However, problems are more severe when the interburden is less than 100 m thick. Ground conditions in upper coalbeds may be disturbed by strata movements associated with previous workings in a lower coalbed. This type of interaction may result in difficult mine roof conditions but has not been identified as a factor contributing to bumps. Stress concentrations occurring in multiple-seam mining scenarios, however, have been associated with bumps; 15 bumps in the database occurred in such settings. In most cases, mining in a lower coalbed encountered zones of high stress beneath barriers or isolated pillar sections in a previously mined upper coalbed.

Rice suggested that "a structurally strong coal" not prone to crushing easily would favor bumps (*27*, p. 4). However, more recent research suggests that the physical properties of coal are not necessarily key factors in bump occurrence. For example, Babcock and Bickel (1984) performed laboratory studies on coal samples from 15 mines in 11 coalbeds. Their study concluded that many, if not most, coals can fail violently given the proper conditions of stress and constraint. The database appears to support this conclusion, for it demonstrates that coal bumps have been experienced in at least 25 U.S. coalbeds (table 3). The height of Eastern U.S. coalbeds ranged from 1 to 3 m; Western U.S. coalbeds were significantly higher, ranging from 1.8 to 4.3 m.

HAZARDS ASSOCIATED WITH BUMPS

Coal mine bumps are dynamic phenomena; numerous fatalities and injuries have been a direct result of miners being struck by coal forcefully ejected during a bump. Approximately 80 pct of the fatalities documented in the database were caused directly by displaced coal either hitting the individual or by forcing the individual into nearby equipment or mine ribs. However, other hazards have also been associated with coal mine bumps, including roof falls and ignitions of methane and coal dust.

Table 3.—U.S. coalbeds associated with coal mine bumps

Coalbed	State	Thickness, m
Eastern United States:		
Beckley	WV	1.8
Blue Creek	AL	1.8
Cedar Grove and Upper Cedar Grove	WV	1.0-1.8
Chilton	WV	1.1
Creech	KY	2.1
Darby	KY-VA	1.0-1.1
Eagle	WV	1.1
Elswick	KY	1.1
Harlan	KY	1.1-2.7
No. 2 Gas	WV	1.5
Pocahontas No. 3	VA	1.3-1.8
Pocahontas No. 4	WV	1.2-2.0
Tiller	VA	1.3-3.0
Upper Banner	VA	1.6
Western United States:		
B	CO	1.9-3.0
Blind Canyon	UT	4.3
C	CO	2.1-2.7
Castlegate D	UT	3.8
Dutch Creek M	CO	2.4
Hiawatha	UT	2.1
Middle B	CO	2.7
Rock Canyon	UT	
Subseam No. 3	UT	1.8-2.4
Upper and Lower Sunnyside	UT	2.1-3.2
Upper O'Connor	UT	2.7

Ten incidents in the database document mine roof falls that occurred in conjunction with bumps. Prior to the widespread use of roof bolting for primary support, bumps had the potential to create roof instabilities simply by dislodging posts and crossbars. With the introduction of roof bolting, however, the effect of bumps on supports was lessened. Nevertheless, bumps appear to continue to contribute to roof falls by disturbing the stability of the roof rock directly. In one case, for example, a bump caused roof rock to be released along a slip between longwall chocks and the face, resulting in a fatality. This associated hazard appears to be most prevalent during pillar mining, particularly in the Uinta Coalfields of Utah.

Ignitions of methane gas and dust associated with coal bumps are somewhat rare, but they are among the most devastating incidents in terms of the numbers of miners killed or injured. For example, on March 14, 1945, a pillar bump at the Kenilworth Mine caused the trailing cable of a loading machine to be pulled with such force that it was severed and created a short circuit that led to arcing (*15*). Thick coal dust resulting from the violent bump, coupled with methane gas, probably from the adjacent gob area, ignited, severely burning 12 miners. Seven of the injured miners eventually died as a result of the accident.

Ignitions are more prevalent in deep pillar extraction areas and during longwall mining. However, one bump-related ignition reportedly occurred during development mining. Mid-Continent Resources has experienced severe problems with extensive methane gas emissions in association with bumps at its mines, which have been referred to as gas outbursts. The most devastating gas-driven bump occurred on April 15, 1981, at the Dutch Creek No. 1 Mine in Colorado. A massive outburst of gas and coal occurred approximately 2 h after mining through a fault on the development section for the No. 102 longwall. Fifteen miners were killed and three were injured in the resultant mine explosion. Five less severe events occurred at the company's L. S. Wood Mine, where significant quantities of methane gas were measured in the mine air after face bumps.

COMPARATIVE MAGNITUDE OF BUMPS

A sense of relative event magnitude can be gained by assessing observed destruction and measured seismicity for a number of events documented in the USBM Coal Bump Database. In terms of observable damage underground, bumps ranged in magnitude from those that dislodged a portion of a single rib to three that partially destroyed large sections of pillars. On June 3, 1985, the Olga Mine in southern West Virginia experienced a series of bumps that eventually affected, to varying degrees, approximately 100 coal pillars (*8*). Fortunately, this event occurred over an idle weekend when no miners were on the section. However, only a few meters of bumped rib coal can have devastating effects. For example, a continuous mining machine helper at the Belina No. 1 Mine was seriously injured on March 19, 1981, while standing next to a rib where only a few meters of coal were expelled.

Numerous reports have been made concerning the degree to which bumps are felt on the surface, sometimes as far as 3 km away. Seismological observatories around the world have recorded some of the more powerful incidents. Eleven bumps from the database have Richter magnitudes of 3 or greater, with three in Virginia having magnitudes of 4 or greater (table 4).

Table 4.—Levels of mining-induced seismicity registered at U.S. coal mines

Mine	State	Richter magnitude	Date
Olga	WV	3.4	Apr. 26, 1965.
Moss No. 2	VA	[1]3.5 and 4.5	July 30, 1970.
Moss No. 2	VA	4.0-4.2	May 20, 1972.
Beatrice	VA	1.0	May 15, 1974.
Jim Walter Resources, Inc., No. 4	AL	3.6	May 7, 1986.
VP No. 3	VA	3.0	Mar. 4, 1987.
Buchanan No. 1	VA	4.0	Apr. 14, 1988.
Buchanan No. 1	VA	3.6	Apr. 10, 1989.
Lynch No. 37	KY	2.3	Nov. 22, 1989.
Deer Creek-Cottonwood	UT	3.0	Mar. 15, 1991.
Soldier Creek	UT	3.6	Jan. 21, 1993.
Lynch No. 37	KY	3.8	Aug. 3, 1994.
Lynch No. 37	KY	3.6	Oct. 5, 1994.

[1]Prebump shock 12 h and 6 h, respectively, before bump occurrence underground.

An explanation for the range in levels of observed seismicity may be found by examining the mechanisms responsible for many of the rock bursts in deep South African and Canadian hard-rock mines. Morrison and MacDonald (*22*) have shown that rock bursts are often associated with slip along preexisting geologic discontinuities adjacent to mine openings. Stick-slip movements on these discontinuities produce a sharp, instantaneous acceleration within the strata around the mine structure. As seismic waves propagate through the mine, pillars are compressed, then extended. This causes an immediate increase in load, resulting in a potentially unstable stress state. During the next instant, load is removed, which lowers confinement and can initiate an unstable state.

The level of mining-induced seismic activity coming from U.S. coalfields suggests that earthquake-like sources may indeed be partially responsible for pillar damage underground. Evidence at one site suggests that the seismic source was over 30 m above the mine opening and may have been associated with slip between large blocks of

strata over or adjacent to longwall gob areas. At other sites, the source of the seismicity appears to be within the mine structure. These events generally have lower values of seismicity, possibly resulting from the dissipation of energy into a mine opening. These data suggest that there is a weak correlation between the magnitude of surface shaking and the degree of destruction experienced underground.

EXAMPLES FROM THE USBM COAL BUMP DATABASE

BUMP EXPERIENCES AT SPECIFIC MINES

The sections below provide an overview of many events represented in the USBM Coal Bump Database. The authors refer often to the L. S. Wood, Gary No. 2 and No. 6, Moss No. 2, and Beatrice Mines to highlight various aspects of U.S. bump experiences. Therefore, a brief description of these operations is warranted.

L. S. Wood Mine

The L. S. Wood Mine near Redstone, CO, was developed in the 2-m-thick B Coalbed in the early 1970's by Mid-Continent Resources. Initially, the mine employed approximately three continuous mining machines and developed pillar sections to the left and right of its main entry system (figure 2). Because the mine was originally a drift mine, overburden in the early years was low. However, overburden rapidly increased as the main entries were developed downdip. By the time the first longwall became operational, the overburden was approaching depths of 500 m. The mine was plagued with methane gas emissions and displacement faults.

Gary No. 2 and No. 6 Mines

The Gary No. 2 and No. 6 Mines, operated by U.S. Steel Mining Co., were first opened in 1903 in the Pocahontas No. 4 Coalbed (*9*). These mines are located adjacent to each other in McDowell County in southern West Virginia. The coalbed crops out on the mine property, but rugged terrain accounts for overburden thicknesses approaching 460 m. In conjunction with thick overburden, strong roof and floor lithologies are present. The mine roof over much of the property includes a massive sandstone up to 45 m thick.

The Gary Mines have a long, fairly well-documented coal bump history. Duckwall (*9*) noted that bumps

Figure 2
Location and Dates of Bumps Reported at L. S. Wood Mine, Redstone, Pitkin County, CO.

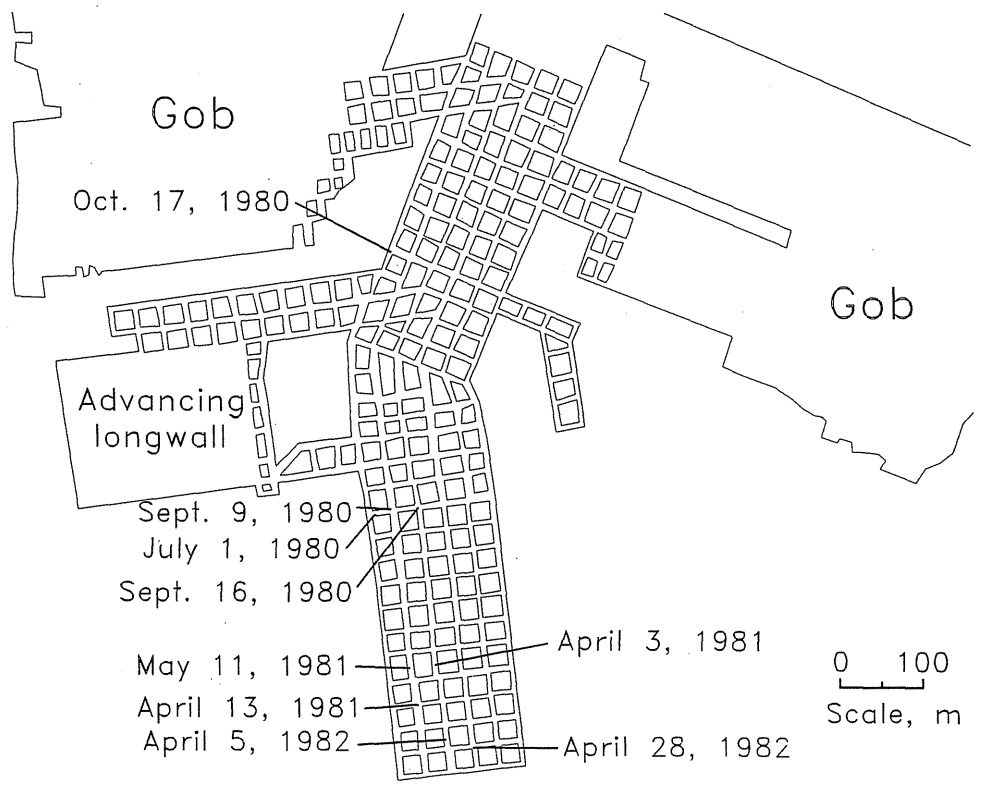

occurred as early as 1930 on the mine property, but they did not appear to be serious events. Records were not maintained until 1945, when injuries were associated with bumps. From 1945 through the 1950's, the history of bumps at these mines and U.S. Steel's efforts to prevent them were well documented through company memoranda, USBM reports, journal articles, and conference papers.

Bumps at the Gary Mines in the 1950's were associated with a variety of factors (figure 3). Mining in the first half of the 20th century undoubtedly resulted in the bump-prone mining scenarios faced in the 1950's. For example, mining was conducted adjacent to gob areas created decades earlier, retreat sections operated on groups of pillars of irregular sizes and shapes, and much of the mining was directed to recovering barriers between old workings.

Moss No. 2 Mine

The Moss No. 2 Mine near Dante, VA, was extensively mined by Clinchfield Coal Co., from the 1950's to the 1970's in 1.2 m of the Tiller Coalbed. During this time, five bumps were recorded and are part of the USBM database (figure 4). The mine utilized a multientry development system, followed by room-and-pillar mining. Extraction of pillars was accomplished primarily by the split-and-fender method. Rooms were typically driven 23 m apart and 6 m wide with crosscuts every 23 m. More than 100 sections were developed and pillared using some variation of this method. One of the first longwall sections in the United States was employed at this site in the late 1960's and 1970's. Twenty-two longwall panels of varying length were extracted.

Many conditions associated with bumps were found at this mine. Overburden at the mine ranged from zero at outcrop to greater than 400 m under the highest ridges. The roof stratum was dominated by thick sequences of massive sandstone. Numerous paleochannels scoured the coalbed, limiting the development of the mine in several areas. Locally, this massive roof had the ability to span large areas of the gob. Additionally, thick pockets of shale were noted adjacent to the sandstone channels. The floor stratum was almost always referred to as a hard, dense, silty shale. The Moss No. 2 Mine property was also overlain by the minable Upper and Lower Banner Coalbeds. The Upper Banner Coalbed was about 250 m above the Tiller Coalbed, but it undoubtedly had a considerable effect on the stress transfer process.

Beatrice Mine

The Beatrice Mine near Keen Mountain, VA, reported 24 bumps between 1972 and 1981 (figure 5). This high number of occurrences spanned the spectrum of mining conditions. Therefore, examples from this operation will be referred to often in this paper. The Beatrice Mine worked about 2 m of the Pocahontas No. 3 Coalbed at overburden ranging from 300 m near the shaft bottom to over 700 m under the highest ridges. A massive, quartzite-rich sandstone was found throughout the property. In places, this extremely hard stratum came in direct contact with the coalbed. However, in most locations, a very competent siltstone occupied the interval between the coalbed and the overlying sandstone. The floor was often reported as a sandy shale. No mining occurred above or below the Beatrice Mine.

BUMPS ASSOCIATED WITH VARIOUS MINING METHODS

The examples below have been grouped according to the type of mining system at various bump sites. These mining systems can generally be categorized as (1) development mining, (2) pillar retreat mining, (3) barrier splitting, and (4) longwall mining. This grouping facilitates descriptions of the impact of the particular mining method on bump occurrence. Examples of bumps associated with the various mining methods are intended to highlight the shortcomings and/or successes of each mining method and related practices and to indicate the influence of conditions and circumstances unrelated to mining method.

Development Mining

Development mining refers to the extension of entries and crosscuts into undeveloped portions of the coal reserve. Generally, extension of mains, submains, butt sections, gate roads, and setup and bleeder entries represent development work. Because this activity involves the initial stages of mining and does not produce abutment loading, bumps should be generated less frequently.

Twenty-one bumps were identified in the total USBM database as occurring during development mining (table 5). Three were in the Eastern United States and 18 were in Utah and Colorado.

The L. S. Wood Mine experienced nine bumps during development of the Main Slope section between July 1980 and April 1982. All these bumps were associated with overburden greater than 600 m. Four bumps took place near one of two adjacent gobs (figure 2). Although the bumps exhibited tremendous force, the skilled work force at the mine was always able to avoid being "caught" by the bump so no miners were injured in any of these events. Eight bumps occurred during or shortly after mining and displaced large volumes of rib coal near the mining zone.

Figure 3
Location of Bumps Reported at Gary No. 2 and 6 Mines, McDowell County, WV.

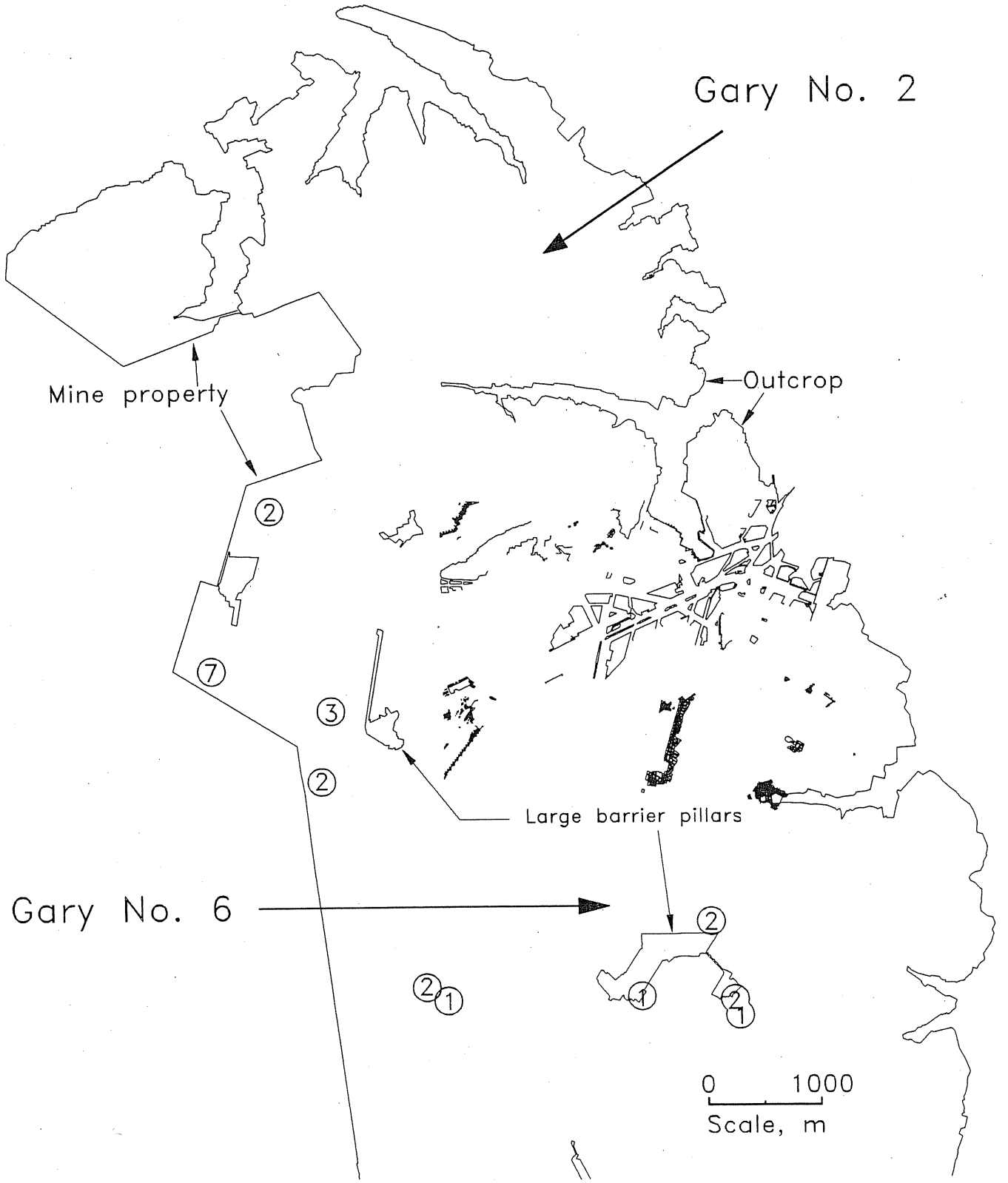

Circled numbers indicate number of bumps at various locations.

Figure 4
Location and Dates of Bumps Reported at Moss No. 2 Mine, Russell County, VA.

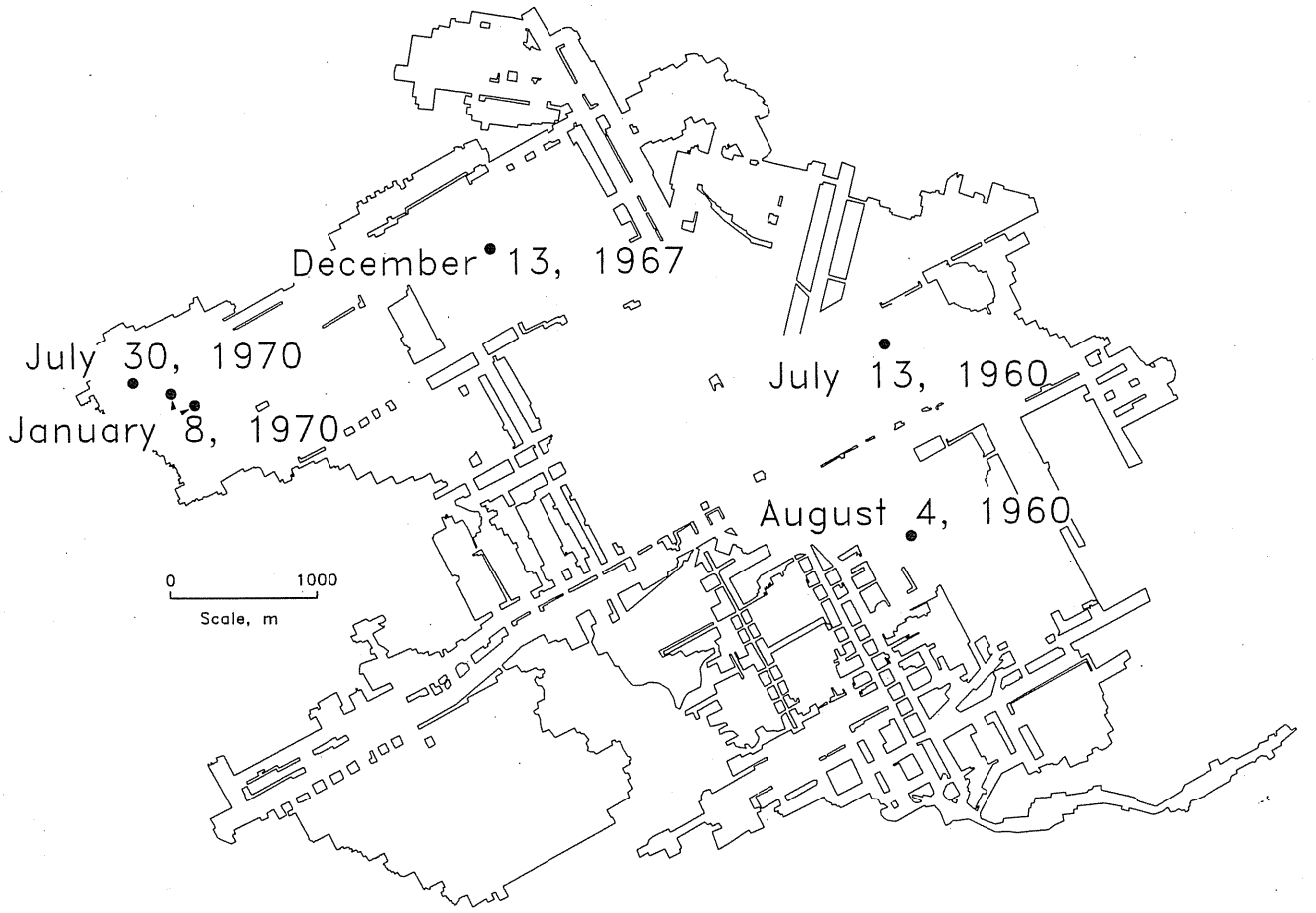

Significant quantities of methane gas were liberated in association with several bumps. After the bump on April 13, 1981, methane concentrations measured as high as 5 pct. Five of the bumps occurred under more than 750 m of overburden far from the gob or faults. In situ coalbed gas pressures were undoubtedly high, for these bumps showed high methane emission characteristics. These events may be better defined as gas outbursts. The bump problems at the L. S. Wood Mine and two other Mid-Continent operations were severe enough to warrant the elimination of gate entries by employing the advancing longwall system.

At the Beatrice Mine, development work was underway in the No. 9 unit section off the Skip South Mains, approximately 70 m from an adjacent gob area (figure 6), when there was a violent bump in the face area on July 24, 1976, that injured three miners. Abutment loading from the adjacent gob area may have contributed to the bump. Therefore, this event could be explained as resulting from the barrier-splitting operations. However, because the gob was 70 m away and the solid block of coal being mined was approximately 230 m wide, it appears more appropriate to categorize it as a development bump. Other significant factors at this site were the very massive, stiff, siltstone roof and floor strata and overburden averaging 600 m in depth.

Table 5.—Conditions associated with development mining

Mine	Number of bumps	Condition
L.S. Wood	4	Close to gob section.
	9	Overburden deeper than 600 m.
	2	Destressing.
Beatrice Mine ..	1	Close to gob section.
	1	Overburden deeper than 600 m.
Deer Creek	1	Close to gob section.
Dutch Creek No. 1	1	Displacement faults.
Sunnyside No. 2	1	Displacement faults.
Total ...	21	

Figure 5
Location and Dates of Bumps Reported at Beatrice Mine, Buchanan County, VA.

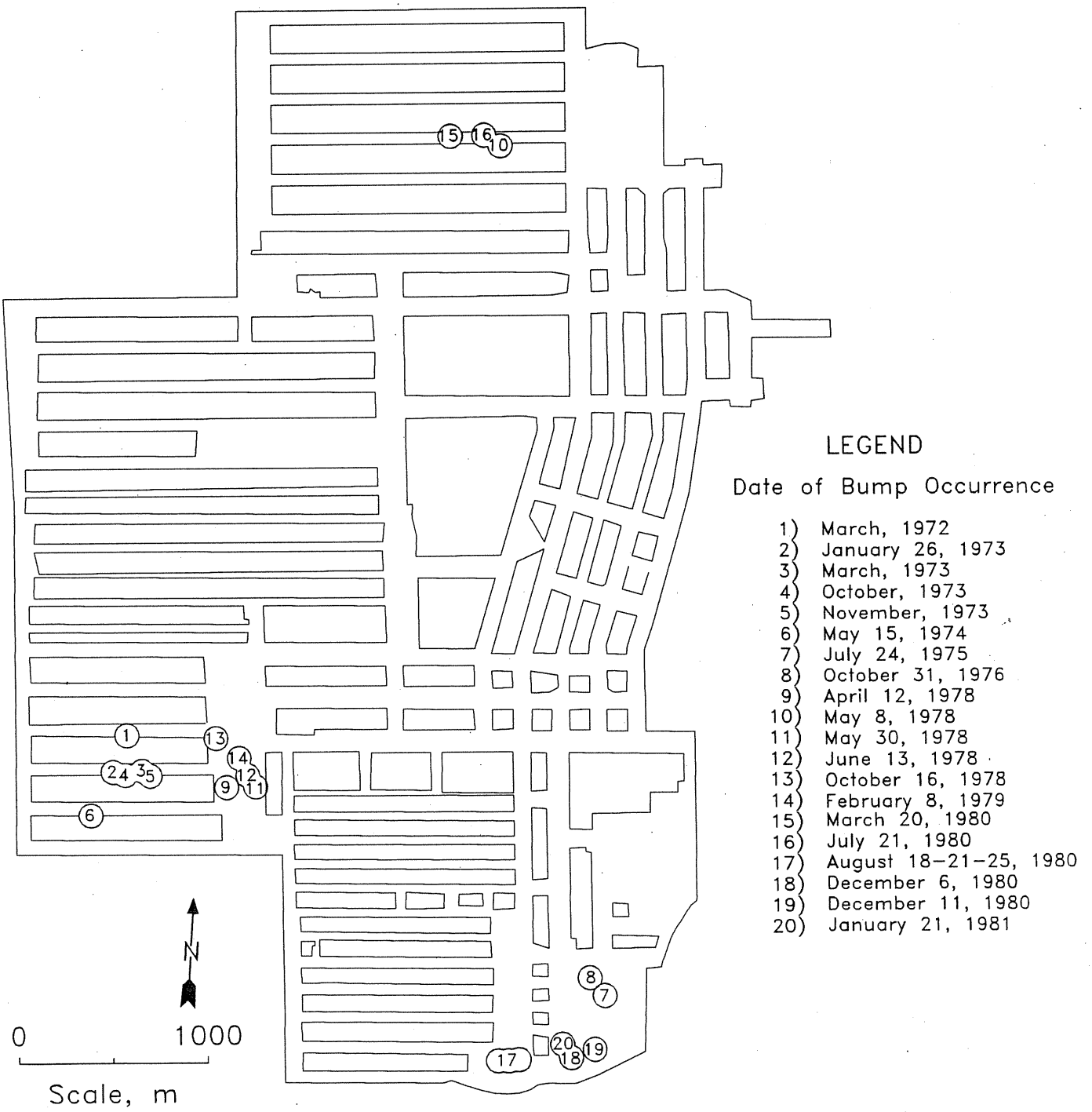

Figure 6
Violent Bump During Development of Pillar Section Within Beatrice Mine That Injured Three Miners.

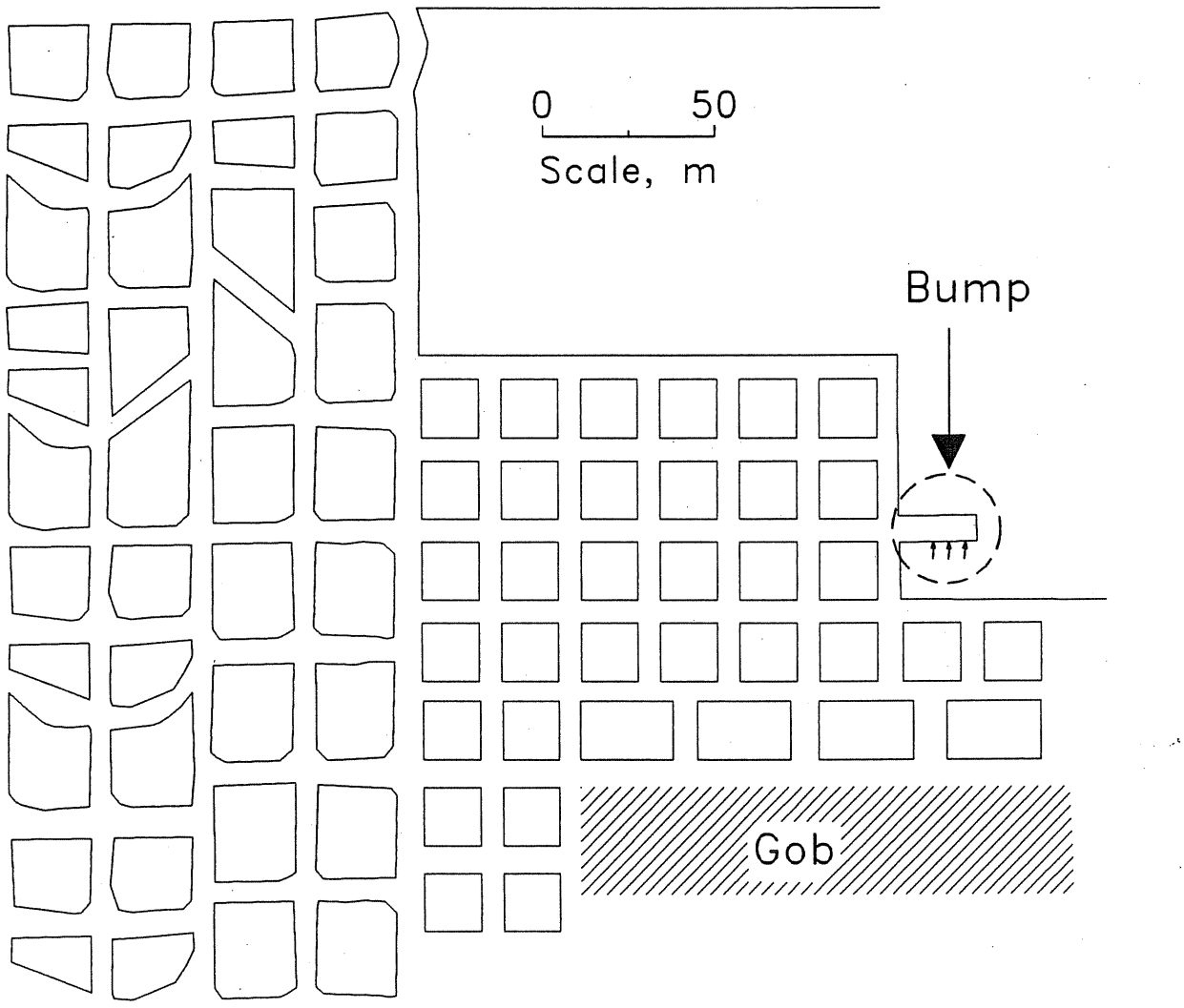

Pillar Retreat Mining

Many bumps have been recorded on continuous miner sections where rows of chain pillars 15 to 30 m wide were extracted near the gob. Individual chain pillars are extracted very rapidly, causing loads to shift before the adjacent pillars can redistribute load in a controlled manner. Pillars in such a range of sizes appear to have difficulty accommodating excessive amounts of strain energy, thereby increasing the likelihood that the pillars will bump. When a pillar is adjacent to the gob, the combination of considerable rib crushing and abutment loading can produce great confining pressures on the solid core (figure 7). With few exceptions, massive strata exist in the immediate and main roof overlying bump-prone coal. These strata can cantilever, adding load to the pillar. Mining in the yielded rib releases confinement and may result in violent solid-core failure.

Pillars adjacent to gob areas experience elevated loading conditions from the unsupported strata above the gob (figure 8*A*). Certain mining geometries, such as a large pillar surrounded by smaller pillars, can concentrate stress (figure 8*B*). Large pillars can be imagined as stiff structures that tend to deform or converge less than smaller, less stiff pillars. These larger structures tend to gather load, increasing the potential for violent failure as the smaller pillars are extracted within and around them.

In addition, section-wide mine plans and extraction sequences can contribute to bumps. For example, overlapping abutment pressures from converging gob lines

Figure 7
Generalized Vertical Stress Distribution Within Coal Pillar.

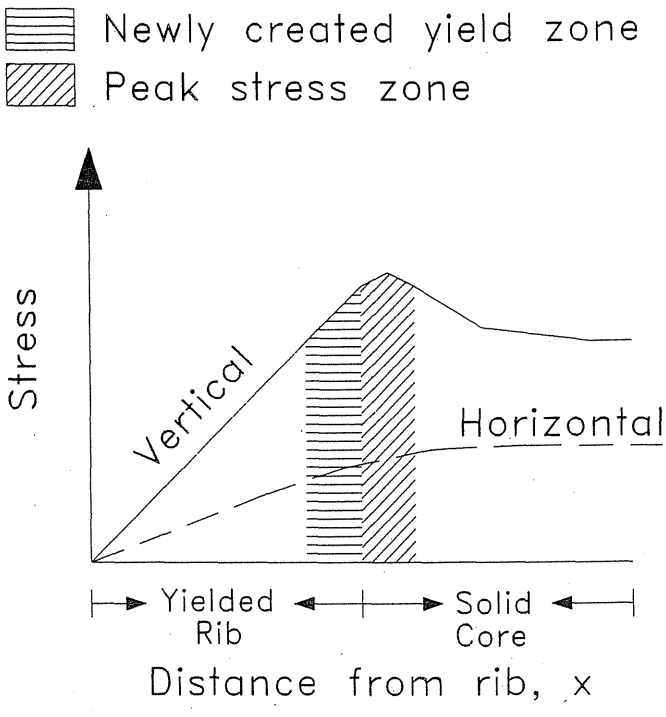

(figures 8*C* and 8*D*) and overlying large pillars or barriers in multiple-seam mining operations can cause excessive pressures (figure 8*E*). Fortunately, all of the preceding conditions lend themselves to engineering solutions, many of which are discussed later with actual examples.

Fifty pillar retreat bumps have been identified in the USBM database. Forty-eight occurred in conjunction with full-extraction mining, whereas two occurred during partial pillar mining. Geology, destressing, and multiple-seam mining were the principal contributing conditions associated with bumps during pillar retreat mining operations. Six events were associated with unique geologic conditions, three with destressing, and two with multiple-seam mining.

On February 16, 1951, a large bump occurred in the Gary No. 2 Mine, killing four miners and injuring six (figure 9). The force of the bump threw four miners against the loading machine, while others were thrown against cribs and timbers. One miner 50 m away was injured by the force of the bump. Earth tremors were felt on the surface within a 3-km radius of the bump's center. This bump, however, dislodged only a relatively small amount of coal. This event may well exemplify mining-induced seismicity with magnitudes similar to those shown in table 4. Possibly the overlying strata had shifted by a considerable amount toward the gob, releasing large amounts of energy but not significantly damaging the mine workings.

Three pillar retreat bumps were reported at the Moss No. 2 Mine. The first occurred on August 4, 1960, in the 2 Right section (figure 10). Extensive arrangements of pillars and pillar remnants had been left during mining, giving the strata above the gob a support system that inhibited the roof caving process.

The second bump occurred on December 12, 1967, in the 6 Right section (figure 11). This bump was associated with a small overhang of roof that was in turn associated with a distinctive change in roof lithology. The inby part of the section had been free of bumps because of the weaker interbedded shale-and-sandstone roof. The second bump took place within the transition zone to the more competent sandstone roof.

The third bump, on July 30, 1970, had several contributing factors (figure 12). The Upper Banner Coalbed was mined 250 m above the Moss No. 2 Mine. The bump occurred as the section was retreating from under the overlying remnant pillars. A considerable amount of stress must have been transferred through these remnant pillars. The bump was obviously violent, for it displaced the continuous mining machine several meters (figure 13).

A bump in the No. 1 South section of the Beatrice Mine on May 30, 1978 (figure 14), was similar to those experienced earlier at the Olga Mine, which had led to the development of the Olga pillar extraction sequencing technique. This method is discussed in greater detail on page 60. Such a sequence uses a continuous mining machine to mine certain highly stressed pillars selectively and move abutment stresses within a mine section in a controlled manner.

Barrier-Splitting

Barrier-splitting is generally done in association with full-extraction pillar operations, most often during the final stages of a mine's life when the barrier pillars along the main access entries are extracted. However, a barrier block is sometimes mined in conjunction with a pillar retreat section for some operational reason. Typically, a mine will begin to extract barriers in the most remote portions of the mine and work back toward the main portal areas. Use of the barrier-splitting technique has decreased owing to inherent difficulties associated with this process.

The USBM database contains references to 36 bumps associated with barrier-splitting operations. As indicated earlier, barrier-splitting often involves high-stress environments because these pillars are designed to carry abutment

Figure 8
Generalized Examples Showing How Different Full-Extraction Mining Scenarios Transfer Load to Pillar Structures.

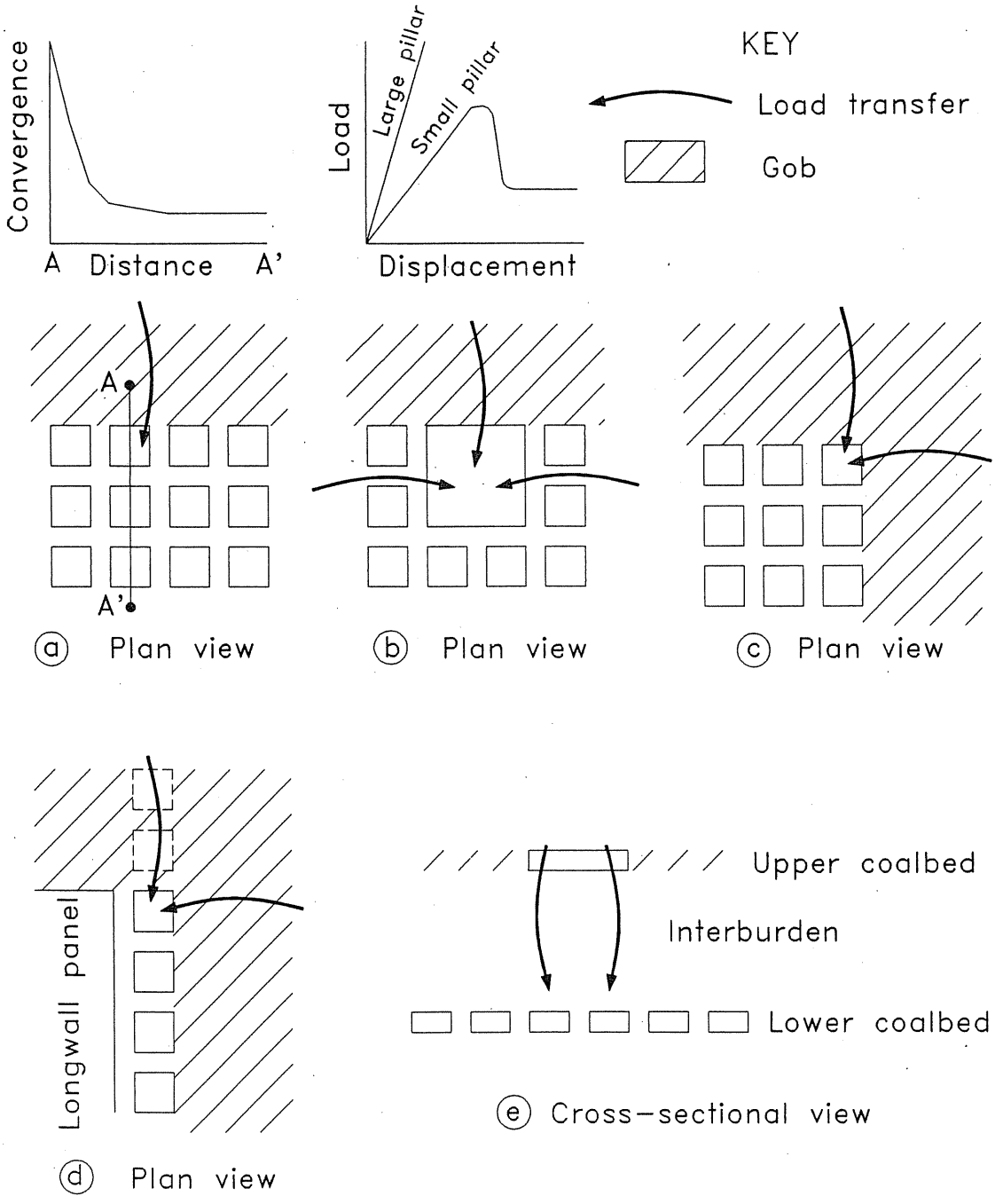

Figure 9
Fatal Pillar Retreat Coal Bump at Gary No. 2 Mine, February 16, 1951.

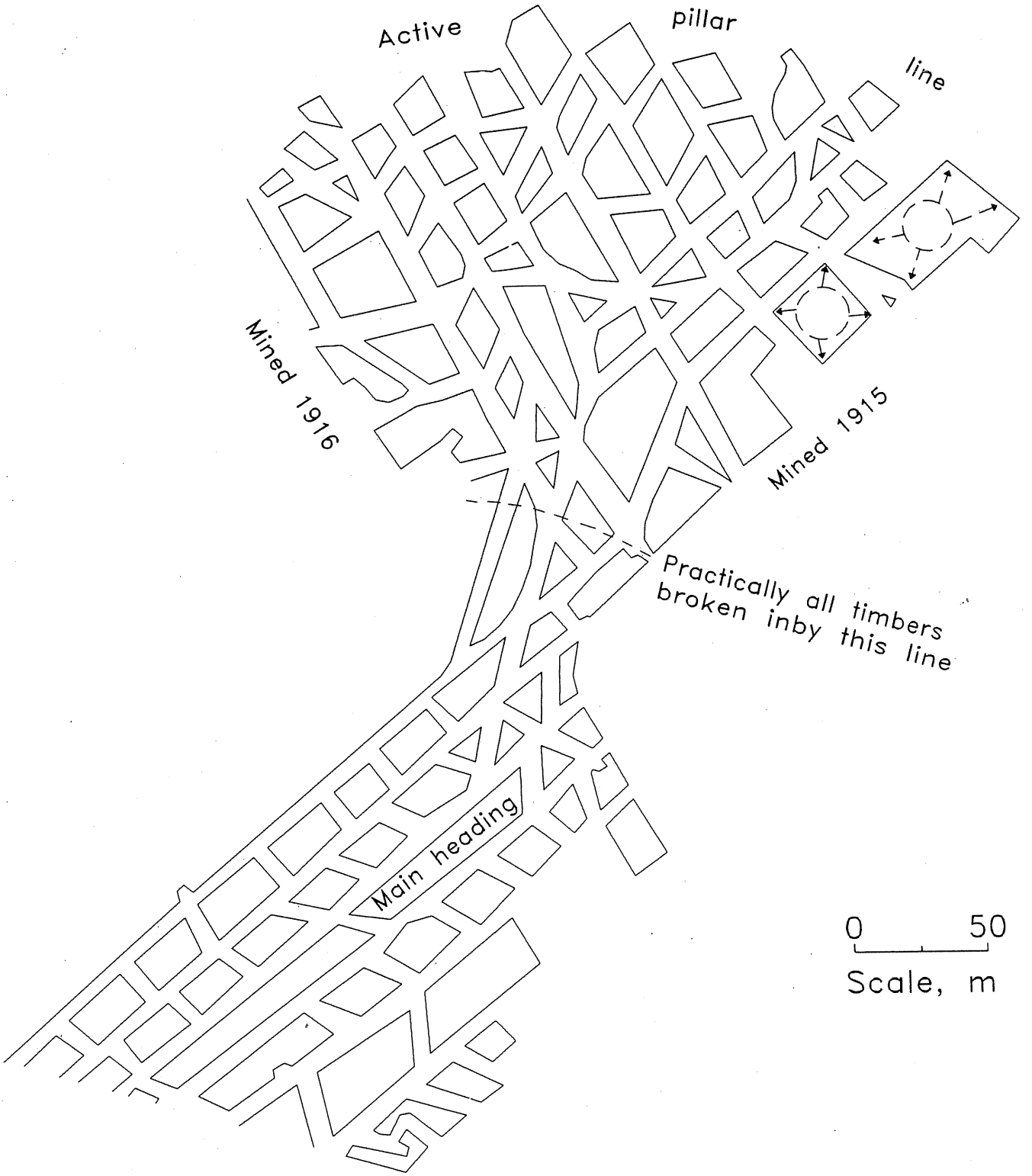

Figure 10
Effects of Pillar Remnants and Hanging Roof Strata on Pillar Retreat Bump at Moss No. 2 Mine, August 4, 1960.

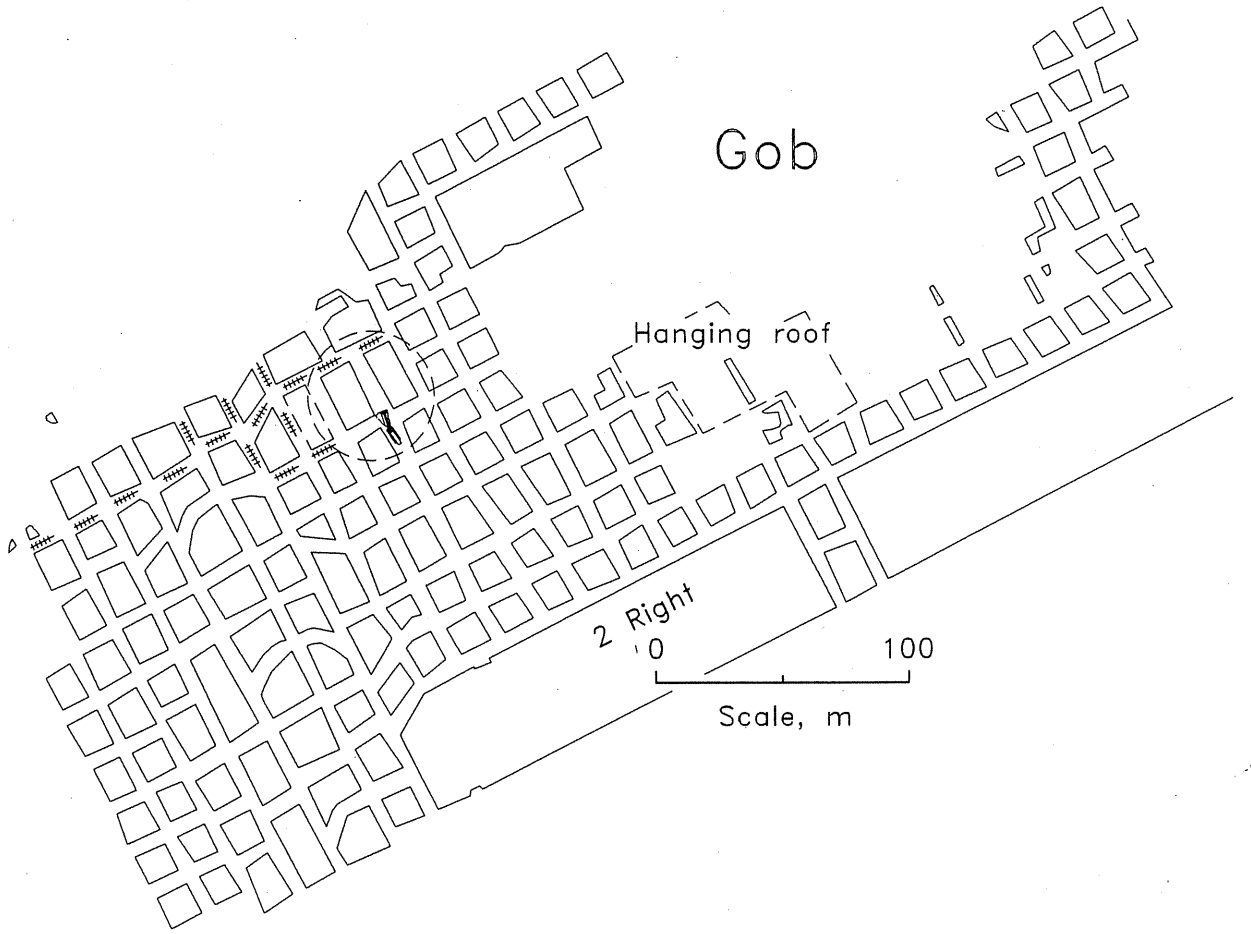

loads. The stress fields and geologies at these operations generally provide conditions conducive to bumps. There were a few instances in which anomalous factors controlled the occurrence of bumps during barrier-splitting. Of the 36 bumps associated with barrier-splitting operations, only two were associated with multiple-seam mining and four were associated with destressing techniques. Also, in most cases, injuries were the result of contact with bumped coal. Associated hazards were limited to one roof fall at the Peabody No. 31 Mine and an ignition at the Gary No. 6 Mine.

Bumps at the Gary No. 2 and No. 6 Mines in the early 1950's illustrate the nature of events typical of barrier-splitting operations. At the No. 6 Mine, barrier-splitting was used in several locations as sections developed decades earlier were retreated. Development of the mine over a long period by hand-loading resulted in an irregular mine plan; bumps occurred under a variety of circumstances and often involved complex geometries that resulted in excessive stress concentrations. Cut sequencing in bump-prone areas at the No. 6 Mine apparently evolved on a case-by-case basis to accommodate the irregular nature of the remaining coal reserves. However, over time, reserves at the Gary No. 2 Mine were developed and retreated using a more consistent method that eventually evolved into the thin-pillar mining system, described on pages 60-61.

Figure 15 illustrates the Gary No. 2 Mine plan in the vicinity of a bump in the 12-Left section in January 1951. In this mining plan, four-entry development sections were driven at intervals off a set of main entries. Sections were separated from one another by a barrier block that was developed just ahead of the retreat line during second mining. However, as indicated in figure 15, bumps were

Figure 11
Effects of Roof Strata Characteristics on Pillar Retreat Bump at Moss No. 2 Mine, December 12, 1967.

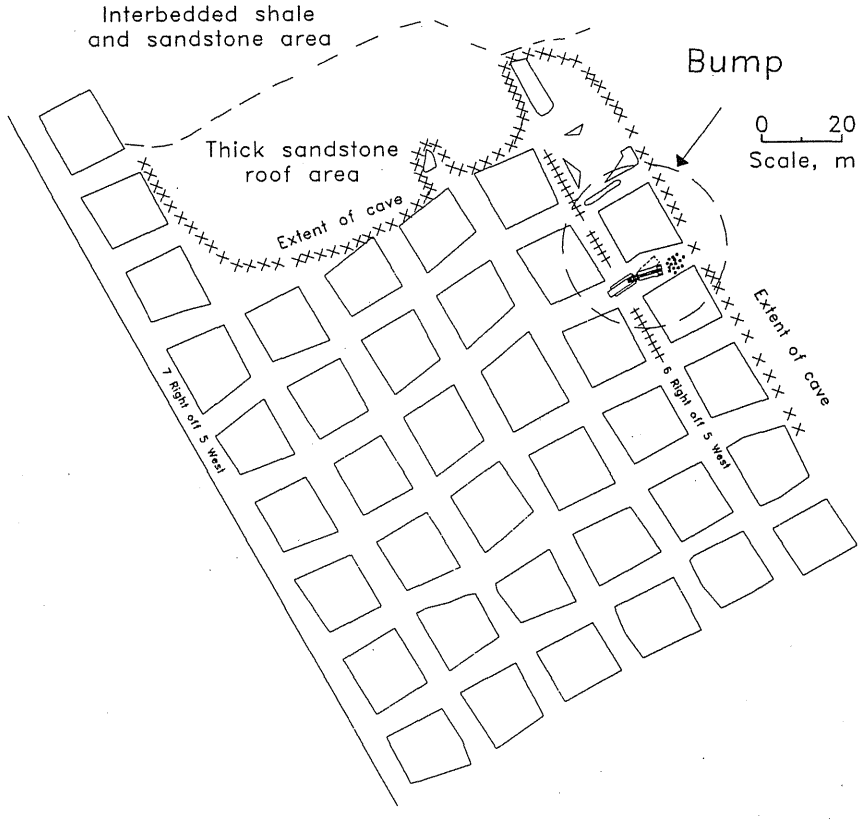

encountered in some locations. USBM researchers, including Holland, found several factors they believed influenced bumps in this system and elsewhere in the Gary No. 2 and No. 6 Mines. For example, pillars of irregular sizes were located adjacent to the retreat line, secondary development was done within the abutment zone, and rooms were not driven in proper sequence. As a result of these and several other related issues, U.S. Steel, the owner, developed another mine plan for the Gary No. 2 Mine.

The next-generation mine plan differed from earlier ones in several respects. Figure 16 indicates, for example, that secondary development took place farther outby the retreat line and adjacent sections were retreated simultaneously; when all sections were activated, the length of the pillar line was approximately 670 m. Nevertheless, bumps were encountered in early 1952. Company personnel indicated that poor caving in the gob inby 18 Left contributed to squeeze and bump conditions. Secondary development well in advance of the retreat line appeared to allow the pillars to crush and the massive sandstone main roof to settle into the gob rather than breaking and falling. Duckwall (c. 1952) notes that "it was possible to travel a distance of [60 m] or more into the mined-out area which was free of falls" in 18 Left. Based on observations of strata behavior and bump experiences at the Gary No. 2 Mine, U.S. Steel engineers sought to incorporate beneficial aspects of each of the mining systems into a new system, which became known as the thin-pillar mining method.

The Gary mines exhibited a long history of coal bumps under a variety of circumstances. The same held true for both the Moss No. 2 Mine (figure 17) and the Beatrice Mine (figure 18). In contrast, the Moss No. 3 Mine in Dickenson County, VA, experienced an isolated bump occurrence; that is, conditions conducive to bumps apparently were not pervasive at the site. Mining began in 1958 at the Moss No. 3 Mine, portal A, and proceeded for nearly 20 years without a reported coal bump event. However, on November 4, 1977, bump conditions were encountered during barrier-splitting operations, resulting in the death of a continuous mining machine helper (figure 19).

The Thick Tiller Coalbed reportedly averaged 3 m thick, in the area of the Moss No. 3 bump. The barrier

Figure 12
Effects of Overlying Remnant Pillars on Pillar Retreat Bump at Moss No. 2 Mine, July 30, 1970.

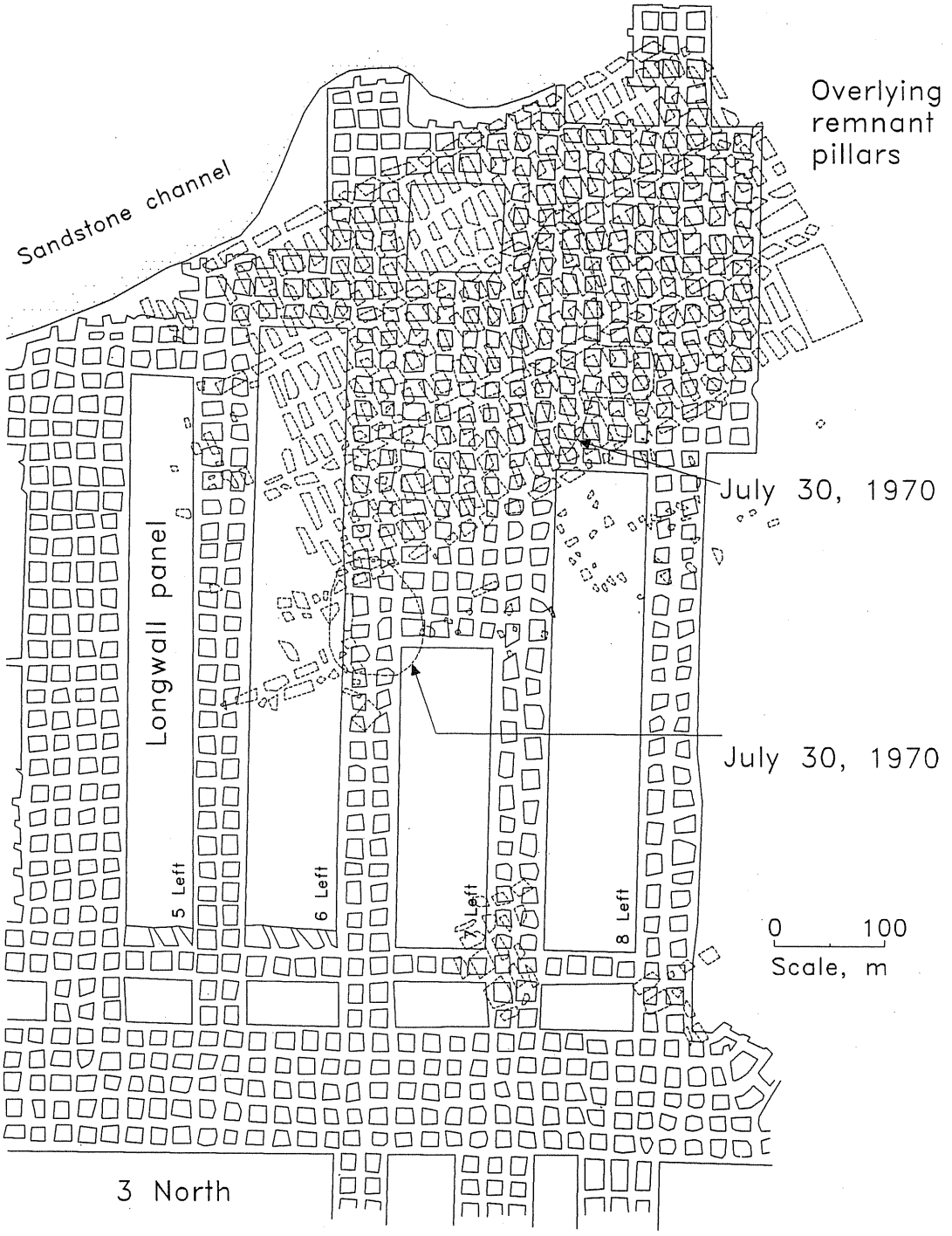

Figure 13
Detailed View of Bump at Moss No. 2 Mine, July 30, 1970.

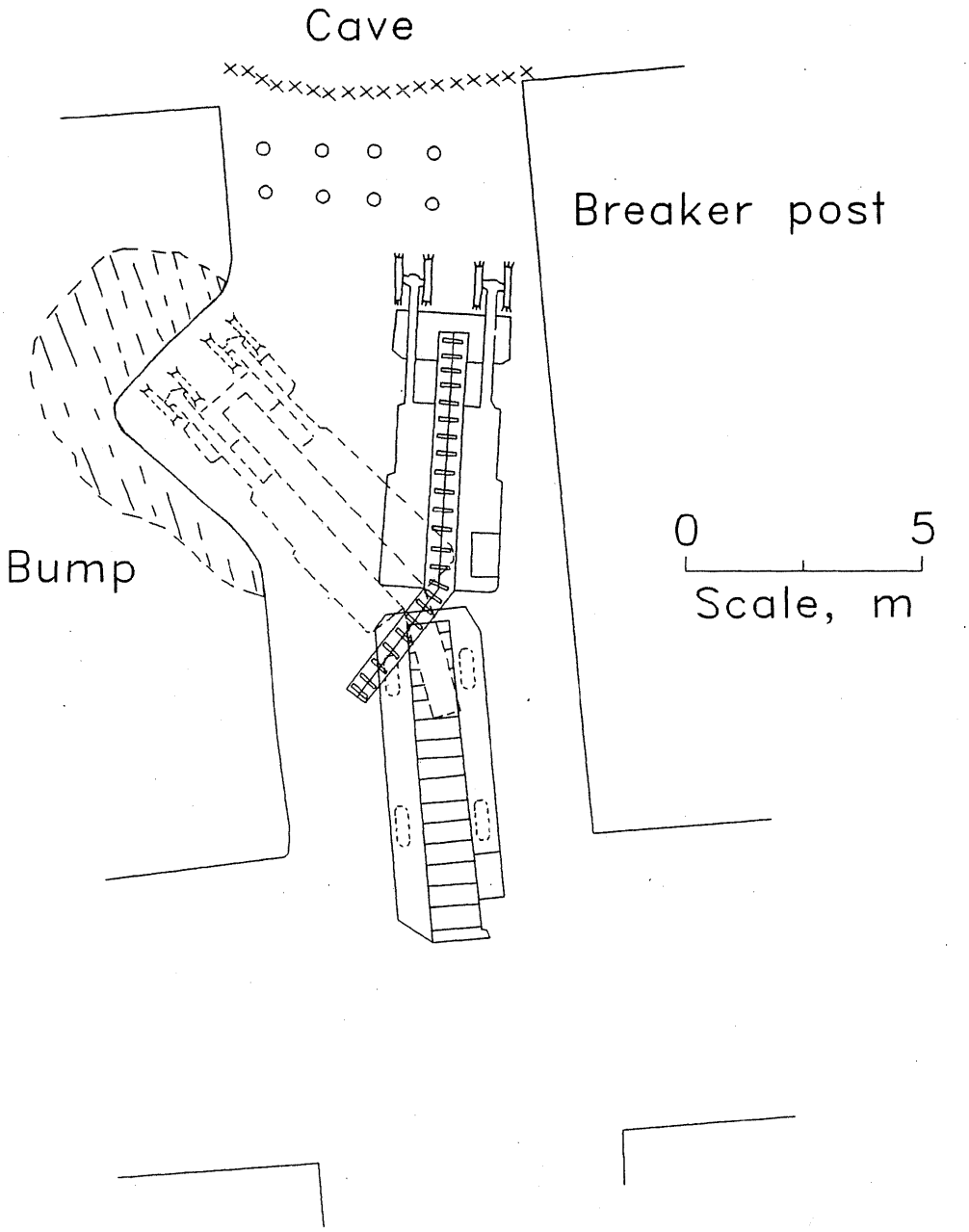

Note position of caved roof line and postbump continuous mining machine (solid lines).

Figure 14
Pillar Retreat Bump at Beatrice Mine, May 30, 1978.

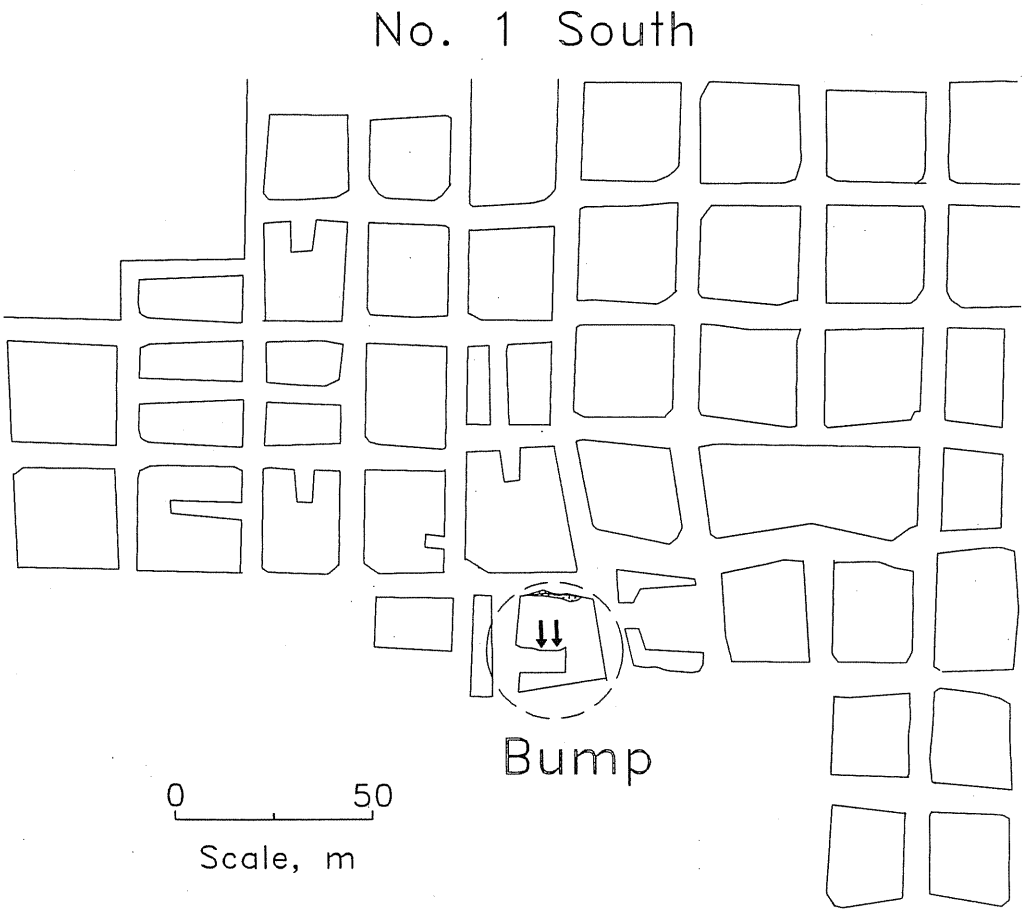

Note use of sequential pillar mining technique.

Figure 15
Barrier-Splitting Bumps in Adjacent Sections With Similar Layout Positions, Gary No. 2 Mine, January 1951.

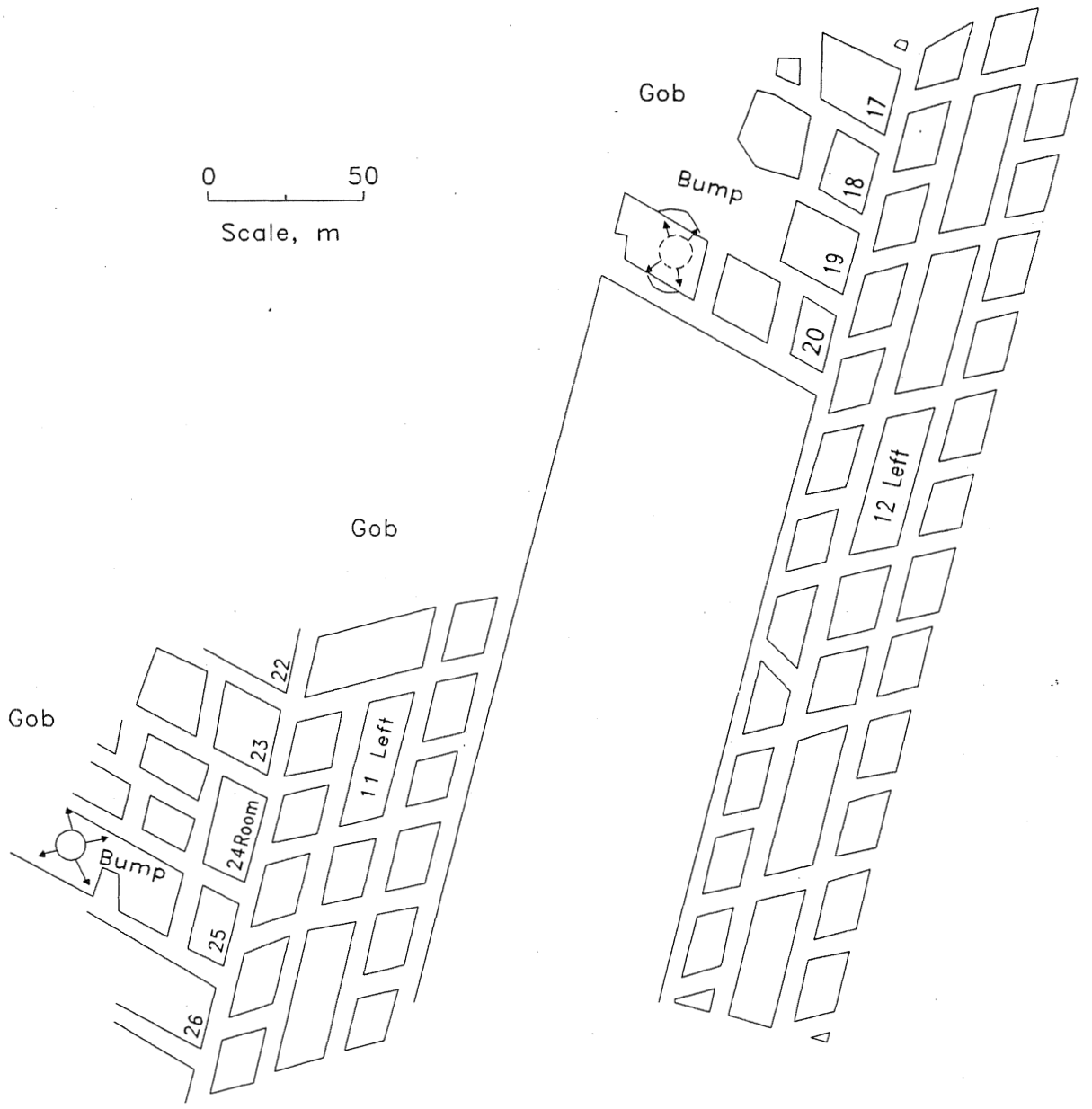

Figure 16
Multiple Bump Events During Splitting of 18 Left Barrier at Gary No. 2 Mine, 1952.

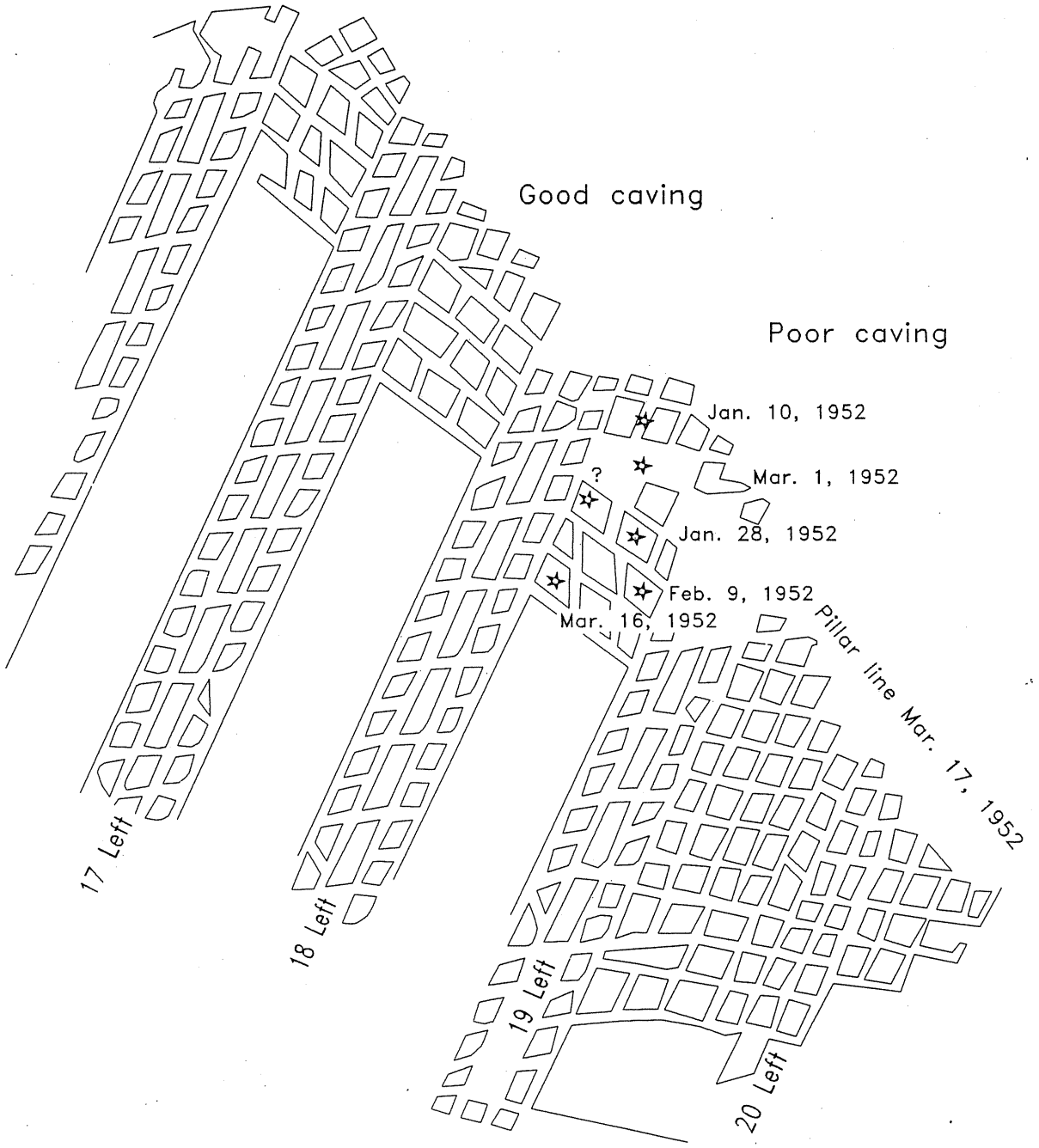

Star denotes location of mountain bump.

Figure 17
Barrier-Splitting Bump at Moss No. 2 Mine, July 13, 1960.

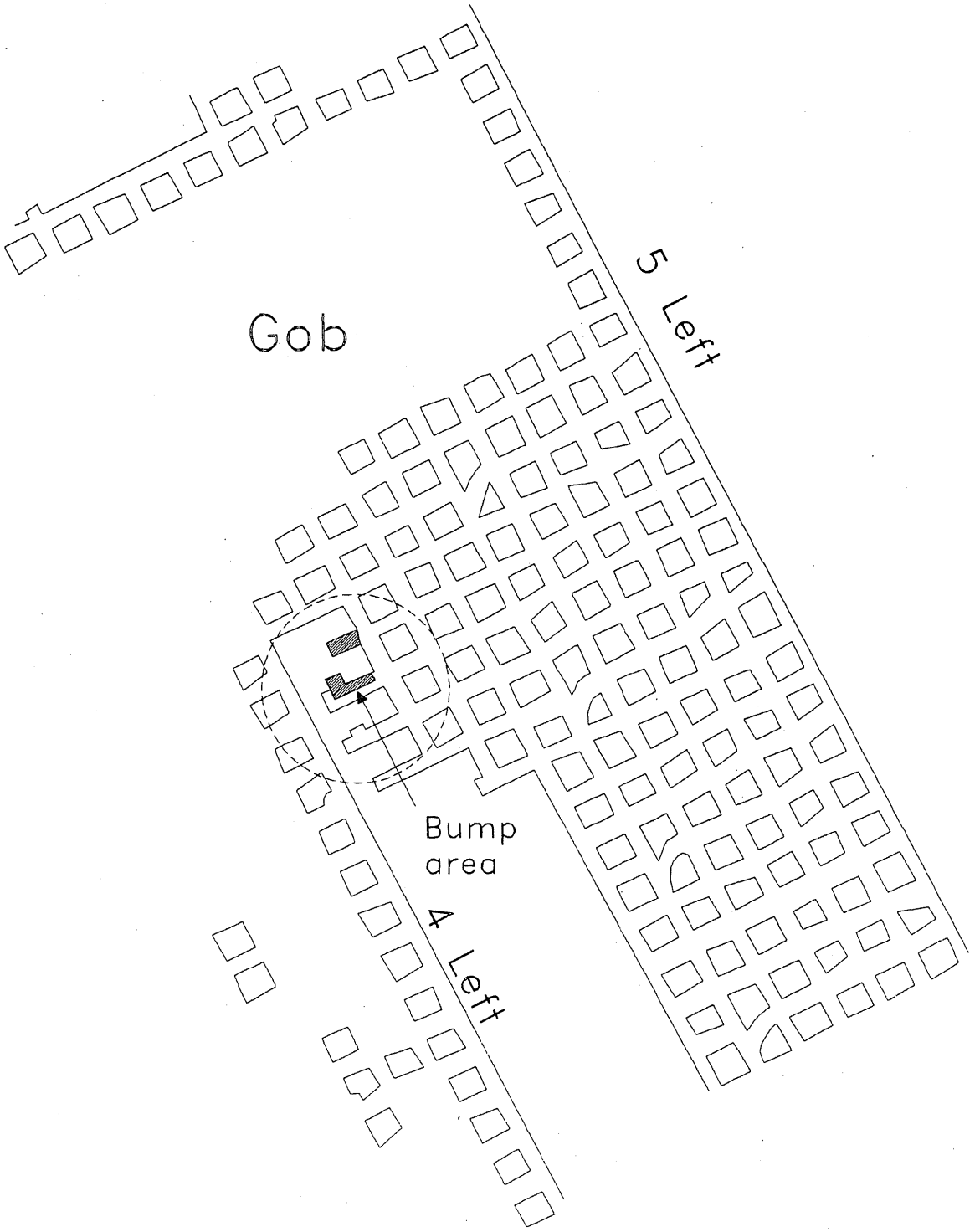

Figure 18
Barrier-Splitting Bump at Beatrice Mine, December 11, 1980.

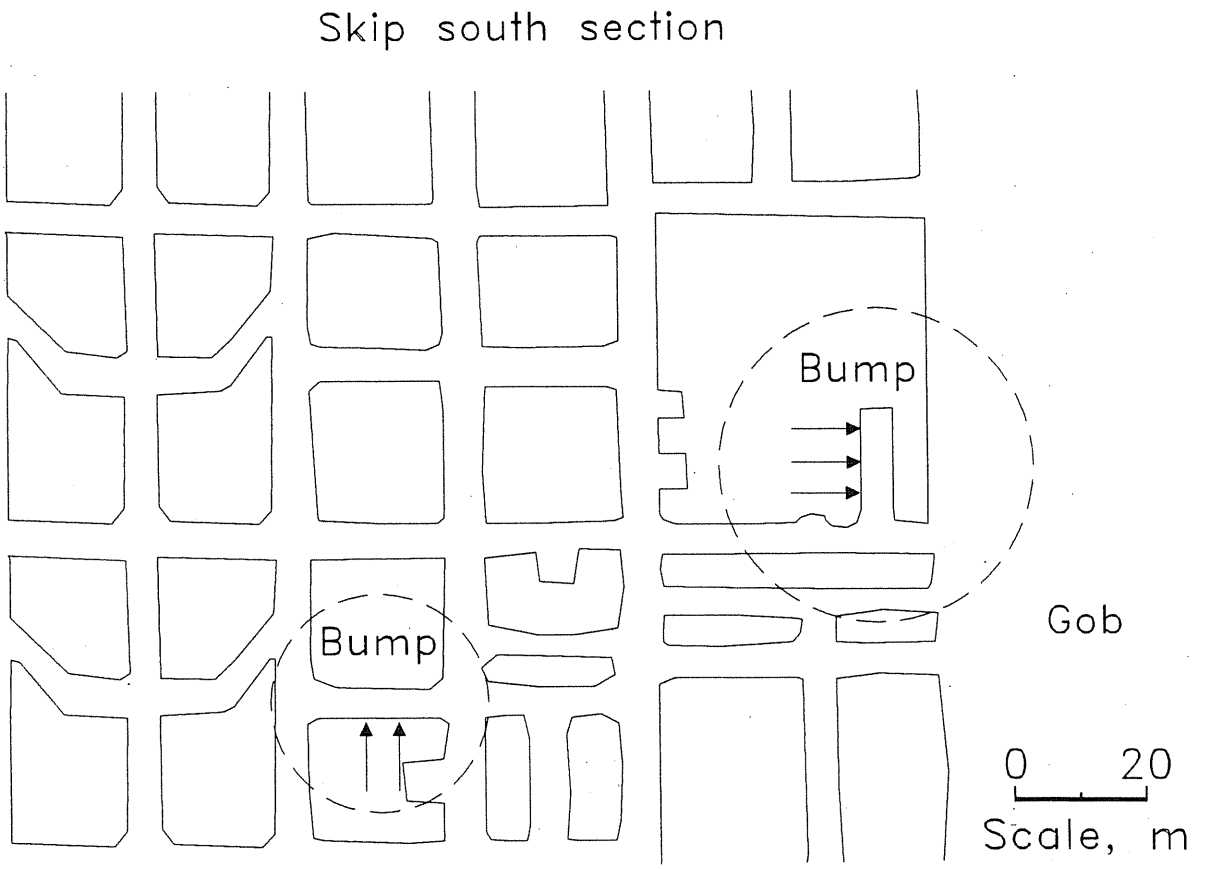

Figure 19
Effects of Multiple-Seam Mining on Barrier-Splitting Bumps at Moss No. 3 Mine, November 4, 1977.

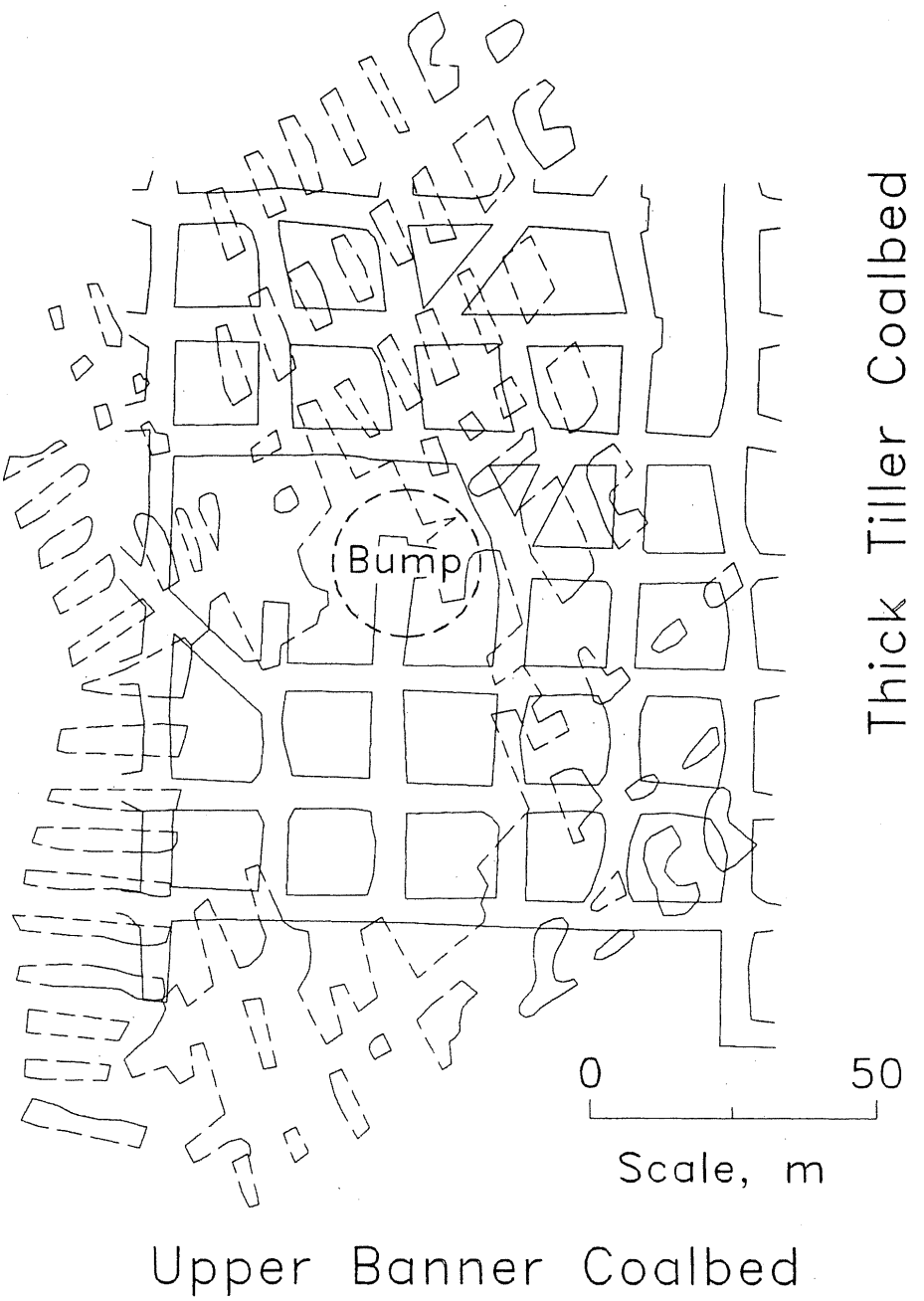

pillar measured about 116 m long by 43 m wide. Adjacent pillars were generally square and appeared to be spaced on 24-m centers. Reports of the Moss No. 3 coal bump did not indicate overburden or interburden thickness between the Thick Tiller and superjacent Upper Banner Coalbeds at the bump site. However, it was concluded that the combined effects of abutment loads generated as a result of barrier-splitting and retreating, along with concentrated stresses caused by overmining, created an excessive stress condition. Isolated pillars that were left in the Upper Banner Coalbed during second mining apparently intensified the stress interaction (figure 19).

Longwall Mining

Since 1970, coal bumps have occurred within gate entry systems and along the faces of U.S. longwall mines. In many cases, these bumps were located where the gate entry pillars were unable to prevent abutment loads from "riding over" onto the mined longwall panel (*17*). In other instances, the bumps responded to either gob caving adjacent to the longwall face or were associated with excessive gas pressures.

The USBM database contains 36 longwall coal bumps. Of these, 12 occurred along the longwall face, 7 within the tailgate, 2 within the headgate, 13 both along the face and within the tailgate entries, and 2 in setup or bleeder entries adjacent to the longwall panels. The most influential condition was the presence of multiple-seam mining, which was found in seven of the events. Five bumps occurred during destressing. Rolls in the structure of the coalbed being mined played an important function in two bumps at the Beatrice Mine. The most significant hazard associated with longwall mining bumps was ignition. Four such events were identified in the database, all of which occurred in Western U.S. longwall mines.

The early experience of longwall mining at the Moss No. 2 Mine clearly exemplifies how inadequate gate entry pillar design can contribute to bumps. Clinchfield Coal Co., the owner, was one of the first companies to implement longwall technology in the United States. The first longwall was laid out next to a mined-out room-and-pillar section approximately 480 m long and 170 m wide. This longwall panel was 60 m wide and 530 m long and was completed on October 11, 1969. Owing to the industry's lack of experience with the longwall mining system at that time, chain pillars measuring 17 by 17 m were believed to be an appropriate size between the first and second longwall panels (figure 20). The second longwall was 80 m wide and 600 m long. At the time of the bump, in which the longwall foreman was injured, the longwall face had retreated approximately 400 m.

Several contributing conditions were readily apparent. Multiple-seam mining occurred in the overlying Lower and Upper Banner Coalbeds. At the time of the bump, the longwall itself was progressing from under a group of unmined pillars (figure 20). Additionally, a large sandstone channel was located about 450 m inby the face and evidently contributed to the poor caving characteristics in the main roof member. Finally, the chain pillars left to protect the longwall panel were of inadequate size and too weak to withstand abutment loading from the adjacent gob areas.

The Beatrice Mine had extensive experience with bumps during longwall mining in its southern portion during the early 1970's (figure 5). Early longwall equipment included a plow and 94 hydraulic legs and canopy units having a capacity of 127 t. Many of the same conditions responsible for bumps at the Moss No. 2 Mine were also found at the Beatrice Mine. Overburden in the south longwall district ranged from 700 to 760 m. Roof strata in these areas apparently changed from a laminated shale and sandstone sequence with coal streaks to predominately sandstone intermixed with siltstone layers. The gate entry design at the Beatrice Mine consisted of a yield-yield-abutment system. The pillars were 24 m long and none were offset. The yield and abutment pillars were 9 and 24 m wide, respectively.

The first coal bumps associated with longwall mining at the Beatrice Mine took place in March 1972 on the tailgate of No. 3 development. At approximately the same panel location on the next panel, another bump occurred on January 26, 1973 (figure 21). Twenty minutes before, the section had been quiet. The bump exploded three chain pillars and completely filled the adjacent entries with loose coal. Several more bumps occurred during the mining of this and the adjacent panel. These events did not appear to be particularly difficult to address and did not result in any injuries.

A devastating bump two panels later in the tailgate entry of No. 6 development (figure 22) killed one miner and significantly injured three others. One of these miners was approximately 150 m away from the immediate bump location. The event was 350 m from the startup rooms in a longwall panel 140 m wide by 910 m long. A stall machine was utilized to keep the tail side of the longwall face advanced about 10 m ahead of the face conveyor (figure 23). This system was used to eliminate removal of the previously set cribs during retreat of the longwall face. James Gilley, a recognized authority on coal bumps (*31*), referred to this occurrence as a "shock impact bump." The

Figure 20
Effects of Overlying Remnant Pillars and Underdesigned Entry Pillars on Longwall Pillar Bump at Moss No. 2 Mine, January 8, 1970.

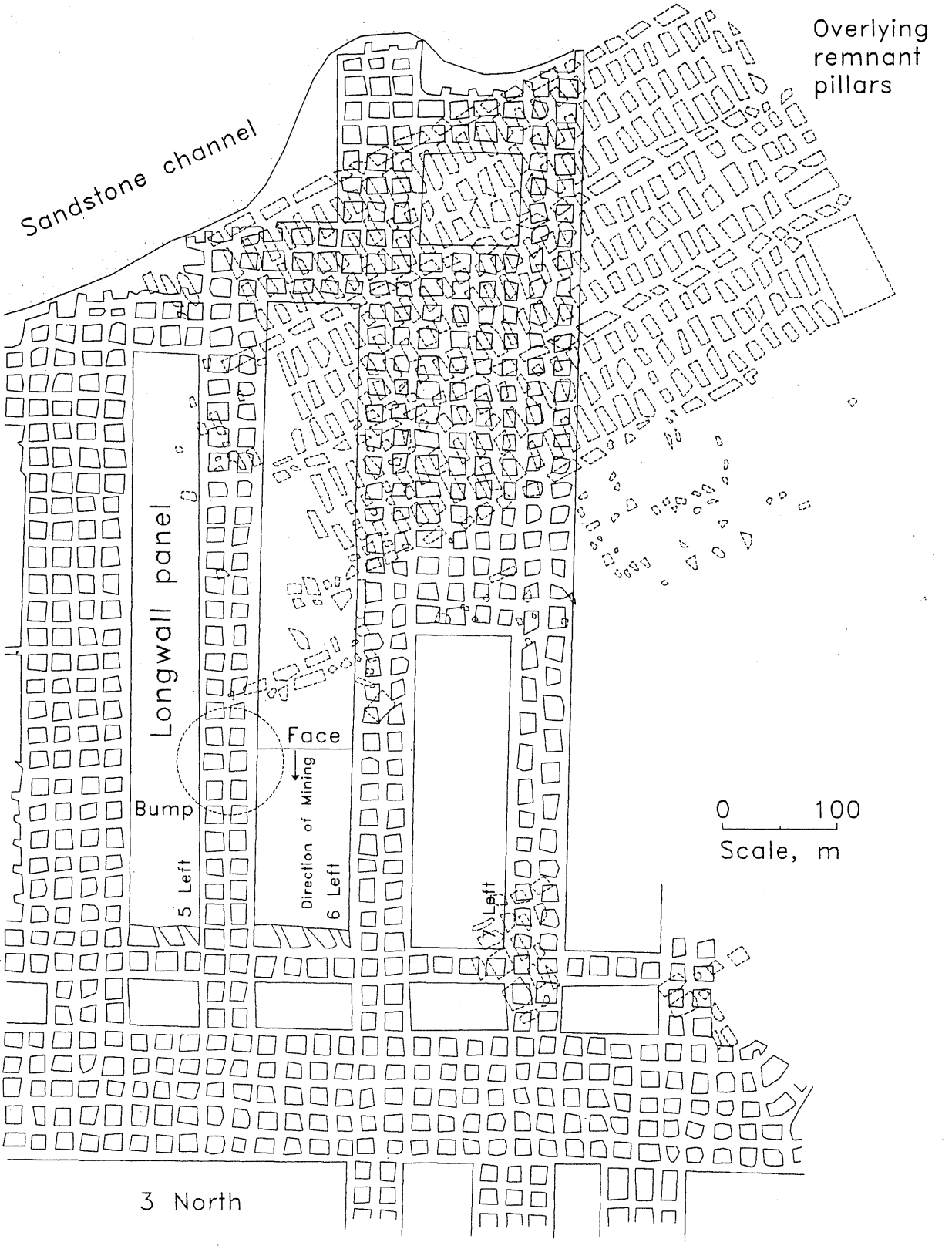

Figure 21
Longwall Tailgate Entry Pillar Bump at Beatrice Mine, January 26, 1973.

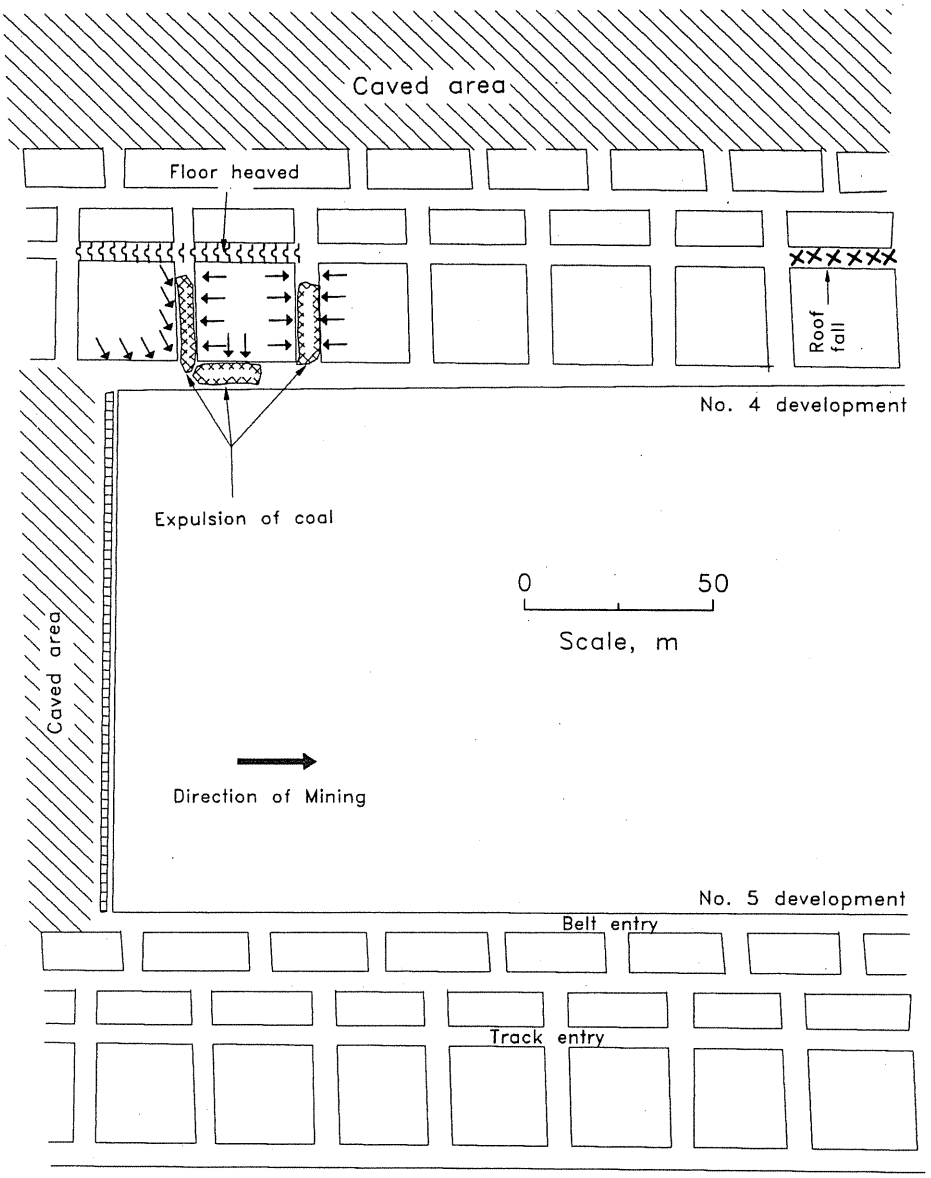

Figure 22
Fatal Longwall Panel Bump Near Tailgate Entry at Beatrice Mine, May 15, 1974.

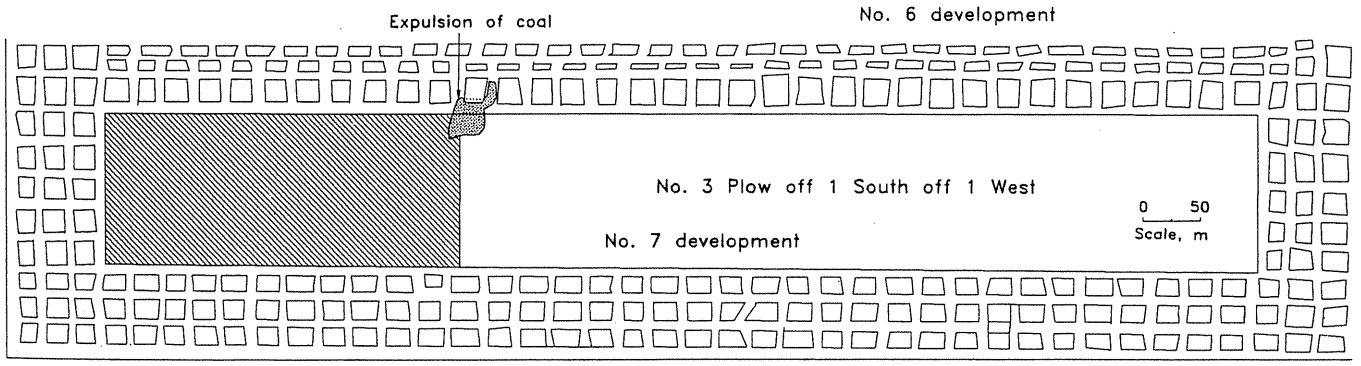

Figure 23
Detailed View of Bump at Beatrice Mine, May 15, 1974.

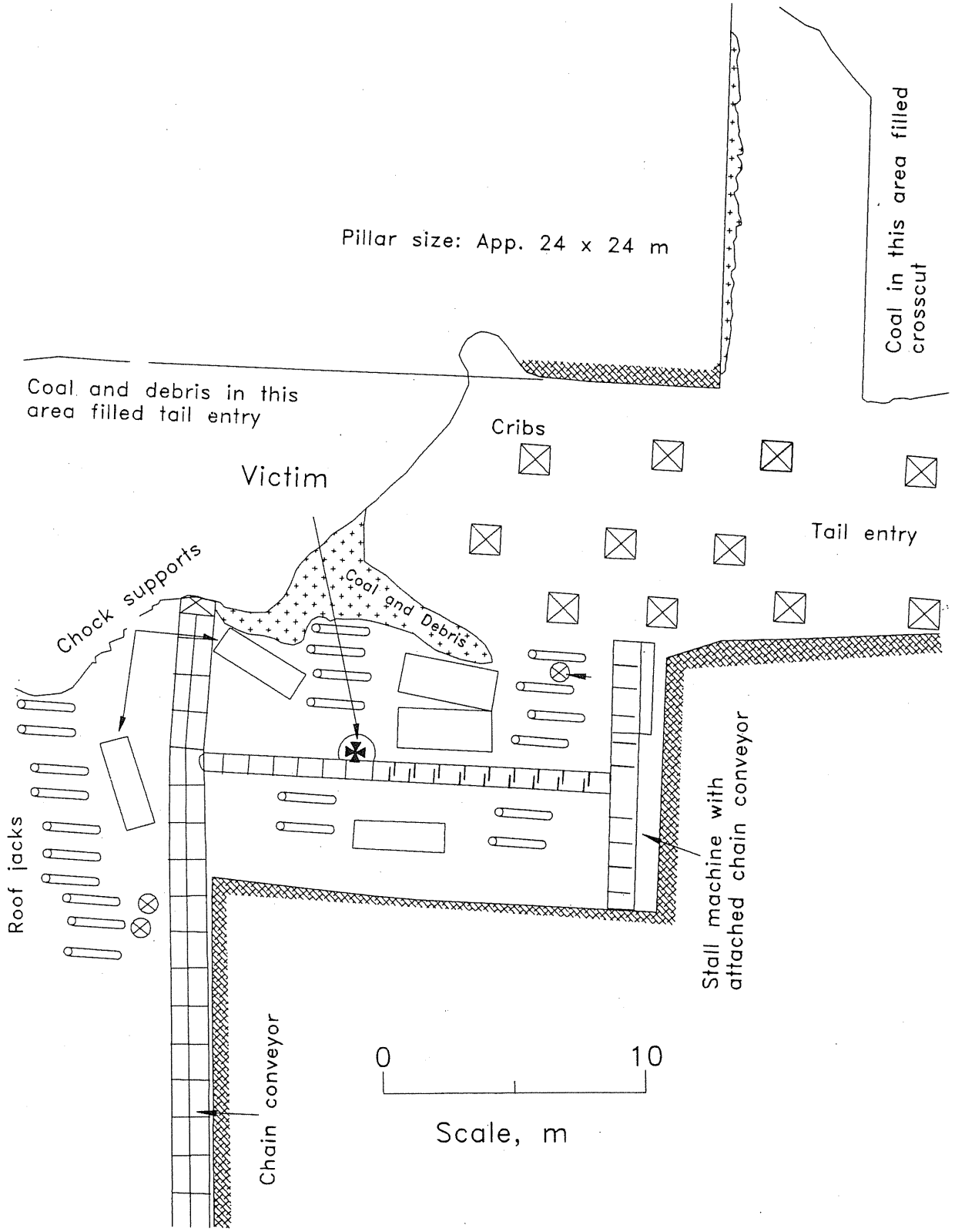

This section of longwall panel was referred to as the "stall area." ⊗ indicates miners.

Virginia Polytechnic Institute and State University's Seismological Observatory in Blacksburg, VA, registered this event as 1.0 on the Richter scale. The destruction underground did not translate into the high levels of seismic energy that had been recorded for several other events.

Several years later, during mining in the northern portion of the Beatrice Mine, three bumps occurred in one location at different times, but in association with a distinctive geologic condition. A large "swag," or roll, in the Pocahontas No. 3 Coalbed was reported across the No. 1-3 developments (figure 24). In this area, the structural elevation of the coalbed changed rapidly with an associated thickening of the coal. Because of the lack of detailed data, one can only infer the exact manner in which this geologic condition influenced bump occurrence. However, rolls are often associated with changes in depositional environments, which are in turn responsible for significant stratigraphic changes. Indeed, a localized increase in floor strength was suggested because of a decrease in the degree of floor heave within the roll area (*10*). The localized thickening of coal may have also contributed to lower pillar strength in the roll area, for the 670 m of overburden in the area did not appear to be excessive for this mine.

The first of these three bumps was generated in a narrow pillar of the No. 2 development headgate entry on May 8, 1978. No miners were injured, but there must have been considerable concern because headgate pillar bumps are rare. In addition, the headgate pillar next to the longwall face was one of the most heavily traveled areas in the mine. Owing to the importance of this area and the significant changes in the character of the floor rock and coalbed, it was recommended that floor holes be drilled and shot along the middle gate entry (*10*). No other bumps were reported until the face of the next

Figure 24
Effects of Large-Scale Structural Roll on Three Headgate and Tailgate Entry Bumps at Beatrice Mine.

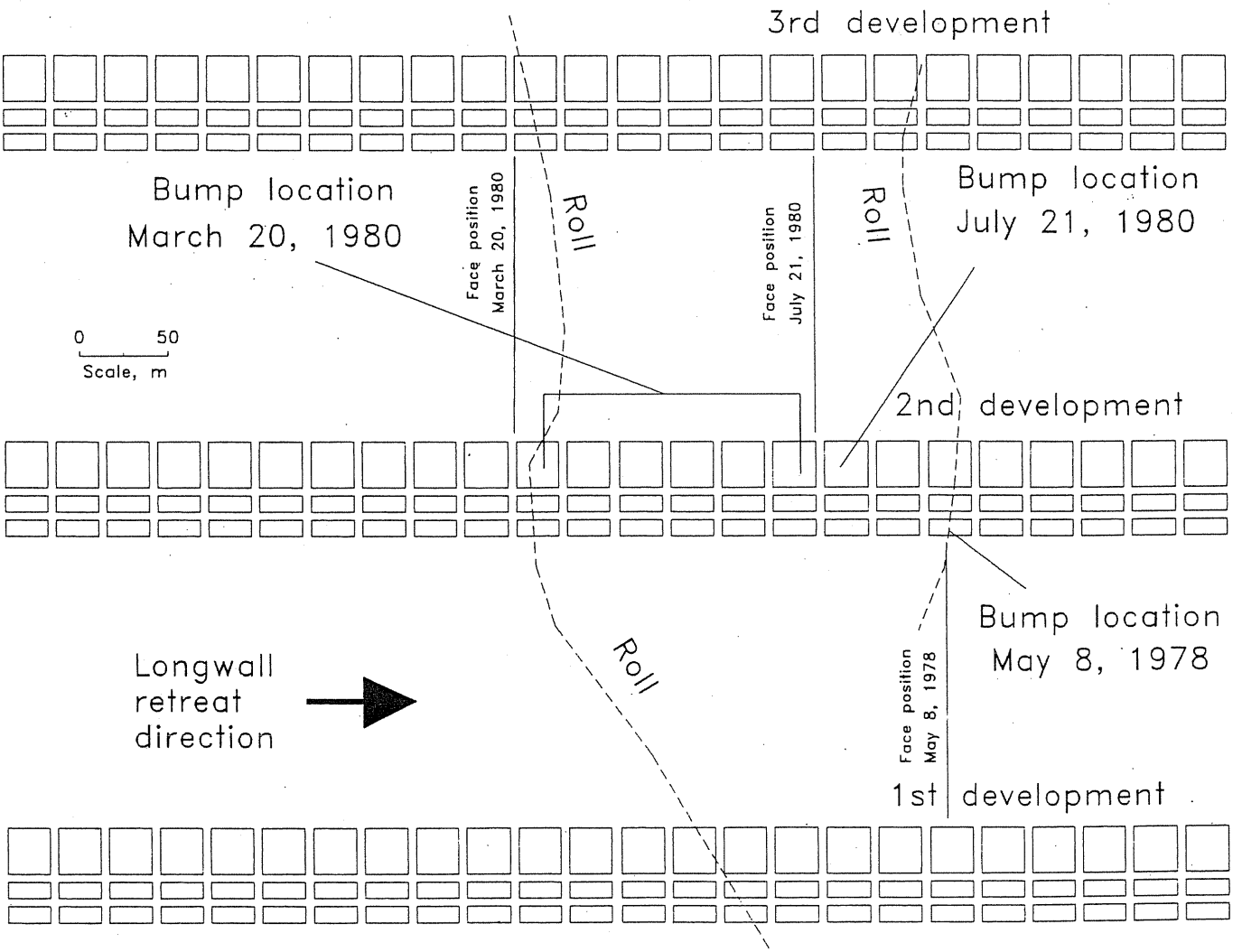

longwall panel approached this same roll (figure 24). Then, on March 20, 1980, six narrow pillars bumped, two of them violently (*11*). No miners were injured in this tailgate bump. Because the floor in the roll area resisted heaving for a distance of 200 m, the operator decided to volley fire or shot fire ribs of three abutment pillars outby the longwall face. The final bump in this area was on July 21, 1980, approximately 50 m from the location of the bump occurring on May 8, 1978. The July 21 bump took place over a weekend, so no miners were on the section; the exact time of occurrence could not be estimated.

SUMMARY OF RECOMMENDATIONS TO MITIGATE COAL MINE BUMPS

When coal pillar bumps first occurred in eastern Kentucky (*3*), local mine officials, workers, mining engineers, and many others tried to explain their cause. Numerous methods of prevention were suggested and attempted unsuccessfully. Most of the bumps were located along the retreating pillar line where several of the following conditions existed: (1) uneven pillar lines, (2) irregular pillar sizes, (3) overburden greater than 300 m, (4) strong mine roof and floor strata, and (5) overhanging or cantilevering gob. Since that time, several prominent mining engineers, consultants, inspectors, and researchers have developed recommendations and methods to mitigate bump hazards in room-and-pillar mines.

RECOMMENDATIONS BY HISTORICAL EXPERTS

Recommendations by Rice

Rice (*27*) proposed that two types of bumps, termed "pressure bumps" and "shock bumps," caused the observed mining problems. Pressure bumps were caused when stress on moderately sized coal pillars became too great for the pillars' bearing strength. Shock bumps were induced by breaking of thick, massive strata above the coalbed, which transmitted a shock wave through the rock to the stressed coal pillars. Faulty mining methods were then identified where (1) pillars were too small, (2) projecting pillars were left behind the retreat line, (3) pillars were narrowed to points, and (4) pillars were extracted in separate groups without any attention being paid to a long, continuous retreat line.

Based on these observations, Rice recommended two operational methods for controlling bumps: straight retreat lines and rock-filled cribs. Keeping retreating pillar lines straight eliminated pillar points projecting into the gob. This practice was fairly easy to initiate and had favorable results. Rock-filled cribs, for a cushioned support of the roof rock, were also tried with positive results. Generally, the cribs were ordinary mine post timbers 1.1 m long, not less than 0.2 m thick, set on 6-m centers. Each crib was tightly packed with a fill of rock material. The cribs were designed and placed so that the mine roof could converge gently without rupture of the immediate strata. This action decreased the potential for sandstone breaks within the gob, which were believed to cause many shock bumps.

Bryson (*3*) described a detailed field test of this design method at a deep mine in the Harlan Coalbed, Cumberland Mining District, under 430 m of cover. Bumps had killed five miners at this particular site. Figure 25 shows the test area, which was approximately 210 m wide and adjacent to a large gob area. Rooms were driven approximately 91 m between the support entries, which were about 10.7 m wide. Prior to the extraction phase, the study area was composed of a series of narrow (10.7 m wide) and large (43 m wide) pillars. As the section was mined, 16 roof-to-floor convergence stations and 64 rock-filled cribs were installed.

After the area was extracted, convergence began. Bryson reported that a few roof rock cracks gradually widened to as much as 41 cm without causing mine roof collapse. Convergence continued until the roof and floor almost met. In general, the strata settled by cracking and grinding noisily, but did not develop many large breaks. Only one bump occurred during coal extraction when the pillar line was not kept straight.

Recommendations by Holland and Thomas

Holland and Thomas (*14*) expanded on Rice's general recommendations regarding pillar extraction procedures and offered the following 10 measures to minimize pillar bumps:

1. Recover all coal in a pillar operation.
2. Avoid pillar line points.
3. Keep the roof spans projecting over the gob as short as possible or provide support so that the roof beds do not fracture.
4. Do not conduct development work in abutment areas.
5. Do not split pillars on or near the extraction line.

Figure 25
Suggested Plan of Pillar Extraction Under Deep Cover Using Rock-Filled Cribs (After *17*).

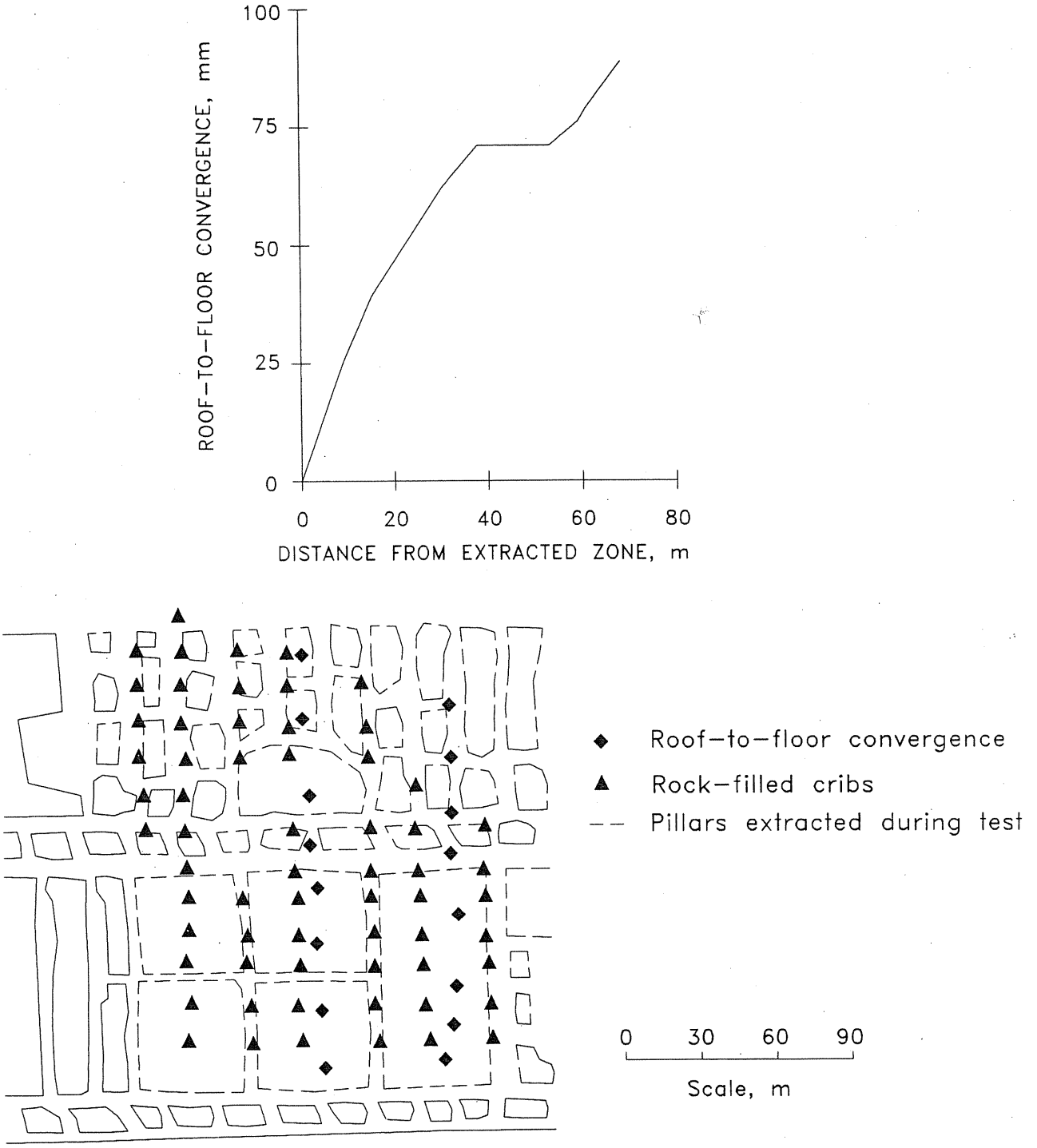

6. Use the open-ended extraction technique with lifts of not more than 4.3 m.
7. Leave one or two rows of pillars adjacent to old gob areas.
8. Maintain pillars at the same size and shape.
9. Keep development entries narrow, approximately 4.3 m.
10. Note areas of rolls, changes in dip, and changes in coal thickness and hardness. Use this information in designing the mining system.

Although many of the rules still apply to modern room-and-pillar operations, several are no longer pertinent by today's standards, however they may be useful as new mining methods are developed. For example, continuous mining machines require regular mining patterns and entries larger than 4.3 m to operate. It is also necessary to conduct development work in abutment areas during the final stages of a mine's life. This is necessary as the mine pulls back along main entries, extracting the remaining large barriers. The practice of a retreating longwall through existing openings may change this assumption.

Recommendations by Peperakis

Peperakis (*25*) summarized experiences in the use of novel engineering designs at the Sunnyside Mines prior to the introduction of longwall mining techniques in the early 1960's. Many of Sunnyside's bumps initiated roof falls of the immediate shales and thin laminated sandstones beneath the massive main sandstone roof rock. Bumps initiated during development were associated with a series of faults trending along strike. Displacements ranged from 1 to 8 m. Peperakis identified the following seven measures to minimize bumps:

1. Conduct long-hole shooting.
2. Cut up large blocks into smaller, more uniform pillars ahead of the retreating pillar line.
3. Do not split large blocks during development.
4. Break large development blocks ahead of retreat pillar lines into uniformly sized blocks.
5. Use substantial supplemental support.
6. Use yieldable steel arch supports to minimize roof falls associated with bumps.
7. Use hydraulic backfill to reduce stress transfer during bumps.

Osterwald (*23*) noted that many other oriented structural features (for example, shatter zones, cleavage, pyrite veins, and cylindrical and smooth fractures) were found in bump-prone areas. He suggested that mine layouts could take advantage of these features to reduce stress concentrations, thereby decreasing bump incidences.

OTHER BUMP MITIGATION RECOMMENDATIONS

Olga Pillar Extraction Sequencing Technique

A novel pillar extraction sequencing technique was developed principally by Olga Mining Co. in the 1970's to control bumps. This technique involved mining numerous places over three to four rows of pillars to direct the overburden loads gradually away from the pillar line where most miners and machines were located. An idealized schematic of the extraction sequence is shown in figure 26. By design, all coal pillars three rows away from the retreating pillar line have at least a "bump" cut. This bump cut is a 6.1- by 6.1-m cut of coal taken from a typical size of chain pillar (18.3 by 21.3 m). The frequent audible thumps during extraction explain the terminology. The two pillar rows closest to the gob line are split in half by extending the bump cut entirely through the pillar. Finally, the pillar wings, or fenders, are extracted in the row closest to the gob line.

This innovative design was evaluated by the USBM using an extensive rock mechanics instrument array to determine how the strata responded during mining (*4*). The response of the strata was measured by 44 coal cells (borehole platened flatjacks) and more than 70 convergence stations. Observations at the field site indicated that the technique redistributed stress effectively. Pressures were transferred farther than would normally be expected—up to eight pillar rows away from the pillar line. This redistribution effectively transferred the load over a very large area, greatly minimizing bump hazards.

Recently, USBM researchers have attempted to evaluate this extraction technique using numerical modeling (*33*). Several idealized mining scenarios were modeled by a USBM-developed boundary-element program with nonlinear material types and an energy-release-rate subroutine. The study found this novel pillar splitting and extraction sequencing method superior in reducing bump potential to more traditional techniques, such as single split-and-fender, pocket-and-wing, and open-ending.

U.S. Steel's Thin-Pillar Method

Coal bumps often occur during extraction of the large barriers adjacent to main entries. Violent bumps during barrier-splitting appeared to be especially troublesome during the 1950's in southern West Virginia. Engineers at U.S. Steel Mining Co., a major coal producer in the

Figure 26
Idealized Pillar Extraction Sequencing Technique for Bump Control During Room-and-Pillar Mining.

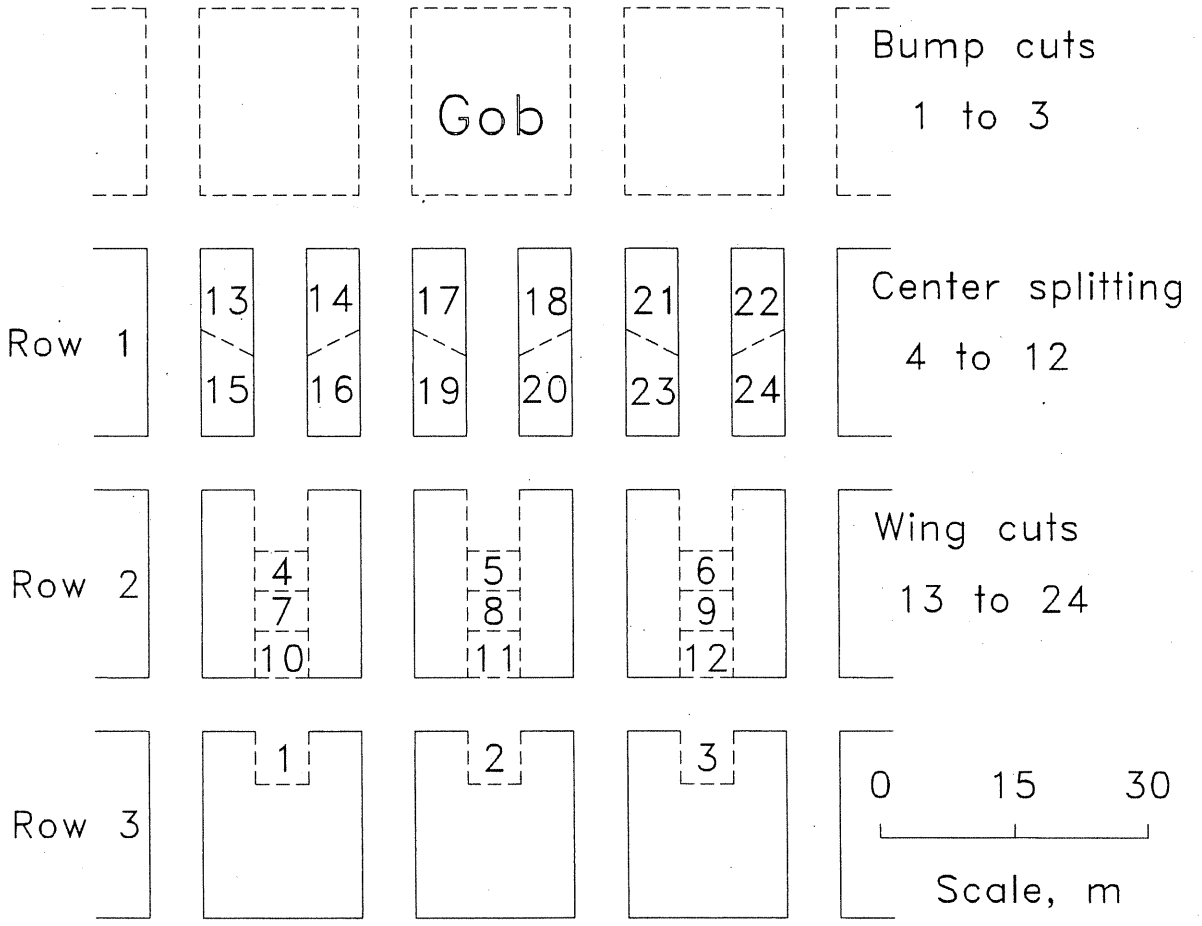

This technique was developed by Olga Mining in the 1970's. Numbers indicate cutting sequence.

region, developed a method of splitting large barriers adjacent to main entry systems (*29*). They found that pillars smaller than 14 m or larger than 49 m almost never bumped. An extraction method known as thin-pillar mining was developed that systematically cut the large barriers into pillars with widths smaller than 14 m, leaving a barrier pillar remnant, which was either destressed or left in place.

When implementing a thin-pillar mining system for barrier extraction, multiple entries are first driven within the barrier directly adjacent to the main entries. The remaining solid barrier is located between the newly advanced headings and the stabilized gob. The mining of barrier and predeveloped chain pillars proceeds simultaneously (figure 27). Barriers are split from the recently driven headings adjacent to the active gob back toward the next solid barrier. These headings are very close, isolating yield pillars about 6.1 m wide. These yield pillars fail in a controlled manner, shedding high stresses both to the active gob areas and farther into the solid barrier. When the remaining barrier approaches 49 by 49 m, a critical-size pillar is formed. This large abutment pillar is called a "bump block" and is left to avert a bump. These large blocks aid in breaking the roof at the pillar line and protecting the remainder of the section from excessive convergence.

The thin-pillar mining system has many forms, but it is generally employed when extracting the barriers left to protect main entries. The smaller pillars tend to yield to the high stresses imposed on them by overburden and normal mining. The adoption of this technique greatly reduced bumps in the Gary Mining District.

Figure 27
Typical Mining Sequence Utilizing Thin-Pillar Method.

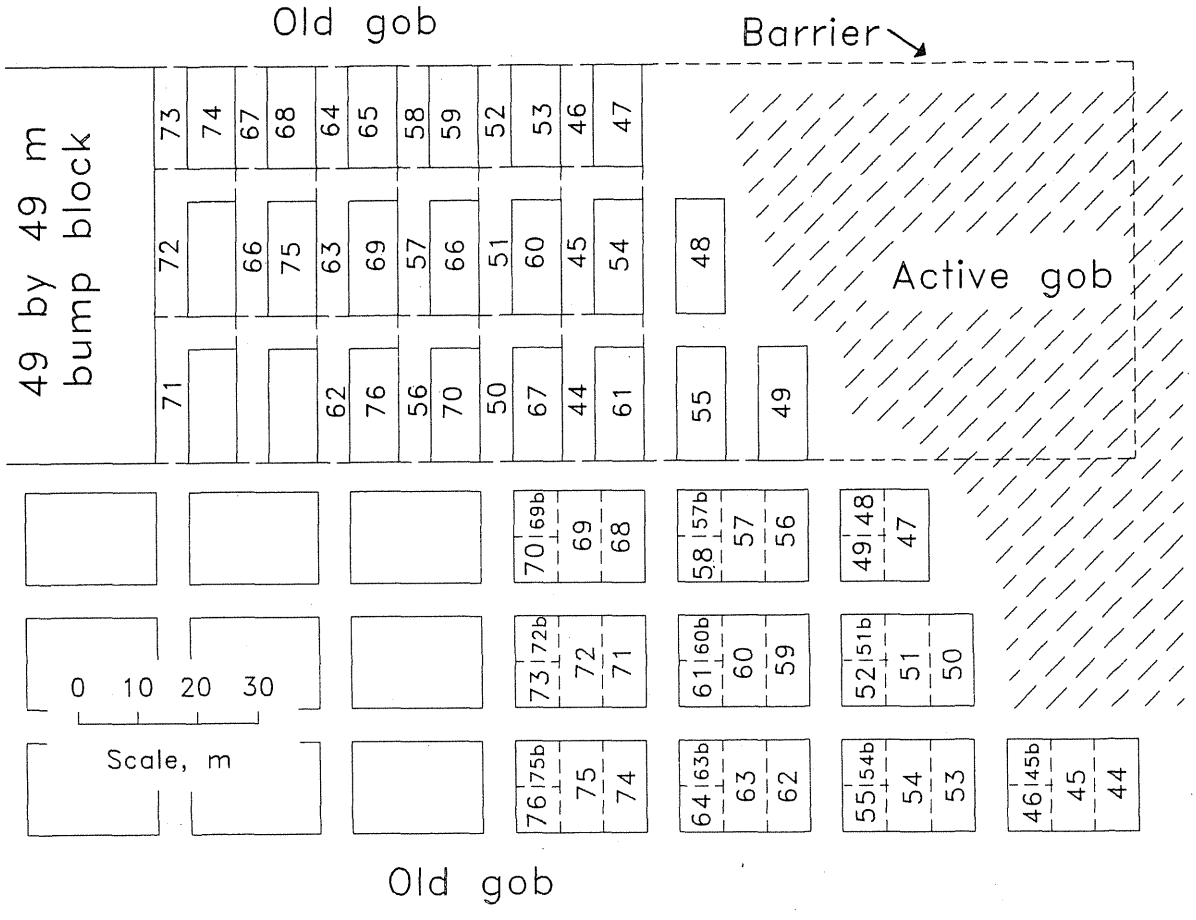

This method was developed by U. S. Steel in the 1950's. Numbers indicate cutting sequence.

Longwall Gate Entry Design Techniques

As a result of the longwall gate entry bump problems discussed above, two different design philosophies have emerged in the United States based primarily upon regional geologic conditions and mining preferences. Standard gate entry designs in the Southern Appalachian coal basin consist of three or more entries with at least one row of *abutment* pillars, whereas two- and three-entry systems with *yield* pillars are a more common gate entry design in the Uinta and Piceance Creek Basins. Many mines in the Southern Appalachian Basin require multiple gate entries because of methane gas emission problems. Several of the bump-prone longwall mines operating in the Southern Appalachian Basin employ three- and four-entry designs with a combination of yield and abutment pillars. The most common designs used in the Uinta and Piceance Creek Basins consist of one or two yield pillars.

Abutment Design

A well-designed abutment gate entry design supports a considerable amount of the abutment loads generated from both the adjacent gob and the approaching longwall face. This method is well suited for longwalls of moderate depth (300 to 600 m) that have substantial methane gas emission problems. In bump-prone ground, typical sizes of gate entry pillars (15 to 25 m wide) fail prior to the passage of the longwall mining face. To control the abutment load ride-over problem, gate entry pillars have been widened so that they do not fail during panel extraction. Redesign of the gate entry was accomplished by increasing

the width of the abutment pillar. This caused the abutment pillars to fail much later in the mining sequence (*13*). This design eliminated abutment load ride-overs from the adjacent gob panels onto the actively mined panel. As a result of implementing this technique, the incidence of bumps at problem mines has been greatly reduced. Although this method has proven successful, it may have limitations when overburden is extreme (about 750 m), depending on coalbed thickness. These conditions may require extremely large abutment pillars, which may be impractical.

Yielding Design

Yield pillar designs allow the gate entry system to deform under the weight of the approaching panel abutments, thereby diverting substantial load to the nearby solid coal panel. This method of stress control for gate entries is well suited for two-entry designs. The first U.S. applications were pioneered in the early 1960's at the Sunnyside Mine in the Uinta Basin (*16*). At that time, longwall mining had been practiced in the United States for only about 10 years, and entry design methods for bump-prone ground were not well developed. Perhaps without fully realizing the advantages of a two- versus a multiple-entry yielding system, operators made the decision to develop only two entries primarily to limit the amount of ground to be opened up prior to panel retreat. Nearly 30 years later, this system has continued to be successful in eliminating entry pillar bumps during panel development and retreat operations, especially in areas overlain by up to 600 m of overburden.

Not all mines have experienced Sunnyside's success with a yield pillar design. A nearby mine attempting to emulate this very profitable design had difficulties in developing small pillars without generating serious bumps and routinely lost significant portions of tailgate entries to large bumps. It soon became evident that the successful application of yielding designs depended partly on the geology surrounding the pillar system. Competent mine roof and floor conditions are necessary to maintain stability during the higher rates of entry closure experienced with this system.

Two-entry gate systems more commonly employ pillar designs that yield during or shortly after development. By design, the narrower gate entries typically generate significant side abutment stresses, which are capable of destroying most conventional chain pillars even at moderate overburden. Where two-entry systems are impractical, yield pillars have been used effectively in multientry systems, but such systems are more commonly used in conjunction with abutment pillar designs. In either application, yield pillar designs have proven to be an effective alternative in mitigating bump hazards in deep U.S. coal mines.

Destressing

Several forms of destressing were identified within the USBM Coal Bump Database. These included (1) volley firing or shot firing, (2) auger drilling, (3) water infusion, (4) hydraulic fracturing, and (5) partial mining. If conducted with deliberation, destressing generally aids in releasing excessive stresses in a controlled manner. However, many examples in the database demonstrate that bumps may occur in conjunction with destressing the coal.

Shot Firing

Shot firing fractures coal, thereby extending the yielded coal zone. This process injects energy into stressed coal, causing seismic shock. The shock waves temporarily release confinement, initiating violent failure under a controlled condition. However, there is little that is engineered about this method. Typically, the shot holes are loaded with explosives, but the amount of explosive needed is poorly defined. The most appropriate lengths and spacings of blastholes are also unknown. Generally, all shots are initiated simultaneously. It is commonly believed that the destressed zone is defined by the length of the blasthole. Jackson (*19*) noted that Mid-Continent Resources mines in Colorado used shot firing to move the peak stress zone into the solid core of the longwall panel when this zone was less than 5 m from the rib. Polish mines have long used shot firing to break and shear cantilevered roof strata.

Auger Drilling

Auger drilling was first practiced at the Gary No. 2 Mine in the mid-1950's when 61-cm holes were drilled from the sides of highly stressed barrier pillars (*29*). Unfortunately, these large-diameter boreholes were prone to triggering large bumps. Up to 1,000 t of coal was ejected from the coal ribs by the largest events, causing this method to be judged too hazardous to use routinely. As a result of European research, which suggested that auger holes less than 10 cm could not initiate a coal bump, auger destress drilling has regained limited favor in recent years.

The Olga Mine routinely used this method to redistribute stress away from active work areas (*4*). As the auger

holes entered the more highly stressed coal 3 to 4 m from the rib, the amount of coal produced rose dramatically. Significant amounts of coal were recovered at a gradual pace, often 10 to 20 times the volume of a 10-cm-diam hole. In effect, augering affected the areas of highest stress in the pillars without removing any of the confining fractured and yielded rib coal. Undoubtedly, this technique is very effective in mining highly stressed coal pillars when other alternatives are unsuccessful.

Water Infusion

Water lubricates fracture surfaces within a rock mass; therefore, water infused into a coalbed can initiate slippage between rock surfaces, thus lowering the state of confinement on the surface and the amount of energy stored within the rock. This technique has been tried successfully in Europe, but has received only limited use in the United States. This probably stems from the difficulty of infusing water into U.S. coalbeds. Water infusion has been attempted in many mines to control respirable dust and methane gas migration. It has been most successful in coalbeds that have a well-developed cleat system that controls permeability.

Because water infusion is impractical when the coalbed is highly stressed, destressing must be completed prior to retreat mining, for holes will not remain open long. Successful water infusion generally requires the coalbed to accept and transmit fluid readily. The equipment must be capable of pumping water at or above hydrostatic pressure.

Two U.S. coal mines have attempted to use water infusion to destress coalbeds. Lessley (*20*) discusses use of the technique in a room-and-pillar section in a Virginia coal mine. Several 4- to 9-m-long holes were drilled into pillars. Injection pressures averaged 3.7 MPa, with the coal pillar accepting between 0.1 and 3 m^3 of fresh water. Microseismic monitoring indicated that only small amounts of energy were released during infusion.

Hydraulic Fracturing

In some mines, it has been difficult to achieve good caving into full-extraction gob areas. This is believed to be a function of the ability of massive units to span the gob. It has been proposed that caving could be induced with hydraulic techniques near vertical breaks within the main roof beam. This technique was attempted at Arch of Kentucky's Lynch No. 37 Mine in southeastern Kentucky, but little data from this experiment are available.

Partial Pillaring

A unique application of pillar destressing was attempted at Energy West Mining Co.'s Deer Creek Mine in Utah in 1987. A remotely controlled continuous mining machine was used to split seven chain pillars outby a retreating longwall face. Pillars in the 7th Right gate entries were progressively narrowed from 12 to 9 m wide to accommodate the change from a three- to a two-entry gate design. Upon retreat, this longwall panel encountered severe pressure in the pillar transition zone, producing bumps and damaging the longwall shearer and adjacent tailgate pillars. It was determined that pillar splitting could provide the safest means of destressing the chain pillars in the transition area (figure 28). Several operational precautions were taken to decrease the dangers of initiating a bump during splitting, with apparent success.

Observational Techniques

Because many bumps are very sensitive to slight changes in geology, considerable attention should be placed on observing the condition of the yielded coal. The depth and character of the fractured coal zone reveals the location of the peak stress zone and therefore the potential for violent failure. Numerous techniques are available to acquire this information. If the ribs are generally crushed, but locally appear straight and solid, the peak stress zone may be close to the pillar edge. If the ribs are difficult to cut or drill, an abnormally high peak stress zone may be present. A sandstone channel scour may signal a change in the character of the contact zone. Generally, the irregular nature of the scours provide higher shearing resistance. The appearance of a "red-coal" zone within the contact zone is perhaps the most dramatic indicator of the imminent occurrence of a coal mine bump. This condition reflects the coalbed's inability to resist the shearing forces generated by the tremendous confinement applied to the coal in a localized area. The red-coal zone probably represents coal that has been mechanically altered because of the presence of excessive amounts of shear strain. USBM researchers have observed this condition at three bump-prone mines: the Olga and Gary Mines in southern West Virginia and the Lynch No. 37 Mine in eastern Kentucky.

Auger drilling also has been used to probe for areas of highly stressed coal (*24*). Often after a particular mining section has bumped, small-diameter (5 cm) auger holes are drilled into the face with hand-held units. Drill hole

Figure 28
Example of Partial Pillar Destressing Method Employed at Deer Creek Mine, Emery County, UT.

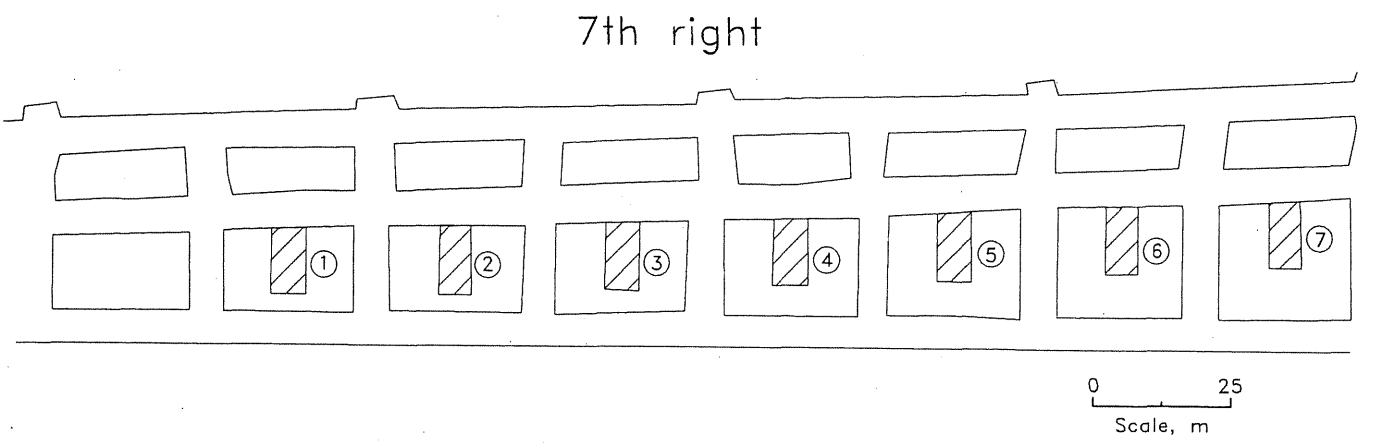

Numbers indicate mining sequence.

cuttings are often monitored, but generally the operator is most interested in determining when drilling difficulty or drill string seizures occur. At these points, it is assumed that the drill hole has entered an area of high stress. Several holes are drilled across the problem working face at distances of 2 to 6 m apart. If the peak stress zone (figure 7) is close to the entry (less than 2 m), the situation is generally considered critical, and mining is temporarily halted or some destressing technique is attempted. If the peak stress zone is greater than 5 m from the entry, conditions are generally considered safe for additional mining at the face. One should note that no reliable criteria exist to guide an operator in selecting how often a face should be probed or in choosing drilling parameters or patterns. Longwall mines such as the Dutch Creek No. 1 and Lynch No. 37 Mines have utilized auger drilling to choose areas to be destressed.

CONCLUSIONS

The Coal Bump Database compiled by the USBM contains a wealth of knowledge from past experience that has undoubtedly reduced the severity of coal mine bumps in the United States. This paper has elaborated on the most successful designs for both room-and-pillar and longwall mining. The following are the principal observations developed from mining in bump-prone strata:

1. The potential for bump occurrence increases when mining in stiff roof and floor rock. Strata of this nature are frequently found within the Southern Appalachian, Uinta, and Piceance Creek Basins.
2. Bumps can occur—
   a. In development sections when faults and igneous dikes are approached,
   b. In room-and-pillar sections when cantilevering roof is encountered,
   c. In longwall sections when geologic structures are encountered, and
   d. In either room-and-pillar or longwall sections when overburden, abutment, or shock loads are excessive.
3. Supplemental support has been useful in minimizing bump damage. Rock-filled cribs allow gob to converge gently without rupturing. Combinations of cribs, crossbars, and props reduce the severity of bumps in main entries. Wood cribs and yielding arches in combination with rock bolts help support weak, immediate mine roof during bumps, which reduces associated roof falls.
4. The use of straight retreating pillar lines and total extraction of all coal can eliminate projections of bump-prone material into the gob.
5. Developing or splitting large blocks of coal into smaller, uniform blocks ahead of the retreating pillar line causes the coal to yield in a controlled manner before it is extracted and allows the roof to bend gently.

6. Sequential splitting of pillars away from the retreating pillar line can effectively move excessive stress away from the working face in a controlled manner.

7. Sizing gate entry pillars large enough to contain induced stresses can effectively reduce bump occurrences.

8. Sizing gate entry pillars to yield in a controlled manner can assist fracturing of the main roof and, in some instances, decrease the magnitude of abutment and/or shock loads onto the longwall face.

Most past and present U.S. bump-control designs have helped control the manner in which the roof rock breaks and have regulated the manner in which stresses are redistributed. These techniques have mostly been very successful, but they have not been applied over a wide range of geologic and mining conditions. As production rates and overburden depths increase and new mining systems are designed, the mining industry will be required to engineer new bump-control techniques. By evaluating past experiences, analyzing current and projected conditions, and investigating innovative design techniques in the field, the requisite technology can be developed to keep bump-prone U.S. mines safer for underground mine workers.

REFERENCES

1. Babcock, C. O., and D. L. Bickel. Constraint - The Missing Variable in the Coal Burst Problem. Paper in Rock Mechanics in Productivity and Protection. Proceedings, 25th Symposium on Rock Mechanics, ed. by C. H. Dowding and M. M. Singh (Northwestern Univ., Evanston, IL, June 25-27, 1984). Soc. Min. Eng., 1984, pp. 639-647.

2. Brauner, G. Rockbursts in Coal Mines and Their Prevention. Balkema, 1994, 144 pp.

3. Bryson, J. F. Method of Eliminating Coal Bumps or Minimizing Their Effect. Trans. AIME, v. 119, 1936, pp. 40-57.

4. Campoli, A. A., D. C. Oyler, and F. E. Chase. Performance of a Novel Bump Control Pillar Extracting Technique During Room-and-Pillar Retreat Coal Mining. USBM RI 9240, 1989, 40 pp.

5. Chekan, G. J., and J. M. Listak. Design Practices for Multiple-Seam Longwall Mines. USBM IC 9360, 1993, 35 pp.

6. ___. Design Practices for Multiple-Seam Room-and-Pillar Mines. USBM IC 9403, 1994, 44 pp.

7. DeMarco, M. J., E. J. Koehler, and H. Maleki. Panel and Gate Road Design Considerations for the Mitigation of Coal Bumps in Western U.S. Longwall Operations. Paper in these Proceedings, 1995.

8. Descour, J. M., and R. J. Miller. Coal Mine Bump Monitoring (contract J0245009, CO Sch. Mines). USBM OFR 32-88, 1987, 111 pp.; NTIS: PB 88-214309/AS.

9. Duckwall, A. E. History and Present Concepts of Mountain Bumps in the Gary District. U.S. Steel Coal Co., c. 1952, 37 pp. Available from A. T. Iannacchione, USBM Pittsburgh Research Center, Pittsburgh, PA.

10. Gaspersich, S. E. Report of Investigation of Coal Mine Bump, Beatrice Mine, Beatrice Pocahontas Company, Keen Mountain, Buchanan County, Virginia. MSHA, July 21, 1980, 2 pp.

11. Gaspersich, S. E., and C. Blankenship. Report of Investigation of Coal Mine Bump, Beatrice Mine, Beatrice Pocahontas Company, Keen Mountain, Buchanan County, Virginia. MSHA, Mar. 20, 1980, 2 pp.

12. Goode, C. A., A. Zona, and A. A. Campoli. Controlling Coal Mine Bumps. Coal Min., v. 21, No. 10, Oct. 1984, pp. 48-53.

13. Heasley, K. A., and K. Barron. A Case Study of Gate Pillar Response to Longwall Mining in Bump-Prone Strata. Paper in Longwall U.S.A., 1988, pp. 92-105.

14. Holland, C. T., and E. Thomas. Coal-Mine Bumps: Some Aspects of Occurrence, Cause, and Control. USBM Bull. 535, 1954, 37 pp.

15. Humphrey, H. B. Historical Summary of Coal-Mine Explosions in the United States. USBM IC 7900, 1959, pp. 204-206.

16. Huntsman, L., and D. C. Pearce. Entry Development for Longwall Mining. Min. Congr. J., July 1981, pp. 29-32, 51.

17. Iannacchione, A. T. Behavior of Coal Pillars Prone to Burst in the Southern Appalachian Basin of the United States. Paper in Rockbursts and Seismicity in Mines, Proceedings of the 2nd International Symposium on Rockbursts and Seismicity in Mines, ed. by C. Fairhurst (Univ. MN, Minneapolis, MN, June 8-10, 1988). Balkema, 1990, pp. 295-300.

18. Iannacchione, A. T., and M. J. DeMarco. Optimum Mine Designs To Minimize Coal Bumps: A Review of Past and Present U.S. Practices. Ch. 24 in New Technology in Mining Health and Safety. Soc. Min. Eng., 1992, pp. 235-247.

19. Jackson, D. Advancing Longwall Mining: A First for Mid-Continent Coal and a First for the U.S. Coal Age, v. 80, No. 10, Sept. 1975, pp. 100-105.

20. Lessley, J. C. Investigation of Coal Bumps in the Pocahontas No. 3 Seam, Buchanan County, Virginia. M.S. Thesis, VA Polytech. Inst. & State Univ., Blacksburg, VA, 1983, 303 pp.

21. Maleki, H. N. and M. Moon. In-Situ Pillar Strength Determination for Two-Entry Longwall Gates. Paper in 7th International Conference on Ground Control in Mining: Proceedings, ed. by S. S. Peng (Morgantown, WV, Aug. 3-5, 1988). Dep. of Min. Eng., WV Univ., 1988, pp. 10-17.

22. Morrison, D. M., and P. MacDonald. Rockbursts at Inco Mines. Paper in Rockbursts and Seismicity in Mines, Proceedings of the 2nd International Symposium on Rockbursts and Seismicity in Mines, ed. by C. Fairhurst (Univ. MN, Minneapolis, MN, June 8-10, 1988). Balkema, 1990, pp. 263-267.

23. Osterwald, F. W. USGS Relates Geologic Structures to Bumps and Deformation in Coal Mine Workings. Min. Eng. (New York), v. 14, Apr. 1962, pp. 63-68.

24. Paul, K. Further Development of Methods for Predicting and Preventing Gas Outbursts. Glückauf (English Translation), July 9, 1981, pp. 334-337.

25. Peperakis, J. Mountain Bumps at the Sunnyside Mines. Trans. AIME, v. 211, Sept. 1958, pp. 982-986.

26. Reeves, John A., Jr. Advancing Longwall Mining at Mid-Continent. Min. Congr. J., v. 64, No. 7, July 1978, pp. 25-29.

27. Rice, G. S. Bumps in Coal Mines of the Cumberland Field, Kentucky and Virginia—Causes and Remedy. USBM RI 3267, 1935, 36 pp.

28. Talman, W. G. Auger Drilling To Control Mountain Bumps. U.S. Steel Corp., Gary-Lynch Districts, Gary, WV, 1955, 22 pp.

29. Talman, W. G., and J. L. Schroder, Jr. Control of Mountain Bumps in the Pocahontas No. 4 Seam. Trans. AIME, 1958, pp. 888-891.

30. Watts, A. C. An Unusual Bounce Condition. Coal Age, v. 14, No. 23, Dec. 1918, pp. 1028-1030.

31. West, M. L., and C. E. McGraw. Report of Fatal Coal-Mine Accident, Beatrice Mine, Beatrice Pocahontas Company, Keen Mountain, Buchanan County, Virginia. MSHA, May 15, 1974, 9 pp.

32. Zelanko, J. C., and K. A. Heasley. Evolution of Conventional Gate Entry Design for Longwall Bump Control: Two Southern Appalachian Case Studies. Paper in Proceedings: Mechanics and Mitigation of Violent Failure in Coal and Hard-Rock Mines. USBM Spec. Publ. 01-95, 1995, pp. 167-180.

33. Zipf, R. K., Jr., and K. A. Heasley. Decreasing Coal Bump Risk Through Optimal Cut Sequencing with a Non-Linear Boundary Element Program. Paper in Rock Mechanics Contributions and Challenges: Proceedings of the 31st U.S. Symposium, ed. by W. A. Hustrulid and G. A. Johnson (CO Sch. Mines, Golden, CO, June 18-20, 1990). Balkema, 1990, pp. 947-954.

BUMP HAZARD CRITERIA DERIVED FROM BASIC GEOLOGIC DATA

By Gary P. Sames[1]

ABSTRACT

The U.S. Bureau of Mines is conducting research to develop a quantitative means of assessing bump-prone geologic conditions using lithologic and topographic information. An engineering software package that includes a spatial relational database, data modeling, and graphic data display is used to apply a set of geologic criteria to assess bump-proneness and produce hazard maps. This paper presents the method and criteria developed through case studies of mine properties in the Pocahontas No. 4 Coalbed in southern West Virginia and the Pocahontas No. 3 Coalbed in western Virginia. Initial results suggest general agreement between the hazard map and field observations. Further development of the criteria and parameter identification are ongoing.

INTRODUCTION

Coal mine bumps are sudden, violent expulsions of coal from a rib or active working face into an adjacent entry or entries. The amount of coal ejected can vary. Small bumps can present a hazard to individual miners, as these events may eject several kilograms of coal under excessive stress. Large bumps can lead to multiple fatalities by generating enough force to eject tons of coal and displace heavy underground machinery.

The literature contains references to bump activity in the United States as early as 1918 (Watts, 1918). Consistent with that long history, a considerable amount of research has been conducted on coal mine bumps. Early work addressed the causes of coal bumps and made recommendations on various mining practices to avert them (Rice, 1935; Holland and Thomas, 1954). Other work focused on the development of mining systems and remediation techniques that could be used safely in bump-prone ground, such as auger drilling and shot firing (Peperakis, 1958; Talman and Schroder, 1958).

Although some mines have successfully addressed the problem, bumps continue to challenge the coal industry. Goode and others (1984) found that 28 fatalities from 1959 to 1984 could be attributed to bumps. Iannacchione and DeMarco (1992) found that at least one fatality, several injuries, and at least one mine closure were attributable to bumps during the preceding decade. However, with ever-increasing mining depths and faster extraction methods associated with increased productivity, in the future more mines will have to contend with geologic environments with high bump potential.

To effectively control coal bumps, a mine operator should have the means available to (1) anticipate bump-prone ground, (2) design mining systems that can be used successfully in bump-prone ground, (3) monitor the effectiveness of a design once it has been implemented, and (4) remediate situations in which bumps were not anticipated or the employed design proved inadequate. Previous U.S. Bureau of Mines (USBM) research has addressed all four topics to varying degrees. For example, successful mine layout designs have been documented in both room-and-pillar and longwall operations (Campoli and Heasley, 1989;

[1]Geologist, Pittsburgh Research Center, U.S. Bureau of Mines, Pittsburgh, PA.

Campoli and others, 1989), and a general methodology for room-and-pillar mine design in bump-prone ground is available (Campoli, 1994). The present paper describes an ongoing USBM research project aimed at characterizing bump-prone geology and establishing geologic criteria to help mine operators anticipate potentially hazardous bump conditions.

BUMP-PRONE GEOLOGY

Throughout the literature on bumps, there are recurring themes regarding geologic conditions associated with bump occurrences. The most basic assumptions accept that "two geologic conditions have been found to cause the occurrence of bumps in the Eastern United States: (1) relatively thick overburden and (2) extremely rigid strata occurring immediately above and below the mine coalbed" (Campoli and others, 1987). Talman and Schroder (1958) noted the importance of "heavy overburden, an overlying stratum of strong nonelastic rock, a structurally strong coal seam which does not crush easily and yet is the weakest stratum in the series, and a floor stratum of more than ordinary firmness" to the occurrence of bumps. Holland and Thomas (1954) listed "a rather definite set of natural conditions" controlling bump occurrences, including 150 m (500 ft) or more of overburden, a strong overlying stratum immediately above or close to the coal, and a strong floor that does not heave readily.

Various descriptions of bump-prone ground provide some insight as to what constitutes bump-prone geology. However, many questions remain unanswered, e.g., how thick is relatively thick, how rigid is extremely rigid, and how close is immediate? The methodology followed in this study to develop bump hazard criteria was to (1) quantify parameters to represent rules of thumb commonly used to describe bump-prone geology, (2) incorporate the various individual parameters into a single bump hazard index, and (3) evaluate the bump hazard index by contrasting predicted bump-proneness with actual bump experience in mines.

The development and evaluation of the bump hazard criteria were facilitated by a relational database management system operating on a computer workstation. Detailed stratigraphic information on bump-prone mines in the southern Appalachian Coalfield is being compiled in an engineering software package called TECHBASE. TECHBASE is a relational database management system with application packages that can, among other capabilities, store and manipulate stratigraphic data, use various modeling techniques to estimate data in two and three dimensions, and create graphics to display the data as plan-view and cross-sectional maps.

BUMP HAZARD CRITERIA

As mentioned earlier, several geologic factors are historically associated with coal bumps, namely, thick overburden and strong, stiff roof and floor members. The most basic approach to quantifying bump-prone ground, therefore, is to find some means to assign relative measures of (1) overburden thickness, (2) strength of mine roof, and (3) strength of floor. In this analysis, index scales were developed for each of these three parameters. Each scale runs from 0 to 100; the higher the value, the greater the degree of bump-proneness.

The overburden index is calculated by extrapolating top-of-coalbed elevation data from core logs into a grid, matching surface elevation data to the grid, subtracting the top-of-coalbed surface grid from the topographic surface grid, subtracting 150 m (500 ft), and normalizing the data by dividing by a number to arrive at a 0-to-100 scale.

This formula assumes a that minimum overburden of 150 m (500 ft) is needed to initiate a bump. Subtracting 150 m (500 ft) from each overburden value in the grid, then normalizing the data to reduce the effective overburden index to a scale of 0 to 100, where 0 represents 150 m (500 ft) of overburden and 100 represents the maximum overburden present at the site, results in a range of values that all carry bump potential. The overburden index is a rather direct measure of overburden thickness; estimating rock strength using roof- and floor-strength indices, however, is less straightforward.

When working with core logs to develop a hazard criterion for strength and stiffness of the roof and floor, one is immediately faced with the variability of the geologic environment. Many researchers point to the presence of specific sandstone units in the immediate roof and floor of bump-prone mines as providing the strength or stiffness necessary to initiate bumps. However, the presence, absence, and/or continuity of any individual unit in coal-measure rocks are generally unpredictable. Named units in core logs can be inconsistent or nonexistent, depending on the ability and requirement for detail originally

assigned to the driller or logger. In addition, sandstone may not be the rock type most directly responsible for bump-prone conditions in every geologic setting.

To overcome these difficulties, a decision was made to develop a geologic criterion based on generic lithologic descriptions, rather than specific lithologic units, and empirical evidence to determine the lithologies most directly related to bumps in each geologic setting. Rather than using named units or beds, code values (Ferm and Weisenfluh, 1981) were assigned to rock types. Code values provide a convenient means of grouping rock types and calculating parameters characteristic of stratigraphic sequences. For example, one approach to estimating the strength of mine roof and floor (and the one used in this study) was simply to determine the percentage of the rock type most directly associated with previous bumps in that geologic setting in an interval above and below the coalbed. Thus, the amount of the targeted rock type present provided a crude measure of mine roof strength or potential to contribute to bump occurrence. Kidybinski (1979) used a similar approach to incorporate a lithologic component into his assessment of "the natural liability of coal to rock bursts."

Roof- and floor-strength indices were calculated in TECHBASE by determining the total thickness of strata identified by three grouped rock-type codes in specified intervals above and below the coalbed. Code group 1 includes sandstones, conglomerates, and sandstones with shale streaks. Code group 2 includes siltstones, sandy shales, and shales with sandstone streaks. Code group 3 is comprised of fine-grained shales, claystones, and coals. This approach eliminated vagaries in named units, the complexity of many lithologic descriptions, and the effect of vertical variability in lithology when deciding which units were to be deemed influential.

A 10-m (33-ft) interval above the coalbed was chosen for examining roof strength. This selection differed from Kidybinski's (1979) recommended interval of 30 m (100 ft). The decision to shorten the interval was made to lessen the effect of averaging the overlying strata to the degree that it began to approach the normal distribution of rock types expected in any given geologic environment. Also considered in the decision was the expectation that using the immediately confining strata as a precursor of bump occurrence was more suited to a hazard index such as this than was using the nature of a large interval of overlying rock. A smaller interval of 3 m (10 ft) was chosen to examine floor strength for more pragmatic reasons—often coreholes do not extend more than a few meters below a coalbed of interest.

The individual index values chosen to represent overburden thickness, roof strength, and floor strength were then combined and averaged to develop a measure of the relative bump hazard. The combined criteria were intended to reflect the conventional wisdom about which geologic conditions constitute bump-prone ground in given geologic settings.

There are, of course, other ways to quantify these parameters. In addition, there are many more parameters that could be quantified and incorporated into a bump hazard index, e.g., roof and floor strength and stiffness as determined by physical property testing, proximity of units of influence to the coalbed, and the number of discrete beds as an indication of the massive nature of the strata. However, before increasing the complexity of the hazard index, the initial criteria are being evaluated by contrasting the predicted hazard level with actual experiences in different geographic locations that have a long history of bump activity.

BUMP-HAZARD ASSESSMENT CASE STUDIES

The bump hazard assessment criteria described above were applied to mine properties in the Pocahontas No. 4 Coalbed in McDowell County, WV, and the Pocahontas No. 3 Coalbed in Buchanan County, VA. The results of this effort are discussed in detail below.

POCAHONTAS NO. 4 COALBED STUDY

The study property in the Pocahontas No. 4 Coalbed in southern West Virginia was first developed in 1903 and ultimately included two mines covering approximately 47 km^2 (18 mi^2). Figure 1 shows the boundary of the mine property, the locations of the diamond coreholes used for the stratigraphic information contained in this paper, and the locations of the three core logs (A, B, and C) shown in figure 2. Also shown in figure 1 is the number of bump occurrences at various locations.

The study property has a long history of coal bumps. The first bumps were reported in the early 1930's. A series of powerful bumps, resulting in many fatalities and serious injuries, occurred from 1945 to 1952. This activity prompted management to aggressively pursue the development of mine designs and remediation techniques, including the successful "thin-pillar" mining method (Talman and Schroder, 1958), to alleviate the problem.

Figure 1
Study Area, Pocahontas No. 4 Coalbed, McDowell County, WV.

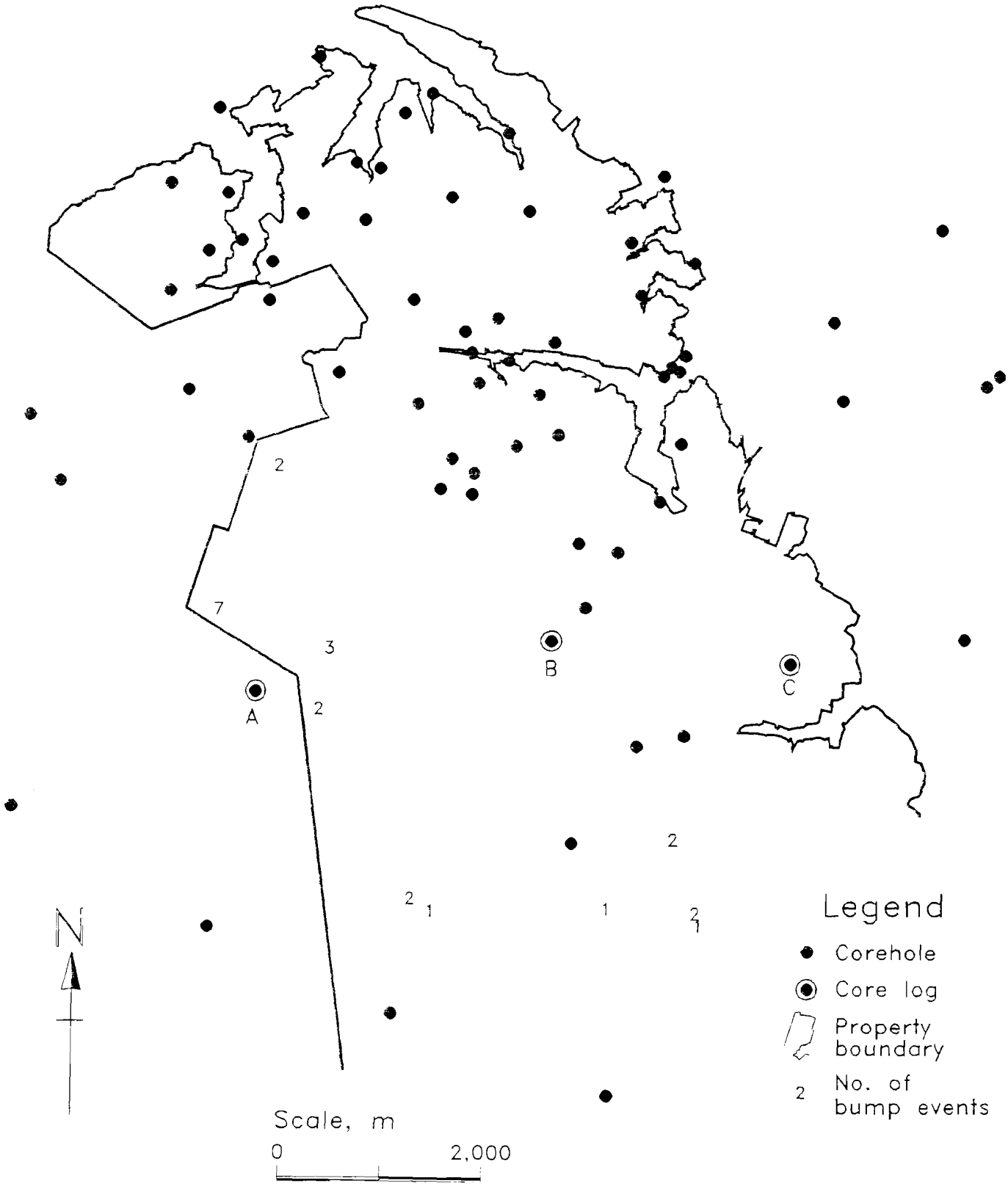

Figure 2
Core Logs A, B, and C, Pocahontas No. 4 Study Area.

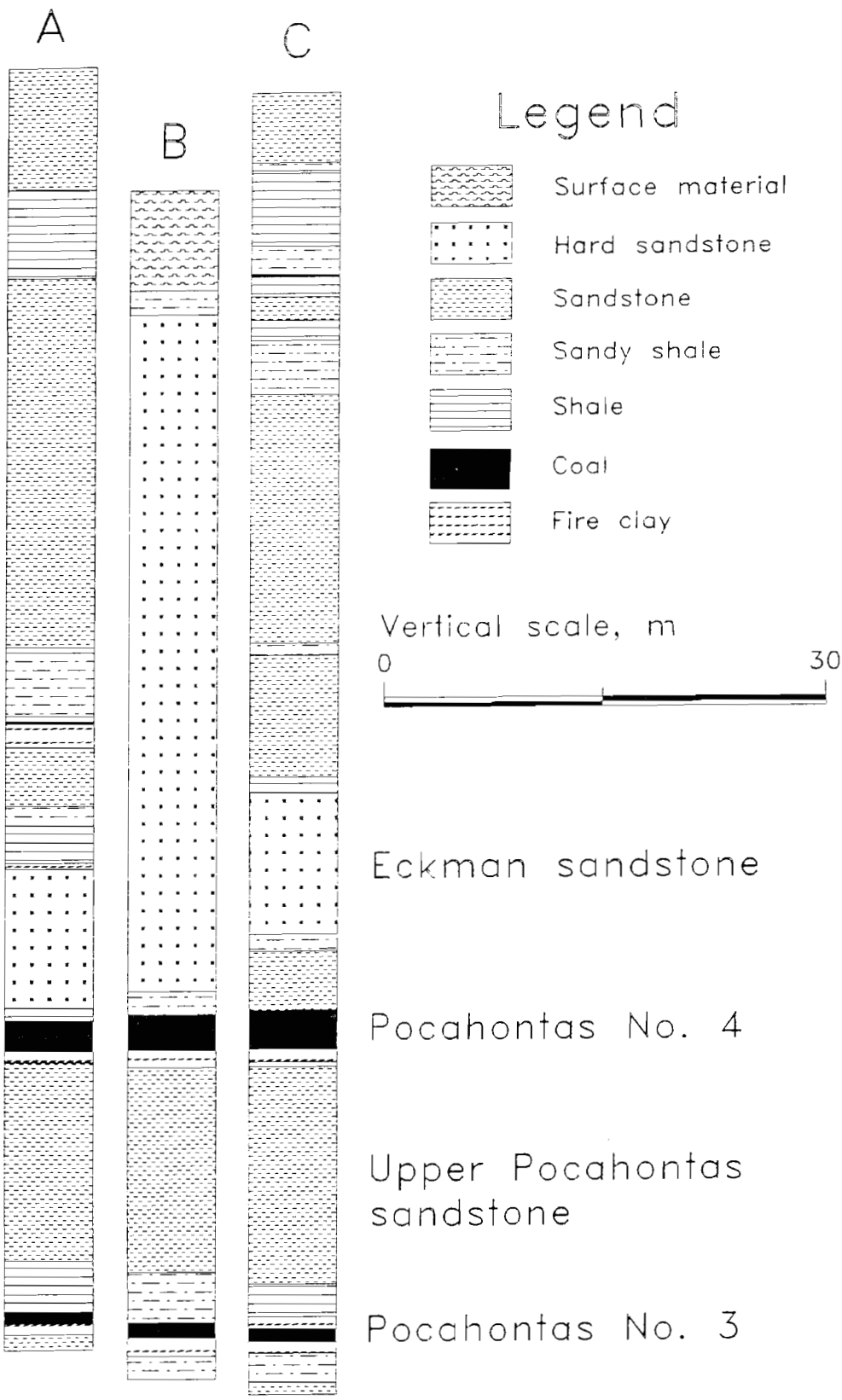

Geologic Setting

The entire minable extent of the Pocahontas No. 4 Coalbed lies within Wyoming and McDowell Counties of southern West Virginia (Hennen, 1915). Wyoming and McDowell Counties are in the Appalachian Plateau physiographic province, a dissected upland with a regional dip to the northwest of less than 20 m/km (110 ft/mi) that is locally interrupted by small, open folds that trend northeast-southwest (Rehbein and others, 1981).

Topography over the mines is rugged, with deep V-shaped valleys and up to 225 m (740 ft) of relief. The coalbed dips from the southeast to the northwest on the western limb of the Dry Fork anticline. The total change in coalbed elevation is approximately 210 m (690 ft) across the mines. From coalbed outcrop, overburden increases to more than 450 m (1,475 ft) under the peaks and ridges in the west and northwest portions of the mines.

The diamond drill core logs shown in figure 2 illustrate typical stratigraphic sequences across the property. The Pocahontas No. 4 Coalbed falls approximately in the middle of the Pocahontas Formation, a coal-bearing sequence of interbedded sandstone, siltstone, shale, and underclay. The coalbed averages about 2 m (7 ft) thick, but locally thickens to 3 m (10 ft) and thins to 0 m. Roof rock varies from a dark gray shale to a hard, stiff, brown micaceous sandstone. The brown micaceous sandstone varies in thickness from about 15 to 55 m (50 to 180 ft) over the mines and is locally interrupted by thin coal and shale interbeds. The mine floor consists of a 0- to 1.5-m (5-ft) thick shale or underclay that grades laterally to siltstone. Below that is the predominant underlying rock, a hard, stiff, fine- to medium-grained sandstone that ranges in thickness from 15 to 23 m (50 to 75 ft) (Hennen, 1915; England, 1974).

Application of Hazard Criteria

The geologic data covering the study mines are from digitized topographic contours and 67 coreholes with known coordinates and collar elevations. Coalbed elevation, topographic data, and lithologic code groups for the roof and floor were modeled using the triangulation method into 150-m (500-ft) grids.

Overburden Index

The coalbed elevation grid was subtracted from the topographic grid to determine overburden thickness. Actual maximum overburden over the properties is 450 m (1,480 ft). Subtracting the 150 m (500 ft) of overburden required to generate bump conditions resulted in a 150- to 450-m (500- to 1480-ft) range of overburden values to be included in the index. These values were then divided by 3 to arrive at an index that ranged from 0 to 100. The resulting overburden index values are shown as four ranges in figure 3.

The significance of the structural change in coalbed elevation becomes evident when viewing the overburden index map (figure 3). Although the prominent topographic highs are to the south and southeast of the property where folded resistant sandstones crop out at the peak of the Dry Fork anticline, overburden thickness increases to the west and northwest due to the 210-m (690-ft) drop in coalbed elevation along the western limb of the anticline.

Roof-Strength Index

The roof-strength index was calculated as the percentage of sandstone within 10 m (33 ft) of the top of the coalbed. Figure 4 shows the range of index values corresponding to roof strength as contoured from the 150-m (500-ft) grid. Empirical and anecdotal evidence, along with accident reports from the U.S. Mine Safety and Health Administration, indicate that the presence of the brown micaceous sandstone immediately above the coalbed is a strong contributing factor to bumps on this property. The sandstone has a compressive strength of 167 MPa (24,200 psi) and a Young's modulus of 3.56×10^4 MPa (5.16×10^6 psi) (Campoli and others, 1989) and is identified in code group 1. This thick sandstone is widely distributed over the mine property, and the roof-strength index map is a good indicator of the proximity of the sandstone to the top of the coal.

Floor-Strength Index

Figure 5 shows the ranges of index values corresponding to floor strength. The floor-strength index was calculated as the percentage of sandstone within 3 m (10 ft) of the bottom of the coalbed. Based on the assumptions discussed in the section on "Bump-Prone Geology," the predominant underlying sandstone on this property meets the requirement of a strong floor rock to generate bump conditions, having a compressive strength of 150 MPa (21,900 psi), and a Young's modulus of 3.77×10^4 MPa (5.45×10^6 psi) (Campoli and others, 1989). It is identified in code group 1.

Figure 3
Overburden Index, Pocahontas No. 4 Coalbed Study Area.

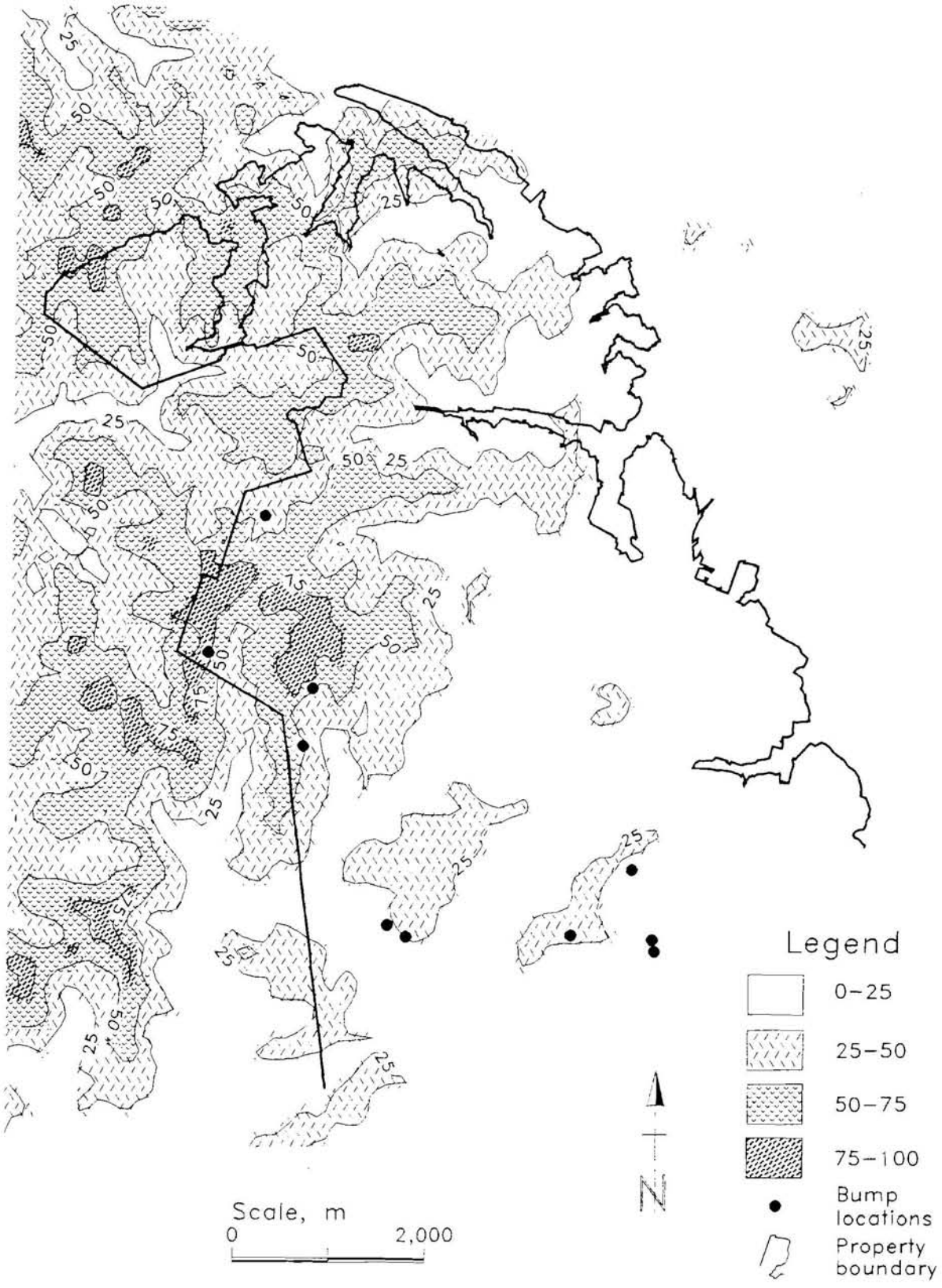

Figure 4
Roof Strength Index, Pocahontas No. 4 Coalbed Study Area.

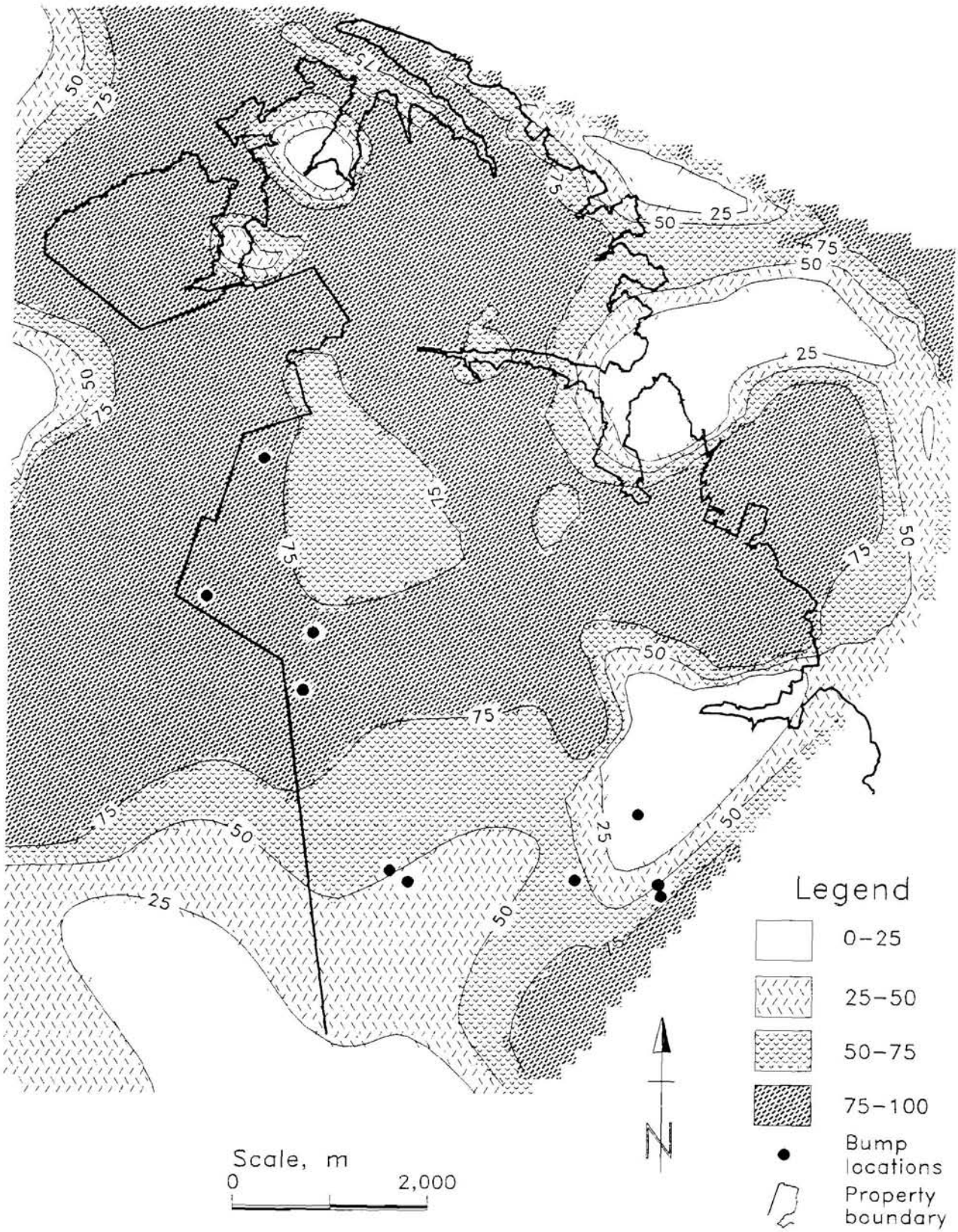

Figure 5
Floor Strength Index, Pocahontas No. 4 Coalbed Study Area.

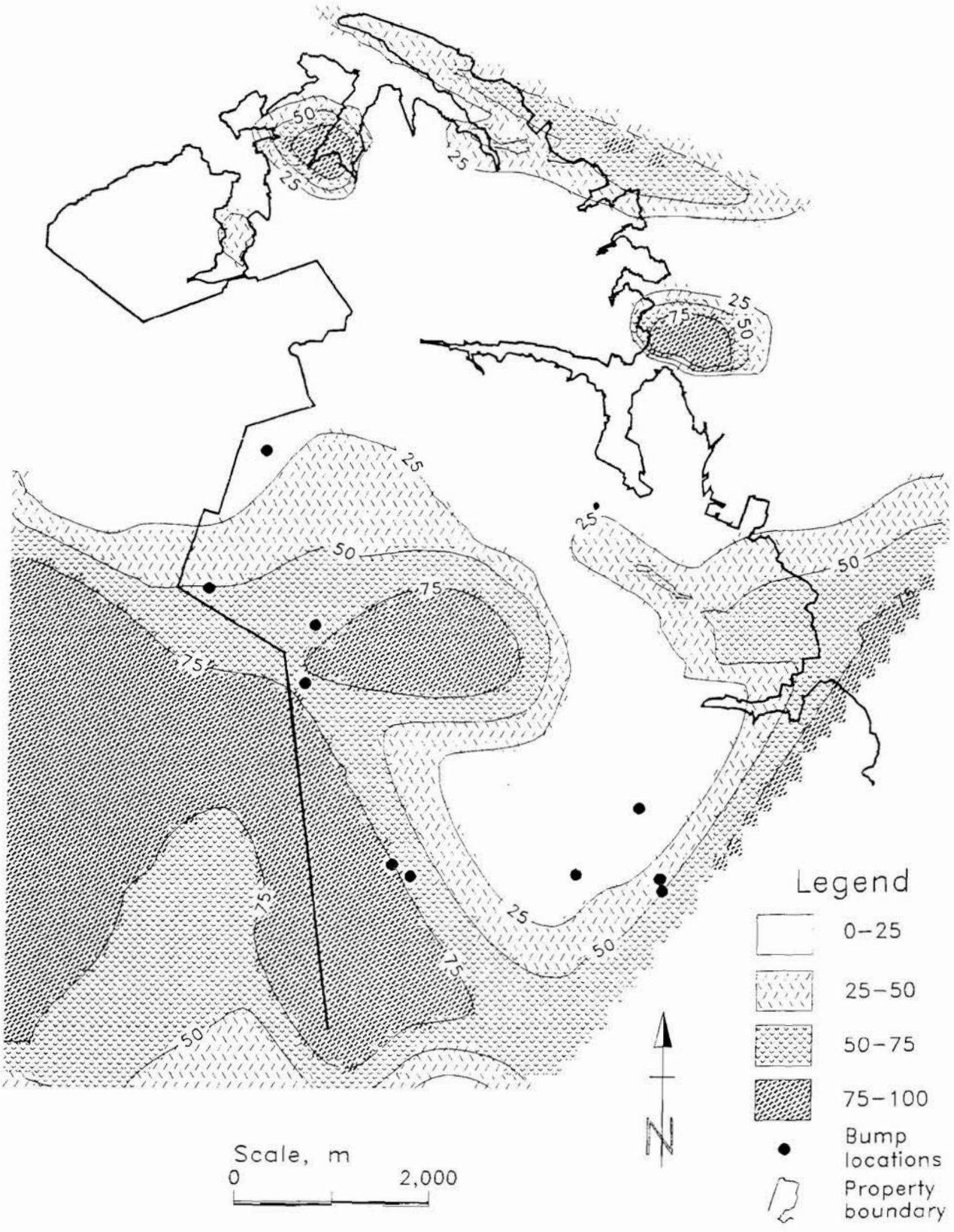

Assessment of Hazard Criteria and Bump-Hazard Index Map

The following paragraphs and table 1 summarize the information contained in the base map in figure 1 (which shows the number of bump events associated with each general bump location), the individual hazard criteria index maps (figures 3-5), and the combined bump-hazard index map (figure 6).

Large areas of the Pocahontas No. 4 study property fall into the lowest overburden index range (0 to 25), but that does not preclude the potential for bumps because most of these areas are under 150 to 225 m (500 to 745 ft) of overburden (figure 3). In fact, the historical locations of bump-prone areas shown on the map are all in areas of at least 185 m (600 ft) of overburden. While the number of bumps is fairly evenly distributed across the overburden index ranges, there is a strong correlation between increasing overburden index values and the number of bumps per square kilometer of index area mined (table 1).

The distribution of index values for high roof strength is much wider over the property (figure 4). This is a direct correlation to the persistent presence of the brown micaceous sandstone and is an indication of the proximity of the sandstone to the top of the coalbed. As shown in table 1, the distribution of the number of bump events shows a definite increase with increasing roof strength index values. However, the number of bumps per square kilometer of index range mined does not increase proportionately due to the large area of the property within the higher index ranges.

Areas of index values indicating high floor strength are less regularly distributed over the property (figure 5). It is common to have at least 1 m of underclay and shale directly beneath the coalbed on this property (see figure 2). The floor-strength index map, then, is a good indicator of the proximity of the hard sandstone to the bottom of the coalbed. As shown in table 1, the distribution of the number of bump events is not consistent with increasing floor-strength index values, although the greatest number occur in the 50 to 75 range, with a corresponding high ratio of bumps per square kilometer of index area mined.

Taken individually, there is a rough correlation between high index values and known bump locations in table 1. However, when the values for the three criteria are combined and averaged to create the bump-hazard index map (figure 6), there appears to be a stronger correlation. Table 1 shows that there is little correlation between the number of bumps per square kilometer of index area mined until the index range reaches 75 to 100, where the ratio increases to 25 to 1.

Although geologic conditions are important contributors to bumps, mining plans and practices are also strongly influential. Holland and Thomas (1954) analyzed 117 bumps and concluded that "most bumps are the result of improper mining methods and practices." Many early bumps at the study property were linked to unfavorable mining practices (Duckwall, c. 1952). In fact, improved mining practices have had a definite effect on the occurrence of bumps; the eventual development of the thin-pillar mining method in the northern half of the study area significantly alleviated bump problems. This area was included, though, in the evaluation of the bump hazard criteria in table 1. Also, the absence of bumps along the central corridor between the two mines where index values range from 25 to greater than 75 corresponds to the absence of retreat mining in extensive development mains and barriers between the mines. Thus, the absence of bumps in areas having high bump index values or the presence of bumps in areas having low bump index values may be the result of the effectiveness of the mining system rather than failure of the criteria to be a true indicator of bump hazard potential.

Table 1.—Number of bumps falling into each index range versus total area of range mined

Index range	Total area of index mined, km^2	Number of bumps within index range	Bumps per square kilometer of index area mined
Overburden:			
0-25	28.0	7	0.25
25-50	12.1	4	0.33
50-75	5.7	5	0.88
75-100	1.2	7	5.83
Roof strength:			
0-25	4.1	2	0.49
25-50	5.9	1	0.17
50-75	12.4	6	0.48
75-100	24.6	14	0.57
Floor strength:			
0-25	24.0	5	0.21
25-50	9.4	2	0.21
50-75	8.5	14	1.65
75-100	5.1	2	0.39
Bump hazard:			
0-25	7.0	2	0.29
25-50	27.7	7	0.25
50-75	11.9	4	0.34
75-100	0.4	10	25.0

Figure 6
Bump Hazard Index, Pocahontas No. 4 Coalbed Study Area.

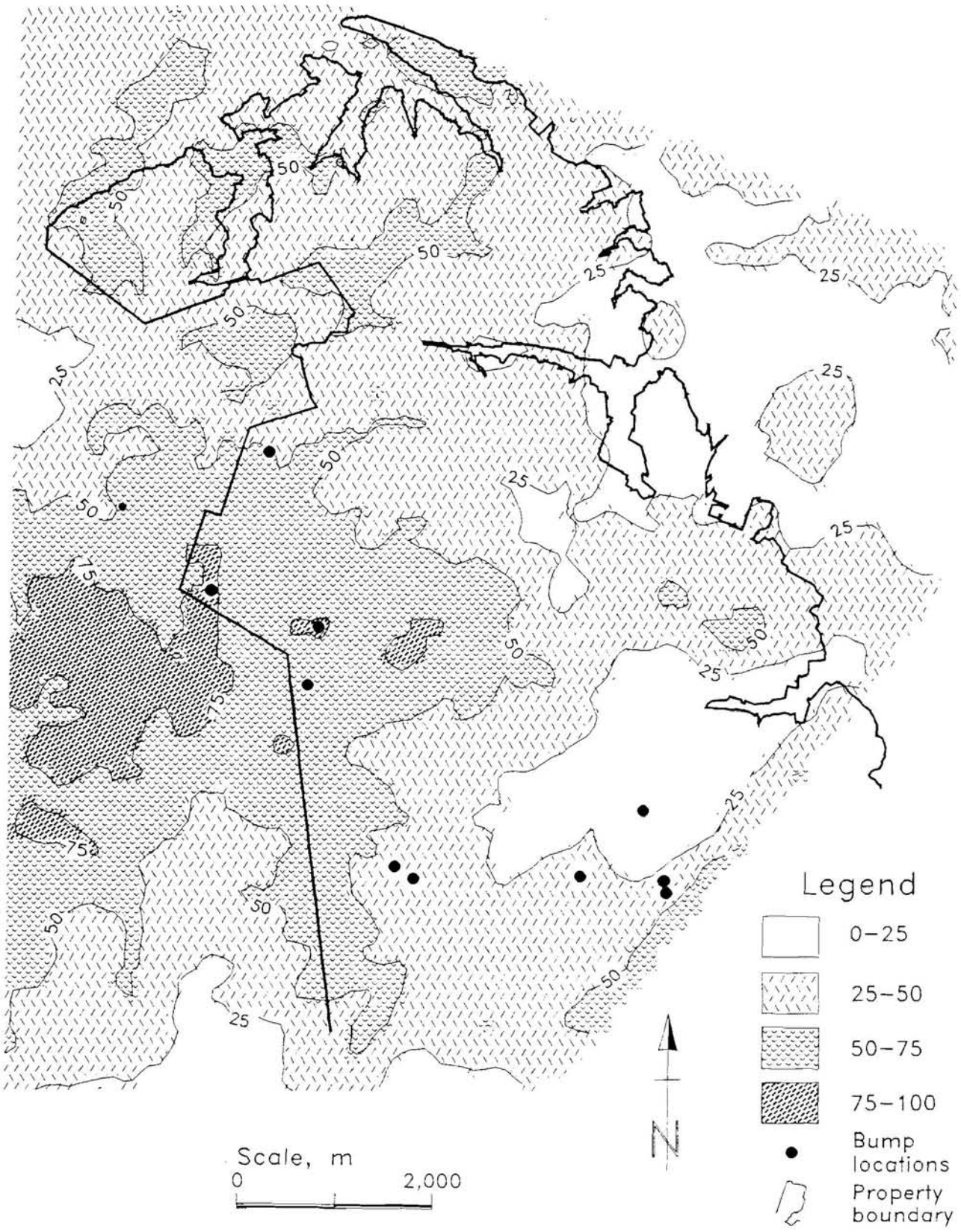

POCAHONTAS NO. 3 COALBED STUDY

The study site in the Pocahontas No. 3 Coalbed is located in a longwall mine in Buchanan County, VA. Figure 7 shows the mine property boundary, the extent of the mine workings at the time of data collection, the locations of the diamond coreholes used for stratigraphic information presented in this paper, and the locations of the three core logs (A, B, and C) shown in figure 8.

Geologic Setting

The study site lies within the Appalachian Plateau physiographic province. Topography over the property is rugged, with steeply sloped ridges, deep V-shaped valleys, and up to 475 m (1,555 ft) of relief. The coalbed dips from east-southeast to west-northwest. The total change in coalbed elevation is approximately 70 m (230 ft) across the mine. The Pocahontas No. 3 Coalbed does not crop out in the area. Overburden ranges from 300 m (985 ft) under the valleys to 778 m (2,550 ft) under the highest peaks and ridges.

The core logs shown in figure 8 illustrate typical stratigraphic sequences within 50 m (165 ft) above and 5 to 7 m (16 to 23 ft) below the coalbed, which averages about 1.7 m (5.6 ft) thick across the property. The Pocahontas No. 3 Coalbed falls near the bottom of the Pocahontas Formation. The Pocahontas Formation sequence in this area consists of interbedded light gray, fine- to medium-grained sandstones, medium to dark gray siltstones, some dark gray shale, and coal (Nolde and Mitchell, 1984).

The immediate roof rock [within 10 m (33 ft) of the top of the coalbed] varies from a highly bedded quartzarenite sandstone, to dark gray, bedded sandstone, to a very hard, dark gray massive sandy shale (siltstone), to dark gray shale. The sandy shale varies in thickness from 0 to 40 m (130 ft). Overlying the whole mine property is the quartzarenite sandstone that ranges in thickness from 40 to 120 m (130 to 395 ft). The distance from the top of the coalbed to the bottom of the quartzarenite is from 5 to 35 m (15 to 115 ft). The mine floor consists of a very competent siltstone and sandstone with shale streaks.

Application of Hazard Criteria

The geologic data covering the Pocahontas No. 3 study property were collected from 57 coreholes with known coordinates and collar elevations. U.S. Geological Survey digital elevation models (DEM's) were used as surface elevation data. Coalbed elevation data and lithologic code groups were modeled using the triangulation method into 30-m (100-ft) grids to match the DEM data.

Overburden Index

The coalbed elevation grid was subtracted from the DEM grid to determine overburden thickness. Actual maximum overburden over the property is 778 m (2,550 ft). Subtracting the 150 m (500 ft) necessary to initiate bump conditions resulted in 628 m (2,050 ft) of maximum effective overburden. These values were then divided by 6.28 to normalize the data to an index range from 0 to 100. The resulting overburden index ranges are shown in figure 9.

Roof Strength Index

The roof-strength index was calculated as the percentage of siltstone within 10 m (33 ft) of the top of the coalbed. Empirical evidence at the study property indicated that the siltstone immediate roof is the overlying rock type contributing most to the potential for coal bumps. The siltstone forms a smooth, widely jointed roof with little or no bed separation or evident sag. Unconfined compressive strengths of the siltstone range from 93.8 to 167.1 MPa (13,600 to 24,230 psi), and Young's modulus ranges from 2.6 to 5.3×10^4 MPa (3.8 to 7.7×10^6 psi) (Campoli and others, 1990). The overlying quartzarenite's unconfined compressive strength of 199.6 MPa (28,950 psi) is also very high (Campoli and others, 1990), but the thinly bedded nature of the sandstone results in good cavability where it is close to the coalbed, and in some areas it causes mine roof control problems resulting from excessive separation and sag. The percentage of siltstone is identified in code group 2; its distribution within 10 m (33 ft) of the top of the coalbed over the property is shown in figure 10.

Floor-Strength Index

The floor-strength index was calculated as the percentage of siltstone within 3 m (10 ft) of the bottom of the coalbed. Unconfined compressive strengths of the siltstone range from 95.8 to 123.6 MPa (13,900 to 17,920 psi) with an average Young's modulus of 4.8×10^4 MPa (6.9×10^6 psi) (Campoli and others, 1990). Floor strength throughout the mined portion of the property was observed to be high, with no evidence of floor heave or failure along pillar edges in advance of the longwall face (Gauna, 1992). The percentage of siltstone is again identified in code group 2. The distribution of the siltstone within 3 m (10 ft) of the bottom of the coalbed over the property is shown in figure 11.

Figure 7
Study Area, Pocahontas No. 3 Coalbed, Buchanan County, VA.

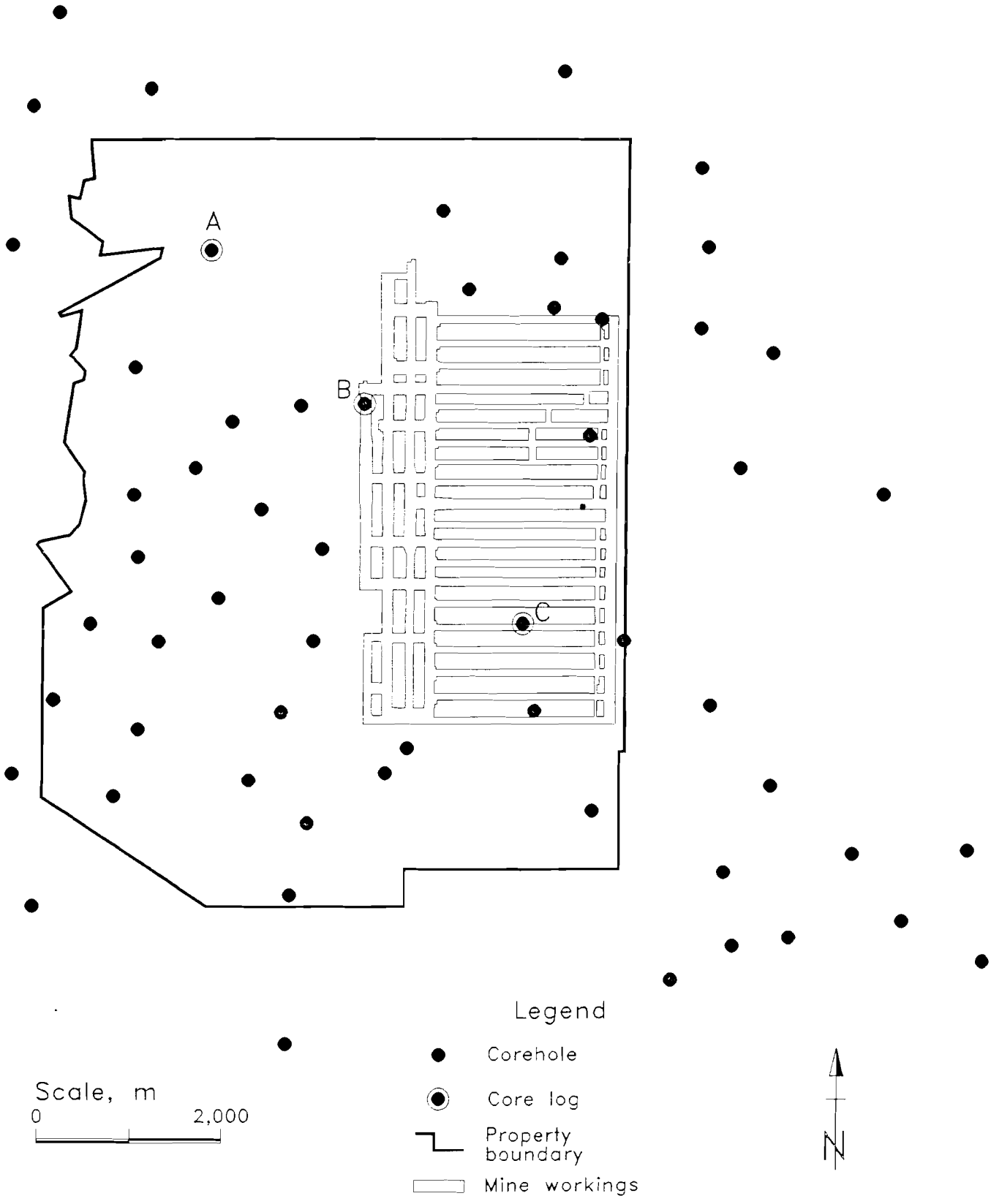

Figure 8
Core Logs A, B, and C, Pocahontas No. 3 Study Area.

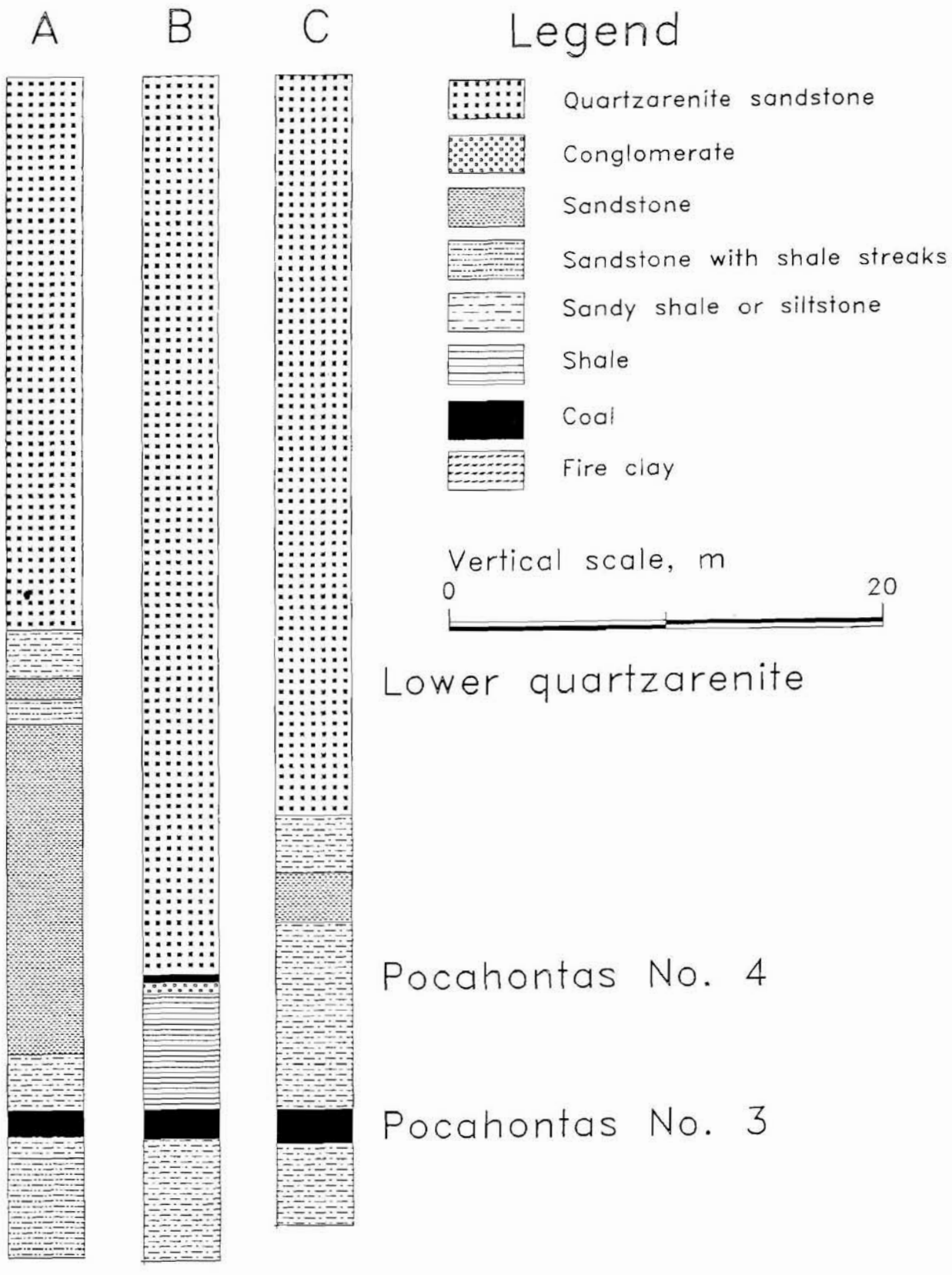

Figure 9
Overburden Index, Pocahontas No. 3 Coalbed Study Area.

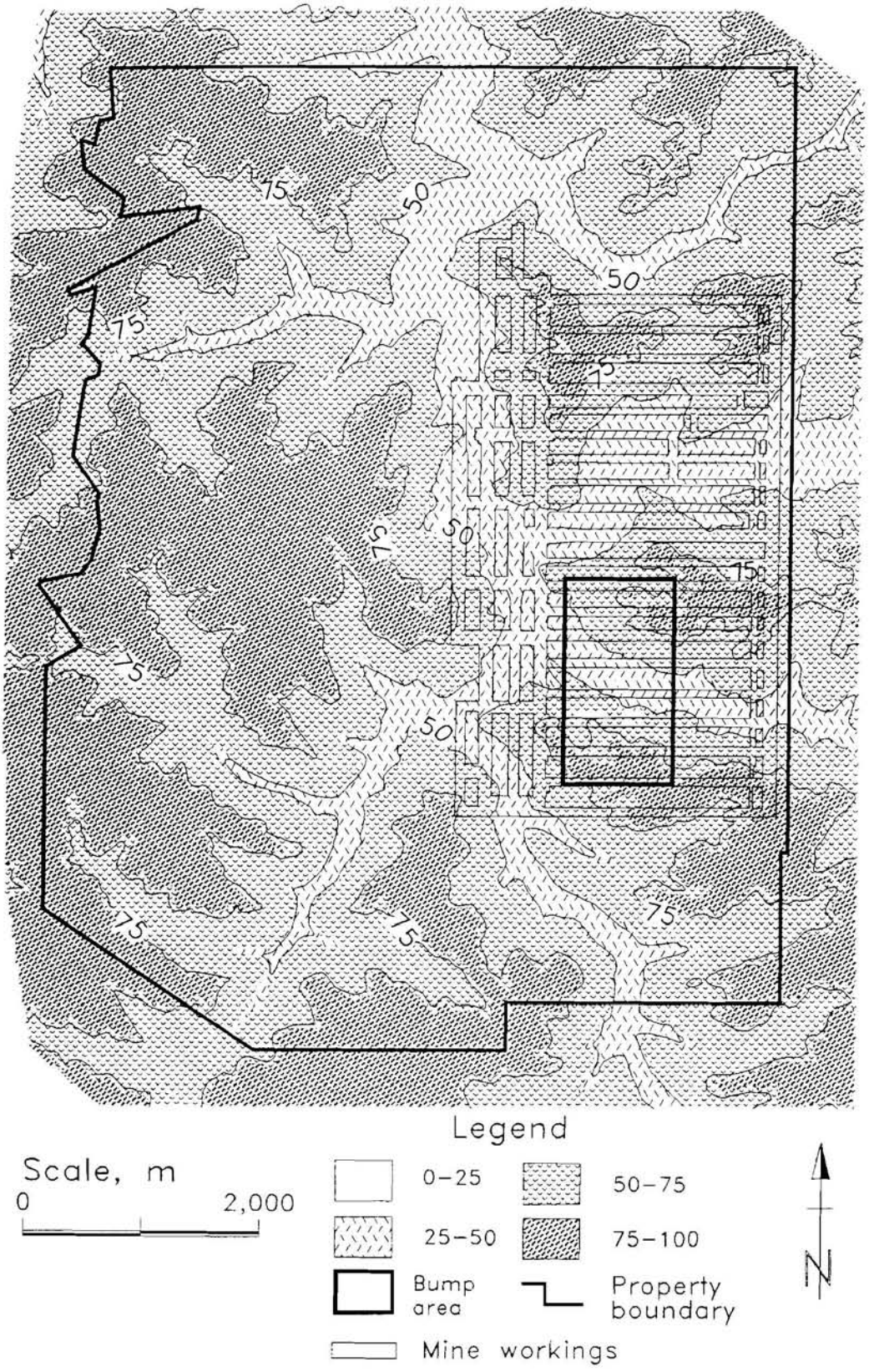

Figure 10
Roof Strength Index, Pocahontas No. 3 Coalbed Study Area.

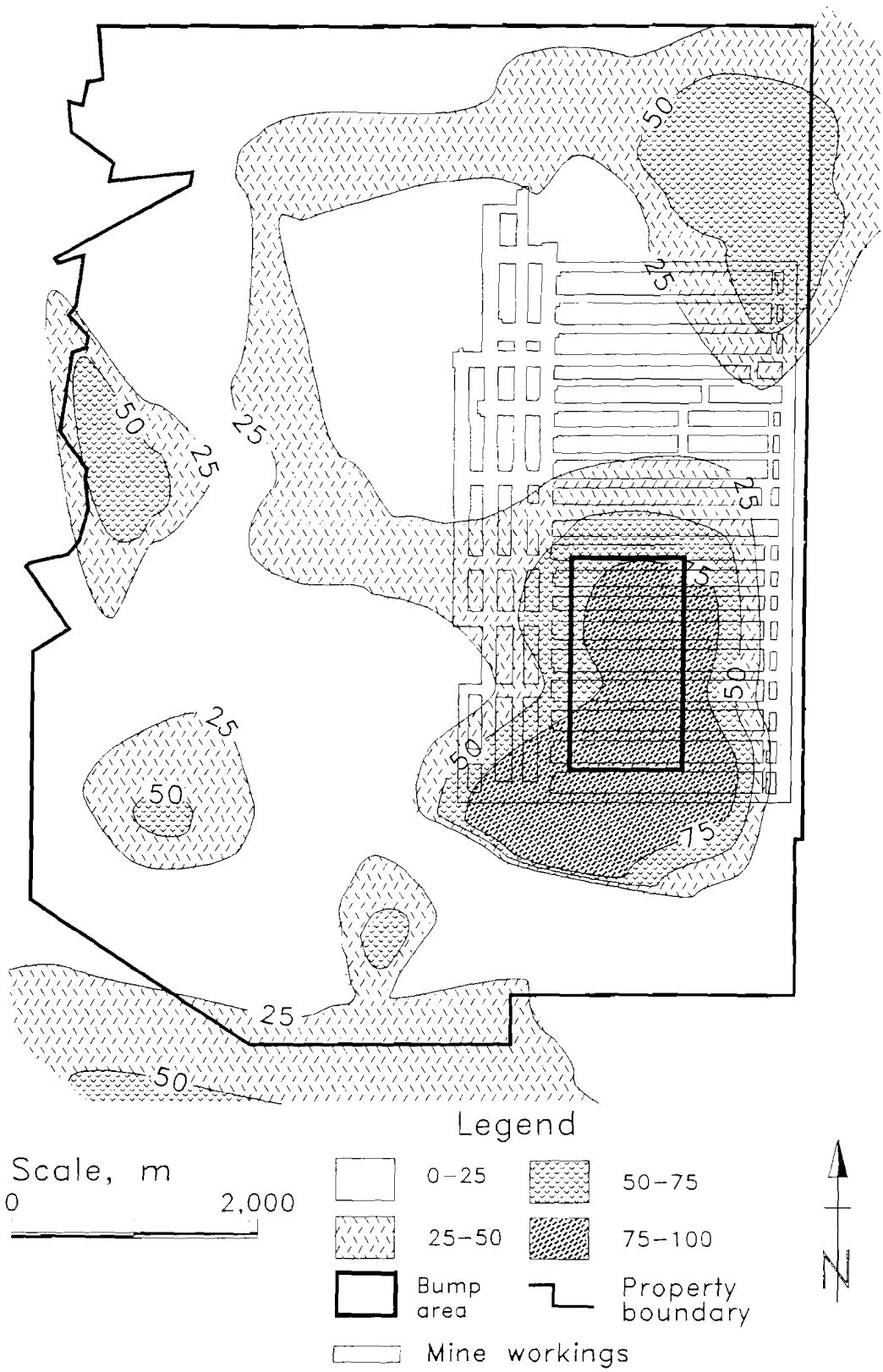

Figure 11
Floor Strength Index, Pocahontas No. 3 Coalbed Study Area.

Assessment of Hazard Criteria and Bump-Hazard Index Map

The significant amount of geologic data covering this property allowed detailed analysis of the geology, and current mining information enabled delineation of a specific area where bump conditions are present. The bump-prone area indicated on the maps has been documented in a previous USBM study (Campoli and others, 1990).

The depth of the Pocahontas No. 3 Coalbed precluded the presence of mine areas falling into the 0 to 25 range of the overburden index (figure 9). Essentially, the entire property is under sufficient overburden to satisfy the condition that deep overburden be present before bumps can be generated. In this case, the overburden criteria simply differentiate between deep versus deeper cover. Although the mine is in the Appalachian Plateau region where peak elevations are approximately equal, the presence of a major stream valley along the eastern half of the property, along with the 70-m (230-ft), east-to-west dip of the coalbed, results in a situation where the largest area of index values in the 75 to 100 range are in the western, unmined portion of the property. The full range of overburden index values lies within the outline of the bump-prone area.

The distribution of high roof-strength index values corresponds neatly with the outline of the bump-prone area (figure 10). The areas of low roof-strength values are areas where the quartzarenite sandstone lies near the top of the coalbed (as in core log B of figure 8) or where the dark gray shale is the predominant immediate roof rock.

Areas of high floor strengths are widely distributed over the mine (figure 11). This finding is consistent with the earlier observation that floor strength throughout the mined portion of the property is high, and there was no evidence of floor heave or failure along pillar edges.

Figure 12 shows the three bump hazard criteria when combined and averaged to form the bump-hazard index map. Correlation between the bump-prone area and areas of high bump-hazard index values is good. Although the northern half of the mine is in the 50 to 75 index range, no bumps have occurred. The relatively high values in this area are the result of the deep cover and a high floor-strength index. The quartzarenite sandstone near the top of the coalbed keeps these values out of the 75 to 100 bump hazard range and would seem to account for the lack of bumps. Figure 13 shows the bump-hazard index map with the areas of solid coal highlighted to reflect more clearly the mining sequence. Two longwalls operate in this mine. Mining began to both the north and south of the two central panel barriers and proceeded in opposite directions.

The panels to the north, to the extent of mining shown, did not experience any bumping of the tailgate pillars or longwall face. In fact, as noted previously, the quartzarenite sandstone is close to the top of the coalbed to the north, and roof stability problems developed in both the headgates and tailgates during extraction of the panels.

Bumping to the south began in the tailgate and at the tailgate side of the longwall face of the second panel and continued with mining of subsequent panels within the area outlined in figures 12 and 13. These events prompted the study by Campoli and others (1990) wherein gate entry design changes eventually controlled bumping at the working face. The tailgate pillars continued to bump behind the face in the gob area, where they posed no danger to miners or equipment.

SUMMARY AND CONCLUSIONS

This paper presents an overview of USBM work in developing a method of assessing coal-bump hazards using basic geologic information. An engineering software package was used to apply a set of geologic criteria to assess bump-proneness and produce hazard maps. The criteria incorporate parameters to reflect overburden thickness and the strength and stiffness of the strata surrounding the coalbed. The roof- and floor-strength indices are a reflection of the percentage of the rock type in the first 10 m (33 ft) of roof and 3 m (10 ft) of floor most directly associated with previous bumps in the given geologic setting.

The bump hazard assessment criteria were applied to mine properties in the Pocahontas No. 4 Coalbed in McDowell County, WV, and the Pocahontas No. 3 Coalbed in Buchanan County, VA. The hazard assessment generally agreed with the information available to document previous bumps on the two properties.

Bump data covering the Pocahontas No. 4 Coalbed study property consisted of historic occurrences that were intense enough to cause fatalities, serious injury, or significant disruption or alteration of existing mining plans and were documented in accident or internal reports.

Figure 12
Bump Hazard Index, Pocahontas No. 3 Coalbed Study Area.

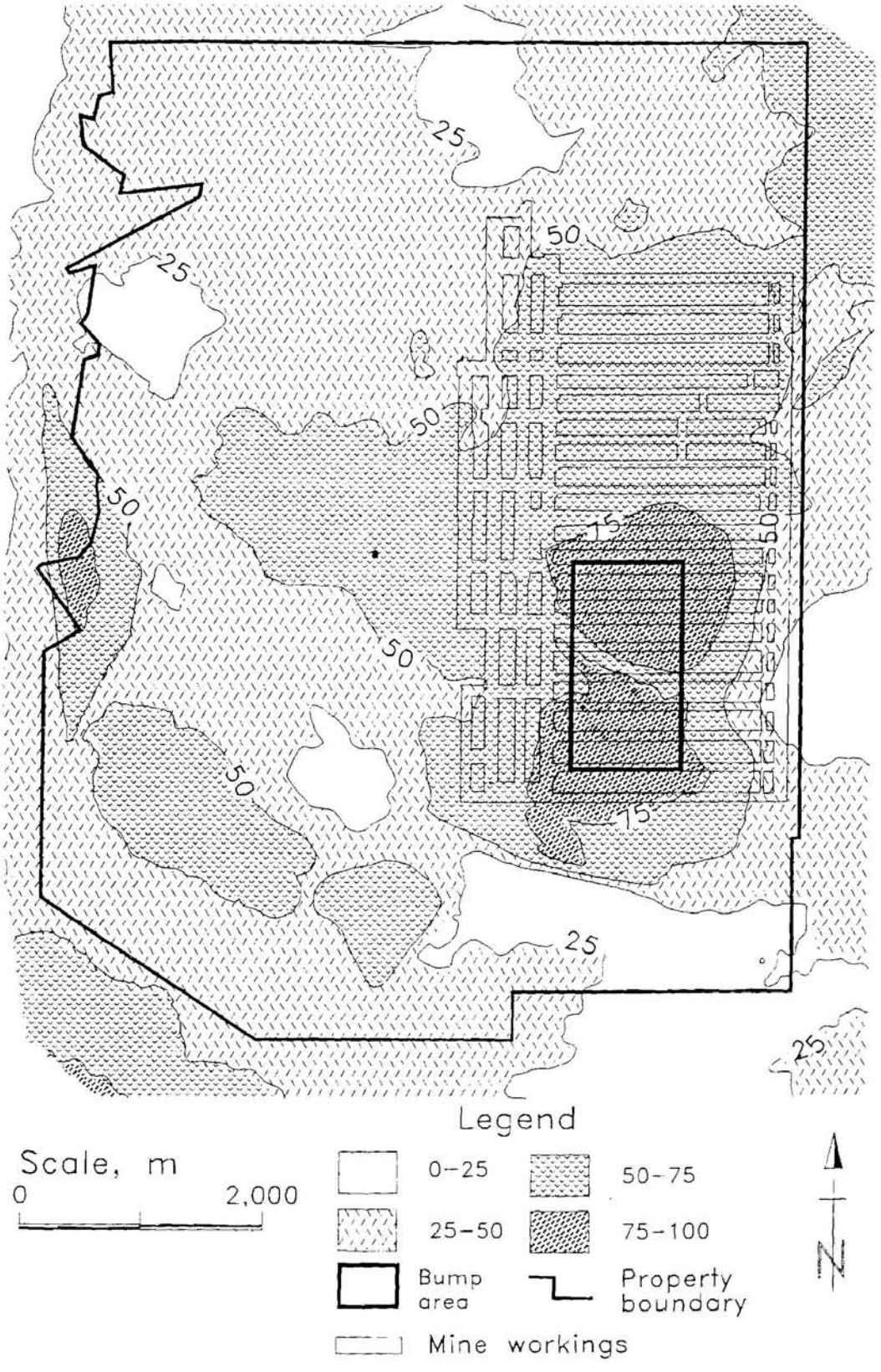

Figure 13
Bump Index Depicting Solid Coal Areas, Pocahontas No. 3 Coalbed Study Area.

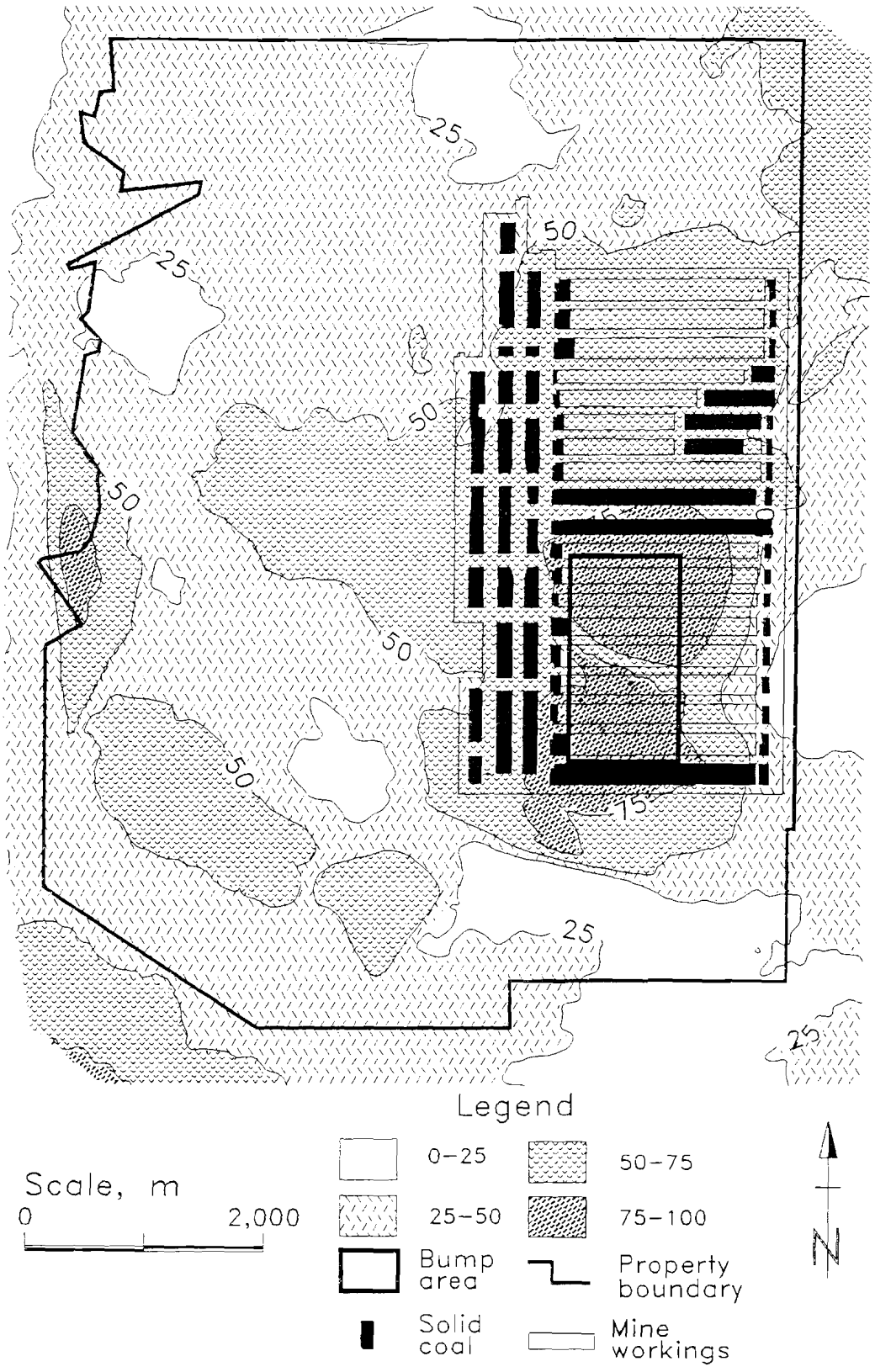

Therefore, generalizations about entire areas that could be considered bump prone were not attempted, and correlation to the bump-hazard index map was based on these isolated events. Comparing the number of events in each index range versus the mined area within that range resulted in reasonable agreement between the criteria and bump occurrences.

Data covering the Pocahontas No. 3 Coalbed study property are more current and delineate a specific area where bump conditions are present. Correlation between the highest bump-hazard index values on the map and the outlined area of known bump conditions in the mine is good. Although the northern half of the mine is in the 50 to 75 index range, no bumps have occurred. The relatively high values in this area are the result of the deep cover and a high floor-strength index. The quartzarenite sandstone near the top of the coalbed keeps these values out of the 75 to 100 bump hazard range and would seem to account for the lack of bumps.

Studies of these two properties showed that the development of universal bump hazard criteria based on predetermined lithologic units and applied generically is impractical. However, identification of the rock types most directly related to bumping in a given mining environment and the availability of good corehole data and coverage greatly increase the usefulness of this type of assessment. In addition, although geologic conditions are important contributors to bumps, mining plans and practices are also strongly influential. Thus, the absence of bumps in areas having high bump index values or the presence of bumps in areas having low bump index values may be the result of the effectiveness of the mining system rather than failure of the criteria to be a true indicator of bump hazard potential. As the database of bump-prone regions to which the geologic criteria are applied is broadened, the USBM will continue to develop and improve the criteria to further delineate bump-prone geologic conditions.

REFERENCES

Campoli, A. A. Bump Control Design Strategy for Room-and-Pillar Coal Mining. SME preprint 94-42, 1994, 9 pp.

Campoli, A. A., T. M. Barton, F. C. Van Dyke, and M. Gauna. Mitigating Destructive Longwall Bumps Through Conventional Gate Entry Design. USBM RI 9325, 1990, 38 pp.

Campoli, A. A., and K. Heasley. Coal Mine Bump Research: Providing Tools for Rational Longwall Design. Paper in Proceedings of the 23rd International Conference of Safety in Mines Research Institutes, comp. by E. T. Wallace and T. H. Koslosky (Washington, DC, Sept. 11-15, 1989). USBM OFR 27-89, pp. 666-676; NTIS: PB 89-225262/AS.

Campoli, A. A., C. A. Kertis, and C. A. Goode. Coal Mine Bumps: Five Case Studies in the Eastern United States. USBM IC 9149, 1987, 34 pp.

Campoli, A. A., D. C. Oyler, and F. E. Chase. Performance of a Novel Bump Control Pillar Extracting Technique During Room-and-Pillar Retreat Coal Mining. USBM RI 9240, 1989, 40 pp.

Duckwall, A. E. History and Present Concepts of Mountain Bumps in the Gary District. U.S. Steel Coal Co., c. 1952, 37 pp.; available from G. P. Sames, USBM Pittsburgh Research Center, Pittsburgh, PA.

England, K. J. Sandstone Distribution Patterns in the Pocahontas Formation of Southwest Virginia and Southern West Virginia. Paper in Carboniferous of the Southeastern United States, ed. by G. Briggs. Geol. Soc. Am. Spec. Paper 148, 1974, pp. 31-45.

Ferm, J. C., and G. A. Weisenfluh. Cored Rocks of the Southern Appalachian Coalfields. Dep. of Geol., Univ. KY, 1981, 93 pp.

Gauna, M. Coal Pillar Design for Deep Conditions: An Operational Approach. Paper in Proceedings of the Workshop on Coal Pillar Mechanics and Design, comp. by A. T. Iannachione, C. Mark, R. C. Repsher, R. J. Tuchman, and C. C. Jones, (Santa Fe, NM, June 7, 1992). USBM IC 9315, 1992, pp. 214-224.

Goode, C. A., A. Zona, and A. A. Campoli. Controlling Coal Mine Bumps. Coal Min., v. 21, No. 10, Oct. 1984, pp. 48-53.

Hennen, R. V. County Report: Wyoming and McDowell Counties. WV Geol. Surv., 1915, 783 pp.

Holland, C. T., and E. Thomas. Coal-Mine Bumps: Some Aspects of Occurrence, Cause, and Control. USBM Bull. 535, 1954, 37 pp.

Iannacchione, A. T., and M. J. DeMarco. Optimum Mine Designs To Minimize Coal Bumps: A Review of Past and Present U.S. Practices. Ch. 24 in New Technology in Mining Health and Safety. Soc. Min. Eng., 1992, pp. 235-247.

Kidybinski, A. Control of High Stresses and Rock Bursts in Mines. Paper in UN Symposium on World Coal Prospects, Katowice, Poland. Oct. 1979, v. 5, pp. 302-328.

Nolde, J. E., and M. L. Mitchell. Geology of the Prater and Vansant Quadrangles, Virginia. VA Div. of Min. Res., Publ. 52, 1984, 28 pp.

Peperakis, J. Mountain Bumps at the Sunnyside Mines. Trans. Soc. Min. Eng. AIME, v. 211, Sept. 1958, pp. 982-986.

Rehbein, E. A., C. D. Douglas, and R. Mullennex. No. 3 Pocahontas Coal in Southern West Virginia—Resources and Depositional Trends. WV Geol. and Econ. Surv. Bull. B-38, 1981, 41 pp.

Rice, G. S. Bumps in Coal Mines of the Cumberland Field, Kentucky and Virginia—Causes and Remedy. USBM RI 3267, 1935, 36 pp.

Talman, W. G., and J. L. Schroder, Jr. Control of Mountain Bumps in the Pocahontas No. 4 Seam. Trans. Soc. Min. Eng. AIME, 1958, pp. 888-891.

Watts, A. C. An Unusual Bounce Condition. Coal Age, v. 14, No. 23, Dec. 1918, pp. 1028-1030.

MAPPING STRESS CHANGES WITH MICROSEISMICS FOR GROUND CONTROL DURING LONGWALL MINING

By P. E. Wilson[1] and R. O. Kneisley[2]

ABSTRACT

Safe and efficient coal mining depends on the rapid identification of hazards that can develop ahead of a mechanized longwall face. The U.S. Bureau of Mines is committed to improving the ability of the mining industry to detect ground control hazards through novel technologies. One of these technologies utilizes microseismic monitoring and analysis to determine stress changes in a mine that might lead to hazardous conditions.

This paper summarizes the results of field studies conducted over several years in four underground coal mines. Microseismic information was collected using geophone arrays situated in the gate road entries of the producing longwalls. Typically, signals were processed to determine source locations and intensities, which were then mapped in relation to longwall coordinates. Frequency and energy distributions of microseismic events were calculated in relation to spatial coordinates and were also determined relative to face position. These distributions show that activity changed with distance from the face, across the panel, and in the support pillars as mining progressed. The data were also compared to concurrent shield and pillar pressure monitoring results and demonstrate the potential of microseismic monitoring to indicate stress changes over a larger area than normally can be examined using conventional techniques.

INTRODUCTION

Sudden, catastrophic failures of a coal seam and/or adjacent strata are a major hazard at a number of underground coal mines in the United States. Greatly improved extraction methods and the pursuit of quality coal at increasing depths have contributed to the isolated, high-stress conditions that generate bumps or bursts. It is necessary to manage stress distributions near active mining areas effectively if the lethal and adverse economic aspects of bumps are to be mitigated. Failure to meet these needs will result in escalating personnel costs in terms of injury and death and economic costs in terms of loss of equipment and regulatory shutdown or suspension of mining. Ultimately, a company may be forced to close the operation, potentially sterilizing minable reserves and seriously affecting the local economy.

The U.S. Bureau of Mines (USBM) has been a leader nationally and internationally in the effort to develop methods to warn of impending ground failures. Part of this effort is aimed toward developing technology that will permit mine operators to better implement effective strata control in highly stressed ground. Dramatic advances in the field of digital computing have led to a resurgence in the use of microseismic monitoring, a method first developed by the USBM in the 1930's (*1-2*),[3] as a means of inferring how mine strata respond to the stresses generated by mining.

Traditionally, in-mine stress-state information is collected using quasistatic methods, such as analyses of pressure cell loading, convergence measurements, and the yield of cuttings while drilling boreholes. Such techniques are

[1]Research physicist.
[2]Mining engineer.
Denver Research Center, U.S. Bureau of Mines, Denver, CO.

[3]Italic numbers in parentheses refer to items in the list of references preceding the appendix at the end of this paper.

usually difficult or expensive to use and only indicate stress at a few discrete locations. By contrast, the acoustic waves generated by microseismic events are detectable throughout most of a mine through the use of sensors that can be attached to any rock surface. Mapping locations and intensities of microseismic events gives dynamic information about how the rock is responding to changes in stress conditions.

A microseismic event is a relatively low-energy acoustic wave produced within a rock mass in response to stress. The stress response can be fault or crack activation, ground motion, and/or slippage along a rock interface, all of which produce an elastic wave that radiates through the ground in all directions. Geophones, which are instruments capable of measuring minute ground motions, are attached to the rock and allow the microseismic wave to be measured. An array of geophones installed around an area enables the detection of a microseismic wave at different times, depending on the distance of each geophone from the source. From an analysis of the time differences observed among arrivals of a wave at each geophone and knowledge of the seismic velocity structure, the point of origin of the microseismic event may be determined. Other important information can also be obtained, such as the amount of energy released, the spectral content of the wave, and the focal mechanism of the event.

Laboratory studies on rock behavior under load indicate that microseismic activity increases as failure is approached (*3*). However, there is some controversy as to what kind of behavior is a precursor to failure under actual mining conditions. Some reports state that activity increases dramatically before failure (*4*), but many researchers believe a high rate of activity with a dramatic decrease immediately before failure is the most reliable indicator (*2, 5*). Additional research is necessary to better characterize the relationship between microseismic activity and failure in underground coal mines.

This paper will present examples of USBM research illustrating the application of microseismic monitoring to the evaluation of ground conditions in underground longwall coal mines. These examples will draw upon data from four mines to show the similarities and differences in microseismic activity among the mines. One example will show that microseismic activity can continue along the longwall face for at least 2 days after mining has halted. Results from another study will be presented showing close parallels between the energy released by microseismic events occurring in zones a fixed distance from the face and stress profiles from numerical models. Evidence will be presented showing that areas of little or no microseismic activity within zones of high activity may be the site of later bumps and bursts. Another analysis will show that pillar pressure measurements correlate well with the energy released by microseismic events occurring in the area of the pillar. Large-energy microseismic events will also be compared over time with shield pressures. This analysis will indicate that a space-time correlation may exist between the advance of the face in the tailgate and the occurrence of large microseismic events.

MINING-INDUCED MICROSEISMIC BEHAVIOR

Data from three of the four mines were collected using a digital microseismic monitoring system developed by the USBM (*6-7*). Velocity gauge geophones were installed in the gate roads of an operating longwall panel, and cables were run to carry the signals to an instrumentation site in the mains. Signal-conditioning equipment and a computer workstation with an integrated analog-to-digital converter that captured and processed the data were placed at the instrumentation site. All sensors, cables, and equipment were constructed so that a permissibility research permit could be obtained from the Mine Safety and Health Administration (MSHA).

EXAMPLE 1—PERSISTENCE OF MICROSEISMIC ACTIVITY

During a 16-month period between 1989 and 1990, the USBM had a digitally based data acquisition system installed in a coal mine in central Utah. This mine had a history of bumping along the face and floor heaving in the tailgates. Mining was conducted using a retreating longwall with a two-entry yield pillar gate road system. The coal seam was under 488 m of cover, and the panel was 183 m wide. There were no ground failures of significance while the study took place; however, production was low during that time for economic reasons. The panel was mined only 3 to 4.5 m during one shift a day. Under normal conditions, the face was retreated 10 to 15 m per shift. However, it was found that even a small amount of mining could generate a significant amount of microseismic activity that could persist for days.

Figure 1*A* shows typical microseismic activity recorded over a 24-h period during a mining day. Mining was conducted during one mid-day shift. Face retreat averaged 3.5 m. More than 800 locatable events were recorded, with the majority being located in a band along the face and from the headgate almost to the tailgate to a depth into the panel of 30 m. This band extended through the headgate pillars into unmined coal. There was some scattered activity far into the panel and in the gob.

The locations of events generated after mining had been halted for 8 to 32 h are displayed in figure 1*B*; events

Figure 1
Postmining Persistence of Microseismic Activity.

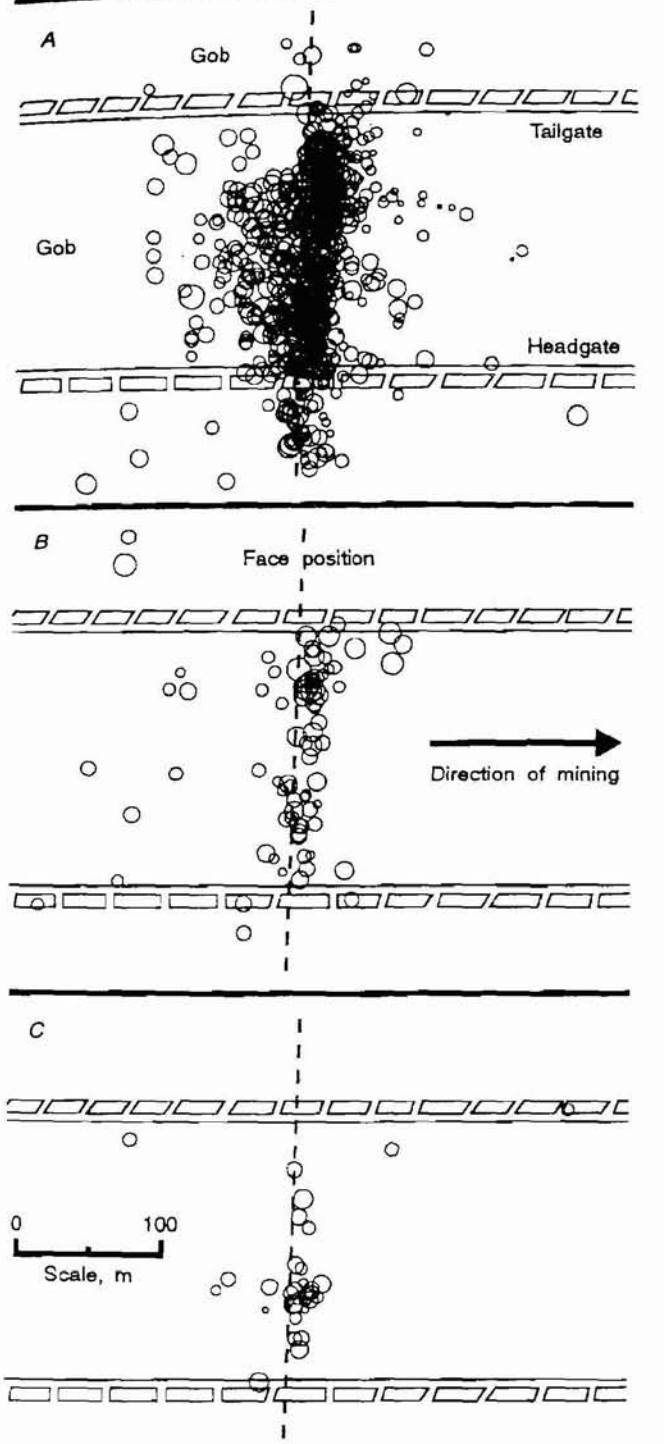

Microseismic event location maps for three time periods. *A*, 24-h period during mining day; *B*, 8 to 32 h after mining was halted; *C*, 32 to 56 h after mining was halted. Sizes of the circles representing event locations are proportional to event energy. Average face positions are marked with broken lines.

occurring 32 to 56 h after mining ceased are shown in figure 1*C*. The number of locatable events recorded during the first day after no mining (figure 1*B*) is less than the number recorded while mining (figure 1*A*) by a factor of 10. The second day of no mining (figure 1*C*) shows a further reduction in the number of located events. The localized clustering of activity into bands along the face is evident for both time periods, showing that equilibrium had not been reached and that the face was still responding to mining-induced stress for at least 2 days after mining stopped.

EXAMPLE 2—BUMPS, BURSTS, AND MICROSEISMIC QUIET ZONES

In a USBM report, Kneisley (*8*) examines microseismic activity associated with both face bumps and floor bursts in a deep coal mine in western Colorado. This mine employed an advancing longwall mining method under more than 900 m of overburden. Face length was 270 m, and there were other active mine workings 120 m above the panel. During the study period, several coal bumps and floor bursts occurred.

Since this study was conducted in 1983, the equipment used to record microseismic activity, was an analog predecessor to the digital systems currently used. This system was adequate for determining arrival time differences at the geophones, but no intensity determinations were made. Locations were calculated using the GBLK method (*2*), with a grid spacing of 15 m. The number of locatable microseismic events recorded ranged from less than 5 to nearly 100 in a day (figure 2). Most events were located at or inby the face, with a distribution that was generally uniform across the panel but sharply reduced near the gate roads.

Based on this report, it was concluded that bumps and floor bursts occur within areas of microseismic "calm," i.e., localized zones of little or no activity. If the premise that microseismic events are generated when rock fails in response to stress is accepted, then these zones represent areas that are not yielding, but are storing strain energy that may be suddenly and violently released. While not all areas characterized by a lack of microseismic events later failed, during the course of the study all documented failures occurred within these calm zones.

Examples of this behavior are shown in figures 3 and 4. In these figures, the size of the circles representing microseismic events indicates location error and not intensity. Also, only events in the failure areas are shown. Figure 3 shows activity in the vicinity of three face bumps. It can be seen that recorded microseismic events occurred outside of the failure areas associated with each bump, and that the areas that failed had been essentially quiet. Figure 4 is a map of microseismic activity relative to a large tailgate floor burst. Overall activity had been

increasing preceding the burst, but the area of eventual failure had been dormant.

EXAMPLE 3—MICROSEISMIC ACTIVITY AND PANEL STRESS

Another experiment was conducted at a coal mine in northwestern Colorado in which microseismic data were collected while pressures on selected shields and tailgate pillars were simultaneously recorded. The panel was 192 m wide, under 330 m of cover, and customarily retreated at 10 m per shift. Usually only one shift was worked per day, but on some days mining was performed over two consecutive shifts. Figure 5 shows typical microseismic event locations on days with two mining shifts, one mining shift, and no mining. Activity was usually centered along the face, with greater concentrations toward the gate roads. Microseismic activity in the headgate pillars always lagged activity at the face by at least 30 m. The number of locatable events collected during a 24-h period was between 300 and 400 on one-shift mining days and rose to between 800 and 1,000 on days when mining was conducted for two consecutive shifts. The number of events was substantially less on days when there was no mining.

Figure 2
Microseismic Event Rate and Bump and Burst Occurrence.

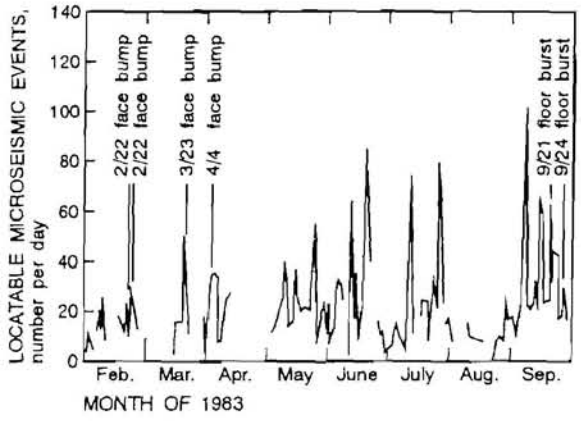

Daily locatable microseismic event rate for the study period, with the time of occurrence of face bumps and floor bursts marked.

Figure 3
Microseismic Event Locations and Face Bump Zones.

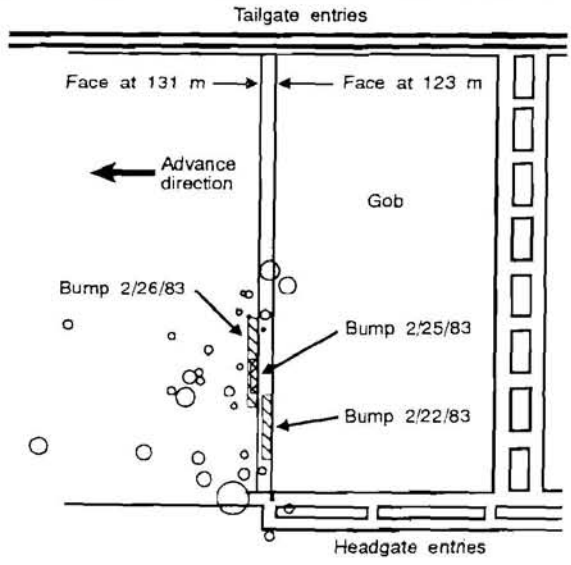

Microseismic event locations mapped in relation to failure zones associated with three face bumps. Sizes of the location circles are proportional to location error.

Microseismic activity was analyzed in another way that produced more insight into the behavior of the rock at this mine. Full waveforms were collected for most events; thus, estimates could be made of the amount of energy necessary to produce each microseismic event. Distributions of these source energies were made by overlaying a two-dimensional grid on the panel map and summing the source energies of events whose locations fell within each accumulation grid cell. These distributions were made both with the grid fixed in space and moving with the face.

Mine stresses had been modeled using the MULSIM/PC computer program and had been found to be in good agreement with field observations (*9*). Microseismic source energy distributions determined using a grid that moved with the face closely paralleled stress profiles obtained from the numerical model analyses. Figure 6 shows numerical modeling stress profiles and cumulative source energy distributions across the panel and pillars. The grid cell size for energy accumulation was 15 m.

Figure 6*A-B* contains graphs of the microseismic energy distribution and modelled stress profiles for a position 44 m ahead of the face. The numerical analysis predicted little change in stress in the headgate pillars as calculated from models for development and mining. The models indicated that panel stresses should increase closer to the tailgate and should be significantly higher in the tailgate pillars. The microseismic energy distribution exhibited similar behavior; little energy was released in the headgate pillars and headgate panel side, but microseismic energy values were greater near the tailgate. Microseismic energy was even greater in the large tailgate pillars, paralleling the stress profile. The only divergence in these graphs is in the small tailgate yield pillars where the microseismic energy was minimal, but the MULSIM results, calculated using linear elastic models with no simulated pillar yielding, indicated that stress should have increased.

Figure 6*C-D* shows similar graphs of the microseismic energy distribution and modelled stress profiles for a

Figure 4
Microseismic Event Locations and Floor Burst Zone.

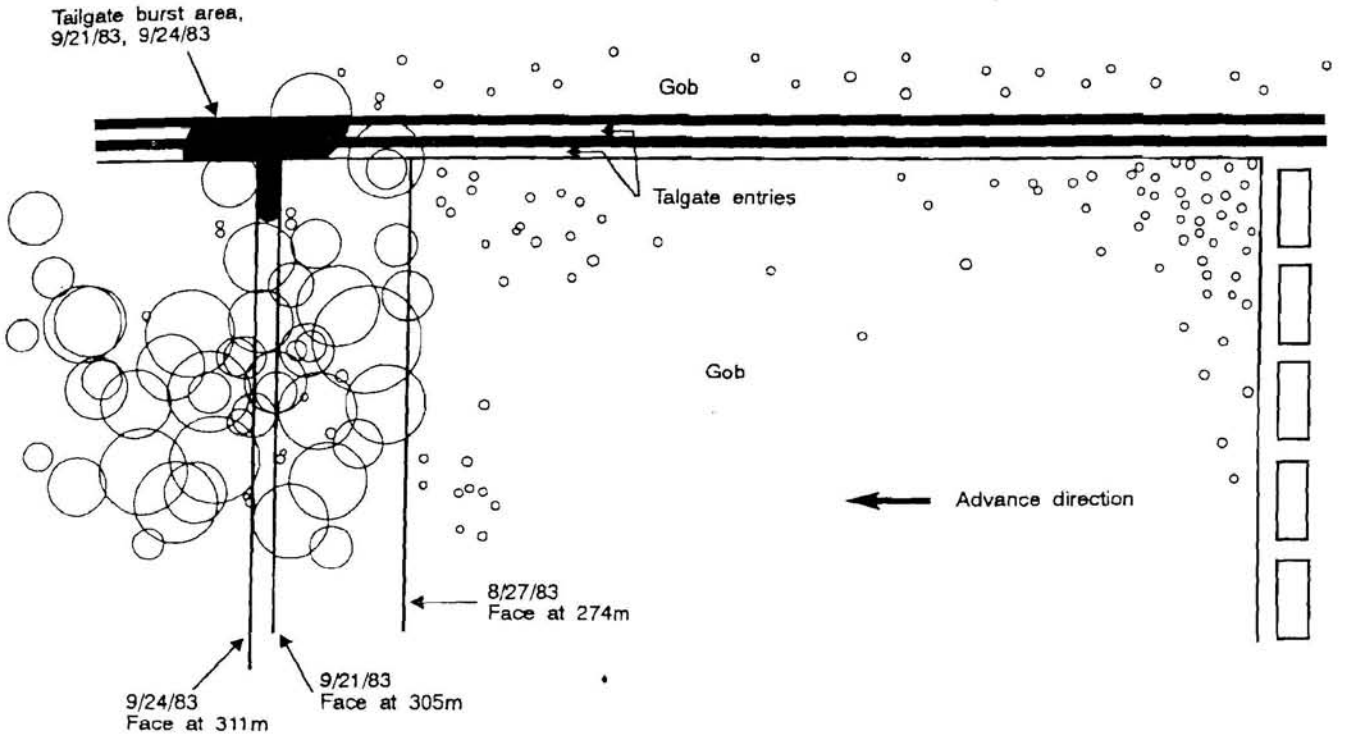

Microseismic event locations mapped in relation to the failure zone associated with two floor bursts. Sizes of the location circles are proportional to location error.

position 78 m behind the face. The stress profiles generated by the models predicted increased stress across the headgate pillars, a stress decrease across the gob, and a large increase in stress across the tailgate pillars. The microseismic energy distribution shows parallel behavior in which energy levels were moderate in the headgate pillars, low across the gob, and substantial in the tailgate pillars.

While the microseismic data were being collected, leg pressures of selected shields were also continuously monitored and digitally recorded (*10*). To investigate a possible relationship between microseismic event occurrence and shield pressure variations, the time of occurrence of large microseismic events and movement of shields were compared. Figure 7 displays such a comparison for a typical period of mining. The frequency distribution in energy of the 23,000+ microseismic events collected during the study period was similar in shape to a normal probability density distribution with a peak value of about 9 J. A 350-J minimum value for large events was chosen as a convenient number that composed the top 4 pct of energies. Advance of the shields, typically 0.76 m, is indicated by a sharp dip and then a return of pressure, but to a lower level than previously. There appears to be some time correlation between the incremental advance of the tailgate shields and the occurrence of large microseismic events. There were 16 shield moves and 19 large microseismic events during the mining cycle. During a time span ranging from 5 min before to 15 min after unset of the tailgate shields, 14 (74 pct) microseismic events occurred. Using the same time span, 11 (69 pct) shield moves were associated with one or more microseismic events. Also, all but one of these microseismic events were located in the vicinity of the tailgate gob and pillar system.

Microseismic activity was also compared to pillar borehole pressure cell (BPC) measurements. These comparisons use microseismic events whose locations fell within rectangular areas encompassing large tailgate pillars, including one-half the width of the passageways surrounding the pillar. BPC's were installed 3, 6, and 13.7 m into the center of the pillar face closest to the panel perpendicular to the mining direction. The 13.7-m depth corresponds to the center of the pillar. Figure 8 is a diagram of BPC placement and the microseismic event accumulation zone for a typical pillar in this study.

Figure 9 shows graphs of the hourly average pressures measured with the BPC closest to the pillar face and the BPC in the center of the pillar, and a running sum of the microseismic source energy for the time period during

Figure 5
Typical Microseismic Activity Related to Mining.

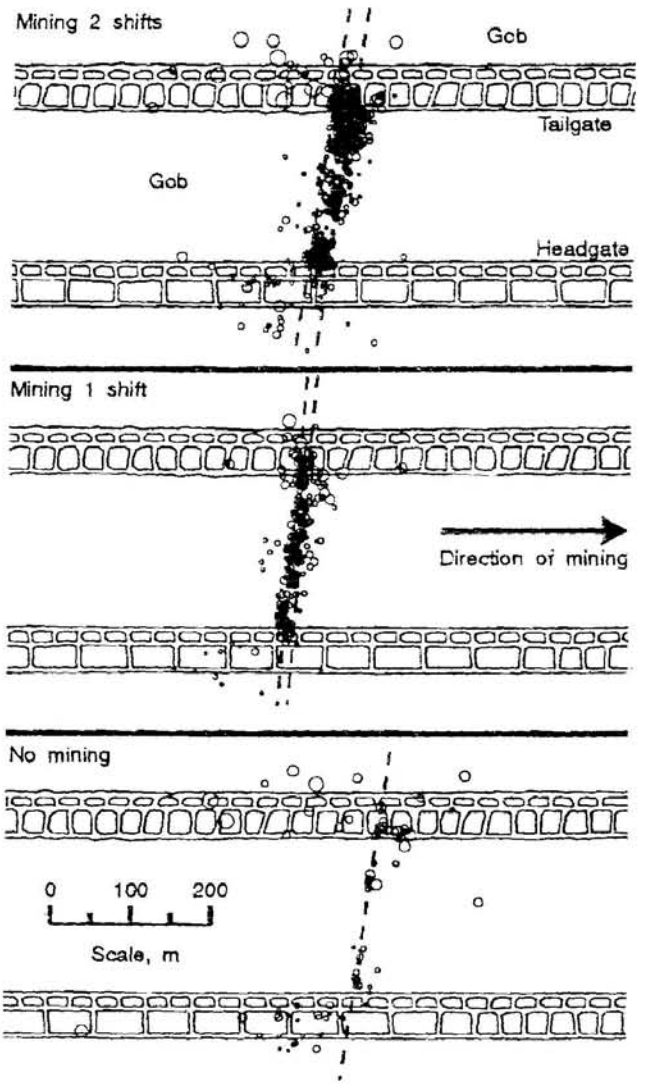

Twenty-four hour microseismic event locations during periods of two-shift mining, one-shift mining, and no mining. Sizes of the location circles are proportional to event energy. Face positions at the start and end of mining are indicated by broken lines.

Figure 6
Microseismic Energy Distribution and Numerical Model Stress Profiles.

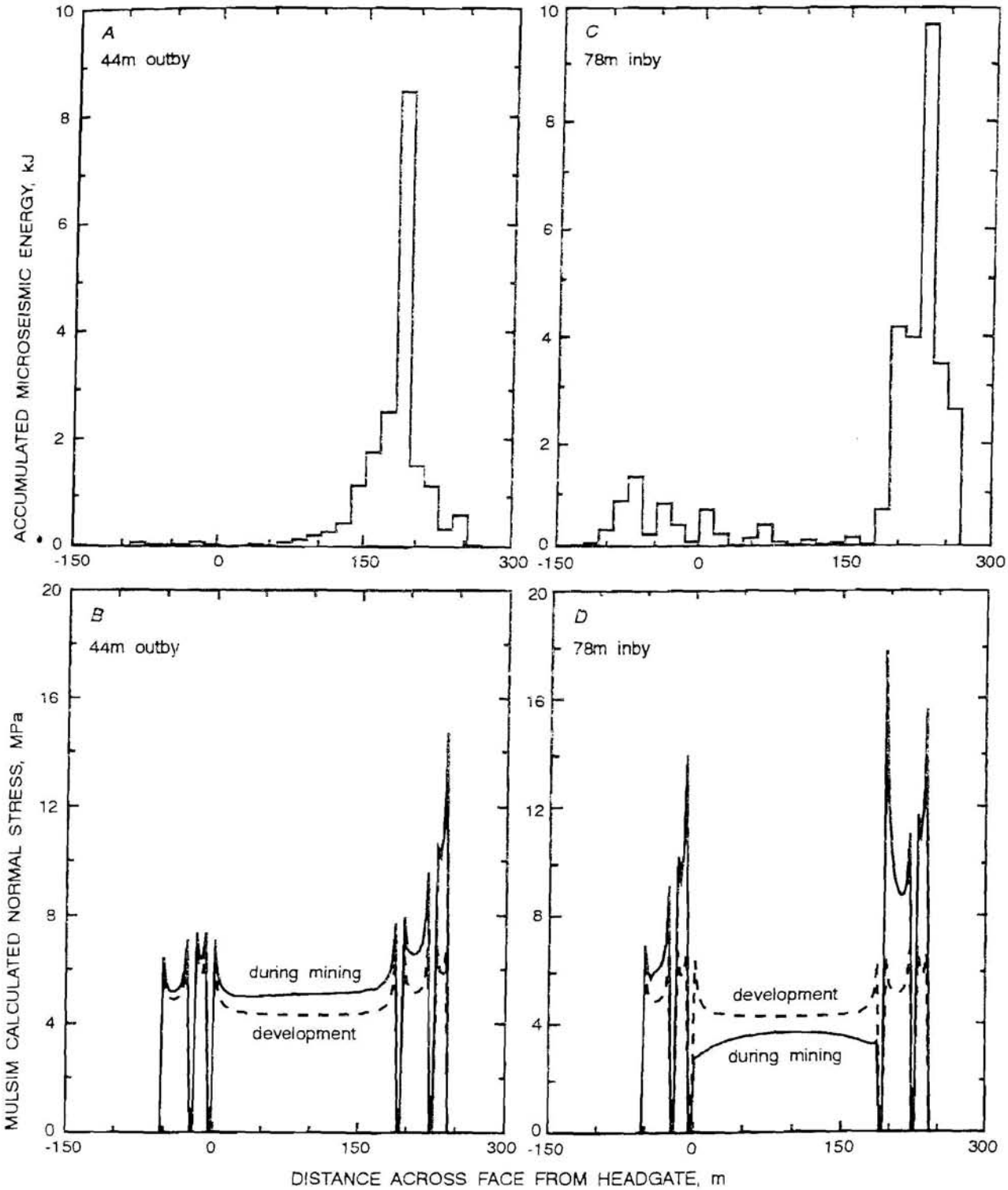

Distributions of microseismic event energies during the study period and numerical model stress profiles as a function of distance across the face and pillars. *A-B* are for a position 44 m ahead of the face; *C-D*, 78 m behind the face. Distance across the face and pillars is perpendicular to mining direction and referenced to the headgate panel edge.

which the greatest change in pillar pressures occurred. Prior to this time period, there was little variation in BPC measurements and no microseismic activity in the pillar area. The decrease at the end of the graph representing the pressure on the BPC at the 3-m depth is believed to indicate progressive failure of the pillar's rib.

There is good visual correlation between accumulated microseismic energy and BPC pressure increases, implying that microseismic event generation in the pillar area appears to be an indicator of increasing pillar pressure. This is in agreement with laboratory tests by Khair (*11*), who studied the production of rock noise from coal specimens under loading. He reported that the specimens exhibited high rates of activity corresponding to local brittle failures as stress was increased.

EXAMPLE 4—MICROSEISMIC DIVERSITY AND PREBUMP BEHAVIOR

In 1989, the USBM was invited to join a cooperative research effort at an underground coal mine in southeastern Kentucky. This mine had experienced two severe face bumps that occurred while mining under a sandstone channel. The USBM installed a variety of equipment, including a microseismic monitoring system, to observe ground behavior while the next panel was being mined under the same conditions (*12*). After the research project was concluded, the microseismic system was used to monitor other longwall panels at the mine for another 3 years.

Even in normal mining situations where there were no geologic anomalies, the microseismic activity recorded at this mine differed from activity at the other three mines discussed in this report. While events clustered in bands parallel to the face as part of normal activity, the density of events was not highest at the face. Often the band was most dense 30 to 40 m into the panel, where the greatest change in forward abutment pressures was found, and little or no activity occurred at the face.

A second type of distribution of activity is shown in figure 10. Data were obtained during a 24-h period in which a 183-m-wide panel under 427 m of cover was mined for 12 m. Microseismic event locations were widely scattered but appeared to follow a trend that crossed from behind the shields into the unmined panel near midface and through the tailgate pillars into the gob from the previous panel. In either distribution of activity, levels were generally significant in the tailgate pillars ahead of mining.

During the initial research at this mine, a severe face bump occurred soon after mining progressed under the sandstone roof, resulting in injuries to miners and damage to shields and the shearer. Damage was so severe that the mine eventually executed an in-panel move of 350 m to a new starting line past the sandstone roof area. When the bump occurred, the width of the panel was 152 m and the

Figure 7

Large Microseismic Event Occurrence and Shield Movement.

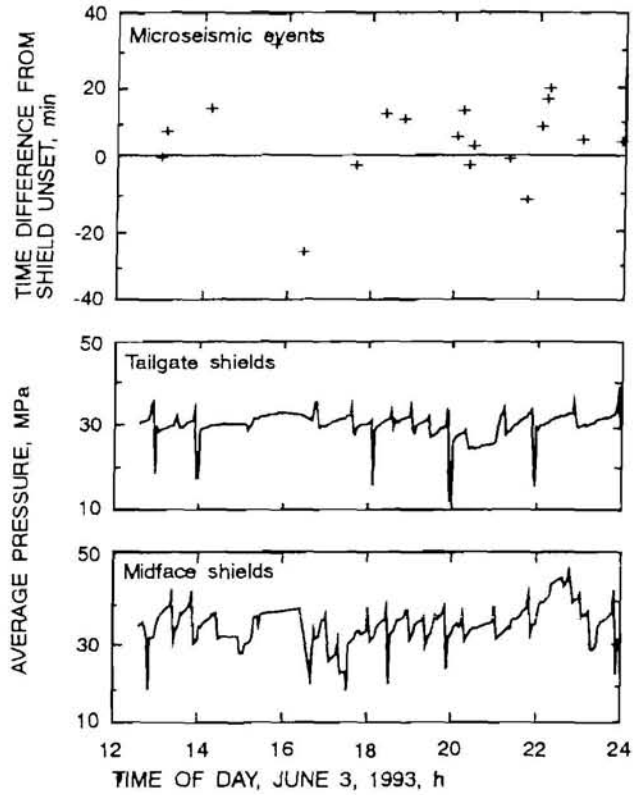

Time differences between microseismic events with energies greater than 350 J and unset of tailgate shields as a function of time. Average pressures of tailgate and midface shields are shown for reference; shield unsets are denoted by sudden pressure drops.

Figure 8

Pillar BPC Placement and Zone of Microseismic Event Accumulation.

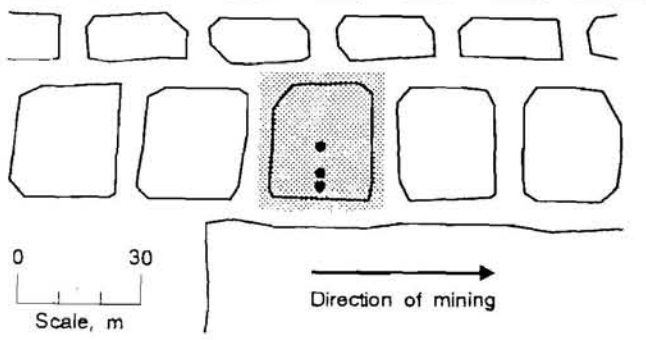

BPC's were installed to measure pillar pressures at depths of 3, 6, and 13.7 m (pillar center). Shaded area shows the microseismic accumulation zone for data displayed in figure 9.

Figure 9
Pillar Microseismic Energy and BPC Pressure Measurements.

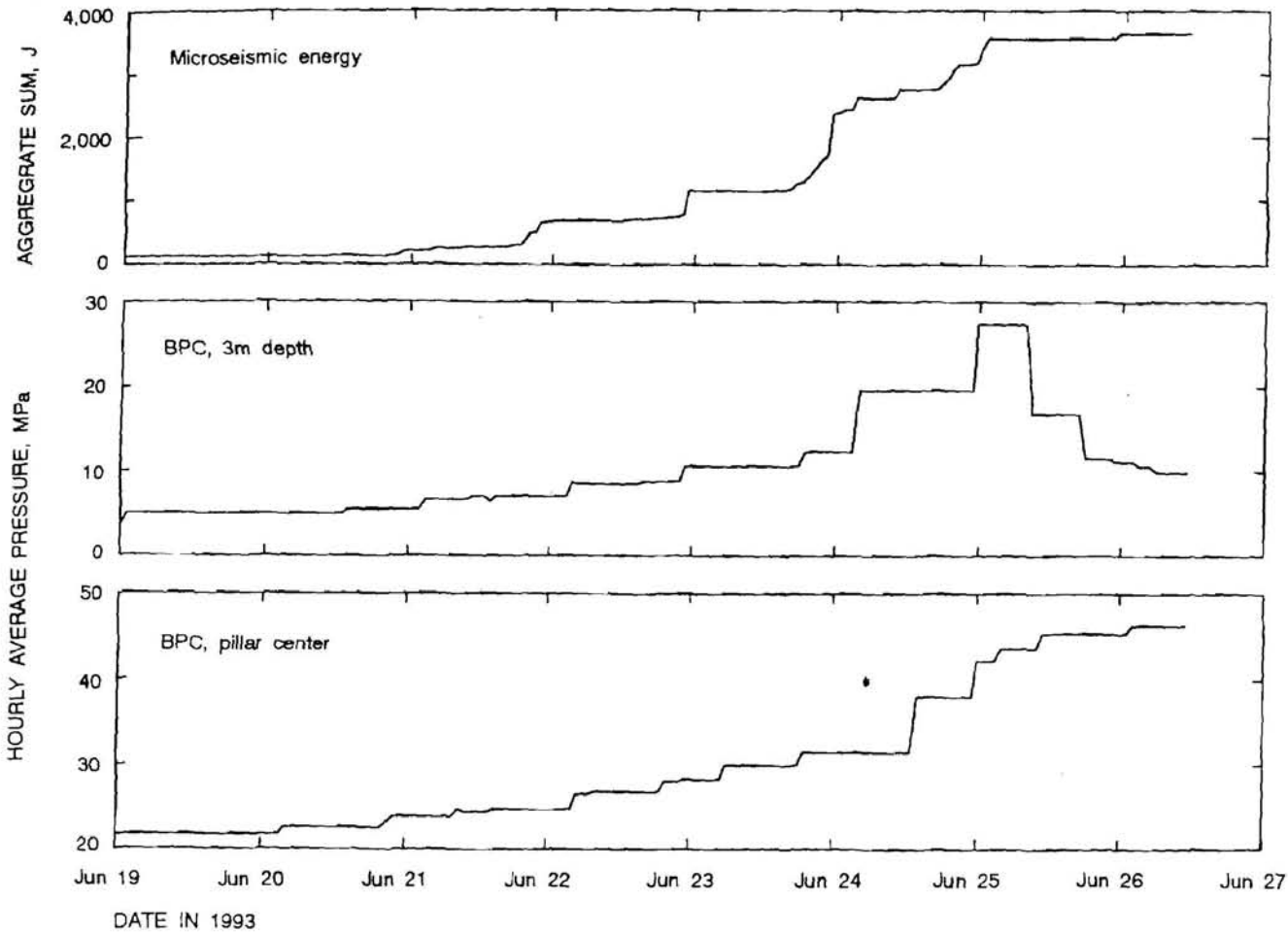

Running sum of microseismic event energies and hourly average pressure measurements as a function of time for a large tailgate pillar.

Figure 10
Another Example of Microseismic Activity During Mining.

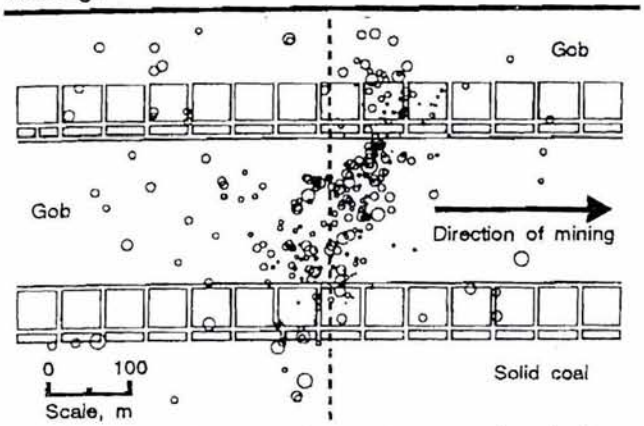

Locations of microseismic events occurring during a 24-h period in an eastern Kentucky coal mine. Sizes of the location circles are proportional to event energies. Average face position is marked with a broken line.

depth of cover was approximately 480 m. An analysis of the microseismic activity preceding the bump was done by Rowell,[4] who found that the activity rate gave no indication of an impending bump but rose and fell in response to mining rate. However, he did note that within a square 100 m on a side centered on the bump location, the number of large events[5] on the day before the bump had increased to 12 from a normal mean daily rate of 6 with a standard deviation of 2.

An analysis of a two-dimensional source energy distribution of microseismic activity preceding the bump provided information as to why the bump originated where it did. Figure 11 displays such a distribution of estimated source energies for microseismic events that occurred during the 72-h period immediately preceding the bump. Areas of accumulation are blocks 15 m on a side. The face position at the time of the bump is denoted with a vertical line. The location of the microseismic event associated with the bump is also marked. This distribution shows there was a significant amount of energy released across the panel near the face, with a peak in the center. More importantly, the distribution also shows the high level of microseismic energy extending into the panel and around toward the tailgate, leaving a ridge of lower energy release jutting into the panel. If microseismic events are produced during deformation, with intensity related to instantaneous yield, then this ridge of low energy represents a low-deformation zone, a place where significant amounts of strain energy were stored. As observed in this situation, this stored energy was violently released, with catastrophic results.

SUMMARY AND CONCLUSION

This paper presented analyses of microseismic data collected at four underground coal mines. Similarities and differences in microseismic activity during normal mining were noted. Three of the mines exhibited bands of microseismic activity along the face. However, an example was shown of a different type of behavior that occurred in the fourth mine, where microseismicity appeared to be banded along a forward abutment and not parallel to the face. Persistence of microseismic activity was demonstrated by presenting data showing that microseismic events occurred for 2 days after mining had stopped. A comparison of microseismic activity with numerical analysis results showed that the energy released during microseismic generation closely paralleled predicted stress profile changes across the panel while mining progressed. Pillar pressure measurements were shown to correlate well with the microseismic energy generated in the area of a pillar. Also, a time comparison done between large-energy microseismic events and average pressures measured in tailgate shields indicated that a space-time correlation may exist between the advance of the face and the occurrence of large microseismic events. Finally, findings were presented relating zones of low microseismic activity to areas of eventual failure.

These findings suggest that microseismic monitoring methods can help to determine characteristics of ground behavior in underground coal mines. Each mine experiences one or more typical behaviors with regard to microseismic activity during normal mining conditions, and any deviations in normal behavior may signal impending problems. The persistence of microseismic activity in the absence of mining indicates that mine stresses can take considerable time to come into equilibrium, and that microseismic monitoring can show where these continuing strain adjustments are occurring. Also, mapping the energy released from microseismic events indicates how strata are responding to stress, which may enable researchers to forecast eventual stress anomalies along the face and shields and in the pillars. Finally, the presence of microseismic quiet zones during times of abnormally high activity rates can point out areas that are potentially at high risk for bumping or bursting.

[4]Presentation by G. A. Rowell and J. S. Lemons entitled "Microseismic Analysis of a Mountain Bump" at the Fifth Conference on Acoustic Emission/Microseismic Activity in Geologic Structures and Materials, PA State Univ., University Park, PA, June 11-13, 1991.

[5]Large events were defined as events in which 6 or more geophones out of the 16 comprising the array were overdriven.

Figure 11
Two-Dimensional Energy Distribution of Microseismic Events Occurring During 72-h Period Preceding a Bump.

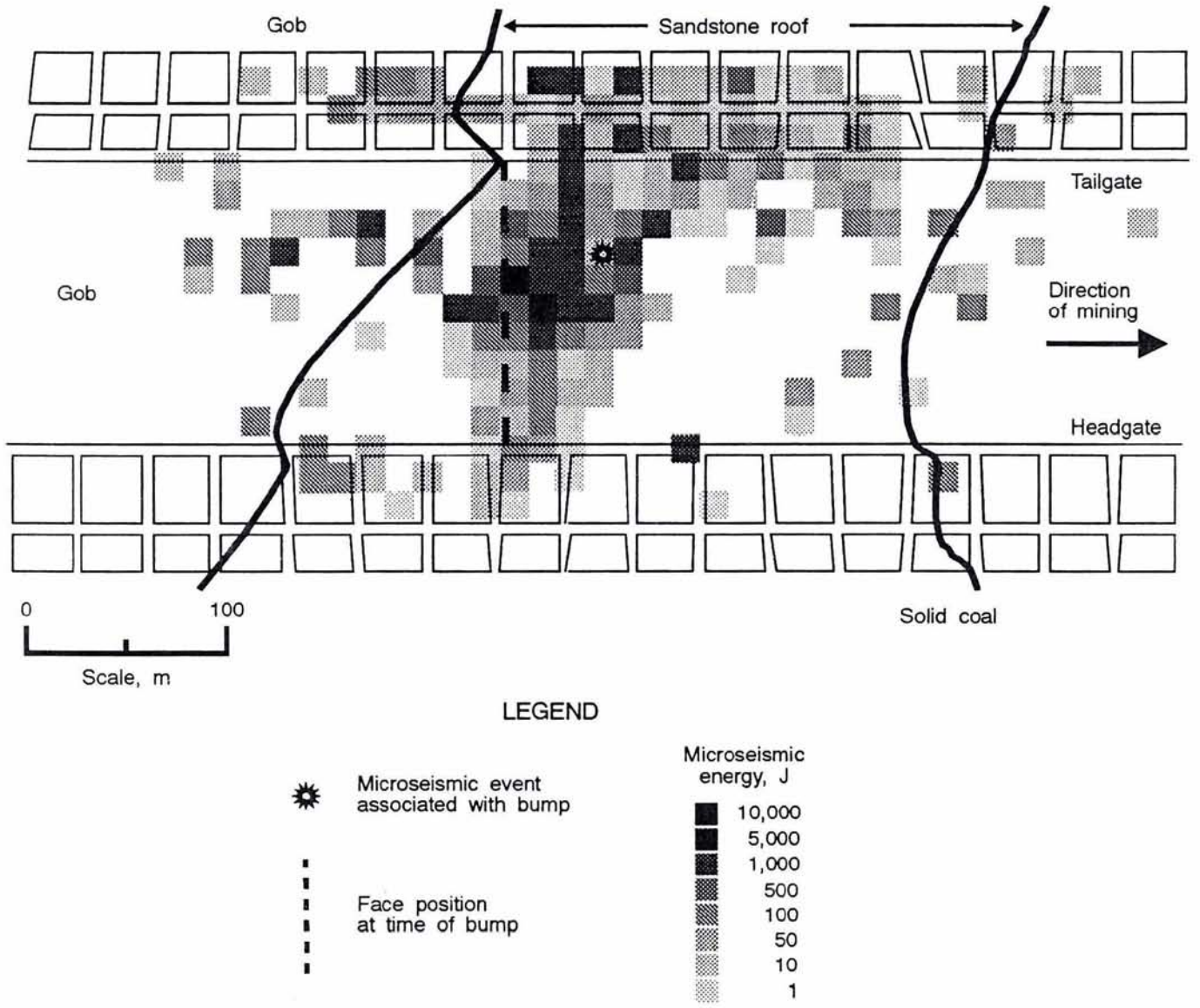

ACKNOWLEDGMENTS

The authors wish to thank those people who assisted significantly in the preparation of this report. Jennifer Riefenberg, geophysical engineer, Denver Research Center, provided the numerical modeling results and stress profiles used in this report. David Conover, mining engineer, also of the Denver Research Center, was responsible for the shield and pillar pressure calculations. Sam Lemons, geophysical engineer, Denver Research Center, collected and organized most of the microseismic data used in this report, and processed it to obtain event locations and energies.

REFERENCES

1. Obert, L. Use of Subaudible Noises for Prediction of Rock Bursts. USBM RI 3555, 1941, 4 pp.

2. Blake, W., F. Leighton, and W. I. Duvall. Microseismic Techniques for Monitoring the Behavior of Rock Structures. USBM Bull. 665, 1974, 65 pp.

3. Lord, A. E., and R. M. Koerner. Acoustic Emissions in Geological Materials. J. Ac. Emis., v. 2, No. 3, 1983, pp. 195-219.

4. Riefenberg, J. Statistical Evaluation and Time Series Analysis of Microseismicity, Mining, and Rock Bursts in a Hard-Rock Mine. USBM RI 9379, 1991, 15pp.

5. Marcak, H. The Relationship of Microstructure in Stressed Coal Seams to Observed Seismo-Acoustic Phenomena. Paper in Proceedings, Third Conference on Acoustic Emission/Microseismic Activity in Geologic Structures and Materials, ed. by H. R. Hardy, Jr., and F. W. Leighton (University Park, PA, Oct. 5-7, 1981). Trans Tech Publ., 1981, pp. 517-528.

6. Wilson, P. E., and J. S. Lemons. Continuous Microseismic Monitoring in a Deep Longwall Coal Mine. Paper in Proceedings, Fourth Conference on Ground Control for Midwestern U.S. Coal Mines, ed. by Y. P. Chungh and G. A. Beasley (Mt. Vernon, IL, Nov. 2-4, 1992). Dep. of Min. Eng., S. IL Univ., 1992, pp. 227-238.

7. Coughlin, J. P., and P. E. Wilson. A UNIX Workstation Monitoring System for Coal-Bump Research. USBM IC 9364, 1993, 12 pp.

8. Kneisley, R. O. Microseismic Data Analysis of Failure Occurrence in a Deep, Western U.S. Coal Mine: A Case Study. USBM RI 9228, 1989, 16 pp.

9. Riefenberg, J., D. Donato, M. Sun, and J. McDonnell. Numerical Modeling Analyses of a Longwall Mining Gateroad System. Paper in Proceedings, Fourth Conference on Ground Control for Midwestern U.S. Coal Mines, ed. by Y. P. Chungh and G. A. Beasley (Mt. Vernon, IL, Nov. 2-4, 1992). Dep. of Min. Eng., S. IL Univ., 1992, pp. 167-177.

10. McDonnell, J. P., R. M. Cox, and J. P. Dunford. Automated Monitoring and Geotechnical Evaluation for Ground Control in Longwall Mining. Paper in New Technology for Longwall Ground Control. Proceedings: U.S. Bureau of Mines Technology Transfer Seminar, comp. by C. Mark, R. J. Tuchman, R. C. Repsher, and C. L. Simon. USBM Spec. Publ. 01-94, 1994, pp. 131-145.

11. Khair, A. W. Acoustic Emission Pattern: An Indicator of Mode of Failure in Geologic Materials as Affected by Their Natural Imperfections. Paper in Proceedings, Third Conference on Acoustic Emission/Microseismic Activity in Geologic Structures and Materials, ed. by H. R. Hardy, Jr., and F. W. Leighton (University Park, PA, Oct. 5-7, 1981). Trans Tech Publ., 1981, pp. 45-66.

12. Zelanko, J. C., G. A. Rowell, and T. M. Barczak. Analysis of Support and Strata Reactions in a Bump-prone Eastern Kentucky Coal Mine. SME Preprint 91-91, 1991, 6 pp.

13. Gibowicz, S. J., and A. Kijko. An Introduction to Mining Seismology. Academic Press, 1994, pp. 264-300.

APPENDIX—SOURCE ENERGY ESTIMATIONS

Extensive research has been done to determine the energy released at the source of a seismic or microseismic event (*13*). However, an accurate determination of an event's source energy depends on access to a complete waveform that represents ground motion at some specific location. The digital data acquisition system used to gather most of the data presented in this paper saved 0.6 s of full waveform signal data from each geophone. These "snapshots" of each geophone signal also included 50 to 250 ms of prior history so that arrival time differences could be determined. This was adequate for most of the microseismic events recorded, but since signals produced by geophones close to large events can produce waveforms that have a duration of over 1 s, there were instances for which complete waveforms were not obtained. The method used to determine the microseismic energies presented in this paper estimates the energy released at the event source by using a fixed window of 0.15 s starting at the time of first arrival, rather than the entire waveform. This gives a conservative measure of event energies but makes it possible to compare large and small events.

The formula[1] used to calculate the source energy E from a velocity gauge geophone signal is

$$E = 2\pi \rho c r^2 V_p^2 T,$$

where ρ = average rock density, kg/m^3,

c = average seismic velocity, m/s,

r = source-to-geophone distance, m,

V_p = root-mean-square particle velocity during time T, m/s,

and T = 0.150 s, the time window.

The calculation is done for each geophone recording a valid signal and then averaged over that number of geophones.

[1]Microseismic Applications for Mining—A Practical Guide, by Wilson Blake. USBM OFR 52-83, 1983, 206 pp.

SEISMIC TOMOGRAPHY TO IMAGE COAL STRUCTURE STRESS DISTRIBUTION

By E. C. Westman,[1] M. J. Friedel,[2] E. M. Williams,[1] and M. J. Jackson[2]

ABSTRACT

Stress anomalies in the vicinity of the longwall face in an underground coal mine can result in violent coal bumps, compromising the safety and efficiency of mine workers. The U.S. Bureau of Mines (USBM) is using seismic tomography to monitor distribution and relative magnitude of stress concentrations throughout a coal pillar or panel. Researchers with the USBM have performed tomographic imaging in pillars and panels of Western underground longwall coal mines in support of the continuing goal of improving safety for and efficiency of underground miners.

Results of three case studies are presented. In the first case study, tomographic images of yield pillars adjacent to a mined panel were calculated. At one site, surveys were completed on subsequent days, resulting in determinations of stress redistribution as the face retreated to within 20 m (65 ft) of the pillar. In the second case study, the results of two surveys across the longwall panel as the forward abutment stress moved into the study area are described. The velocity results were compared to stress levels measured with borehole pressure cells. The final case study reports results of a survey in which a longwall shearer was used as the seismic source, rather than the hammer used in the first two studies.

INTRODUCTION

The rate of advance of longwall faces is the highest in history. With continued acceleration predicted, miners need a technique that will allow them to foresee stress-induced hazards before these hazards cause injury and downtime. Seismic tomography is being developed to create images of the interior of the coal panel in support of the U.S. Bureau of Mines (USBM) program to improve the health, safety, and efficiency of underground miners. The goal of this research is to provide the mining industry with a near real-time methodology for producing a continuously updated contour map of the stress distribution within the interior of a longwall panel and nearby pillars in the forward abutment zone. This paper describes the results of a series of seismic tomographic surveys performed at two Western longwall coal mines. The goal of these studies was to map changing stress concentrations in coal structures during longwall panel mining.

A relationship between stress and seismic wave velocity and attenuation is fundamental to these studies. Previous laboratory research (*1-2*)[3] has shown that as stress increases, alterations to the physical makeup of the material cause cavities within the material to close in the direction of primary stress, resulting in higher seismic wave velocities and lower attenuation. Under continued loading, as failure is approached, microcracks oriented parallel to the direction of primary stress form within the sample; these eventually coalesce into macrocracks just prior to failure. Opening these cracks results in lower seismic

[1]Geophysical engineer, Denver Research Center, U.S. Bureau of Mines, Denver, CO.

[2]Geophysicist, Twin Cities Research Center, U.S. Bureau of Mines, Minneapolis, MN.

[3]Italic numbers in parentheses refer to items in the list of references at the end of this paper.

wave velocities and increased attenuation. A similar response occurs during mining on a larger scale in pillars and panels.

Initiation of a seismic event, whether because of hammer impact, material failure, or some other reason, results in the generation of several different seismic wave types. These wave types have differing sensitivities to physical property changes because their modes of propagation are different. The fastest waves are compressional, or P-, waves. P-waves propagate with particle motion parallel to the direction of propagation. Slower shear, or S-, waves propagate with particle motion orthogonal to the direction of propagation. These different wave modes will also have different sensitivities to fracture orientations. Because the forward abutment stress is primarily a vertical load that closes horizontal fractures, vertically oriented shear waves are the most diagnostic of forward-abutment stress levels (*3*).

Underground tomographic surveys require the proper equipment and methodology. The USBM has developed an intrinsically safe in-seam seismic system (ISISS) to enable seismic studies in return air. The seismic data acquisition system consists of off-the-shelf components chosen because of their low cost and general accessibility. A source that delivers a high-energy signal, that is acceptable to the mine, and that is easy to use is essential. Geophones, small sensors that convert mechanical movement to electrical current, are isolated by circuit barriers housed in a steel enclosure for added durability and safety. The input and output connectors for the barrier box are NK-27 connectors, which are standard for the seismic industry. The recording instrument is a 24-channel digitizing seismograph that converts the analog voltage from the geophones into a digital representation for storage and processing. For use in the field, cables from the geophones to the barrier box are limited to four conductors, or two geophones per cable. This necessitates stringing several individual cables but provides increased safety; in case of a ground fall, there is less chance of the cable housing being compromised and several conductors shorting out.

Tomography is a method of generating images of structural features within a body by propagating energy through the body from multiple viewing angles and reconstructing pictures representative of the interior (*4*). The path followed by a seismic wave from a source to a receiver is represented as a ray (figure 1). Travel-time tomography creates a velocity distribution based on the time it takes for each ray to travel from a source to a receiver. A description of the stress level within the pillar or panel can be interpreted from the velocity tomograms. Successive tomograms taken over time as mining progresses show velocity changes in the coal as a function of changing stresses.

Originally developed for medical purposes, the method has been applied to creating cross sections of the earth using electromagnetic (*5*) and seismic waves (*6*). Recently, seismic tomography has been used to characterize stress in underground hard rock (*7-8*) and coal (*9-10*) mines.

MIGRATOM, a wave migration tomography code developed by the USBM, was used to perform tomographic reconstructions from the travel times for each survey. This code uses the simultaneous iterative reconstruction technique (SIRT) with straight rays or curved rays traced according to Huygen's principle (*11*). The root mean square residual difference between calculated and measured travel times is calculated for each iteration, showing when the solution has stabilized.

The results of three case studies are presented. In the first, the stress-induced velocity changes in the floor beneath two yield pillars were measured. The second study, at a different mine, imaged stress-induced velocity changes measured through the coal in the forward abutment of the longwall panel. The final study, conducted at the same mine as the first study, presents results of attenuation tomography studies in which the vibrations emitted by the longwall shearer were measured in the tailgate roof and analyzed for stress-induced amplitude changes.

Figure 1
Schematic of Seismic Tomography.

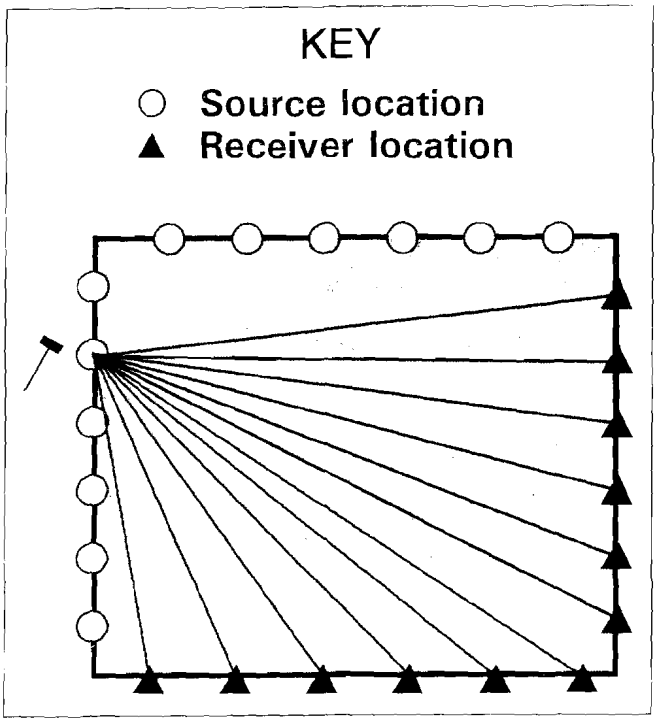

A seismic source, such as a hammer or explosive, transmits an elastic wave that is recorded by several receivers mounted on the opposite side.

CASE STUDY 1

Seismic tomography was performed through a sandstone layer in the floor beneath two yield pillars in the vicinity of the face, yet at separate locations and with different floor conditions, in a Western longwall mine (*9*). At these two underground study sites, seismic energy was excited at points on the mine floor (i.e., the underlying sandstone or mudstone) using a sledgehammer as the impact source. At site A, the propagation path of the first-arrival wave involved travel from the point of impact, across a sandstone member, to the geophones placed in the mine floor. At site B, the refracted wavelet traveled from the point of impact, through a mudstone layer, along the top of the sandstone, and back through the mudstone to the geophones placed on the mine floor (figure 2).

DATA ANALYSIS

Seismic tomography may require making static corrections to the original data. Static corrections are necessary to remove time delays associated with travel through "slow" strata, i.e., strata in which the seismic wave travels significantly less quickly than in the primary strata being observed. Because the objective of this study was to generate images of velocity distributions in the sandstone, it was important to remove time delays associated with travel through the mudstone. To achieve this goal, first-arrival travel-time measurements were plotted as a function of source-receiver separation for each side of the pillar. Because the actual propagation path was not known, the distance between any given source-receiver pair was assumed to be straight. Despite the scattering of data (attributed to the assumption of straight ray paths instead of the probable curved ray paths and local variations in both loading and random noise), linear trends are evident in the time-distance plots shown in figure 3.

VELOCITY DISTRIBUTION: SITE A

Figure 4 shows the velocity tomogram for study site A when the center of the pillar and longwall face were separated by a distance of about 30 m (100 ft). The characteristic velocity structure was heterogeneous, having several seemingly random but localized high-velocity regions [4 km/s (13,000 ft/s)] overprinted on a uniform background velocity [2 km/s (6,500 ft/s)]. The consistent and pervasive nature of these velocity features, despite the use of various starting velocity models and constraints, suggested that they were probably stress related and not artifacts of the tomographic program. While it is tempting to assign a value of stress to the computed velocities, it must be recalled that the accuracy of reconstructed velocity extremes is sensitive to the degree of sampling (number of ray paths) and so are most accurate as indicators of stress distribution, not necessarily absolute stress magnitude.

Figure 5 shows a velocity tomogram generated after a day of mining at site A. In this case, the longwall face had retreated to within 18 m (60 ft) of the center of the pillar. Again, the velocity distribution was heterogeneous, ranging from 2 to 4 km/s (6,500 to 13,000 ft/s); however, the high-velocity regions shifted toward the center of the pillar and intensified. Also notable was the development near the pillar core of a high-velocity region trending perpendicular to the direction of primary cleating.

The change in velocity character at site A from one tomogram to the next implied that temporal variations in stress occurred. To better define those regions of greatest change in mechanical conditions, a difference tomogram was computed (figure 6) by subtracting the first reconstruction from the second. This tomogram indicated that the greatest stress increase occurred along entry 2 from the center of the pillar to the outby end of the pillar, and also in the outby corner of the pillar nearest to the panel. At the center of the pillar, only a minor increase in stress [as indicated by a 0.5-km/s (1,640-ft/s) velocity increase] was observed.

VELOCITY DISTRIBUTION: SITE B

Figure 7 shows the velocity distribution for site B at a time when the longwall face was roughly 18 m (60 ft) inby the center of the pillar. Again, the velocity structure appeared heterogeneous [spanning 2 to 4 km/s (6,500 to 13,000 ft/s)], suggesting that stress was being applied nonuniformly to the pillar. The velocity systematically decreased along the center axis (parallel to the panel) of the pillar and away from the working face. The region of greatest concentrated stress appeared at the pillar end closest to the longwall face, manifesting itself as a region of concentrated stress both directly under and extending away from the pillar. Furthermore, the buildup of stress along a direction perpendicular to the primary cleat was similar to that observed during the second survey at site A; however, in this case, the buildup appeared to have shifted toward the center of the pillar.

CASE STUDY 2

Two seismic surveys were performed across a 215-m (700-ft) wide coal panel in an underground mine in an effort to generate images of the onset of the forward abutment stresses (*12*). Source and receiver locations were spaced at 6-m (20-ft) intervals on opposite sides of the panel. Typically, the forward abutment stress retreats with the face, staying within approximately 30 m (100 ft) of the face. Two surveys were completed, one when the working face was 25 m (80 ft) from the survey area, and the second after the face had retreated to within 8 m (25 ft) of the survey area (figure 8). The 40-Hz, three-component geophones were firmly anchored in 1-m (3-ft) boreholes along the headgate entry 3 panel rib.

The source was a sledgehammer struck against the panel rib at points spaced every 6 m (20 ft) along tailgate entry 1. The occasional presence of soft coal along the panel entry required the use of a steel rod with the hammer to couple the energy to the unfractured coal within the panel. The hammer was swung up to 30 times per location, and for each impact, the data were converted to digital memory. Each record was stacked with the previous ones to increase the signal strength relative to the background noise. It was discovered after the first survey that there was a high amount of microseismic activity that would occasionally mask the signal of the transmitted wave. During the second survey, the stack preview capability of the seismograph was used to delete any records in which significant microseismic noise was present. Records free of microseismic noise were stacked by the seismograph, and the summed record was saved to disk.

PANEL VELOCITY DISTRIBUTIONS

A distinct change in stress distribution at the working face of the panel is illustrated by comparing the velocity tomograms for the two surveys. Velocities of the vertically oriented shear (SV) waves were used because they are the most sensitive to the effects of vertical stresses (*3*). The SV velocity distribution for the first survey (figure 9) is quite uniform, having a mean velocity of 0.89 km/s (2,940 ft/s), with a standard deviation of 0.07 km/s (230 ft/s.) The SV velocity distribution for the survey taken the second day has a mean velocity of 0.89 km/s (2,920 ft/s), with a standard deviation of 0.06 km/s (200 ft/s); however, figure 10 shows two clear velocity peaks within the panel, one near the intersection of the face and the tailgate, and the other 35 m (115 ft) outby the face along the headgate. The peaks result from movement of the forward abutment stresses into the survey area. The stress on the coal panel is greatest in the vicinity of the least support, where the tailgate intersects the working face, resulting in the highest velocity measurements. The second velocity peak shown in the figure occurs outby the face, along the headgate; a low-velocity zone exists at the intersection of the face and headgate. One possible explanation is that the stress in this area bridges over to the adjacent unmined panel, thereby destressing the face. Additionally, the primary cleat direction trends northeast-southwest at this mine, possibly resulting in increased fracturing and a lowered velocity region at the junction of the face and the headgate.

COMPARISON OF PANEL VELOCITIES WITH BOREHOLE PRESSURE CELL MEASUREMENTS

The SV velocity distribution from the second day was compared to measurements obtained with conventional geotechnical instruments at a point near the tailgate side of the panel. Borehole pressure cells were emplaced in the panel to monitor stress changes at a single point during mining. Borehole pressure cells are flat steel bladders, approximately 5 cm wide by 20 cm long (2 in by 8 in), filled with hydraulic oil. The cell is grouted several meters into a borehole, and an initial pressure is established in the cell closely approximating the anticipated load on the cell. A tube connects the cell to a pressure transducer outside the coal. As pressure within the coal increases, the cell is deformed. The pressure transducer converts the subsequent change in oil pressure to a change in electrical voltage, which is recorded on a data logger (*13*). The velocity distribution for a profile located 12 m (40 ft) into the coal from the east side of the panel can be compared to stress change measurements obtained at different times as the face approaches the location of a from a single borehole pressure cell installed 12 m (40 ft) the panel rib (figure 11). The six velocity points displayed are the calculated values within the tomogram along the profile. The figure shows that the SV results correlate well to the stress measurements.

CASE STUDY 3

Studies were performed on a Western longwall panel (at the same mine as case study 1) in an initial effort to determine if a longwall shearer could be used to obtain images of stress distribution in the immediate vicinity of the face and tailgate. Use of the shearer would allow safer and more automated data acquisition, as well as enable the generation of images of the immediate face area of the panel. The amplitude of the grinding action of the longwall shearer was assumed to be approximately constant relative to amplitude changes caused by stress-induced physical property changes within and adjacent to the coal seam. By calculating the amplitude at specific points, tomographic images of attenuation in the longwall panel were obtained.

Surveys were conducted by recording the signals from geophones in the tailgate when the shearer was at specific locations along the face. A display of shearer position on the headgate shield allowed an observer at the headgate to trigger the seismograph manually as the shearer passed every fifth shield, approximately every 7 m (23 ft). Geophones were attached to roof bolts in the tailgate at approximately 15-m (50-ft) intervals. Attaching the geophones to roof bolts was much easier than drilling boreholes into the rib; however, this method resulted in a survey of the immediate roof rather than the coal seam. Receivers could not be attached to roof bolts in the headgate because vibrations from the conveyor belt would mask any signal from the shearer.

Processing the data consisted of calculating the amplitudes and generating the attenuation tomograms. The amplitudes used as input to the tomography program were calculated by obtaining the average periodogram for the recorded signal between 80 and 200 Hz (*14*). These amplitudes were then converted to the appropriate units for input to MIGRATOM (*11*). The calculation required a value for the input amplitude; because no sensor could be placed in the immediate vicinity of the longwall shearer as it moved across the face, the received amplitudes were plotted as a function of distance, and an estimate of the

Figure 2
Refracted Ray Path Beneath Coal Pillar (Not To Scale).

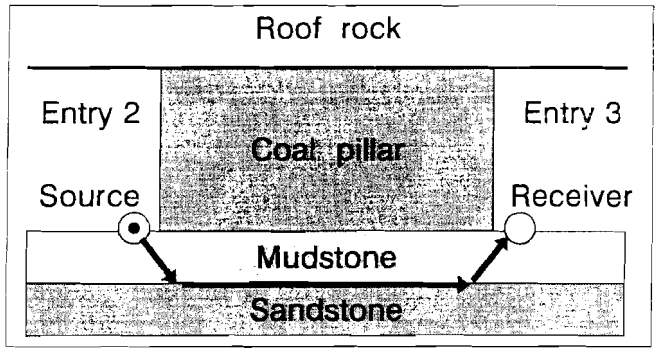

Figure 3
Travel-Time Scatterplots.

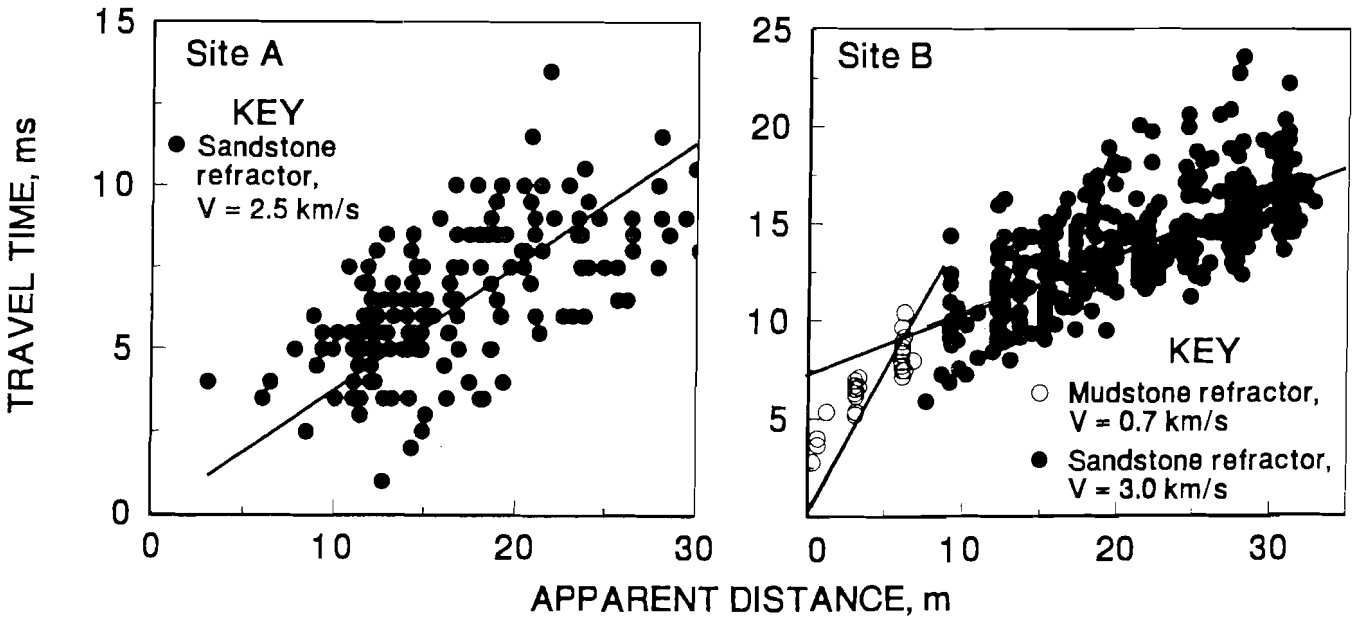

Linear trends indicate refractors and apparent velocity.

input amplitude was obtained by extrapolating back to zero offset.

A triangular image was obtained from the tomographic reconstruction because the receivers were only placed in the tailgate. Limitations in the angle of coverage restricted interpretation of the image to regions approximately 60 m (200 ft) wide along the face and the tailgate. The region along the tailgate was examined for this study, resulting in a rectangular plot 60 m (200 ft) wide by 100 m (330 ft) long.

Figure 12 shows the attenuation tomograms calculated for 2 days as the face retreated. The images are similar between 370 and 430 m east and show several features ahead of the face that were constant from one day to the next, presumably due to geologic anomalies in the roof. Typically, high attenuation identifies a material with open cracks (due either to low stress or failed material); therefore, the high attenuation region at the junction of the face and the tailgate, extending approximately 25 m (80 ft) along the tailgate for both days, indicates a material with open cracks. As this is the location of expected high stress, two explanations are possible: (1) the roof through which these surveys were taken is cantilevering over the gob, opening cracks within it or (2) the stress within the roof is approaching failure stress, and fractures are being created prior to failure. Without additional information it is not possible to determine precisely what is occurring in the roof; however, future studies will allow further development of this potentially useful technology.

Figure 4
P-Wave Tomogram, Site A, Day 1.

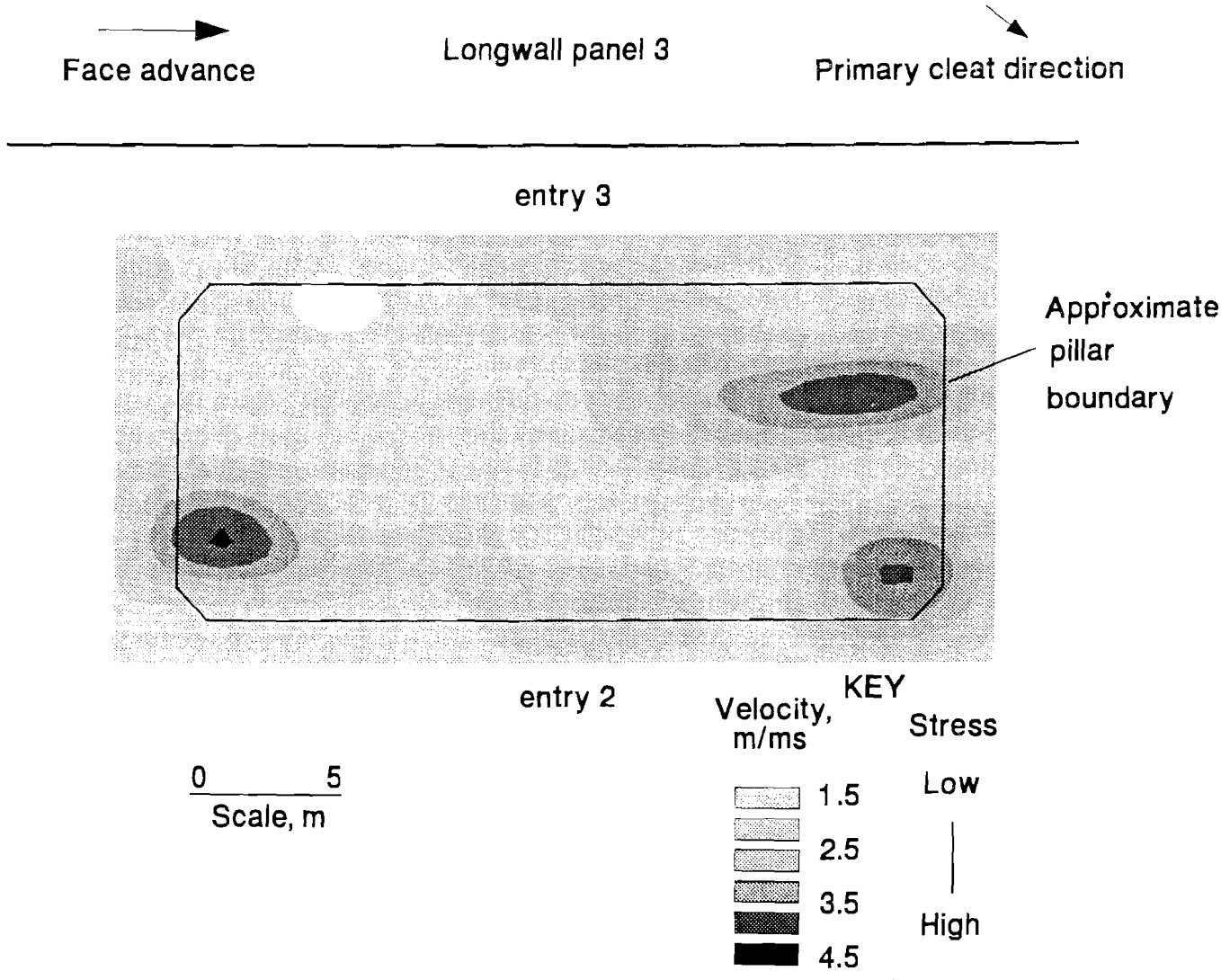

Pillar center is 22 m (72 ft) from face. High-velocity regions indicate concentrated loading.

Figure 5
P-Wave Tomogram, Site A, Day 2.

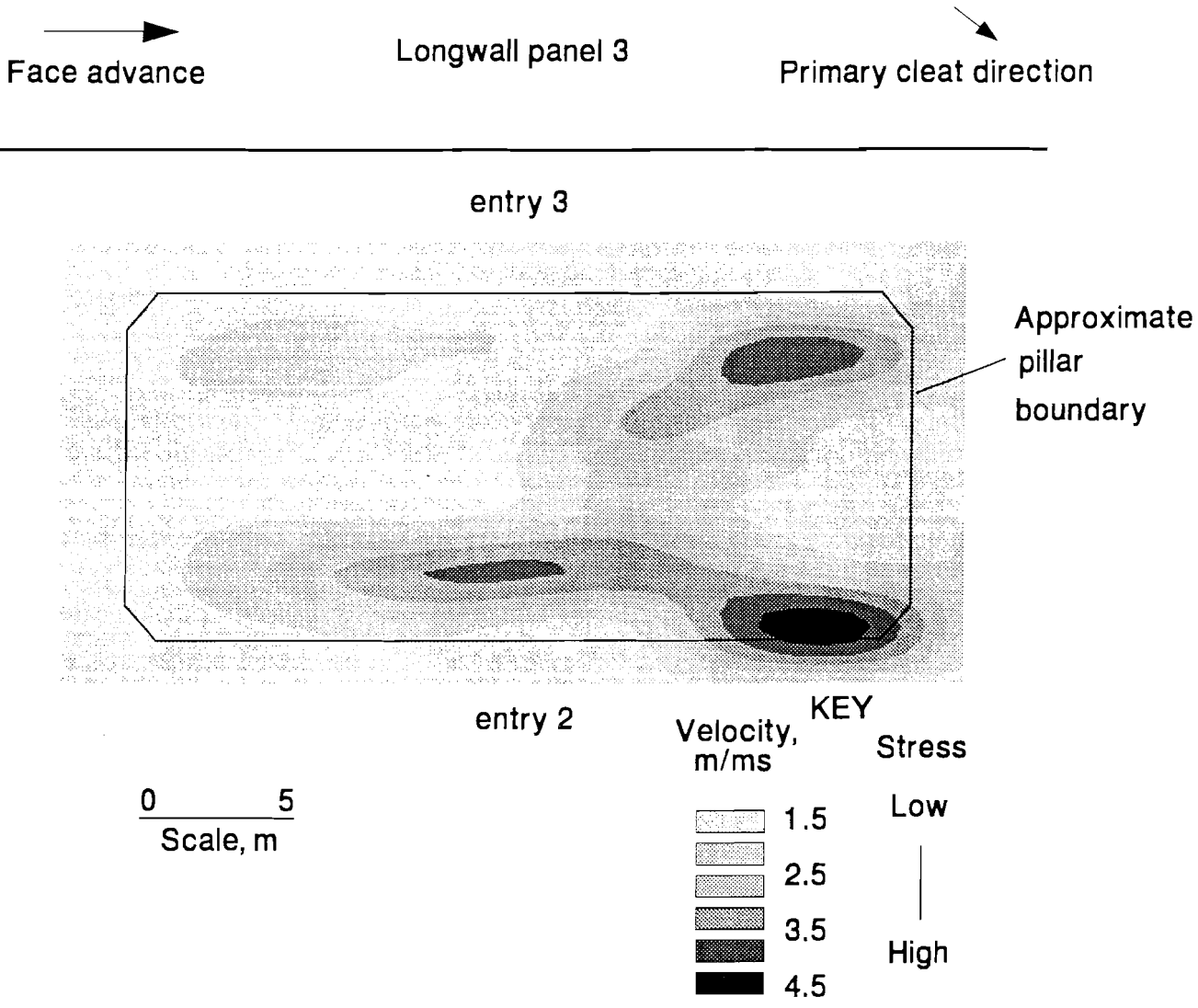

Pillar center is 9.5 m (30 ft) from face. High-velocity regions indicate stress buildup along a trend perpendicular to primary cleat.

Figure 6
P-Wave Difference Tomogram, Site A.

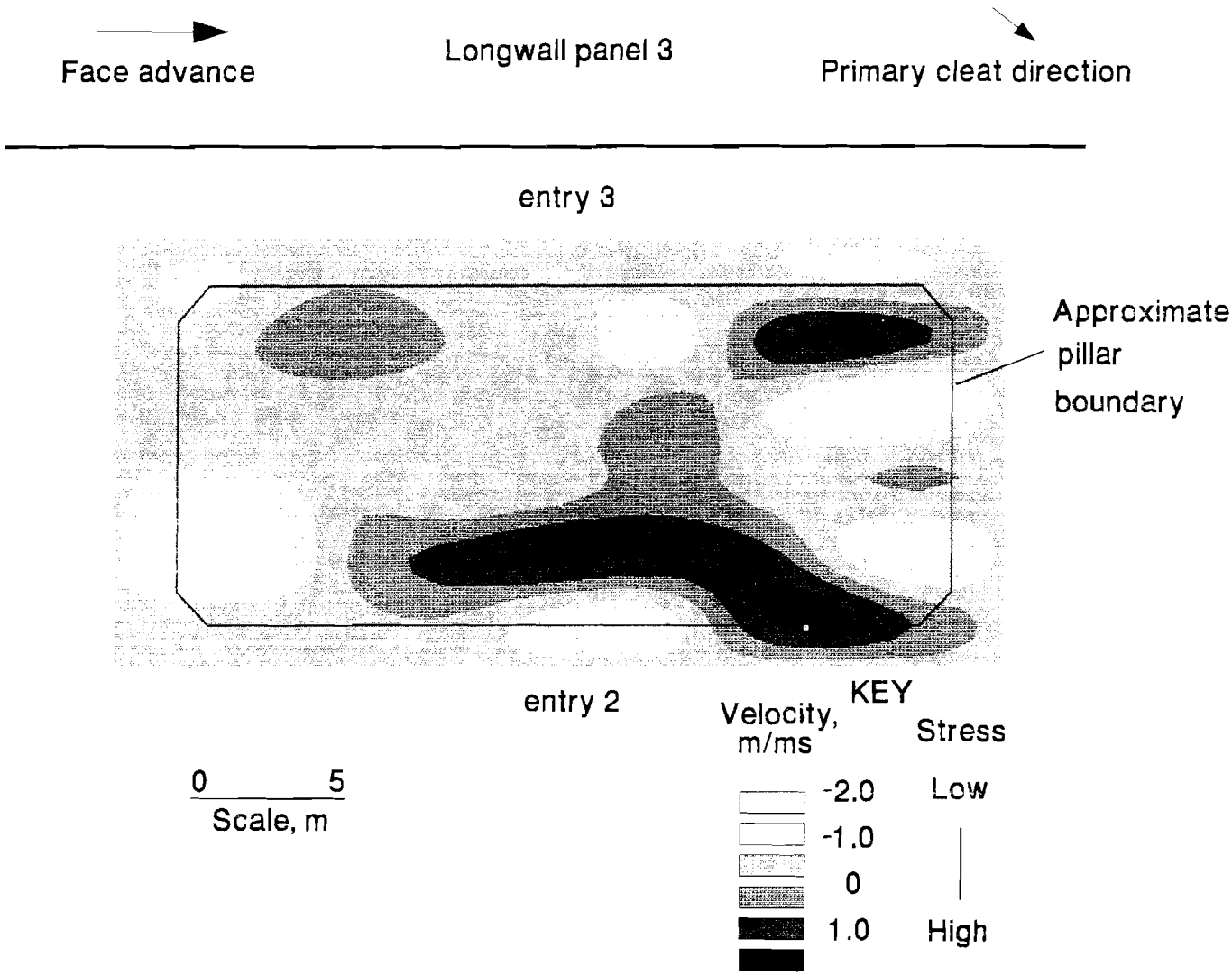

Tomogram indicates buildup (velocity increase) and relaxation (velocity decrease) of mine structure.

Figure 7
P-Wave Tomogram, Site B.

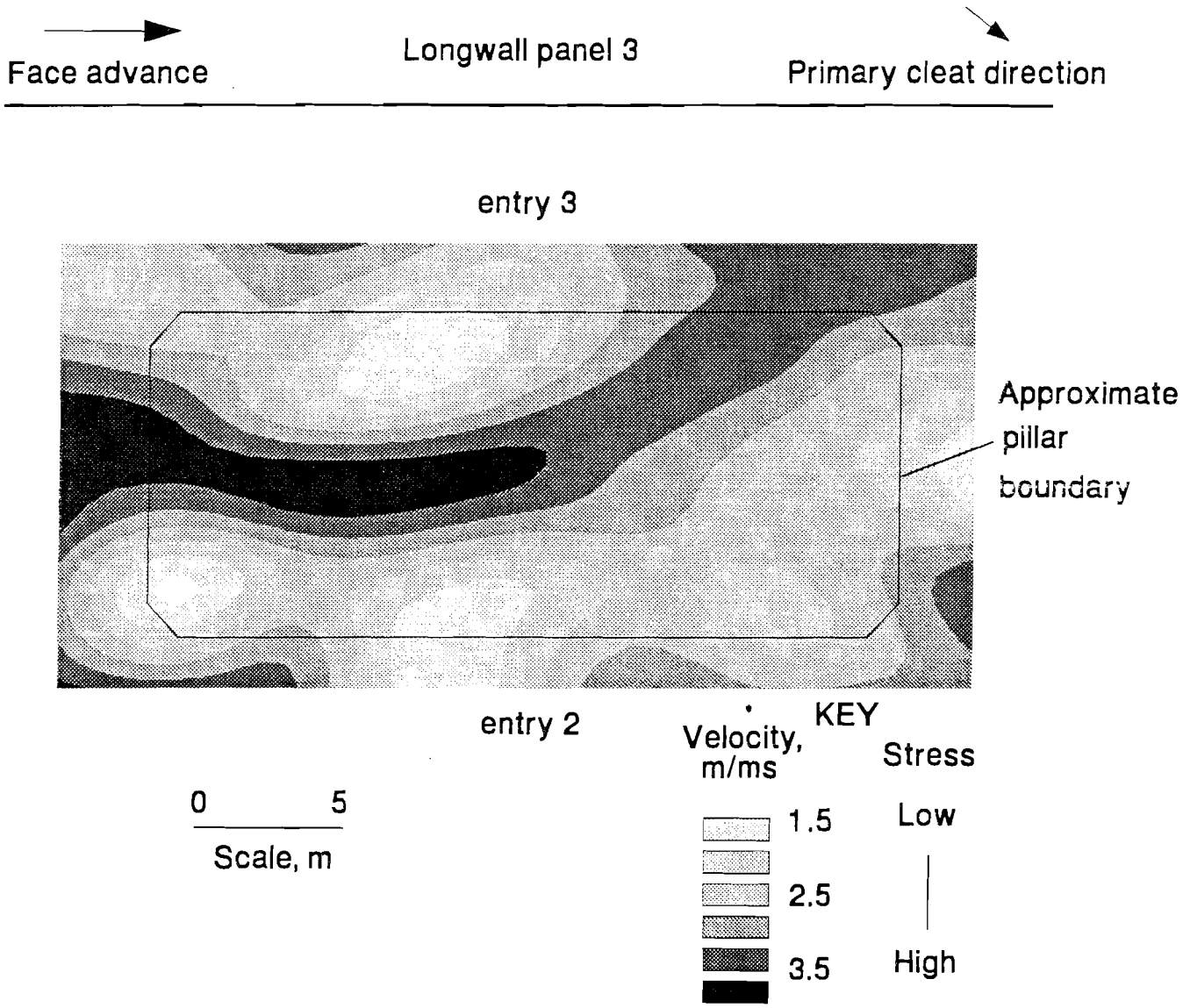

Tomogram indicates stress buildup at pillar end closest to working face and along trend perpendicular to primary cleat.

Figure 8
Map of Survey Area for Panel Study.

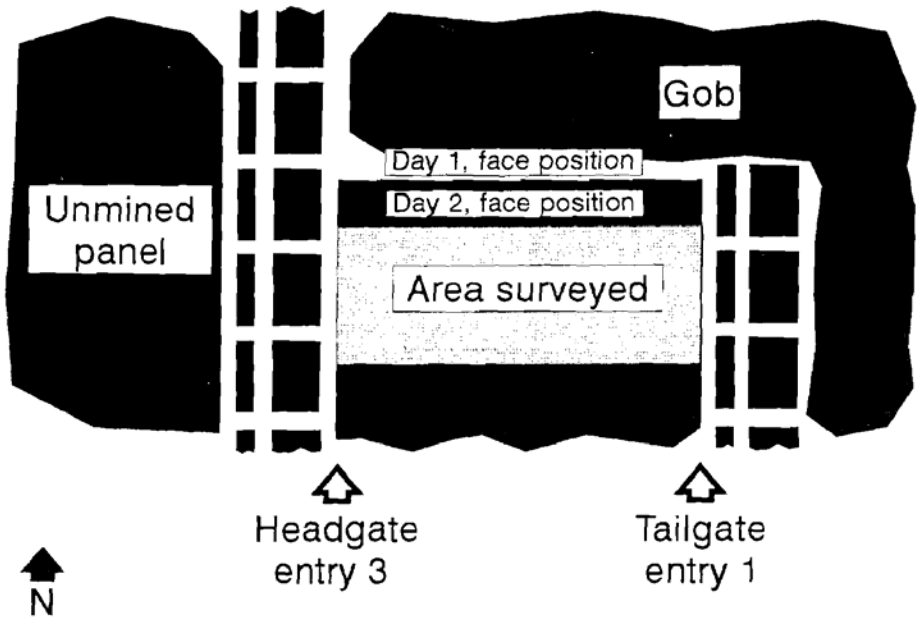

Face locations are indicated for the two study periods.

Figure 9
SV Velocity Tomogram for Survey Taken on Day 1.

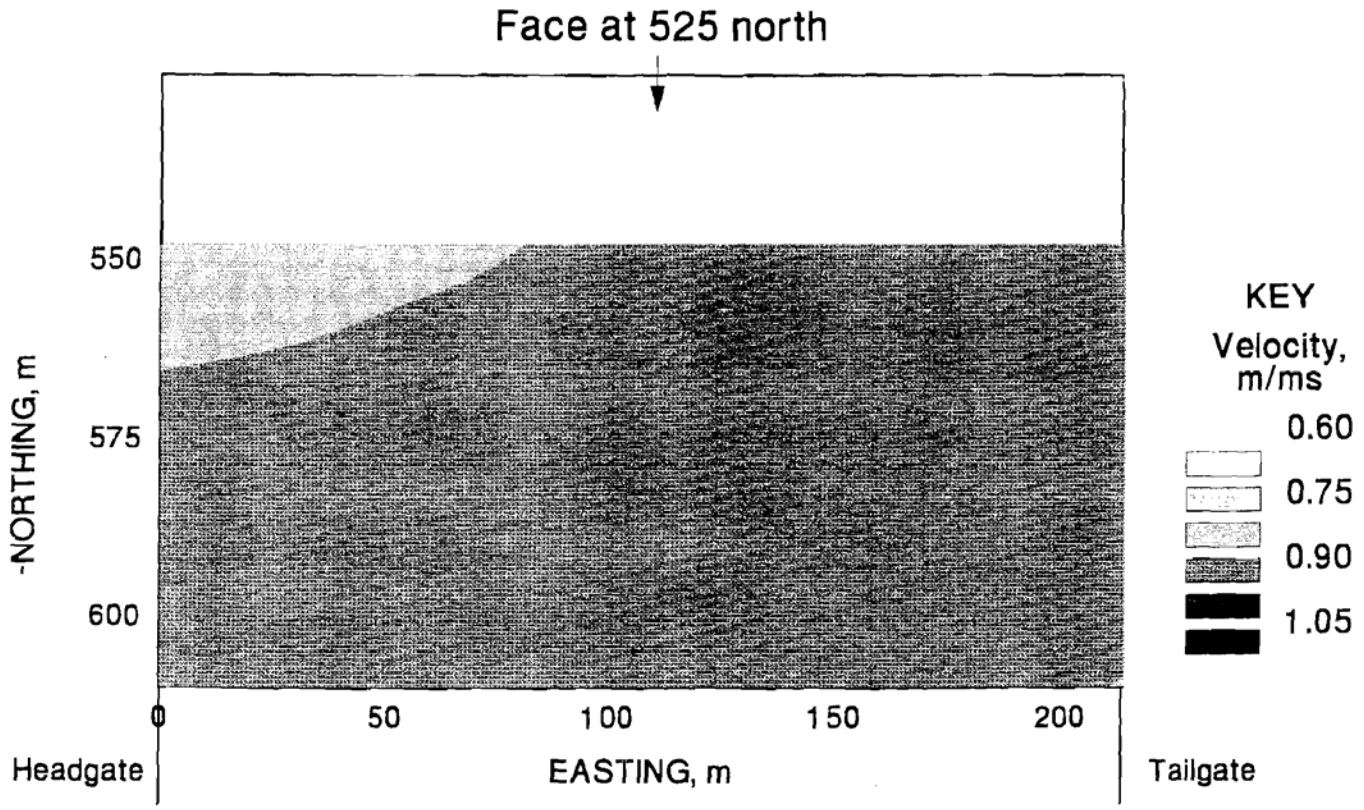

Working face is 24 m (80 ft) north of survey area.

Figure 10
SV Velocity Tomogram for Survey Taken on Day 2

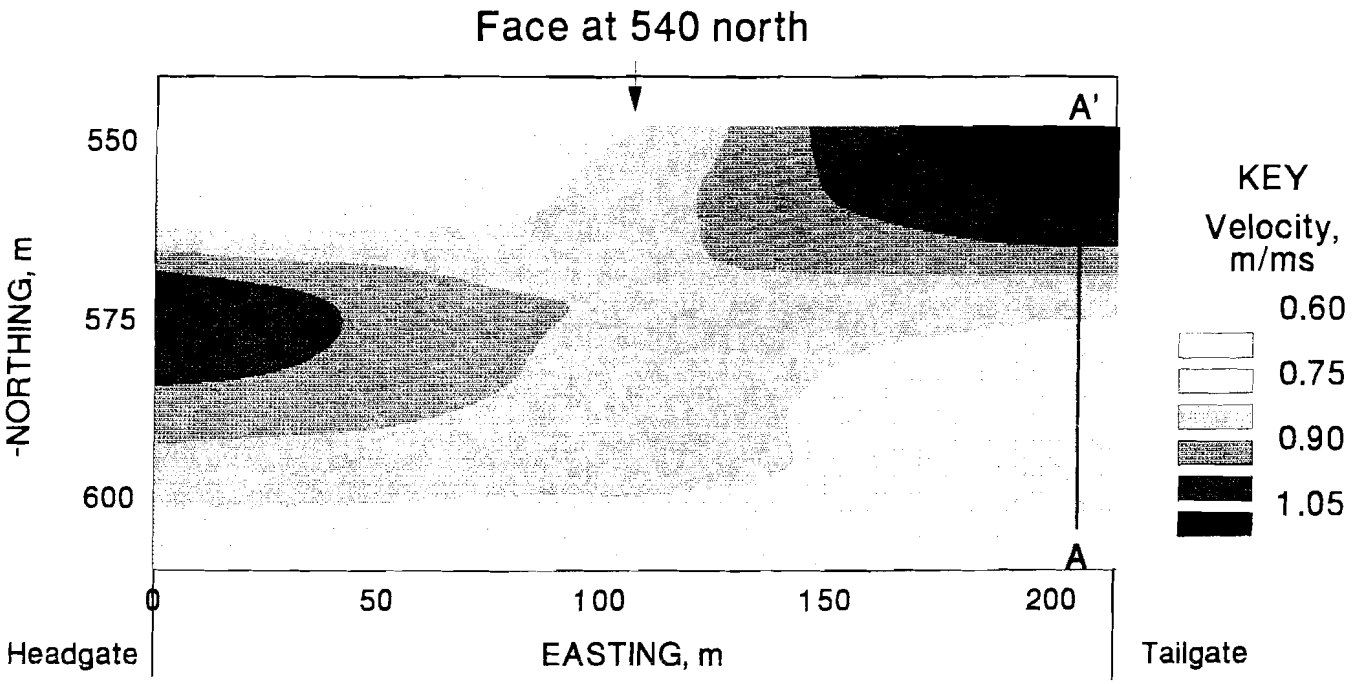

Working face is 8 m (25 ft) north of survey area. Profile A-A' is shown parallel to east edge of panel.

Figure 11
Comparison of Calculated Velocity Profile A-A' (See Figure 10) With Data From BPC.

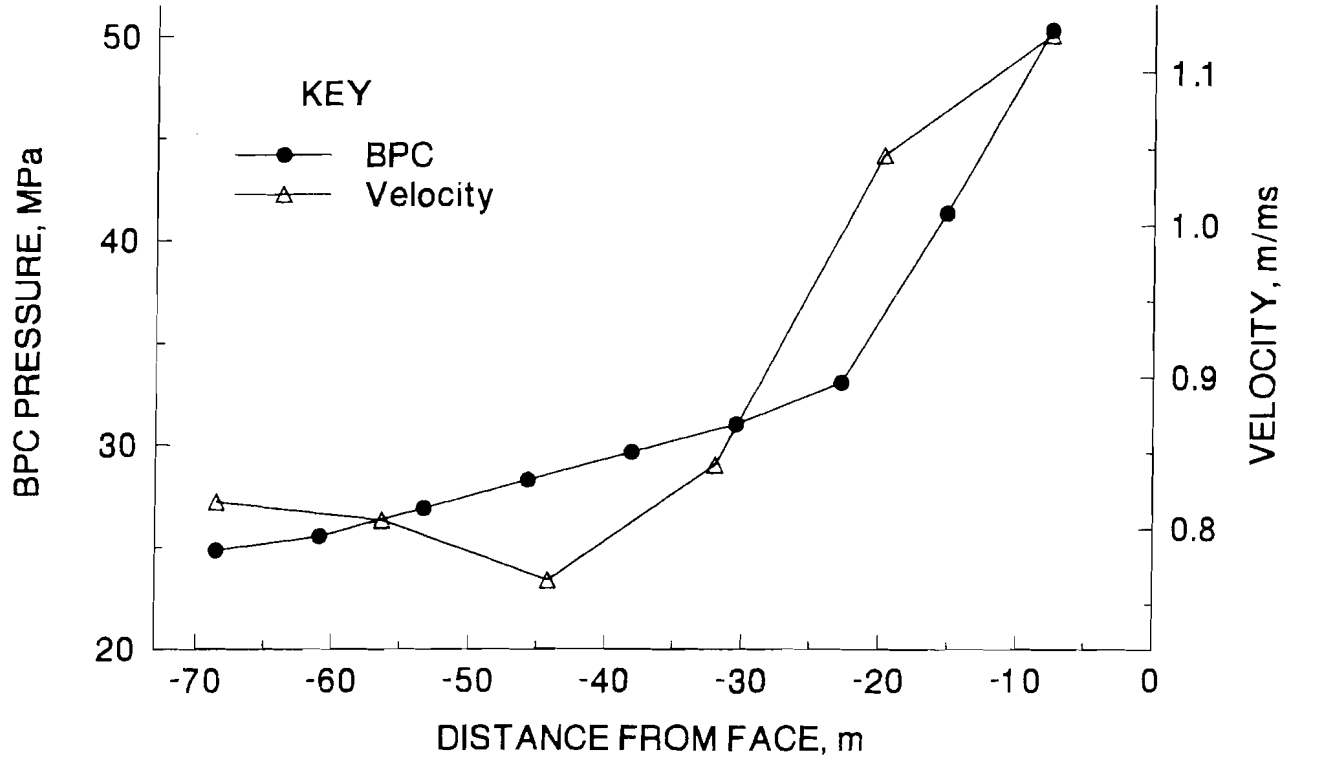

BPC was installed 12 m (40 ft) into panel. Pressure values were collected from different face positions.

Figure 12
Attenuation Tomograms of Panel Within 60 m (200 ft) of Tailgate.

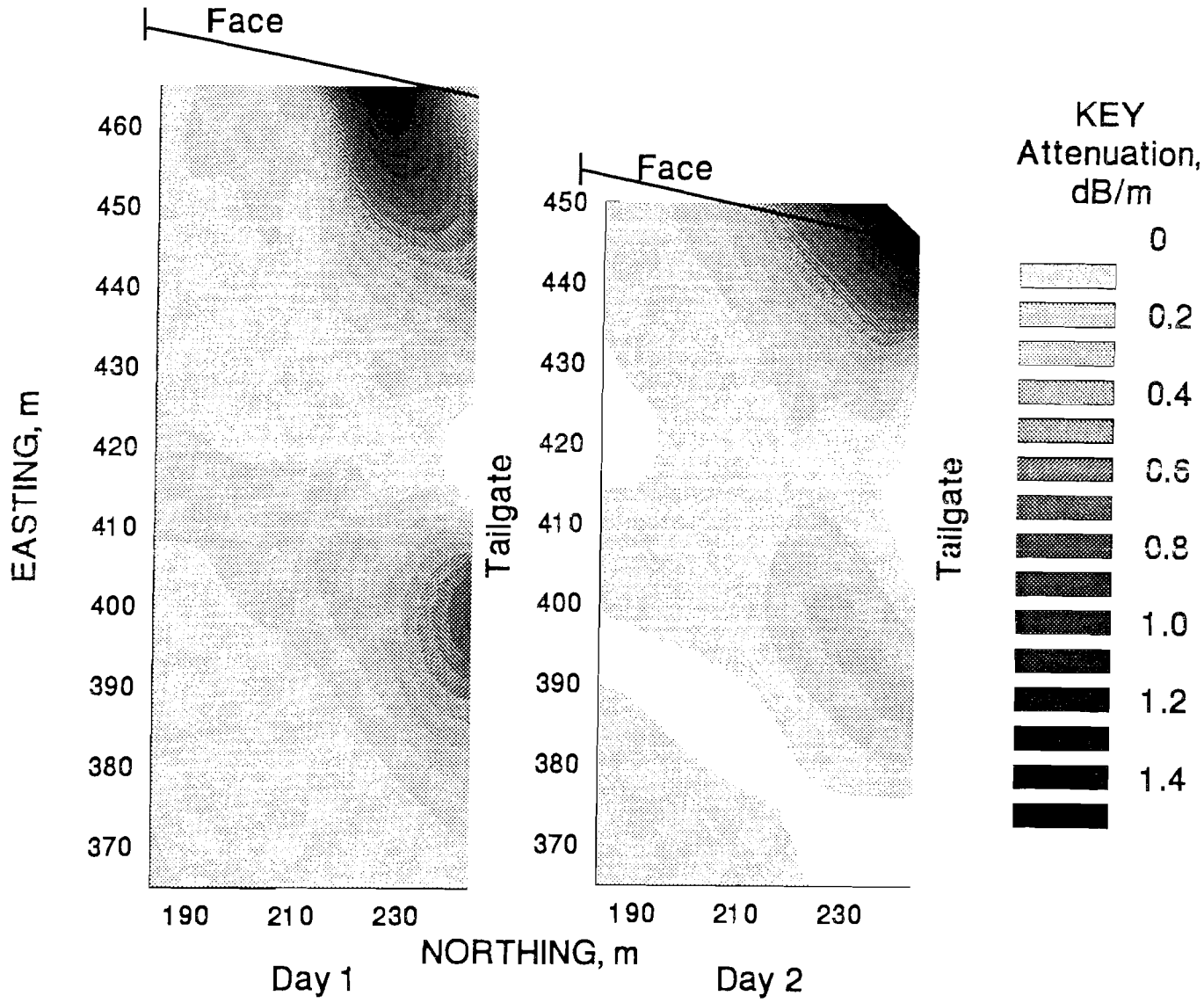

High-attenuation regions near face indicate concentrated loading of forward abutment.

CONCLUSIONS

Seismic tomographic surveys were performed in three case studies. In the first case study, velocity distributions were determined in the floor beneath yield pillars in the headgate near the longwall face. A high-velocity core, which is indicative of high stress, perpendicular to the primary cleat was observed. With the exception of localized failure zones, P-wave velocity increased as the face retreated to within 18 m (60 ft) of the center of the pillar on a subsequent survey, indicating a general stress buildup within the pillar as the face approached.

The second case study mapped the longwall panel as the forward abutment stress moved into the region. An area 60 m (200 ft) long by the entire width of the panel [210 m (700 ft)] was mapped on successive days as the face retreated to within 8 m (25 ft) of the survey area. A region of high shear-wave velocity was observed near the junction of the face and the tailgate. A cross section of the velocity image correlated well with stress measurements obtained from borehole pressure cells.

The final case study detailed an effort to map the panel within 60 m (200 ft) of the tailgate ahead of the face by using the longwall shearer as the seismic source. By assuming a relatively constant level of noise produced by the shearer, attenuation tomograms were generated that allowed inference of geologic and stress anomalies near the junction of the face and the tailgate.

Seismic tomography offers a unique tool to the mining industry. Combining the methods described in this paper with automated acquisition could allow a mine engineer to have continuous updating of the distribution of stress concentrations and geologic anomalies in underground structures. These factors can be examined, and in the case of hazardous conditions, appropriate actions can be taken prior to compromising safe working conditions.

REFERENCES

1. Yu, G. Elastic Properties of Coals. Ph. D. Thesis, MacQuarie Univ., Sydney, Aust., 1992, 133 pp.

2. Shea-Albin, V. R., D. R. Hanson, and R. E. Gerlick. Elastic Wave Velocity and Attenuation as Used To Define Phases of Loading and Failure in Coal. USBM RI 9355, 1991, 43 pp.

3. Westman, E. C., M. M. Foss, and E. M. Williams. Comparison of Stress Distribution Images Generated with P, SH, and SV Velocity Tomograms. Paper in Expanded Abstracts of the 64th Society of Exploration Geophysicists Annual Meeting (Los Angeles, CA, Oct. 23-28, 1994). Soc. Expl. Geophys., 1994, pp. 544-546.

4. Gordon, R. A Tutorial on ART (Algebraic Reconstruction Techniques). IEEE Trans. Nucl. Sci., v. NS-21, June 1974, pp. 78-93.

5. Dines, K. A., and J. R. Lytle. Computerized Geophysical Tomography. Proc., IEEE, v. 67, No. 7, July 1979, pp. 1065-1073.

6. Mason, I. M. Algebraic Reconstruction of a Two-Dimensional Velocity Inhomogeneity in the High Hazles Seam of Thoresby Colliery. Geophys., v. 46, 1981, pp. 298-308.

7. Young, R. P., and S. C. Maxwell. Seismic Characterization of Highly Stressed Rock Mass Using Tomographic Imaging and Induced Seismicity. J. Geophys. Res., v. 97-B9, 1992, pp. 12361-12373.

8. Maleki, H. The Application of Tomographic Methods for the Study of Structural Failure. Paper in Proceedings: Mechanics and Mitigation of Violent Failure in Coal and Hard-Rock Mines. USBM Spec. Publ. 01-95, 1995, pp. 313 to 322.

9. Friedel, M. J., M. J. Jackson, E. M.Williams, and M. S. Olson. Tomographic Imaging of Coal Pillar Conditions: Observations and Implications. Soc. Min. Eng. preprint 94-265, 1994, 19 pp.

10. Westman, E. C. Characterization of Structural Integrity and Stress State via Seismic Methods: A Case Study. Paper in Proceedings of 12th International Conference on Ground Control in Mining, ed. by S. S. Peng (Morgantown, WV, Aug. 3-5, 1994). Dep. of Min. Eng., WV Univ., 1993, pp. 322-329.

11. Jackson, M. J., and D. R. Tweeton. MIGRATOM - Geophysical Tomography Using Wavefront Migration and Fuzzy Constraints. USBM RI 9497, 1994, 35 pp.

12. Williams, E. M., and E. C. Westman. Stability and Stress Evaluation in Mines Using In-Seam Seismic Methods. Paper in Proceedings of 13th International Conference on Ground Control in Mining, ed. by S. S. Peng (Morgantown, WV, Aug. 2-4, 1994). Dep. of Min. Eng., WV Univ., 1994, pp. 290-297.

13. Haramy, K. Y., and R. O. Kneisley. Hydraulic Borehole Pressure Cells: Equipment, Technique, and Theories. USBM IC 9294, 1991. 26 pp.

14. Stearns, S. D., and R. A. David. Signal Processing Algorithms in Fortran and C. Prentice-Hall, 1993, 331 pp.

INTEGRATED SHIELD AND PILLAR MONITORING TECHNIQUES FOR DETECTING CATASTROPHIC FAILURES

By Robert M. Cox,[1] David P. Conover,[1] and John P. McDonnell[1]

ABSTRACT

The Ground Control Management System (GCMS) developed by the U. S. Bureau of Mines has allowed researchers and mine management personnel to monitor geostructural data remotely and evaluate ground stability conditions in real-time during high-speed mechanized extraction of coal from longwall panels. Because of the high rate of advance of mechanized longwall faces and the frequent encounter of changes in geologic structure, mine operators are finding it increasingly difficult to cope with the rapid changing ground conditions encountered during succeeding production shifts. The GCMS offers a solution to these problems by combining existing mine monitoring technology with automated computer analyses specifically formulated for ground control management.

The GCMS has been used to collect and analyze data from several longwall panels instrumented to evaluate (1) shield loading behavior, (2) ground pressure redistribution, and (3) ground failure modes associated with catastrophic floor bumps in tailgate roadways. This paper summarizes practical applications of the GCMS and shows how the system can be used to anticipate and detect ground hazards while mining progresses. Shield loading anomalies and ground pressure changes related to major panel roof failures and catastrophic tailgate roadway closures caused by floor bumps are discussed.

INTRODUCTION

The number of mechanized longwall mining systems installed and operating in U. S. coal mines during the past decade are shown in table 1 (*1*).[2] Also included in table 1 are the annual number of fatal and nonfatal accidents associated with the operation of longwall mining systems and reported by the Mine Safety and Health Administration (MSHA) for the period 1983 through 1993. Figure 1 shows the severity rate of accidents per year associated with longwall coal mining in the United States. The significant coal mine safety hazards associated with the use of high-speed mechanized longwall mining systems are shown in figure 2, and the relative number of accidents per year are shown in figure 3. During the past decade two coal mine disasters have occurred in longwall coal mines: the Wilberg Mine fire (1984), which resulted in 29 fatalities, and the Pyro explosion (1989), which caused 12 fatalities.

The most serious safety problems that frequently occur during the operation of a mechanized longwall panel are those specifically associated with maintenance of the tailgate roadways for adequate face ventilation and as alternative escapeways. Unexpected closures of tailgate roadways because of catastrophic ground failures, defined for the purpose of this paper as roof falls, floor heaves, and pillar bursts, are a constant operating problem for longwall mines and pose continuing dangers to the work force. It is not uncommon to have as many as 5 pct of the longwall faces in the United States idled on a given day because of premature gate road closures. These idle periods typically last about one-half shift, during which time remedial (supplemental) ground supports must be set in the tailgate roadway, under less than ideal working conditions, before

[1]Mining engineer, Denver Research Center, U.S. Bureau of Mines, Denver, CO.

[2]Italic numbers in parentheses refer to items in the list of references at the end of this paper.

Figure 1
Severity Rate of Longwall Mining Accidents.

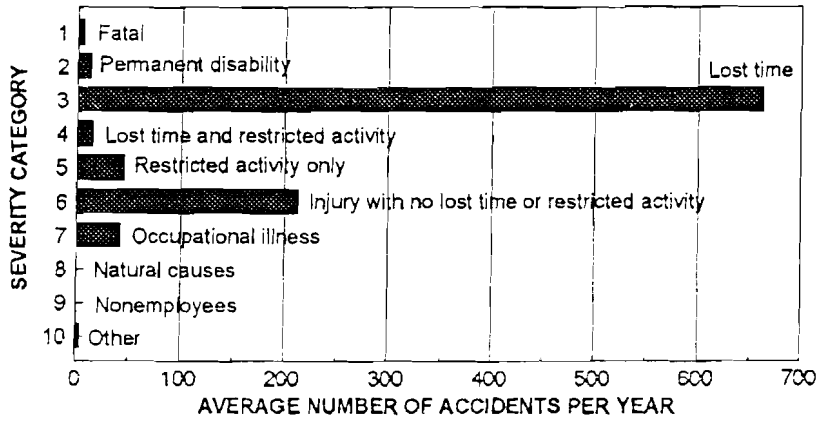

Figure 2
Significant Safety Hazards Associated With Mechanized Longwall Mining.

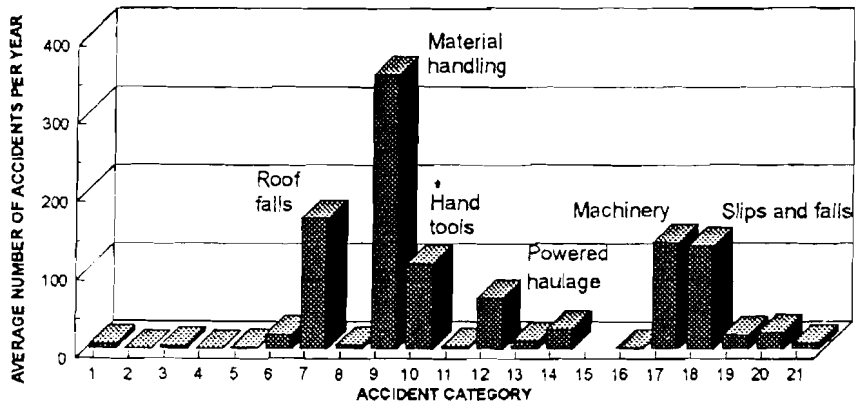

Figure 3
Rate of Significant Longwall Accidents.

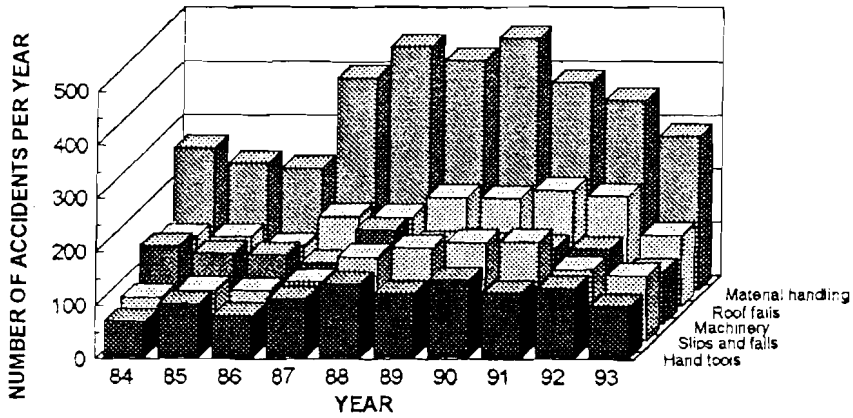

coal extraction can resume in safety. These dangers are significantly increased for longwall faces operating in bump-prone ground. Some longwall faces have been known to be idled for several days or weeks because of catastrophic tailgate closures.

Table 1.—Summary of longwall mines and accidents by year.

Year	Operating longwall mines	Fatal accidents	Nonfatal accidents
1983	118	1	535
1984	112	[1]29	743
1985	108	1	759
1986	99	5	734
1987	96	2	1,047
1988	92	3	1,206
1989	95	[2]12	1,207
1990	96	5	1,239
1991	92	1	1,184
1992	89	1	1,087
1993	89	0	807

[1]Wilberg Mine fire.
[2]Pyro explosion.

The most significant problem facing coal mine operators using modern mechanized longwall mining systems is the difficulty of detecting and responding to changing ground conditions encountered by a rapidly advancing longwall face. Although computer systems have been used extensively to evaluate rock mechanics data (*2*), only recent advances in sensor technology and computer monitoring systems have allowed improved techniques to be incorporated for the remote monitoring and evaluation of geotechnical data from underground coal mines (*3*). Computer-controlled mine-wide monitoring systems are improving safety and productivity in U. S. coal mines (*4*), and such systems have become commonplace for monitoring such diverse items as environmental conditions, electric power distribution, and equipment performance. Ongoing developments are providing additional capability and flexibility, such as control and operation of mining machines and haulage systems (*5-7*).

Although previous ground control studies (*6, 8*) have used data acquisition systems to collect information, the application of these systems in real-time analyses of geotechnical data for ground control planning has not been widespread. Real-time acquisition of data, coupled with automated computer processing, can provide important decision-making tools for mine management (*6, 9*). The current trend in monitoring system development is to integrate separate monitoring systems under the control of a central computer (*5-7, 10*). New computerized ground control technology must be compatible with existing monitoring systems to be of maximum benefit to the mining industry.

The automated Ground Control Management System (GCMS) developed by the U. S. Bureau of Mines (USBM) uses computerized mine monitoring and electronic sensor technology for the continuous acquisition and analysis of geostructural data (*10- 12*). The mine operator now has available a real-time ground control information tool for the effective management of ground stability on high-speed mechanized longwall panels. The computerized GCMS is designed to monitor ground response to the high-speed extraction of longwall panels continuously and to display geotechnical data, such as shield loads and ground pressures, in real time. The GCMS also processes and stores the data and can be used to create graphic displays for both real-time examination of ground stability conditions and to analyze historical trends in the geomechanics data for future mine layouts.

The GCMS is currently being used to monitor geostructural data and evaluate ground stability conditions during the high-speed extraction of coal from mechanized longwall panels in an underground coal mine in northwestern Colorado. To date, the capabilities of the GCMS have been demonstrated during the continuous monitoring and evaluation of data during the extraction of five consecutive longwall panels at the test mine. The resulting data have improved understanding of shield-loading behavior during face operations and ground failure modes associated with catastrophic tailgate roadway failures. A review of characteristic shield pressure patterns and the occurrence of shield pressure anomalies associated with ground failures are presented in this paper.

MONITORING SCHEME

A schematic of the GCMS instrument network is shown in figure 4. The entire system is comprised of commercially available equipment, and all underground components are MSHA approved for permissible use in underground coal mines. The existing system has been configured to monitor continuously shield-loading behavior across the longwall face and ground pressure changes associated with various gate road pillar systems. From time to time, various other sensors have been connected to the system to monitor strata movements. The actual numbers and locations of sensors and trunk cables can be adjusted as necessary to support a wide variety of monitoring programs. The system has also served as a test facility for evaluating the effectiveness of various prototype sensors being developed to measure ground control parameters.

Figure 4
Schematic of GCMS Instrument Network.

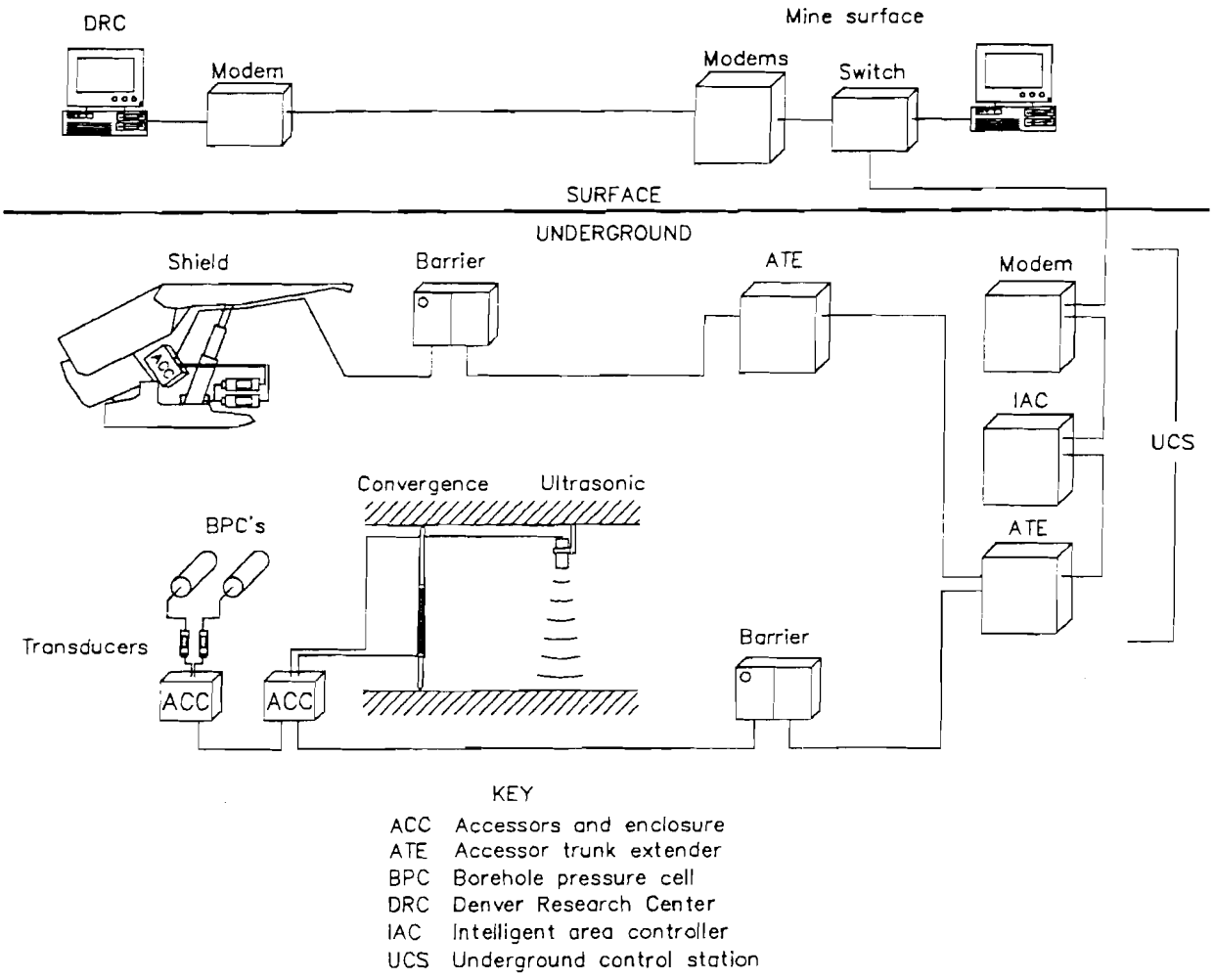

The test site mine is located in the Yampa Coalfield in north west Colorado, about 20 km (12 miles) west of Oak Creek, CO. The coal seam within the test area of the mine is about 340 m (1,100 ft) deep, has a uniform geologic structure, and an average thickness of 3 m (10 ft) (figure 5). The floor consists of interbedded mudstones and bony coal underlain by stronger sandstones and a lower rider coal seam. The immediate roof extends about 31 m (100 ft) above the coal and consists of four distinct layers (A, B, C, and D) of interbedded sandstones and shales overlain by two small rider coal seams occurring beneath a prominent sandstone unit (the Lennox). The remaining overburden consists of several hundred meters of shale beds capped by the massive Twentymile Sandstone.

The mine was developed using a three-entry gate road system with panels approximately 200 m (640 ft) wide and 3,000 m (10,000 ft) long. Panels are mined from west to east. Roadways are 6 m (18 ft) wide, small pillars are 9 m (30 ft) wide by 21 m (80 ft) long, and large pillars are 21 m (80 ft) square. Figure 6 is a map of the mine layout indicating the geometry of the longwall panels, pertinent geologic features, and the locations of gate road instrument sites.

Figure 5
Geophysical Log and Stratigraphy of Test Mine Site.

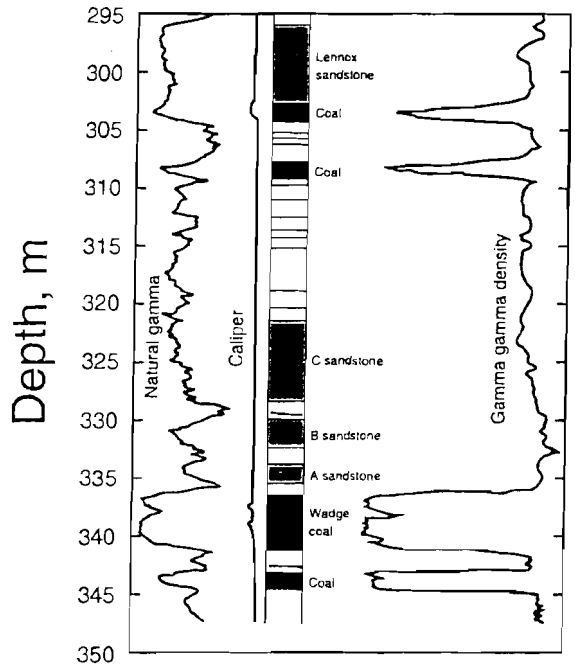

A double ranging drum shearer is being used to mine coal from the longwall face in 76-cm (30-in) cuts using a modified half-face cutting method. In the first pass (from headgate to tailgate), the center of the coal face is cut about 40 cm (16 in) deep, and on the return pass (from tailgate to headgate), the full seam is cut 76 cm (30 in) deep. About 15 cm (6 in) of top coal is left for product quality control. Experience at the mine has shown that this method of mining has improved longwall face roof control and miner safety by reducing stress concentrations along the face and minimizing the hazard of serious face spalling. The method also provides even loading of the face conveyor and section belts.

The longwall face roof is supported by 560-mt (620-st), state-of-the-art, two-legged, electrohydraulic lemniscate shields. The average rate of advance of the high-speed mechanized longwall panels is shown in figure 7 and has increased from 9.4 m/d (30 ft/d) for the first panel to approximately 12 m/d (40 ft/d) for panels 4 and 5. The average panel rate of mining has been about 300 m (1,000 ft) per calendar month, with the mine typically working eight 10-h shifts per week.

The computerized GCMS instrumentation plan was designed to monitor ground behavior continuously during the mining of successive longwall panels. To date, a total of nine gate road ground pressure sites have been instrumented and monitored during the mining of the five longwall panels shown in figure 6. The layout of a typical gate road instrument site is shown in figure 8. Each site consists of borehole pressure cells (BPC's) installed at various depths within boreholes drilled into the coal pillars and panel ribs. These sites are designed to monitor abutment loading characteristics of the coal pillars and panel ribs as adjacent longwall panels are mined.

Although gate road ground pressure instrument sites provide valuable ground control information, they are very labor intensive to install, expensive, and of limited utility for continuous panel-wide monitoring of geostructural conditions. Shield leg pressure monitoring, on the other hand, requires only a single installation per panel and provides continuous data during the extraction of the complete panel. Thus the real-time monitoring of shield-loading behavior is ideally suited for the continuous dynamic analysis of ground stability in and around an active longwall face (*11*).

The locations of instrumented shields across the longwall face were varied for successive panels, as shown in figure 9, to study typical shield-loading behavior along the face and relative behavior between adjacent shields, and to monitor roof-loading characteristics near the tailgate roadway. For practical purposes, such as the close working space along the face and the power limits imposed by the permissible power barriers, no more than 10 shields could be instrumented with one trunk cable (i.e., 20 sensors, 2 legs per shield).

The automated GCMS permits the continuous viewing of the status of all the geotechnical instruments in real time, either in numerical text or graphic form. For example, figure 10 shows a real-time computer display of the positions and current pressure readings of each of the shield pressure transducers located along the panel 4 face and the BPC's at gate road pillar sites 7, 8, and 9 located between panels 4 and 5, as indicated in figure 6.

Figure 6
Test Mine Layout, Geotechnical Features, and Instrument Sites.

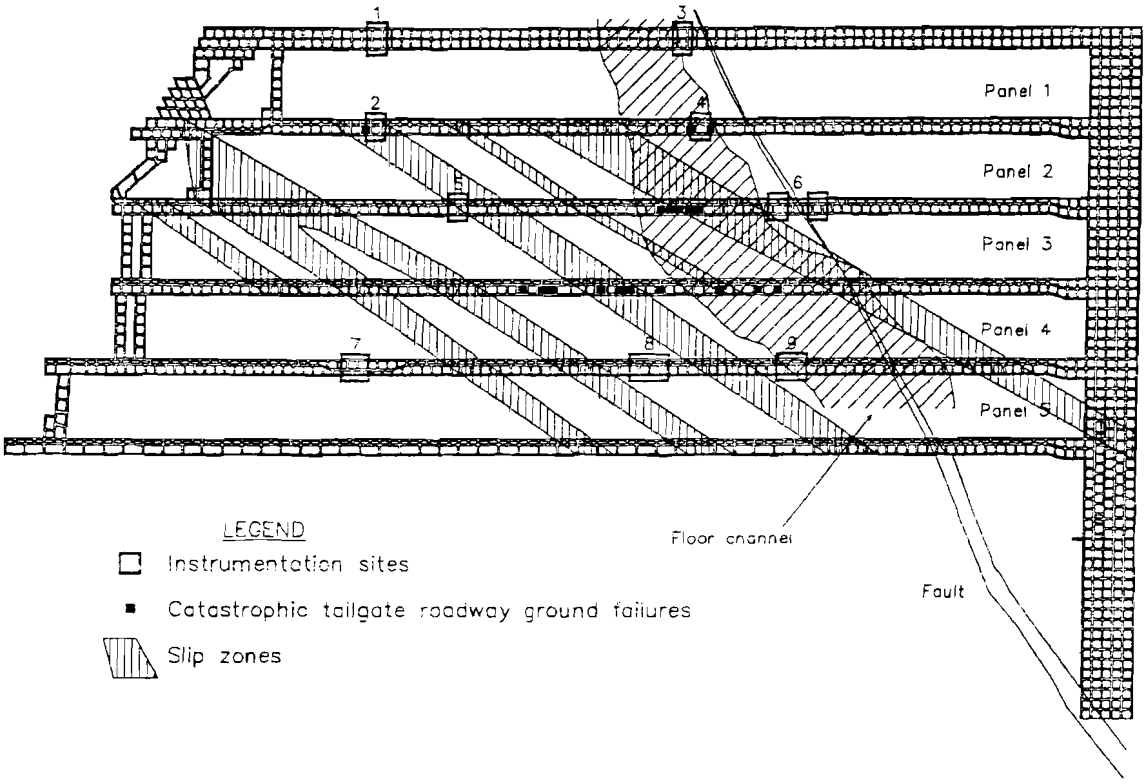

Figure 7
Rate of Advance of High-Speed Mechanized Longwall Panels.

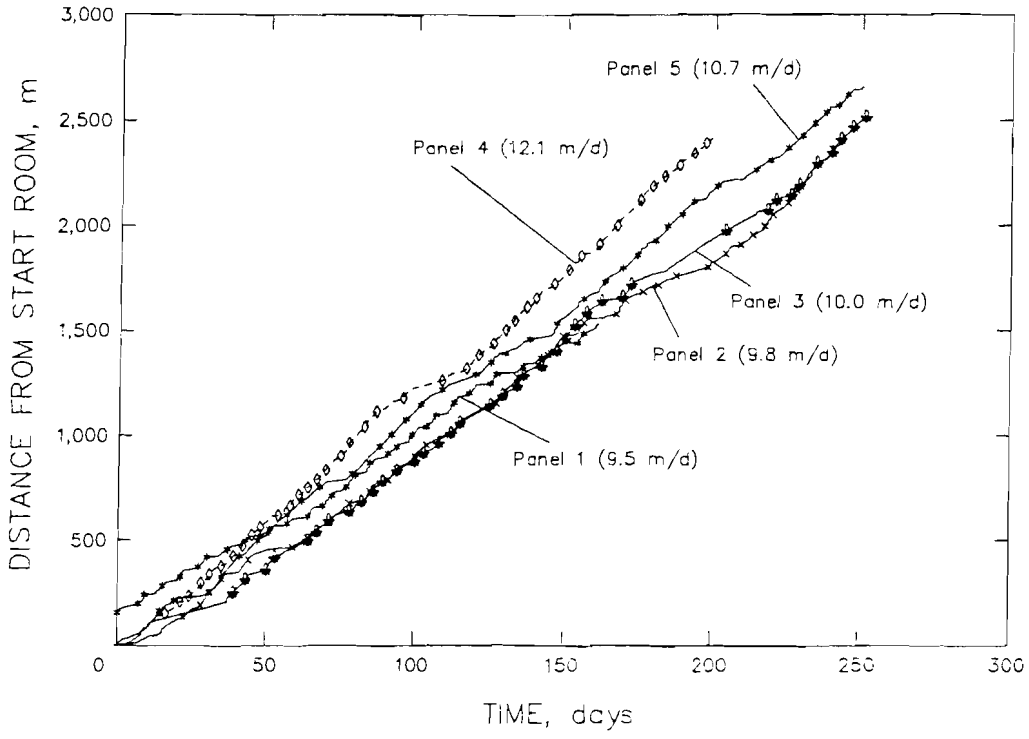

Figure 8
Layout of Typical Gate Road Instrument Site.

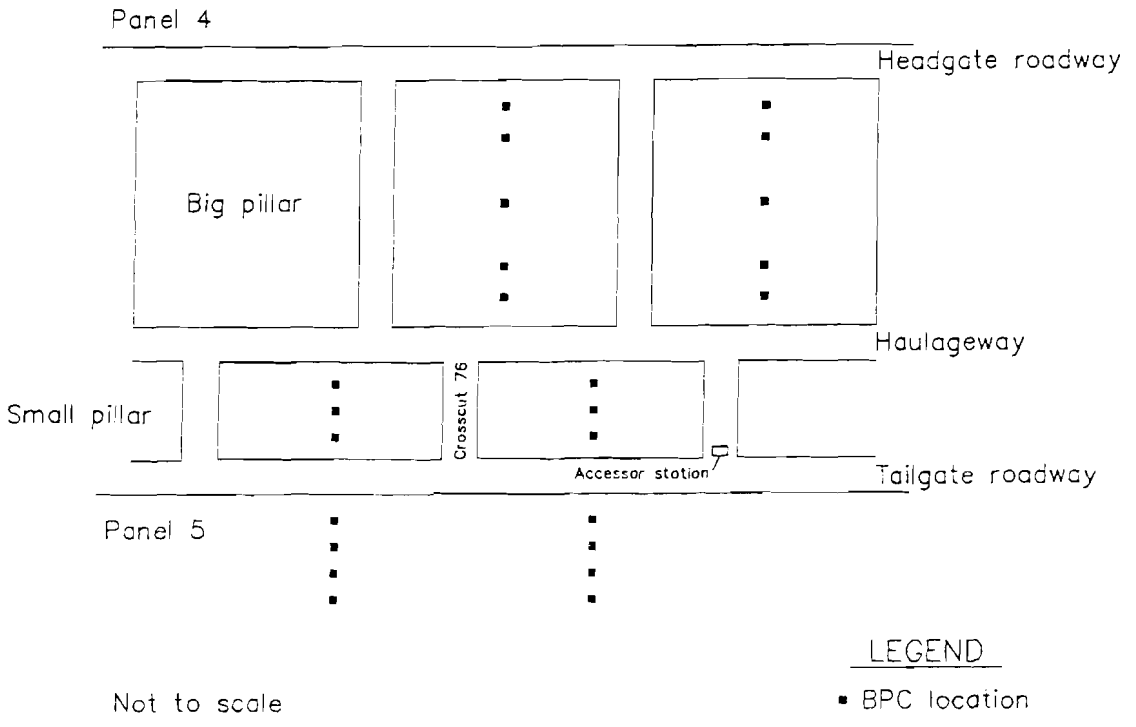

Figure 9
Shield Pressure Monitoring Locations Along Each Longwall Panel Face.

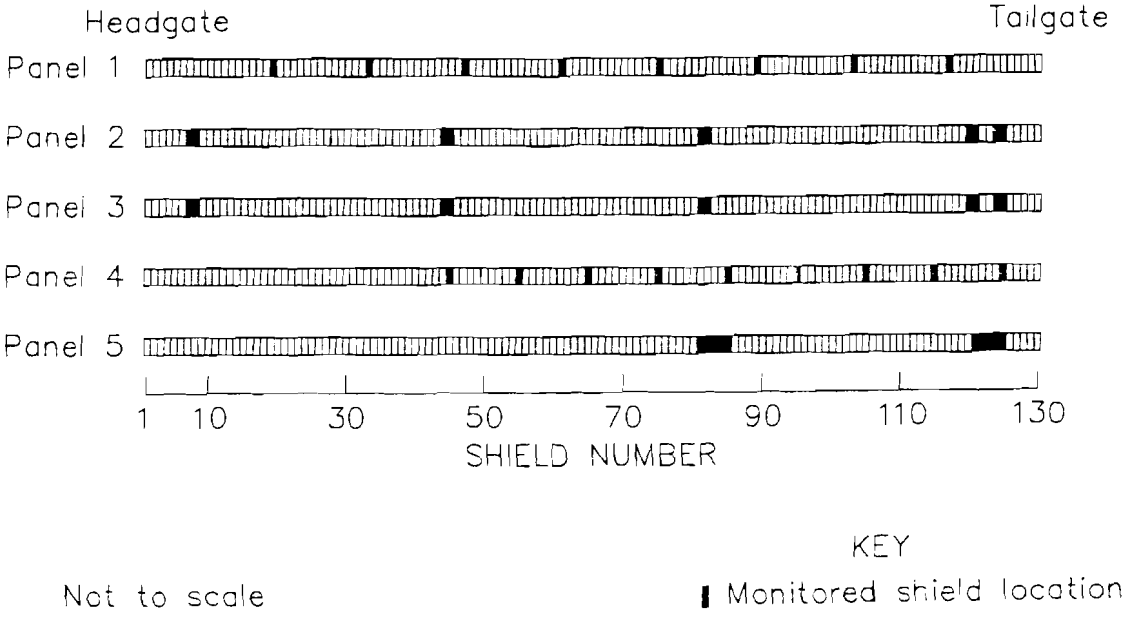

Figure 10
Typical Computer Display of Real-Time GCMS Data.

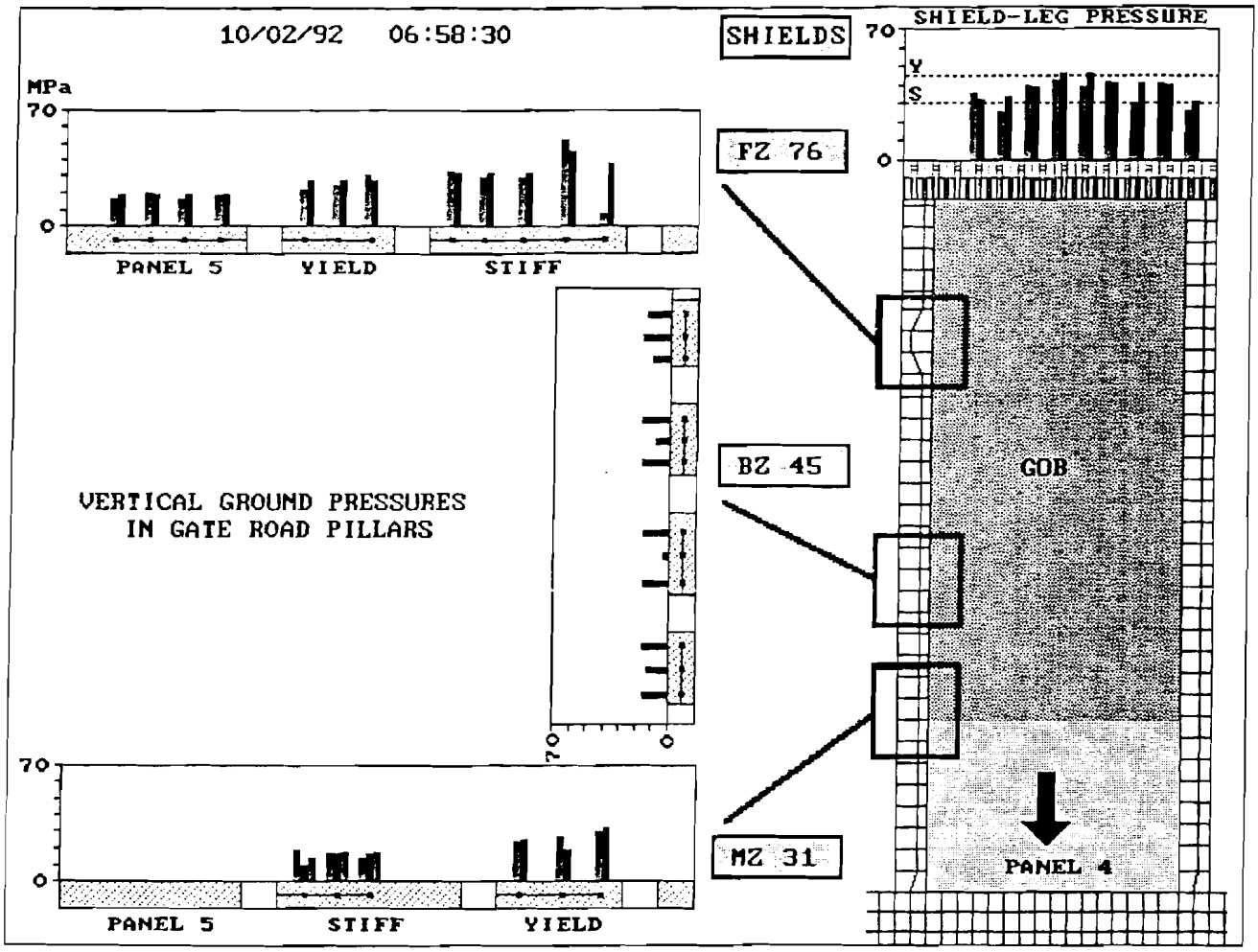

SHIELD AND PILLAR LOADING PATTERNS

To date, the GCMS has been used to collect, store, process, analyze, and evaluate field data from five longwall panels. Typical shield loading as a function of mining cycle time is shown in figure 11 for a typical work day. Normal shield duty cycles for each mining cut across the longwall face usually vary between 30 and 45 min. Longer duty cycles, varying from hours to days, occur during breakdowns, between shifts, and over idle periods such as weekends and vacations. Generally, shield loads continue to increase during these longer cycles, as shown in figure 11, often approaching the yield load of the shields within a few hours. During panel 1 mining, the face typically experienced heavy spalling across the face during the initial cut of a work shift after the face had been idle for several days. The mine subsequently altered its production schedule to reduce the duration of idle periods and now schedules at least one longwall production shift per day (*10*).

Panel-wide shield-loading behavior was analyzed by reducing the shield pressure data for evaluation by calculating the time-weighted average pressure (TWAP) for each shield duty cycle that corresponded to each 0.75-m

Figure 11
Computer Display of Typical Shield-Loading Behavior.

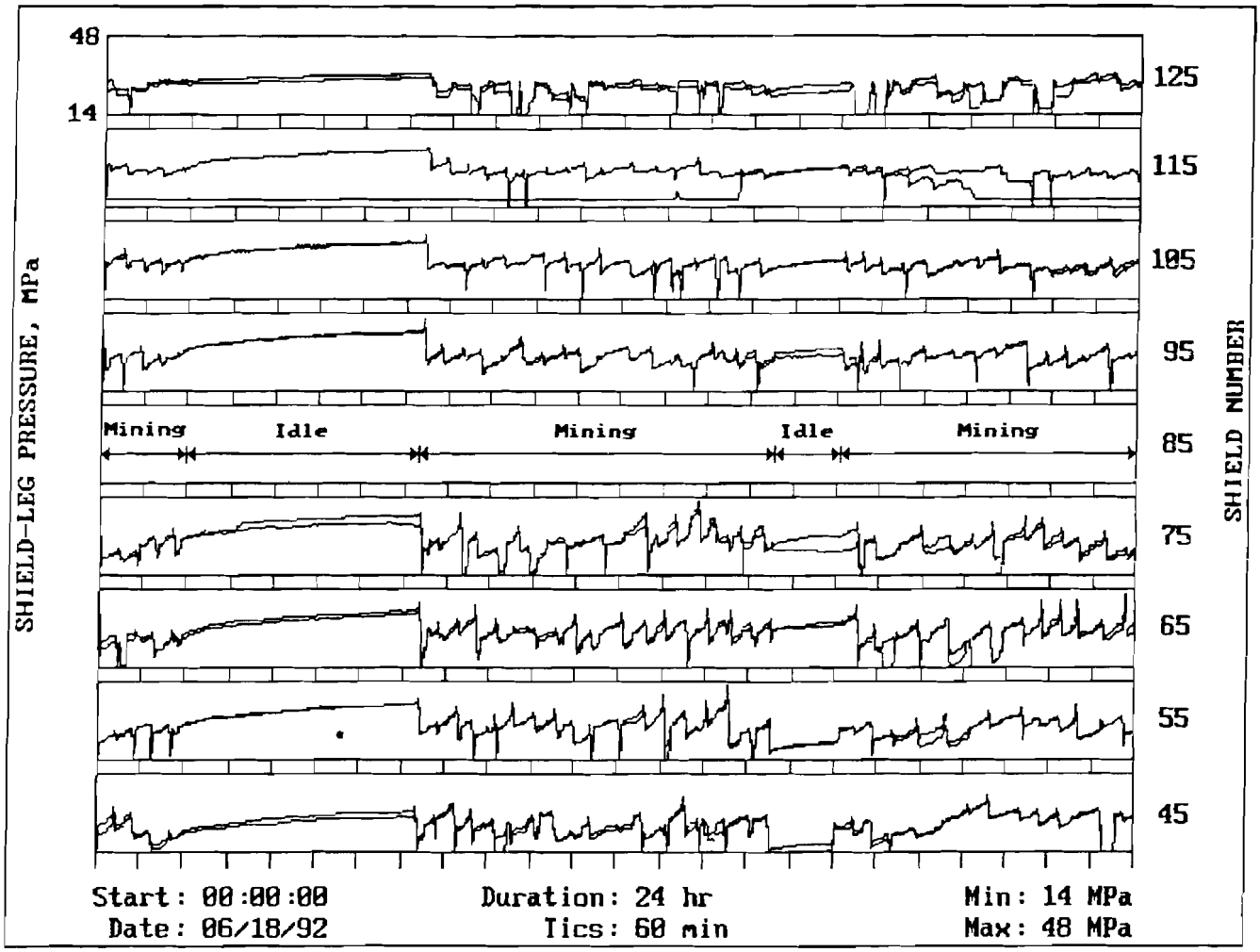

cut (about 30 in) across the face. The TWAP is assumed to be representative of the average support pressure of each shield for each mining cut. The difference between the TWAP and the setting pressure (SP) for each duty cycle (TWAP-SP) has also been calculated to evaluate the behavior of the shields. The TWAP-SP represents the variation in shield loading during a duty cycle. Figure 12 illustrates the typical variations in both the average TWAP and the average TWAP-SP across the longwall face during an operating shift. Although the TWAP distribution is relatively uniform, the TWAP-SP distribution shows significantly greater shield-loading variations in the central portion of the longwall face. Three-dimensional plots of the TWAP data for panels 2 and 3 are shown in figure 13. A review of the data indicates that the average shield pressure tends to be about 3.5 MPa (500 psi) higher in the tailgate third of the panel. The analysis also indicates that the average shield pressure near the headgate roadway is approximately equal to the setting pressure of the shields. This finding suggests that the face area near the headgate edge of the panel is typically protected from high ground pressures by the structural integrity of the headgate roadway pillar system.

Anomalous shield-loading patterns have been observed in association with catastrophic ground failure events at the test mine, such as major roof caves and/or abrupt tailgate roadway closures. Anomalous shield loading was first detected while analyzing the shield data collected during the initial roof caving of panel 2. As shown in figure 14, pressure on the four midpanel shields increased rapidly to yield pressure during two consecutive cycles several hours before the initial roof cave. Also, note that shield pressures did not relieve after the cave but remained at the yield pressure until the shields were advanced at the start of the next shift (*10*).

Anomalous shield loading has also been indicative of catastrophic tailgate roadway ground failures, typically referred to as "floor bumps" by the miners. As shown in computer displays of shield loading behavior presented as figures 15, 17, 20, 21, and 22, the midpanel shields appear to experience greater-than-normal pressure increases during consecutive mining cycles for about 3 to 6 h preceding the occurrence of a tailgate floor bump, whereas the near-tailgate shields experience a rapid increase in pressure several minutes before or during the occurrence of a floor bump. This phenomenon has been designated as a shield pressure "bump signature" that is associated with the occurrence of all known tailgate floor bumps monitored at the test mine.

During the mining of panel 2, a significant tailgate floor bump occurred near gate road instrument site 6L-74 (figure 6) at about 10:30 p.m. on October 18, 1990. A computer display of shield loading behavior during this event is shown in figure 15 and corresponds to the characteristic bump signature previously described. Figure 16 is a computer display of ground pressure changes monitored in the adjacent instrumented gate road pillar site. An analysis of these data indicates a series of increasingly severe ground failures over a period of about 6 h, which culminated in a severe floor bump around 10:30 p.m. The tailgate roadway was closed for the remainder of the shift, and mining did not resume until the tailgate roadway supports were replaced two shifts later.

Three additional floor bumps were monitored during the mining of panel 2 in the vicinity of gate road instrument site 6L-40 (figure 6). Figure 17 is a computer display of shield-loading behavior monitored during the first of these floor bumps reported by the miners to have occurred about 1 p.m. on January 29, 1991, at crosscut 6L-41. The characteristic bump signature is very evident in the plot of the shield pressure data shown in figure 17. Figure 18 is a computer display of the gate road ground pressure changes monitored during the same floor bump. These data show significant ground pressure increases in the pillar site located approximately 45 m (150 ft) outby the longwall face at the time of the floor bump. Figure 19 is a computer display of gate road ground pressure changes associated with the second floor bump that occurred on January 31, 1991, at crosscut 6L-40 adjacent to the instrument site. These data indicate abrupt failure of both the pillar and panel coal ribs adjacent to the tailgate roadway to a depth of at least 6 m (20 ft) inside the original entry rib line. Shield pressure data were not being collected at this time because of problems with the trunk line serving the longwall face instruments. The third significant floor bump occurred as the face passed through crosscut 39 on February 6, 1991, at about 4:45 p.m. just prior to the start of the evening production shift. The characteristic bump signature is very evident in the computer display of the shield pressure data shown in figure 20.

During the mining of panel 3, at least five consecutive tailgate floor bumps occurred as the longwall face passed through crosscuts 44, 43, 42, 41, and 40 during November of 1991 (figure 6). The characteristic bump signature was evident in shield pressure data for each of these events, as shown in figure 21, which is presented here as a representative computer display of panel 3 data. Three of these floor bumps caused severe damage to the tailgate roadway support structures (cribs and posts) outby the face, resulting in cessation of mining operations until resupport of the roadway could be effected.

A similar set of data was collected for floor bump events that occurred during the mining of panel 4 (figure 6). Each of the tailgate floor bumps monitored during the mining of panel 4 produced the same characteristic floor bump signature, as shown by the example computer display presented as figure 22.

Figure 12
Average Values of TWAP and TWAP-SP Variations Across Longwall Face.

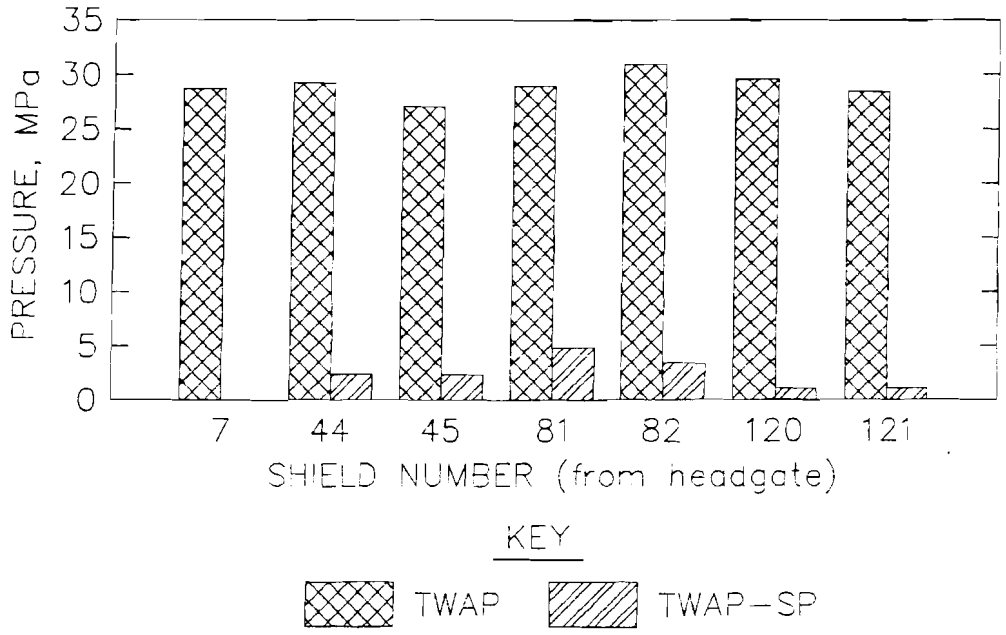

Figure 13
Three-Dimensional Plot of Panel-Wide TWAP Data.

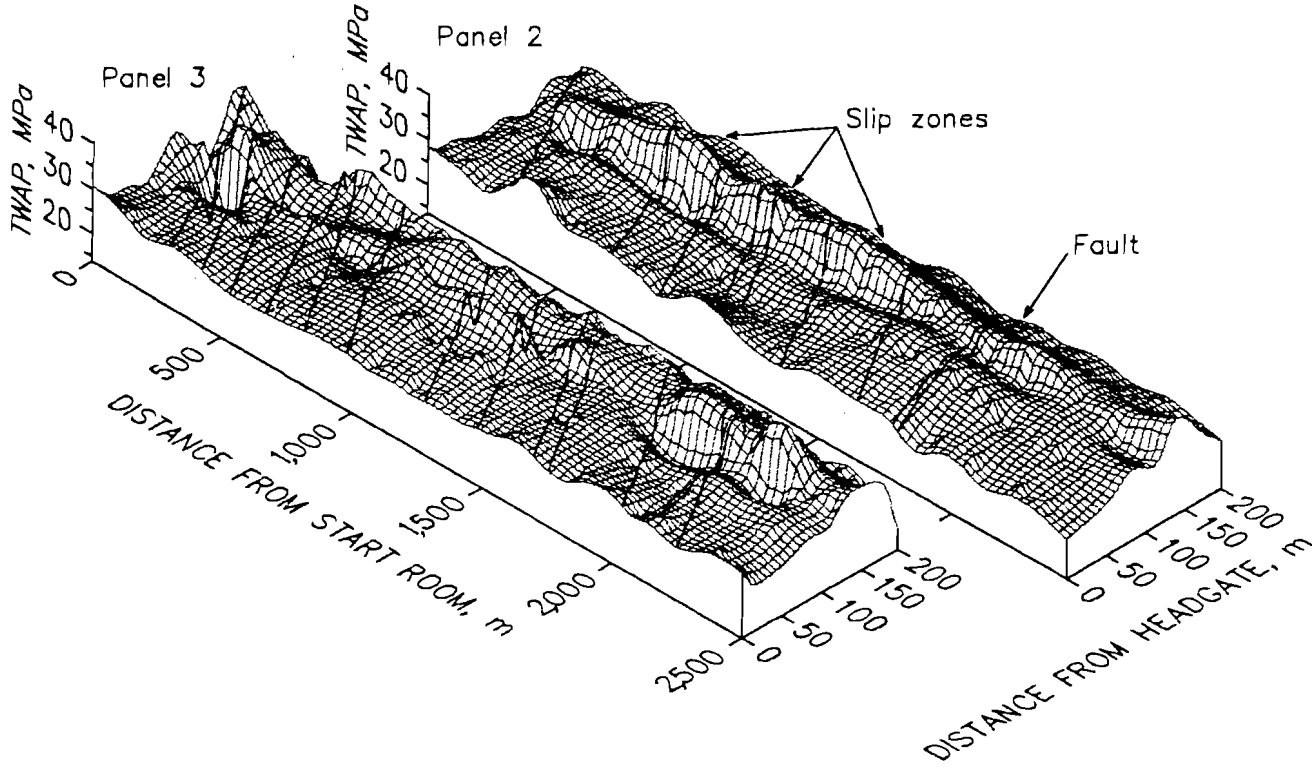

Figure 14
Computer Display of Shield-Loading Behavior Associated With Panel 2 First Cave.

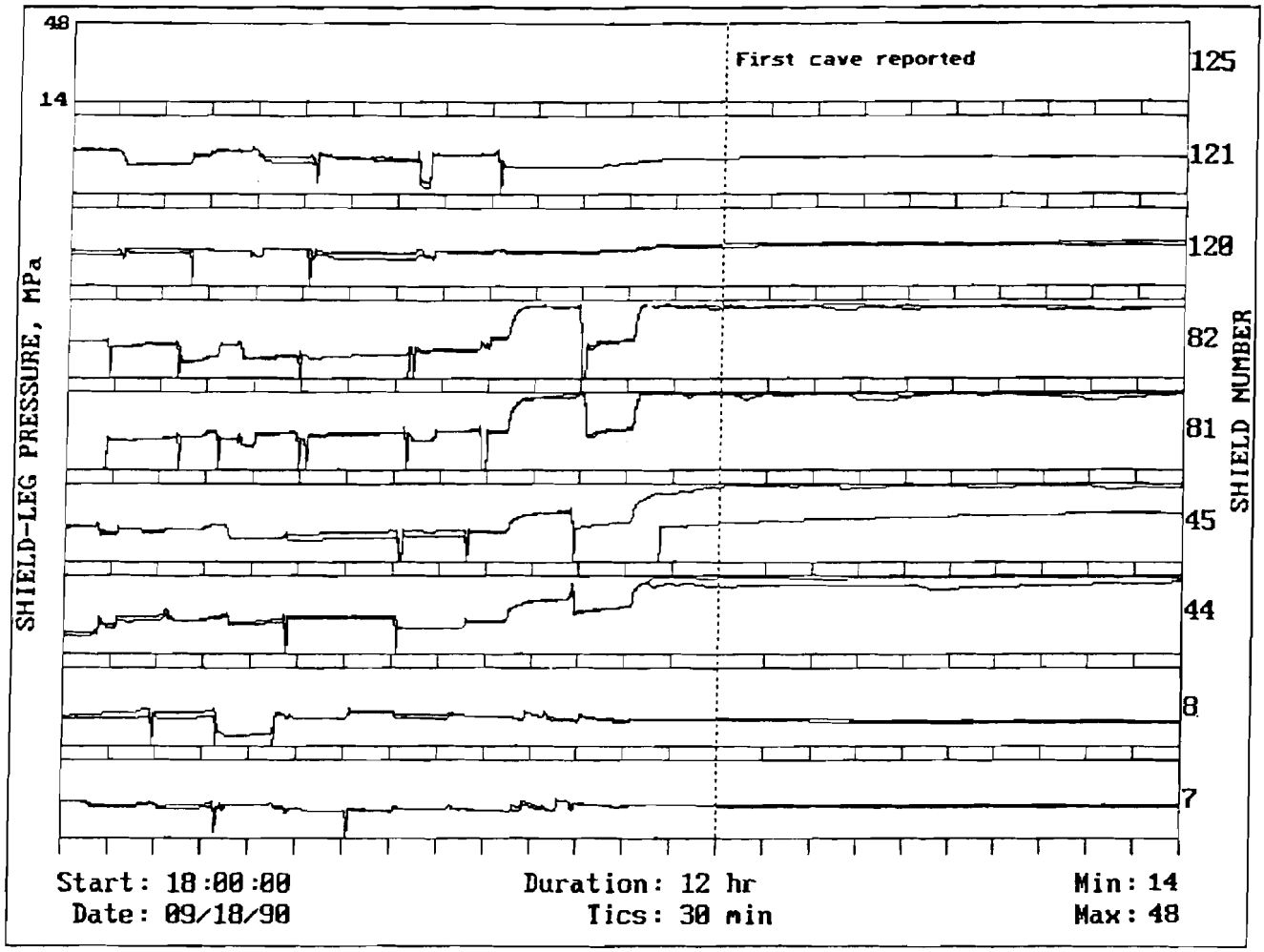

Figure 15
Computer Display of Shield-Loading Behavior Associated With Catastrophic Floor Bump Near Panel 2 Tailgate Roadway Instrument Site 6L-74.

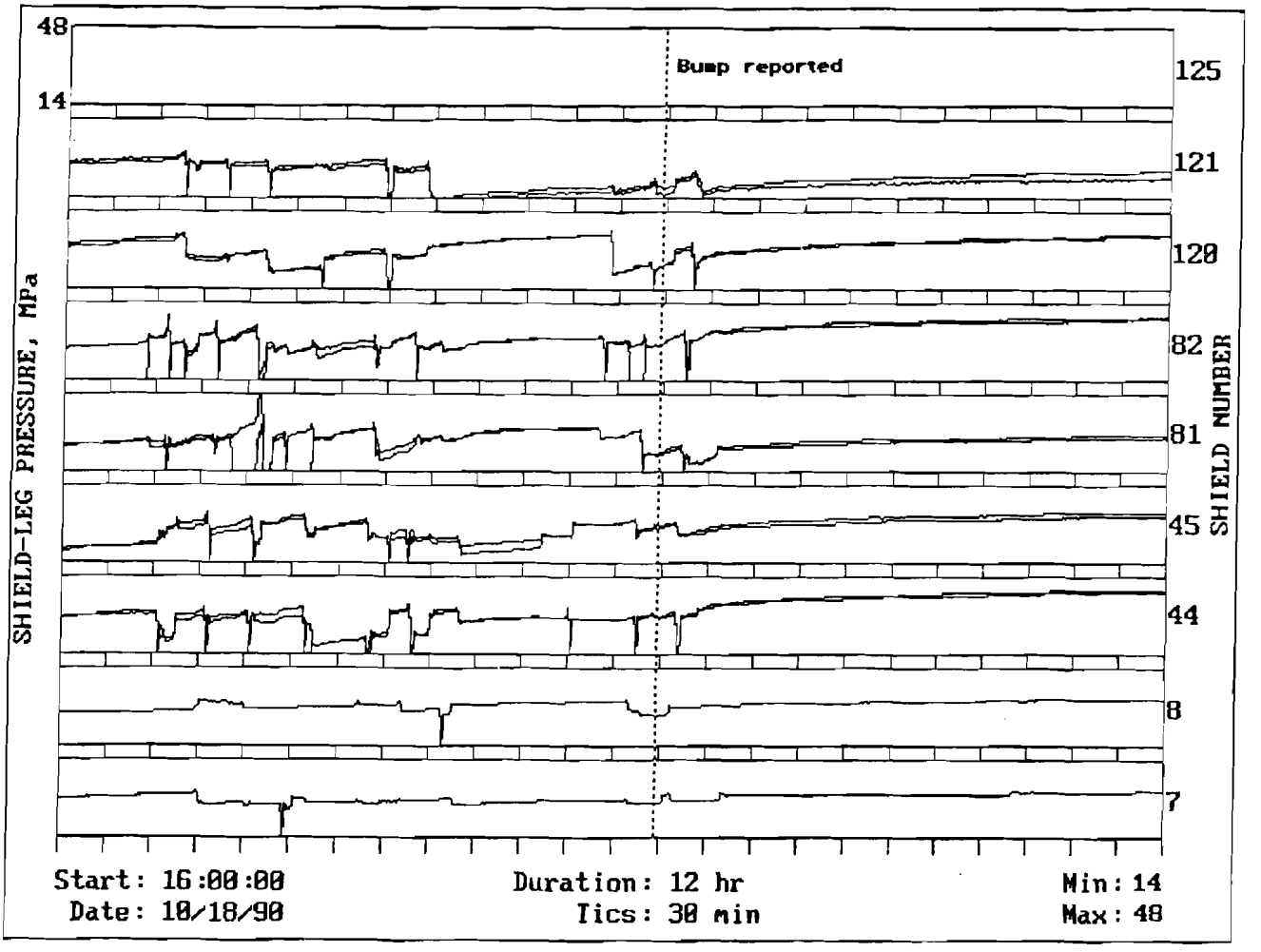

Figure 16
Computer Display of Ground Pressure Changes Associated With Floor Bump Monitored at Instrument Site 6L-74.

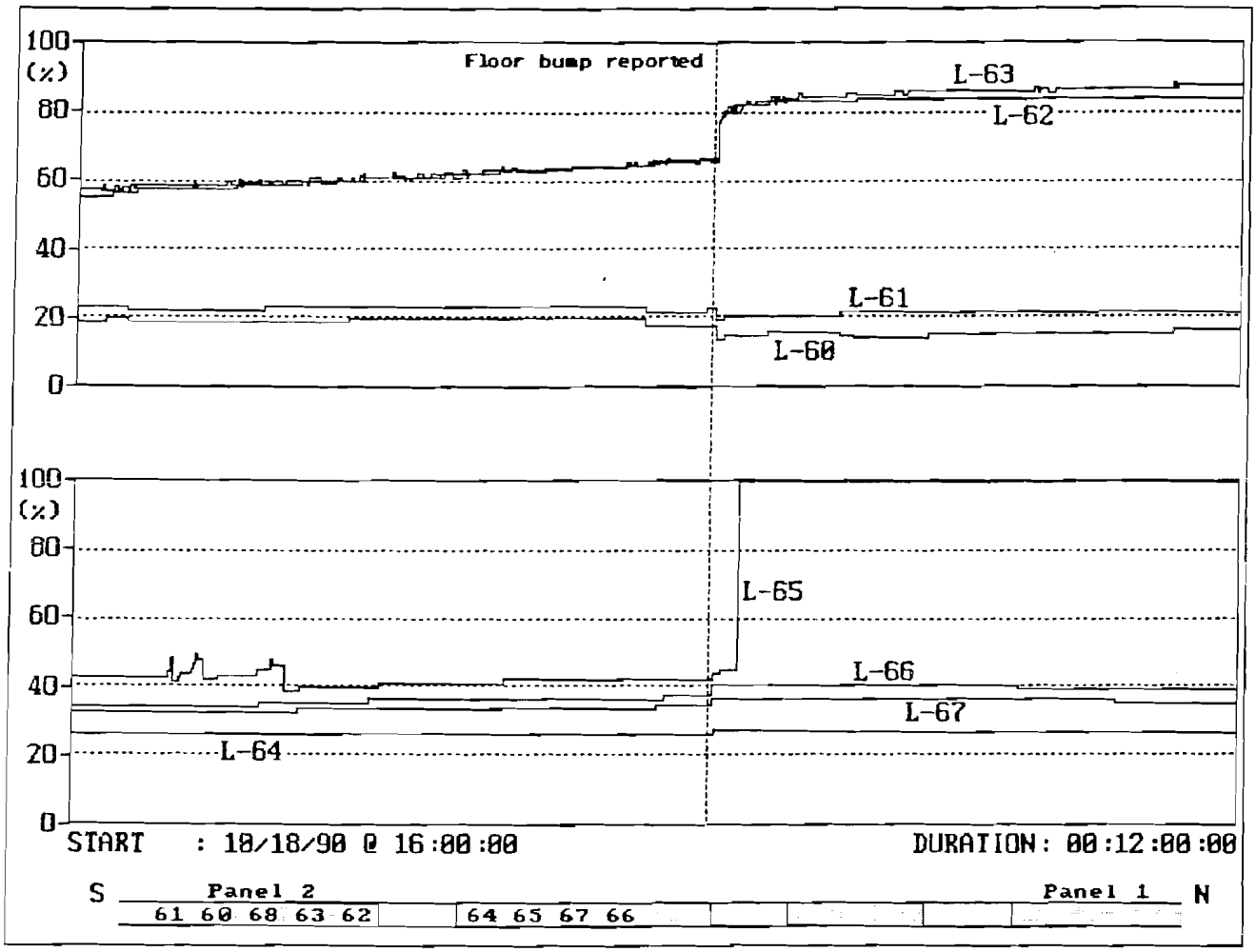

Figure 17
Computer Display of Characteristic Signature Plot of Shield-Loading Behavior During Floor Bump Monitored at Crosscut 6L-41.

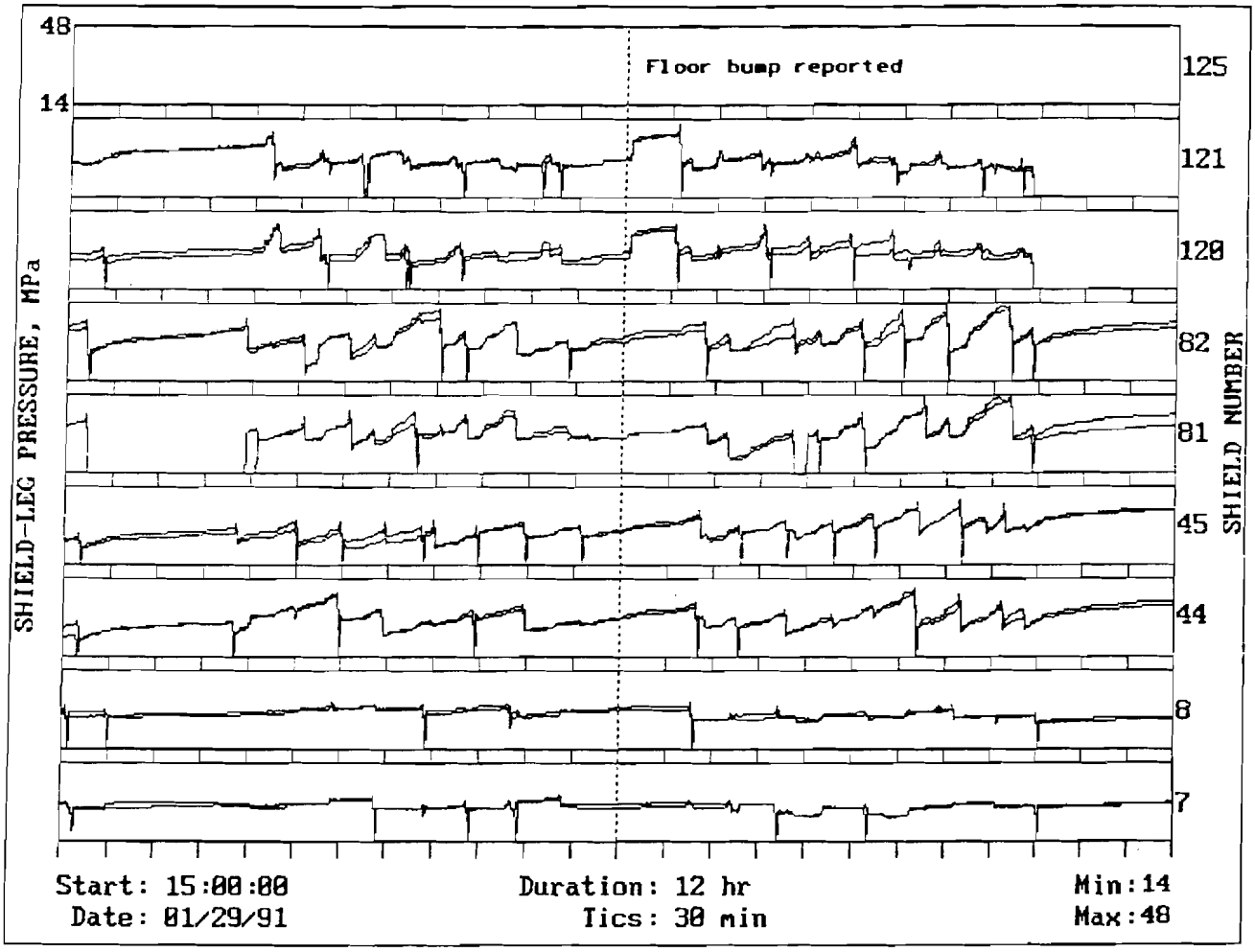

Figure 18
Computer Display of Gate Road Ground Pressure Changes Monitored During Floor Bump at Crosscut 6L-41.

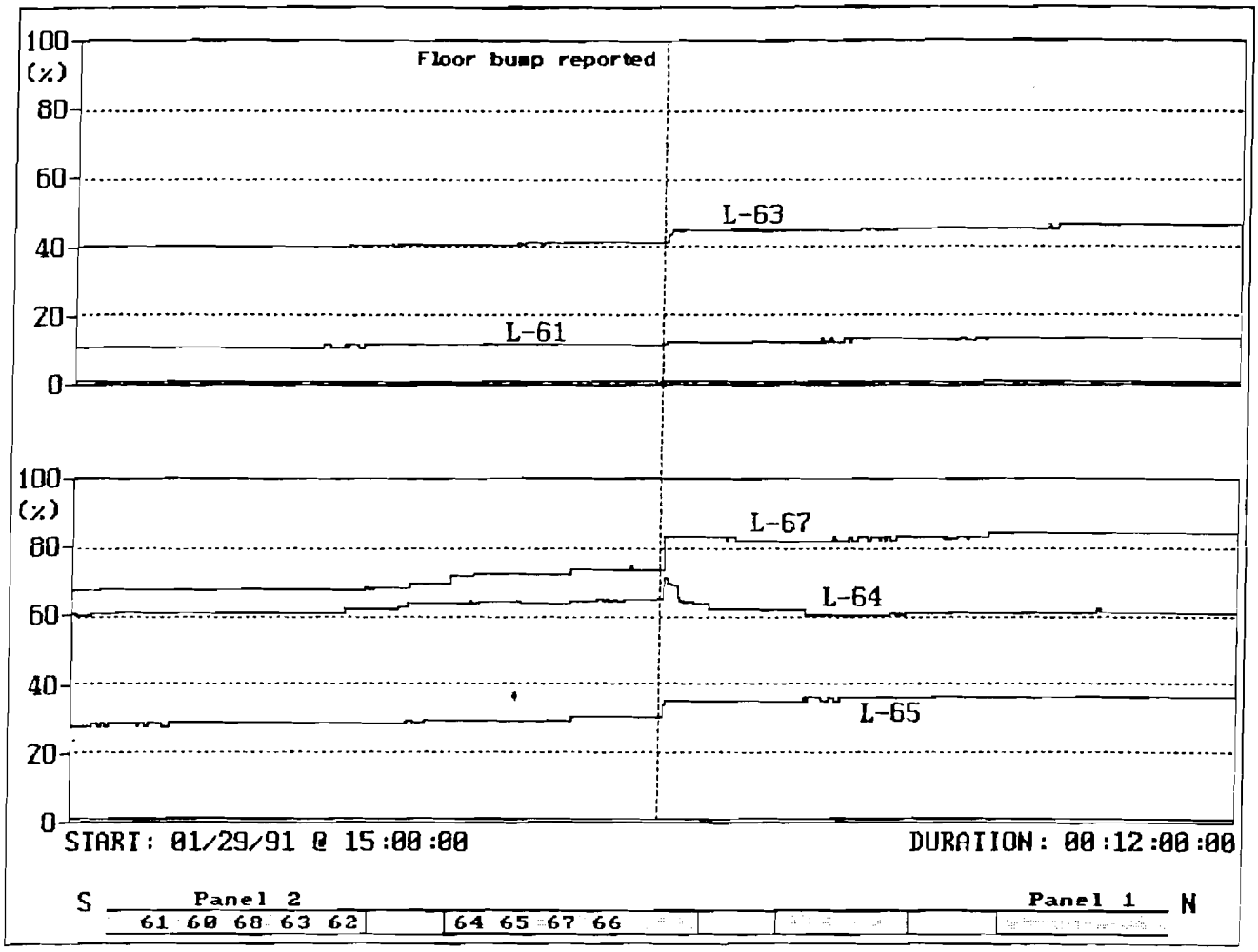

Figure 19
Computer Display of Ground Pressure Changes Associated With Floor Bump Monitored Adjacent to Instrument Site 6L-40.

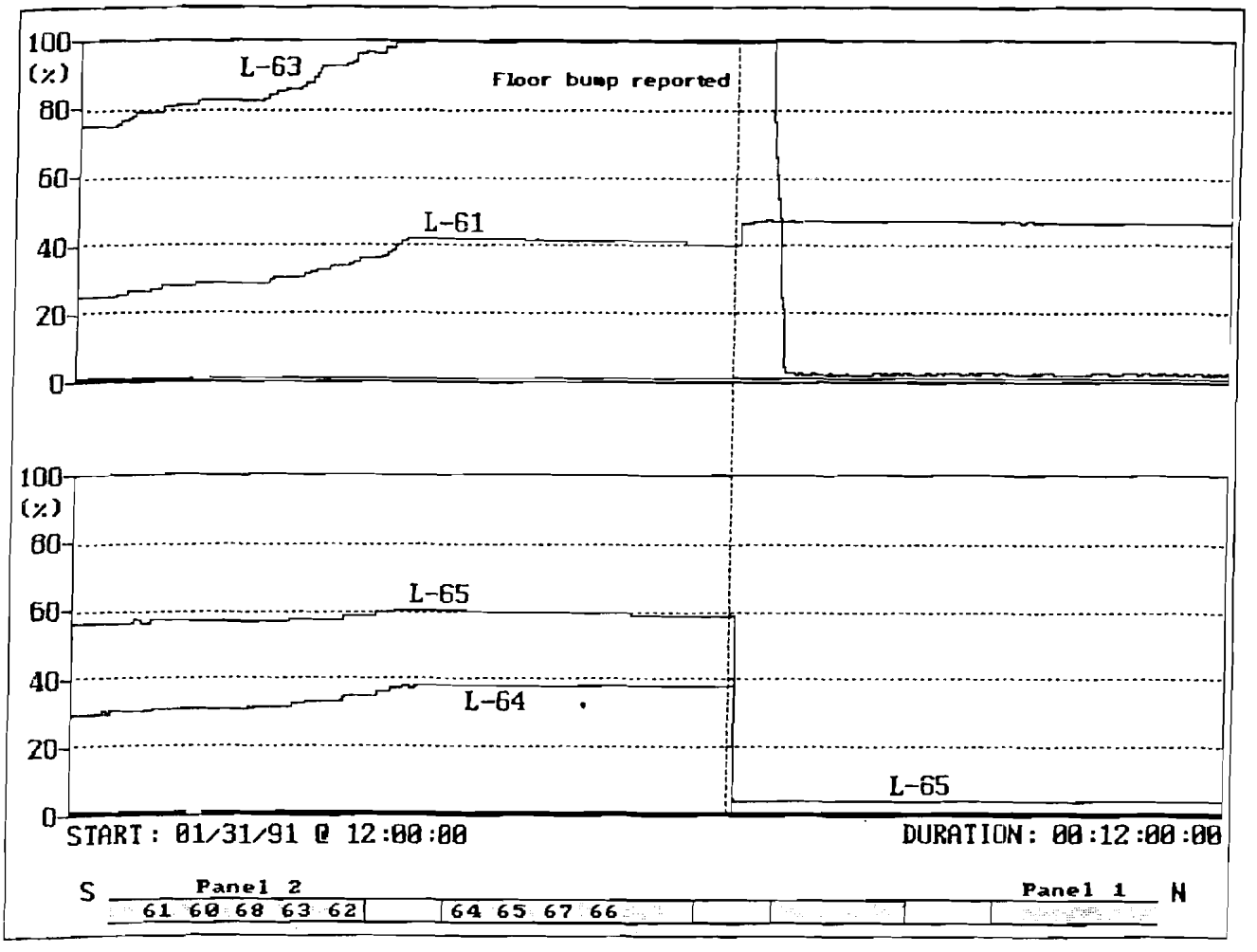

Figure 20
Computer Display of Characteristic Signature Plot of Shield-Loading Behavior During Floor Bump Monitored at Crosscut 6L-39.

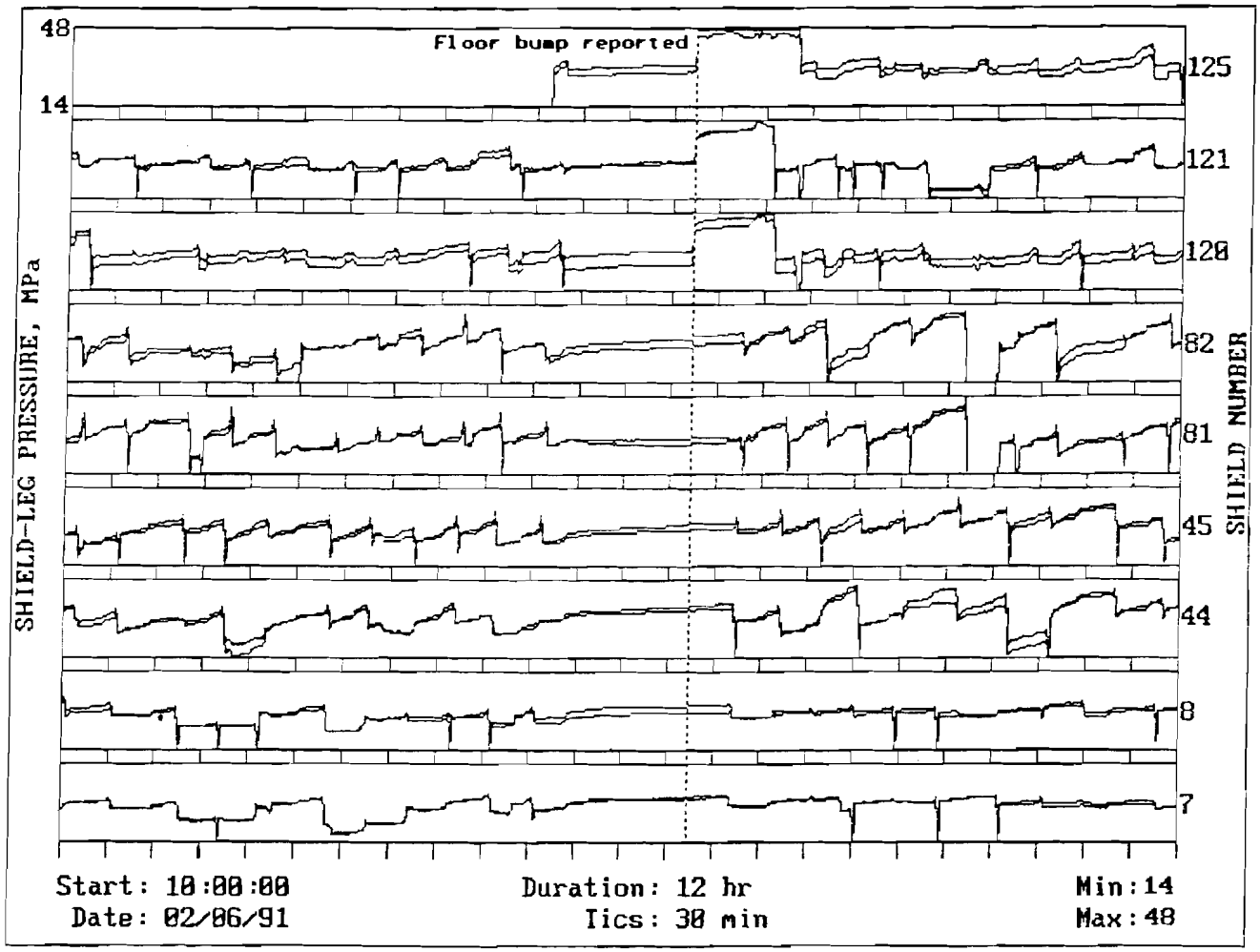

Figure 21
Representative Computer Display of Panel 3 Shield-Loading Behavior During Tailgate Roadway Floor Bumps.

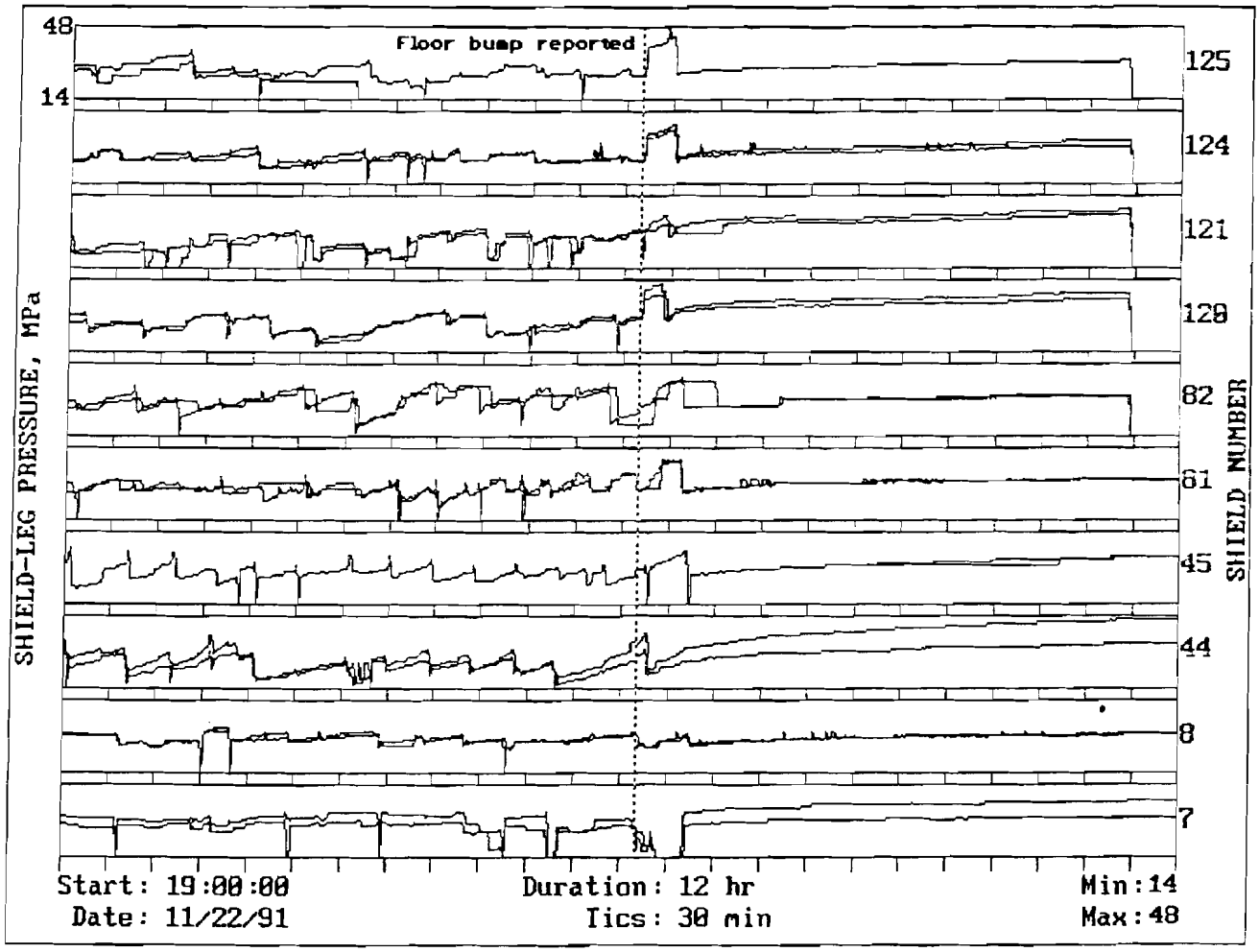

Figure 22
Representative Computer Display of Panel 4 Shield-Loading Behavior During Tailgate Roadway Floor Bumps.

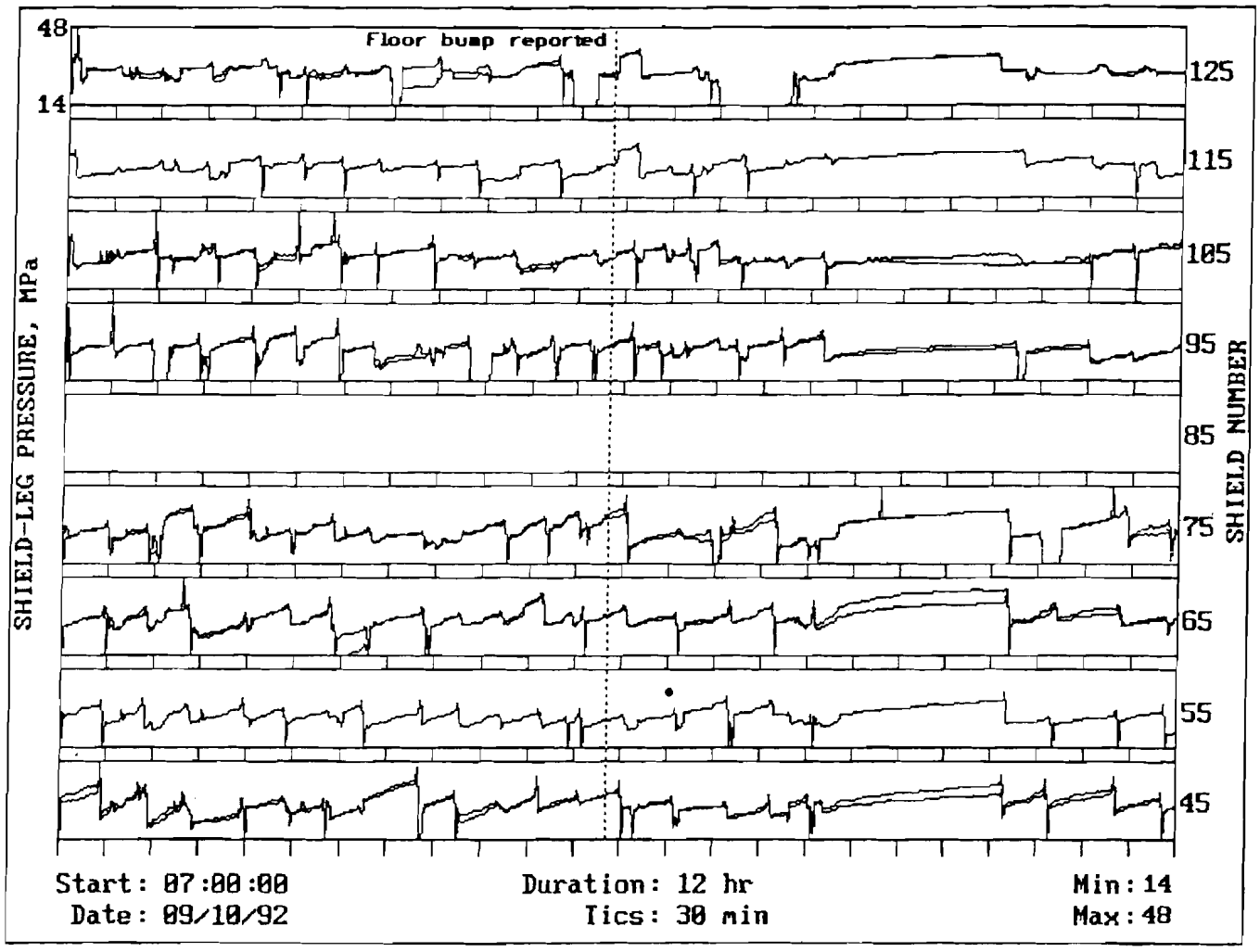

MECHANISM OF TAILGATE ROADWAY GROUND FAILURES

In-mine observations and analyses of available rock mechanics data indicate that the major pressure abutment zones surrounding the longwall panels extend at least 36 m (120 ft) beyond the limits of coal extraction from each of the panels. The sequential extraction of longwall panels has created overlapping abutment zones in the regions enclosing the gate road pillar systems left between the panels. This mining method has created a "pillar-line point" known to be conducive to catastrophic failures in bump-prone ground (*13*). The overlapping pressure abutments apparently overload the pillars left between the panels and create excessive ground pressures, which are a contributing factor related to the cause of the abrupt floor bump phenomenan being observed during the extraction of the longwall panels at the test mine. It was observed that the floor bumps always occurred as the tailgate of the longwall face was passing by an adjacent tailgate roadway crosscut forming, essentially, a four-way intersection. Upon reflection, it is obvious that this would be the location of the greatest ground stress buildup in and around the longwall panel.

The catastrophic tailgate roadway closures typically involved instantaneous floor heave associated with rib spalling and pillar sloughing for a distance of approximately 25 m (80 ft) outby the active face (*14*). In general, the floor bump problem is believed to be related to stiff floor rock conditions. It has been observed that when the tailgate ground conditions are "soft" and roadway convergence is in the range of 15 cm (0.5 ft) or more, catastrophic failure of the tailgate floor and adjacent pillar does not occur. However, when the tailgate ground conditions are "stiff" and entry closure is less than 10 cm (0.4 ft) at the tailgate, catastrophic gate road ground failures usually occur as the face passes through the roadway crosscut. The catastrophic ground failures are usually severe enough to dislodge support structures (i.e., cribs and props) and shut down face operations until the roadway ground structures can be repaired or replaced. In the bump-prone regions of the mine, the immediate floor consists of a relatively strong bed of thin sandstone underlain by a much weaker layer of interbedded coal and clay stringers. This weak layer forms the initial failure plane for the abrupt failure and extrusion of the immediate floor from beneath the adjacent coal ribs when the instantaneous floor heave and associated rib sloughing occur, as shown schematically in figure 23 (*15*). Thus the relative thickness and strength of the immediate floor strata are thought to be the critical factors in determining the relative stability of the tailgate roadway as it is subjected to the increasing ground pressures of the abutment zone created by the retreating longwall panel. Several methods of preventing and/or controlling the floor bumps were devised to facilitate the safe and efficient operation of the longwall panels. Destress blasting of the immediate floor of the tailgate roadway was adopted as being one of the most effective methods of preventing abrupt tailgate floor heave (*15*) and was used successfully to prevent serious floor bump problems during mining of the fifth longwall panel at the test mine.

Figure 23
Schematic of Floor Bump Failure Mechanism.

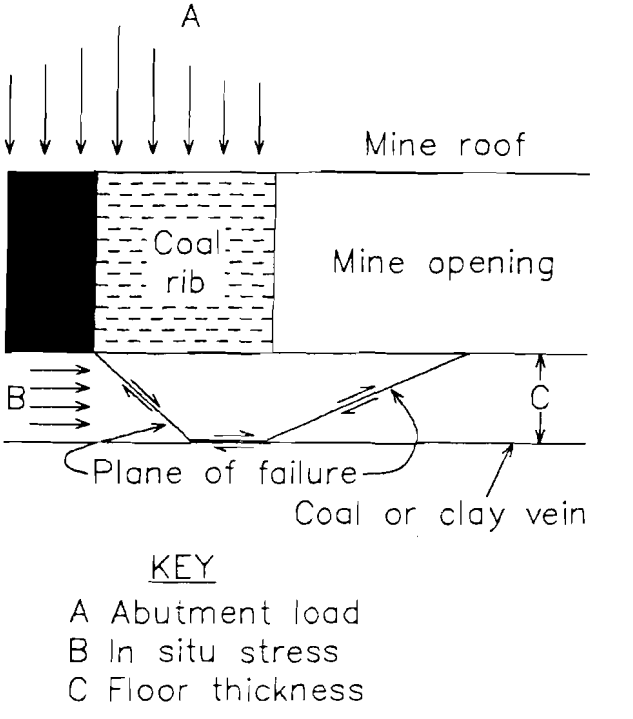

SUMMARY AND CONCLUSIONS

The use of the computerized GCMS to monitor shield-loading behavior and gate road pillar pressure changes continuously has significantly improved understanding of ground behavior during the high-speed extraction of longwall panels using mechanized mining equipment. Much has been learned about the abutment load transfer phenomenon as it relates to gate road stability. The demonstrated correlations between variations in shield pressure and ground failures (i.e., floor bumps and major roof caves) offer mining engineers the first real possibility of developing a real-time alarm system to anticipate impending ground failures associated with high-speed mechanized longwall mining systems. Analyses of anomalous shield pressure data and catastrophic ground failure events associated with these anomalies suggest that shield pressures may be used as precursors of impending ground hazards associated with the high-speed mechanized extraction of longwall panels in underground coal mines. The data indicate that these precursors may precede ground hazard events by several minutes to several hours, thus allowing the mine operator the time needed to take the appropriate action to protect mine workers and prepare for the installation of additional strata support. This early warning capability clearly indicates the need for a continuous monitoring program.

The GCMS provides a continuous flow of geotechnical data from the operating longwall panel. The GCMS is rapidly evolving into a knowledge-based expert system incorporating automatic data collection and analysis techniques that can function both as a real-time ground stability evaluation tool and provide historical data for future mine design and mine planning studies.

REFERENCES

1. Merritt, P. C. Annual Longwall Census. Coal Min. (formerly Coal Age), February issues, 1983 to 1994.

2. Cox, R. M. The Use of a Graphic Mini-Computer System as a Rock Mechanics and Roof Support Design Tool. Paper in Proceedings of the Second Conference on Ground Control in Mining, ed. by S. S. Peng and J. H. Kelley (Morgantown, WV, July 19-21, 1982). Dep. Min. Eng., WV Univ., Morgantown, WV, 1982, pp. 159-170.

3. McDonnell, J. P., R. M. Cox, and J. P. Dunford. Automated Monitoring and Geotechnical Evaluation for Ground Control in Longwall Mining. Paper in New Technology for Longwall Ground Control - Proceedings: U.S. Bureau of Mines Technology Transfer Seminar, comp. by C. Mark, R. J. Tuchman, R. C. Repsher, and C. L. Simon. USBM Spec. Publ. 01-94, 1994, pp. 131-145.

4. Jackson, D. Deserado Gains Edge Through Computer Monitoring. Coal Min., v. 24, No. 12, Dec. 1987, pp. 31-45.

5. Zaburunov, S. A., and A. P. Sanda. Mine Monitoring in America. Coal, v. 24, No. 6, June 1988, pp. 34-40.

6. Barrett, P. British Boost Longwall Efficiency Through Monitoring and Control. Coal, v. 24, No. 6, June 1988, pp. 44-47.

7. Ostermann, W. Utilization of Data Transmission in Modern Mining. Paper in Proceedings of the 8th International Conference on Coal Research (Tokyo, Japan, Oct. 16-20, 1988). 1988, pp. 51-65.

8. Deguchi, G., A. Fukushima, and K. Nishimura. Integrated Monitoring for the Prediction of Outbursts. Paper in the Proceedings of the 8th International Conference on Coal Research (Tokyo, Japan, Oct. 16-20, 1988). 1988, pp. 66-80.

9. Garrity, P., and K. W. Mills. Intelligent Longwall Support Management Systems. Paper in Computer Systems in the Australian Mining Industry (Queensland, N.S.W., Australia, Sept. 1989). CSIRO Div. of Geomech., Univ. Wollongong, Queensland,N.S.W., Australia, 1989, pp. 152-158.

10. Hanna, K., K. Haramy, and T. R. Ritzel. Automated Longwall Mining for Improved Health and Safety at the Foidel Creek Mine. SME preprint No. 91-165, 1991, 8 pp.

11. Conover, D., and K. Hanna. Shield Pressure Monitoring To Detect Longwall Ground Control Hazards. Paper in Proceedings, Forth Conference on Ground Control for Midwestern U.S. Coal Mines, ed. by Y. P. Chungh and G. A. Beasley (Mt. Vernon, IL, Nov. 2-4, 1992). Dep. Min. Eng., S. IL Univ., 1992, pp. 217-226.

12. Hanna, K., and R. Cox. Automated Ground Control Management System for Coal Mine Hazard Detection. Paper in Proceedings of the Second International Symposium on Mine Mechanization and Automation, ed. by G. Almgren, U. Kumar, and N. Vagenas (Lulea Univ. of Tech., Lulea, Sweden, June 7-10, 1993). Balkema, 1993, pp. 681-689.

13. Holland, C. T., and E. Thomas. Coal-Mine Bumps: Some Aspects of Occurrence, Cause and Control. USBM Bull. 535, 1954, 37 pp.

14. Cox, R. M. Tailgate Roadway Convergence: A Key Indicator of Potential Ground Control Problems. Paper in Proceedings of the 13th International Conference on Ground Control in Mining, ed. by S. S. Peng (Morgantown, WV, Aug. 2-4, 1994). Dep. Min. Eng., WV Univ., Morgantown, WV, 1994, pp. 185-189.

15. Buchan, G. M., and R. M. Cox. Cause and Control of Longwall Floor Heave. Paper in Proceedings of the Longwall U.S.A. International Exhibition & Conference (Pittsburgh, PA, June 7-9, 1994). Maclean Hunter, Ormand Beach, FL, 1994, pp. 165-172.

GATE ROAD DESIGN CONSIDERATIONS FOR MITIGATION OF COAL BUMPS IN WESTERN U.S. LONGWALL OPERATIONS

By Matthew J. DeMarco,[1] J. R. Koehler,[1] and Hamid Maleki[2]

ABSTRACT

Longwall mining in the Western United States has long had to contend with the regular occurrence of pillar and panel coal bumps, primarily resulting from deep cover [generally 450+ m (1,500+ ft)], massive sandstone units in the main roof, strong immediate roof and floor strata bounding the coal seam, and the high stress concentrations created along panel peripheries, particularly in multiple-seam workings. To assist mine operators in recognizing bump-prone geologic conditions and, ultimately, in avoiding those entry configurations that further contribute to bump-inducing stress concentrations, this paper summarizes the experience of Western U.S. longwall operations over the past decade. More specifically, this paper highlights those mining conditions that most greatly contribute to bump occurrences, several mining practices that tend to aggravate bump-prone settings, and the problems associated with "critical pillars," the primary contributors to gate road bumps. While U.S. Bureau of Mines research continues to develop proven gate road design technologies, this report serves as a summary of bump control through mine design for Western longwall mines.

INTRODUCTION

Some of the most significant coal-bump problems in U.S. longwall history have been encountered in the Book Cliffs and Wasatch Plateau regions of central Utah, with several fatalities and numerous injuries attributable to this catastrophic failure phenomenon over the past few decades (Koehler, 1994b). Novel gate design approaches and well-planned multiseam mining have largely eliminated the threat of major bumps in the region in more recent years, but with today's higher productivity operations mining seams at even greater depths, the potential for these disastrous events has once again become of serious concern for virtually all of the region's operators. Today, most of the mines in the region are confronted with at least some degree of bump problem, primarily related to mine setting and/or panel design factors. This fact has been all too recently illustrated by the occurrence of serious bump events in longwall *headgates* at two major operations in the region, which is a situation that will continue to plague operators as several mining companies look at moving into areas of the coal district with histories of serious bump problems. This paper presents an overview of the conditions that contribute to bumping in the Wasatch and Book Cliffs Coalfields. It further examines a few of the more major problems with mine design that may aggravate already bump-prone mine settings and emphasizes the severity of bump problems resulting from the misapplication of gate road designs. A very recent example of critical pillar usage at the Sunnyside Coal Co.'s No. 1 Mine, near Sunnyside, UT, is also given.

[1]Mining engineer, Denver Research Center, U.S. Bureau of Mines, Denver, CO.

[2]Mining engineer, Spokane Research Center, U.S. Bureau of Mines, Spokane, WA.

GROUND CONDITIONS CONDUCIVE TO BUMPING IN WESTERN LONGWALL MINES

Western longwall operations often contend with a number of mining conditions conducive to the development of serious coal bump problems. Among these conditions are some of the greatest cover depths in the United States [up to 900 m (3,000 ft)], dramatic variations in overburden depths along the length of a panel because of ridge-and-canyon topography, massive sandstone units in the main roof, strong immediate roof and floor strata, strong coal seams with impersistent cleat systems, persistent sand channeling in the immediate roof, and, at some locations, a variety of structural discontinuities such as faults and shear zones. Many mines along the Wasatch Plateau and Book Cliffs escarpments encounter a critical combination of these conditions at some point. Not surprisingly, these conditions have been well cited as the primary contributors to coal bumps in Eastern coalfields (Iannacchione and DeMarco, 1992).

DEEP, VARIABLE COVER

Western coal mines susceptible to bump-prone conditions are generally situated either in the mountainous regions of Colorado or the plateau escarpments of central Utah (figures 1 and 2). As a result, cover depths can be extremely variable over very short distances, commonly exceeding 300 m (1,000 ft) just inby the mine portal. Currently, longwalling in the Wasatch Plateau and Book Cliffs regions is conducted at mining depths ranging from 300 m (1,000 ft) to nearly 900 m (3,000 ft), with average depths of approximately 600 m (2,000 ft). The trend of future mining in this region should involve deeper operations for many years to come.

At most operations, the onset of bump problems has occurred around a depth of 450 m (1,500 ft); however, there are exceptions to this rule of thumb because of panel and/or pillar geometry, number of panels mined, site geology, etc. In some cases, bumps have occurred at depths as shallow as 225 m (750 ft) (Koehler, 1994b). Experience has demonstrated that, in many instances, proper mine design can largely eliminate bumps altogether, as has been the case at several mines operating at depths in excess of 600 m (2,000 ft).

The mountainous topography of central Utah not only engenders coal bumps attributable to great mining depths, but also creates problems along panels where large variations in mining cover occur. For example, a recent study at the Sunnyside operation (described later in this paper) reported cover depths ranging from approximately 840 m (2,800 ft) near the start-up room to 420 m (1,400 ft) at midpanel to 870 m (2,900 ft) near the projected face stopline along approximately 1,500 m (5,000 ft) of panel. This widely varying ridge-and-canyon setting created considerable problems in predicting when and where bump-prone conditions might be encountered, which is a situation common to area mines. In addition, due to inherent spatial variations of sandstone channels and large sandstone units, and their stress-concentrating properties (Maleki, 1988), overall stress distribution near the seam can vary over a short distance, complicating coal bump predictions.

This problem was also seen at the now-idle Castle Gate No. 3 Mine, where rapid changes in topography made it almost impossible to determine when bumps would occur along the longwall face (figure 3). Face destressing near the tailgate of the 9th East panel (6th panel), a technique that employed a combination of face and tailgate high-pressure hydrofracture holes, was suspended when the longwall came out from under 600 m (2,000 ft) of cover and overburden loads became much lower [depths of 330 m (1,100 ft) to 420 m (1,400 ft) along the face]. The massive Castle Gate sandstone was not present over this portion of the panel and mining proceeded smoothly.

As the face advanced beneath the canyon escarpment once again, stress-relief drilling and hydrofracturing were resumed in an effort to reduce potential face bump conditions; however, the complicated nature of panel loading beneath the edge of the cliffs relegated the success of the destressing program to speculation. The result was that use of these stress-relief techniques was discontinuous and

Figure 1
Ridge-and-Canyon Topography Typical of Book Cliffs and Wasatch Plateau Coalfields.

Figure 2
Escarpment of Wasatch Plateau Near Huntington, UT.

erratic until some form of verification was obtained that the drilling was indeed necessary. Such verification came shortly after when a severe face bump stopped mining for several days, indicating the ineffectiveness of the destressing effort. The mine was idled a couple of months later, in April 1989, after the occurrence of several additional bump events (Barron, 1994).

Maleki (1995) has also documented the occurrence of a severe coal bump in an Eastern coalfield due to sudden changes in stress gradient near a ridge providing 660 m (2,200 ft) of mining cover.

MASSIVE SANDSTONE UNITS

One of the leading contributors to coal bumps in the Wasatch-Book Cliffs Coalfields is several massive sandstone units that commonly make up the main mine roof and floor. Among these, in ascending order, are the Starpoint, Spring Canyon (often considered a tongue of the Starpoint), Aberdeen, Kenilworth, Sunnyside, and Castle Gate sandstones (Barron, 1994). Most of these sandstones either bound or are located within the coal-bearing Blackhawk Formation, as shown in figure 4. These sandstones are by no means the only units of strong, competent strata within the Blackhawk; numerous smaller sandstone units and exceptionally strong siltstones make up much of the main roof overburden in the region (figure 5).

The presence of these units contributes to bump-proneness in several ways. Their strength and continuity, particularly in the Castle Gate Sandstone, allow load transfer over the gobs of several panels before they fail and reach a state of maximum subsidence. The result can be, and often is, the transference of considerable abutment loads over relatively large distances. Canyons naturally help to alleviate this problem, but the potential still exists for this excessive load transfer at most of the mines operating along the escarpment front. Case studies have demonstrated good ground conditions typically exist on the first, and possibly the second, panel; however, the third panel tailgate often takes the brunt of the severe abutment loads. Once good caving has been established, these problems generally decline in severity. The use of wider panels has been often recommended to enhance cave conditions (Barron, 1994; Maleki, 1988).

The sudden failure of these massive units is also a contributing factor in the initiation of coal bumps (Maleki, 1995). A recent analysis of a severe coal bump in a Book Cliffs mine has emphasized that the failure of surrounding

Figure 3
Longwall Panel Layouts at Castle Gate No. 3 Mine.

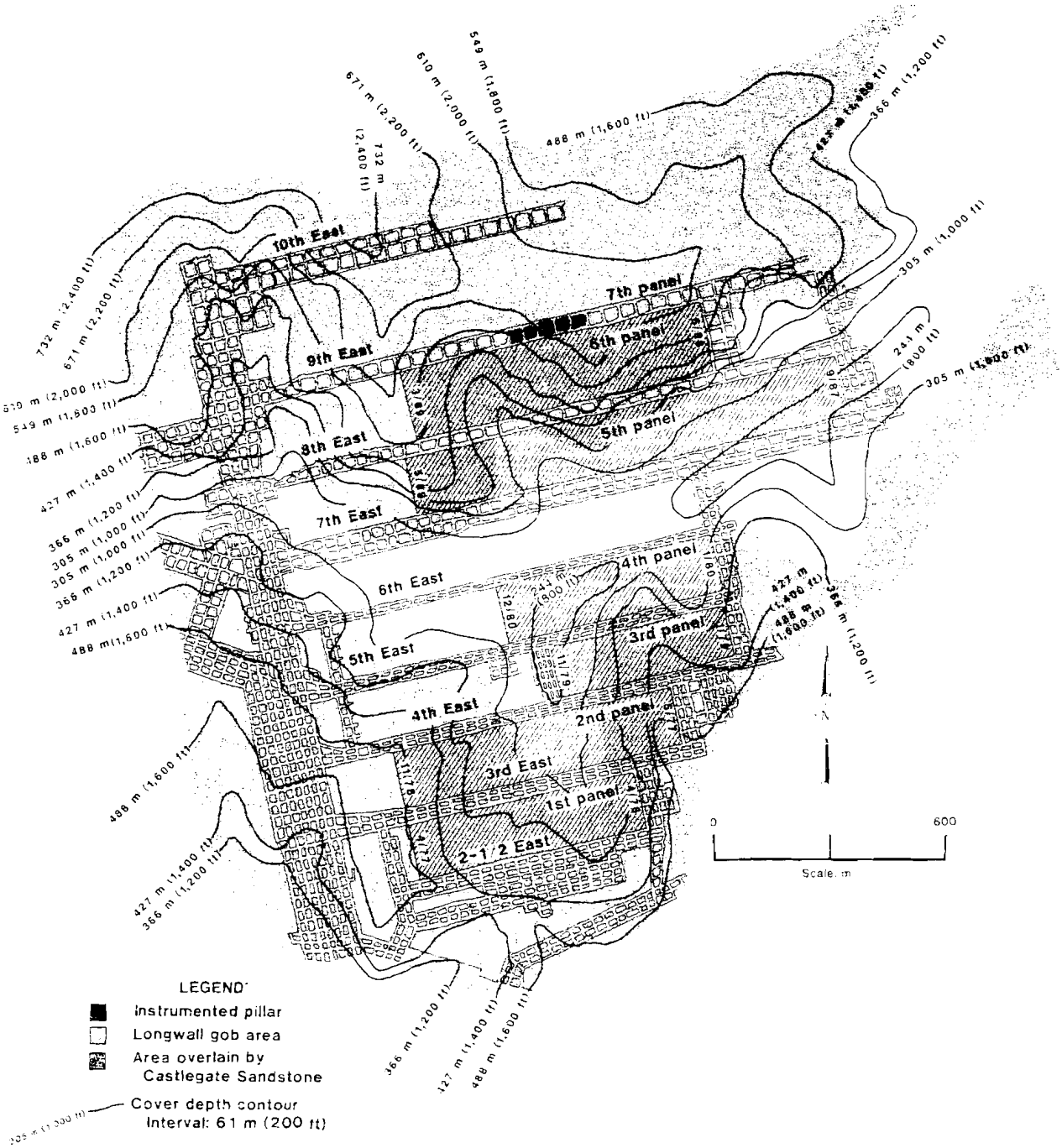

Figure 4
Generalized Stratigraphic Sections, Wasatch Plateau and Book Cliffs Coalfields.

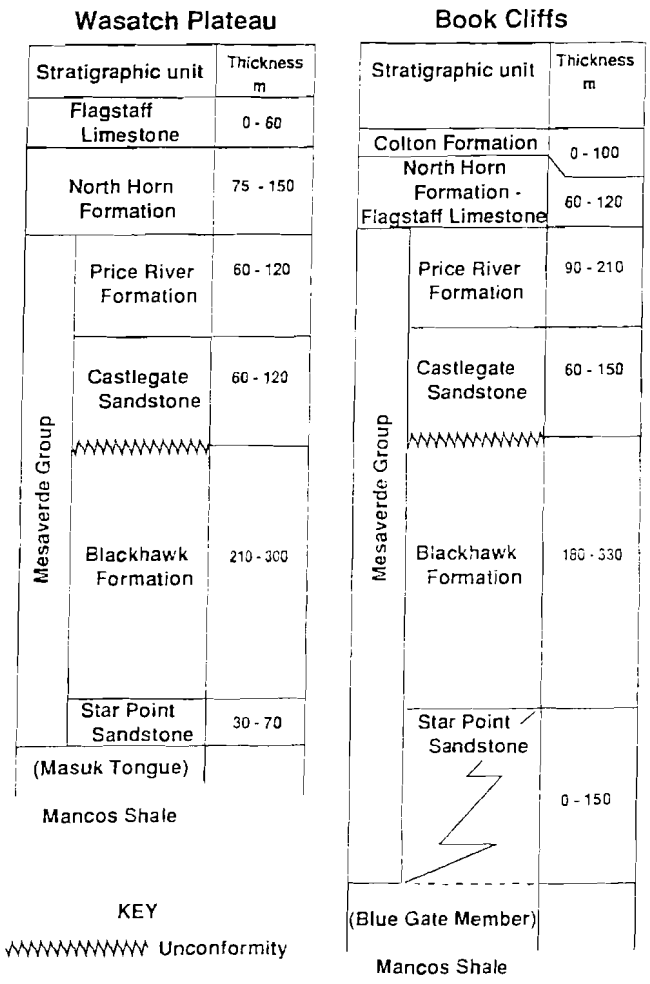

Figure 5
Exposure of Star Point Sandstone at Cottonwood Mine Loading Facility.

Upper portion of unit is below Hiawatha Seam located even with small cubical building above concrete silo. Numerous strong sandstone and siltstone units can be seen to overlie seam workings as well.

strata provided the triggering mechanism for failure of marginally stable coal pillars. It was shown that the coal pillars were critically loaded prior to the event with a factor of safety of 0.75. The bump occurred when the upper sandstone strata failed as the face retreated a distance equal to the panel width. The failure of these strata was interpreted as a dynamic pulse that triggered failure of the critically loaded pillar (Maleki, 1995). Seismic analysis of strain energy released from this 3.6 Richter-magnitude event also confirmed that a source of energy from the upper strata, in addition to pillar strain energy, was needed to balance energy calculations (Boler, 1994).

STRONG ROOF AND FLOOR STRATA

Strong floor strata immediate to the coal seam and strong roof strata within 9 to 15 m (30 to 50 ft) of the seam have long been recognized as major contributors to coal bumps (Holland and Thomas, 1954; Iannacchione and DeMarco, 1992; Peparakis, 1958). In fact, the confinement offered to the coal seam by these stronger, stiffer strata appears necessary to generate levels of stored energy sufficient to cause bumps within and immediate to the coal seam structure (Babcock, 1984). Conversely, weak roof and floor strata do not allow the accumulation of high loads and excessive strain energy on the coal structure because of stress-dissipating deformation into the mine openings (figure 6). Soft ground conditions may actually help lessen the integrity of the coal seam near the periphery of the entry as the strata migrate into the opening, thereby concentrating the high stresses deeper in the structure where the strength of the confined coal is much greater than the applied load.

Figure 6
Illustration of Pillar Confinement Offered by Strong Roof and Floor Strata (Left) Versus Weak Strata (Right).

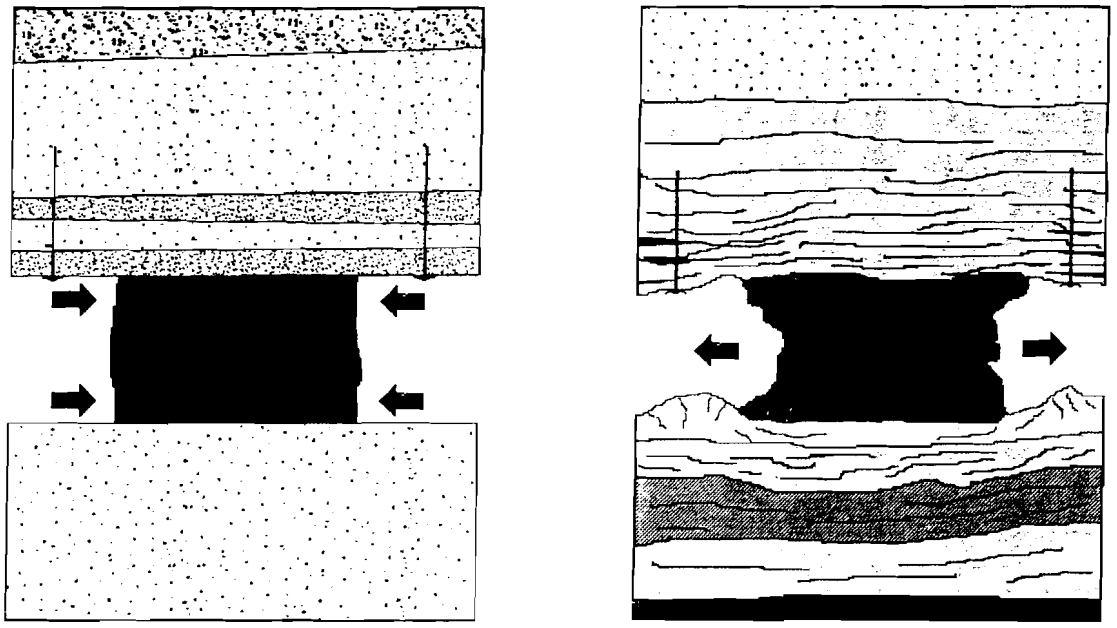

In the Wasatch-Book Cliffs coal region, the strata immediate to the seam are conducive to bumping in a number of mines. In these mines, the floor is commonly composed of thick sandstones overlain by thin siltstones and mudstones, and, as a result, floor heave is rarely experienced. The intervals of weaker materials separating the sandstones from the overlying seam can vary considerably across a given property, and it is not uncommon to find these massive sandstone units immediately contacting the bottom of the seam. This has been noted by the authors in those operations working in the Sub-3 Seam and the Hiawatha Seam where the Starpoint Sandstone is often found next to the seam.

Roof strata at some bump-prone operations are considerably more variable than the floor strata. At these mines, it is not uncommon to find significant changes in the thickness of individual roof units over very short lateral distances, particularly in areas where channel deposits are frequently encountered. This condition was present at the Sunnyside No. 1 Mine, near Sunnyside, UT (figure 7). Clearly, highly variable roof strata create difficult ground control problems with regard to roof support, but these relatively stiff roof members (siltstones and sandstones isolated at various points along the gate road and longwall face) also tend to concentrate bump-initiating stresses. This was certainly the case at Sunnyside and has been the case at many operations where channel features are common.

The primary roof strata encountered in bump-prone operations include massive mudstones, siltstones, fine-grained sandstones, and massive weak sandstones (figure 8). While the mudstones are generally of moderate strength, the lack of bedding structures or slickenside features may provide for good confinement along seam contacts. The strongest units commonly encountered in bump-prone operations are unquestionably dense siltstones and fine-grained sandstones. Whereas the unconfined compressive strength of mudstone may range from 41.4 to 69.0 Mpa (6,000 to 10,000 psi), recent tests on siltstone and fine-grained sandstone from the Sunnyside operation showed strengths ranging from 151.7 to 220.7 MPa (22,000 to 32,000 psi). Such numbers are often found in the mines throughout the region and are considered high even for strong roof conditions.

Barron (1994) describes the geology at four Wasatch-Book Cliffs mining operations that have experienced bumping to different degrees at one time or another. Bumps at two of the operations, the Sunnyside No. 1 Mine and the Castle Gate No. 3 Mine, resulted from the effects of highly variable, yet strong, roof strata. The other two operations, the Wilberg Mine and the Starpoint No. 2 Mine,[3] both experienced bumping related not to average mine roof conditions, but rather to the presence of sandstone channels in the immediate mine roof.

[3]Private communication from J. M. Mercier, supervisory geologist, Cyprus Plateau Mining Corp., Starpoint No. 2 Mine, Price, UT.

Figure 7
Roof Logs From Sunnyside No. 1 Mine.

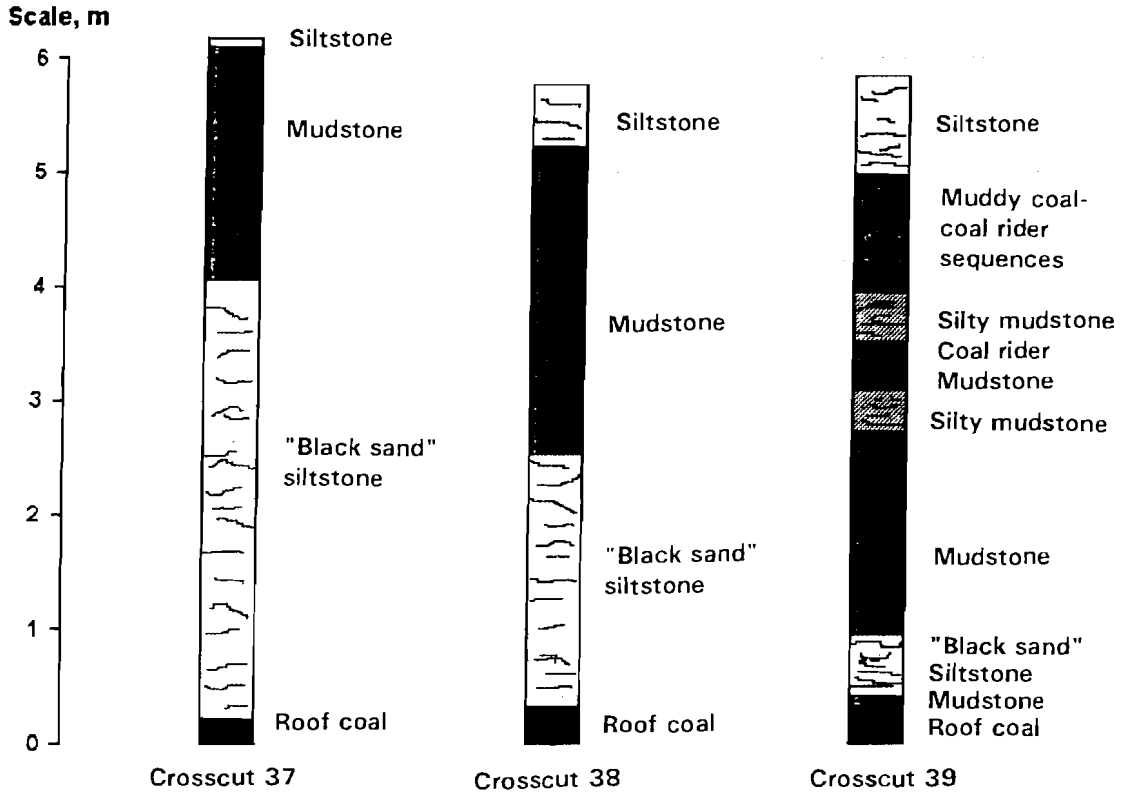

Logs illustrate widely varying nature of roof lithologies encountered in many Wasatch Plateau-Book Cliffs Coalfield mines.

SANDSTONE CHANNELS IN IMMEDIATE ROOF

Considering the combination of massive, weak roof members and extremely strong units distributed in a discontinuous manner along the length of the gate entries (figure 7), it becomes clear why it is difficult to pinpoint likely areas of bumping in most of the region's operations.

An exception to this problem involves the occurrence of sandstone channels in the immediate roof. Sandstone channels are stress-concentrating structures that are directly related to bumping along longwall panels nationwide. These features are common to the region's mines (Barron, 1994) and are seen both as deep channel cuts of limited lateral extent (less than a hundred meters across) that may or may not scour the seam and broad washes that may extend for several hundred meters laterally along the entry system within the bolted horizon of the roof. The unconfined compressive strengths of these units can vary considerably, but they are generally lower than the unconfined compressive strengths of the siltstone and fine-grained sandstone units described above. The massive nature of many of these units (or lack of bedding and joint structures) appears to be the major factor affecting bump initiation immediate to these features. That is to say, the *rock mass* strength of the entire channel deposit is of more concern than the absolute intact unit rock strength of the sandstone comprising the channel. Many of these units do possess considerable structure in the form of distinct bedding and/or regular jointing (Maleki, 1988), but it is not uncommon to find the channels as large, relatively solid structural units.

Both channel types have contributed to coal bumps in U.S. mines. Narrower channels tend to concentrate loads along the tailgate, which creates the potential for isolated bumping problems within tailgate pillars and along the tailgate portion of the panel face (DeMarco, 1988). Unless these features are clearly identified during gate development, either by direct observation or by logs of roof conditions obtained during bolting, bumps related to these channel features will occur without apparent reason. To forestall such problems in mines where numerous, narrow channel deposits are present, it is a requirement that channel locations and distributions be mapped accurately. Only in this way can changes in gate support design and/or destressing be effectively employed.

Figure 8
Typical Stratigraphic Section for Hiawatha/Blind Canyon Seams.

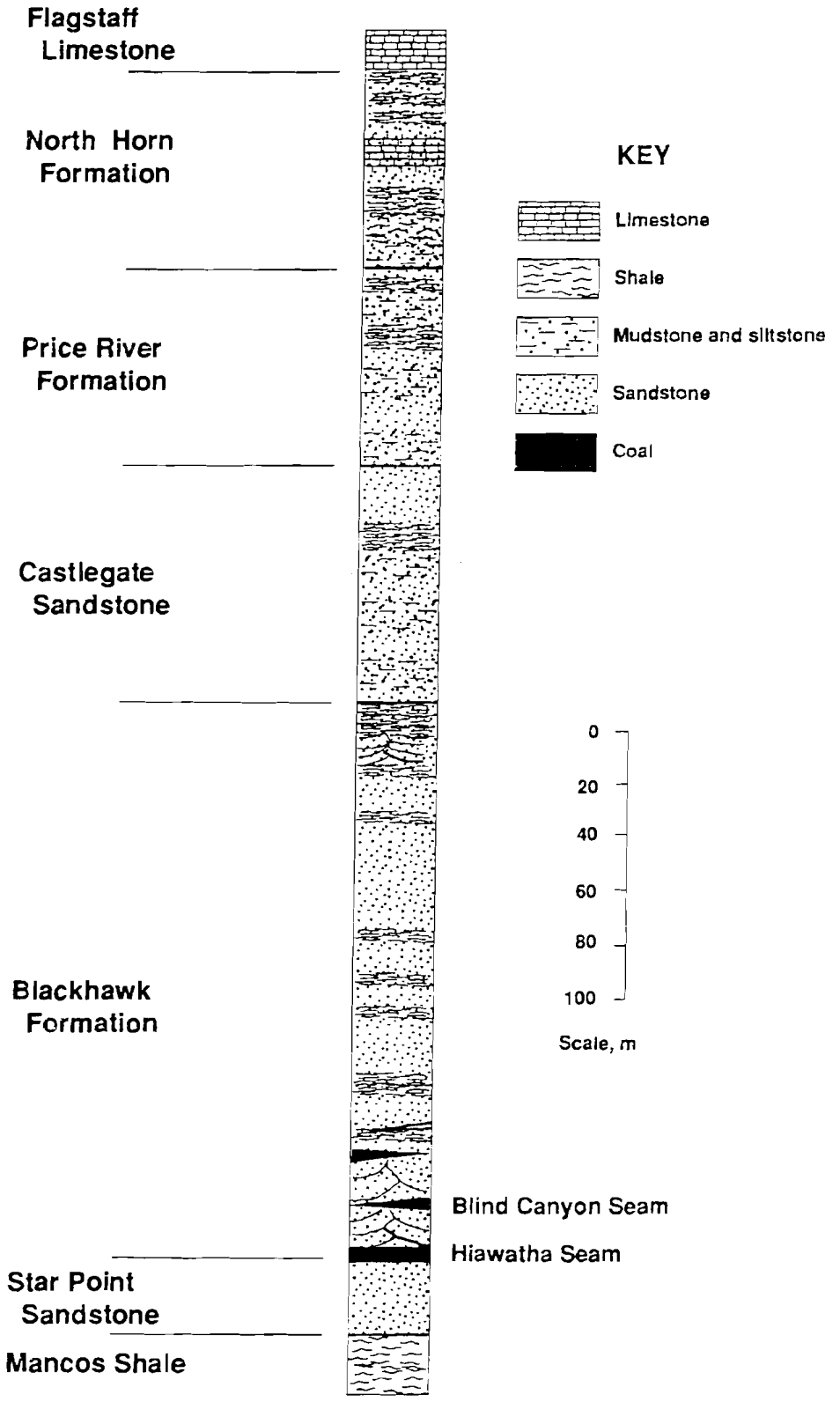

Broad channel features are common in Wasatch Plateau operations and, because they are easier to identify underground, afford a certain degree of predictability where bump-prone conditions are concerned. As with the less-easily located and identified narrow channel deposits, the primary concern appears to be excessive loading along the tailgate. Stresses about gate peripheries are generally better distributed by broad deposits, yet the magnitudes of stress along tailgate panel abutments are higher than those recorded under normal mining conditions. These higher loads can be dealt with most effectively through proper gate design, employing either full-yielding pillar or abutment-yield pillar entry systems. Gate designs that inadequately minimize stress concentrations along the tailgate entry and face areas will require extensive panel destressing in the tailgate immediate to overlying channel sandstones (DeMarco, 1994).

STRONG COAL SEAMS

While it has been shown that most U.S. coals can be made to bump under the right combination of confinement and loading conditions (Babcock, 1984), it is worthwhile to discuss seam characteristics in some Western operations that appear to influence bumps. The two most prominent contributors are (1) impersistent cleating and (2) the presence of strong rock splits in the mid-to-upper portion of the seam. While it is not necessary for these conditions to be present for bumps to occur, they have been linked to some of the worst bump conditions documented in Western mining.

During a USBM study at the Castle Gate No. 3 Mine (Barron, 1994), numerous bumps occurred on the longwall face and within the tailgate pillars that eventually led to the closure of this operation. In addition to very strong roof and floor conditions, strong seam conditions were observed. Cleating in the coal was difficult to discern and did not appear to contribute significantly to rib-side yielding along the gate entries during panel mining (figure 9). A hard siltstone parting at approximately midseam height was also present throughout the mine. The confinement effects of the stiffer roof and floor strata, coupled with the seam-strengthening effects of the parting, assisted in generating extremely high loads immediate to pillar and panel riblines. This was seen very clearly in pressure cell load data. Forward abutment loads peaked within 0.3 m (1 ft) of the faceline, and pillar yield zones were limited in depth, often within 1 to 1.5 m (3 to 5 ft) of the rib. As a result, the coal was incapable of supporting these high loads and severe bumping occurred, particularly along the tailgate (figure 10).

Similar conditions have been experienced at the Sunnyside mining complex over the past 30 years of longwalling (Koehler, 1994). A recent USBM study on gate road pillar sizes at this mine showed that large abutment pillars exhibited high loads close to the ribline during mining of the first panel and just prior to bumping. While the Lower Sunnyside Seam does yield fairly readily, a strong parting in the upper portion of the seam appears to strengthen the composite coal-parting material. Stress-detection drilling indicated that high loads in these pillars were concentrated between 1 to 3 m (3 to 9 ft) from the ribline, although experience suggests a much deeper yield zone should exist at the nearly 900 m (3,000 ft) of cover to which these pillars were subjected. As a consequence of the high loads, many of the oversized yield pillars (critical pillars) bumped violently with passage of the first face.

Again, it must be noted that numerous cases of bumping have occurred in the Wasatch-Book Cliffs coal regions where these seam conditions did not exist. However, it appears that enough bumps have taken place in strong, structureless coal seams and rock splits to warrant their being considered where bump potential is a concern.

FAULTS AND SHEAR ZONE STRUCTURES

Investigations of fault and shear zone structures in the central Utah coalfields point to two basic concerns: (1) the effect of significant changes in the stress field in the vicinity of these discontinuities and (2) the loading potential of isolated blocks of strata above the seam. Whether stick-slip movement along fault structures is responsible for dynamic load changes has yet to be more thoroughly determined (Boler, 1994), but changes in loading conditions have been noted as major contributors to bumping when mining approaches a discontinuity (Iannacchione and DeMarco, 1992; Peparakis, 1958). Maleki (1981) has also documented large increases in vertical loading dependent upon fault orientation to retreat mining layouts, furthering this assertion.

A bump resulting from an isolated block of roof strata coming to bear on a section of the gate road pillars was recently seen at an operation along the Wasatch escarpment. This operation utilizes a two-entry yield-pillar system at cover depths averaging around 450 m (1,500 ft). Once pillar yielding began following development, it became apparent that a four-pillar-long section of the gate road was not being subjected to appreciable loading, because the yield pillars showed no sign of rib failure. In fact, long after the other gate pillars had shown considerable rib yielding, this section continued to look as though it had only recently been developed. It was soon discovered that the section was bounded by diverging, high-angle shear zones running through the roof, seam, and floor, with observed offsets of 0.3 to 0.75 m (1 to 2.5 ft). During mining of the first panel, the panel abutment was mined out from under the overlying isolated wedge of roof rock between the shear zones, and the subsequent immediate weighting of the pillars resulted in severe bumping adjacent to the face stage loader and belt structure. This block of rock effectively bridged the gate entry until first panel mining allowed the full weight of the block to bear upon the unyielded gate pillars.

Figure 9
Intake Entry of 9th East Gate Road, Sub-3 Seam, Castle Gate No. 3 Mine.

Note typical lack of rib failure. Cover depth is 600 m (2,000 ft). This entry stood open for several years prior to longwalling.

Figure 10
Tailgate Pillar Bump in 8th East Gate Road, Castle Gate No. 3 Mine.

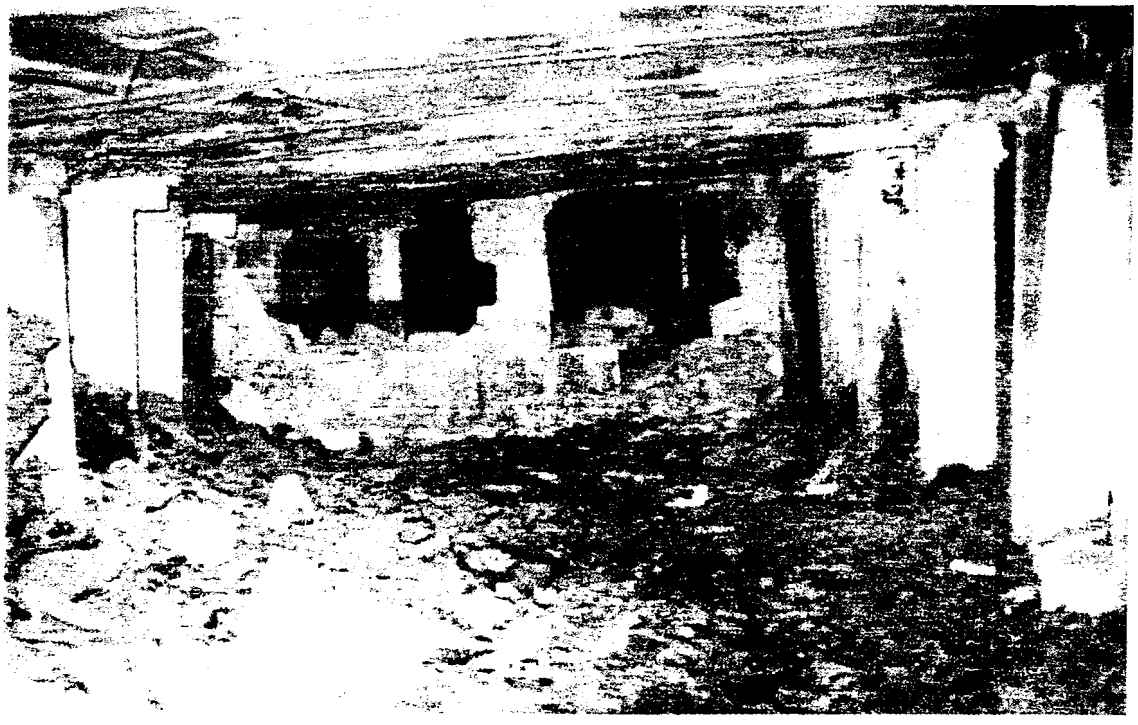

MINING PRACTICES THAT AGGRAVATE DIFFICULT GROUND CONDITIONS

To mitigate the frequency of gate road pillar bumps, over the years mine operators in the Wasatch-Book Cliffs Coalfields have implemented the use of two-entry, yielding-pillar gate road configurations. This approach attempts to soften the ground around the gate system, thereby diverting bump-inducing stresses to deep within the confines of the adjacent panel abutment. In general, the approach has been very successful when employed correctly. Problems arise, however, where pillar sizes are such that inadequate yielding occurs. These improperly sized pillars are termed "critical pillars," and their use can result in the most extreme bump hazard possible.

This section describes the critical-pillar concept and discusses the historical misapplication of these structures in Western mining operations. Also discussed are applications of abutment-yield pillar gate configurations and some considerations for using two rather than three entries.

CRITICAL-PILLAR GATE ROAD SYSTEMS

Where the use of pillars with width-to-height ratios greater than 4 to 5 is concerned, the concept of the *critical pillar* has often governed the performance experienced in *deep* Western coal mines (DeMarco, 1994). A critical pillar can most simply be defined as one that is too large to yield either nonviolently or before the roof and floor sustain permanent damage, and yet is too small to support full longwall abutment loads. The relationship between critical-pillar designs and yield and abutment pillar designs is presented in figure 11. The horizontal axis represents the minimum performance standard separating stable from unstable gate road configurations. A pillar design whose performance falls above the horizontal axis is considered successful (stable), whereas a design whose performance falls below the horizontal axis is considered unsuccessful (unstable).

An important aspect of this concept is the rate at which a successful gate road design can become unsuccessful. Ground conditions deteriorate more gradually in abutment pillar systems as pillar size decreases. Changes in performance are observed as the onset of minor amounts of floor heave, increases in audible coal popping and minor bumping, and increases in the frequency of roof-related problems (DeMarco, 1994). In comparison, the performance of yield-pillar-based gate roads may rapidly decline with only a few meters of increase in pillar size; the transition between a fully successful yielding gate road and the worst of possible conditions for a critical pillar is often abrupt.

It cannot be overemphasized that increasing pillar width toward the critical-pillar range only invites the full weight of the overburden to be transmitted to a gate system that cannot possibly support it. As a result, critical pillars are to be considered *extremely* bump prone, even at shallow depths, when strong mine roof and floor conditions exist. Unlike the abutment-to-critical-pillar transition, where coal bumps are generally first witnessed in the tailgate, the yield-to-critical-pillar transition allows severe bumping in the headgate entries immediate to the face. An all-too-graphic example of this problem recently occurred at a Western operation where unyielded pillars adjacent to the face in the headgate bumped violently as the first panel abutment was mined. Although it was fortunate that no one was injured, considerable damage was sustained by the stage loader and face-end belt structure. In settings not readily conducive to pillar bumping, prolonged loading of the gate pillars will certainly result in severe roof, floor, and/or rib instabilities, requiring at least extensive supplemental support along the entire tailgate entry, assuming that gate closure can be avoided.

Figure 11 is a useful graphic representation of the critical-pillar concept; however, it should not be used to suggest that pillar width (or size) alone determines whether a pillar design falls in the critical range. Other mining parameters, such as seam height, depth of cover, and the physical properties of the roof and floor strata, can have a profound effect on the final disposition of a specific pillar geometry. For example, a pillar configuration that readily and gently yields under moderate roof conditions may bump violently under strong roof members. In this comparison, the pillar configuration that is considered a successful yield pillar application in one setting becomes an unsuccessful critical pillar in another. Similar changes in pillar behavior have been noted by mine operators when significant increases in mining depth appear to have hindered pillar yielding, possibly because of added roof and floor confining stresses, thereby requiring *smaller* pillar dimensions to avoid bump-prone, critical-pillar designs.[5] DeMarco (1994), in a qualitative analysis of case histories of Western mines, noted that, in general, yield pillars should be sized with width-to-height ratios less than 5 to ensure proper yielding and that a Coal Mine Roof Rating (CMRR) (Molinda and Mark, 1993) of greater than 50 should exist to ensure roof stability in a high-deformation environment. Maleki (1988) has also suggested additional criteria based on pillar postfailure behavior for yield pillar design.

Because the range of pillar widths that make up the critical-pillar zone is unquestionably different for each

[4]Private communication from J. M. Mercier, supervisory geologist, Cyprus Plateau Mining Corp., Starpoint No. 2 Mine, Price, UT.

[5]Private communication from M. Moon, chief engineer, Energy West Mining Co., Huntingdon, UT.

Figure 11
Conceptualization of Critical-Pillar Concept.

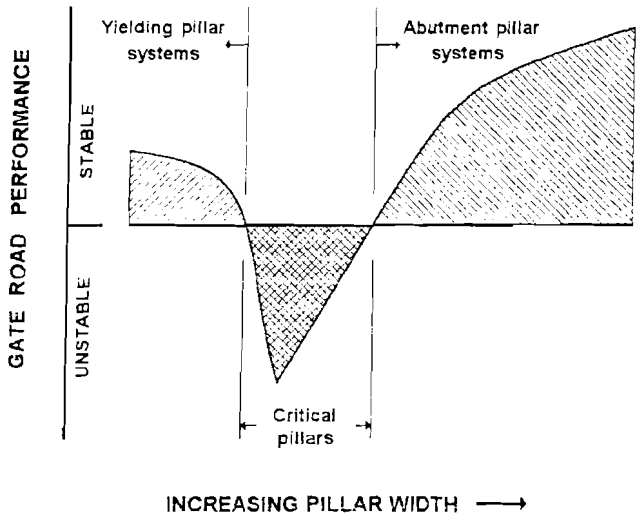

This figure shows transition from successful yield pillar systems through unsuccessful critical designs to successful abutment pillar systems for cases with competent roof rock.

mine setting, so is the failure mode (as described by the influence of pillar failure on the surrounding ground conditions). Critical pillars have been shown to fail in one of three ways, depending on the pillar size employed and the geologic conditions present: coal bumps, roof falls, and floor heave (DeMarco, 1994).

The primary mode of failure of the critical pillars-gate-entry system studied during the recent Sunnyside Mines investigation was coal bumping. In contrast, a field study of a three-entry, critical-pillar configuration at another deep Western U.S. coal mine by DeMarco and others (1988) revealed the primary entry-pillar failure mode to be roof falls. Although one of these three types of ground instabilities is usually the predominant or primary mode of failure, it is also possible that a combination of primary and secondary modes of failure can be experienced along the length of a gate road because of variations in geology. For example, whereas coal bumps proved to be the primary mode of failure of the critically sized pillars at the Sunnyside test site, localized floor heave and roof falls were also observed during adjacent panel mining.

In the section on "Recent Examples of Critical Pillars and Gate Road Bumps" in this paper, the importance of the critical-pillar concept will be emphasized with a recent case study at the Sunnyside operation, where a variety of pillar sizes were employed under various conditions. It cannot be overstated that perhaps the single, most-frequent contributor to gate road bumps is the use of designs that result in critical-pillar behavior.

ABUTMENT-YIELD PILLAR GATE ROAD SYSTEMS

Full yielding-pillar gate road systems are largely unique to mining in the West and are most generally preferred to cope with the deep, multiseam, bump-prone conditions common to most of the region's operations. However, the use of the three-entry, abutment-yield pillar configuration should not be discounted as it has some advantages in bump-prone ground when subseam mining is not an issue. The application of this design stems from two considerations: (1) a transition at a given property from traditional full-abutment systems (common among Eastern mine operations) toward yield-pillar-based designs and (2) the need to cope with thin seams or extremely strong roof and floor conditions that preclude the successful deployment of yield pillars; that is, pillar sizes that initiate effective yielding are too small to satisfy operational needs and/or requirements mandated by law. While the first consideration may be largely based on the marginal-to-significant economic advantages gained in switching from costly full-abutment systems, the second consideration is firmly rooted in the need to maintain a safe, travelable tailgate escapeway *in a bump-prone environment.*

When deploying an abutment-yield pillar gate system design, *where the primary purpose of the design is to mitigate coal bumps*, it is often a prudent practice to place the larger abutment pillar against the first panel gob and the smaller yield pillar adjacent to the tailgate entry (although there are some variations; for example, in nonbump-prone conditions, operational advantages may be realized by reversing this configuration). Appropriately sizing the abutment pillar ensures that excessive loads from the first panel side abutment are shielded from the future tailgate. The end result is an effective barrier (abutment pillar) established between the first panel abutment loads and the new tailgate, and a softened tailgate entry system (yield pillar) that is incapable of bumping with the advance of the second panel.

This arrangement should be considered very practical under strong roof and floor conditions where the presence of the larger abutment pillar allows the width of the yield pillar to be minimized beyond the limits mandated for full-yielding gate system designs. For instance, whereas a full-yielding design may limit minimum pillar widths to no less than 9 m (30 ft) for operational reasons, the abutment-yield design may employ yield pillars much smaller without the need to consider these same concerns. An added advantage is that in the event the abutment pillar bumps because of insufficient design (the critical-pillar case described previously), the yield pillar will act as an effective "bump curtain" protecting the tailgate entry from ejected coal (Zelanko and Heasley, 1995). This entire system approach may not be conducive to adequate caving, however,

and may be less desirable than a full-yielding pillar gate design, particularly when multiseam mining is a concern.

The potential for bumps to occur may actually increase when the configuration is reversed; that is, when the yield pillar is placed against the first panel gob. As the pillar yields, the overlying roof cantilevers onto the adjacent large pillar abutment. Not only are side abutment loads transferred, but so are the additional loads from above the yield pillar and the entry span between the yield and abutment pillars. For the case of a 9-m (30-ft) wide yield pillar, the additional span cantilevering onto the abutment pillar is nearly 15 m (50 ft), plus whatever overhang has developed on the gob side of the yield pillar. Although the yield pillar will support a portion of this additional span, the combined effect of these cantilevered sections is to concentrate higher loads onto the abutment pillar. If the abutment pillar is marginally designed to handle side abutment loads, considerable pillar yielding may occur along the gob side of the pillar. The end result is effectively to concentrate the highest of the side abutment loads immediate to the tailgate escapeway.

In the presence of strong ground conditions (the sandstones and siltstones described previously), this pillar configuration may create an environment with severe bump potential, as described in the previous section on "Critical-Pillar Gate Road Systems." In weaker ground conditions, failures often appear as severe floor heave and roof falls. In either case, the stress concentrations within the vicinity of the tailgate entry are often excessive compared to the preferred configuration, as was recently illustrated at a Colorado operation where the "typical" configuration placed the yield pillar against the first panel gob. A USBM comparative study of abutment-yield and yield-abutment designs (figure 12) gave the following results, as reported by McDonnell (1995):

Figure 12
Plan View of Study Site Locations.

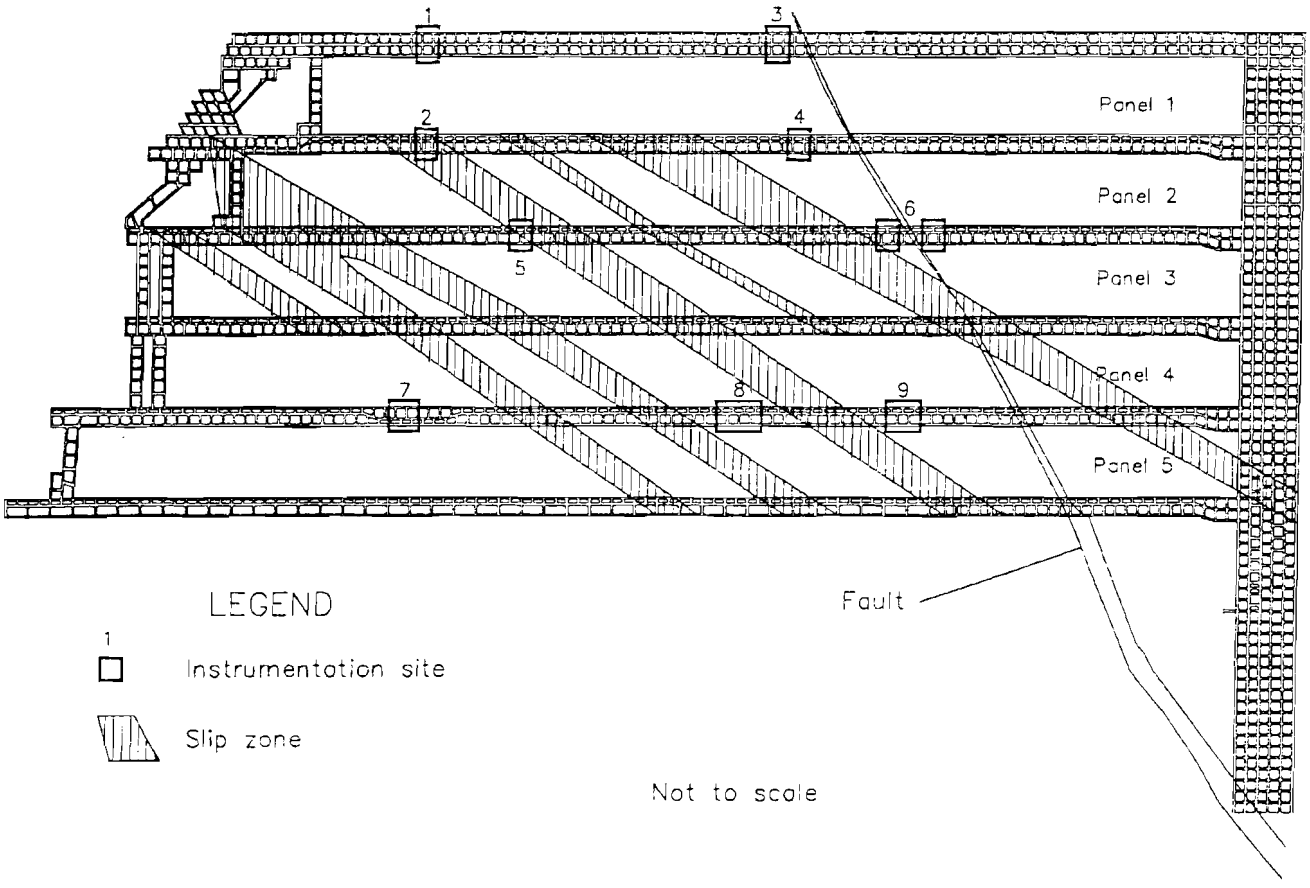

Site 7 illustrates preferred arrangement for controlling bump-related problems (McDonnell, 1994).

USBM and mine personnel conducted on-site observations of tailgate conditions throughout longwall mining at the study mine. At each gate road instrumentation site with the typical pillar layout [yield pillar against the first gob] during second panel mining, significant cutter-type roof problems were observed within 23 m (75 ft) outby the face at the panel-roof line. Cutter-type roof problems and floor heave in the zone immediately outby the tailgate end of the longwall panel face were observed at numerous locations during longwall panel mining at the study mine. While panels 2, 3, and 4 had experienced cutter-type roof failures and dynamic floor heave events at the panel-tailgate edge outby the face, the roof and entry conditions outby the panel 5 face through the site 7 gate road area were generally good [section where abutment pillar was against the first gob].

High pressures, as measured by borehole pressure cell (BPC) instrumentation, surrounded the tailgate entry during second panel mining through all the gate road test areas with the typical pillar arrangement (sites 2, 4, 6, 8, and 9). Conversely, the measured pressure in the mine structure around the tailgate entry at site 7 during panel 5 mine-through was considerably less. The abutment loads from longwall mining at site 7 were shifted away from the tailgate entry and the panel edge and were being carried by the big pillar core and the panel, away from the tailgate entry.

Had mining conditions been more conducive to bumps [the mine has a moderate roof and floor and operates under 330 m (1,100 ft) of cover], severe conditions would likely have prevailed long before the study determined that the preferred configuration may actually be an improvement for this operation. Figure 13 demonstrates the pillar loading sequences along the tailgate that make this configuration especially viable for deployment in more bump-prone conditions. It should not, however, be concluded from this study that the "typical" configuration was unacceptable for this particular operation. Decisions regarding the appropriate configuration must take into account both ground control and operational considerations.

It should also be noted that although strong roof and floor conditions have been encountered by most operations in the Wasatch Plateau and Book Cliffs Coalfields, and have been dealt with most effectively with full-yielding-pillar gate road systems, conditions do exist that may preclude the sole use of yield pillars. As previously mentioned in the discussion on critical pillars, failure to achieve a successful yield pillar at a property can be catastrophic in terms of creating severe bump conditions. This situation can arise in exceptionally strong ground, as was the case at the Castle Gate No. 3 operation near Helper, UT (Barron, 1994). Over the course of mining several panels at this mine, a successful yield pillar was never achieved, and the mine opted to use larger abutment pillars instead. Evidence suggests that the maximum width for a successful yield pillar design at this property falls within the range of 4.6 to 6.1 m (15 to 20 ft), which is below the minimum allowed by law in a two-entry configuration. In this particular case, the use of the abutment-yield pillar configuration may have offered relief to the persistent tailgate bumping problem that plagued the operation.

MULTIPLE-ENTRY VERSUS TWO-ENTRY GATE ROAD SYSTEMS

Two-entry systems have evolved over the years in Western mines as the preferred design when employing full-yielding-pillar gate configurations. The basis for this preference is largely rooted in historical practice rather than in the economics of developing additional entries. It was determined many years ago, shortly after longwalling was introduced to Western U.S. coalfields, that in bump-prone conditions, the less ground opened up, the better (Koehler, 1994a, 1994b). Past studies have shown that multientry gates may incur higher loads than two-entry systems, but room does exist to consider the use of multientry systems when the quality of the roof warrants allowing wider gate spans (DeMarco, 1988; Koehler, 1994a).

One situation that calls for minimizing the number of entries involves the presence of sand channels in overlying roof strata. As previously mentioned, these structural features are common to many Western mines and are notorious for creating poor roof conditions along the margins. Minimizing entry development reduces the overall areal exposure of this potential roof-fall hazard (Maleki, 1988). This hazard is exacerbated by the large amount of deformation imparted to the immediate roof in the yielding gate system. Also, a potential problem is created by the additional length of cantilever arm possible when channels span a multientry system. The result may be to increase loading on the tailgate region of the face and possibly the initiation of more frequent bump events. This was suspected to be the case for at least one Western operation in recent years where the use of a three-entry yielding system was replaced with a two-entry system to minimize tailgate face-end loading resulting from the possible cantilevering of stiff channel sandstones. Escapeway conditions improved greatly in the forward abutment zone [45 to 75 m (150 to 300 ft) outby the tailgate face corner] when the entry system was switched to the two-entry design (though it should be noted that no quantitative data exist to prove the contribution of the channel cantilever to the face-end bumps experienced).

Figure 13
Overall Yield Sequence of Site 7 During Panel 5 Mining.

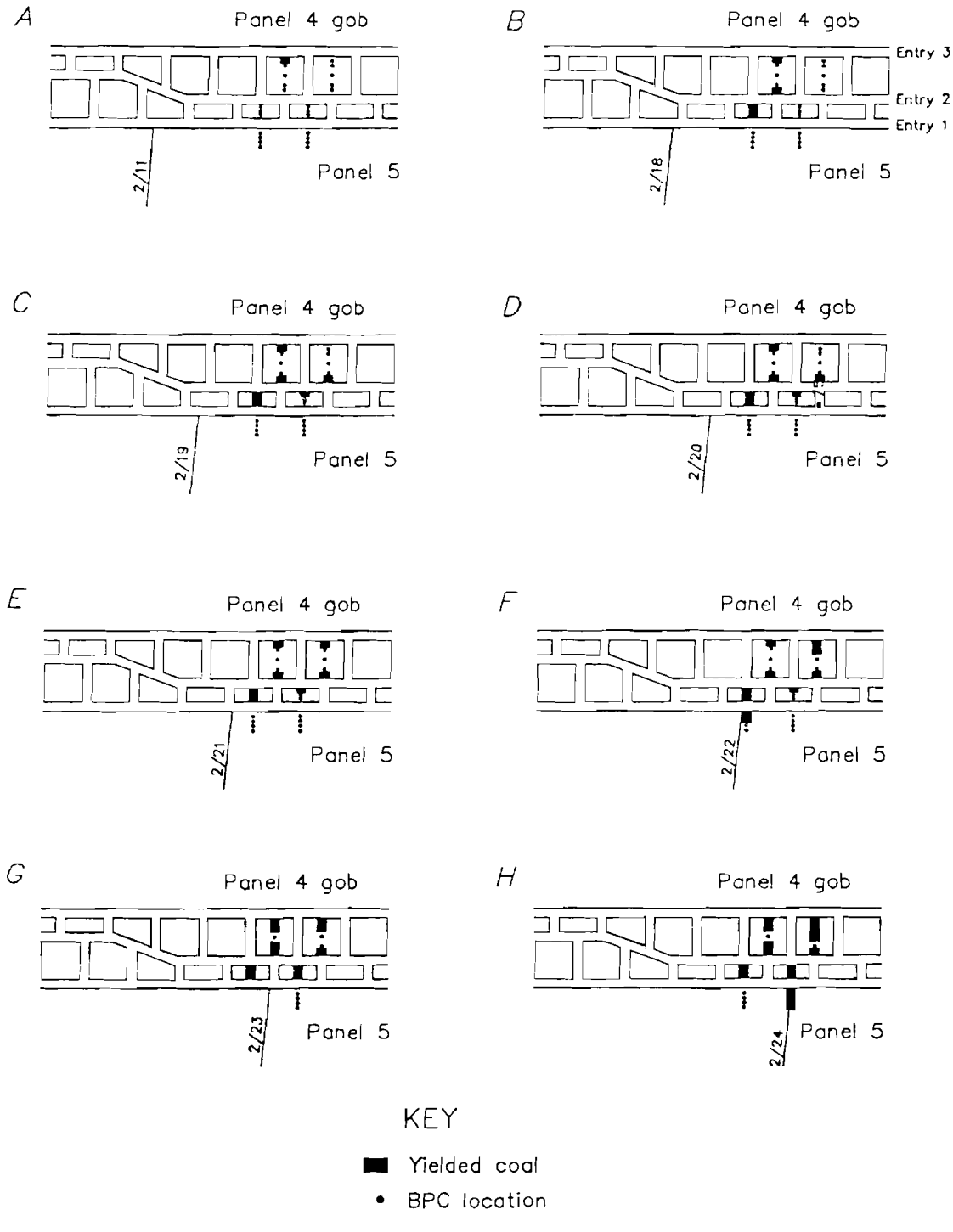

Face positions are given at end of day shift from 2/11/93 to 2/24/93 (McDonnell, 1994).

RECENT EXAMPLE OF CRITICAL PILLARS AND GATE ROAD BUMPS

To develop a clearer understanding of critical-pillar behavior, a field investigation was recently completed at the Sunnyside No. 1 Mine in a two-entry gate road where pillars were uniformly decreased in width from 17 to 10 m (56 to 32 ft) along the length of the entry system from the startup room outby. Ground pressure and probehole drilling measurements collected during the study provided a physical explanation for the ground conditions observed at several sites during adjacent panel mining. The following sections present an overview of the mine setting, as well as study results, from the perspective of graphically demonstrating the critical-pillar concept.

STUDY SITE HISTORY

The Sunnyside Nos. 1, 2, and 3 Mines are located in eastern Carbon County, UT, approximately 44 km (26 mi) east of the town of Price. Under varied ownership, underground coal mining has been conducted on the Sunnyside property since at least 1896. In March 1989, the Sunnyside Coal Co. reopened the mines after they had been idle for approximately 2 years; unfortunately, the mines were once again idled for business reasons in March 1994.

The longwall mining system was first introduced at Sunnyside in 1961 to improve worker safety in the difficult, bump-prone conditions found on the property. Natural factors conducive to coal bumps at the mines include great depth [as much as 900 m (3,000 ft)], rapid variations in relief, tectonic movement associated with faulting, and massive sandstone strata above and below the coalbeds (Jackson, 1971; Wong, 1985). Through a lengthy trial-and-error process during which many different gate road configurations were tried, Sunnyside engineers developed a two-entry, yield-pillar-based entry system that provided excellent ground control in the face of these difficult conditions. This system, which employs nominal 10-m (32-ft) wide chain pillars, virtually eliminated pillar bumps, greatly reduced face bumps, and substantially mitigated floor heave (Koehler, 1994a).

During the evolution of this system, several panel entry configurations were tried that employed critical-pillar designs. These designs were quickly abandoned because of severe coal bumps, bump-related roof falls, and floor heaving associated with their use. In fact, critical-pillar designs would likely have never been used at Sunnyside again if not for an accidental surveying error that resulted in the development of a tapered two-entry gate road.

STUDY SITE GEOLOGY

The mine portals are located near the base of the steep western Book Cliffs. The cliffs rise sharply approximately 1,000 m (3,330 ft) above the valley floor, resulting in abrupt changes in mining cover depth over very short horizontal distances. Cover depth ranges from 100 m (330 ft) at the outcrop to nearly 900 m (3,000 ft) within the current mining area. The strata comprising the Book Cliffs dip 3° to 12° to the north-northeast. The coalbeds of economic significance in the Book Cliffs Coalfield are confined to the Blackhawk Formation of the Mesaverde Group (figure 14). The coal-bearing portion of the Blackhawk Formation lies above the Kenilworth Sandstone and includes the Sunnyside member. The Sunnyside member is dominated by massive cliff-forming sandstone, but near the top there are lagoonal deposits that include the Upper and Lower Sunnyside Coalbeds.

The cliff-forming Castle Gate Sandstone overlies the Blackhawk Formation. It is approximately 55 m (180 ft) thick in the mine area and is composed mainly of fine- to medium-grained sandstone. The 150-m (490-ft) thick Price River Formation overlies the Castle Gate Sandstone and is composed of interbedded sandstones and shales, the sandstone grading from thin-bedded to massive ascending through the sequence.[6] The remaining overburden at the mine site is composed of the geologic units of the North Horn, Colton, Wasatch, and Green River Formations.

The Sunnyside Seam varies in thickness from 10 cm (4 in) in the west near Kenilworth, UT, to as much as 7.3 m (24 ft) in a single bed in parts of the Sunnyside district. At the mine site, the coal seam often separates into two distinct beds with as much as 23 m (75 ft) of siltstone intervening; however, in general, the upper and lower beds are considered localized splits of the same formation (Osterwald and others, 1981). The gate road in which this study was conducted was located in the Lower Sunnyside Seam. Typically, the Lower Sunnyside Seam is 1 to 2 m (3 to 7 ft) thick and is characteristically very hard and relatively unfractured, and forms a competent rib.[7]

The composition of the roof and floor of the Lower Sunnyside Seam can vary substantially over distances as little as 100 m (330 ft). Five basic rock types are found in the immediate roof, floor, and interburden surrounding the Lower (and Upper) split. They are (1) dark brown mudstone, (2) gray-brown silty sandstone, (3) interbedded siltstone and sandstone, (4) fine-grained quartzose sandstone, and (5) fine-grained calcareous sandstone. In general, the dark brown mudstone occurs immediately above and below

[6]Dames and Moore. Report to Kaiser Steel Company for coal slurry pond permit application, 1973, 9 pp., available upon request from J. R. Koehler, Denver Research Center, USBM, Denver, CO.

[7]Diamond, W. P. (Pittsburgh Research Center, USBM, Pittsburgh, PA). Private communications, 1977; available upon request from B. J. Scheibner, Spokane Research Center, USBM, Spokane, WA.

Figure 14
Generalized Stratigraphic Section of Mesaverde Group for Sunnyside Mining District.

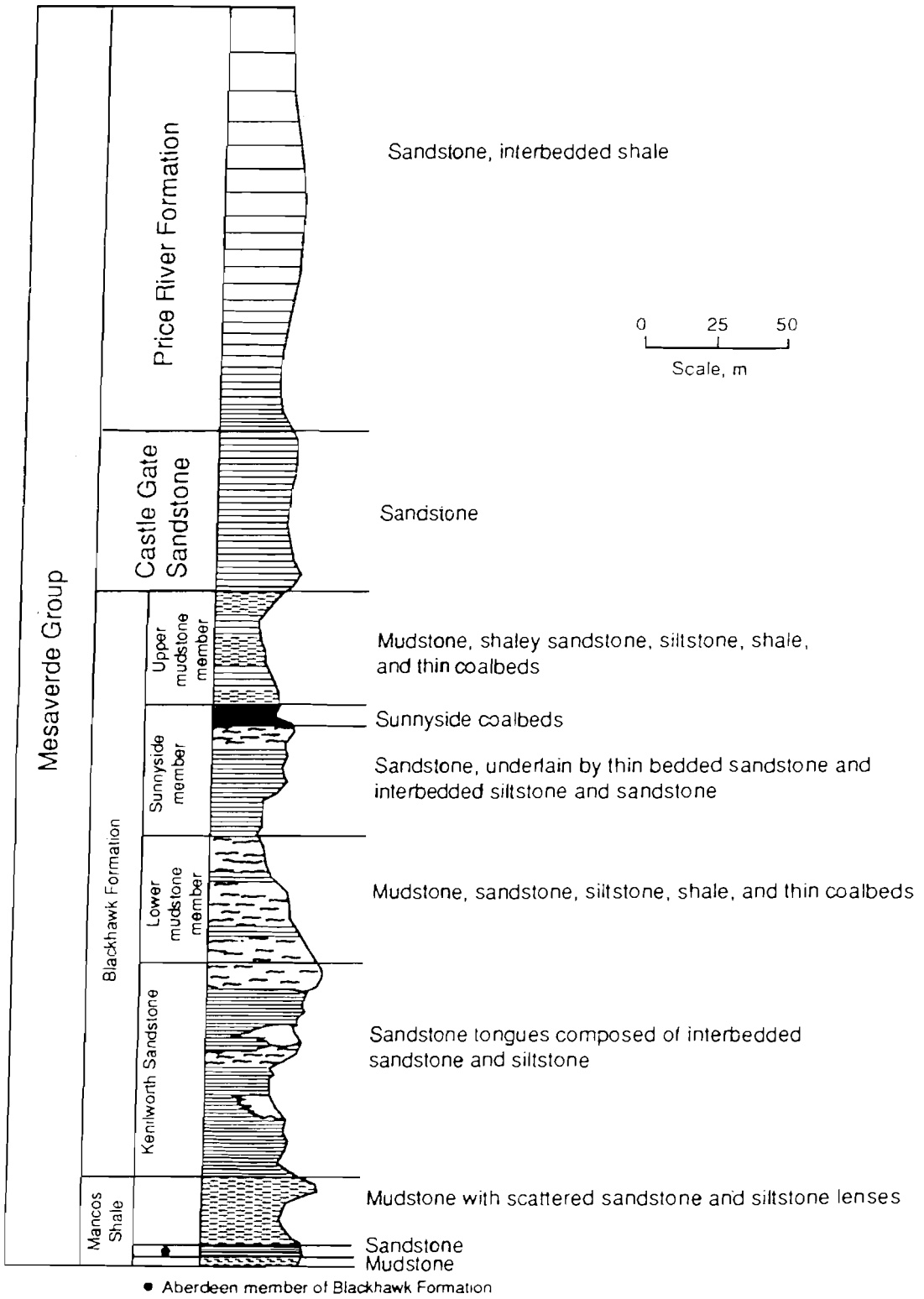

(Scheibner, 1979).

the Lower Sunnyside Seam and varies in thickness from 10 cm (4 in) to 8 m (26 ft). The gray-brown sandy siltstone is generally found in the rock parting between the splits and varies in thickness from 0.3 to 2.4 m (1 to 8 ft). The interbedded siltstone and sandstone usually occurs as "sandbar-type" features in the parting between the seams and can be as much as 8 m (26 ft) thick. Lastly, the fine-grained quartzose and calcareous sandstones occur irregularly as lenses or channel-fill deposits above, below, or between the coal splits (Koehler, 1994a; Scheibner, 1979).

STUDY SITE INSTRUMENTATION AND MEASUREMENTS

The location for the field study was the two-entry 23rd Left gate road in the Sunnyside No. 1 Mine (figure 15). As previously reported, an accidental surveying error resulted in the development of diverging entries and chain pillars that uniformly decreased in width from 17 m to 10 m (56 ft to 32 ft) with further outby positions. Two permanent instrumentation sites were established along the gate in pillars 17 and 12 m (55 and 40 ft) wide (figures 16 and 17). A planned third set of instruments in pillars 10.6 m (35 ft) wide was not installed because mining operations were prematurely halted; however, probehole drilling in two chain pillars and at two locations within the adjacent panel (figure 18) at the planned site 3 was completed before the No. 1 Mine was closed.

Permanent instruments at sites 1 and 2 consisted of USBM hydraulic borehole pressure cells (BPC's) installed in the pillars and adjacent 24th Left panel and oriented to measure changes in vertical ground pressures. Circular chart-type hydraulic pressure recorders attached to the BPC's with steel tubing ensured nearly continuous collection of ground-pressure data during adjacent panel mining. As at site 3, probehole drilling was conducted at sites 1 and 2 to delineate high-stress zones and determine the degree of pillar and panel yielding.

All probehole drilling was accomplished using a hand-held pneumatic auger-type drill. Boreholes 5 cm (2 in) in diameter and up to 9 m (30 ft) in length were drilled approximately midseam at all three sites. Data collected during the probehole drilling program included estimates of the depth of yielded or high-stress zones based upon the difficulty of drilling experienced by the operator. Also, a qualitative evaluation of the relative rock noise emitted during the drilling process was utilized to further indicate the presence of high stress levels.

ANALYSIS OF FIELD DATA

The locations of the three instrument-drill sites in the 23rd Left gate road are shown in figure 15. The 23rd Left panel was mined first but was not completed because of mine closure; the 24th Left panel was not mined. The "actual face stopline" marker found on figure 15 indicates the extent of 23rd Left panel extraction.

Site 1

Site 1 was established in the chain pillars and a section of the adjacent 24th Left panel between crosscuts 46 and 48 (figure 16). The pillars at site 1 were 17 m (55 ft) wide by 32 m (105 ft) long, and the cover depth was approximately 800 m (2,600 ft). Installed BPC's included four cells placed at regular intervals across the width of one chain pillar and five cells placed up to 16 m (52 ft) deep in the 24th Left panel. Twelve stress-detection probeholes were drilled in two pillars and at two locations in the 24th Left panel during instrument installation.

The probehole drilling data, collected when the face was approximately 185 m (607 ft) inby site 1, indicated pillar and panel rib yield zones were only about 1 m (3 ft) deep. Zones of competent coal under moderate stress began approximately 1.5 m (5 ft) into the ribs and extended as much as 3 m (10 ft) deep into both the chain pillars and the 24th Left panel. These data suggest that little yielding of either the pillar or panel ribs at site 1 occurred during the 6 months between development of the area and initiation of panel retreat operations.

Ground pressure profiles across the instrumented pillar and panel for three longwall face positions (FP) relative to the line of BPC's are presented in figure 19. The 78-m (256-ft) inby FP profile shows pillar and panel pressures as the forward stress abutment began to affect the site noticeably. Both pillar and panel stresses remained relatively low at this point in the mining cycle; however, observations taken in the gate road at this time noted an increase in the frequency and magnitude of rock noise emanating from the coal and surrounding strata. No significant bump events had been reported as yet.

As mining progressed to the 8-m (26-ft) inby FP, pillar pressures increased dramatically as a result of the onset of the full forward abutment. Examination of the 8-m (26-ft) inby pressure profile shows that peak BPC pressure was nearly 65 MPa (9,425 psi); the remaining functional BPC's were reporting pressures between two and three times those recorded at the 78-m (256-ft) inby FP. BPC data suggest that the 23rd Left panel side of the chain pillar had yielded to a depth of 3 to 4 m (10 to 13 ft); however, most of the pillar was still intact as evidenced by the very high loads on the remaining cross section.

At the 8-m (26-ft) inby FP, ground stresses in the 24th Left panel also increased substantially. BPC data suggest that the first 3 to 5 m (10 to 16 ft) of the panel rib had yielded, and the stress abutment had moved deeper into the 24th Left panel. In-mine observations made at this time noted excessive, often severe, rock failure noise at the

Figure 15
Study Site locations in 23rd Left Gate Roads, Sunnyside No. 1 Mine.

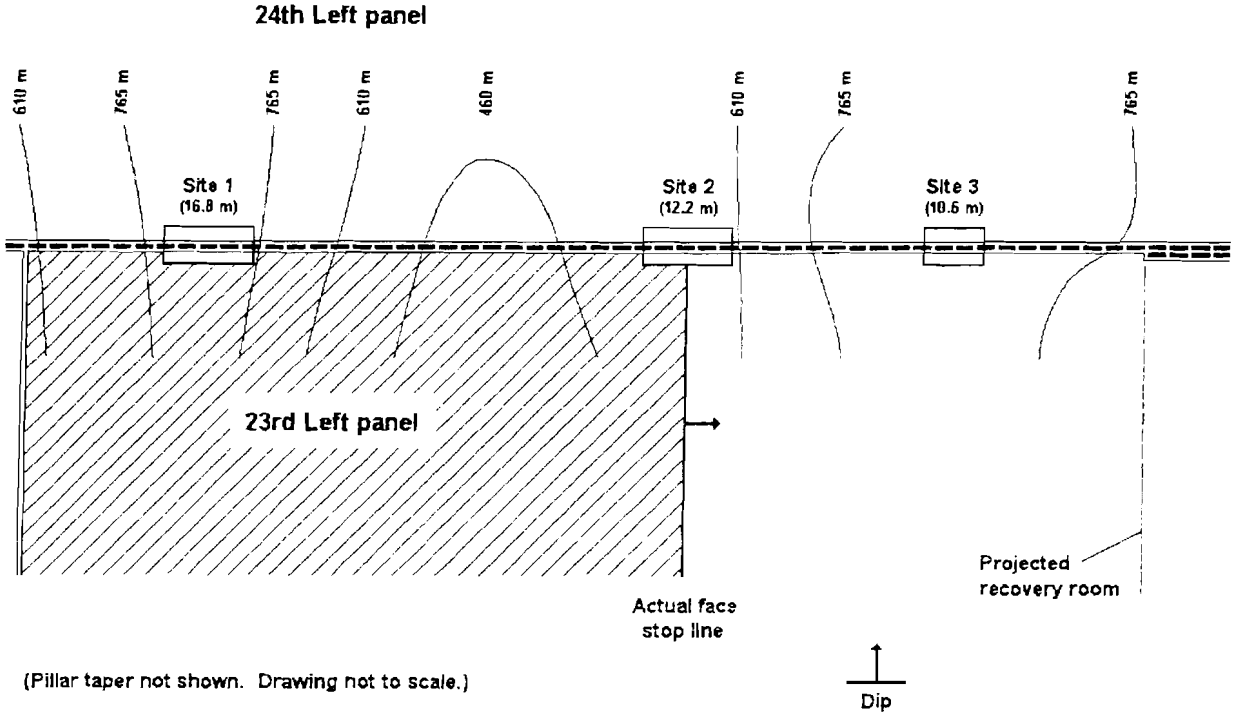

Figure 16
Instrumentation and Probehole Drilling Map for Crosscuts 46 to 49, Site 1.

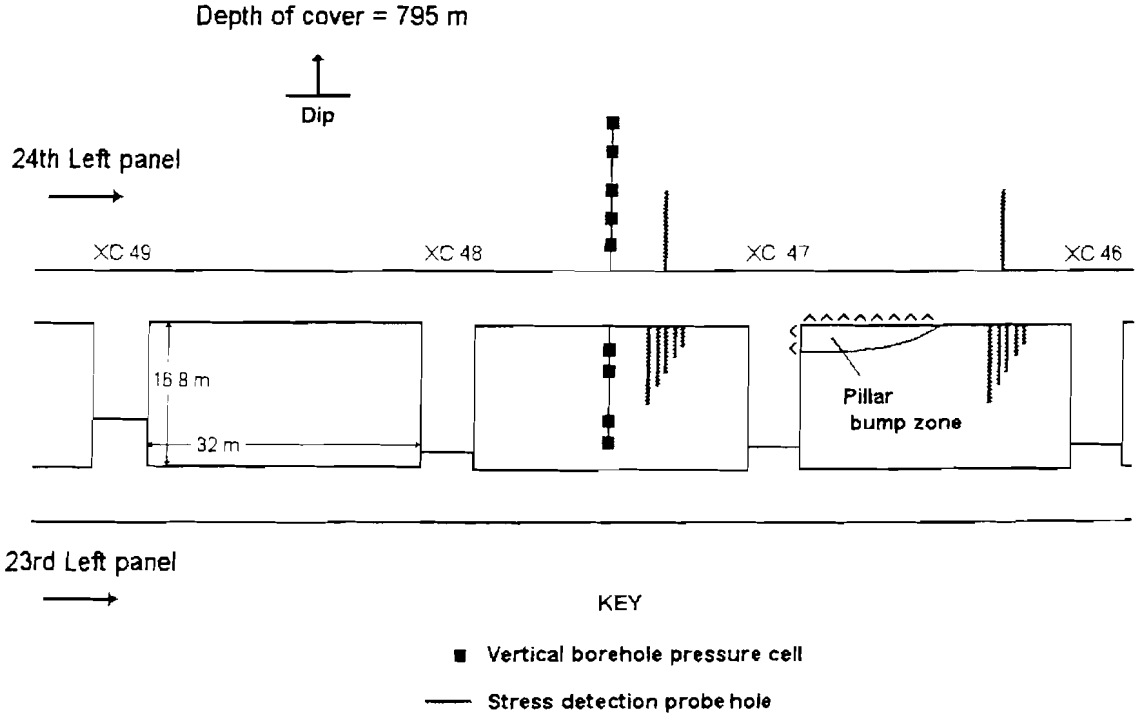

Figure 17
Instrumentation and Probehole Drilling Map for Crosscuts 24 to 27, Site 2.

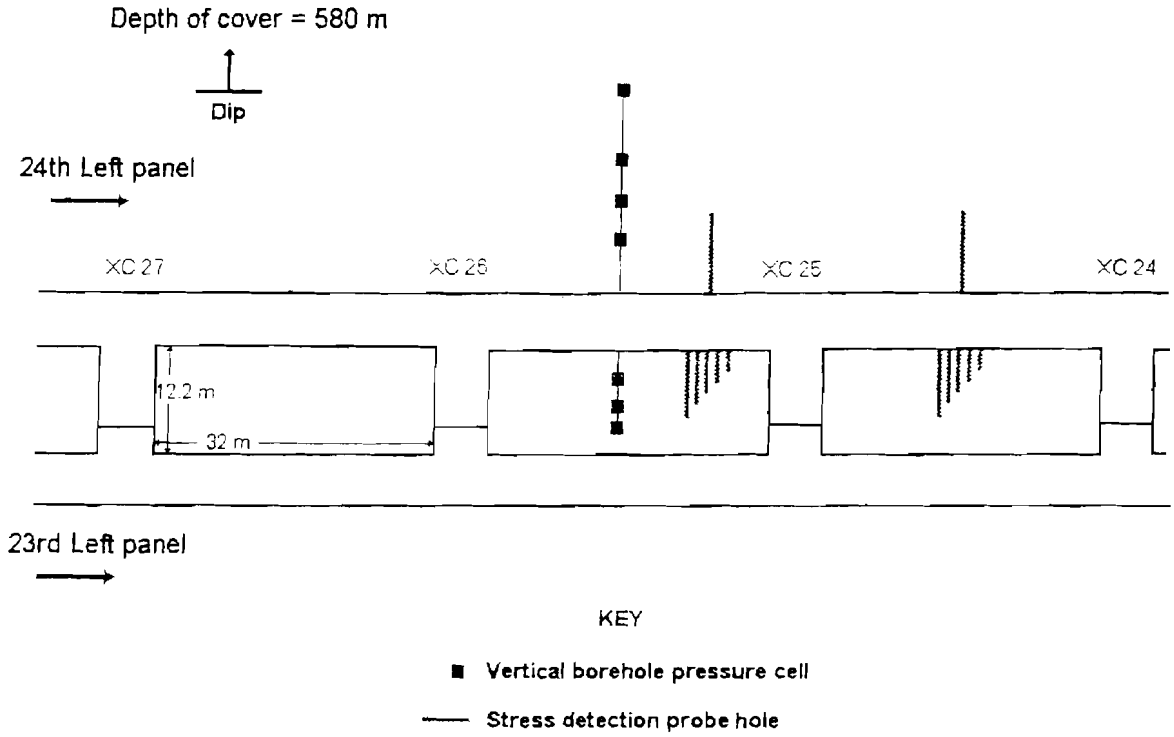

Figure 18
Probehole Drilling Map for Crosscuts 12 to 15, Site 3.

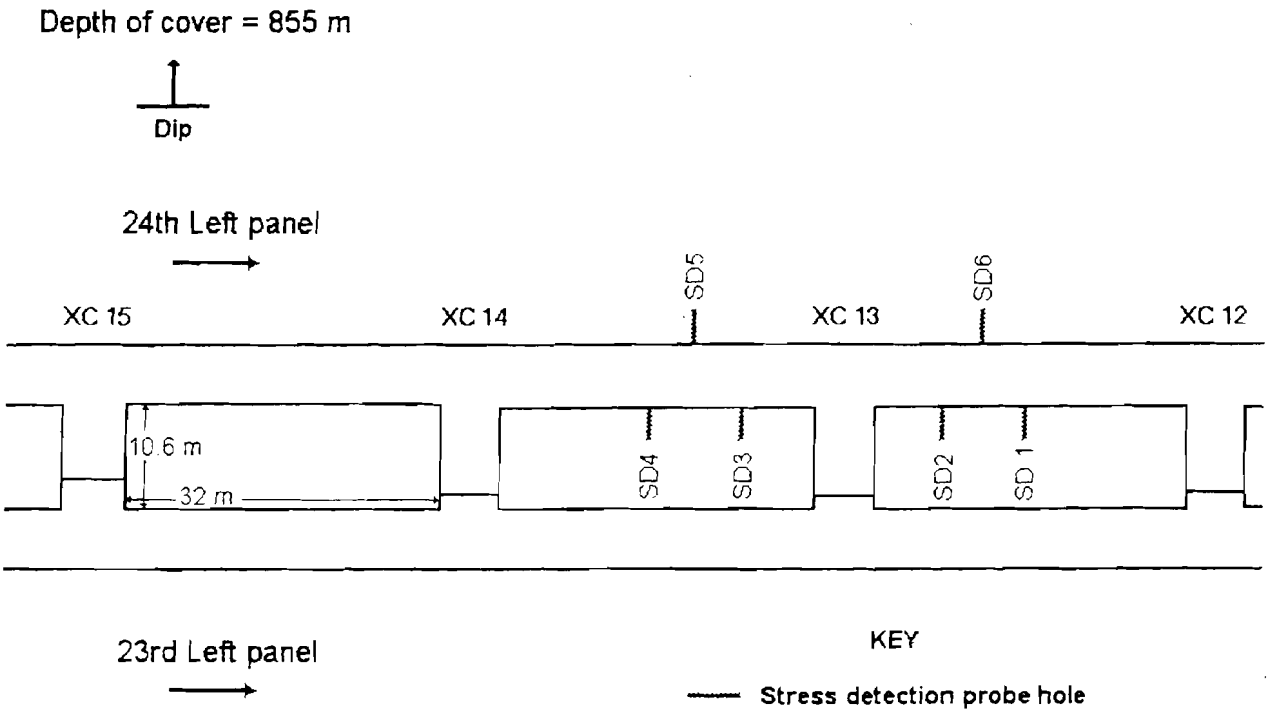

Figure 19
Ground Pressure Profiles for Select Longwall Face Positions, Site 1.

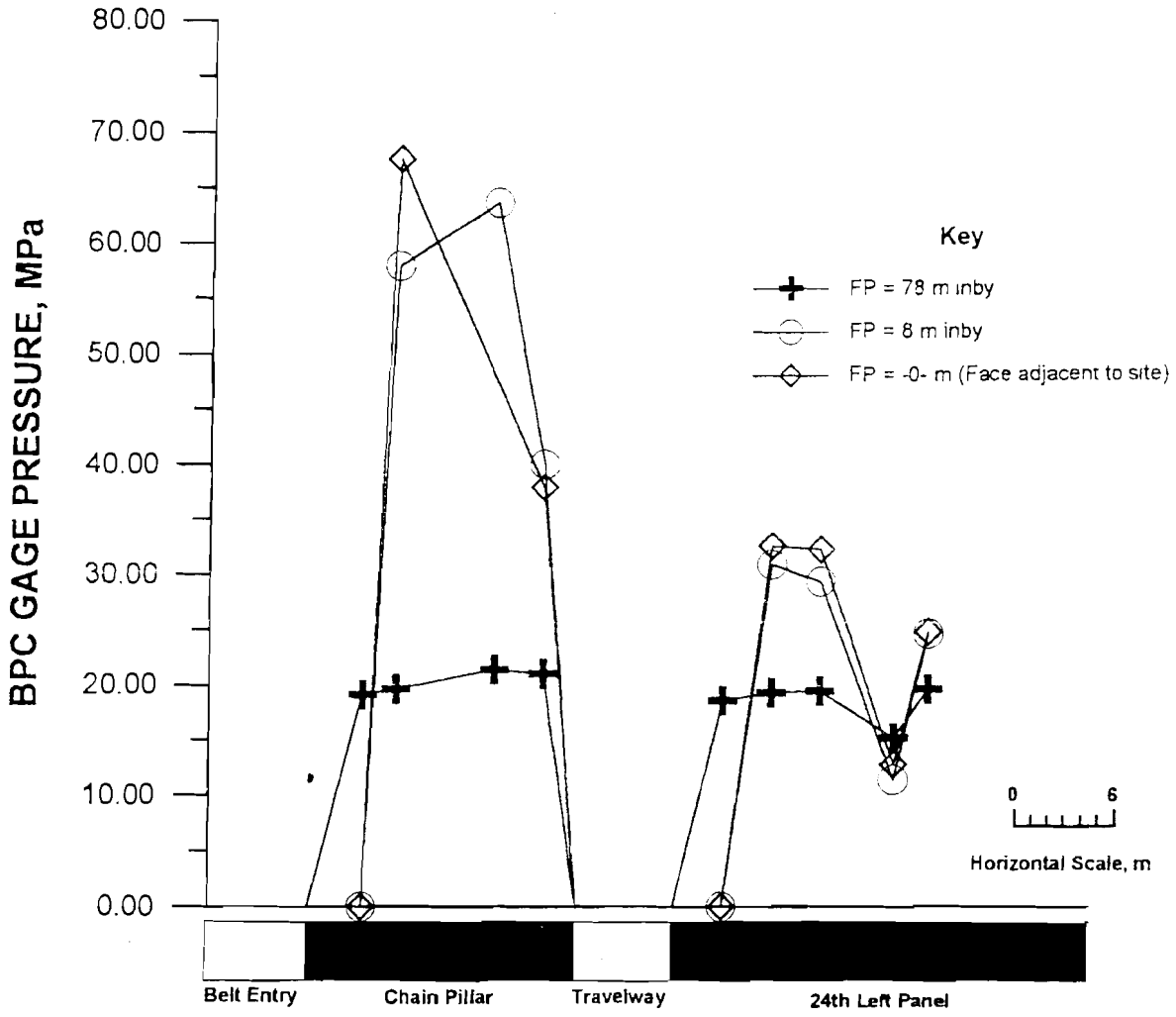

23rd Left panel extraction, looking inby.

study site. In addition, two pillars 30 to 40 m (100 to 130 ft) inby the instrumentation site [20 to 30 m (65 to 100 ft) behind the face] bumped heavily, ejecting coal into the future tailgate and knocking down several cribs.

When the longwall face advanced to the study site (FP = 0), peak pillar pressures were approaching 70 MPa (10,150 psi), and only two functioning pillar BPC's remained. Examination of the pressure charts from the failed BPC's reveals the occurrence of *instantaneous* pressure spikes of as much as 40 MPa (5,800 psi), which apparently destroyed the hydraulic integrity of the instruments. These extreme pressure changes were believed to be caused by the heavy bump activity emanating from the chain pillars immediately inby the site. This speculation was later demonstrated to be true when a documented bump event in the adjacent outby pillar resulted in pressure spikes that ruptured the remaining pillar BPC's and most of the panel instruments.

Although the pillar pressure profile at 0 FP shows a very highly loaded chain pillar, 24th Left panel pressures had not increased substantially since the 8-m (26-ft) inby FP, and no further panel rib yielding was indicated. These data suggested that most of the chain pillar continued to behave elastically. After the 0 FP, BPC data collection at the site was discontinued because of the damage inflicted on the instruments by the aforementioned pillar bump. This bump occurred when the face was approximately 60 m (197 ft) outby site 1. Documented damage from this event included the shattering of many of the 20- by 20-cm (8- by 8-in) wooden blocks making up two 1- by 1-m (3- by 3-ft) four-point cribs, with an additional four cribs being blown down by flying coal. Also, an estimated *36* m^3

1,270 ft^3) of in-place coal was forcibly ejected from the pillar rib (figure 16) into the future tailgate entry, making passage through this area very difficult.

In summary, the 17-m (55-ft) wide pillar at site 1 yielded little from the time of development until onset of the full forward stress abutment despite the 800-m (2,600-ft) depth. Limited yielding of the pillar did occur under the weight of the front abutment; however, a large, competent core of coal remained. As the longwall face passed the site, the already highly loaded pillar core was subjected to further loading from the side abutment. The addition of this load drove several of the pillars in this area to bump violently soon after the face passed. These data clearly indicate that the 17-m (55-ft) wide configuration was a critical-pillar design for the given mining conditions. In addition, the occurrence of these severe pillar bumps in the headgate strongly suggests that the 17-m (55-ft) wide pillar was probably closer in width to a successful yield pillar design than it was to a successful abutment design.

Site 2

Site 2 was established in the chain pillars and a section of the adjacent 24th Left panel between crosscuts 24 and 26 (figure 17). The pillars at site 2 were 12 m (40 ft) wide by 32 m (105 ft) long, and the cover depth was approximately 580 m (1,900 ft). Installed BPC's included three pressure cells placed at regular intervals across the width of one chain pillar and four pressure cells placed up to 24 m (77 ft) deep in the 24th Left panel. Twelve stress-detection probeholes were drilled in two pillars and at two locations in the 24th Left panel during instrument installation.

The probehole drilling data, collected when the face was approximately 600 m (2,000 ft) inby site 2, indicated pillar yield zones were from 2.5 to 3 m (8 to 10 ft) deep. Zones of moderate stress began approximately 3 m (10 ft) into the pillar ribs and were estimated to be approximately 1 m (3 ft) wide. Similarly, probehole drilling in the 24th Left panel indicated the existence of a 3- to 4-m (10- to 13-ft) deep yield zone along the panel rib. These data suggested that the chain pillars and 24th Left panel ribs at site 2 began yielding under gate road development loads.

Ground pressure profiles across the instrumented pillar and panel for three longwall face positions relative to the line of BPC's are presented in figure 20. The 159-m (522-ft) inby FP profile shows pillar and panel pressures before the forward stress abutment had reached the instrumentation site. Pillar and panel ground pressures are seen to be low, and the 3- to 4-m (10- to 13-ft) deep panel rib yield zone indicated by the probehole drilling is reflected by the very low BPC pressure 6 m (20 ft) from the panel rib.

As mining progressed to the 65-m (213-ft) inby FP, panel and (especially) pillar pressures rose significantly with the initial onset of the forward stress abutment. In fact, the highest pillar pressures recorded during the study of site 2 occurred when the face was 65 m (213 ft) inby the line of BPC's. Peak pillar pressure was approximately 40 MPa (5,800 psi); however, pressures on either side of the pillar center dropped rapidly with proximity to the pillar rib. In comparison, substantially higher loads were seen across a much greater portion of the pillar width at site 1 than at site 2. The panel pressure profile for the 65-m (213-ft) inby FP suggests that the panel yield zone had expanded to approximately 7 to 8 m (23 to 26 ft) in depth. This finding indicates that the forward abutment loads were being more evenly distributed between the chain pillar and the panel and suggests the occurrence of widespread softening of the ground surrounding the openings.

Ground pressures significantly changed once again as the longwall face moved to within 24 m (79 ft) inby site 2. Examination of the 24-m (79-ft) inby FP profile reveals that pillar pressures had returned to levels similar to those recorded at the 159-m (522-ft) inby FP. In addition, the panel pressure profile indicates that the panel rib yield zone extended to a depth of at least 10 m (33 ft). In-mine observations noted significant rock noise emanating from the coal and surrounding strata during the period of mining from the 65-m (213-ft) inby FP to the 24-m (79-ft) inby FP; however, *no* coal bumps were known to have occurred in and around site 2 during this time. Collectively, these data suggest that the pillars and a significant portion of the panel rib at site 2 had yielded in a nonviolent fashion, creating a protective "soft" zone of broken coal surrounding the gate entry.

In summary, the 12-m (40-ft) wide pillar at site 2 began yielding sometime after development but before the initial onset of the forward stress abutment; yielding of the adjacent 24th Left panel rib also started during this time period. As pillar and panel loads began to increase with the approach of the forward stress abutment, further pillar yielding occurred until pillar pressures returned to pre-longwalling levels. Forward abutment loads were consequently transferred to the 24th Left panel, causing additional yielding of the panel rib and completing the softening process around the gate. This information suggests that a 12-m (40-ft) wide pillar *approaches* proper yield pillar dimensions for the mining conditions found at Sunnyside. In fact, this configuration has been demonstrated to be a *marginal* yield pillar design at Sunnyside; in a previous study, Koehler (1994b) reported the occurrence of tailgate pillar bumps when a 12-m (40-ft) wide pillar was used. Incomplete pillar and panel rib yielding because of localized variations in geologic structure along the gate length was probably responsible for the behavior reported in that study.

Figure 20
Ground Pressure Profiles for Select Longwall Face Positions, Site 2.

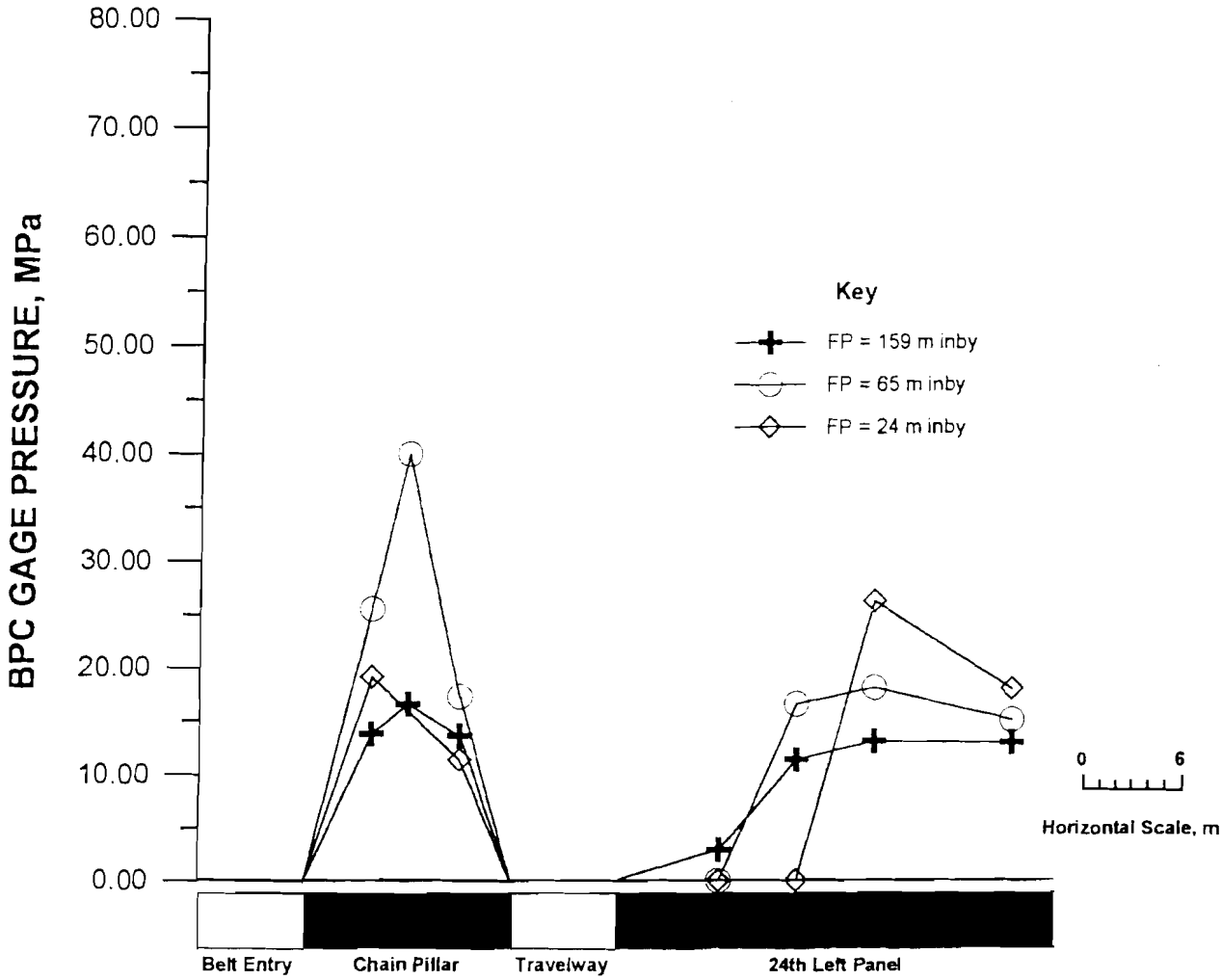

23rd Left panel extraction, looking inby.

Site 3

Site 3 was established in the chain pillars and a section of the adjacent 24th Left panel between crosscuts 12 and 14 (figure 18). The pillars at site 3 were 10.6 m (35 ft) wide by 32 m (105 ft) long, and the cover depth was approximately 855 m (2,800 ft). As previously reported, BPC's could not be installed at site 3 because of the unexpected closure of the Sunnyside No. 1 Mine; however, six stress-detection probeholes were drilled in two chain pillars and at two locations within the 24th Left panel before the mine was closed.

The probehole drilling data from site 3 were collected when the face was approximately 425 m (1,394 ft) inby the site. Data from chain pillar holes SD1, SD2, and SD4 indicated pillar rib yield zones were from 2 to 3 m (6 to 10 ft) deep, with a low-to-moderately stressed zone of intact coal approximately 0.5 m (2 ft) wide from 3 to 3.5 m (10 to 12 ft) deep. Intact coal under low stress was found from 3.5 m (12 ft) to the pillar center. Data from probehole SD3 suggested that pillar rib conditions at this location were different from those at the other three pillar holes. The pillar rib at SD3 was found to be solid, and moderate loads were encountered for the first 2 m (6 ft) of probehole. Drilling data indicated the presence of intact coal under low apparent stress from 2 m (6 ft) to the pillar center. Following completion of hole SD3, moderate rock failure noise was emitted from the coal surrounding the hole collar for approximately 15 min.

The pillar probehole data suggest that the chain pillars at site 3, like those at site 2, began to yield sometime after development. The data from probehole SD3, however, indicated that pillar rib yielding was not entirely uniform along the pillar perimeter. This result is not surprising; field study of 9.6-m (32-ft) wide pillars in the 20th Left gate roads of the Sunnyside No. 1 Mine demonstrated that some variability in the degree of pillar yielding can be expected (Haramy, 1990).

Probehole drilling data from panel holes SD5 and SD6 indicate that the degree of yielding along the 24th Left panel rib was also variable at the time of data collection. At probehole SD5, the panel rib yield zone was approximately 3 m (10 ft) deep, with a 1-m (3-ft) wide zone of moderate-to-high stress between 3 and 4 m (10 and 13 ft) into the panel rib. In comparison, at probehole SD6 the yield zone was estimated to be between 1.5 and 2 m (4 and 6 ft), deep, with a 2-m (6-ft) wide zone of high stress between 2 and 4 m into the panel rib.

In summary, the 10.6-m (35-ft) wide pillars, as well as the 24th Left panel rib, at site 3 began yielding sometime after development. The degree of pillar and panel rib yielding at this site was found to be variable; however, in general, the pillars and panel at site 3 were in the same approximate state of yielding (at prelongwalling load levels) as those found at site 2. As previously reported, in-mine experience with the 12-m (40-ft) wide pillars at site 2 has demonstrated that this configuration is a marginally successful yield pillar design for Sunnyside conditions. In comparison, employing yield pillars ranging in width from 9 to 10.6 m (30 to 35 ft) has met with favorable results at Sunnyside (Koehler, 1994a, 1994b).

CONCLUSIONS

Experience in Western mining operations shows that gate road coal bumps are the often the result of a combination of in-mine ground conditions and the actual gate design employed. The primary setting influences have historically thick, competent sandstone units in the main roof, strong roof and floor strata immediate to the seam, sand channels in the immediate roof, strong and largely unstructured coal seams, and faults and shear zone structures immediate to the seam, all of which are subject to deep, variable cover. Gate design practices that aggravate adverse mine settings include the misapplication of abutment-yield pillar configurations, the use of too many entries with full-yielding entry system designs, and, above all, the use of critical pillars. It cannot be overstated that critical pillars are perhaps the single greatest design problem where gate road ground instabilities are of concern. Such instabilities are not just limited to bump occurrences, but the entire spectrum of entry ground-control problems, including roof, rib, and floor failures.

To develop a clearer understanding of critical-pillar behavior, a field study of a tapering gate road was conducted at the Sunnyside No. 1 Mine. Three study sites were established along the length of the 23rd Left gate road in chain pillars 17 m (55 ft), 12 m (40 ft), and 10.6 m (35 ft) wide. A summary of the results of this field investigation follows.

- The 17-m (55-ft) wide pillars yielded little from development until onset of the forward stress abutment, despite the 800 m (2,600 ft) of cover. As a result, most of the abutment loads were borne by the chain pillars and not the adjacent panel. The combined weight of the forward and side abutment loads drove several of the pillars in this area to bump violently soon after the first longwall face passed by. Damage from these bumps included shattered and blown-down cribs and partial blockage of the future tailgate by ejected coal. The data and observations collected at this site clearly indicate that the 17-m (55-ft) wide configuration was a critical-pillar design for the given mining conditions.

- The 12-m (40-ft) wide pillars began yielding sometime after development but before the initial onset of the forward stress abutment; yielding of the adjacent 24th Left panel rib also started during this time period. Further pillar yielding occurred with the onset of forward abutment loads until pillar pressures returned to prelongwalling levels. Consequently, load transfer caused additional yielding of the adjacent panel rib, completing the softening process around the gate. No pillar bumps were reported. The data and observations collected at this site suggest that the 12-m (40-ft) wide pillar configuration approaches proper yield pillar dimensions for the mining conditions found at Sunnyside.

- The 10.6-m (35-ft) wide pillars and adjacent 24th Left panel rib began yielding following development. The degree of pillar and panel yielding was variable; however, in general, the pillars and panel at this site were in the same approximate state of yielding (at prelongwalling load levels) as those at the 12.2-m (40-ft) wide pillar location. Although the collection of data from the 10.6-m (35-ft) wide pillars was prematurely terminated by mine closure, significant on-site experience employing yield pillars of this width suggests that a nominal 10-m (33-ft) wide pillar provides excellent gate road ground control through the complete mining cycle (Koehler, 1994a, 1994b).

The failure of yield pillar designs to provide adequate ground control and reduce or eliminate those conditions responsible for the initiation of bumps is primarily related to the misapplication of these designs in coal seams having unfavorable roof and floor characteristics and/or the use of critical pillars, which actually *promote* poor ground conditions. A critical pillar is defined as one that is too large to yield nonviolently or to yield before the roof and floor sustain permanent damage, but too small to support full longwall abutment loads. Often, yield pillar widths are mistakenly increased to accommodate deepening cover in the same manner that abutment pillar widths might be increased. This situation is to be avoided because the difference between a fully successful yielding gate road and the *worst* possible critical-pillar condition may be as little as a few meters of increase in yield pillar size. Mine operators who unknowingly employ a critical-pillar design often abandon the concept of yielding gate roads prematurely, mistakenly labeling them as inapplicable to their given minesite conditions.

REFERENCES

Babcock, C. O. Constraint—The Missing Variable in the Coal Burst Problem. Paper in Proceedings of the 25th U.S. Symposium on Rock Mechanics (Evanston, IL, June 25-27, 1984). Soc. Min. Eng., AIME, 1984, pp. 539-547.

Barron, L. R., M. J. DeMarco, and R. O. Kneisley. Longwall Gate Road Stability in Four Deep Western U.S. Coal Mines. USBM IC 9406, 1994, 84 pp.

Boler, F. M., S. Billington, and R. K. Zipf. Estimations of Radiated Energy and Strain Energy Release for a Magnitude 3.6 Coal Mine Event (Pres. at Seismo. Soc. Am. 89th Annu. Meet., Pasadena, CA, April 5-7, 1994). Seismo. Res. Lett., v. 65, No. 1, Jan.-Mar., 1994, p. 34.

DeMarco, M. J. Yielding Pillar Gate Road Design Considerations for Longwall Mining. Paper in New Technology for Longwall Ground Control. Proceedings: U.S. Bureau of Mines Technology Transfer Seminar, comp. by C. Mark, R. J. Tuchman, R. C. Repsher, and C. L. Simon. USBM Spec. Publ. 01-94, 1994, pp. 19-36.

DeMarco, M. J., J. R. Koehler, and P. H. Lu. Characterization of Chain Pillar Stability in a Deep Western Coal Mine—Case Study (Phoenix, AZ, Jan. 25-28, 1988). Soc. Min. Eng. preprint 88-76, 1988, 12 pp.

Haramy, K. Y., and R. O. Kneisley. Yield Pillars for Stress Control in Longwall Mines-Case Study. Int. J. Min. Geol. Eng., v. 8, 1990, pp. 287-304.

Holland, C. T., and E. Thomas. Coal Mine Bumps—Some Aspects of Occurrence, Causes, and Control. USBM Bull. 535, 1954, 37 pp.

Iannacchione, A. T., and M. J. DeMarco. Optimum Mine Designs to Minimize Coal Bumps: A Review of Past and Present U.S. Practices. Ch. 24 in New Technology in Mining Health and Safety. Soc. Min. Eng., AIME, 1992, pp. 235-247.

Koehler, J. R. Longwall Gate Road Evolution and Performance at the Sunnyside Coal Mines (Albuquerque, NM, Feb. 14-17, 1994). Soc. Min. Eng., preprint 94-179, 1994a, 11 pp.

Koehler, J. R. The History of Gate Road Performance at the Sunnyside Mines: Summary of U.S. Bureau of Mines Field Notes. USBM IC 9393, 1994b, 43 pp.

Maleki, H. N. Analysis of Violent Failure in U.S. Coal Mines: Case Studies. Paper in Proceedings: Mechanics and Mitigation of Violent Failure in Coal and Hard-Rock Mines. USBM Spec. Publ. 01-95, 1995, pp. 5-25.

___. Ground Response to Longwall Mining: A Case Study of Two-Entry Yield Pillar Evolution in Weak Rock. CO Sch. Mines Q., v. 83, No. 3, 1988, 52 pp.

___. Coal Mine Ground Control. Ph.D. Thesis, CO Sch. Mines, Golden, CO, 1981, 432 pp.

McDonnell, J. P., D. P. Conover, and R. M. Cox. Evaluation of an Alternative Longwall Gate Road Design. USBM RI 9541, 1995, 15 pp.

Molinda, G. M., and C. Mark. The Coal Mine Roof Rating (CMRR): A Practical Rock Mass Classification for Coal Mines. Paper in Proceedings of the 12th Conference on Ground Control in Mining, ed. by S. S. Peng (Morgantown, WV, Aug. 3-5, 1993). Dep. Min. Eng., WV Univ., Morgantown, WV, 1993, pp. 92-103.

Osterwald, F. W., J. O. Mayberry, and C. R. Dunrud. Bedrock, Surficial, and Economic Geology of the Sunnyside Coal Mining District, Carbon and Emery Counties, Utah. U.S. Geol. Surv. Prof. Paper 1166, 1981, 68 pp.

Peparakis, J. Mountain Bumps at the Sunnyside Mines. Trans. AIME, v. 211, Sept. 1958, pp. 982-986.

Scheibner, B. J. Geology of the Single-Entry Project at Sunnyside Coal Mines 1 and 2, Sunnyside, Utah. USBM RI 8402, 1979, 106 pp.

Zelanko, J. C., and K. A. Heasley. Evolution of Conventional Gate-Entry Design for Longwall Bump Control: Two Southern Appalachian Case Studies. Paper in Proceedings: Mechanics and Mitigation of Violent Failure in Coal and Hard-Rock Mines. USBM Spec. Publ. 01-95, 1995, pp. 167-180.

EVOLUTION OF CONVENTIONAL GATE ENTRY DESIGN FOR LONGWALL BUMP CONTROL: TWO SOUTHERN APPALACHIAN CASE STUDIES

By Joseph C. Zelanko[1] and Keith A. Heasley[1]

ABSTRACT

This paper focuses on the conventional design of gate roads for minimizing bump hazards in longwall mining. The paper describes bump occurrences and the evolution of gate road designs to combat bumps at two southern Appalachian longwall mines. An analysis of gate road system stability at these mines is presented, along with a discussion of the apparent effect of the strength-load ratio on the occurrence of coal bumps. It is suggested that properly sized gate pillars can mitigate tailgate face bumps in many situations by limiting the transfer of abutment stresses to the longwall face.

INTRODUCTION

Coal mine bumps are the sudden, violent expulsion of coal from a rib or active working face into an adjacent entry or entries. (In a coal bump, as opposed to a gas outburst, only a minimal amount of gas is released in conjunction with the ejected coal.) Coal bumps are an extremely debilitating problem, for they can result in personnel injuries and fatalities, damaged equipment, reduced production, and lost reserves. Additionally, the unpredictable nature of bumps has a profoundly negative effect on the morale of the work force. Commensurate with the seriousness of the problem, a significant effort has been expended to better understand the coal bump phenomenon. The U.S. Bureau of Mines (USBM) and several coal companies and universities have been active in this research.

Historically, the coal bump problem has been mitigated through design recommendations that proposed modifying extraction sequences and mine geometry and through various destressing operations. Holland and Thomas (1954) examined 117 bumps that occurred in the United States between 1925 and 1950 and determined that, in many instances, bumps could be alleviated by avoiding unfavorable mining configurations. Iannacchione and DeMarco (1992) presented a review of bump research in the United States that emphasized the success of previous work in (1) identifying the various factors that contribute to bumps and (2) developing mining methods and recommendations to minimize bump hazards. However, an analysis of accident statistics from 1959 to 1984 by Goode and others (1984) confirmed that coal mine bumps constituted a persistent problem and had led to 28 fatalities during that time. These fatalities were equally divided between Eastern and Western U.S. coalfields.

Because the vast majority of the underground coal produced in the United States has been mined by room-and-pillar methods, many of the approaches developed historically to address bump-prone conditions apply only to this method. Room-and-pillar mining provides great flexibility, particularly in terms of cut sequencing, which has been advantageous in several cases (Campoli and others, 1989; Mucho and others, 1993). In contrast, longwall mining follows a fairly rigid extraction sequence and, as a result, innovative design practices are required to address bump problems on longwall faces.

[1]Mining engineer, Pittsburgh Research Center, U.S. Bureau of Mines, Pittsburgh, PA.

Challenging bump problems have been encountered with longwall mining as this method has become more prominent in the United States. At least one fatality, several injuries, and one mine closure have been attributed to bumps on longwall sections (Iannacchione and DeMarco, 1992). To date, several different approaches have been undertaken to mitigate bumps in longwall mining operations. In the Eastern United States, a conventional coal pillar design approach appears to have been successful in curtailing bumps at the working face. Alternate approaches adopted in the Western U.S. coalfields include yielding pillar systems in several Utah coal mines (Maleki, 1988; Koehler, 1994) and advancing longwalls in Colorado (Jackson, 1975).

Conventional gate road design is based on the premise that, in some instances, properly sized gate pillars can mitigate tailgate face bumps by limiting the transfer of abutment stresses to the longwall face. Essentially, if tailgate abutment pillar failures and/or bumps are prevented or at least delayed, the abutment pillars may support gob load that would otherwise be transferred to the tailgate corner of the longwall face. However, conventional coal pillar design is not a panacea. Certainly, conditions may be encountered where gate system design will have little influence on bumps. For example, excessive stress conditions could be encountered that would contribute to the occurrence of bumps at midface despite the presence of stable gate pillars. In extreme instances, excessive stress conditions have resulted in bumps during development (Iannacchione and Zelanko, 1995).

This paper focuses on the conventional design of gate roads for minimizing bump hazards in longwall mining. The authors describe bump occurrences and the evolution of gate road design at two southern Appalachian longwall mines.

CASE STUDY MINE 1

The first case study is a longwall mine in Buchanan County in southwestern Virginia. At this mine, eight successive longwall panels have been mined to the north and 10 successive panels have been mined to the south of twin barrier pillars (figure 1). The gate entry system between the sixth and seventh panels to the south contains what is referred to as the 7 development study area. This was the first of three areas studied in detail by the USBM. The other study areas are in 8 development and 10 development, as shown in figure 1.

The mine extracts the Pocahontas No. 3 Coalbed, which is located in the Pocahontas Formation and averages 1.7 m (5.5 ft) thick. Overburden in the three study areas ranges from 400 to 700 m (1,300 to 2,200 ft) thick, and the coalbed dips 1° from east to west (Campoli and others, 1990). The immediate roof in the south end of the mine consists of a widely jointed siltstone overlain by a massive quartzarenite sandstone. In the study areas, the siltstone ranges from 9 to 18 m (30 to 60 ft) thick, and the sandstone ranges from 60 to 75 m (200 to 250 ft) thick. The mine floor consists of a combination of very competent siltstones and sandstones. Underground observations by Iannacchione (1990) indicate a persistent absence of prominent fractures or joints in the immediate roof and floor, and the main roof, dominated by the thick sandstone, is exceedingly difficult to break. In situ stress measurements in the 8 development study area also indicate that the maximum horizontal stress is 23 MPa (3,400 psi) at N. 76° E., and the minimum horizontal stress is 11 Mpa (1,600 psi) (Campoli and others, 1990).

The original gate pillar configuration employed at case study mine 1 consisted of a yield-yield-abutment design in which the yield pillars were 9 m (30 ft) wide, the abutment pillar was 24 m (80 ft) wide, and the crosscuts were spaced on 30-m (100-ft) centers. Throughout the mine, the longwall panels were 183 m (600 ft) wide and roughly 1,800 m (6,000 ft) long. In the original design, the larger abutment pillars were located directly adjacent to the tailgate. During the tailgate phase of the gate road, these 24-m (80-ft) square pillars frequently experienced heavy bumps directly adjacent to the tail drive, causing coal to be thrown into the face area where miners were working.

The second gate pillar design, evaluated in the 7 development study area, was a yield-abutment-yield design with the same size abutment pillar [24 m (80 ft) square] flanked on either side by 9-m (30-ft) wide yield pillars. The crosscuts were again on 30-m (100-ft) centers (figure 2). In this design, the 9- by 24-m (30- by 80-ft) yield pillars apparently yielded during the headgate pass of the longwall (Campoli and others, 1990), thereby eliminating their potential to bump. Then, on the tailgate pass of the longwall, the yielded pillars effectively shielded face workers from thrown coal if the 24-m (80-ft) square abutment pillar bumped in the tailgate.

The 7 development study area (figure 1) was centered approximately 1,430 m (4,700 ft) from the startup entry of panel 6 under approximately 595 m (1,950 ft) of overburden. The 24-m (80-ft) square tailgate abutment pillars in this gate entry system were observed to bump as the abutment load from the panel 7 gob was superimposed

Figure 1
Map of Mine 1.

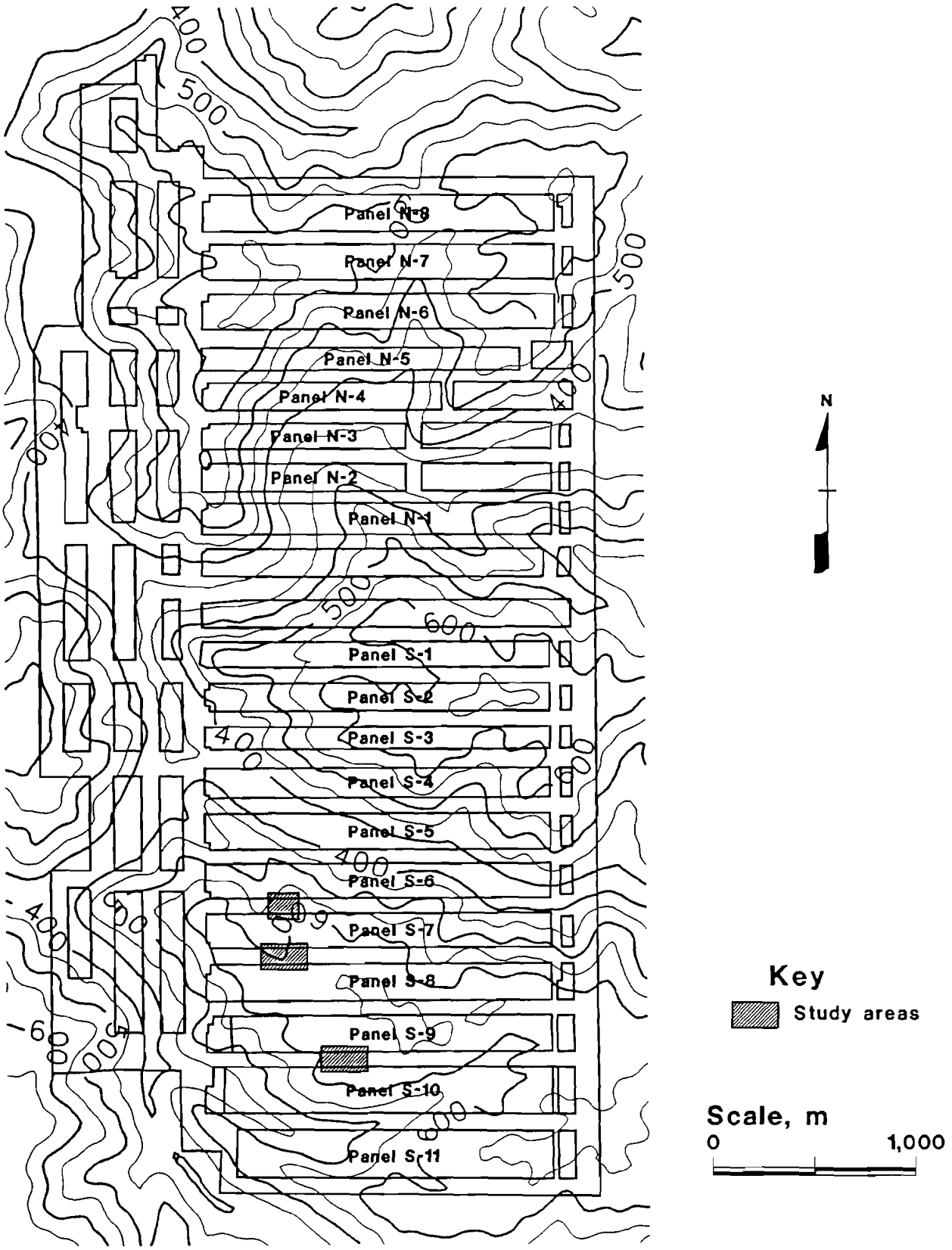

Figure 2
Pillar Designs in 7 and 8 Development.

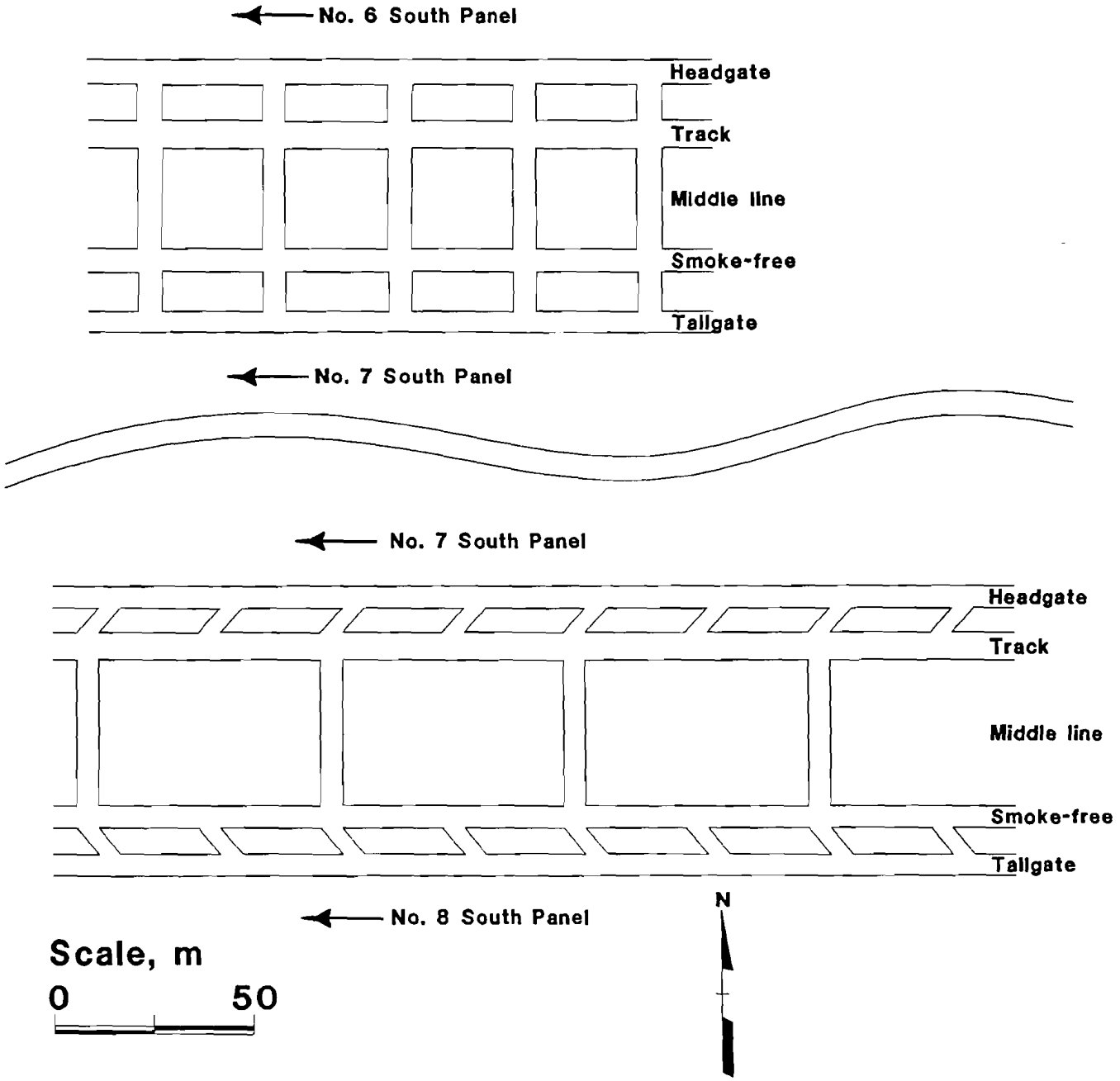

on the pillars. Initially, the abutment pillars bumped inby the longwall face. However, at mid-panel, the abutment pillars were bumping adjacent to the longwall face. After about 1,200 m (4,000 ft) of the panel had been mined, the 24-m (80-ft) square tailgate abutment pillars within this gate entry system were observed to bump up to five pillar rows [150 m (500 ft)] in front of panel 7 (figure 3). Apparently, the failure of the abutment pillars in advance of mining resulted in load transfer to the tailgate corner of panel 7 and subsequent face bumps (Campoli and others, 1990).

To better control ventilation between previous and active gobs, improve tailgate entry stability, control tailgate face bumps, and standardize gate entry system design, mine 1 modified the yield-abutment-yield configuration for 8 development and subsequent gate roads. This new design consisted of 6- by 24-m (20- by 80-ft) yield pillars on each side of a 37- by 55-m (120- by 180-ft) abutment pillar (figure 2). Between the yield pillars, the crosscuts were driven at 60° angles on 30-m (100-ft) centers, whereas between the abutment pillars, the crosscuts were driven at 90° angles on 60-m (200-ft) centers.

The 8 development study area (figure 1) was centered approximately 1,400 m (4,600 ft) from the startup entry of panel 7 under approximately 625 m (2,050 ft) of overburden. Under worst-case conditions, after approximately 1,400 m (4,600 ft) of panel 8 had been extracted (near the center of the 8 development study area), the abutment pillars did not begin to bump until they were approximately 30 m (100 ft) inby the longwall face. Furthermore, the intensity of tailgate abutment pillar bumps was greatly reduced by the new design (Campoli and others, 1990); in fact, many of the observed bump areas may have only been the edge of the abutment pillar. Thus, the 37- by 55-m (120- by 180-ft) abutment pillars supported the applied abutment loads and prevented ground stresses from overriding to the longwall face during panel 8 mining (Heasley and Barron, 1988).

Figure 3
Schematic of Face Bump in 7 Development.

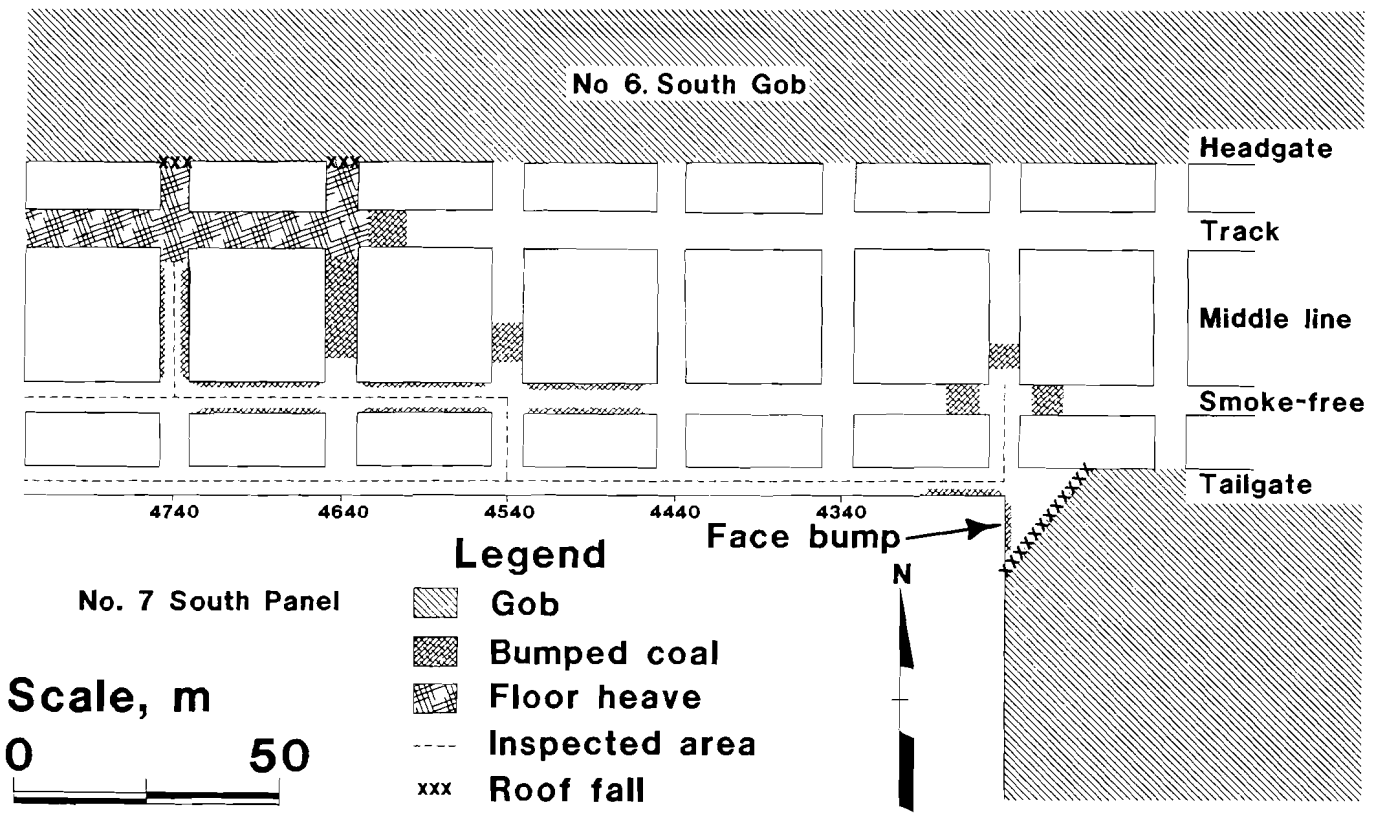

CASE STUDY MINE 2

The second case study is a longwall mine in the Upper Cumberland coal district of the southern Appalachian Coalfield in Harlan County in southeastern Kentucky. This coal district covers an area approximately 160 km (100 mi) long and 13 km (8 mi) wide between Pine Mountain on the northwest and Cumberland Mountain on the southeast (Brant and others, 1983). The mine operates in the Harlan Coalbed. Within the extent of the property, the mined height of the coalbed varies from 2.5 to 3.7 m (8.0 to 12.0 ft). Two other coalbeds, the Kellioka and the High Splint, have been mined on the property. They are located approximately 45 m (150 ft) and 450 m (1,500 ft), respectively, above the Harlan Coalbed.

The Harlan Coalbed is underlain by the subHarlan Sandstone over the entire mine property. However, in many areas an intermediate shale member ranging up to approximately 4.6 m (15 ft) thick also appears between the coal and the underlying sandstone. The immediate roof varies considerably across mine 2. Generally, the roof consists of a laminated gray shale; however, in places, the roof varies from a weak, highly fossilized and slickensided black shale to a strong siltstone. In addition, a sandstone channel system was encountered on the south side of the mine property (figure 4). This channel has been characterized as a deltaic formation with fingerlike projections extending radially outward from a central main channel.

Whereas conditions at mine 1 were relatively consistent across much of the mine property, a number of conditions, which correlate with bumps, varied considerably across mine 2. For example, the sandstone channel system

Figure 4
Map of Mine 2.

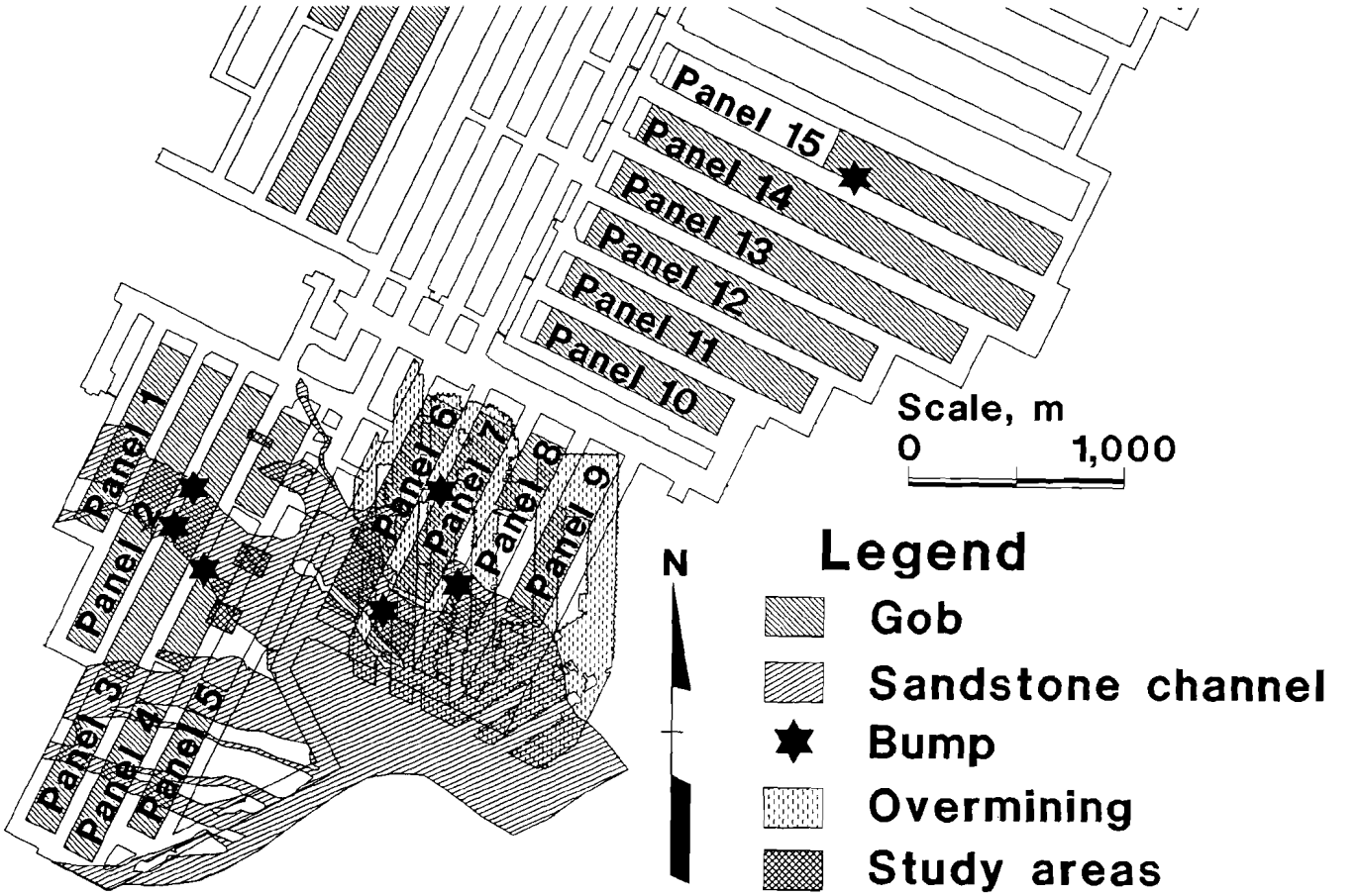

caused sudden changes in the geologic and mechanical composition of the immediate roof. Also, topographic relief varied dramatically across the property, and multiple-seam interactions were evident in some areas of the mine. The following is a description of the history of coal bumps at mine 2 and some of the conditions believed to have contributed to these events.

Within the last 5 years, at least six different gate road designs were utilized at case study mine 2 (figure 5). Although the current design is a four-entry, yield-abutment-yield layout, the coal pillar configuration historically had been a three-entry yield-abutment design. Pillar dimensions frequently varied from one gate road to the next. However, all of the three-entry systems were configured similarly, with the abutment pillar placed adjacent to the longwall panel in the headgate. In the earlier three-entry designs (figure 5*A* through 5*C*), the dimensions of both pillars were increased in successive designs, ostensibly to account for increasing overburden. The smaller pillar's least dimension was increased from 15 to 21 m (50 to 70 ft) and the larger pillar's least dimension was increased from 27 to 37 m (90 to 120 ft). The smaller pillar in these gates did not perform necessarily as a true yield pillar. However, in later designs (figure 5*D* and 5*E*), the dimensions of the smaller pillar were reduced and the dimensions of the abutment pillar were increased. Mine management has come to believe through visual observation that the 12-m (40-ft) wide pillar (figure 5*F*) currently acts as a true yield pillar and has improved roof control.

Longwall mining began at mine 2 in 1982 (Schuerger, 1985) and progressed through 10 panels, or portions of these panels, without a coal bump. However, in mid-April 1989, a large bump occurred on the longwall face (panel 3, as shown in figure 4). Investigations following the face bump revealed that the tailgate abutment pillars adjacent to the face and immediately outby had bumped as well. At the time of the bump, the longwall face had begun to advance under a sandstone channel that crossed the panel. The longwall panel was approximately 152 m (500 ft) wide, and the tailgate was a three-entry arrangement with coal pillars 15 and 27 m (50 and 90 ft) wide by 30 m (100 ft) long (figure 5*A*).

Production was resumed from the site of the first bump in late April 1989. In early May 1989, after an additional advance of about 180 m (600 ft), a second large face bump occurred as the face was nearing the outby margin of the sandstone channel. The height of the overburden at this second bump site was approximately 380 m (1,250 ft). Reports indicated that the tailgate abutment pillars were completely crushed and the floor was broken and heaved adjacent to the face and at least two pillar rows outby.

The longwall was advanced from the second bump site to the end of panel 3 without further incident. However, in anticipation of similar bump-prone conditions in panel 4, mine management implemented a stress detection and destressing program. A hand-held pneumatic auger drill was used to detect zones of high stress in the longwall face. Drilling yield (cuttings volume) was monitored, and drilling resistance was observed to determine whether shot firing should be used for destressing. When zones of high stress were encountered, 5-cm (2-in) diam holes were drilled 3 to 6 m (10 to 20 ft) deep within the suspect zone and shot with permissible explosives. In addition, Lexan acrylic sheets were suspended on chains from the shield canopies to help isolate the walkway behind the panline from coal thrown from the working face.

Despite these measures, a major coal bump occurred on the panel 4 longwall face and in the adjacent tailgate pillars. As before, the face was advancing under the sandstone channel, with an overburden thickness of 358 m (1,175 ft). Investigations again revealed that the panel 4 tailgate pillars [18 and 30 m (60 and 100 ft) wide by 30 m (100 ft) long] had bumped at least two pillar rows outby the face (Zelanko and others, 1992). After this bump, management opted for an unplanned face move around the remainder of the channel in this panel rather than risking another such event. Setup entries were mined just outby the channel, and mining was resumed from that location, as indicated in figure 4.

A major arm of the sandstone channel system in the vicinity of the three bumps was apparently a deciding factor in the bump occurrence. The cross section of the channel was generally lens shaped, with a maximum thickness of approximately 15 m (50 ft) in the center, thinning to 0 m (0 ft) near the edges. The channel crossed perpendicular to the longwall panels (figure 4) and thus affected a relatively short distance during panel retreat. Scouring or removal of some of the coalbed during deposition of the channel was evident in the gate entries near the channel.

The potential for coal bumps initially appeared to be diminished significantly in the next series of panels scheduled to be mined (panels 6 through 9) (figure 4). The sandstone channel was less apparent in this area; it appeared to be broader and had not scoured the coalbed to the extent observed in the panels mined previously. Although the overburden thickness increased beneath a ridgeline, the abutment pillar dimensions had been increased to 43 by 37 m (140 by 120 ft). In addition, a significant barrier remained between the next series of panels (6 through 9) and the previous gob; the barrier was created by leaving a large portion of panel 5 unmined. Although these attributes reduced the likelihood of bumps, the potential for multiple-seam mining interactions existed in these panels. The Kellioka Coalbed, approximately 45 m (150 ft) above the Harlan Coalbed, had been mined and, in limited areas, partially retreated using room-and-pillar methods (figure 4).

Figure 5
Gate Road Configurations Utilized at Mine 2.

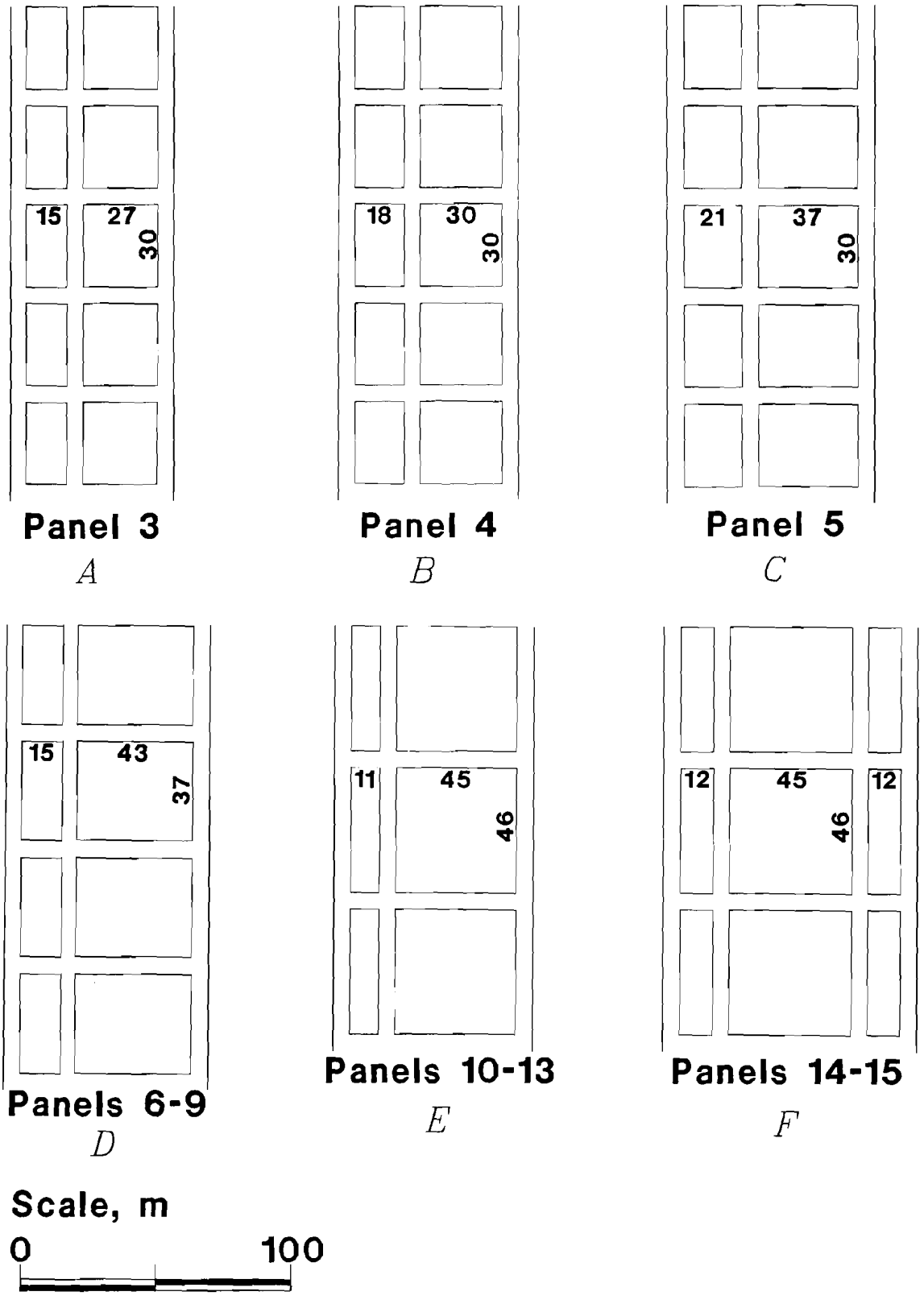

Numbers indicate pillar dimensions in meters.

Although several seismic shocks were reported early in the extraction of panel 6, no evidence of thrown coal was observed on the face or in the gate roads or bleeders, and this panel was extracted without incident. However, a major bump occurred in panel 7 near the tailgate when the face had progressed about 170 m (550 ft) from the startup entry. At the point of this second bump, the face had encountered a zone of heavy scouring. After the bump, coal pillars adjacent to the tailgate and immediately outby one row appeared to be yielding and spalling. Pillars farther inby and outby appeared to be more competent, but as much as 1 m (3 ft) of floor heave was noted. Dimensions of these pillars are shown in figure 5*D*.

At the location of the face bumps in panel 7, it was noted that a barrier approximately 75 m (250 ft) wide was left between two room-and-pillar panels in the superjacent Kellioka Coalbed. The upper seam workings were not aligned with the lower seam longwall panels. As mining progressed in panel 7, the potential for zones of stress concentration and relief existed based on the condition of the upper seam and the extent of interaction between seams. After the major face bump in panel 7, the face was moved approximately 110 m (350 ft) outby and restarted. Several subsequent minor events appeared to coincide with the position of abutment zones in the overlying Kellioka Coalbed. In addition, a second serious event, in which the shearer sustained some damage, occurred subjacent to a room-and-pillar development area. Although this second major bump in panel 7 did not occur beneath a barrier, it was noted that the bump occurred near the point of maximum overburden at the juncture of three ridge lines.

Experiences in panel 7 were repeated to some extent in panel 8. Panel 8 was moved ahead 240 m (800 ft) to avoid mining beneath the sandstone channel. A major face bump occurred when the face had advanced about 170 m (550 ft). In the tailgate, yield pillars for six rows outby the face were crushed and yielded; tailgate abutment pillars adjacent to the face showed heavy spalling and displacement into the entries, but no bumping was apparent. At five pillar rows farther outby, portions of several abutment pillars were noted to have bumped. At the time of the bump, the face had advanced so that the tailgate corner was positioned beneath a barrier in the Kellioka workings. The bumped tailgate pillar was similarly positioned beneath an overlying abutment pillar (figure 4).

After the bump, the face was moved outby approximately 430 m (1,400 ft) in panel 8 to avoid superjacent barriers and high cover. No significant bumps were reported as the remainder of this panel and panel 9 were mined. Portions of panel 9 were mined under barriers in high cover; however, the tailgate in most of these areas was adjacent to the unmined length of the previous panel.

Panels 10 through 15 were developed using 45- by 46-m (147- by 152-ft) abutment pillars and either one 11-m (35-ft) wide or two 12-m (40-ft) wide yield pillars. These designs performed well during the extraction of five successive panels; however, a tailgate pillar bump occurred at midlength in panel 15. At the time of the bump, the longwall face had advanced to within 9 m (30 ft) of the outby edge of the adjacent tailgate abutment pillar. Although the face experienced a significant seismic shock, a large volume of material was not involved. Overburden thickness at the bump site was approximately 670 m (2,200 ft). During extraction of the remainder of panel 15, seismic events were reported in the headgate, but no serious events have been encountered to date.

COAL PILLAR DESIGN METHODOLOGY

Traditionally, coal pillar design has been accomplished by determining pillar strength and anticipated loads, then selecting the pillar size with a suitable margin of safety of strength over load. Mark (1987, 1990) developed a method for gate road pillar design called analysis of longwall pillar stability (ALPS), which provides estimates of both pillar strength (load-bearing capacity) and loading associated with longwall extraction. In the basic ALPS approach, pillar strength is determined using the Bieniawski formula, while pillar loading is a combination of tributary area development loading and angle-of-draw abutment loading. Total gate road load-bearing capacity and the total gate road load form a ratio that provides an estimate of the stability of the gate road. Mark analyzed this stability factor using a database of more than 100 case histories of failed and unfailed gate road pillars.

Generally, Mark recommends an ALPS stability factor range between 0.7 and 1.3 for a satisfactory tailgate roof condition, depending on the roof quality. Mark found that mines operating under exceptionally strong roof can utilize lower stability factors, whereas those under weaker, slickensided roof should employ higher stability factors (Mark and others, 1994).

Although ALPS was not developed for design in bump-prone conditions, the ALPS stability factor can provide a simple, quick quantification of the relative stability (or strength-load capacity) of various gate-pillar situations. In the present study, ALPS was used as a method to compare various gate road designs utilizing the same mechanical considerations. Table 1 presents stability factors and pertinent parameters for 10 different gate road situations from the two mines. In all instances, these stability factors represent the strength-load ratio corresponding to a pillar at the tailgate T-junction during second panel mining. Pillar and panel dimensions are given, as well as overburden thickness and coalbed height.

Table 1.—Stability factors and pertinent parameters for different gate road configurations

	Mine 1[1]				Mine 2[2]							
	6 development	7 development		8 development		Panel 3	Panel 4	Panel 5	Panel 7	Panel 8	Panel 13	Panel 15
Pillar width, m:												
1	9	9		6		15	18	21	15	15	11	12
2	24	24			37	27	30	37	43	43	45	45
3	9	9		6		NAp	NAp	NAp	NAp	NAp	NAp	12
Pillar length, m	24	24		24	55	30	30	30	37	37	46	46
Panel width, m	183	183		183		152	152	152	183	183	183	183
Comparative overburden:[3]												
ALPS stability factor	0.46	0.46		0.88		0.44	0.54	0.63	0.67	0.67	0.82	0.81
Maximum overburden:[4]												
Overburden, m	520	600		670		520	550	460	630	630	630	670
ALPS stability factor	0.40	0.33		0.56		0.38	0.44	0.63	0.45	0.45	0.54	0.52
Coal bump:												
Observations	Pillar bumps	Pillar bumps	Face bumps	No bumps		Face bump[5-6]	Face bump[6]	Face bump[6]	No bumps	Face bump[6-7]	Face bump[6-7]	No bumps	Pillar bump
Overburden, m	410	530	600	670		350	440	440	610	640	550	640	670
ALPS stability factor	0.53	0.38	0.33	0.55		0.57	0.48	0.56	0.45	0.45	0.54	0.54	0.52

NAp Not applicable.
[1]Coal seam thickness = 1.7 m.
[2]Coal seam thickness = 2.7 m.
[3]Solely to compare gate road designs, an overburden of 460 m was used.
[4]Maximum overburden experienced by that particular panel.
[5]Under a stream valley.
[6]Under a sandstone stream channel.
[7]Multiple-seam interaction.

COMPARATIVE EVALUATION OF GATE ROAD DESIGNS

Gate road systems at the two mines evolved in response to a variety of issues, one of which was coal bumps. At mine 1, a change from a yield-yield-abutment to a yield-abutment-yield system resulted in improved performance in bump-prone ground. The support capacity of the two gate road systems remained essentially the same, but the yield pillar adjacent to the tail drive effectively shielded workers on the face from coal thrown when the abutment pillars bumped. The next change in the gate road design—from a 24-m (80-ft) square pillar to a larger 37- by 56-m (120- by 180-ft) abutment pillar—involved a significant increase in load-bearing capacity of the system. In fact, the ALPS stability factor [for a uniform overburden of 460 m (1,500 ft)] rose from 0.46 to 0.88 (table 1); this was an increase in calculated load-bearing capacity of more than 90 pct. This increase in strength of the gate pillar system appears to have eliminated face bumps at mine 1.

The calculated load-bearing capacity of the gate road systems at mine 2 also showed a significant increase from the earliest three-entry design to the most recent four-entry system. However, each successive design at mine 2 only resulted in incremental changes in the stability factor (table 1). The incremental design changes from panels 3 to 5 reflected an effort to increase gate road stability as maximum overburden increased over each successive panel in this area. However, the more drastic design changes implemented in panel 7 and again in panel 13 were made specifically in response to coal bumps. Overall, the current four-entry gate road system represents an 84 pct increase in calculated load-bearing capacity over the capacity of the panel 3 tailgate, where the first serious face bump at mine 2 occurred.

Assuming that a stronger gate road system can mitigate tailgate face bumps by limiting the transfer of abutment stresses to the longwall face, one would expect different bump responses based on differing gate pillar strength-load ratios. If the tailgate pillars remain stable as second panel mining proceeds, then both pillar bumps and face bumps should be eliminated. If the pillars are slightly inadequate, pillar bumps may result as the tailgate pillars proceed into the gob. As the strength-load ratio decreases, pillar bumps may occur adjacent to the tail drive or even outby the face. Ultimately, abutment pillar failure outby the face may lead to face bumps. Based on this premise, it follows that the bump hazard should increase from no bumps to pillar bumps to face bumps as the ALPS stability factor decreases.

To evaluate the validity of this assumption, coal bumps at the case study mines were examined for decreases in bump activity and severity associated with increases in the ALPS stability factor table 1. The stability factors are also presented in a chart in figure 6. Although this chart represents the experience of only 10 gate road situations, a couple noteworthy observations concerning stability factor and bumps can be made. First, there have been no bumps at either of these mines when the ALPS stability factor for the gate road was greater than 0.6. This supports the premise that a sufficiently strong gate pillar system can help eliminate bumps. Second, both pillar bumps and face bumps occurred in the range of ALPS stability factors from about 0.3 to 0.6; however, as figure 6 shows, the five face bumps associated with stability factors greater than 0.48 were also associated with some geologic, topographic, or geometric anomaly that appeared to be the overriding factor in the bump occurrence. For example, at mine 2 in panels 3 and 4, all of the bumps occurred at the edge of a sandstone channel even though the stability factor of the gate road was lower at some other point. Similarly, at mine 2 in panel 7, the bumps occurred at locations underlying barrier pillars in a superjacent mine (figure 4).

It appears that a simplistic analysis using only ALPS can provide some insight into the bump potential of a particular gate road design. However, where sandstone channels, multiple seams, and/or multipanel interactions are present, the ALPS stability factor alone (which does not consider these conditions) is not sufficient for generating a practical bump control design. Under these anomalous conditions, a more detailed analysis of bump potential may be needed.

One method that can supplement a stability factor analysis in bump-prone ground is a geologic bump hazard analysis such as described by Sames (1995). This analysis uses a relational database to evaluate geologic information against a given set of criteria. The approach provides a means of quantifying geologic parameters and the interactions among them that can affect bump-proneness.

The assumptions incorporated into ALPS for estimating pillar loads are not appropriate for anomalous situations, such as those encountered in multiple-seam mining. In such a situation, a more detailed mechanistic analysis of the site should be utilized in which the complete elastic response is investigated and the multiple-seam interactions and the overall panel geometry are considered. For example, a boundary-element analysis performed by USBM researchers at mine 1 showed that the calculated elastic strain energy released from the tailgate corner of the longwall face was halved owing to the change in gate road design between 7 development and 8 development. In a similar analysis by Heasley and Zelanko (1992), the energy released from the tailgate corner of a longwall face at mine 2 was 15 pct greater when the face was overlain by a barrier pillar than when the face was overlain by a pillared section (figure 4). Energy release has proved useful as a tool in several other bump investigations (Maleki and others, 1987; Zipf and Heasley, 1990; Heasley, 1991).

Figure 6
Comparison of Coal Mine Bumps Using ALPS Stability Factors.

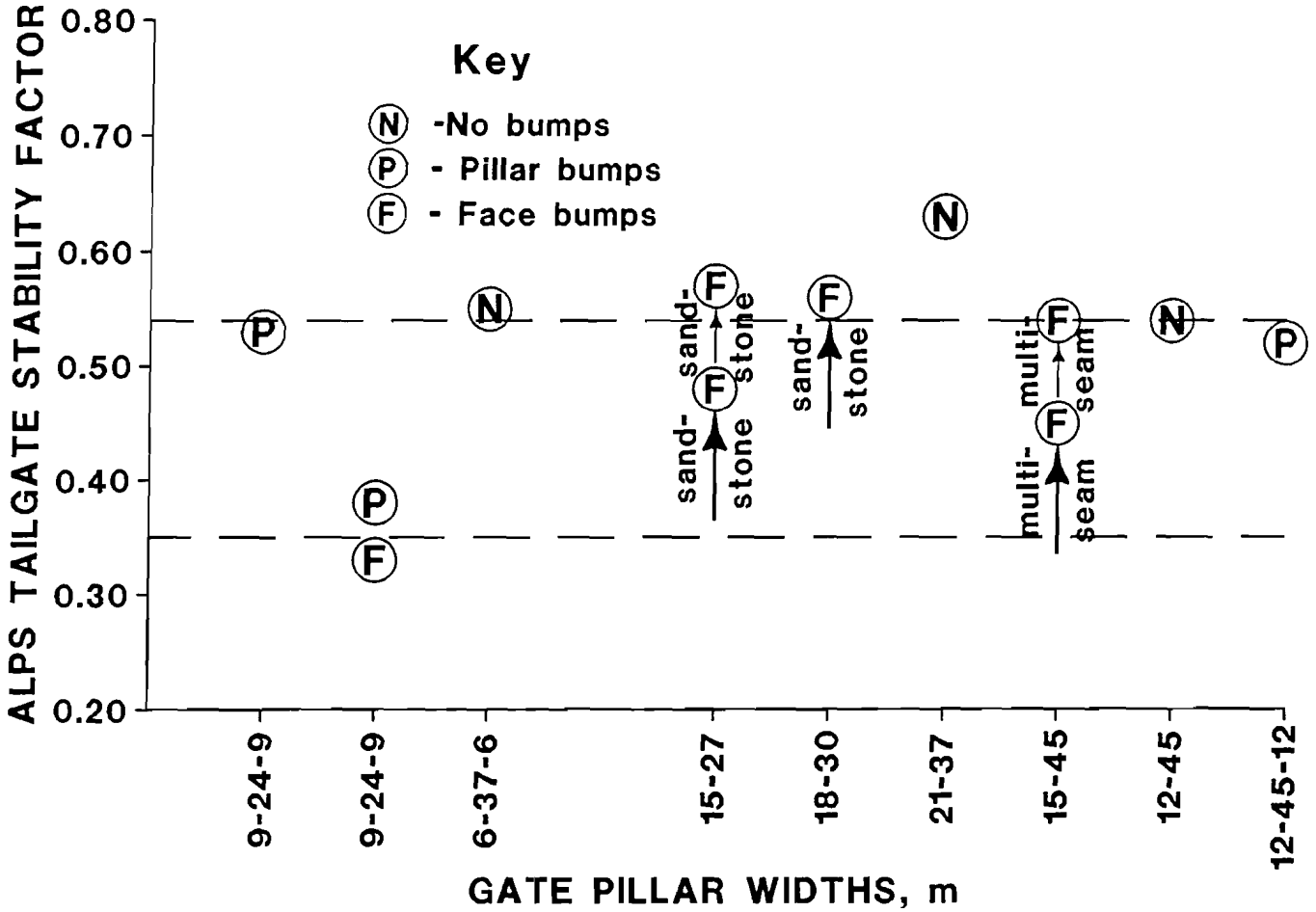

DISCUSSION AND CONCLUSIONS

Although the specific mechanisms responsible for coal mine bumps are not completely understood, one established factor in their occurrence is the presence of high vertical stress. The case studies of two mines presented in this paper support the premise that, in some instances, properly sized gate pillars can mitigate tailgate face bumps by limiting the transfer of abutment stresses to the longwall face. Both studies demonstrated that an increase in the effective strength-load ratio of the gate road pillars helped eliminate or reduce longwall face bumps.

The case studies of these two mines, particularly that of mine 2, also underscore the fact that coal pillar design has limitations regarding the control of longwall face bumps. In several instances, geologic anomalies and multiple-seam interactions apparently instigated face bumps in specific locations even though the gate road design had been used successfully elsewhere in the mine under similar or deeper cover. There are also certain longwall face bump situations where increasing gate road strength would not apply to bump mitigation. For instance, under extremely deep cover, abutment stresses on the longwall face may be sufficient to facilitate face bumps regardless of the strength of a conventional gate road design. Midface bumps, for example, would probably be affected very little by increases in gate system load-bearing capacity. In these extreme stress conditions, yield-pillar systems (DeMarco and Koehler, 1995) may effectively eliminate gate road pillar bumps, and destressing techniques (Haramy and others, 1995) would be more appropriate for effective bump control at the face. Moreover, operational, economic,

and/or legal constraints often determine the maximum abutment pillar size that can be used.

The two case studies demonstrate several additional interesting aspects of longwall design for coal bump control. First, the technique of placing a yield pillar between the abutment pillar and the tailgate to shield the tailgate drive area from an abutment pillar bump has been quite effective. This location for a yield pillar can also help reduce floor heave in the tailgate by physically separating the high-stress abutment pillar from the high-stress tailgate corner of the face. Second, in addition to the geologic, multiple-seam, and overburden factors mentioned above, several geometric factors pertaining to longwalls in the case studies appear to enhance the likelihood of face bumps. For example, on several occasions there appeared to be some correlation between single and/or multipanel gob size and bumps. In two instances at mine 2, the face had advanced approximately 170 m (550 ft) when bumps occurred. This amount of advance made the open gob area just about square. Although the panels had already had a first fall, this geometric configuration would conceivably cause the largest stress concentration on the face because it would create a suspended main roof. Similarly, but on a larger scale, the 6th and 7th panels at mine 1 and the 15th panel at mine 2 experienced bumps after the multipanel gob was approximately square.

An intuitive feeling is that at a deep mine there should be overburden interaction between successive panels and that the magnitude of this interaction should increase until the accumulated width of the panels is essentially equal to their length. Therefore, a given gate road design may not experience a maximum abutment load until both a full panel abutment load and a full multipanel abutment have been achieved. This implies that a gate road design can be successful in supporting the immediate panel's abutment load in the tailgate of the first few panels, but may not be strong enough to support both the immediate panel's abutment load and the cumulative multipanel abutment load as successive panels are mined.

REFERENCES

Brant, R. A., D. R. Chesnut, E. R. Portig, and R. A. Smath. Coal Resources of the Upper Cumberland District, Kentucky. Energy Resources Series IMMR83/088, Univ. KY Inst. for Min. and Miner. Res., Nov. 1983, 41 pp.

Campoli, A. A., T. M. Barton, F. C. Van Dyke, and M. Gauna. Mitigating Destructive Longwall Bumps Through Conventional Gate Entry Design. USBM RI 9325, 1990, 38 pp.

Campoli, A. A., D. C. Oyler, and F. E. Chase. Performance of a Novel Bump Control Pillar Extracting Technique During Room-and-Pillar Retreat Coal Mining. USBM RI 9240, 1989, 40 pp.

DeMarco, M. J., E. J. Koehler and H. Maleki. Gate Road Design Considerations for Mitigation of Coal Bumps in Western U.S. Longwall Operations. Paper in Proceedings: Mechanics and Mitigation of Violent Failure in Coal and Hard-Rock Mines. USBM Spec. Publ. 95-01, 1995, pp. 141-165.

Goode, C. A., A. Zona, and A. A. Campoli. Controlling Coal Mine Bumps. Coal Min., v. 21, No. 10, Oct. 1984, pp. 48-53.

Haramy, K. Y., H. Maleki, and D. E. Swanson. Practical Techniques To Control Coal Mine Bumps. Paper in Proceedings: Mechanics and Mitigation of Violent Failure in Coal and Hard-Rock Mines. USBM Spec. Publ. 95-01, 1995, pp. 201-216.

Heasley, K. A. An Examination of Energy Calculations Applied to Coal Bump Prediction. Paper in Rock Mechanics as a Multidisciplinary Science: Proceedings of the 32nd U.S. Symposium, ed. by J.-C. Roegiers (Univ. OK, Norman, OK, July 10-12, 1991). Balkema, 1991, pp. 481-490.

Heasley, K. A., and K. Barron. A Case Study of Gate Pillar Response to Longwall Mining in Bump-Prone Strata. Paper in Longwall U.S.A., 1988, pp. 92-105.

Heasley, K. A., and J. C. Zelanko. Pillar Design in Bump-Prone Ground Using Numerical Models With Energy Calculations. Paper in Proceedings of the Workshop on Coal Pillar Mechanics and Design. USBM IC 9315, 1992, pp. 50-60.

Holland, C. T., and E. Thomas. Coal-Mine Bumps: Some Aspects of Occurrence, Cause, and Control. USBM Bull. 535, 1954, 37 pp.

Iannacchione, A. T. Behavior of Coal Pillars Prone to Burst in the Southern Appalachian Basin of the United States. Paper in Rockbursts and Seismicity in Mines, Proceedings of the 2nd International Symposium of Rockbursts and Seismicity in Mines, ed. by C. Fairhurst (Univ. MN, Minneapolis, MN, June 8-10, 1988). Balkema, 1990, pp. 295-300.

Iannacchione, A. T., and M. J. DeMarco. Optimum Mine Designs To Minimize Coal Bumps: A Review of Past and Present U.S. Practices. Ch. 24 in New Technology in Mining Health and Safety. Soc. Min. Eng., 1992, pp. 235-247.

Iannacchione, A. T., and J. C. Zelanko. Occurrence and Remediation of Coal Bumps: A Historical Review. Paper in Proceedings: Mechanics and Mitigation of Violent Failure in Coal and Hard-Rock Mines. USBM Spec. Publ. 95-01, 1995, pp. 27-68.

Jackson, D. Advancing Longwall Mining: A First for Mid-Continent Coal and a First for the U.S. Coal Age, v. 80, No. 10, Sept. 1975, pp. 100-105.

Koehler, J. R. Longwall Gateroad Evolution and Performance at the Sunnyside Coal Mines. SME preprint 94-179, 1994, 11 pp.

Maleki, H. Ground Response to Longwall Mining: A Case Study of Two-Entry Yield Pillar Evolution in Weak Rock. CO Sch. Mines Q., v. 83, No. 3, 1988, 52 pp.

Maleki, H., J. Aggson, F. Miller, and J. F. T. Agapito. Mine Layout Design for Coal Bump Control. Paper in 6th International Conference on Ground Control in Mining: Proceedings, ed. by S. S. Peng (Morgantown, WV, June 9-11, 1987). Dep. of Min. Eng., WV Univ., 1987, pp. 32-46.

Mark, C. Analysis of Longwall Pillar Stability. Ph.D. Thesis, PA State University, University Park, PA, 1987, 414 pp.

___. Pillar Design Methods for Longwall Mining. USBM IC 9247, 1990, 53 pp.

Mark, C., F. E. Chase, and G. M. Molinda. Design of Longwall Gate Entry Systems Using Roof Classification. Paper in New Technology for Longwall Ground Control, Proceedings: U.S. Bureau of Mines Technology Transfer Seminar. USBM Spec. Publ. 01-94, 1994, pp. 5-17.

Mucho, T. P., T. M. Barton, and C. S. Compton. Room-and-Pillar Mining in Bump-Prone Conditions and Thin Pillar Mining as a Bump Mitigation Technique. USBM RI 9489, 1993, 18 pp.

Sames, G. P. Bump Hazard Criteria Derived From Basic Geologic Data. Paper in Proceedings: Mechanics and Mitigation of Violent Failure in Coal and Hard-Rock Mines. USBM Spec. Publ. 95-01, 1995, pp. 69-89.

Schuerger, M. G. An Investigation of Longwall Pillar Stress History. Paper in 4th Conference on Ground Control in Mining, ed. by S. S. Peng and J. H. Kelley (July 22-24, 1985). WV Univ., Morgantown, WV, 1985, pp. 41-50.

Zelanko, J. C., G. A. Rowell, and T. M. Barczak. Analysis of Support and Strata Reactions in a Bump-Prone Eastern Kentucky Coal Mine. Trans. SME, v. 290, 1992, pp. 1894-1900.

Zipf, R. K., Jr., and K. A. Heasley. Decreasing Coal Bump Risk Through Optimal Cut Sequencing with a Non-Linear Boundary Element Program. Paper in Rock Mechanics Contributions and Challenges: Proceedings of the 31st U.S. Symposium, ed. by W.A. Hustrulid and G. A. Johnson (CO Sch. Mines, Golden, CO, June 18-20, 1990). Balkema, 1990, pp. 947-954.

BUMP CONTROL DESIGN PROTOCOL FOR ROOM-AND-PILLAR COAL MINING

By Alan A. Campoli,[1] Thomas P. Mucho,[1] and R. Karl Zipf, Jr.[2]

ABSTRACT

The U.S. Bureau of Mines (USBM) developed a stress control design protocol to minimize coal mine bumps—the violent failure of overly stressed coal pillars. The protocol was developed for room-and-pillar retreat mining conducted with available continuous miner technology. A model of pseudoductile coal pillar strength was used to develop unlimited-width and limited-width section design criteria. The unlimited-width design assumes an infinitely long pillar line composed of uniformly sized pillars extracted against an infinitely wide gob area. Tributary-area theory was combined with a linear shear-angle concept to estimate loads applied to total-extraction pillars adjacent to gob areas. Overburden increases eventually prohibit unlimited-width sections and force the use of barrier pillars between limited-width sections. The USBM-developed boundary-element code MULSIM/NL was used to develop and implement a systematic limited-width section design procedure. The complex distribution of gob-side abutment load between side abutment pillars and chain pillars in the total-extraction zone necessitated computer simulation. The USBM created a spreadsheet program, LAYOUT, to summarize and provide for efficient utilization of the bump control design protocol. Based on overburden thickness, coalbed thickness, and coal pillar dimensions entered by the user, LAYOUT calculates a stability factor for the first and second pillar rows outby the expanding gob for unlimited-width sections. If overburden and coalbed thickness conditions do not allow an unlimited-width section design, LAYOUT suggests a limited-width design. LAYOUT results were verified against four case studies of coal mine bumps.

INTRODUCTION

Room-and-pillar retreat mining requires that coal pillars intended for total extraction support the combination of development and gob-side abutment loads. Pillar design must also facilitate safe and efficient retreat mining. Mechanical properties of a coalbed and associated strata, depth of overburden, and in situ stress conditions impact design of a total-extraction pillar. In particular, the hard, immediate roof and floor often associated with coal mine bumps impose unique design requirements.

Analysis of bumps during room-and-pillar retreat mining with continuous mining machines yields the following design rules of thumb:

1. Coal pillars should be uniformly sized and shaped, large enough to support the development load, yet small enough to permit bump-free total extraction under abutment zone loading.
2. The coal should be mined as completely as possible.
3. Pillar lines should be as straight as possible, avoiding points at the intersection of gob areas.
4. Barrier pillars should be split in advance of approaching gob areas prior to abutment zone loading.
5. Designs that require multiple working places in a single pillar should be avoided, because bumps are triggered by mining-induced stress adjustment.

When prudently implemented, these rules allow successful retreat mining until the weight of overburden requires coal pillars to become too large to permit bump-free total extraction under butment zone loading at the

[1]Mining engineer, Pittsburgh Research Center, U.S. Bureau of Mines, Pittsburgh, PA.
[2]Mining engineer, Denver Research Center, U.S. Bureau of Mines, Denver, CO.

gob edge (Campoli and others, 1990). Successful designs for deeper bump-prone mines must prevent excessive stress accumulations in total-extraction pillars adjacent to gob areas.

The goal of this U.S. Bureau of Mines (USBM) research was to facilitate safe and efficient room-and-pillar retreat mining of bump-prone coalbeds by limiting coalbed stress adjacent to expanding gob areas through variation of section layouts. The first step was design of total-extraction pillars and their associated pillar extraction plans. The second step was development of a coalbed strength model. The third step was development of stress limit design criteria. The fourth and final step was development of a methodology to estimate the magnitude and distribution of development and abutment loads applied to the pillar line.

The linear geometry of unlimited-width sections allowed for the accomplishment of step four using tributary-area and linear shear-angle concepts. Increasing overburden depths required limited-width sections separated by barrier pillars to control stress within total-extraction panels. The accomplishment of step four with limited-width section designs required prediction of abutment load distributions for rectangular gobs and apportionment of these loads over pillars of mixed sizes. A parametric study of the complicated interaction of various combinations of overburden depths, total-extraction panel widths, and abutment pillar widths was conducted with the USBM-developed boundary-element program MULSIM/NL.

TOTAL-EXTRACTION PILLAR DESIGN

The split-and-fender pillar extraction method has been successfully used in numerous bump-prone mines (Campoli and others, 1989). This method does not require multiple working places within pillars; thus, roof support and ventilation personnel are not subjected to the extreme bump hazard of working within a pillar while it is being mined. The Olga Mine, McDowell Co., WV, used the split-and-fender pillar extraction method with 6.1-m (20-ft) deep cuts to extract 16.8- by 21.3-m (55- by 70-ft) pillars in the 1.8-m (6-ft) high Pocahontas No. 4 Coalbed (figure 1). Three rows of pillars outby the gob were simultaneously mined to increase dispersion of abutment loads. Generally, the first two rows of pillars outby the gob were split along their long axes, leaving two 5.3- by 21.3-m (17.5- by 70-ft) wings that yielded under abutment zone loading. The splitting of the third row generally was begun prior to the removal of the wings adjacent to the gob. Figure 1 depicts the cut sequence on three rows of chain pillars. Only the cuts taken from a block of pillars three rows on a side are numbered. Cuts from the inby pillars in the area labeled "Gob" are in the sequence, as well as cuts in the adjacent pillars. Neither were labeled for the sake of clarity.

Ideally, the chain pillar's ability to store strain energy and thus bump is destroyed by the time the third center splitting cut is completed. For example, the pillars in row 2 will not bump after cuts 22, 23, and 24 are extracted. This simultaneous mining of the first three pillar rows outby the gob spreads the abutment load over six pillar rows outby. This, combined with the abutment pillars left between the section and the previous gob, allowed the 16.8- by 21.3-m (55- by 70-ft) pillar to be safely extracted under overburden that ranged from 430 to 490 m (1,400 to 1,600 ft) deep (Campoli and others, 1989). However, the reduction in confined core mining bump hazard came at the expense of production efficiency because of the dramatic increase in miner place-change time.

Figure 1
Split-and-Fender Pillar Extraction Plan.

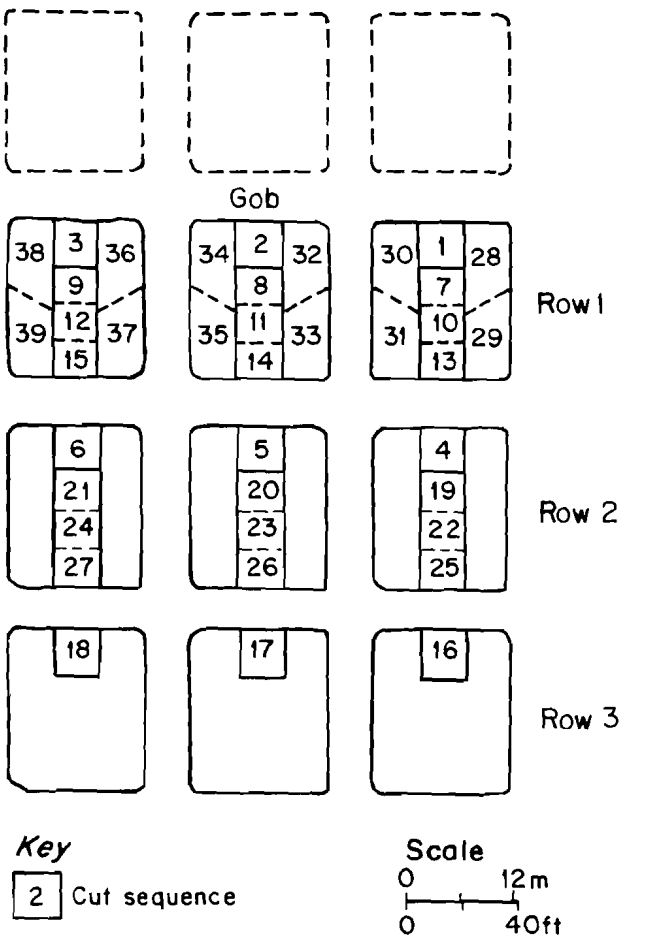

Split-and-fender pillar extraction plan for 16.8- by 21.3-m (55- by 70-ft) pillars using standard 6.1-m (20-ft) deep continuous miner cut.

Figure 2
"Christmas Tree" Pillar Extraction Plan.

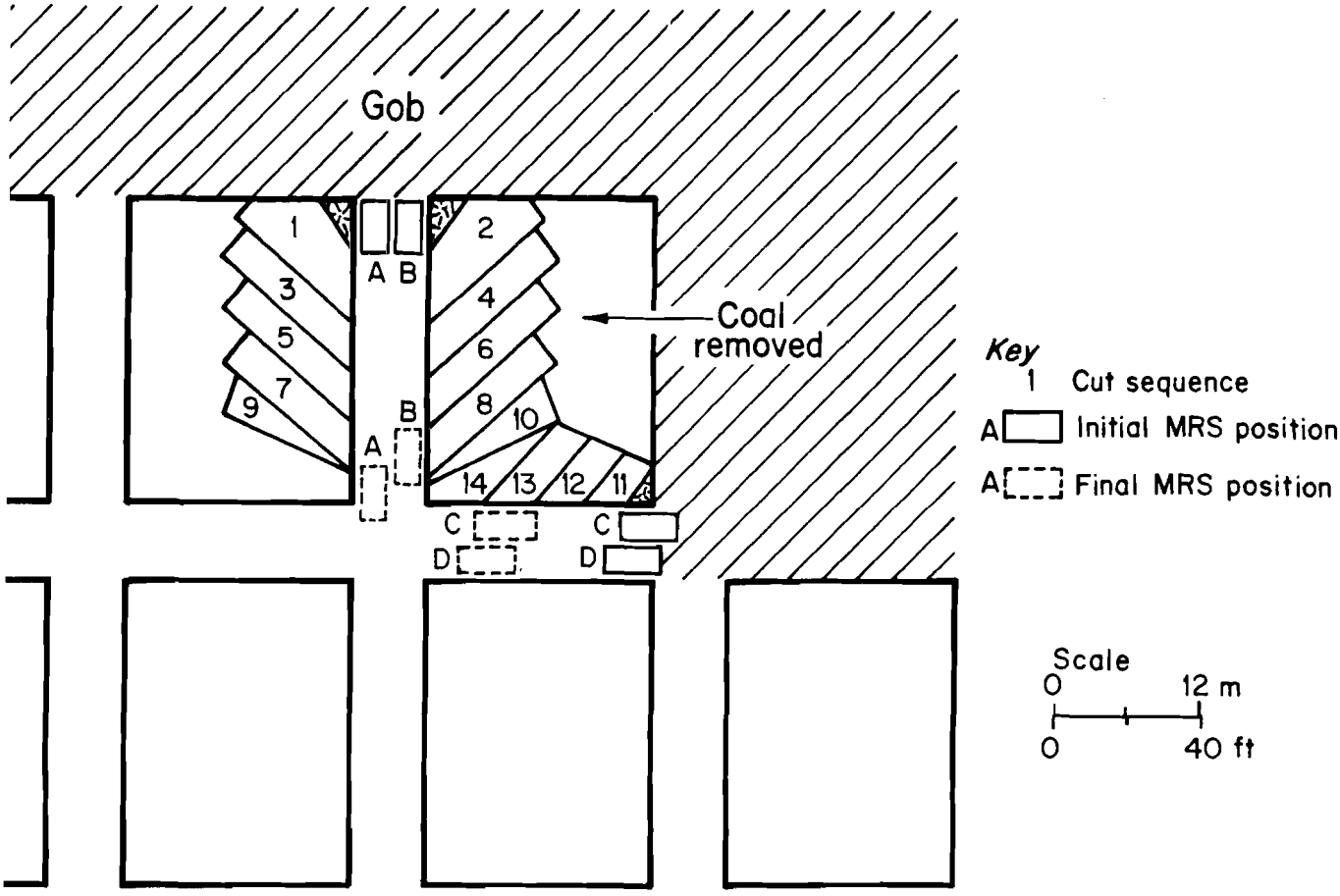

Christmas tree pillar extraction plan for 18.3- by 24.4-m (60- by 80-ft) pillars using 12.2-m (40-ft) continuous miner cuts and four mobile roof supports (MRS).

As pillar width and length increase, the ability of the pillar to support the combination of development and abutment loading increases. Therefore, as overburden depth increases, so must pillar size, while allowing for efficient and bump-free extraction. However, even nominal pillar size increases can dramatically complicate pillar extraction with the split-and-fender method. Bump control pillar extraction plans have been developed for total-extraction pillars up to 27.4 m (90 ft) square. Although extraction of a pillar this large is theoretically possible, it would be inefficient and difficult to implement.

Pillar extraction plans using extended-cut mining could allow for the efficient extraction of relatively large pillars. A "Christmas tree" extended-cut pillar extraction plan, approved by the U.S. Mine Safety and Health Administration (MSHA) and currently used at Marrowbone Development Co., Naugatuck, WV, employs four mobile roof supports to extract 18.3- by 24.4-m (60- by 80-ft) pillars.[3] This pillar extraction plan, requiring 6.1-m (40-ft) continuous miner cuts (figure 2), minimizes the cutting of confined core. The Christmas tree extraction plan does not require multiple working places within pillars.

[3]Personal communication from F. E. Chase, geologist, Pittsburgh Research Center, Feb. 1994.

PSEUDODUCTILE COAL PILLAR STRENGTH MODEL

To facilitate consistent coal strength input for the design methodologies for both the analytical unlimited-width section and the numerical (MULSIM/NL) limited-width section, the USBM developed a coal pillar strength model. The model is a simplification of the Barron pseudoductile model (Barron, 1984). Confined pillar core is assumed to reach a maximum stress of 55.2 MPa (8,000 psi). The stress in the yielded perimeter is assumed to average 20.7 MPa (3,000 psi). The depth of the yielded perimeter is assumed to be 4.6 m (15 ft) in a 1.8-m (6-ft) thick coalbed based on geotechnical evaluations conducted at the Olga Mine (Campoli and others, 1989) and the VP No. 3 Mine, Buchanan Co., VA (Campoli and others, 1993). The depth of the yield zone in the 3.7-m (12-ft) thick Harlan Coalbed was shown to be 9.1 m (30 ft) in a geotechnical evaluation using similar instruments (Zelanko and others, 1991). The depth of the yielded perimeter is assumed to be 2.5 times the coalbed thickness in the 0.9- to 3.7-m (3- to 12-ft) coalbed thickness range. Figure 3 shows this relationship for a 21.3-m (70-ft) square pillar in a 1.8-m (6-ft) thick coalbed. The predicted maximum pillar strength for selected coalbed thicknesses and total-extraction pillar sizes is shown in table 1.

Figure 3
Confined Pillar Core and Yielded Perimeter.

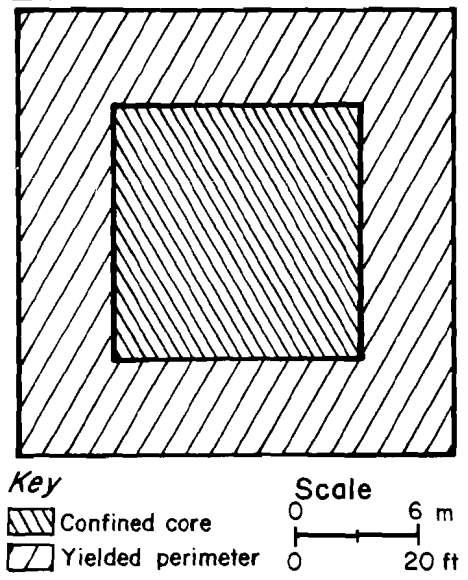

Assumed apportionment of yield zone and confined core in a 21.3-m (70-ft) square pillar in a 1.8-m (6-ft) thick coalbed at maximum load-bearing capacity.

Table 1.—Predicted maximum pillar load[1] for selected coalbed thicknesses, meters (feet)

Coalbed thickness	Coal pillar size			
	27.4 × 27.4 (90 × 90)	21.3 × 21.3 (70 × 70)	18.3 × 24.4 (60 × 80)	16.2 × 21.3 (55 × 70)
0.9 (3)	33.58 (7.55)	19.08 (4.29)	18.59 (4.18)	14.46 (3.25)
1.8 (6)	27.09 (6.09)	14.55 (3.27)	14.01 (3.15)	10.59 (2.38)
2.7 (9)	22.06 (4.96)	11.43 (2.57)	10.90 (2.45)	8.18 (1.84)
3.7 (12)	18.46 (4.15)	9.74 (2.19)	9.21 (2.07)	7.25 (1.63)

[1]Maximum pillar load = 1×10^9 N (1×10^9 lbf)

STRESS LIMIT DESIGN CRITERIA

The criteria for selecting the appropriate section design for a given overburden thickness are twofold: (1) Total-extraction pillars at maximum strength must be confined to the first pillar row outby the active gob and (2) the barrier pillar separating the previous gob and the active gob must not yield until the total-extraction panels on both sides of the abutment pillar have been mined. The total-extraction pillar criteria eliminate the simultaneous mining of multiple rows and the associated inefficient production rates associated with the Olga Mine mining method (Campoli and others, 1989). The first row of total-extraction pillars is designed not to yield under the combination of development and abutment loads.

The abutment pillar criteria ensure that the abutment pillar does not yield until it is encompassed by gob on both sides. The abutment pillar is analogous to the tailgate entry in longwall mining. These stress limits were based on in-mine geotechnical evaluations of two successful bump control mine designs: the Olga Mine room-and-pillar design (Campoli and others, 1989) and the VP No. 3 Mine longwall design (Campoli and others, 1990).

UNLIMITED-WIDTH SECTION DESIGN

The unlimited-width section consists of uniformly sized pillars extracted against an infinitely wide gob. The model compares the previously discussed assumptions concerning simplified pseudoductile pillar strength to approximations of development and gob-side abutment loading. Development loads are the result of the weight of the overburden directly over the coal pillar. Tributary-area theory predicts these loads by the following equation:

$$L_d = (w + \frac{e}{2})\ (\ell + \frac{e}{2})\ (H)\ (\gamma), \quad (1)$$

where L_d = development load, N (lbf),

w = pillar width, m (ft),

e = entry width, m (ft),

ℓ = pillar length, m (ft),

H = overburden depth, m (ft),

and γ = rock density, N/m^3 (lbf/ft^3).

Note that the pillar dimensions parallel and perpendicular to the gob line are referred to as the pillar width and length, respectively.

Wilson (1973), King and Whittaker (1971), Mark (1990), and Chase and Mark (1993) have used linear shear-angle concepts to predict gob-side abutment loads. A section becomes supercritical when increases in gob width no longer result in increases in abutment loading (L_s) (figure 4). An infinitely wide (supercritical) gob in the unlimited-width section design model results in a section that is under maximum abutment load from a single gob. Mark (1990) quantified this abutment load condition with the following equation:

$$L_s = (H^2)\ (\tan \beta)\ (\gamma/2)\ (w), \quad (2)$$

where L_s = supercritical abutment load, N (lbf),

H = overburden depth, m (ft),

β = shear angle, deg,

γ = rock density, N/m^3 (lbf/ft^3),

and w = pillar width, m (ft).

The angle β has been fixed at 21° based on extensive field studies of more than 50 longwalls by Mark (1990) and more than 50 room-and-pillar operations by Chase and Mark (1993).

Distribution of the abutment load on pillars adjacent to the gob edge has been approximated by Mark (1990). He used an approximation of the width of abutment influence zone (D) determined by Peng and Chiang (1984) from field measurements. They determined that D is a function of overburden depth. Mark combined this with an inverse square stress decay function to form the relationship described in figure 5. Integration of the abutment stress distribution function and evaluation over the limits from zero to pillar length (ℓ) approximates the portion of the abutment load (L_s) carried by the pillars occupying the first row outby the gob (L_t).

Figure 4
Unlimited-Width Linear Shear-Angle Abutment Load.

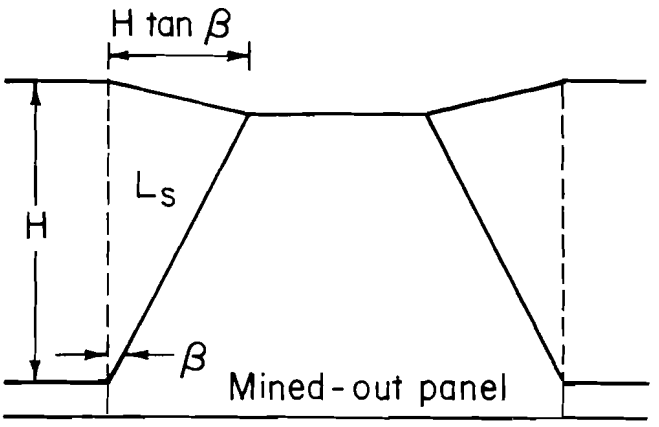

Conceptualization of unlimited-width linear shear-angle abutment load (after Mark, 1990). L_s = supercritical side abutment load, H = overburden depth, and β = shear angle.

Figure 5
Distribution of Side Abutment Load.

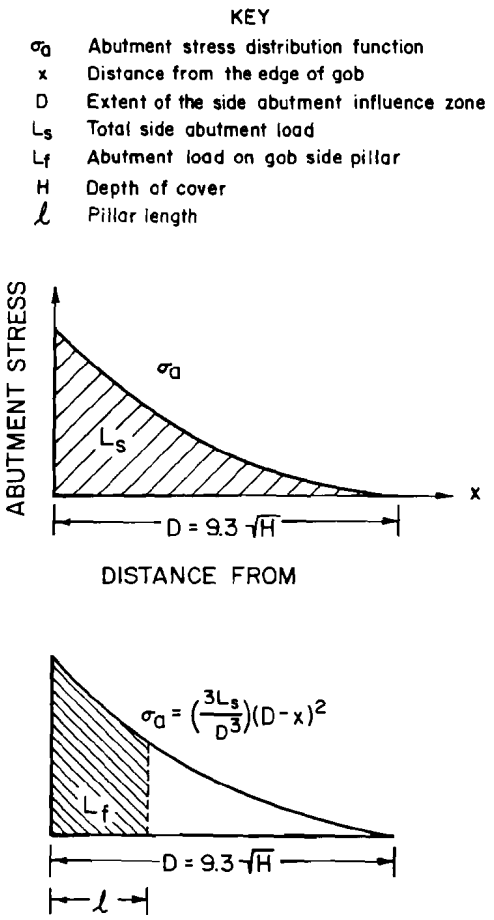

Given the total-extraction pillar dimensions, overburden thickness, and coalbed thickness, a stability factor can be calculated for the unlimited-width section. The stability factor is the coal pillar strength as predicted by the simplified pseudoductile model divided by the sum of the development (L_d) and the gob-side abutment pillar load (L_f).

$$SF = \frac{P}{L_d + L_f}, \qquad (3)$$

where SF = stability factor,

P = pillar load capacity, N (lbf),

L_d = development load, N (lbf),

and L_f = abutment load on gob-side pillar, N (lbf).

Thus, the stability factor is unity when the pillar row directly outby the gob is at maximum load-bearing capacity.

The stability factor is inversely proportional to both coalbed thickness and overburden thickness. Setting the stability factor to unity permits direct comparison of the predicted performance of four pillar sizes representative of the range of pillar sizes that provide considerable load resistance while allowing high-stress extraction under bump-prone conditions (table 2). The most-difficult-to-extract 27.4-m (90-ft) square pillar is predicted to support unlimited-width designs to 386.2 m (1,267 ft) of overburden for a 1.8-m (6-ft) thick coalbed. The least-difficult-to-extract 16.8- by 21.3-m (55- by 70-ft) pillar is predicted to support unlimited-width designs to 292.6 m (960 ft) of overburden for a 1.8-m (6-ft) thick coalbed. Table 2 shows that the 18.3- by 24.4-m (60- by 80-ft) and 21.3-m (70-ft) square pillars are predicted to perform nearly identically. Beyond these overburden depths, a limited-width or subcritical section design with barrier pillars between sections must be employed.

Because of haulage constraints, actual continuous miner sections cannot be of unlimited width. The unlimited-width design procedure assumes that the section is not subjected to side abutment loads from previously extracted panels. This abutment load interaction can be prevented by separating the total-extraction areas with abutment pillars. The Ashley, or Pennsylvania Mine Inspector's, formula (Ashley, 1930) has been used to design barrier pillars for this purpose for many years.[4]

$$B = 6.1 + 4T + 0.1\,H, \qquad (4A)$$

where B = abutment pillar width, m,

T = coalbed thickness, m,

and H = overburden depth, m; or

$$B = 20 + 4T + 0.1\,H, \qquad (4B)$$

where B = abutment pillar width, ft,

T = coalbed thickness, ft,

and H = overburden depth, ft.

[4]Equation 4*A* is for use with metric units, and equation 4*B* is for use with U.S. customary units.

Table 2.—Thickness of overburden resulting in a stability factor of 1 for given coal pillar sizes and coalbed thicknesses, meters (feet)

Coal pillar size	Coalbed thickness			
	0.9 (3)	1.8 (6)	2.7 (9)	3.7 (12)
16.8 × 21.3 (55 × 70) . .	365.8 (1,200)	292.6 (960)	242.3 (795)	218.8 (718)
18.3 × 24.4 (60 × 80) . .	393.5 (1,291)	321.3 (1,054)	267.0 (876)	235.9 (774)
21.3 × 21.3 (70 × 70) . .	393.5 (1,291)	323.7 (1,062)	270.7 (888)	240.5 (789)
27.4 × 27.4 (90 × 90) . .	451.1 (1,480)	386.2 (1,267)	333.1 (1,093)	292.6 (960)

Recall that the abutment pillar is required to remain stable only until it is encompassed by gob on both sides. Thus, the abutment pillars are not sterilized, as they may be weakened by mining as total-extraction mining progresses. The thin-pillar mining method has been used to extract barrier pillars located between total-extraction areas. Figure 6 illustrates this method as conducted at the Gary No. 2 Mine, McDowell Co., WV, in the Pocahontas No. 4 Coalbed (Mucho and others, 1993).

Figure 6
Thin-Pillar Abutment Pillar-Extraction Method.

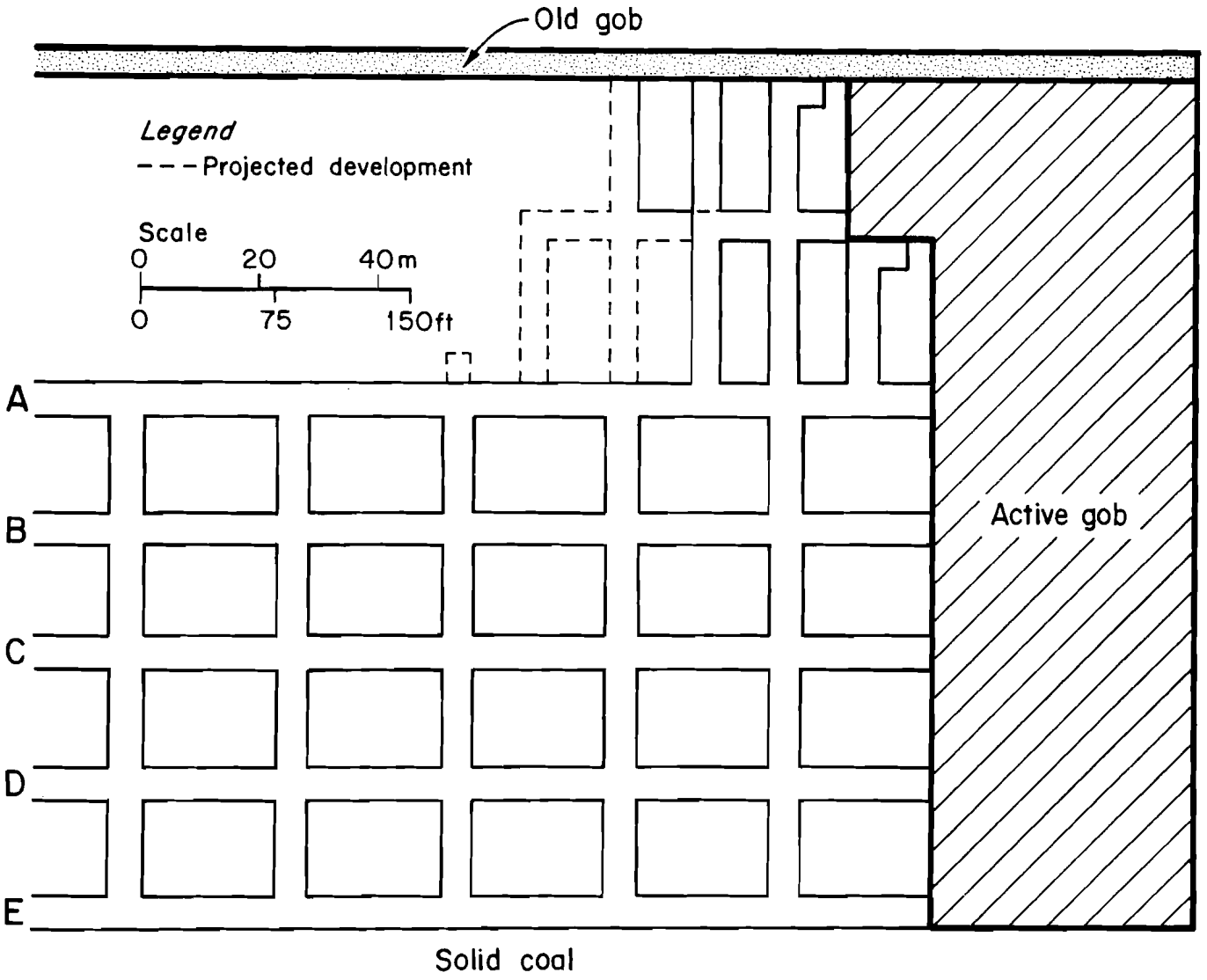

LIMITED-WIDTH SECTION DESIGN

Mining at overburden thicknesses greater than those listed in table 2 results in a stability factor less than 1.0 for a given total-extraction pillar size. Such a stability factor indicates that with the unlimited-width design procedure, the strength of the gob-side pillar row is insufficient to carry the combined development and abutment loads. The simple linear geometry of unlimited-width sections requires approximation of in situ tributary load, infinitely wide gob edge behavior, and uniformly sized total-extraction pillar strength. The limited-width design criteria require prediction of abutment load distributions for rectangular gobs and apportionment of these loads over mixed pillar sizes. A parametric study of the complicated interaction of various combinations of overburden depths, total-extraction panel widths, and abutment pillar widths was conducted with the boundary-element program MULSIM/NL.

MULSIM/NL was developed by the USBM to assist in alleviating safety hazards associated with bumps in U.S. coal mines (Zipf 1992a, 1992b). The program provides a means for calculating stress, displacement, and energy changes for various mining configurations in bump-prone conditions. The outputs permit evaluation of various mine designs that could decrease coal bumps.

The program does not account for the effect of the Earth's surface and assumes that seams are planes at great depth. It can accommodate up to four parallel seams having any orientation with respect to the Earth's surface. A continuous, homogeneous, linear-elastic rock mass is assumed to surround the seams. MULSIM/NL incorporates six nonlinear in-seam material properties via the boundary conditions. Unmined in-seam coal material may be represented as linear-elastic, strain-softening, or elastic-plastic. The gob or backfill material left in the wake of mining may be represented as bilinear-hardening, strain-hardening, or linear-elastic.

The accuracy of calibration determines the accuracy and usefulness of the model predictions. This is especially true in geologic models because of the uncertainty of input material properties. USBM researchers are concluding an extensive model calibration based on in-mine geotechnical evaluation of strata response to longwall mining in the bump-prone VP No. 3 Mine. Longwall gate road pillar failure observed through hydraulic stressmeters was used to calibrate the input failure strength of coal material. Gate road entry convergence was used to calibrate the elastic moduli of the coal and surrounding media. The limited-width section parametric studies used material property values tested as part of this effort.

In the parametric studies, overburden depth and section configuration in a 1.8-m (6-ft) thick coalbed were varied. The single-step models assigned surrounding media a modulus of elasticity of 6,890 MPa (1 million psi) and a Poisson's ratio of 0.25. Horizontal stress was assumed to be one-half the induced vertical stress.

The coalbed was represented by a strain-softening coal material. Peak stress, peak strain, residual stress, residual strain, and Poisson's ratio are required input parameters for the strain-softening model. The stress-strain response of four coalbed strain-softening materials is shown in figure 7. The distance of an element from a mine entry determines which of the four stress-strain curves represents a particular element. The external coal material makes up the perimeter of the pillar. The peak and residual strengths of each coal material increases with the distance from the entry. Core material, of maximum peak strength and residual strength make up the center of the pillar. Poisson's ratio was assumed to be 0.3 for all of the strain-softening coal materials. These properties were used with 15.2-m (50-ft) square coarse-mesh elements, each of which formed a five-by-five row square of 3-m (10-ft) square fine-mesh elements. Based on these assumptions, a 21.3-m (70-ft) square pillar contains only one core material element at its geometric center (figure 8).

Retreat mining allows the roof to cave as the panel is extracted. The volume of broken material is greater than that of the intact rock. This bulking effect, combined with bending and sagging of the main roof, allows for mechanical loading of the gob floor. The measurement of gob loading during the consolidation cycle is difficult. Accurate characterization of this cycle is important in modeling the complex ground behavior associated with limited-width section design.

Figure 7

Stress-Strain Response of Four Coalbed Strain-Softening Materials.

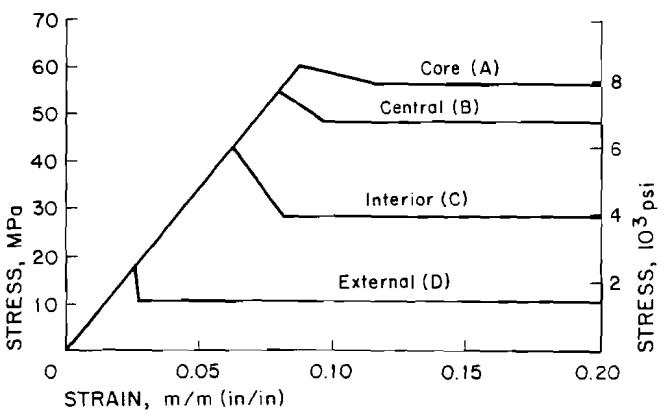

Figure 8
Assignment of Strain-Softening Material Properties.

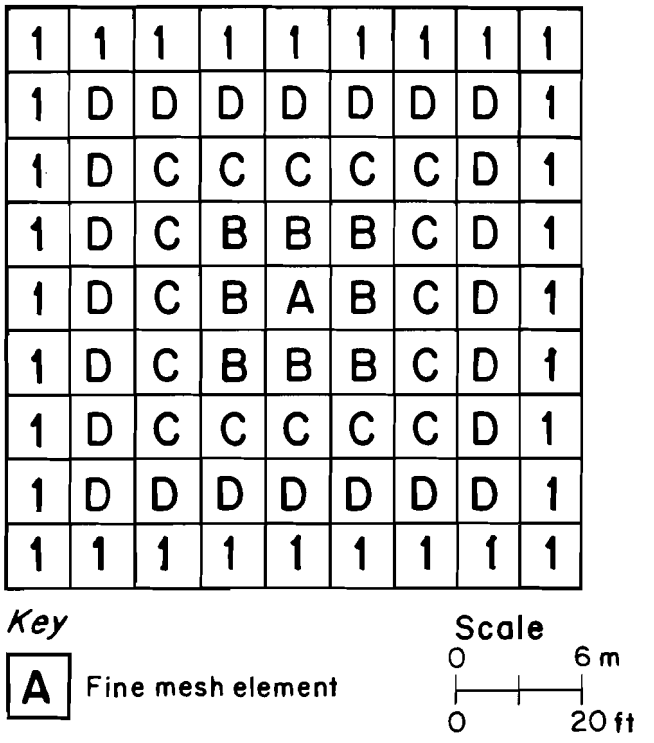

Assignment of strain-softening material properties in a 21.3-m (70-ft) square pillar. The numeral 1 represents one-half of the entry width, which was assumed to be 6.1 m (20 ft).

A three-pronged approach was used in an effort to develop an accurate representation of the mechanical behavior of gob in the consolidation cycle. First, the material properties of simulated gob material were determined in the laboratory, and the best form of a stress-strain equation was determined (Pappas and Mark, 1993). Second, a field investigation was conducted to measure longwall gob consolidation in the bump-prone VP No. 3 Mine (Campoli and others, 1993). Third, MULSIM/NL was revised to incorporate the laboratory-determined stress-strain equation, and the new gob material was used in a calibration of the model based on the in-mine geotechnical response.[5]

Laboratory results showed that the stress-strain relationship of the simulated gob material was nonlinear, but the stress-secant modulus relationship was approximately linear. A solution proposed by Salamon (1990) best describes the compressive behavior of backfill material with the stress-strain equation shown in equation 5. Solving equation 5 for the slope of the stress-strain curve (σ/ϵ) defines the secant modulus (E_s). Equation 6 shows that the secant modulus of Salamon's solution is a linear function of the stress, where the Y intercept is the initial secant modulus and the slope of the line is the reciprocal of the maximum strain. This linear relationship between secant modulus and stress agrees with laboratory gob tests (Pappas and Mark, 1993); therefore, this equation was chosen as the best fit to the data.[6]

$$\sigma = \frac{E_o \epsilon}{(1 - \epsilon/\epsilon_m)}, \quad (5)$$

$$E_s = \frac{\sigma}{\epsilon} = \left[\frac{1}{\epsilon_m}\right] \sigma + E_o, \quad (6)$$

where σ = applied stress, MPa (psi),

E_o = initial secant modulus, MPa (psi),

ϵ = strain, m/m (in/in),

ϵ_m = maximum strain, m/m (in/in),

and $_s$ = secant modulus, MPa (psi).

Implementation and testing of this new gob material in MULSIM/NL proved the material to be an improvement over linear-elastic gob material and capable of providing a reasonable fit to measured field data (Campoli and others, 1990, 1993). The two major input parameters to Salamon's strain-hardening gob model (equation 5) are maximum strain and initial elastic modulus. The parametric analysis of limited-width section design used a 0.4-m/m (in/in) maximum strain and 2.1-MPa (300-psi) initial modulus. The resultant stress-strain curve is shown in figure 9. The maximum strain parameter determines directly the strain value at which the stress-strain curve becomes asymptotic. The magnitude of gob stress is inversely proportional to the maximum strain. The initial modulus is directly proportional to magnitude of gob stress, with maximum effect on the gob edge stress.[7]

The MULSIM/NL output, when subjected to the previously described stress limit criteria, resulted in seven

[5]This work will be published in 1995 as a USBM Report of Investigations entitled "Gate Road Design Decreases Energy Release and Eliminates Face Bumps," by K. A. Heasley and D. M. Pappas.

[6, 7]See footnote 5.

Figure 9
Salamon Strain-Hardening Gob Model Stress-Strain Assumptions.

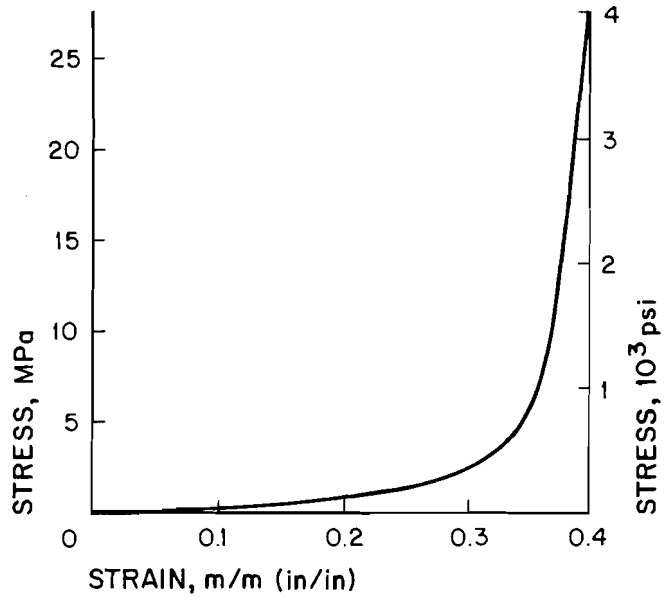

section designs appropriate for overburden depths from 305 to 671 m (1,000 to 2,200 ft) at 61-m (200-ft) increments. The sections are combinations of 21.9-m (72-ft) square pillars; 5.5-m (18-ft) wide entries; and 21.9-, 49.4-, and 76.8-m (72-, 162-, and 252-ft) wide abutment pillars. These dimensions are mesh-generation-forced approximations of the 18.3- by 24.4-m (60- by 80-ft) pillars and 12.2-m (20-ft) entries recommended for ease of extraction under bump-prone conditions. The three discrete abutment pillar widths were also influenced by mesh design considerations and are multiples of the square pillar centers.

The general section configuration is illustrated in figure 10. The square pillars on the right and top of the fine mesh form the main and submain haulage of the mine. A two-pillar-wide barrier protects the main haulage from abutment loads generated from previous mining of the initial panel. The six-pillar-wide panels are mined from the bottom up. The two rows of square pillars at the bottom form the bleeder entries. The skin-to-skin extraction of the panels between continuous barrier pillars is not prohibited by MSHA regulations and should be acceptable because the hard sandstone roof associated with bump-prone mines should bridge over the barrier pillars, forming a void facilitating gob ventilation. A three-pillar-wide barrier pillar is left between the total-extraction panels.

In figure 10, a worst-case stress scenario is evaluated in the one-step MULSIM/NL model. One-half of the 610-m (2,000-ft) long second panel has been extracted under 610 m (2,000 ft) of overburden. Although the scale of this plot does not facilitate detailed stress pattern analysis, it provides insight into the parametric analysis of the limited-width section. The darker the shading, the greater the stress. The solid black areas represent coal at or near its maximum stress of 55.2 MPa (8,000 psi). The white areas represent entries and gob areas whose stress is less than 5.5 MPa (800 psi).

Vertical stress in the first seven pillar rows outby the expanding gob and the barrier separating the total-extraction areas is more closely examined in figure 11. The section configuration meets the stress limit criteria at an overburden depth of 610 m (2,000 ft). Coal at or near its maximum strength is confined to the first pillar row outby the gob. The barrier pillar core stress is at or below 27.6 MPa (4,000 psi) adjacent to the first row of pillars outby the gob. Thus, the barrier provides an effective stress shield for the total-extraction panel, and total-extraction pillar failure is confined to the first outby pillar row.

The required abutment pillar width increases with depth, whereas the permissible section width decreases with depth. Table 3 summarizes the suggested section configuration and resultant extraction ratio for each of seven overburden thickness levels in a 1.8-m (6-ft) thick coalbed. Increases in coalbed thickness decrease coal pillar strength, thus reducing permissible overburden thickness for a given design; decreases in coalbed thickness have the opposite effect. This effect decreases total-extraction pillar strength more than barrier pillar strength. Subsequent MULSIM/NL parametric analyses could further refine the effect of coalbed thickness variation on limited-width section design. The concessions to MULSIM/NL mesh formulation requirements, the vagaries of material property specification, and the somewhat subjective stress limit design criteria are reflected in the wide 61-m (200-ft) overburden interval between section designs.

Table 3.—Summary of limited-width section design parametric study, meters (feet)

Design	Overburden depth	Panel width	Barrier width	Extraction ratio, pct
A	304.8 (1,000)	Unlimited	None required	100
B	365.8 (1,200)	224.9 (738)	21.3 (70)	91
C	426.7 (1,400)	224.9 (738)	48.2 (158)	82
D	487.7 (1,600)	197.5 (648)	48.2 (158)	80
E	548.6 (1,800)	170.1 (558)	48.2 (158)	78
F	609.6 (2,000)	170.1 (558)	75.0 (246)	69
G	670.6 (2,200)	142.6 (468)	75.0 (246)	66

Figure 10
Section Design Appropriate for 610 m (2,000 ft) of Overburden.

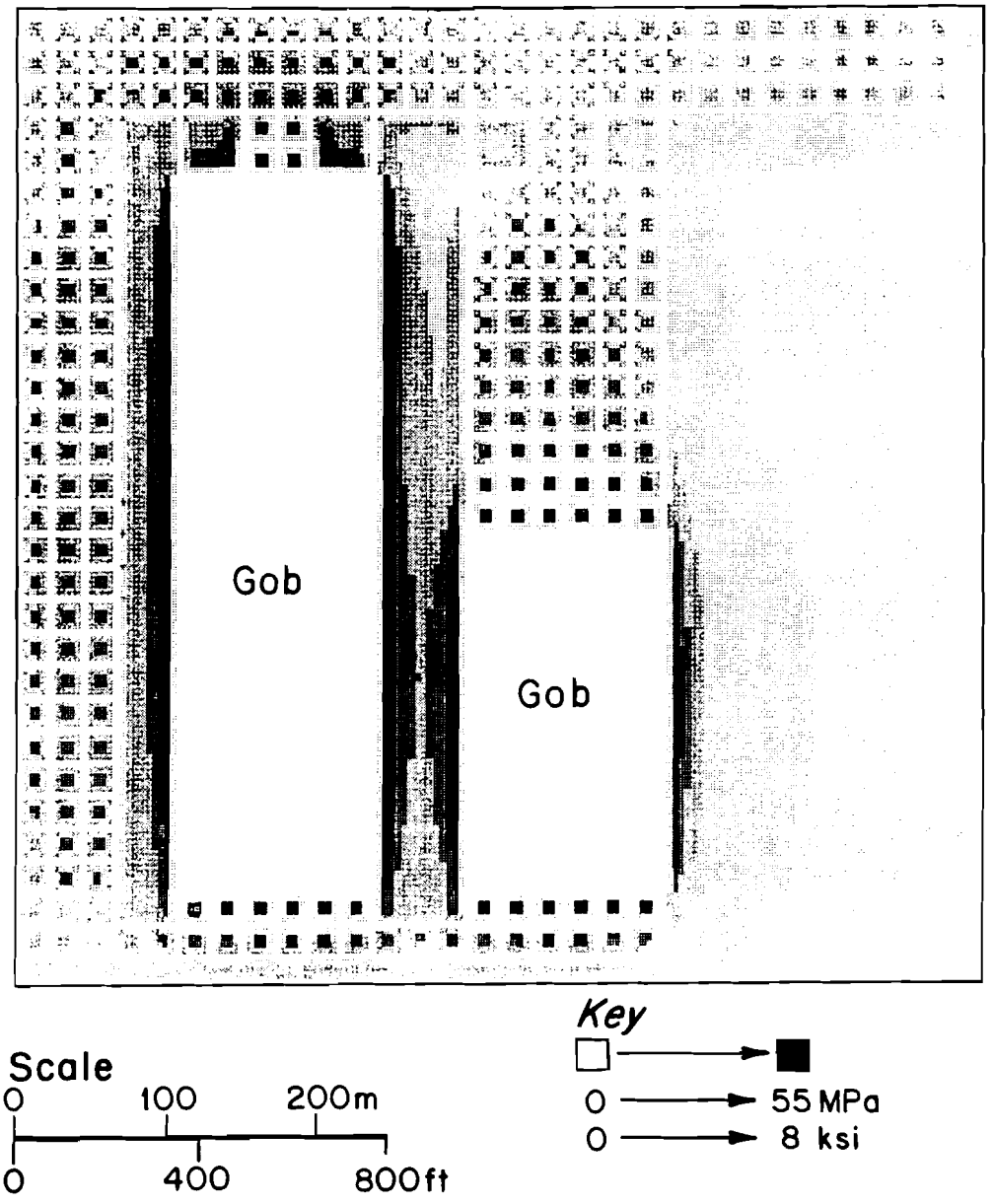

Figure 11
Vertical Stress Design for 610 m (2,000 ft) of Overburden.

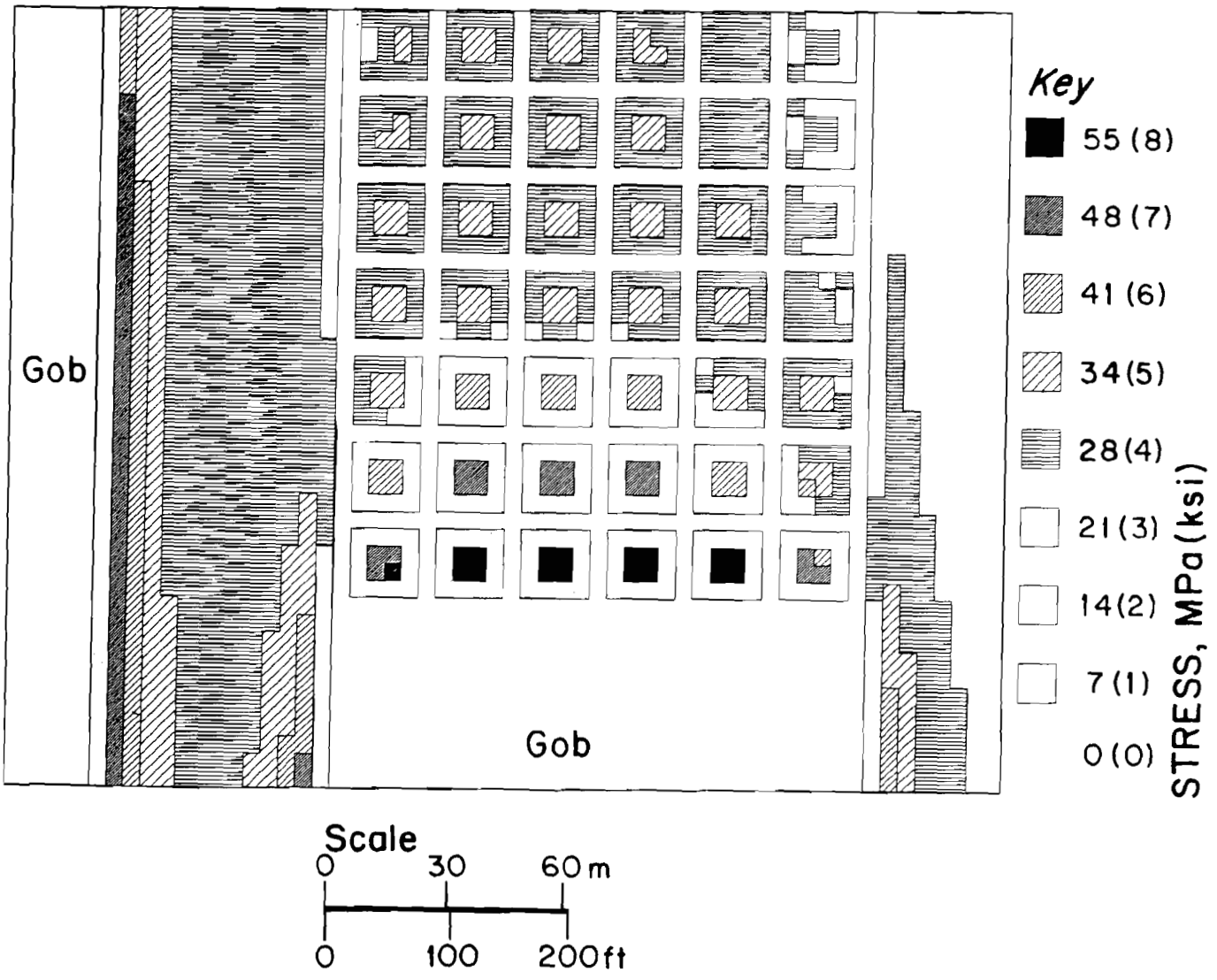

The parametric studies were limited to a 1.8-m (6-ft) thick coalbed and seven discrete overburden depths. The results can be generalized to accommodate variation in coalbed thickness and overburden depth. The MULSIM/NL analysis suggested that barrier pillar widths are less conservative than those suggested by the Ashley equation (equation 4) for a 1.8-m (6-ft) thick coalbed (figure 12). The Ashley equation accounts for variation in coalbed and overburden thicknesses and is used to suggest barrier pillar width for the limited-width section.

The width of the limited-width section is based on the ratio of total-extraction pillar strength in user-specified coalbed thickness to strength of a total-extraction pillar in a 1.8-m (6-ft) thick coalbed. The first step in this process is to fit a continuous function to the section width used in the parametric analysis. Equation 7 accounts for 99.6 pct of the variation in results of the parametric analysis where the section width is a 1.8-m (6-ft) thick coalbed (figure 13).[8]

$$P = -0.01053\ H + 12.1, \qquad (7A)$$

where P = section width in 21.3-m total-extraction pillars,

and H = overburden depth, m; or,

$$P = -0.00321\ H + 12.1, \qquad (7B)$$

where P = section width in 70-ft total-extraction pillars,

and H = overburden depth, ft.

By multiplying the output of equation 7 by the ratio of 21.3-m (70-ft) square total-extraction pillar strength for the specified coalbed thickness over the strength of a 21.3-m (70-ft) square pillar in a 1.8-m (6-ft) thick coalbed and rounding to the nearest whole number, one obtains a suggested width for the limited-width section. Note that the 18.3- by 24.4-m (60- by 80-ft) and the 21.3-m (70-ft) square pillars have similar maximum load values (table 1) and are considered to be interchangeable as the basic building blocks of the limited-width section design procedure.

[8]Equation 7*A* is used with metric units, and equation 7*B* is used with U.S. customary units.

Figure 12
Comparison of Ashley and Parametric Analysis Abutment Pillar Width Suggestions.

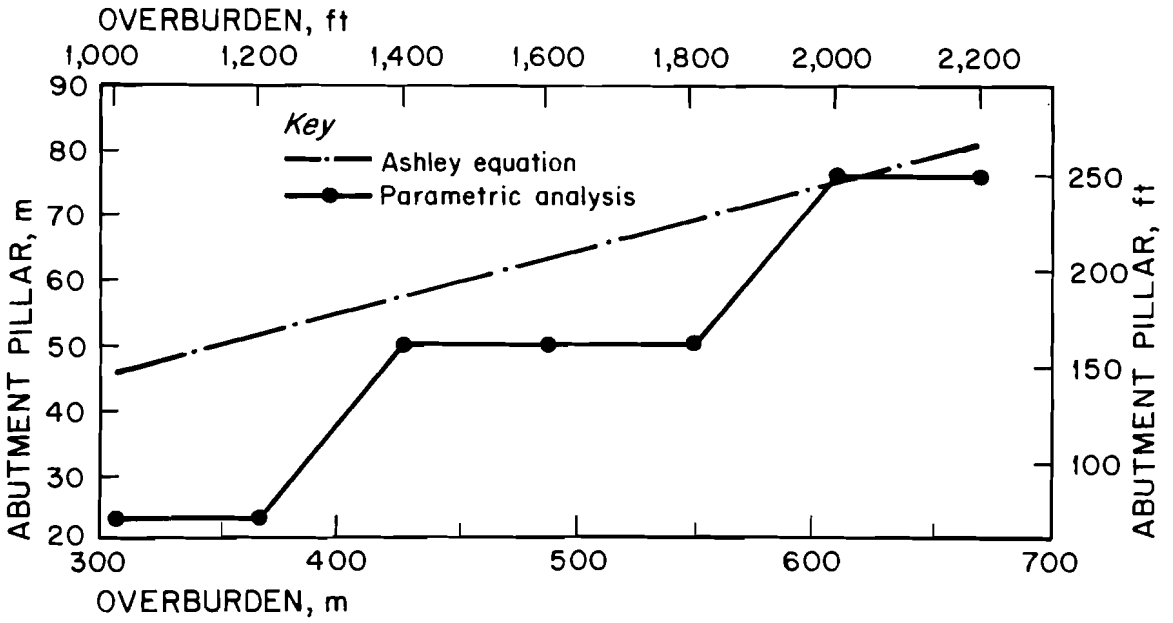

Figure 13
Fit of Limited-Width Section Design Equation to Parametric Analysis Results.

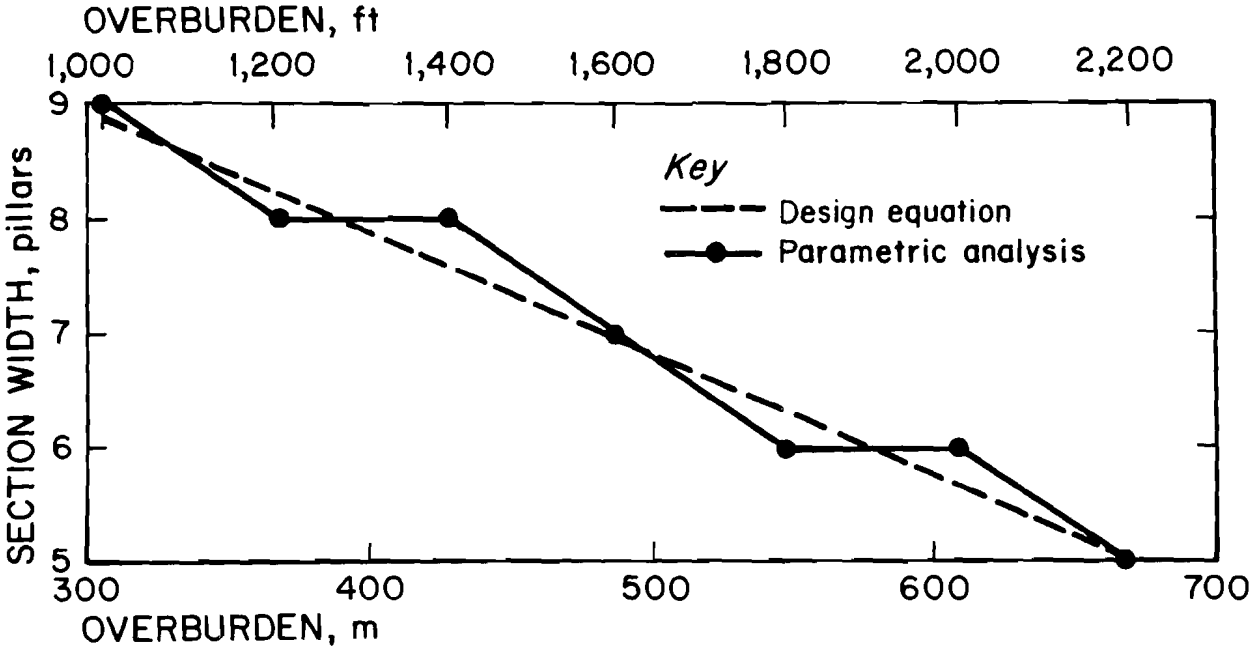

LAYOUT: A BUMP HAZARD ASSESSMENT MODEL

The USBM developed a bump hazard assessment model, LAYOUT, as a spreadsheet template to use with LOTUS 1-2-3 in which unlimited-width and limited-width section design criteria are employed. The model assists a mining engineer in the design of room-and-pillar retreat sections for continuous miner extraction of bump-prone coalbeds. The model LAYOUT provides an essential first step in the mine design process. LAYOUT assumes that the mined coalbed is contained within bump-prone strata. The appendix to this paper is a user's guide to LAYOUT.

The user is requested to specify overburden depth, coalbed thickness, and total-extraction pillar dimensions. Based on this input, LAYOUT calculates (1) the stability factor for the first two pillar rows in an unlimited-width section, (2) a suggested barrier pillar width to separate adjoining sections, and (3) a suggested limited-width section design.

The LAYOUT model was verified against four case studies of coal mine bumps. In the first case study, W-P No. 21 Mine extracted the 1.2-m (4-ft) thick Chilton Coalbed under a maximum overburden of 244 m (800 ft). A bump-related fatality occurred during mining of 18.3-m (60-ft) square pillars with the split-and-fender method (figure 14) (Campoli and others, 1987). Analysis using LAYOUT resulted in a stability factor of 1.51 for an unlimited-width section with 18.3-m (60-ft) square pillars. Thus, pillar size was sufficient to meet stress limit design criteria. The case study confirmed this conclusion, inasmuch as numerous panels were extracted without significant ground control problems. However, the bump fatality was caused by the use of mixed pillar sizes (see figure 14). This case study highlights the need for strict adherence to the design rules of thumb listed in the introduction of this paper in conjunction with the LAYOUT program.

In the second case study, the Olga Mine extracted the 1.8-m (6-ft) thick Pocahontas No. 4 Coalbed under 396 m (1,300 ft) of overburden (Campoli and others, 1989). Analysis of LAYOUT output suggested that the limited-width design procedure, as the 27.4-m (90-ft) square total-extraction pillar design, results in a safety factor of only 0.98. The limited-width design procedure recommends eight-pillar-wide extraction panels separated by 53-m (174-ft) wide continuous barrier pillars. This was consistent with the successful stress shield layout implemented in the 9-Right study area (figure 15).

In the third case study, the VP No. 3 Mine extracted the 1.8-m (6-ft) thick Pocahontas No. 3 Coalbed under 610 m (2,000 ft) of overburden (Campoli and others, 1993). Analysis of LAYOUT output suggested that the limited-width design procedure, as the 27.4-m (90-ft)

Figure 14
Bump Accident Area at W-P No. 21 Mine.

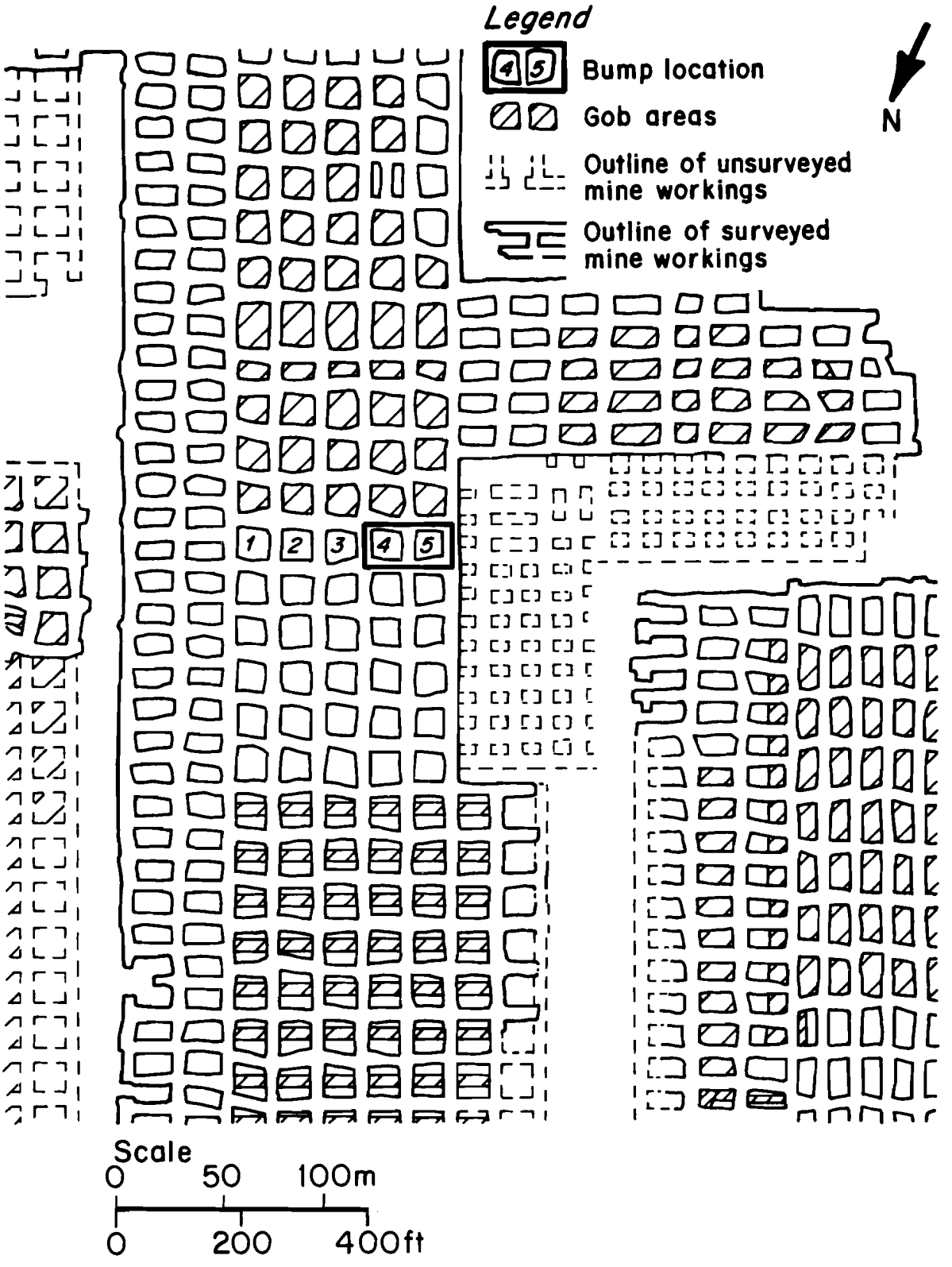

Figure 15
9-Right Study Area at Olga Mine.

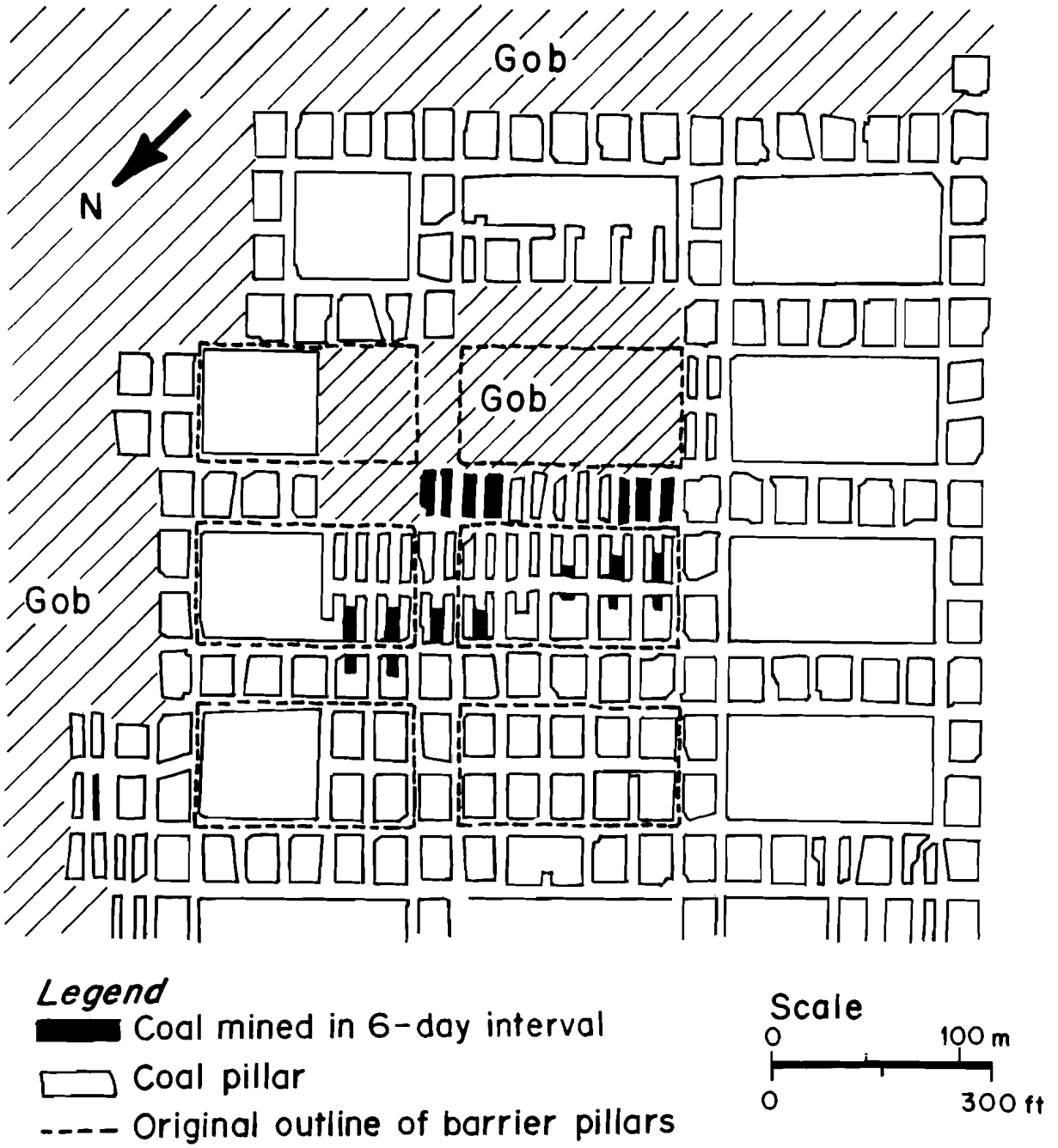

square total-extraction pillar design, results in a safety factor of only 0.76. The limited-width design procedure recommends six-pillar, 170-m (558-ft) wide extraction panels separated by 74-m (244-ft) wide continuous barrier pillars. The successful stress shield layout implemented in the retreat longwall section extracted 183-m (600-ft) wide panels separated by 72.5-m (238-ft) wide gate roads.

In the fourth case study, the Soldier Creek Mine extracted the 3.4-m (11-ft) thick Rock Canyon Coalbed under 518 m (1,700 ft) of overburden. Analysis of LAYOUT output suggested that the limited-width design procedure, as the 27.4-m (90-ft) square total-extraction pillar design, results in a safety factor of only 0.47. The limited-width design procedure recommends five-pillar, 137-m (450-ft) wide extraction panels separated by 71-m (234-ft) wide continuous barrier pillars. The mine experienced coal bumps while attempting to extract five-pillar, 128-m (420-ft) wide panels comprising 18.3-m (60-ft) square total-extraction pillars (figure 16). The first panel was extracted without bumps because it was between solid coal barriers. However, the second panel retreat experienced severe coal pillar bumps resulting from insufficient side abutment load protection provided by 42.7-m (140-ft) and 18.3-m (60-ft) barrier pillars and was therefore abandoned.

Single copies of the LAYOUT program may be obtained by sending a blank, formatted diskette to—

Alan A. Campoli
U.S. Bureau of Mines
Pittsburgh Research Center
Cochrans Mill Rd.
P.O. Box 18070
Pittsburgh, PA 15236-0070

Figure 16
Bump Activity Area at Soldier Creek Mine.

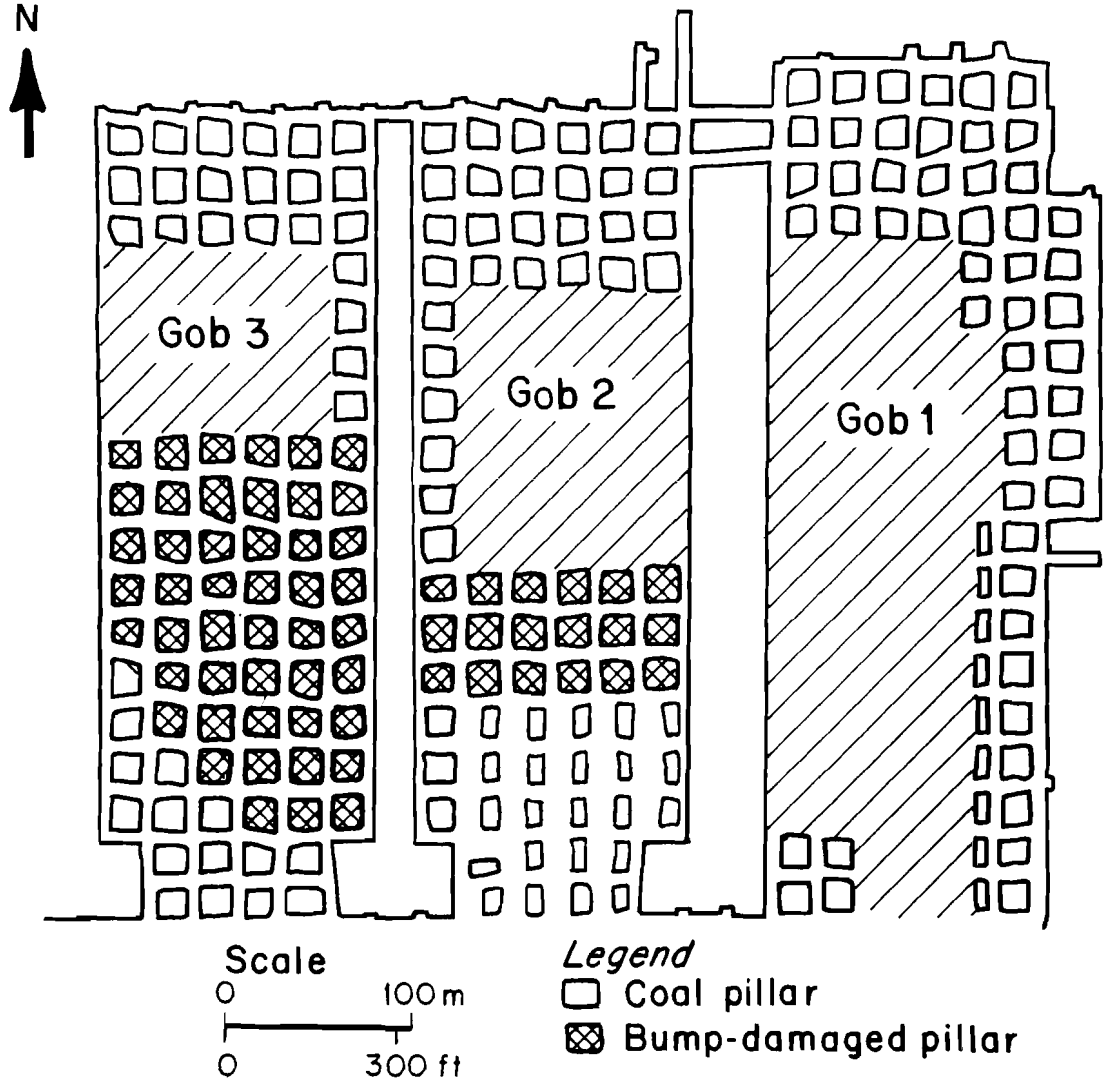

CONCLUSIONS

The risk of coal mine bumps becomes critical when the mined coalbed is under significant overburden and encased in rigid strata. Coal mine design is the only factor under significant control of the mine operator. The USBM therefore developed LAYOUT, a bump hazard assessment model, as a LOTUS 1-2-3 spreadsheet template using linear, shear-angle-based, unlimited-width and boundary-element-based, limited-width section design criteria. Both approaches use a pseudoductile coal pillar strength model. LAYOUT assists in the design of room-and-pillar retreat sections for continuous miner extraction of bump-prone coalbeds and provides an essential first step in the mine design process.

REFERENCES

Ashley, G. H. Barrier Pillar Legislation in Pennsylvania. Trans. AIME, Coal Div., 1930, pp. 76-97.

Barron, K. An Analytical Approach to the Design of Coal Pillars. CIM Bull., v. 77, No. 868, 1984, 272 pp.

Campoli, A. A., T. M. Barton, F. C. Van Dyke, and M. Gauna. Gob and Gate Road Reaction to Longwall Mining in Bump-Prone Strata. USBM RI 9445, 1993, 48 pp.

___. Mitigating Destructive Longwall Bumps Through Conventional Gate Entry Design. USBM RI 9325, 1990, 38 pp.

Campoli, A. A., C. A. Kertis, and C. A. Goode. Coal Mine Bumps: Five Case Studies in the Eastern United States. USBM RI 9149, 1987, 34 pp.

Campoli, A. A., D. C. Oyler, and F. E. Chase. Performance of a Novel Bump Control Pillar Extracting Technique During Room-and-Pillar Retreat Coal Mining. USBM RI 9240, 1989, 40 pp.

Chase, F. E., and C. Mark. Ground Control Design for Pillar Extraction. SME preprint 93-282, 1993, 12 pp.

King, H. J., and B. N. Whittaker. A Review of Current Knowledge on Roadway Behavior. Paper in Proceedings of the Symposium on Roadway Strata Control. Instit. Min. and Metall., 1971, pp. 73-87.

Mark, C. Pillar Design Methods for Longwall Mining. USBM IC 9247, 1990, 53 pp.

Mucho, T. P., T. M. Barton, and C. S. Compton. Room-and-Pillar Mining in Bump-Prone Conditions and Thin-Pillar Mining as a Bump Mitigation Technique. USBM RI 9489, 1993, 18 pp.

Pappas, D. M.. and C. Mark. Behavior of Simulated Longwall Gob Material. USBM RI 9458, 1993, 39 pp.

Peng, S. S., and H. S. Chiang. Longwall Mining. Wiley, 1984, 708 pp.

Salamon, M. D. G. Mechanism of Caving in Longwall Coal Mining. Paper in Rock Mechanics Contributions and Challenges: Proceedings of the 31st U.S. Symposium, ed. by W. A. Hustrulid and G. A. Johnson (CO Sch. Mines, Golden, CO, June 18-20, 1990). Balkema, 1990, pp. 161-168.

Wilson, A. H. A Hypothesis Concerning Pillar Stability. Min. Eng. (London), v. 131, 1973, pp. 409-417.

Zelanko, J. C., G. A. Rowell, and T. M. Barczak. Analysis of Support and Strata Reactions in a Bump-Prone Eastern Kentucky Coal Mine. SME preprint 91-91, 1991, 14 pp.

Zipf, R. K., Jr. MULSIM/NL Application and Practitioner's Manual. USBM IC 9322, 1992a, 48 pp.

___. MULSIM/NL Theoretical and Programmer's Manual. USBM IC 9321, 1992b, 52 pp.

APPENDIX.—USER'S GUIDE TO LAYOUT: A BUMP HAZARD ASSESSMENT MODEL

by Alan A. Campoli[1]

The USBM developed LAYOUT, a bump hazard assessment model, as a spreadsheet template in LOTUS 1-2-3, release 3.1. The model assists the mining engineer in the design of room-and-pillar retreat sections for continuous miner extraction of bump-prone coalbeds. LAYOUT provides an essential first step in the mine design process. It assumes that the mined coalbed is contained within bump-prone strata.

Use of LAYOUT begins with retrieval of the file labeled "LAYOUT.WK3." LAYOUT can be used in all versions of EXCEL and LOTUS 1-2-3, release 3.1 and later, by converting the spreadsheet to the appropriate format. The user specifies overburden depth, coalbed thickness, total-extraction pillar width, and total-extraction pillar length in cells E19, E20, E21, and E22, respectively. Note that pillar dimensions parallel and perpendicular to the gob line are referred to as pillar width and length, respectively. The spreadsheet is protected and cannot be changed except for initial data input. Based on this input, LAYOUT calculates the total-extraction pillar strength (cell E30), development load (cell E33), abutment load (cell E34), and pillar stability factor for the first (cell E40) and second (cell E41) total-extraction pillar rows outby the gob. If the stability factor for the first pillar row outby the gob is less than 1, the instruction "INCREASE PILLAR SIZE or EMPLOY LIMITED-WIDTH SECTION" appears in cell A42. At that point, the user may either change the pillar dimension input (cells A21 and A22) or consider the suggested limited-width section design. The section width in multiples of either 21.3-m (70-ft) square or 18.3- by 24.4-m (60- by 80-ft) total-extraction pillars is displayed in cell E47. The barrier pillar width suggested to separate both the unlimited- and limited-width sections is displayed in cell E50.

One must consider the following assumptions and limitations associated with LAYOUT.

1. In the unlimited-width design procedure, the abutment loads are modeled as if sufficient gob has been formed to allow a portion of the overburden weight to be applied to the gob floor as defined by the linear shear angle. Thus, LAYOUT does not account for first-fall effects.

2. After analysis of the few case studies available, it appears that an unlimited-width stability factor of greater than 1 should be applied. However, LAYOUT assumes that all of the gob-side total-extraction pillars are the same size. Care must be taken during advance mining to ensure that this is the case.

3. LAYOUT does not account for faults or any geologic structure in the mine roof. It is assumed that the roof behaves uniformly. If such structure is known to exist, the possibility of anomalous stress concentrations should be considered.

[1]Mining engineer, Pittsburgh Research Center, U.S. Bureau of Mines, Pittsburgh, PA.

STRESS DETECTION AND DESTRESSING TECHNIQUES TO CONTROL COAL MINE BUMPS

By K. Y. Haramy,[1] H. Maleki,[2] and D. Swanson[3]

ABSTRACT

Dangerously high stress areas in underground coal mines can be controlled by proper mine planning and/or destressing. This paper reviews practical methods to detect and destress high-stress zones within coal faces and mine pillars. The U.S. Bureau of Mines investigated stress-related problems in several underground mines. Laboratory and field test results of the drilling-yield method for high-stress detection were conducted to determine the correlation between the volume of cuttings obtained and the magnitude of applied stress. The results indicate that this method can be used effectively to locate high-stress zones within longwall panels. In-mine experiences and a three-dimensional computer modeling program were used to evaluate the effectiveness of stress-relief methods. These studies show that the occurrence of coal bumps can be reduced by properly implementing destressing techniques. However, careless use of stress-relief methods may increase the potential for a coal bump. Areas within different mines have site-specific characteristics that will indicate how the effective the stress-relief methods are.

Techniques applicable to longwall and room-and-pillar mining for both Eastern and Western U.S. coal mines are discussed.

INTRODUCTION

In many parts of the world, coal bounces, bumps, and outbursts are major hazards to underground mining. Bump is a term used to describe rock and coal failures ranging in magnitude from an explosion of small rock fragments from faces or ribs to a sudden collapse of a large section of a mine. A bump is defined as a sudden and violent explosion of rock and coal in or around an excavation. Failure is normally associated with high stress and brittle or brittle-elastic materials. Bumps may also be associated with desorbed gas. This type of failure is termed an outburst. These events have the potential to inflict severe injury to mining personnel. Invariably, production is disrupted and entry or mine closure may result. Bumps can induce damaging effects on adjacent strata that may lead to roof and/or floor problems.

The severity of bumps usually increases with depth. The cause of this increase is attributed to increased overburden weight. However, depth is not the only factor that can contribute to bumps. Although bumps have been reported in mines under less than 305 m (1,000 ft) of cover, in general, bumps in shallow mines occur infrequently and are not as severe. Whereas localized, high-stress zones are common to all bump occurrences, other factors, such as geological conditions, mine design, and rock physical properties and mining practice, may act independently or in combination to cause a bump. For example, in deep coal mines, strong roof beds induce excessively high abutment stresses and tremendous amounts of strain energy in the coal. When coupled with confinement provided by strong adjacent strata and horizontal stresses, the potential for the sudden release of stored

[1]Supervisory mining engineer, Denver Research Center, U.S. Bureau of Mines, Denver, CO.

[2]Mining engineer, Spokane Research Center, U.S. Bureau of Mines, Spokane, WA.

[3]Mining engineer, Twin Cities Research Center, U.S. Bureau of Mines, Minneapolis, MN.

energy and dynamic failure increases. The location and orientation of geological anomalies such as faults, folds, dikes, and joints may also contribute to stress buildup and bump frequencies (*1*).[4]

Investigations of seismic-induced energy releases caused by underground coal mining have found strong evidence for a relationship between sudden dynamic failures and mining activity (*2-9*). Good correlations for mining-induced seismicity are well documented for the Book Cliffs-eastern Wasatch Plateau area in Utah; the upper Silesia Coal Basin, Poland; the North Staffordshire Coalfield, England; and the Myntaogou Coalfield, China. These coal-mining areas are similar in that regional tectonic stress fields are high because of unfavorable geology, mining depth, dipping coal seams, and highly irregular topography. The severity and magnitude of seismic events range from near-field bumps to a magnitude 4.0 earthquake. Identifying critical factors, such as mine design, rock properties, and the existence of strong roof and floor members, that contribute to sudden energy releases is essential in the development of remedial measures to lessen the effects of these failures.

Independent seismic monitoring studies conducted in coalfields in various parts of the world show a strong similarity in findings (*2, 6, 8-9*), that is, zones of high seismicity correlate well with the directions and locations of the greatest amount of mining activity in major coal mining districts. These studies also show good correlation between increased production in the area and increased seismicity.

- During the monitoring period in the Book Cliffs-eastern Wasatch Plateau, the University of Utah, Salt Lake City, UT, and the U.S. Geological Survey (USGS) detected several hundred events per day, with the largest being a 4.0-magnitude earthquake. The epicenter of most of the stronger seismic events appeared to be away from the immediate vicinity of the mine. Also, the most seismically active areas had shifted from the Book Cliffs toward the more actively mined areas near Soldier Canyon (*7*). McKee and Arabasz have shown that, for the Utah coalfields, the highest number of seismic events corresponded to areas where coal extraction rates were greater than one-half million metric tons per year (*7*).
- Among the most violent coal regions in China is the Myntaogou Coalfield. Since 1957, seismic events associated with rock bursts became more prevalent as more mining took place. A surface seismic monitoring program detected 4,187 events of varying magnitudes between 1960 and 1962 (*6*). Of this number, 120 events were of tectonic origin and possibly not related to coal mining, leaving 4,067 events that showed some effects of mining in terms of spatial and temporal relationships. Although the magnitudes of the earthquakes were not reported, some were severe; over 80 homes on the surface were destroyed, as well as concrete structures underground (*6*).
- During a 2-year period (1975-1977) Keele University, the Institute of Geological Sciences, and the National Coal Board in the United Kingdom began measuring seismic events in the North Staffordshire Coalfield and vicinity (*8*). A total of 711 seismic events was detected, with 54 events being felt by local residents. The largest event measured was nearly 3.0 on the Richter scale. The highest incidence of seismic events appeared to be related to the position of the actively mined coal face to old workings in an upper and a lower seam.
- Seismic activity has been particularly high in the upper Silesian Coalfields, and 23,078 events greater than 1.5 on the Richter scale were measured between 1977 and 1986 (*9-10*). During this period, seven events with a magnitude greater than or equal to 3.5 were detected. In this study, a strong relationship was found between the cumulative seismic energy released per year and coal production.

Recognizing the effect of dynamic failures on the health and safety of miners, the U.S. Bureau of Mines (USBM) conducted research to evaluate the drilling-yield method for use in mines to locate potential bump zones rapidly. This research also involved an evaluation of practical methods of controlling bumps. These methods included volley firing, auger drilling, hydro fracturing, and other methods that can be used to induce fracturing in noncaving roof strata.

DETECTION OF HIGH STRESS IN COAL

Many attempts have been made to detect bump-prone areas ahead of mining. Detection of bump-prone areas has involved locating high-stress zones in the coal seam and/or surrounding rock mass. One widely used practical method is the drilling-yield method.

The drilling-yield detection method, also known as probehole drilling, has been used in Russia since the 1950's. In the early 1960's, the method was modified and adapted to local and geological conditions in a few European coalfields. Recently, the method was introduced to U.S. mines and was favorably received.

[4]Italic numbers in parentheses refer to items in the list of references at the end of this paper.

volume of drill cuttings. A volume of cuttings can be expected from a drill hole of a known diameter and length. If the actual volume of generated cuttings exceeds the volume of the hole by a significant amount, the zone around that particular hole is determined to be highly stressed. Drilling in a previously stressed zone produces compression in the borehole, and various dynamic effects are observed, such as audible knocking (bumping) and jamming of the drilling rod in the borehole. Typical curves from a 2.3-m (7-ft) high coal seam are presented in figure 1 and show the drilling-yield results for low- and high-stress zones. The closer to the pillar edge a highly stressed zone is, the greater the danger of rock bumping. Based on past studies (*1*), the bump potential is determined from the drilling-yield results and seam thickness. These relationships are summarized as follows:

- If the increased stress zone is detected at a distance greater than 3.5 times the mining height (T) measured from the rib side, a ***FAVORABLE*** mining state is assumed. Mining can progress, and no destressing is required.
- If the increased stress zone is detected at a distance between 1.5 T and 3.5 T from the ribside, a ***DANGEROUS*** mining state exists. Mining may or may not progress, depending on many other factors, such as physical properties of the rock, geologic conditions, and the amount of stress increase in the zone.
- If the increased stress zone is detected at a distance less than 1.5 T from the ribside, a ***CRITICAL*** bumping condition exists. Mining should stop, and destressing should be practiced.

Since geologic conditions and rock physical properties vary, these results may need to be confirmed before they are applied in a specific mine.

THEORY AND FIELD RESULTS

The idea of probehole drilling is based on the theory of stress around a circular opening. Stress magnitude and distribution around a single, circular opening, such as a drill hole, have been determined analytically and from laboratory studies (*11*). Stress concentrations around a circular opening in a bidirectional stress field are shown in figure 2. This figure shows the boundary stress concentration around the circular opening for a material with a Poisson's ratio of 0.25. When the boundary stress exceeds the strength of the material, the hole begins to deform and fail. In highly stressed areas, such as the forward abutment region ahead of a longwall face, the coal around the drill hole behaves plastically and flows into the hole.

The drilling-yield detection method was used at several mines to locate high-stress zones in the longwall face and

Figure 1
Drilling-Yield Results.

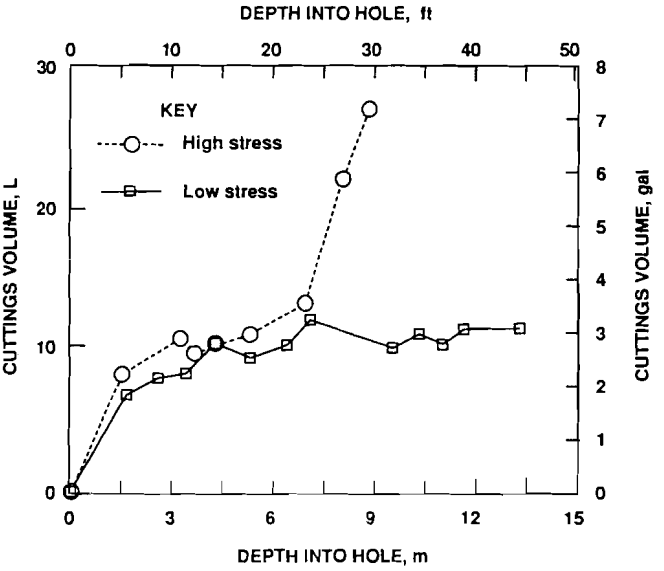

Figure 2
Boundary Stress Concentration for Circular Opening.

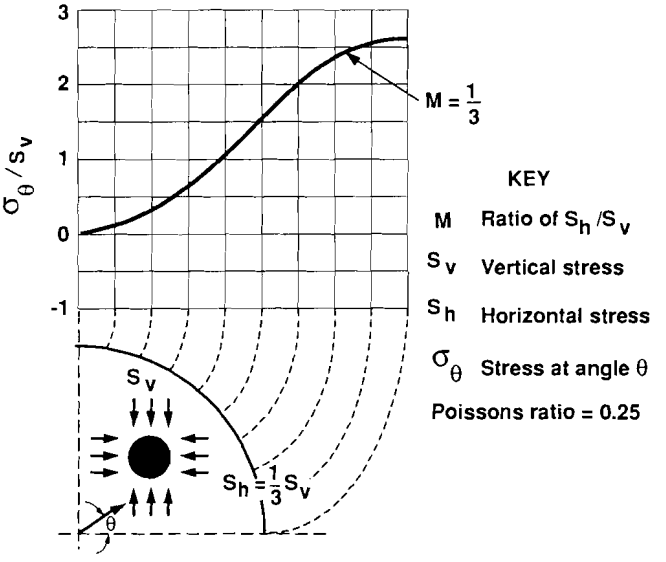

in the panel ahead of mining. Probehole drilling was conducted using a hand-held, air-powered auger drill with auger rods 1 to 1.5 m (3 to 5 ft) long. Along with the auger rods, a two-wing, 5-cm (2-in) diam, carbide-insert drag bit was used. Drilling operations were conducted by a two-person crew (one driller and one helper) who added auger rods and recorded the following information: volume of cutting produced per length of hole drilled, occurrence of bounces, location of gas in the hole, and squeezing of the hole on the drill rod. Site preparation

currence of bounces, location of gas in the hole, and squeezing of the hole on the drill rod. Site preparation involved scaling the rib or face to provide a solid, stable surface for the collar of the hole. Actual drilling involved controlling the penetration rate to prevent the auger steel from sticking in the hole. Because the drill was hand-held, the driller's experiences were critical to locating the high-stress zone. Drilling was always performed while the longwall face was idle.

The area was determined to be stressed if the volume of cuttings from the hole exceeded 19 L/m (5 gal/yd), if the driller heard or felt minor bouncing or constant hole squeezing, or the auger steel was recorded as jamming or getting drawn into the hole during drilling. The presence of large volumes of gas also indicated high-stress zones.

The drilling pattern at one test site consisted of 5-cm (2-in) diam probeholes drilled on 15- to 31-m (50- to 100-ft) centers 4 to 4.5 m (13 to 15 ft) deep. Each hole was roughly perpendicular to the seam at midseam height along the length of the longwall face on a daily basis. The results were plotted to show the areas of high stress ahead of the face. Figure 3 shows typical drilling-yield data from three drill holes. The abutment zone, which fits the criteria for critical stress, occurred at a depth of approximately 14 m (45 ft) ahead of the face. At this mine, if drilling-yield results show an abutment zone farther from the face than at least three times the seam height [9 m (30 ft)], the face is generally determined to be nonbump-prone, and no destressing is performed.

Figure 3
Drilling-Yield Data from Three Drill Holes.

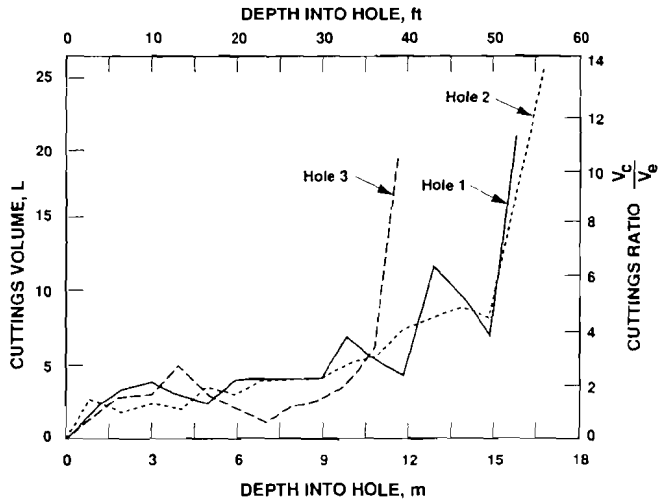

Cuttings ratio V_c/V_e is obtained from 1-m (3-ft) sections of 5-cm (2-in) diam borehole.

At another mine, the drilling-yield method was effective in detecting stress zones in the panel ahead of mining at two separate locations. Drilling was terminated when the steel was drawn into the hole, cuttings exceeded 19 L/m (5 gal/yd) of drilling, a bounce or a squeeze on the drill steel occurred, or after approximately 9 m (30 ft) of drilling. The steel drawn into the hole is a feeling similar to that experienced when driving a screw in a piece of wood with a power drill. If drilling ceased a distance of less than 6 m (20 ft) into the panel because of such conditions, the area would be considered a potential problem area. Holes were drilled in the tailgate entry at every crosscut and adjacent to the pillar centerline in the panel [approximately 15-m (50-ft) centers]. Drilling began at a distance greater than 0.25 times the overburden depth outby the face. All drilling was conducted during idle shifts, and the results are shown in figure 4. At this mine, no dangerously high stress zones were detected within the critical distance into the panel rib, and, therefore, no destressing was required.

LABORATORY TESTS AND RESULTS

Probehole drilling, as proven by in-mine experience, can give reliable information on the general stress condition in a coal seam. Absolute stress magnitude is not determined, however. Laboratory tests were performed to determine the relationship between stress magnitude and volume of cuttings. The tests were conducted using 10-cm (4-in) simulated coal (coalcrete) cubes that had been compressed using a developed test frame (*12*). The average compressive strength of the samples was 10 MPa (1,500 psi), and Young's modulus was 2×10^3 MPa (3×10^5 psi). The results shown in figure 5 indicated a linear relationship between the applied vertical stress and the log of $\frac{V_c}{V_e}$.

$$\sigma_v = 123 \left[\log \frac{V_c}{V_e} \right] + 18 \qquad (1)$$

where σ_v = applied vertical stress, MPa,

V_c = actual volume of cuttings obtained, MPa,

and V_e = volume of cuttings expected from the hole drilled.

Results indicate that drill yield may be used to indicate the general stress level in the mine.

Figure 4
Drilling-Yield Results at Western Coal Mine.

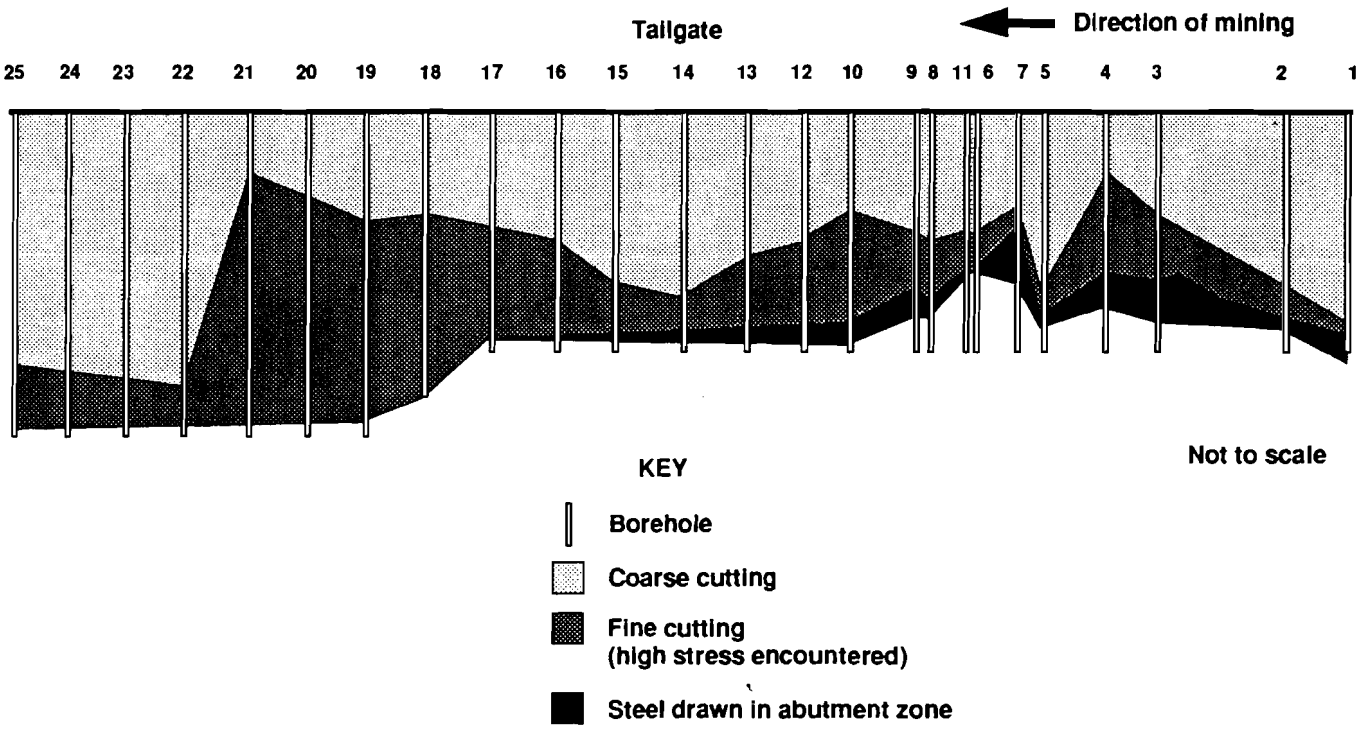

Figure 5
Laboratory Test Results from Drilling-Yield Method.

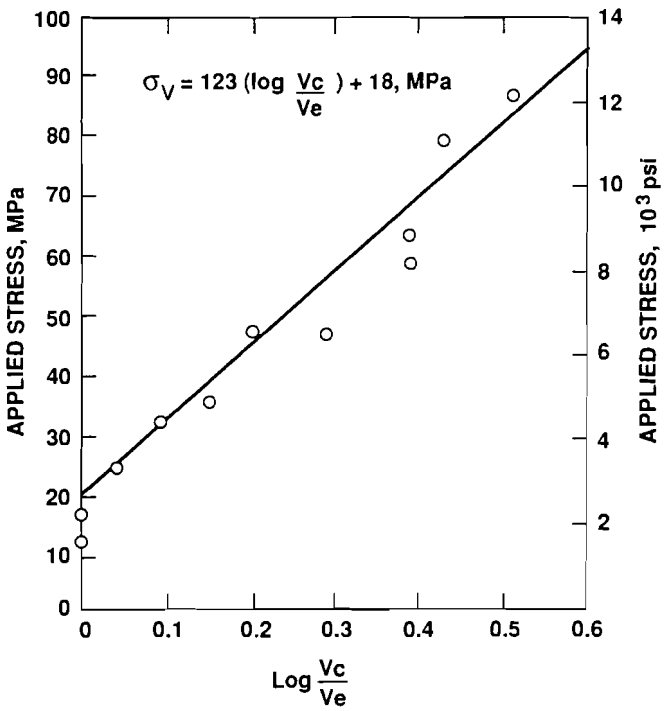

DESTRESSING METHODS FOR BUMP CONTROL

High stress is the common denominator in the bump problem. Causes of high stress can be traced to a number of factors, such as pillar size and shape, roof and floor confinement, coal material properties, mining method, rate of advance, cutting depth, and orientation of panel with respect to in situ stress fields. The contributing factors are numerous and present very complicated problems in predicting potential bump locations. Prevention of bumps may be achieved by proper planning and mine design and sometimes should include an active stress-relief program incorporated into the mining cycle.

The basic concept of stress relief or transference of high stress concentrations from one portion of a mine structure to another is not new. Fracturing or softening rock or coal to control stress buildup has been practiced in various mines. In coal mines, if mine planning does not eliminate bumps, destressing the active working face is a logical method of preventing bumps.

Although different destressing methods have been used, all methods are based on the same theory. Coal, or in some instances roof and/or floor rock, is intentionally fractured and made to fail. As a result, high stress accumulations can not occur in the fractured zone, and load is transferred onto an unfractured part of the mine structure. If stress cannot build up, the area will not bump violently. The theory is simple, but controlling the extent of fracturing and the rate of load transfer is not always feasible. Occasionally, destressing itself may trigger a bump, but mine personnel are usually remote from the working face during stress relief operations. For example, in volley firing, workers drill only small-diameter holes and then retreat a safe distance while the holes are fired. Overall, worker safety is increased by a stress relief program.

Three major destressing methods have been used in underground coal mines.

VOLLEY FIRING

Destressing by volley firing has successfully reduced the number of bumps in several Western coal mines (*12*). In this method, explosives are used to fracture the coal face to a certain depth before mining. The method is used prior to face advance or entry development to advance the abutment zone away from the active working face.

Longwall face stress relief is accomplished by drilling into previously identified high-stress zones, as illustrated in figure 6. The blast holes are loaded with 1.35 kg (3 lb) of permissible explosives, stemmed, and detonated. The drill pattern consists of a series of 5-cm (2-in) diam holes 4 to 4.6 m (13 to 15 ft) deep, drilled on approximately 1.25-m (4-ft) centers. Hole depth depends on the required daily advance of the face and on the location and magnitude of the stress abutment ahead of the face. Local conditions and site-specific experience dictate exact hole parameters. The corners of the longwall face require a specific drilling pattern, using combinations of two or three holes, as shown in figure 6, to relieve high stress on the face.

When developing entries, the cut sequence should be designed to transfer the abutment zone ahead of mining. The multiple-entry sequence shown in figure 7 was the most effective system used at the test site. Advancing entry 1 created an abutment zone represented by the stress profile shown in the figure. As entries 2 through 4 were advanced the same distance in sequence, the abutment zones also advanced, and the crosscuts were mined safely in the destressed zone. If destressing was not done prior to mining these zones, advancing these entries would have been dangerous. This process was repeated after all the crosscuts were mined. Destressing a longwall development section or the working face of a room-and-pillar entry working face may also be required. Figure 8 illustrates a volley-fire drill-hole pattern for a development section, where holes are angled into the rib in a specific pattern. The drill holes do not extend deeply into the rib because blasting the rib effectively reduces the load-carrying area

Figure 6
Volley Firing Drill-Hole Pattern for Longwall Faces.

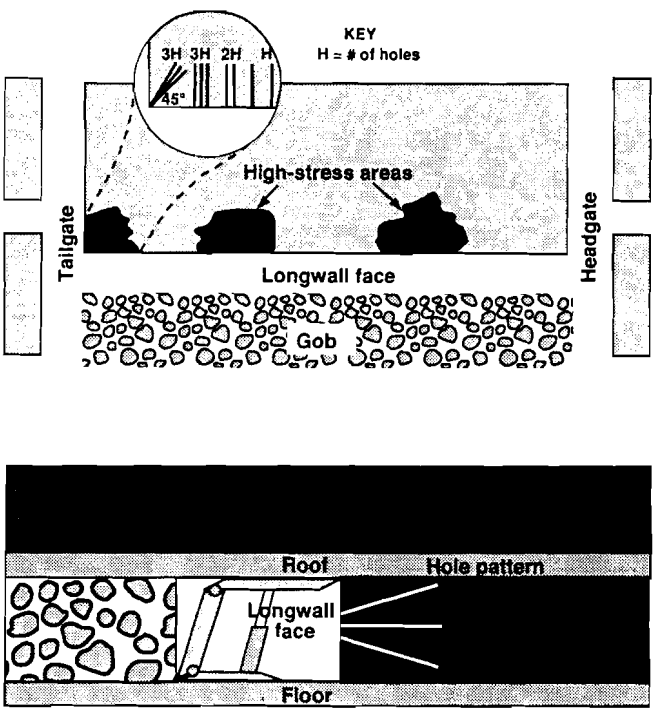

Hole specifications are 5-cm (2-in) diam, 4 to 4.5 m (13-15 ft) deep, on 1.2-m (4-ft) centers.

Figure 7
Effective Mining Sequence for Advancing Development Section in Bump-Prone Mine.

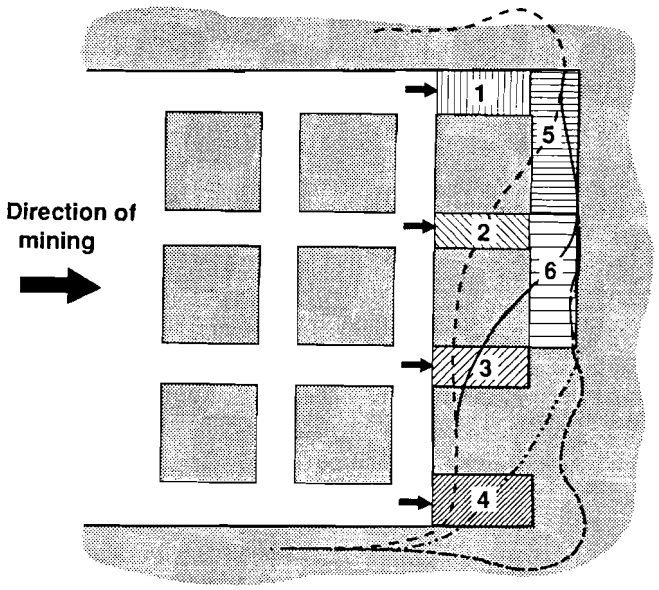

of the pillar. The depth and angle of the rib holes depend on the size of the pillar, the distance of the abutment zone from the face and entry, and other local conditions. At an Eastern mine *(13)*, the volley-firing technique was applied to reduce the load-bearing capacity of pillars during room-and-pillar retreat mining. The effectiveness of this method at this mine was monitored using roof-to-floor convergence. The results published by Campoli and others *(13)* suggested that the effectiveness of volley firing increases with the amount of explosives used.

HYDRAULIC FRACTURING

This method involves the injection of fluid under pressure to cause material failure by creating fractures or fracture systems. Hydraulic fracturing is most effective in the roof and coal seam ahead of the longwall face. Although this method has been used to destress longwall

Figure 8
Volley Firing Drill-Hole Pattern for Development Entries.

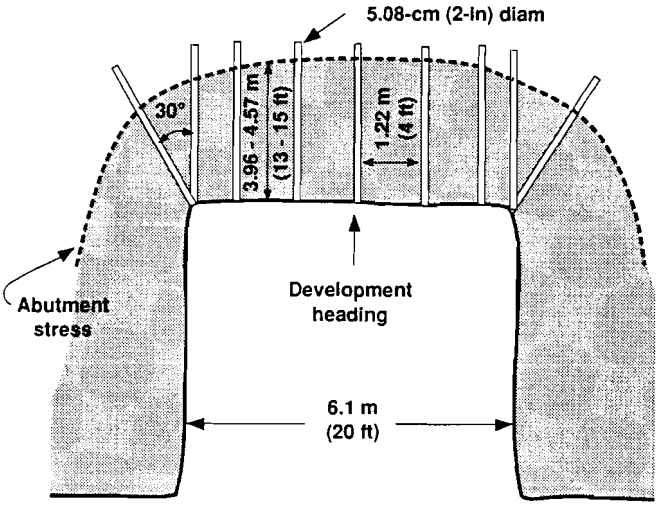

faces, it is time consuming and not recommended for use on the face because it may interfere with production.

Experiments conducted in Poland *(14)* have shown the beneficial effects of hydraulic fracturing of the roof ahead of the longwall face. The number of seismic events during mining decreased significantly in zones where the roof had been hydraulically fractured as compared to zones that had not been fractured. During fluid infusion, the number of seismic events increased, an indication that the fracturing process caused stress redistribution.

Hydraulic fracturing of the coal seam ahead of the face is also practiced. Figure 9 shows a sample drill-hole pattern into the rib of a longwall panel. Fluid under high pressure is injected into the holes. The pressure needed for fracturing is dependent on the physical properties and in situ stresses for coal and adjacent strata. At the study site, the fluid pressure was calculated using the following equation:

$$\Psi = (1 - \nu)\,(C_x + \tau), \qquad (2)$$

where Ψ = fluid pressure,

ν = Poisson's ratio,

C_x = rock bed strength,

and τ = tensile strength.

Numerous variables affect hydraulic fracturing, including prevailing rock stress, rock tensile strength, modulus of elasticity and Poisson's ratio of the rock, rate of fluid injection, injection time, fracture clearance, formation

Figure 9
Hydraulic Fracturing Pattern Ahead of Longwall Face.

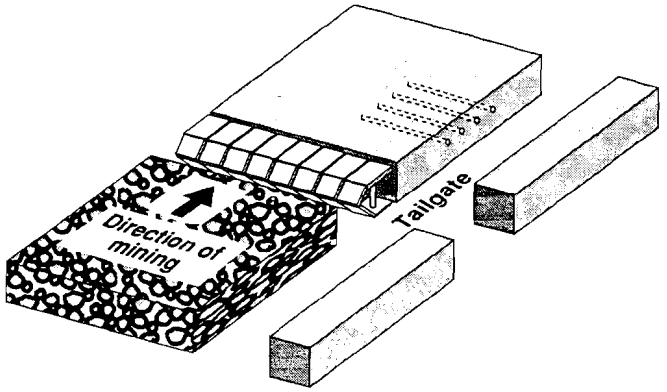

Hole specifications are 5-cm (2-in) diam, 30.5-m (100-ft) deep, on 30.5- to 61-m (100-to 200-ft) centers.

permeability and porosity, fracture fluid viscosity and pressure, and total fluid volume injected. Controlling the extent of the fracture zone is very difficult because of the many variables associated with hydraulic fracturing. Fracturing a very large and highly stressed area causes loads to be redistributed and may create bump conditions in the mine.

Destressing efforts in a Western longwall mine were concentrated in the tailgate end of the longwall face. The tailgate consisted of two 6-m (20-ft) wide entries with 25- by 36-m (85- by 120-ft) chain pillars. The panel width was 185 m (610 ft), and the planned retreat distance was approximately 1,064 m (3,500 ft). After the face had retreated approximately 182 m (600 ft), severe bumping occurred at the face and in the tailgate pillars and continued for the next 243 m (800 ft) of retreat. No major bumps occurred for the next 305 m (1,000 ft) of retreat, and mining progressed rapidly with high production. Bumping resumed between approximately 736 m (2,420 ft) of face retreat and continued until the face was halted after 809 m (2,660 ft) of retreat because of a major face bump. The bumping occurred at this mine when the face was beneath ridges and overlain by greater than 486 m (1,600 ft) of overburden, whereas during the relatively bump-free period, overburden depths were less than 486 m (1,600 ft).

Panel coal destressing by water infusion was initiated when bumps were encountered after 182 m (600 ft) of advance and continued until the face was halted. Two infusion procedures were developed and used concurrently, as shown in figure 10.

In the first procedure, (figure 10*A*) 5-cm (2-in) diam holes spaced 9 m (30 ft) apart were drilled 6 to 28 m (20 to 90 ft) into the tailgate panel rib, beginning at least 12 m (40 ft) outby the face, and a high-pressure hose with a packer was inserted into each hole. Whenever the face had progressed to within 3 m (10 ft) inby a hole, the hose was connected to a pump, and face-support-shield hydraulic fluid, which is an emulsion of water and soluble oil, was pumped into the hole at an approximate pressure of 28 MPa (4,000 psi). Each hole was pressurized for a duration of 30 min or until a minor bump was induced. When the tailgate panel rib holes were drilled with a handheld drill, it proved very difficult to maintain hole alignment parallel to the local seam dip at midseam height. Because secondary support timbers had been installed in advance of the face, working space and equipment access in the tailgate entry were limited, and use of a machine-mounted drill was not feasible.

Figure 10
Fluid Injection Patterns Used at Western Longwall Mine.

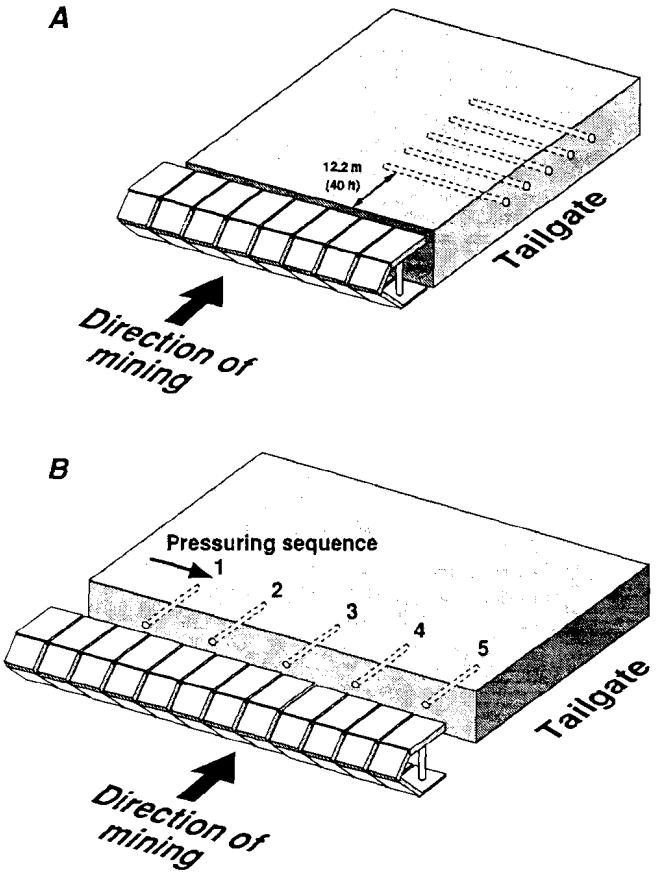

The second procedure (figure 10*B*) consisted of drilling three or four holes 6 m (20 ft) into the face. These holes were evenly spaced along the face between a point approximately 40 m (130 ft) from the tailgate rib and the tailgate panel corner. After all holes were drilled, they were successively pressurized in the same manner as the tailgate rib holes, starting at the hole farthest from the tailgate and progressing toward the tailgate. This procedure was conducted at intervals of 10 cuts by the shearer, approximately

7.5 m (25 ft). Face-hole destressing was time consuming and precluded shearer cutting at the section of the face being destressed until the procedure was completed, thus causing significant production delays.

These procedures were used concurrently and generally proved effective in destressing the tailgate area of the face and alleviating severe unanticipated bumping. However, the difficulty of identifying optimum destressing times and locations, the inability to assess the effectiveness of each destressing attempt, the limited time available for face destressing (to avoid production interruptions), and adverse drilling conditions inhibited the overall success of the effort.

At another Eastern mine, the operator switched from destressing to fluid infusion after attempts with volley firing failed to mitigate coal bumps. At this mine, it had not been possible to mine through the bump-prone areas without destressing. Fluid infusion was used to facilitate coal fracturing at lower stress levels because this method reduced confining pressures or friction at coal and rock interfaces (*15*). Coal fracturing ahead of the longwall face reduced the potential for buildup of high stresses at the face and the violent release of strain energy.

A Mohr-Coulomb failure criterion, shown in figure 11, was used to demonstrate both strengthening and weakening resulting from changes in confining pressures of an Appalachian coal seam. The in situ strength of the coal was 30 MPa (4,400 psi) at typical confining stresses of 6 MPa (875 psi). Under noncaving sandstone channels, higher confinement stresses could be formed in the seam (*16*), increasing coal strength to 35 MPa (5,100 psi) and contributing to coal bumps.

Fluid infusion reduces confining pressures and enhances coal fracturing at lower stress levels. The infusion replaces the air in voids in the seam, lubricates cleats and geologic interfaces, and increases pore pressure. As shown in figure 11, a 12° reduction in the angle of internal friction could reduce the in situ coal strength to 24 MPa (3,500 psi). Coal strength could be reduced further if the pore pressure was increased by 3.5 MPa (500 psi), as shown in figure 11*C*.

Both low- and high-pressure fluid infusion have been used in this mine to enhance coal fracturing. Low-pressure [less than 8 MPa (1,200 psi)] water infusion holes were drilled in the coal from the headgate and the tailgate during panel development in an attempt to saturate the entire seam in a mine experiencing severe coal bumps at the face-tailgate position. Figure 12 illustrates the locations of coal bumps and fluid infusion holes. All holes were planned to reach midpanel. Few holes were shortened because of drilling difficulties in rock splays, which are persistent in this seam. Packers were used to seal sections of the hole, and water under low pressure was injected until the coal was saturated (*17*).

The effectiveness of this method for coal bump control is highly influenced by a variety of geologic and operational factors, such as directional permeability of the coal seam, poroelasticity, presence of coal-rock interfaces, drilling limitations, and availability of mine water. One bump occurred adjacent to an unsuccessful fluid infusion hole. This indicated that other mitigation measures may be needed to soften localized high-stress zones near the tailgate. High-pressure fluid infusion tests were used at the tailgate corners. Four 4.5-m (15-ft) shallow holes were

Figure 11
Mohr-Coulomb Circles to Demonstrate Effect of Fluid Injection on Rock Strength.

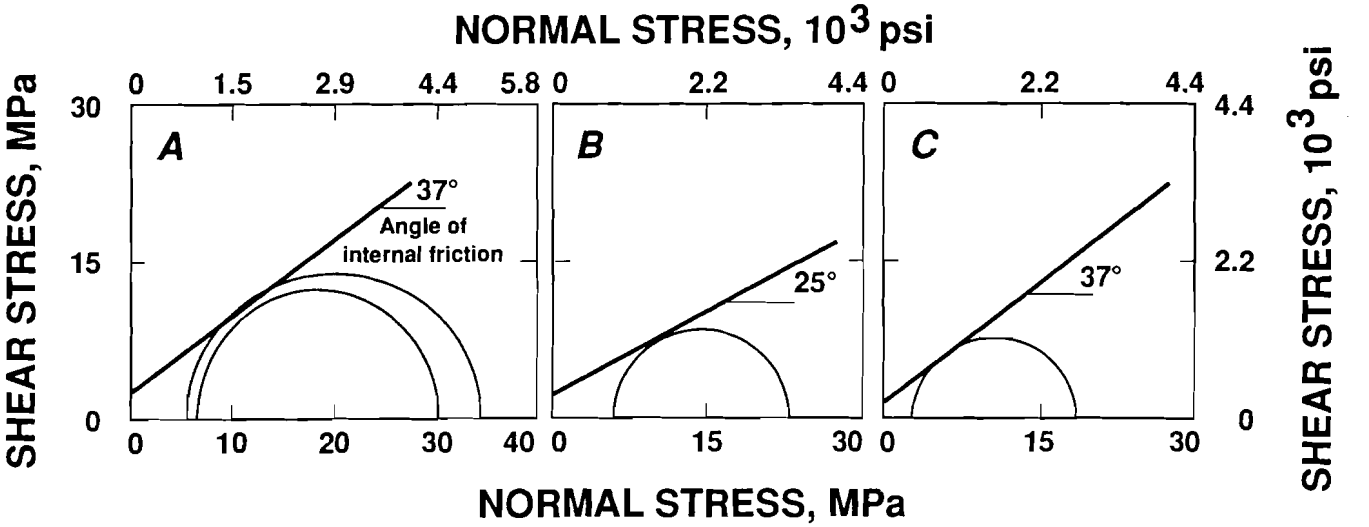

Figure 12
Water Infusion-Hole Pattern of Eastern Coal Mine.

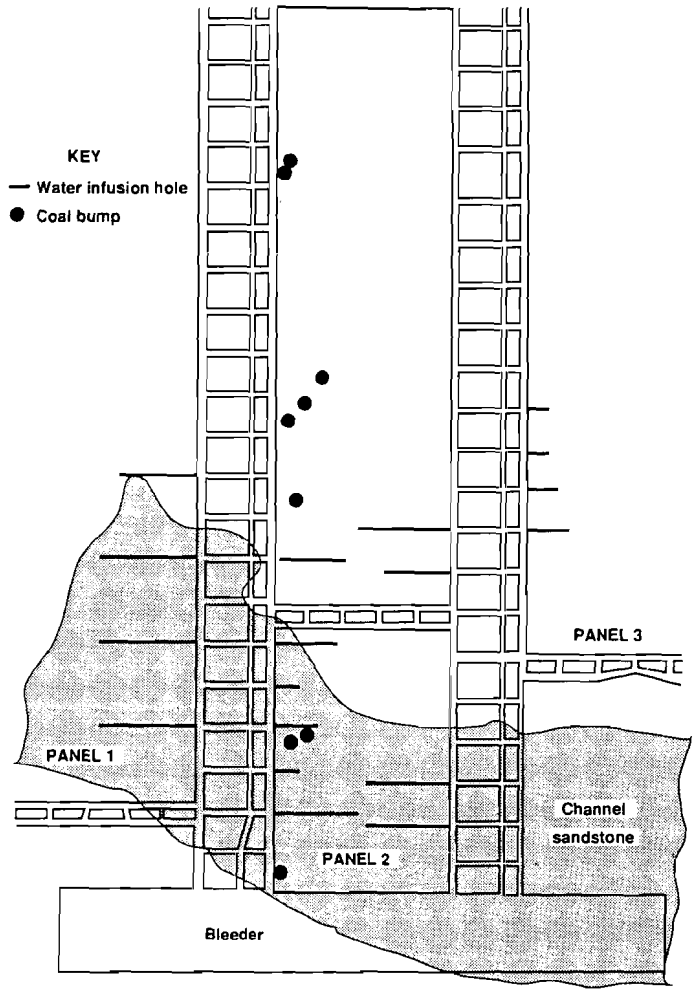

drilled perpendicular to the longwall face from the tailgate corner at 10.6-m (35-ft) spacings. The holes were individually sealed and pressurized at 33 MPa (4,800 psi) with hydraulic fluid, until a minor bump or fracture resulted. Fracturing of the coal surrounding the hole took generally less than 10 to 15 min. However, the drilling and pressurization cycle could only be repeated twice a shift. This limited the advance rate significantly.

AUGER DRILLING

In this method, stress relief is induced by drilling holes into a highly stressed area. Depending on the magnitude of the stress, a hole or series of holes in a coal seam will structurally weaken the seam and cause failure of the coal; stress buildup cannot occur once the coal has failed. Talman (*18*) reported experiences with large-diameter, auger-drilled holes as a stress-relief method. The holes were 15 cm (6 in) in diameter and were maintained not less than 10 m (33 ft) ahead of the face. The drill was positioned approximately 15 m (50 ft) from the face, and barricades were constructed between the drill and the coal face. Violent bumps were triggered during drilling; however, mine personnel were protected by the barricades. In addition, the auger-drilling operation was performed during nonproduction shifts to minimize the number of workers present in the mine.

Long boreholes [15.24 to 24.4 m (50 to 80 ft)] with large diameters [11.4 to 30.5 cm (4.5 to 12 in)] spaced on 4- to 4.57-m (13- to 15-ft) centers have been used to relieve stress at mining faces in foreign mines. The relationship among hole diameter, number of boreholes, and relief depends on conditions at each mine. In the United Kingdom, for example, the borehole length does not exceed 9 m (30 ft), even for a 5- to 7.5-cm (2- to 3-in) diam hole. In France and Belgium, the spacing between holes on the longwall face is 3 to 5 m (10 to 16 ft). In development entries, a fan-shaped pattern with five boreholes is drilled in the direction of advance. The maximum possible borehole diameter depends on the sensitivity of the

seam or the location being drilled; violent occurrences during drilling indicated that smaller diameter holes should be used.

Experience in European coal mines, as well as conclusions from Talman (*18*), has shown that drilling from a distance, even when drilling small-diameter boreholes, is required to drill safely in areas that are highly stressed. Furthermore, two adjacent holes should not be drilled simultaneously.

This method was used at an Eastern mine during a room-and-pillar retreat mining operation (*13*). The holes were drilled using 10-cm (4-in) diam holes. Room convergence and the cutting volume measurements were recorded during drilling. A direct correlation between convergence and cutting volume existed and was repeated by Compoli and others (*13*). The data show that at this mine, high stress levels [4,900 MPa (710,000 psi)] are necessary if the auger drilling for stress reduction is to be effective.

The auger-drilling stress-relief method was analyzed by the USBM in a controlled setting using laboratory tests (*19*). The tests involved drilling holes of different diameters into triaxially loaded cubes to determine what combination of applied stress and drill hole size would produce failure of the cube. The test apparatus consisted of a steel test frame that allowed compressive vertical loading in a hydraulic press while applying confining pressure to all sides using hydraulic flatjacks. The cubes were first subjected to a vertical load of approximately 44,480 N (10,000 lbf), using approximately 3.5-MPa (500-psi) confining pressures. Holes of different diameters were then drilled into the loaded cubes still in the apparatus, after which the vertical load was increased to cause material failure. The results illustrated in figure 13 show a definite relationship between the magnitude of applied stress and the diameter of the drill hole.

Figure 13
Relationship Between Failure Stress Magnitude and Hole Diameter Causing Failure.

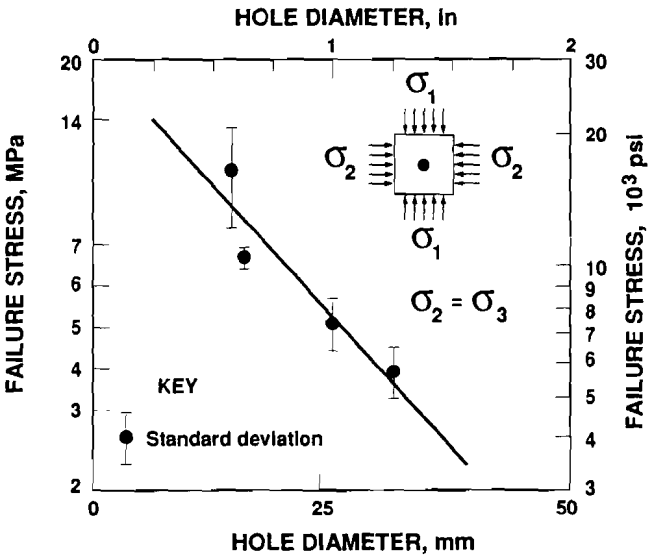

In highly stressed areas, a small drill hole can produce failure and hence relieve stress. In-mine experiences of the relationship between hole diameter and failure are needed to determine the optimum solutions for each site-specific location.

STRESS-RELIEF ANALYSIS USING NUMERICAL MODELING

Computer analysis was used to evaluate stress redistribution patterns resulting from destressing a longwall face. The initial structural analysis used a two-dimensional, finite-element model to provide an understanding of the pressure abutment surrounding the longwall panel and to predict the extent of the weakened zone ahead of the longwall face. Then, to simulate the true stress distribution patterns caused by destressing, further analyses were conducted using a modified version of the MULSIM computer program (*19-20*), which is a three-dimensional, boundary-element method.

Using the location and magnitude of front abutment stresses determined from the finite-element results, a boundary-element baseline model was created to fit these conditions. This model, shown in figure 14, represents a plan view of the longwall panel at the test site. Although the actual panel width was 244 m (800 ft), only 85 m (280 ft) could be modeled within the available grid size. All elements were 3 m (10 ft) wide, and the stiffness of the weakened coal at the face was set at one-half the stiffness of the intact coal.

After the baseline model was constructed, eight other models were developed to analyze the effects of various face destressing patterns. The models ranged from destressing a small isolated area to destressing the entire longwall face.

Results for every destressing model were reduced to graphs of the calculated distribution of vertical stresses in the seam and are shown in figure 15. Cross section A-A′ shows the stress profile on the face, and cross section B-B′ shows the stress profile approximately 4.5 m (15 ft) ahead of the face.

In general, the results showed that destressing only a portion of the face redistributed stresses to adjacent areas that had not been destressed, resulting in higher stress peaks on the face in these areas. The simulated destressing caused maximum stress increases from 1.2 to 1.3 times along A-A′ and from 1.4 to 1.7 times along B-B′.

Figure 14
MULSIM Computer Program Grid Showing Destressing Zones on Face.

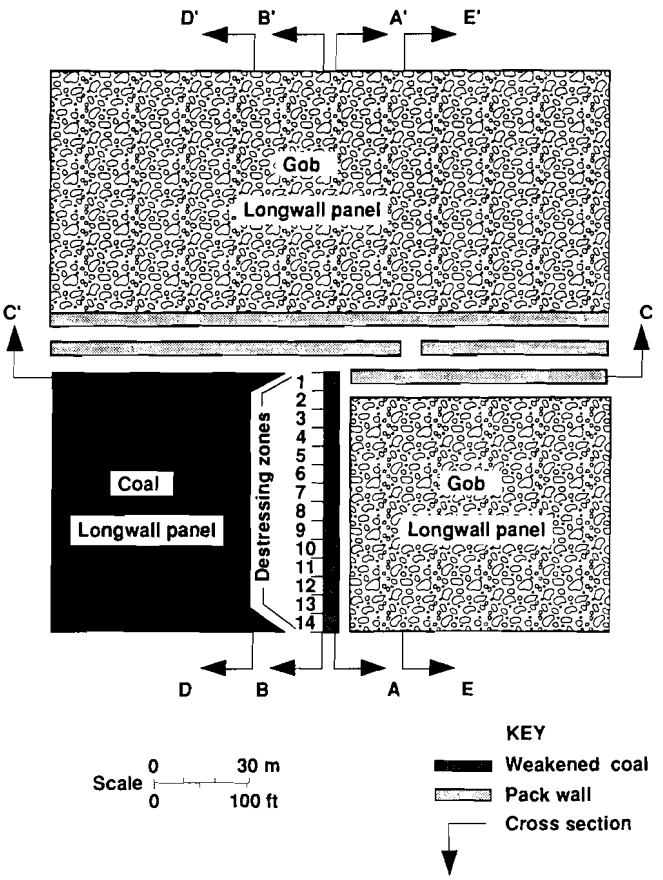

Figure 15
Vertical Stress Profiles for Lines A-A′ and B-B′.

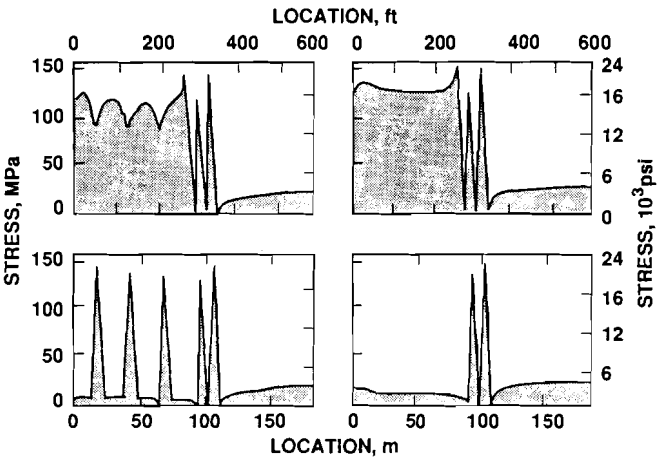

The larger increases for each of the two cross sections occurred primarily in the models in which most of the face had been destressed, leaving smaller regions intact to carry increased stresses.

Destressing the entire face resulted in (1) a stress increase 1.5 times the previous abutment stress 4.5 m (15 ft) *ahead* of the face and (2) a substantial decrease in stress *at* the face. The stress distribution along cross section C-C′ for this model indicates that a stress abutment extended about 30 m (100 ft) adjacent to the tailgate entry in advance of the longwall face. Therefore, it would be desirable to destress the panel for at least 30 m (100 ft) alongside the entry. Any of the three destressing methods discussed might be effective.

Vertical stresses were also analyzed at 30 m (100 ft) ahead of the face (cross section D-D′) and 30 m (100 ft) behind the face (cross section E-E′). No stress changes resulting from destressing were discerned along these cross sections.

In conclusion, dangerous high-stress conditions may occur if portions of the longwall face are destressed and isolated areas are left untreated. Achieving the lowest attainable stress levels adjacent to the face of the panel requires destressing the entire face.

INDUCED FRACTURING IN NONCAVING ROOF STRATA

Strong, competent roof strata contribute to bumps and should be considered in mine design. These types of strata often overhang behind longwall face supports and, in retreat room-and-pillar mining, generate excessive stress on the face by creating a cantilever effect. If caving is inadequate, the abutment zone does not advance with mining, and so stress on the face may increase to a critical points, resulting in a bump. This critical point is reached when stress in the abutment zone exceeds the ability of coal to store strain energy.

As the face advances, the roof may overhang a large span before it caves. Eventually, the cantilever beam becomes so long and stores so much strain energy that it fails (*21-22*). Depending on the overhang length and site-specific conditions, the rate of caving can range from slow to rapid and has a significant impact on the scope and severity of failure. The sudden failure of a massive roof beam is a dynamic event usually accompanied by air blasts, ground stability problems, and major bumps caused by roof shocks (*23*). Air displacement caused by dynamic roof caves may produce air velocities in excess of 90 m/s (200 mi/h) in underground mines and contributes to significant hazardous conditions.

An apparent solution is to induce regular roof caving in strata that do not cave readily. However, caving is complicated by the dangerous working conditions created by the hanging roof, the inaccessibility of the caving zone, the large expanse of rock that must be dealt with, and the inability to forecast the location and length of hanging roof. Hence, although it may be easier to prevent than to remediate a hanging roof condition, the need for prevention cannot easily be foreseen. Consequently, the most efficient induced-caving methods are those that make the best use of limited access to a roof before it hangs.

Control techniques for hanging roofs can be divided into two general classes according to whether the problem roof is suspended prior to first fall or cantilevered after first fall. The USBM has been involved in the evaluation of an induced-caving method for mitigation of violent first-fall hazards. Several methods of induced caving have also been tried in underground coal mines. Objectives ranged from forced and immediate caving to roof weakening and caving only after a substantial increase in unsupported roof span. The success of these methods is greatly affected by local ground control conditions and by the degree to which they are applied.

SETUP ENTRY ROOF BLASTING TO CONTROL FIRST FALL

To control the effects of first falls, roof fracturing techniques can be used to create a vertical free surface that interrupts the continuity of the suspended lower main roof in the startup room between the retreating face and the bleeder pillars. To prevent possible closure that might result from precaving roof deflections, this free surface should be part of an open slot rather than a narrow crack. Of several potential fracturing approaches, roof blasting offers the integration of conventional longwall setup procedures and a high degree of reliability. Rather than a single, large-scale dynamic event, the first fall should consist of several inconsequential falls.

A plan, illustrated in figure 16, was developed to create a fracture along the startup room (setup entry) parallel to the longwall face. Such a fracture should be located as close to the bleeder pillars as is practical; it should be wide enough to permit movement of newly fractured material; and it should be approximately as high as the anticipated caving height (usually two to three times the mining height). Drilling equipment limitations and site-specific conditions may lead to longer or shorter drilling lengths.

A drilling pattern for a blast round tested in an underground mine consisted of two closely spaced rows with holes arranged in a 1:1 staggered pattern. Twenty holes were drilled in two rows. Spacing between holes was 1.2 m (4 ft) and between rows was 0.6 m (2 ft), as shown in figure 17. The first row of holes was spaced 0.6 m

Figure 16
Fracturing Pattern in Startup Room.

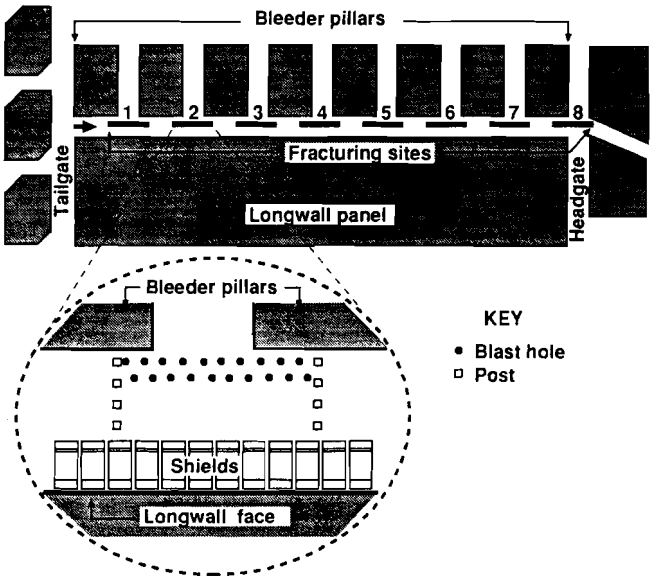

Figure 17
Blast-Hole Pattern in Each Fracturing Site.

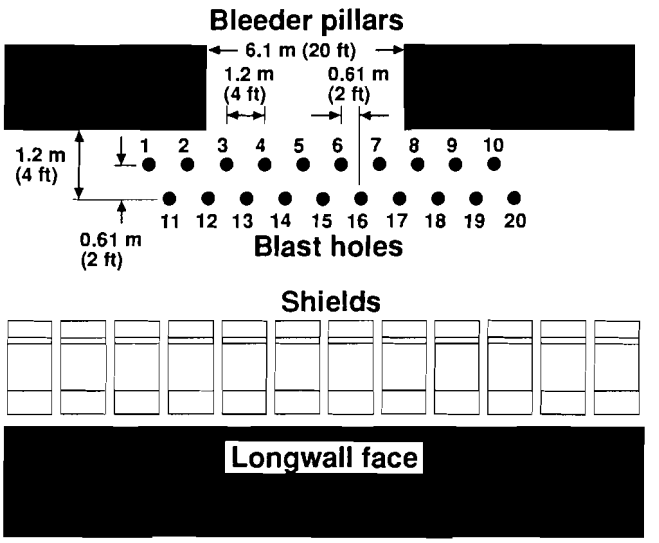

(2 ft) off the bleeder pillar line, and the second row was offset by 1.2 m (4 ft). The blastholes were drilled vertically into the massive sandstone roof strata using conventional roof bolters.

Penetration difficulties and unusual bit wear can be avoided by proper bit selection. Drilling can be conducted between completion of setup entry development and installation of longwall face equipment. Blasthole drilling can alternatively be integrated into the roof bolt drilling

task during setup entry development. Dedicating a double-drill roof bolter and a single operator per shift to the task of drilling 5.5-m (18-ft) blastholes will result in about 32 blastholes per 8-h shift being drilled.

Longwalls may be initiated prior to blasting. Face advance may provide more space for casting blasted material. In addition, separation of an immediate shale roof from an overlying massive sandstone main roof may benefit by an increased roof span. However, threat of immediate roof caving may require artificial support in the form of cribbing or posts.

Depending on the mine plan and permit approvals, the holes may either be loaded and shot together or in separate rounds across the full length of the setup entry, as shown in figure 17. If shot in separate rounds, a span of unblasted roof should be left between rounds, and this span should be supported with cribbing or posts to ensure safe working conditions for the next round. Working away from side abutment pressures, multiple-blast rounds should proceed from the tailgate to the headgate side of the setup entry. Each designated hole is loaded with permissible explosive, cap and wires, and stemming. The blast rounds should be shot with delays between successive holes according to MSHA requirements.

During blast detonations, shields can be at full setting pressure. Shock loads resulting from blasting the small-diameter holes do not pose a significant threat to the shields if there is a proper delay in sequencing. Each shot can be examined as soon as ventilation permits by visual inspection through the shields. The blasted rock should cave behind the shields. If the blast round has been designed correctly, overbreak of immediate roof and caving into the pan lines should not occur. However, temporary stoppings at the back of the bleeder section may be blown down after blasting.

INDUCED CAVING BY LONG-HOLE BLASTING

Long-hole blasting is a technique adapted from sublevel stoping and block caving in underground metal mining. Blastholes are drilled from tailgate entries in sufficient numbers and density so that the rock mass will be weakened after it is blasted. Fan, parallel holes, and radiating blast patterns are among several options. In addition to blasting from gate roads, long-hole blasting can be done at some mines from the face area, the surface, or from overlying workings. The difference in fracturing capacity between conventional and permissible explosives should be considered.

Mine stress conditions at the time of drilling and blasting have a great effect on the success of this method. Ahead of the face abutment, holes may be drilled in less altered rock, but blast fragmentation may be less effective owing to greater confinement. Within the abutment zone, high stress may cause excessive closure of blast holes during drilling and "dead compression" of explosives after loading. Along the face, drilling and blasting are greatly constrained by production requirements and roof supports. Over the gob, roof instability may cause problems during blasting. Differential horizontal movement of roof strata between drilling and blasting may cause misalignment of strata, resulting in unusable blastholes. The time interval between explosive loading and detonation presents the risk that untimely natural caving may result in a situation where undetonated explosives and detonators lie unconfined and irretrievable in the gob.

In response to potential implementation difficulties, some long-hole practices have gained greater acceptance. Of these, practices, blasting a line of holes drilled at a 30° angle between face supports is the most effective, and repeated blasts of this type in conjunction with face moves between blasts increases the prospect of favorable results.

This method was applied in a Polish mine to initiate caving behind the shields. At this mine, depending on roof thickness and rock physical properties, hole specifications varied as follows:

- Hole length = 4 to 7 m (13 to 23 ft).
- Hole diameter = 4 cm (1.6 in).
- Hole angle = 60° from horizontal.
- Horizontal hole spacing = 6 to 10 m (20 to 33 ft).
- Distance from blast hole canopy = 0.61 m (2 ft).

OTHER METHODS

Other techniques, such as hydraulic fracturing in the roof and fluid-saturation weakening, may be used in certain mines. Hydraulic fracturing offers a potential means of reducing drilling requirements for induced caving through generation of far-reaching fractures from a single borehole. However, with hydraulic fracturing, it is difficult to control the extent of the fracture area; fracturing too large an area may create, rather than reduce, ground control problems. Water saturation techniques can induce caving by reducing the strength of coal-measure rock. Unfortunately, massive sandstone roof strata cannot be easily saturated because of its low permeability. Another method is to orient the longwall 30° to the major fracture zone in the strong roof member. This allows the roof to break through existing fractures.

CONCLUSIONS

The drilling-yield method is an effective technique that can be rapidly and inexpensively used to locate abutment zones prior to destressing. This method involves drilling a small-diameter hole into the coal seam and recording the volume of drill cuttings and other pertinent information. Because experiences with this method are limited, predetermined drilling patterns should be developed. The hazard of a coal bump can be reduced by properly implementing volley firing, hydraulic fracturing, or auger drilling. A complete discussion of several experiences using these methods was presented and can be used as a guideline for assisting a mine engineer in determining which distressing method is not applicable in a given mine. In-mine experiences and computer analyses also indicate that incorrect use of stress-relief methods may actually increase the potential for a coal bump at the face. Although hydraulic fracturing and fluid infusion have been used at the face, these techniques are time consuming and are more useful ahead of the face in the tailgate entries.

The effects of first falls on structural instability may be reduced by creating a fracture parallel to the longwall face before mining. Although these methods have not been tested at many mines, the information presented in this paper may assist a mining engineer in designing and reducing first-fall effects.

REFERENCES

1. Haramy, K. H., and J. P. McDonnell. Causes and Control of Coal Mine Bumps. USBM RI 9225, 1988, 35 pp.

2. Wong, I. G. Mining-Induced Earthquakes in the Book Cliffs and Eastern Wasatch Plateau, Utah, U.S.A. Int. J. Rock Mech. Min. Sci. & Geomech. Abstr., v. 22, No. 4, 1985, pp. 263-270.

3. Dunrud, C. R., and F. W. Osterwald. Seismic Study of Coal Mine Bumps, Carbon and Emery Counties, Utah. Trans., Soc. Min. Eng. AIME, v. 232, No. 2, 1995, pp. 174-182.

4. Iannacchione, A. T., and M. J. DeMarco. Optimum Mine Designs to Minimize Coal Bumps: A Review of Past and Present U.S. Practices. Paper in Proceedings of the New Technology and Mine Health and Safety. Soc. Min. Eng., 1992, pp. 235-247.

5. Gibowicz, S. J. The Mechanism of Seismic Events Induced By Mining: A Review. Paper in Rockburst and Seismicity in Mines, Proceeeding of the 2nd International Symposium on Rockbursts and Seismicity in Mines, ed. C. Fairhurst (Univ. MN, Minneapolis, MN, June 8-10, 1988). Balkema, 1990, pp 2-27.

6. Chu, K., G. Ma, B. Lju, and D. Tja. Rock Bursts and Provisions for Preventing Them in the Chinese People's Republic. Paper in Proceedings of the 7th "Landertreffen." Int. Bur for Rock Mech. Leipzig, German Democratic Republic, Translation No. 14, 1965, 8 pp.

7. McKee, M. E., and W. J. Arabasz. Microearthquake Studies Across the Basin and Range-Colorado Plateau in Central Utah. Paper in Overthrust Belt of Utah, ed. by D. L. Nelson (Proc., Symp. and Field Conf., 1982). UT Geol. Assoc. Publ. 10, 1986, pp. 137-149.

8. Kusnir N. J., D. P. Ashwin, and A. G. Bradley. Mining Induced Seismicity in the North Staffordshire Coalfield, England. Int. J. Rock Mech. Min. Sci. & Geomech. Abstr., v. 17, 1980, pp. 45-55.

9. Dubinski, J. Characteristics of Seismicity Induced by Mining Operations in the Upper Silesian Coal Field. Paper in Proceedings of the 18th Czechoslovakia-Poland Conference on Geophysics, v. 83, 1990, pp. 115-127.

10. Neyman, B., A. Szecowka, and W. Zuberek. Effective Methods for Fighting Rock Bursts in Polish Collieries. Paper in 5th International Strata Control Conference (London, Eng., 1972). Nat. Coal Board, preprint, 1972, 9 pp.

11. Obert, L., and W. Duvall. Rock Mechanics and Design of Structures in Rock. Wiley, 1967, 650 pp.

12. McDonnell, J. P., and K. Y. Haramy. Probe-Hole Drilling: High-Stress Detection in Coal. USBM IC 9179, 1988, 11 pp.

13. Campoli, A. A., D. C. Oyler, and F. E. Chase. Performance of a Novel Bump Control Pillar Extraction Techniques During Room-and-Pillar Retreat Coal Mining. USBM RI 9240, 1990, 40 pp.

14. Sikora, W., A. Kidybinski, and K. Saltysek. Designing of Hard Roof-Rock Destressing Systems for Safe Warning of Rock Burst Prone Coal Seams. Central Min. Inst., Katowice, Poland, 1978, 26 pp.

15. Maleki, H. In Situ Pillar Strength and Failure Mechanisms for U.S. Coal Seams. Paper in Proceedings of the Workshop on Coal Pillar Mechanics and Design, comp. by A. T. Iannacchione, C. Mark, R. C. Repsher, R. J. Tuchman, and C. C. Jones (Santa Fe, NM, June 7, 1992). USBM IC 9315, 1992, pp. 73-77.

16. Maleki, H. Coal Bump Mechanics for U.S. Coal Mines. Paper in Mechanics and Mitigation of Violent Failure in Coal and Hard-Rock Mines. USBM Spec. Publ. 01-95, 1995, pp. 5-25.

17. Cervik, J., A. Sainato, and M. Deul. Water Infusion of Coal Beds for Methane and Dust Control. USBM RI 8241, 1977, 27 pp.

18. Talman, W. G., and J. L. Shrooder. Control of Mountain Bumps in the Pocahontas No. 4 Seam. Trans., Soc. Min. Eng. AIME, v. 211, 1958, pp. 888-891.

19. Haramy, K., J. McDonnell, and L. Beckett. Stress Relief to Control Coal Bursts. Soc. Min. Eng. preprint 87-57, 1987, 12 pp.

20. Kripakov, N. P., L. A. Beckett, and D. A. Donato. Loading on Mine Structures Influenced by Multiple Seam Interactions. Paper in Proceedings of the International Symposium on Application of Rock Characterization Techniques in Mine Design, ed. by M. Karmis (New Orleans, LA, Mar. 1986). Soc. Min. Eng. AIME, 1986, pp. 225-235.

21. Haramy, K. Y., J. A. Magers, and J. P. McDonnell. Mining Under Strong Roof. Paper in Proceedings of the 7th Conference on Ground Control in Mining, ed. by S. S. Peng (WV Univ., Morgantown, WV, Aug. 10, 1988). Dep. Min. Eng., WV Univ., 1988, pp. 179-194.

22. Wu, X., and M. G. Karafakis. Mathematical Modeling of Strong Roof Bed in Longwall Mining. Paper in Proceedings of the 12th Conference on Ground Control in Mining, ed. by S. S. Peng (WV Univ., Morgantown, WV, Aug. 3-5, 1993). Dep. Min. Eng., WV Univ., 1993, pp. 175-184.

23. Brady, B. T., and K. Y. Haramy. High Amplitude Stress Wave Generation and Damage Induced by Roof Caving in Mines. Paper in Rock Mechanics Models and Measurements Challenges from the Industry. Proceedings of the 1st North American Rock Mechanics Symposium, ed. by P. P. Nelson and S. E. Laubach (Univ. TX at Austin, June 1994). Balkema, 1994, pp. 1033-1040.

GEOLOGICAL FACTORS IN ROCK BURSTS IN THE COEUR D'ALENE MINING DISTRICT: STRUCTURE

By B. G. White,[1] J. K. Whyatt,[2] and D. F. Scott[1]

ABSTRACT

Research conducted by the U.S. Bureau of Mines indicates that both rock bursts and nonviolent wall rock deformation in the Coeur d'Alene Mining District are strongly controlled by preexisting structures. These structures include sheared, steeply dipping bedding; gouge-filled faults; and variably oriented joints. The locations and extent of burst damage are strongly influenced by the orientation of mine openings with respect to these structures.

Burst damage related to preexisting structures results primarily from (1) buckling of narrow, tabular rock masses into mine openings and (2) fault-slip on bedding planes or preexisting faults. Buckling-type failures occur when development openings intersect bedding, faults, or joints at acute angles. Fault-slip failures most typically occur along bedding or fault planes that intersect veins near pillar-stope margins as wall rock moves into mine openings.

Rock-burst damage and related ground support problems may be reduced by (1) planning development openings so they cut bedding, faults, and joints at angles greater than 50°, (2) giving extra attention to ground support in situations where unfavorable geometries cannot be avoided, and (3) destressing or eliminating pillars.

INTRODUCTION

To reduce the risk of injury and death from rock bursts, the U.S. Bureau of Mines has conducted rock-burst research in the Coeur d'Alene Mining District for more than 40 years. Much of this research has addressed the seismic aspects of rock bursts. Such work has made it increasingly evident that rock bursts are often associated with specific geologic features such as faults. The present research has been directed toward better understanding the mechanical influence of geology on the generation of rock bursts.

The Coeur d'Alene Mining District (figure 1) has produced more than 110,000,000 t of high-grade lead-zinc-silver ore in little more than a century of nearly continuous operation. Only two mines are currently active. One is the Sunshine Mine, which has produced more than 8,500 million grams of silver from numerous veins. The second is the Lucky Friday Mine, a lead-silver mine with minor zinc production. Recently, reopening the silver-rich Galena Mine, which has been temporarily closed because of low silver prices, has been under consideration. All three of these mines have experienced rock bursts. In particular, the Lucky Friday Mine has experienced abundant low-level seismicity and several rock bursts each year, which have caused damage to major haulageways. Conclusions presented in this paper are strongly influenced by observations made at this mine.

Once mining in the district had progressed to depths of more than 800 m, rock bursts became fairly common. Their frequency has usually been attributed to the presence of hard, brittle quartzite or to the high horizontal stresses documented by various researchers. We believe each of these factors is locally important in rock-burst and general ground-control problems. However, we also believe most rock bursts and other ground failures in the

[1]Geologist.
[2]Mining engineer.
Spokane Research Center, U.S. Bureau of Mines, Spokane, WA.

Figure 1
Selected Major Faults and Mines of Coeur d'Alene Mining District.

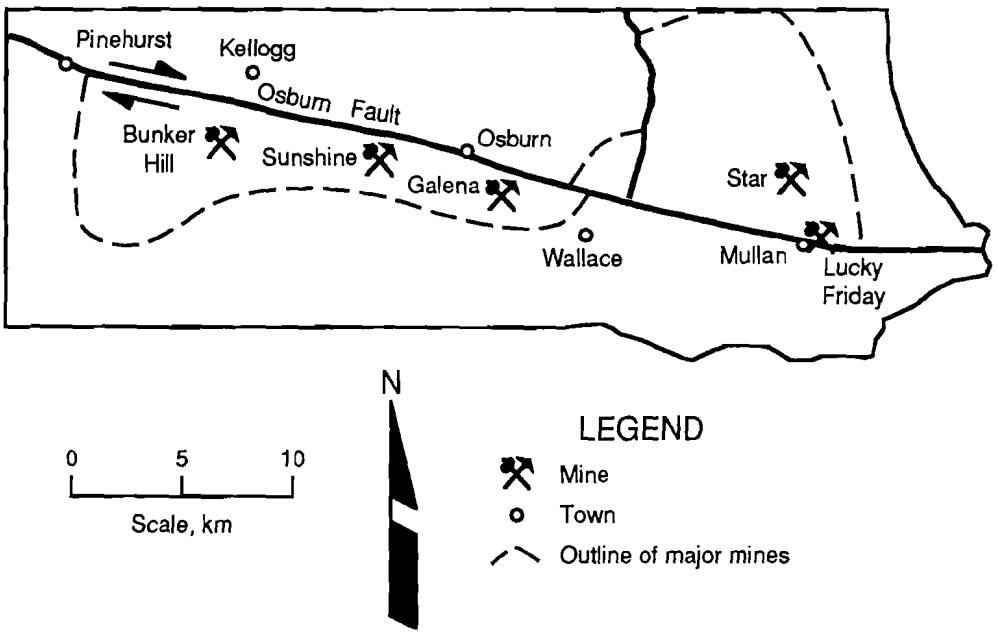

Note that Osburn Fault offsets productive parts of district (dashed lines).

district result directly from the presence of preexisting, planar rock discontinuities. These discontinuities are primarily steeply dipping beds and faults, but locally include closely spaced joints. All of these structures promote failure under less stress than would be required if the host rocks were unfractured and unlayered.

In this paper, we emphasize the influence of these structures on rock bursts and ground-control problems. Understanding the specific mechanics of ground failure caused by such structures should increase the effectiveness of ground-control measures. We conclude with specific suggestions that may reduce rock-burst hazards.

GEOLOGY

HOST ROCK

Host rocks of Coeur d'Alene ore bodies are slightly metamorphosed sedimentary strata of the Precambrian-aged Belt Supergroup (Hobbs and others, 1965). These strata are characterized by great thicknesses of relatively uniform, thin-bedded, fine-grained rock types. Most formations contain only silt- and clay-sized original sediment, now siltite-argillite. A few Belt formations important as ore hosts are characterized by original sand, now metamorphosed to quartzite. However, thick-bedded quartzitic strata of the district are often thinly laminated and contain numerous thin interbeds of argillite. These bedding features greatly influence the mechanical response of quartzite and its role in rock bursts and other ground-control problems (Scott, 1993).

All district production is closely associated with quartzite. Most of this production has been hosted by the Revett Formation, which is particularly characterized by the presence of quartzite layers (Hobbs and others, 1965). At the Lucky Friday Mine, rock bursts have been frequent in quartzite-dominated strata of upper and lower members of the Revett (Blake and Cuvelier, 1990; Scott, 1993). In contrast, bursts were uncommon when mining took place in the middle Revett member, which contains mostly softer, weaker, siltite-argillite strata. Elsewhere in the district, rock bursts are also commonly associated with quartzite.

STRUCTURE

The long history of diverse tectonism in the Coeur d'Alene district[3] began with the formation of tight, large-scale folds that created uniformly steep bedding dips on the scale of individual mines. The steeply dipping vein-type ore bodies postdate these folds. In addition, post-mineralization tectonism in the form of normal faults and strike-slip faults has been intense. The younger tectonism also caused extensive shearing along steeply dipping argillite interbeds and locally intense fracturing of quartzite.

Most Coeur d'Alene ore bodies trend west-northwest, roughly parallel to the strikes of faults and bedding. Some veins cut directly across these usual trends and directly truncate bedding. The Lucky Friday ore body is unusual in that the Lucky Friday vein follows the trend of beds that have been locally reoriented to northeast strikes by prior tectonism. Consequently, the vein has the more typical habit of lying relatively parallel to bedding strike, despite its northeasterly trend.

ROCK BURST TYPES

In this paper, a rock burst is considered to be a violent expulsion of highly stressed rock into a mine opening. However, the authors recognize that the term is also used in a more practical sense to include any mining-induced seismic event that causes damage to openings.

Three basic types of rock bursts are known to occur in district mines. Hedley (1992) distinguishes these as strain bursts, pillar bursts, and fault-slip bursts. At the Lucky Friday, and probably at other mines, specific geologic and geometric aspects of a burst site influence the type of burst that occurs.

1. *Strain bursts* result from the concentration of stress and high stress differentials near the surfaces of openings. These bursts typically affect development openings such as crosscuts, raises, and initial cuts in overhand stopes. Shafts and raise boreholes are also damaged by strain bursts. Similar deformation patterns develop in small-diameter drill holes, such as diamond drill holes.

Strain bursts are commonly thought to represent failure at the immediate surface of a mine opening. However, the failure of a surficial layer of rock exposes yet another surface, which may fail and expose a third layer, and so on. A progressive series of surface-type failures to great depth in the rock may ultimately involve a substantial volume of rock. If such deformation at a given site occurred almost instantaneously, the result would be a fairly massive strain burst. Consequently, we regard strain bursts as bursts that include deformation that penetrates to some depth beneath the initial surface of an opening, to several meters or more in the case of an extensive strain burst.

The most characteristic strain bursts at the Lucky Friday Mine affect ribs and rib-back and floor-back junctures (figure 2). Rock bursts that affect ribs are generally thought to characterize mining districts with high vertical stress loading, rather than horizontal loading, as is the case in the Coeur d'Alene district. This observation emphasizes that factors other than in situ stress often influence rock bursts.

2. *Pillar bursts* are caused by the instantaneous crushing of pillars. In the Coeur d'Alene district, by the time pillars have been mined to heights that would make them unstable, about 20 m or less, the pillars have commonly been destressed by drilling and blasting. Destress blasting of pillars has been used successfully in the district for more than 20 years. However, in highly stressed pillars, destress drilling has occasionally proven impossible because of the difficulty of keeping the drill holes open. In these cases, abandonment of the pillars has sometimes been the only reasonable recourse.

3. *Fault-slip bursts* have been documented in the district by distinctive seismic signatures and through interpretations of burst damage and local geology (Scott, 1993; Williams and others, 1992). Damage caused by fault-slip bursts involves rock being heaved into mine openings and typically accompanies a fairly large seismic event. Such events are frequently centered some distance from the damage site.

CONCEPTS OF ROCK BURSTING: MASSIVE ROCK

Nearly all rock bursts at the Lucky Friday Mine seem directly controlled by preexisting planes of weakness represented by bedding, faults, and joints. However, to fully appreciate the importance of these structures on development of bursts, a review of rock burst mechanisms in rock where such structures are absent or ineffective is useful. The immediate discussion is most relevant to

[3]A detailed discussion of this topic will be published early in 1995 in the proceedings of Belt Symposium III in the paper, "Diverse Tectonism in the Coeur d'Alene Mining District, Idaho," by B. G. White.

Figure 2
Rib Failures at Lucky Friday Mine.

A, Typical burst damage; note undamaged back and rock bolts and mesh displaced from ribs. *B*, Burst-modified shape of lateral from original rectangular cross-section. Damage affected upper left and lower right ribs.

strain bursts and pillar bursts. Slip bursts will be considered separately.

In massive rocks, both strain bursts and pillar bursts result from high in situ stress that is locally concentrated and reoriented around mine openings. These two burst types are fundamentally identical in their failure mechanism. They differ primarily in scale, the result of the mine geometries involved and the effect of these geometries on the ability of surrounding wall rock to contribute the energy that ultimately drives the burst.

It has been suggested (Fairhurst and Cook, 1966; Cook, 1966) that bursting involves two separate, independent mechanisms. Observations at the Lucky Friday support this concept. These two fundamental mechanisms are thought to operate whether failure is instantaneous, producing rock bursts, or gradual, causing undramatic opening failures.

1. First, the involved rock develops discontinuous fractures parallel to the surfaces of the openings. Affected mine openings include crosscuts, drifts, shafts, raises, stopes, and drill holes. If fracturing is not extreme and fractured rock remains in place, significant ground-support problems may not arise. However, if conditions are such that these fractures continue to develop, they begin to separate the wall rock into slabs that approximately parallel the surfaces of the opening.

2. Second, the slabs ultimately deform by buckling into the opening. Buckling, in turn, causes brittle rock to fracture. This failure mode is active when the discontinuous fractures develop to such an extent that the tabular rock layers formed can no longer support load and become unstable. According to descriptions of buckling behavior found in standard references on material strength (e.g., Timoshenko and Gere, 1961), this point is reached at a certain ratio of thickness to length for the load and material involved. While gradual buckling may only cause nuisance damage, instantaneous buckling may represent a rock burst.

The elastic strain energy that exists within individual slabs when buckling deformation is initiated is regarded as inadequate to drive violent failure of the slab (Blake, 1972; Hedley, 1992). To generate a burst, elastic energy must be supplied from the rock mass surrounding the buckling rock. This extra contribution of elastic energy has been called "following load" (e.g., Fairhurst, 1986).

A fundamental difference between pillar bursts and strain bursts lies in the relative capability of the surrounding wall rock to supply following load. This can be illustrated by first comparing these types of bursts with a simpler case. For example, if only a single unstable slab were to develop adjacent to a mine opening (figure 3*A*), attachment of the ends of the slab to adjoining, rigid wall rock would limit the capability of the surrounding rock mass to contribute elastic energy. The adjoining rock is regarded as "stiff" relative to the deforming slab. The surface rock layer could detach itself or spall, but such an event would necessarily be relatively low in energy.

At the other extreme, pillar bursts involve complete pillar failure. Pillar bursts apparently develop from the formation and essentially simultaneous buckling of many unstable slabs throughout the pillar (figure 3*B*). Here, stored elastic energy from a large volume of surrounding wall rock is released by initiation of buckling. This enables elastic strain energy from this large volume of a rock mass to be directed to the bursting pillar. An extensive strain burst involving development of multiple slabs that buckle essentially simultaneously (figure 3*C*) represents an intermediate case, and stored elastic energy from a moderate volume of a surrounding rock mass becomes available to drive the burst.

CONCEPTS OF ROCK BURSTING: LAYERED ROCK

Consideration of rock bursts in massive rock highlights the contrast in rock behavior in the Coeur d'Alene district that results from the presence of preexisting structures. Wall rock in this district is everywhere layered as a result of its sedimentary origin. In all mines, these layers mainly dip steeply, the product of tight, large-scale folding during the early tectonic history of the district (Hobbs and others, 1965). Subsequent tectonism has split apart many of these sedimentary layers. Even thick, relatively homogeneous beds are internally layered on a fine scale and have been subjected to partial mechanical delamination as a result of tectonism. Wall rock and ribs are thus inherently separated into steeply dipping slabs of variable thickness. As a result, the mechanism of ground failure is reduced to a single stage of buckling-type deformation.

In addition to nearly ubiquitous, steeply dipping sedimentary layers, steeply dipping, gouge-filled faults are common in all mines of the district. Where these structures are subparallel to ribs and lie a short distance behind the surface of a rib, they form narrow, steeply dipping columns that are frequently involved in bursts.

The pervasive layering of wall rocks has two direct effects on ground support that greatly contribute to rock bursts and ground-support problems in general. These two factors may be most responsible for the high incidence of rock bursts in the district.

Figure 3
Mechanisms of Buckling-Type Failures.

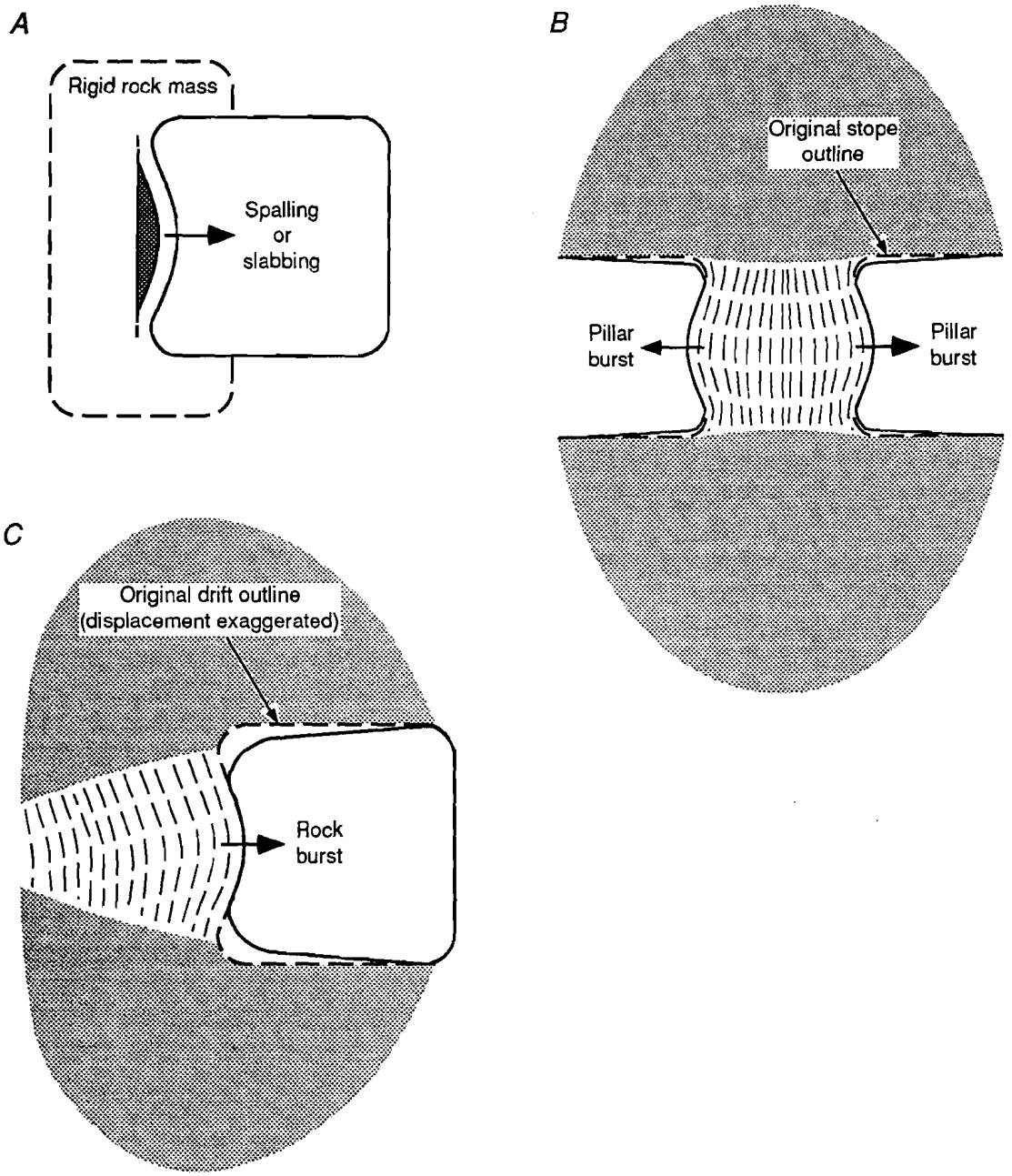

A, Single slab failure; *B*, pillar failure; *C*, extensive strain burst failure. Shaded areas identify inferred source of elastic strain energy that drives bursting. Bending of rock slabs is exaggerated; brittle deformation is expected before bending reaches the extent shown.

1. Less stress is required to buckle preexisting layers of rock than to split massive, unfractured rock of the same composition into comparable layers. This can be illustrated by reference to general equations that describe critical stress necessary to cause buckling as a function of thickness divided by length (e.g., Timoshenko and Gere, 1961). For example, the critical stress necessary to cause a rock layer to buckle approaches 0 as thickness approaches 0. Thus, unbolted, thinly layered, near-vertical-dipping strata should be easily deformed by buckling at relatively shallow depths because of the load generated by the overlying rock alone. Closely spaced, preexisting joints are also locally involved in rock bursts for this reason.

2. Faults and bedding planes physically isolate buckling layers from the adjoining rock mass. Slip along these planes is unimpeded by attachment to the rock mass on the opposite side of the structure (figures 4 and 5). This enables elastic strain energy from a fairly large volume of a surrounding rock mass to actively supply following load to the deforming rock. We define this as a *fault-bounded strain burst*. We believe the capability of rock to fail by this mechanism is a major reason for the high incidence of rock bursts in district mines. Fault-bounded strain bursts in steeply dipping structures also account for the common occurrence of rib bursts in the district, which would not ordinarily be expected in mines where the greatest tectonic loading is horizontal.

Fault-bounded strain bursts, like ordinary strain bursts and pillar bursts, derive their relatively large energies from elastic strain energy contributed by the surrounding rock mass. We speculate that the rock mass can deliver this energy from the greatest volume of rock when the affected

Figure 4
Mechanism of Fault-Bounded Strain Burst.

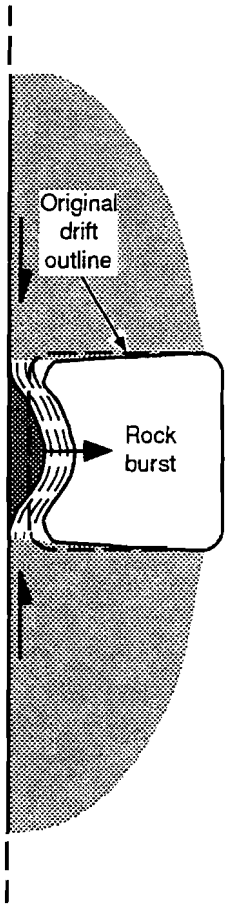

Bedding or fault plane physically separates rock mass involved in burst from adjacent portions of rock mass. Slip along these planes enables relatively large amounts of elastic strain energy to be supplied to relatively small volumes of bursting rock. Compare to figure 3*A*.

Figure 5
Fault-Bounded Strain Burst.

Burst damage in Lucky Friday 5400-01 haulage ramp. Plates have been stripped from roof bolts by downward impulse and localized back failure. Most expelled rock came from narrow rock column in right rib formed between rib and fault immediately behind original surface of rib. It is not known whether these fractures formed during or preceded burst event.

layers nearly parallel the longest dimension of an available opening. As a result, the stress direction that is most effective in causing a burst is relatively perpendicular to drifts, crosscuts, or other linear openings. Where structures dip steeply, bursts that occur in drifts and crosscuts inevitably affect ribs, a result that would ordinarily be interpreted as indicating that greatest loading is steep. Instead, such bursts may primarily reflect the orientation of the long dimension of the opening in relation to planar features.

FACTORS THAT PROMOTE FAULT-BOUNDED STRAIN BURSTS

Several factors greatly increase the likelihood of fault-bounded strain bursts. For example, where mine openings cross strata or faults at a low angle, the probability increases that the opening will expose layers that are at a critical level of stress. Some of these layers are also likely to be "fault-bounded" along sheared bedding planes or actual faults and therefore to be vulnerable to the fault-bounded strain burst mechanism. In addition, steeply dipping strata that are truncated at low angles by drifts and that are mechanically detached from adjacent strata by gouge-filled argillite bedding planes have greater effective spans across openings than does competent unstratified rock. These conditions amplify the load parallel to the surface where these strata form ribs. Strata that are cut off by a fault on one side of an opening are also thought to acquire disproportionately high loads on the opposite side of the opening. Finally, because quartzite has a higher elastic modulus than argillite, an equal amount of layer-parallel strain causes disproportionately higher load in quartzite layers (and correspondingly less load in adjacent argillite beds). This partially accounts for the higher incidence of rock bursts observed in quartzite.

Although ground failure resulting from buckling ribs is strongly favored when the affected layers are nearly parallel to the ribs, we have observed instances of this type of deformation at locations where bedding strikes were as great as 50° from the trend of subhorizontal development openings and where bedding dips were as low as 50°. In these cases, ground failures have tended to be gradual, resulting in progressive breakup of shotcrete, loosening of rock bolts, and localized rib collapse (figure 6). These observations emphasize the effectiveness of preexisting structures on promoting ground support failures.

As noted, fault-bounded strain bursts affect horizontal openings, such as crosscuts and drifts. However, steep openings, such as shafts, raises, and raisebore holes, are particularly susceptible to this type of failure. Because faults and strata in district mines generally dip steeply, steeply oriented openings generally lie at a low angle to these structures. In addition, the common west-northwesterly strikes of steeply dipping strata and faults approximate the direction of greatest tectonic loading. Thus, the direction of greatest stress also coincides with the direction of greatest following load potential. At the Lucky Friday Mine, ore passes where these relationships are evident have been sites of especially bothersome ground-control problems.

Figure 6
Buckling Failure in Rib.

Gradual buckling-type deformation in Lucky Friday 5570-07 ramp. Deformed layers have separated from intact layers by slip along bedding plane. Beds strike 50° from rib and dip 70° to the right. Rock layers have broken into short pieces.

BUCKLING STABILITY OF SLABS AND EFFECTIVENESS OF ROCK BOLTS

The critical stress necessary to cause buckling failure of narrow slabs is actually proportional to the square of thickness divided by length (e.g., Timoshenko and Gere, 1961). The dependence of critical stress on the square of thickness divided by length partially accounts for the effectiveness of rock bolts as ground support, in that bolts reduce the effective length of slabs that could potentially fail by buckling. While bolts that bisect slabs reduce length by one-half, the critical stress necessary to cause buckling increases by a factor of four. Experience in deep South African mines (Wagner and Godfrey, 1976) has led to several standard bolting guidelines that take advantage of this concept for burst-prone ground. These are (1) bolt length in ribs should equal or exceed one-half the height of the opening and (2) bolt spacings should not exceed one-half the length of the bolt. Bolts used in such a manner clamp rock together to produce units of greater total thickness and reduce the effective length of thin slabs.

We reason that intact slabs are able to support significantly greater loads than partially buckled slabs. Similarly, we infer that greater bolt strength is required to restrain a partially buckled slab than is required to prevent buckling from being initiated. Consequently, it would be best to prevent the start of buckling failure by bolting slabbed rock solidly at the outset (Cook, 1966). Highly rigid (high-modulus) rock bolts should be most effective in preventing the initiation of buckling-type failures (Cook, 1966). However, once buckling has begun, bolts that resist breaking are probably most effective (Wagner and Godfrey, 1976). Yieldable bolts, such as the South African cone bolt, may be particularly well adapted for such situations (Ortlepp, 1992). In many cases, a combination of high-modulus rigid bolts and yieldable bolts may prevent most problems.

Since buckling-type deformation requires the existence of slabs, it follows that bolting practices should emphasize containment of these slabs. Bolts are likely to be most effective where they cross bedding or other tabular structures at nearly right angles. Such an orientation maximizes the component of clamping stress and also penetrates the greatest thicknesses of rock layers. This suggests that bolts should be installed more nearly perpendicular to rock layers than to mine surfaces or at some intermediate, compromise angle.

FAULT-SLIP BURSTS

Burst damage in the district sometimes results from slip on faults or other structures, but evidence for such slip is rarely observed directly (Williams and others, 1992; Scott, 1993). However, hypocenters frequently approximate the locations of known faults, and seismic data support the fault-slip interpretation.

Major damage caused by these events occurs primarily where slip surfaces intersect mine openings. Such damage appears to result from rock being heaved from the surfaces of openings. It is also thought to result when seismic waves from fault-slip events encounter openings. Such damage is thought to especially affect ground that is already highly fractured, usually as a result of prior tectonic deformation, so such ground is already unstable.

Fault-slip bursts at the Lucky Friday have often been associated with pillar or stope margins. This suggests that stoping may increase shear stress on preexisting faults and argillite interbeds or may promote slip by decreasing normal stress on fault planes. Such slippage is commonly interpreted as tending to close mined-out stopes.

Much low-level seismicity and shotcrete damage in Lucky Friday development ramps appear to reflect nearly continuous movements along bedding planes in the immediate footwall of the Lucky Friday vein. Such movements apparently represent progressive accommodation of the wall rock to mining. These movements also suggest that slip-type seismic events are probably inevitable. Consistent ground-support measures are needed that are adequate to contain the most commonly occurring types of damage.

Large fault-slip-type events in the Richter magnitude range of 2 to 4 have been documented in the hanging wall of the Lucky Friday vein. These events typically have hypocenters 30 to 70 m from the nearest mine workings. Such events seem best interpreted as indicating closure of mined-out stopes by movement on preexisting faults. Despite the amount of energy released in such events, actual damage is often minor and is expressed as sand squeeze, sill fracturing, and localized, relatively nonviolent rib failures. We interpret an August 1994 burst at the Lucky Friday Mine (figure 7) as resulting from strike-slip movement when highly stressed wall rock moved by slipping along preexisting fault planes. Interpretation is based, in part, on observations of locally intensified squeeze of sandfill in stopes and inferred fracturing and buckling-type heave of the unmined vein.

During previous overhand mining at the Lucky Friday, fault-slip bursts that affected access crosscuts were somewhat common. Damage to the crosscuts was usually dominated by sill heave on the pillar side of a bedding slip plane and down-drop on the opposite side (figure 8). Damage was usually interpreted as indicating a significant

dip component of slip (figures 8 and 9). This type of damage has been less frequent and less severe since underhand mining replaced the overhand method.

Fault-slip seismic events may also cause secondary damage as seismic waves intersect mine openings, displacing rock into the opening. "Shakedown" is thought to originate from highly fractured, weak back and wall rocks, which are dislodged relatively nonviolently. "Flyrock" originates when rock is conspicuously flung away from its parent surface. Seismic waves may also trigger buckling failure in layers that have already been stressed almost to their critical points. In such cases, the ensuing damage may bear no direct relationship to the mechanism most responsible for the event.

Figure 7
Interpretation of Fault-Slip Burst Near 5570-07 Stope.

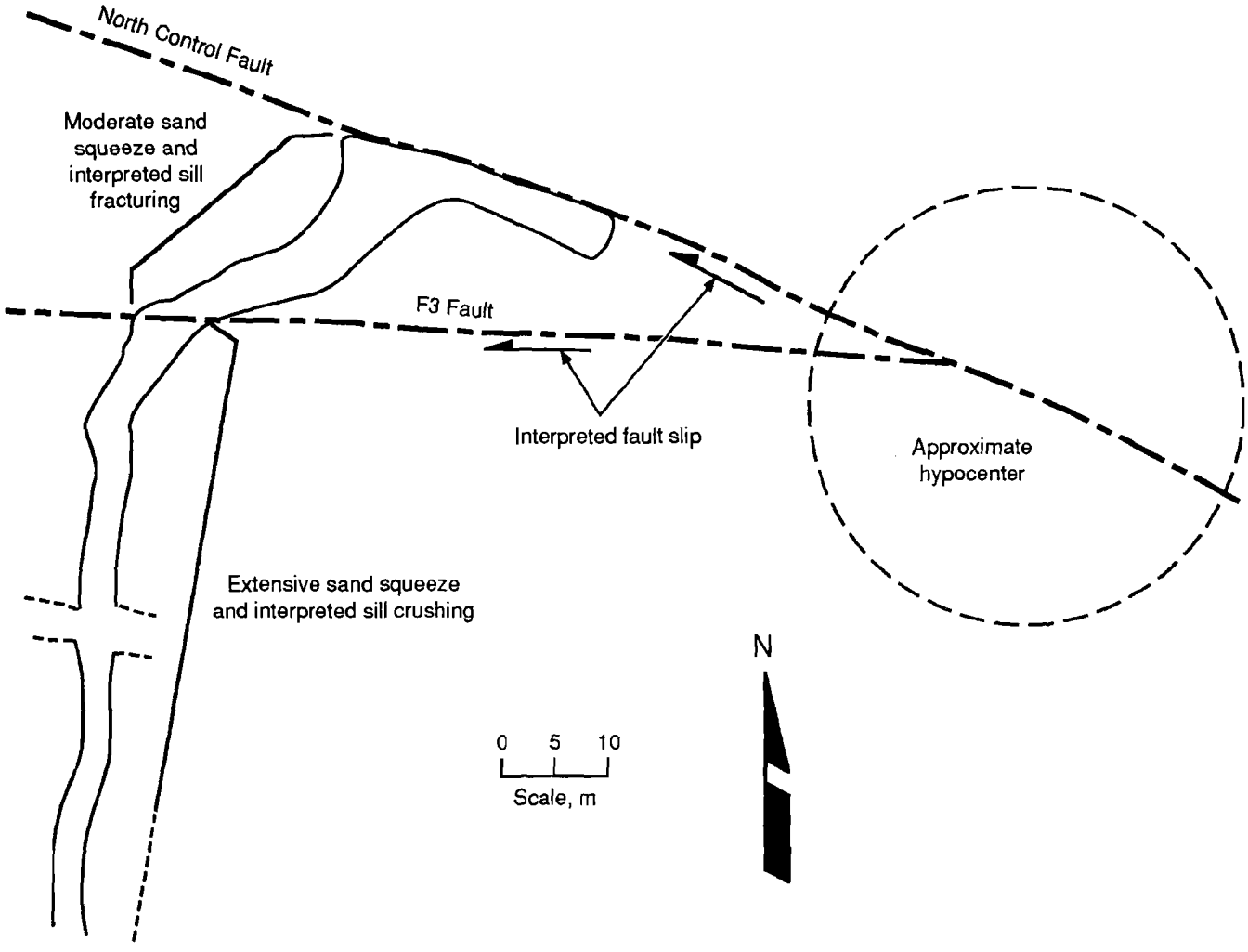

A Richter-magnitude 4 event centered east of 5580-07 stope in Lucky Friday Mine squeezed sand and locally fractured and heaved sill. This event probably resulted from strike-slip movements on known faults, which tended to close stope.

Figure 8
Burst Damage in Lateral, Lucky Friday Mine.

Photo shows that track heaved upward and illustrates inferred fault slip on an underlying bedding plane approximately beneath and parallel to exposed rail. Debris on track fell from right rib.

Figure 9
Stope Closure Resulting From Slip Along Bedding.

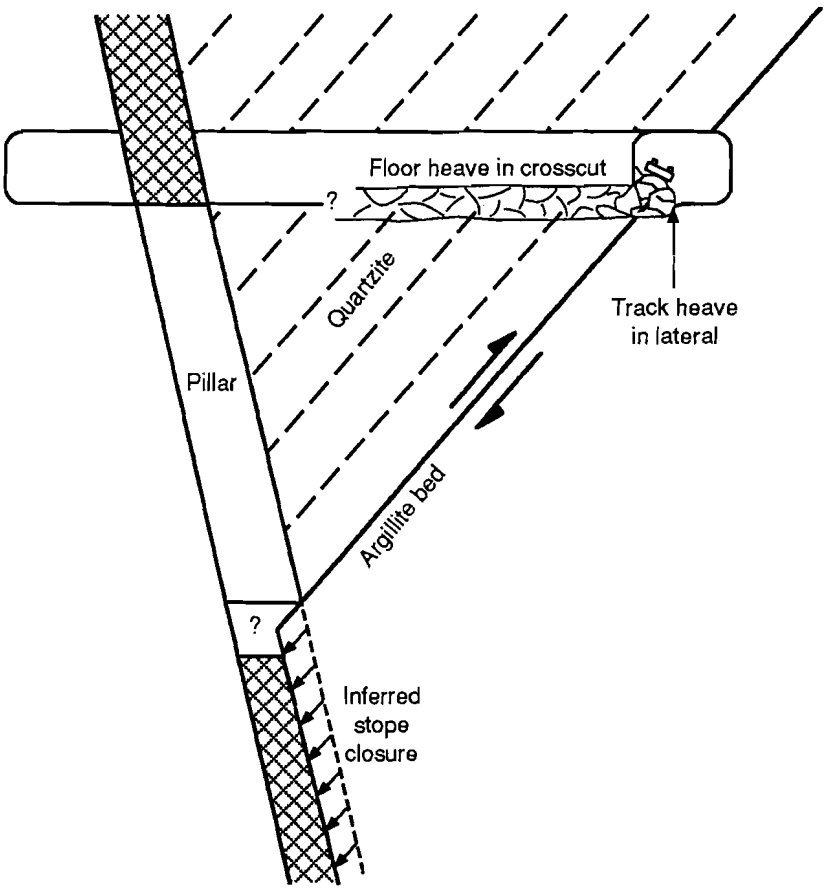

Interpretation of movement indicated by damage shown in figure 8. (After Williams and others, 1992.)

SUMMARY AND RECOMMENDATIONS

We conclude that, in the Coeur d'Alene Mining District, many rock bursts are controlled by steeply dipping bedding planes and faults. These structures are a major reason for the high incidence of rock bursts and mining-induced seismicity. We presume that these planes of weakness cause failure under significantly less stress than that required to cause bursts in massive, unlayered rock. In addition, the orientations of steeply dipping structures with respect to mine openings influence the surface that is damaged, regardless of the direction of greatest stress.

Consideration of the effects of preexisting structures on ground failure affirms the usefulness of several standard measures used to alleviate ground failure problems. These measures include (1) longwall underhand mining, which eliminates stress-concentrating pillars; (2) the use of shotcrete and mesh for containing shakedown and minor slabbing; and (3) use of bolts to stabilize the rock mass on a large scale.

We particularly emphasize that, where possible, openings should be planned so as to cross structures at large angles (as near to 90° as possible) rather than at low angles. In some cases, aligning accessways and positioning and inclining raise boreholes may enable them to be driven at large enough angles to inclined faults and bedding that many ground-control problems may be prevented.

Where development openings at low angles to steeply dipping beds or faults cannot be avoided, we recommend special attention to ground support. A primary objective should be to bolt rock layers tightly together so as to constrain these layers from buckling. We suggest that—

1. Bolts should be driven so as to cross bedding or faults at angles as near to perpendicular as practicable.
2. Rocks should be bolted as soon as possible after blasting and mucking to secure rock slabs before buckling is initiated and while the immediate face is still providing significant support.
3. Mine openings, such as slot ramps, that will later be deepened should be bolted with bolts that approach one-half the ultimate height of the opening; the use of stulls with blocking sufficient to permit limited squeeze without failure and extension of cemented sand into slots is also suggested.
4. If wall rocks are bolted before buckling begins, bolts with high modulus (resistance to stretching) should be most helpful. However, if buckling takes place despite initial bolting, strong, yieldable bolts are likely to provide the greatest long-term usefulness. A combination of high-modulus bolts and yielding bolts may be most useful.

REFERENCES

Blake, W. Rock Burst Mechanisms. CO Sch Mines Q, v. 67, No. 1, 64 pp.

Blake, W., and D. J. Cuvelier. Developing Reinforcement Requirements for Rockburst Conditions at Hecla's Lucky Friday Mine. Paper in Rockbursts and Seismicity in Mines, Proceedings of the 2nd International Symposium on Rockbursts and Seismicity in Mines, ed. by C. Fairhurst (Univ. of MN, Minneapolis, MN, June 8-10, 1988). Balkema, 1990, pp. 401-410.

Cook, N. G. W. The Design of Underground Excavations. Paper in Failure and Breakage of Rock. 8th Symposium on Rock Mechanics, ed. by C. Fairhurst (Univ. of MN, Minneapolis, MN, 1966). AIME, 1966, pp. 167-193.

Fairhurst, C. In-Situ Stress Determination—An Appraisal of Its Significance in Rock Mechanics. Paper in Rock Stress and Rock Stress Measurements: Proceedings of the International Symposium on Rock Stress and Rock Stress Measurements, ed. by O. Stephansson (Stockholm, Sept. 1-3, 1986). Centek, Lulea, Sweden, 1986, pp. 3-17

Fairhurst, C., and N. G. W. Cook. The Phenomenon of Rock Splitting Parallel to the Direction of Maximum Compression in the Neighborhood of a Surface. Paper in Proceedings of the First Congress on the International Society of Rock Mechanics (Lisbon, Portugal, Sept. 25-Oct. 1, 1966). V. 1, Nat. Lab. of Civil Eng., Lisbon, Portugal, 1966, pp. 687-692.

Hedley, D. G. F. Rockburst Handbook for Ontario Hardrock Mines. Spec. Rep. SP92-1E, CANMET, 1992, 305 pp.

Hobbs, S. W., A. B. Griggs, R. E. Wallace, and A. B. Campbell. Geology of the Coeur d'Alene Mining District, Shoshone County, Idaho. U.S. Geol. Surv. Prof. Paper 478, 1965, 139 pp.

Ortlepp, W. D. The Design of Support for the Containment of Rockburst Damage in Tunnels: An Engineering Approach. Paper in Rock Support in Mining and Underground Construction: Proceedings of the International Symposium on Rock Support, ed. by P.K. Kaiser and D.R. McCreath (Sudbury, ON, June 16-19, 1992). 1992, Balkema, pp. 593-609.

Scott, D. F. Geologic Investigations Near an Underhand Cut-and-Fill Stope, Lucky Friday Mine, Mullan, ID. USBM RI 9470, 1993, 21 pp.

Timoshenko, S. P., and J. M. Gere. Theory of Elastic Stability. McGraw-Hill, 1961, 541 pp.

Wagner, H, and J. B. Godfrey. Location and Support of Tunnels in Deep-Level Gold Mines. Paper in Tunnelling '76, ed. by M. J. Jones (London, Eng., Mar. 1-5, 1976). Inst. Min. Metall., 1976, 341-347.

Williams, T. J., C. J. Wideman, and D. F. Scott, D. F. Case History of a Slip-Type Rockburst. PAGEOPH, v. 139, No. 3/4, 1992, pp. 627-637.

INFLUENCE OF MINING-INDUCED SEISMICITY ON POTENTIAL FOR ROCK BURSTING

By P. L. Swanson[1]

ABSTRACT

Relationships between the locations of mining-induced seismic events, local fault structures, and mine geometry were examined by the U.S. Bureau of Mines in the Galena Mine, a deep hard-rock mine in northern Idaho. Stopes in the Galena Mine experiencing rock bursts and other large seismic events were found to fall into two structural regimes: the Silver vein and the N. 48° W. trend. The latter is a steeply dipping plane of seismic activity that is subparallel to major, locally steeply dipping faults that bound blocky structures. The N. 48° W. trend also intersects a shaft that was seriously damaged when fault gouge was expelled into the opening during a 3-month period of high seismic energy release. Models of stress interaction were developed to support the hypothesis that mining-induced deformation was mobilized along a 1.5-km length of the N. 48° W. trend. Specifically, numerical models were used to simulate rupture of seismic events and estimate induced changes in the quasistatic stress field. A Coulomb failure criterion was used with these results to estimate spatial variations in the potential for slip on planes parallel to local faults. Increases in the potential for slip on fault planes subparallel to the N. 48° W. trend were consistent with activation of deformation along the trend's 1.5-km length.

INTRODUCTION

Certain mine geometries and geologic structures play critical roles in the generation of rock bursts and other large mining-induced seismic events (Cook and others, 1966). To develop effective strategies for the reduction of rock-burst hazards at a particular mine site, the underlying mechanisms, whether controlled by mine geometry, geology, or both, must first be identified. Toward this end, the relationships among large seismic events, mining geometry, and local fault structures were examined in a burst-prone mine (Galena) in the Coeur d'Alene Mining District of northern Idaho.

Rock bursts in deep hard-rock mines have been classified into two groups: those associated with high stresses induced by mine geometry and those linked to the interaction of these stresses with preexisting geologic structures, such as faults and dikes (e.g., Gibowicz, 1990). The high-stress-induced events occurring in the immediate vicinity of mine workings and pillars are often considered to be less damaging (i.e., result in a smaller area of damage) and of lower magnitude than those associated with large-scale slip along faults (Gay and others, 1984; Brummer and Rorke, 1990). Nevertheless, fault-slip events can be triggered far out in the host rock without significant, or any, in-mine damage.

Rock bursts in the Coeur d'Alene district are often triggered during mining into remnant (sill) pillars produced by the commonly used overhand cut-and-fill mining method (Blake, 1972). In this case, both geology and mine geometry influence rock bursting; fault structures are present in the immediate vicinity of mining and are subjected to the high stresses present in the pillars. An attempt to reduce rock bursting by eliminating pillars in an experimental underhand longwall cut-and-fill mining operation is in progress at one mine in the district (Williams and

[1]Geophysicist, Denver Research Center, U.S. Bureau of Mines, Denver, CO.

Cuvelier, 1990). Eliminating pillars, however, does not reduce the frequency of encounters with faults. Studies of rock bursts in the Coeur d'Alene district show that many are consistent with slip along faults and other planar geologic structures (Jenkins and others, 1990; Williams and others, 1992; Boler and Swanson, 1993; Lourence and others, 1993).

This study was initiated by researchers at the U.S. Bureau of Mines (USBM) after a 3-month sequence of large seismic events occurred in six separate stopes that fell along a well-defined plane. This 1.5- by 0.5-km near-vertical plane, hereafter referred to as the N. 48° W. trend, was generally parallel to the trend of, and approximately coincident with, major local faults. During the same time period, the main entry shaft, which intersects the N. 48° W. trend, experienced significant ground control problems, resulting in a 3-month shutdown. Evidence is presented here that suggests that deformation was mobilized over the entire length of the mine along the N. 48° W. trend in a series of Richter-magnitude (M_L) 1 to 3 seismic events. A stress-interaction mechanism for this mobilization is investigated.

In this paper, the structural geology typical of the region is described, followed by descriptions of the stress field and vein geometry. Then, the N. 48° W. trend is identified along with other structures known to be associated with rock bursting. The paper then focuses on a short period of high seismic energy release along the N. 48° W. trend. Using seismic source size and stress-drop estimates and calculations of induced fault-slip potential, a case for stress interaction among these large seismic events is argued.

STRUCTURAL GEOLOGY

The Coeur d'Alene Mining District has been described as being located in an intensely faulted and sheared structural knot (Hobbs and others, 1965; Wallace and Morris, 1986). The slightly metamorphosed Precambrian rocks were compressed into a series of folds having varying amplitudes and wavelengths (synclinorium) and were subsequently faulted. Figure 1 shows that portion of the district surrounding the Galena Mine. Two locally dominant structural features, the right-lateral, strike-slip

Figure 1
Silver Valley Near Galena Mine Showing Major Faults.

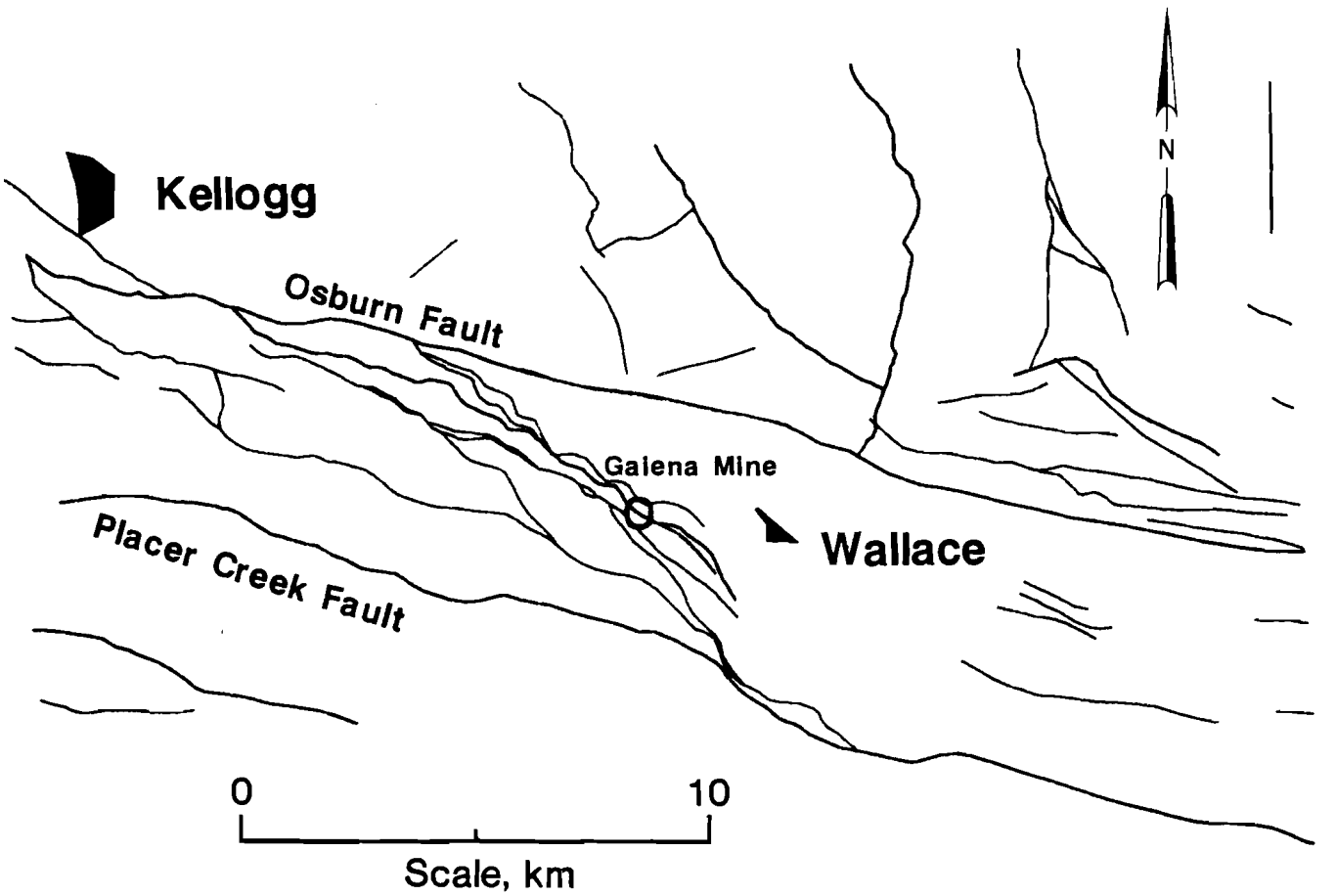

Osburn and Placer Creek Faults, can be traced for over 100 km and make up part of the extensive Lewis and Clark lineament (Wallace and others, 1990). These two faults are connected by a dense concentration of lesser faults (e.g., Polaris, Silver Standard, Killbuck, Argentine) that are found in the vicinity of the mine along a line that trends approximately N. 50° to 60° W. Most of these faults dip steeply to the southwest, and some approach near-vertical in the vicinity of the Galena Mine. Segmentation into complex strands is common. The following discussion refers to the geologic structure in the vicinity of the Galena Mine.

Figures 2 and 3 are maps of fault structure at depth. Only faults that can be traced with certainty across mine levels, diamond-drill holes, and sequential vertical cross sections (250-m spacing) are shown in figure 2. Many other faults are observed in mine openings (figure 3) but, because of their vast numbers and the fact that they can end abruptly, they have not been traced between levels. The northwest-trend of faulting persists down to the scale of a few meters.

The country rock surrounding the mine workings in figure 3 is the Revett Formation. The Revett is locally made up of 0.2- to 1.0-m-thick beds of brittle, high-strength, high-modulus quartzite interbedded with thin beds of argillite (typically <2 cm thick, with rare zones up to 0.7 m thick). In the vicinity of much of the present mining activity, the beds strike northwest and dip steeply (~75° to 80°) to the northeast. Bedding plane faults are ubiquitous, with typical spacings of a few meters. Bedding plane fault offsets average well under 5 m. Many other faults and joints with various orientations are present, producing a complex blocky structure. Throughout the mine, the maximum size block that is free of visible faults is estimated to be only 5 to 7 m on a side.

Rock bursting is prevalent in the Revett Quartzite throughout the Coeur d'Alene Mining District. The Polaris Fault separates the Revett Quartzite from the St. Regis argillites in certain parts of the mine (figure 4). A layer of gouge and sheared rock (0.3 to 10 m thick, with 1 m being typical) is commonly observed in mine openings driven through the Polaris Fault. Such crossings indicate the weak and highly permeable nature of these larger faults, as do the obvious signs of moisture, and enlarged (eroded) mine openings that often need timbered support. Until it dries out following exposure to air circulated by the mine's ventilation system, the soft plastic gouge can be molded by hand.

Mine workings that penetrate the Polaris Fault, and those in the St. Regis Formation, often experience considerable "squeeze" (obvious deformation without significant seismic activity, i.e., M_L <-1), but few, if any, rock-bursting problems. Apparently, the St. Regis argillites consume strain energy by deforming plastically, thus reducing the severity of rock bursts.

Figure 2
Faults Intersecting 4300 Level of Galena Mine.

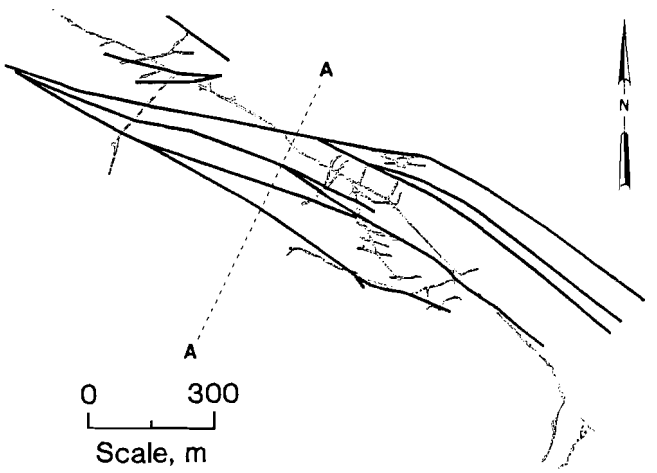

These faults (heavy lines) can be traced between levels and cross sections. Cross section A-A' is shown in figure 4.

Figure 3
Finer Scale Fault Structure Intersecting Veins 97, 104, and 120 on 4300 Level.

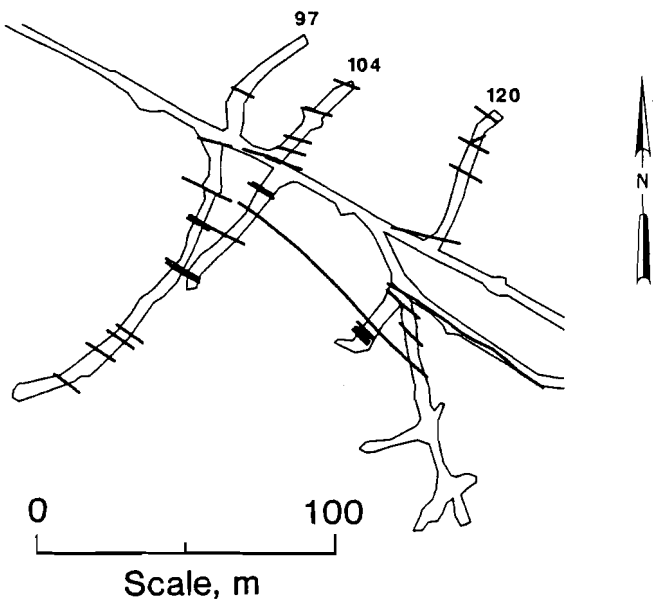

Faults range from a few grains in width, with clean, discrete surfaces, to the larger shear zones exhibited by the Polaris Fault, with cataclasis and gouge. In general, fault zones in the quartzite are narrower than in the argillites. The width, however, may depend upon the scale at which observations are made; a single discrete interface may represent one small facet of a large, complex, anastomosing shear zone involving many structural blocks. The blocky nature of the rock mass found at the scale of individual stopes may be interpreted, in certain instances, as

Figure 4
Vertical Cross Section Through Galena Mine as Depicted in Figure 2.

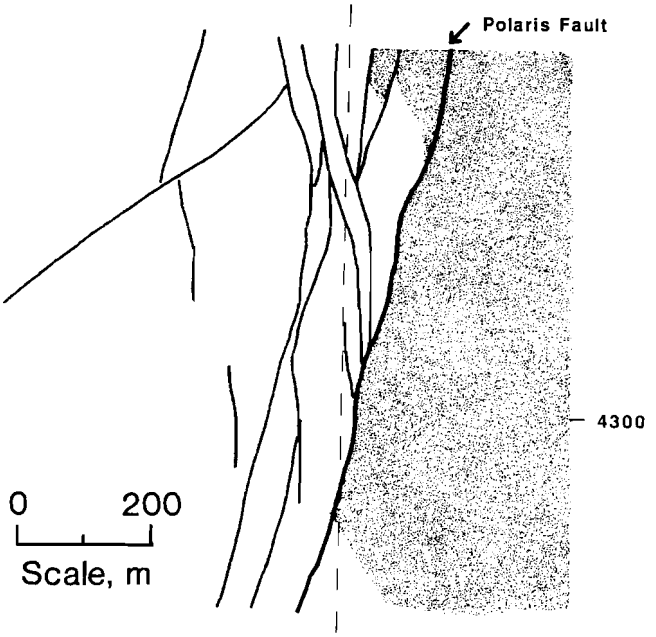

Shading indicates St. Regis argillites. Dashed line is approximate trace of N. 48° W. trend.

representing deformable elements that belong to much larger fault structures.

In summary, stiff quartzite blocks are bounded by compliant fault structures and argillites and are elongated parallel to these structures. As these structures are commonplace in the Galena Mine, mining-induced deformation may be strongly influenced by rigid-block mechanics.

IN SITU STRESS, VEIN GEOMETRY, AND SLIP POTENTIAL

Studies of in situ stress in the district (Board and Beus, 1984; Whyatt, 1986; Sprenke and others, 1991) indicate that the predominant direction of maximum horizontal compressive stress is N. 45° W. ±15°. In the vicinity of the Galena Mine, this direction is parallel to the strike of local faulting and the near-vertical bedding. Limited observations of borehole breakouts in the Galena Mine are consistent with a maximum principal stress direction of N. 45° W. Based on empirical relationships fit to in situ stress data collected throughout the district (Whyatt, 1986), the vertical, maximum, and minimum horizontal principal stresses in the central part of the mine are estimated to be 38, 51, and 39 MPa, respectively.

All but one of the steeply dipping burst-prone veins strike N. 35° E. to N. 65° E., or roughly perpendicular to both the N. 48° W. trend and the maximum horizontal stress direction (see, for example, figure 3). Faults that intersect these veins strike between N. 45° W. and N. 80° W. (e.g., figure 2) with most clustering between N. 50° W. and N. 65° W. Thus the faults generally strike perpendicular to the veins and subparallel to the N. 48° W. trend.

The vein-normal maximum horizontal stress orientation gives rise to local stress distributions similar to those found in gravity-loaded horizontal tabular deposits with large end lobes where shear stress is high (e.g., Jaeger and Cook, 1976). Alignment of these lobes with preexisting fault surfaces and argillite (and other) beds provides optimum conditions for aiding stope closure through both stable and unstable right-lateral and left-lateral slip. These conditions for slip can be illustrated by examining changes in normal and shear stresses across such beds upon mining a vein. The Coulomb failure criterion (e.g., Jaeger and Cook, 1976) is considered in a form that describes the difference between the shear stress required for slip on a surface and the actual stress on that surface. In this paper, this quantity is called the slip potential and is expressed by the equation,

$$\text{Slip potential} = |\tau| - s_o - \mu\sigma_n, \qquad (1)$$

where $|\tau|$ = shear stress on the surface in question,

$s_o + \mu\sigma_n$ = Coulomb stress required for slip,

s_o = cohesive shear strength,

μ = coefficient of friction (internal friction for intact rock),

and σ_n = normal stress acting on the plane.

Equation 1 is identical to the excess shear stress (ESS) parameter of Ryder (1988) and other researchers in which the difference between static shear stress prior to slip and the dynamic strength of the plane is expressed when μ is the dynamic coefficient of friction.

Figure 5 is a schematic showing one excavated vein intersecting the N. 48° W. trend at nearly 90°. Absolute values of slip potential are shown for slip on planes trending N. 48° W. The direction of σ_1 in figure 5 was taken to be N. 30° W., representing one end of the reported range of the maximum principal stress direction (i.e., N. 45° W. ±15°). Symmetry of contour lobe size and orientation occurs when σ_1 is oriented N. 45° W. The elevated slip-potential lobes are thus elongated to the northwest over the reported range of σ_1 orientation. Localized fault structures (figures 1-4) and bedding planes parallel to these elevated slip-potential lobes are prime

candidates for seismic and aseismic slip (both right- and left-lateral) that accommodate closure.

SPATIAL DISTRIBUTION OF ROCK BURSTS

At a depth of 1 to 1.7 km, the silver ore vein deposits of the Galena Mine are extracted using the overhand cut-and-fill method. There are more than 40 near-vertical veins that are distributed, in subparallel fashion, over a horizontal distance of 1.5 km. Up to 20 different stopes are mined at any one time. Of these, 10 may be prone to rock bursting.

The seismicity data described in this paper were initially examined to constrain the design of a full seismic waveform recording system. Richter magnitudes were estimated from a calibrated short-period vertical seismometer operating on the surface. Seismic events were located (Swanson and Sines, 1991) using one of eight 16-channel accelerometer arrays in a networked microseismic monitoring system (Steblay and others, 1990; Estey, 1995). This system provides real-time hypocenter locations for events with magnitudes greater than approximately -5. Each array is roughly 150 m on a side and is centered around individual rock-burst-prone stopes. Location errors for events falling within an individual array, where the detection and location sensitivity are greatest, are ±10 m at best (Swanson and others, 1992).

Approximately 200 of the largest mining-induced seismic events with M_L ranging from 0.0 to +3.0 were located. Figure 6 is a histogram showing all located seismic events and a subset of damaging seismic events. A damaging seismic event is defined here as one that requires at least one-half day of stope cleanup and/or repair.

Ten rock-burst-prone stopes fell into two different structural regimes: the Silver vein and the N. 48° W. trend (figure 7). Figure 7 illustrates the two structural regimes and the 4300 level at a depth of approximately 1.3 km. The Silver vein is the largest vein in the mine and has been associated with rock bursts since the 1950's. It extends at least 1 km vertically and as much as 400 m horizontally. The mined horizontal extent of more typical veins is 80 to 120 m. The near-vertical veins have a height that is typically two to four times their breadth and an excavation width of 2 to 5 m.

Six stopes with recurring seismic activity plus the damaged shaft define the N. 48° W. trend. In one 11-month period, 30 of 32 events having an M_L >1.0 occurred exclusively along the N. 48° W. trend despite the fact that mining was progressing in at least 25 different stope and development headings that were not aligned with this trend. Several particularly large seismic events (M_L >2.5)

Figure 5
Absolute Slip-Potential Contours for Slip on N.48°W.-Oriented Planes.

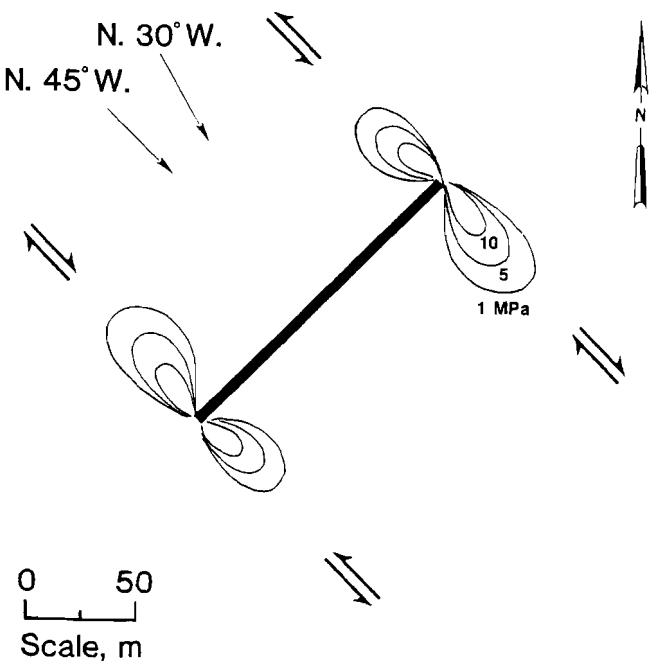

Contours (in MPa) are calculated near vicinity of mined-out vein on N.30°W. trend. Direction of σ_1 is N.30° W. Perfect contour symmetry occurs for σ_1 oriented at N.45°W.

Figure 6
Distribution of Seismic Magnitudes for January 1989 Through June 1991.

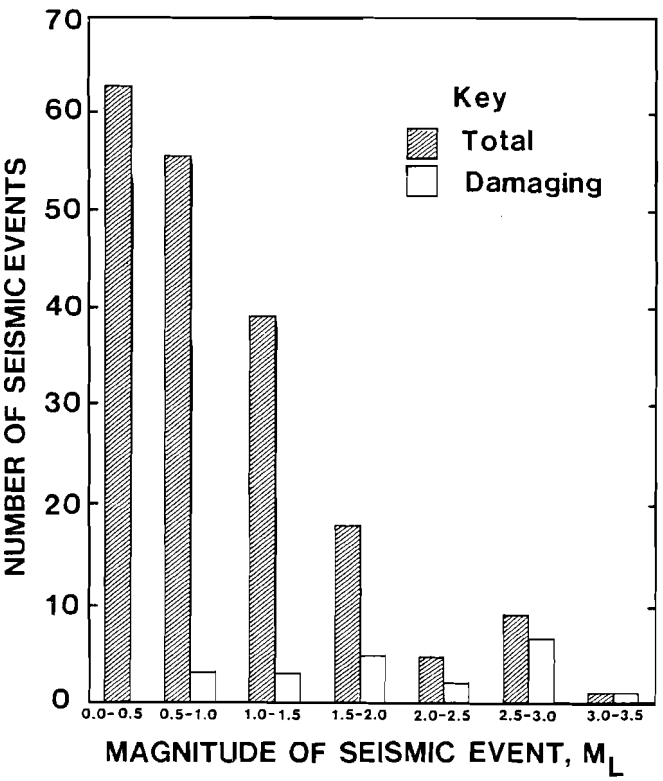

Figure 7

N.48°W. Trend of Stopes (Solid Circles) Experiencing Rock Bursting and Other Large Seismic Events.

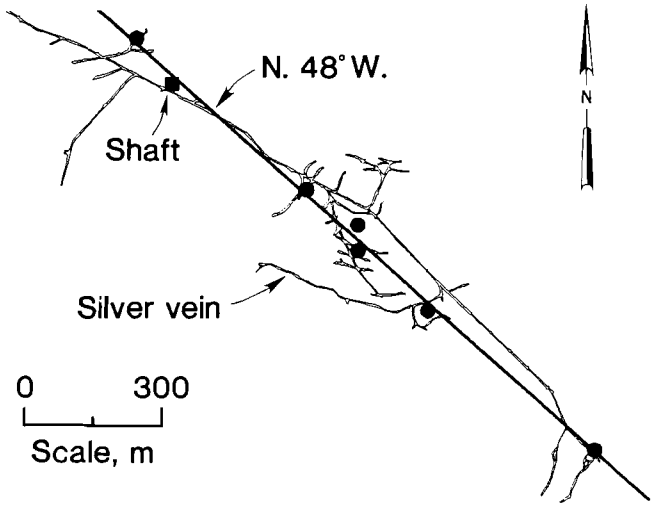

Rock-burst-prone stopes on Silver vein are omitted for clarity. Plan view shows 4300 level at a depth of 1.3 km.

occurred in the last 3 months of this 11-month period. The remainder of this paper focuses on this short period of high seismic activity along the N. 48° W. trend.

CONCENTRATED RELEASE OF SEISMIC ENERGY

Periods of elevated rock-burst activity, or rock-burst "seasons", have long been recognized by old-time Galena miners. One such period of elevated activity occurred in the first 3 months of 1990 (figure 8). Over 90 pct of the seismic energy released from the mine in 1990 was released during this time. Seismic energy E (in ergs) was estimated using Gutenberg and Richter's (1956) relation log E = 11.8 + 1.5 M, with M_L as magnitude M. The seismic energy emitted along the N. 48° W. trend occurred in a series of 11 events having an M_L of 1.1 to 2.9. Four events, ranging from M_L 2.6 to M_L 2.9, dominated the periods of energy release, labeled a, b, d, and e in figure 8. The main entry shaft damage at c occurred shortly after the largest event of the sequence at b. Following this short period of high seismic energy release, the rate remained below the average long-term rate, which is indicated by the slope of the dashed line in figure 8, for 10 months. Mining productivity was nearly constant during this entire period.

The temporal coincidence of a rapid sequence of large seismic events and shaft damage (all occurring on the N. 48° W. trend), followed by a significant quiet period, suggests large-scale release of stored elastic strain energy through activation of fault-slip along one of the major

Figure 8

Cumulative Seismic Energy Released Along N.48°W. Trend.

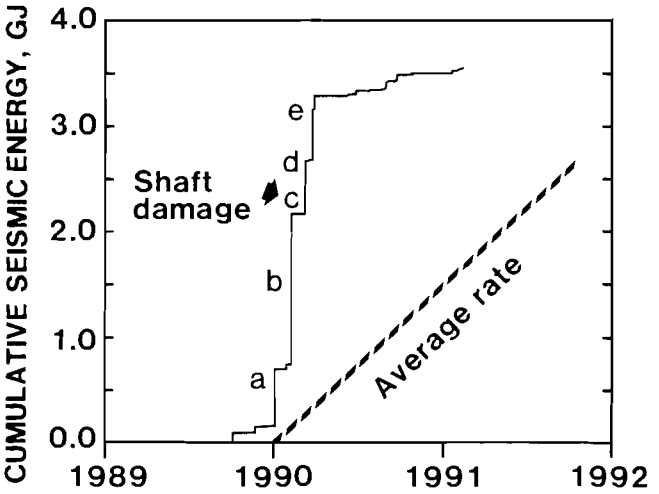

Periods of energy release a, b, d, and e are associated with events shown in figure 10. Time of fault-gouge expulsion into main entry shaft is denoted by c. Dashed line shows long-term average energy release rate.

northwest-trending faults. However, a single major discontinuity surface cannot be traced through the N. 48° W. trend. It should be reemphasized that faults on the scale of the mine in the Coeur d'Alene Mining District are not simple planar structures, but are complex, multiple, anastomosing surfaces that can vary rapidly in character over very short distances (Wallace and Morris, 1986). Therefore, even if one envisaged a complex 3-month-long propagation of a shear-slip event that was periodically triggered by mining activity, the presence of a single, continuous discontinuity surface does not seem to be required for fault structure and fault movement at this scale. An alternate interpretation involves the transmission of seismicity-induced changes in stress by relatively rigid quartzite blocks that are elongated parallel to the dominant northwest fault structures. The latter view is consistent with the expected mechanical response of the local geologic structure.

RELATIONSHIP BETWEEN SEISMIC SOURCE SIZE AND EVENT MAGNITUDE

To evaluate the degree to which ruptures generated in a particular stope affect the stress field in adjacent stopes, an approximate measure of rupture size is required (figure 8). Such interaction may promote stope closure and release of stored energy along the N. 48° W. trend. Earthquake seismologists routinely estimate fault-slip areas and resulting stress drops through quantitative analyses of

seismic waveforms (Gibowicz, 1990). Numerous estimates of rupture dimensions and shear stress drop have been reported for mining-induced seismicity in hard-rock mines (Spottiswoode and McGarr, 1975; McGarr and others, 1981; Spottiswoode, 1984; McGarr and others, 1990). These published values were fit to an equation relating seismic magnitude to the logarithm of seismic source dimension r, where r is the radius of a circular rupture area.

$$M_L = 2.4 * \log r(m) - 2.7. \quad (2)$$

The best fit occurs for a stress drop of 2.2 MPa (319 psi), which is consistent with the typically small values (1 to 10 MPa) reported for mining-induced seismicity (Gibowicz, 1990).

As a check on the assumed relationship between magnitude and source dimension, the mine volume exhibiting microseismicity ($M_L \geq -5$) following a M_L 2.9 event was estimated using the data collected by the microseismic monitoring system. The event occurred in the country rock between the stopes covered by four separate arrays of the monitoring system (figure 9). Damage was restricted to rock falls on several levels and one M_L 0.9 aftershock on the 4300 level that lifted a train track a few centimeters. The observed volume of aftershock microseismicity was a minimum due to the extremely low detection sensitivity beyond individual accelerometer arrays.

Nearly 4,000 microseismic events were detected during the 10½ hours following the M_L 2.9 event. Less than 700 events were actually located; the remainder did not meet the location criteria used in the routine monitoring system (Swanson and others, 1992).

An order of magnitude fewer events are typically located with these four arrays when there have been no large rock bursts. Figure 9 is a graphic representation of the seismic source estimated from equation 2 (r = 201 m). Both estimates of source dimension (equation 2 and figure 6) are of the same order of magnitude.

HYPOTHESIS: MOBILIZATION OF DEFORMATION ALONG LENGTH OF MINE

The relationship between magnitude and source size (equation 2) is now used to illustrate what portion of the N. 48° W. trend could be occupied by a slipped area if all events had a N. 48° W. orientation. The case for making this assumption rests not on seismic waveform data and analyses (for no such data are available), but rather on structural geology, compatibility between N. 48° W. slip and stope closure, and alignment of observed events. Figure 10 shows a vertical section of the plane of induced seismic activity, looking northeast. Estimated sizes and

Figure 9
Source Dimension Estimate for M_L2.9 Event.

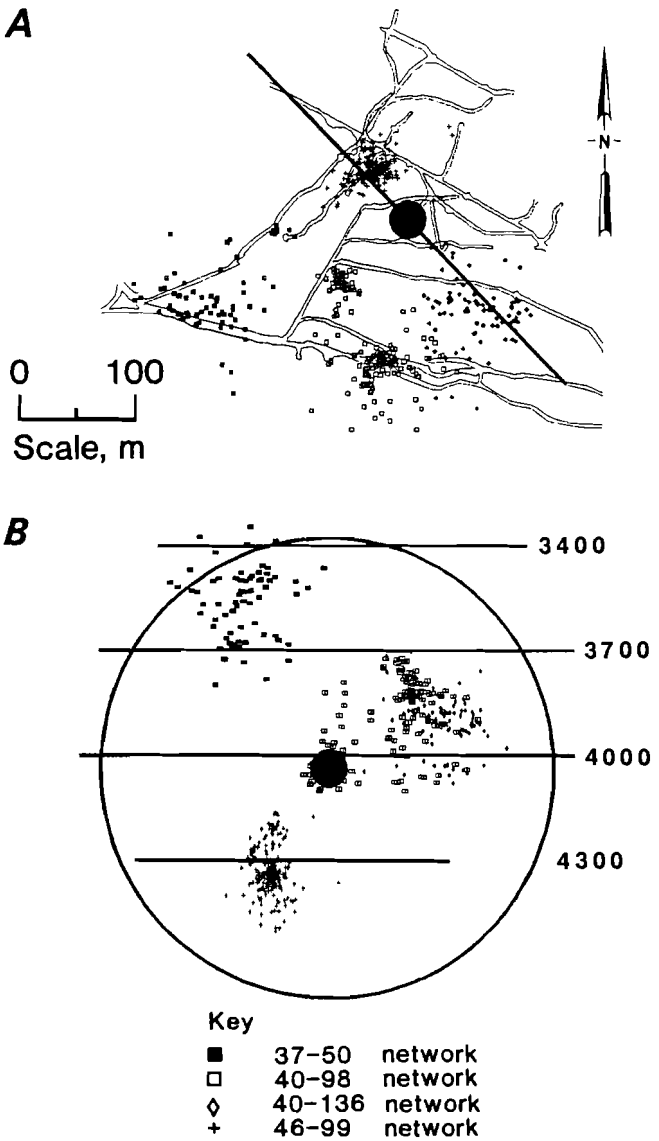

Estimate is based on volume distribution of microseismicity recorded for 10-1/2 hours by four arrays of networked monitoring system. Hypocenter is shown as large solid dot. Apparent clustering is due largely to low detection sensitivity in regions between the four arrays. Source dimension estimate from equation 2 (text) shown as 201-m-radius circle in (*A*) plan view and (*B*) vertical section looking northeast.

positions of rupture planes correspond to individual events (M >1) occurring during periods of energy release (a-e) shown in figure 8. A significant fraction of the 1.5- by 0.5-km plane of seismic activity is covered by the rupture sources.

To investigate the degree of stress interaction among these events, elementary two-dimensional elastic stress

analyses were used to calculate quasistatic stress changes resulting from simple shear rupture sources. In particular, the increase in the potential for slip along the N. 48° W. trend resulting from simple shear rupture at other positions on this plane is examined.

When geologic and/or mine structures are stressed almost to the point of failure, minute perturbations in the stress field may trigger instability. The change in the potential for slip [also called change in the Coulomb failure function (Oppenheimer and others, 1988; Reasenberg and Simpson, 1992)] resulting from stress-altering events is given by equation 3.

$$\Delta(\text{slip potential}) = \Delta\tau + \mu\Delta\sigma_n, \qquad (3)$$

where $\Delta\tau$ = change in shear stress and $\Delta\sigma_n$ = change in normal stress (positive for increased tension).

Stress changes associated with the first three events (a) in the sequence of figure 10 are estimated. These events occurred within a 24-h period. The boundary-element method of Crouch and Starfield (1983) was modified to maintain contact between crack surfaces. The ruptures are represented by elements placed at each event location and oriented N. 48° W. Rupture dimensions are scaled by the appropriate event magnitude. A right-lateral shear stress of 2.2 MPa, corresponding to the stress drop determined from the fit to seismic data in equation 2, is applied across each slip plane, and field stresses are calculated. μ and s_o (see equation 1) are taken to be 0.6 and 0.3 MPa, respectively.

For simplicity, a homogeneous isotropic medium is first considered. This example neglects two influences. First, a nonuniform stress distribution is expected in a deforming faulted block medium. However, at the present time, there is not sufficient information to determine which of the ubiquitous potential slip planes should be included in a tractable model. Appropriate constitutive relations and initial boundary conditions are also unknown. Second, the stress-concentrating effect of stope geometry is neglected. In these initial calculations, the intent is to estimate the distance over which significant stress *changes* occur because of simple rupture. Neglect of the lower elastic modulus of the sandfill in adjacent stopes results in lower bound estimates of induced stress.

Figure 11 shows contours of increased slip potential (equation 3) resulting from slip on the first three ruptures (a events) for planes oriented N. 48° W. For clarity, contours are shown for only the positive changes in slip potential. If desired, contour maps of decreased slip potential can also be constructed. A band of elevated slip potential encompasses the N. 48° W. trend and beyond. Similar results are found for planes oriented parallel to the strike of most major faults (N. 45° W. to N. 65° W.) near stopes along the N. 48° W. trend. Imposing higher stress drops increases the magnitude of the change in the slip potential along the N. 48° W. trend. When the stress drops for the three events do not all have the same sign, slip potential along the N. 48° W. trend is decreased relative to figure 11.

Figure 10
Vertical Section View of N.48°W. Plane of Seismic Activity (Looking Northeast).

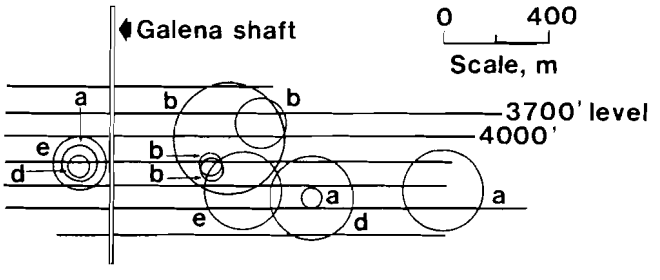

Estimated sizes and positions of circular rupture planes correspond to periods of energy release (a-e) shown in figure 8. The Galena shaft (c) is shown as vertical lines.

Figure 11
Plan View of Boundary-Element Model.

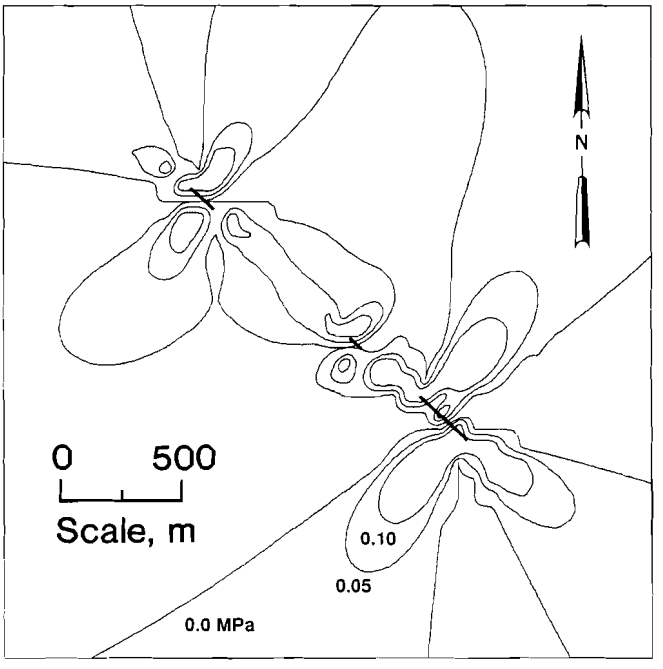

Model of first three ruptures (dark lines) in sequence a of figure 10, where M_L = 1.8, 1.1, and 2.6 from upper left to lower right. Contours (in MPa) indicate values of increased slip potential for N.48°W.-oriented planes as a result of 2.2-MPa, right-lateral stress drops across the three ruptures.

DISCUSSION

The changes in slip potential, or static Coulomb stress, associated with the seismic events shown in figure 10 represent only a few percent of the total stress drop that drives these events. While these stress increments are too small to cause rupture by themselves, they may be sufficient to trigger instabilities in structures that are already critically stressed. In many recent studies, small increases in slip potential have been linked to the triggering of seismic and aseismic crustal deformation on a very large scale. Increases in slip potential greater than 0.01 MPa have been identified with zones of earthquake aftershocks triggered by crustal near-vertical strike-slip faults (Oppenheimer and others, 1988; Reasenberg and Simpson, 1992; Stein and others, 1992). Stein and Lisowski (1983) have found correlations between aftershock locations and increases in slip potential of >0.03 MPa. Similarly small values are suggested for triggering reservoir-induced seismicity (Grasso, 1992; Roeloffs, 1988). Fault creep, which is one interpretation of an event producing the shaft damage, has also been observed to be accelerated by changes in slip potential of a few tenths of an MPa (Simpson and others, 1988). Models of stress transfer developed for a southern California earthquake sequence extending back for 50 years (Stein and others, 1994) show that each event increased slip potential at the site of future earthquakes. This sequence recently culminated in the damaging 1994 Northridge earthquake. Evidence is also mounting that favorable incremental stressing caused by earlier earthquakes precedes future large seismic events across the globe (Kagan, 1994).

Small stress changes that trigger local instabilities in the Galena Mine have long been inferred from observations of (1) microseismic activity occurring several hundred meters from, but concurrent with, small-volume (~10 m^3) production blasting; (2) rock bursts and other large seismic events that are occasionally triggered at significant distances from, but concurrent with, blasting (~100 m); and (3) the high occurrence rates of seismic doublets or pairs of events in space and time (Swanson and Sines, 1990; Estey, 1995). The values of increased slip potential in figure 11 are of the same order of magnitude or larger than those reported in the above-mentioned field studies and cover multiple stopes along the N. 48° W. trend. Similar results are found in models of the other large events in figure 10. This is taken as evidence that supports the idea that seismicity- and blasting-induced quasistatic stress changes may link deformation of highly stressed areas over the observed distances.

Similarity of rupture slip direction (i.e., left-lateral versus right-lateral) is not a requirement for triggered slip in adjacent working areas; the slip need only accommodate stope closure. (This is at least the case when stress resulting from closure in a preexisting stress field is the dominant local force driving rock bursts and seismic events. This may not be the case for tectonically driven events triggered by mining.) As shown in figure 5, each stope has elevated potential for both left- and right-lateral strike-slip.

Model results shown in figure 5 apply to an isolated stope. Preliminary modeling efforts, in which seismic slip surfaces and multiple mine openings are considered together, indicate that (1) significant interaction between stopes occurs under static, nonseismic loading conditions, (2) N. 48° W.-oriented seismic events further perturb the slip potential throughout multiple stopes along the N. 48° W. trend, and (3) the change in slip potential may be positive or negative depending upon the relative orientations of the slip plane, slip direction, and strike of the stope (vein), and the relative positions of the slip plane and stope. Such perturbation of slip potential represents one possible mechanism by which deformation may be mobilized in several working areas throughout the Galena Mine.

The evidence presented to support the hypothesis that mining-induced deformation was mobilized along the entire length of the mine cannot be considered as unequivocal proof of the hypothesis. It can be argued, however, that it is reasonable, that the evidence is consistent, and that these results deserve further consideration in developing hazard forecasting and destressing methods in other mines with similar conditions.

SUMMARY

The relationship among local geology, vein and stope layout, and the locations of large seismic events and rock bursts has been examined in a deep hard-rock mine in northern Idaho. Two structural regimes were found to be associated with rock bursting: (1) the Silver vein, the largest vein in the mine, which has a long history of rock bursting and (2) the N. 48° W. trend, a near-vertical plane striking N. 48° W. throughout the length of the mine. This plane is subparallel to the strikes of the major faults in the mine.

Over 90 pct of the seismic energy emanating from the mine in 1990 was released in one 3-month period in a series of large seismic events and rock bursts along the N. 48° W. trend. During this time, the main access shaft,

which is coincident with the N. 48° W. trend, was damaged when fault gouge was expelled into the shaft opening. While a single, discrete fault surface cannot be traced continuously throughout the length of the plane of activity, steeply dipping fault structures trending N. 45° W. to N. 70° W. permeate the mine. These blocky structures are thought to provide preferential slip surfaces that facilitate stope closure and stress transfer between adjacent working areas.

The degree to which calculated seismic slip surfaces fill the N. 48° W. plane of activity was examined using published relationships between magnitude and source dimension. Boundary-element models of simple shear slip were used to estimate quasistatic stress changes associated with three seismic events that initiated a rapid period of energy release. Attendant changes in slip potential for planes parallel to fault structures were calculated. For stress drops greater than or approximately equal to 2.2 MPa (the average of published results), a zone of elevated slip potential extends along the entire N. 48° W. trend, and values approach and/or exceed those reported prior to large southern California earthquakes. Such values may trigger earthquake aftershock activity, fault creep, and reservoir-induced seismicity. The evidence presented here supports the hypothesis that mining-induced deformation was mobilized along the N. 48° W. trend throughout the mine.

ACKNOWLEDGMENTS

The author thanks ASARCO, Inc., for its cooperation with the USBM in the field experiments at the Galena Mine. Mine geologists, J. Lucini and H. Lenhardt contributed substantially to the author's understanding of Coeur d'Alene geology. Jeffrey Whyatt, mining engineer, Spokane Research Center, provided the modified boundary-element code and instruction in its use.

REFERENCES

Blake, W. Rock Burst Mechanics. CO Sch. Mines Q, No. 67, 1972, pp. 1-64.

Boler, F. M., and P. L. Swanson. Seismicity and Stress Changes Subsequent to Destress Blasting at the Galena Mine and Implications for Stress Control Strategies. USBM RI 9448, 1993, 21 pp.

Board, M., and M. Beus. Instrumentation and Preliminary Analysis of a 6,200-ft Deep Circular Shaft in Northern Idaho. Paper in Geomechanics Applications in Underground Hardrock Mining (Denver, CO, Oct. 24-26, 1984). Soc. Min. Eng. AIME, 1984, pp. 127-135.

Brummer, R. K., and A. J. Rorke. Case Studies on Large Rockbursts in South African Gold Mines. Paper in Rockbursts and Seismicity in Mines, Proceedings of the 2nd International Symposium on Rockbursts and Seismicity in Mines, ed. by C. Fairhurst (Univ. MN, Minneapolis, MN, June 8-10, 1988). Balkema, 1990, pp. 323-330.

Cook, N. G. W., E. Hoek, J. P. G. Pretorius, W. D. Ortlepp, and M. D. G. Salamon, Rock Mechanics Applied to the Study of Rockbursts. J. S. Afr. Inst. Min. Metall., v. 66, 1966, pp. 436-528.

Crouch, S. L., and A. M. Starfield. Boundary Elements in Solid Mechanics. Allen and Unwin, London, 1983, 322 pp.

Estey, L. H. Overview of USBM Microseismic Instrumentation and Research for Rock Burst Mitigation at the Galena Mine from 1987 - 1993. USBM Spec. Publ. 01-95, 1995, pp. 283-302.

Gay, N. C., D. Spencer, J. J. Vanwyk, and P. K. Van der Heever. The Control of Geological and Mining Parameters on Seismicity in the Klerksdorp Gold Mining District. Paper in Rockbursts and Seismicity in Mines, ed. by N. C. Gay and E. H. Wainwright (Proc. of Symp. on Seismicity in Mines, Johannesburg, 1982). Symp. Ser. 6, S. Afr. Inst. of Min. and Metall., Johannesburg, S. Afr., 1984, pp. 107-120.

Gibowicz, S. J. The Mechanism of Seismic Events Induced by Mining: A Review. Paper in Rockbursts and Seismicity in Mines. Proceedings of the 2nd International Symposium on Rockbursts and Seismicity in Mines, ed. by C. Fairhurst (Univ. MN, Minneapolis, MN, June 8-10, 1988). Balkema, 1990, pp. 3-27.

Grasso, J. R. Mechanics of Seismic Instabilities Induced by the Recovery of Hydrocarbons. Pure and Appl. Geophys., v. 139, 1992, pp. 507-534.

Gutenberg, B., and C. F. Richter. Magnitude and Energy of Earthquakes. Ann. Geofis., v. 9, 1956, pp. 1-15.

Hobbs, S. W., A. B. Griggs, R. E. Wallace, and A. B. Campbell. Geology of the Coeur d'Alene District, Shoshone County, Idaho. U.S. Geol. Surv. Prof. Paper. 478, 1965, 139 pp.

Jaeger, J. C., and N. G. W. Cook. Fundamentals of Rock Mechanics. Chapman and Hall, 1976, 585 pp.

Jenkins, F. M., T. J. Williams, and C. J. Wideman. Analysis of Four Rock Bursts in the Lucky Friday Mine: Mullan, Idaho, USA. Paper in International Deep Mining Conference: Technical Challenges in Deep Level Mining, ed. by D. A. J. Ross-Watt and P. D. K. Robinson (Johannesburg, S. Afr., Sept. 17-21, 1990). S. Afr. Inst. of Min. and Metall., Johannesburg, S. Afr., pp. 1201-1212,

Kagan, Y. Y. Incremental Stress and Earthquakes. Geophys. J. Int., v. 117, 1994, pp. 345-364.

Lourence, P. B., S. J. Jung, and K. F. Sprenke. Source Mechanism at the Lucky Friday Mine: Initial Results from the North Idaho Seismic Network. Paper in Rockbursts and Seismicity in Mines 93. Proceedings of the 3rd International Symposium on Rockbursts and Seismicity in Mines, ed. by R. P. Young (Kingston, ON, Aug. 16-18, 1993). Balkema, 1993, pp. 217-222.

McGarr, A., J. Bicknell, J. Churcher, and S. Spottiswoode. Comparison of Ground Motion from Tremors and Explosions in Deep Gold Mines. J. Geophys. Res. v. 95, 1990, pp. 21,777-21,792.

McGarr, A., R. W. E. Green, and S. M. Spottiswoode. Strong Motion of Mine Tremors: Some Implications for Near-Source Ground Motion Parameters. Bull. Seism. Soc. Am., v. 71, 1981, pp. 295-320.

Oppenheimer, D. H., P. A. Reasenberg, and R. W. Simpson. Fault Plane Solutions for the 1984 Morgan Hill, California, Earthquake Sequence: Evidence for the State of Stress on the Calaveras Fault. J. Geophys. Res., v. 93, No. B8, 1988, pp. 9007-9026.

Reasenberg, P. A., and R. W. Simpson. Response of Regional Seismicity to the Static Stress Change Produced by the Loma Prieta Earthquake. Science, v. 255, 1992, pp. 1687-1690.

Roeloffs, E. Fault Stability Changes Induced Beneath a Reservoir with Cyclic Variations in Water Level. J. Geophys. Res., v. 93, 1988, pp. 2107-2124.

Ryder, J. A. Excess Shear Stress in the Assessment of Geologically Hazardous Situations. J. S. Afr. Inst. Min. Metall., v. 88, No. 1, 1988, pp. 27-39.

Simpson, R. W., S. S. Schulz, L. D. Dietz, and R. O. Burford. The Response of Creeping Parts of the San Andreas Fault to Earthquakes on Nearby Faults: Two Examples. Pure and Appl. Geophys., v. 126, 1988, pp. 665-685.

Spottiswoode, S. M. Source Mechanisms of Mine Tremors at Blyvooruitzicht Gold Mine. Paper in Rockbursts and Seismicity in Mines, ed. by N. C. Gay and E. H. Wainwright (Proc. of Symp. on Seismicity in Mines, Johannesburg, 1982). Symp. Ser. 6, S. Afr. Inst. of Min. and Metall., Johannesburg, S. Afr., 1984, pp. 29-38.

Spottiswoode, S. M., and A. McGarr. Source Parameters of Tremors in a Deep-Level Gold Mine. Bull. Seism. Soc. Am., v. 65, 1975, pp. 93-112.

Sprenke, K. F., M. C. Stickney, D. A. Dodge, and W. R. Hammond. Seismicity and Tectonic Stress in the Coeur d'Alene Mining District. Bull. Seism. Soc. Am., v. 81, 1991, pp. 1145-1156.

Steblay, B. J., T. Swendseid, and B. Brady. Innovative Microseismic Rock Burst Monitoring System. Paper in Rockbursts and Seismicity in Mines. Proceedings of the 2nd International Symposium on Rockbursts and Seismicity in Mines, ed. by C. Fairhurst (Univ. MN, Minneapolis, MN, June 8-10, 1988). Balkema, 1990, pp. 259-262.

Stein, R. S., G. C. P. King, and J. Lin. Change in Failure Stress on the Southern San Andreas Fault System Caused by the 1992 Magnitude = 7.4 Landers Earthquake. Nature, v. 258, 1992, pp. 1328-1332.

Stein, R. S., G. C. P. King, and J. Lin. Stress Triggering of the 1994 M = 6.7 Northridge, California, Earthquake by Its Predecessors. Science, v. 265, 1994, pp. 1432-1435.

Stein, R. S., and M. Lisowski. The 1979 Homestead Valley Earthquake Sequence, California: Control of Aftershocks and Postseismic Deformation. J. Geophys. Res., v. 88, No. B8, 1983, pp. 6477-6490.

Swanson, P. L., L. H. Estey, F. M. Boler, and S. Billington. Mining-Induced Microseismic Event Location Errors: Accuracy and Precision of Mining-Induced Event Locations. Pure and Appl. Geophys., v. 139, 1992, pp. 375-404.

Swanson, P. L., and C. D. Sines. Repetitive Seismicity and Rock Bursting along a Plane Parallel to Known Faulting in the Coeur d'Alene District, ID. Trans. Am. Geophys. Union, v. 71, 1990, p. 1453.

___. Characteristics of Mining-Induced Seismicity and Rock Bursting in a Deep Hard-Rock Mine. USBM RI 9393, 1991, 12 pp.

Wallace, C. A., D. J. Lidke, and R. G. Schmidt. Faults of the Central Part of the Lewis and Clark Line and Fragmentation of the Late Cretaceous Foreland Basin in West-Central Montana. Geol. Soc. Am. Bull. 102, 1990, pp. 1021-1037.

Wallace, R. E., and H. T. Morris. Characteristics of Faults and Shear Zones in Deep Mines. Pure and Appl. Geophys., v. 124, 1986, pp. 107-125.

Whyatt, J. K. Geomechanics of the Caladay Shaft. M.S. Thesis, Univ. Idaho, Moscow, ID, 1986, 195 pp.

Williams, T. J., and D. J. Cuvelier. Report on a Field Trial of an Underhand Longwall Mining-Method to Alleviate Rockburst Hazards. Paper in Rockbursts and Seismicity in Mines. Proceedings of the 2nd International Symposium on Rockbursts and Seismicity in Mines, ed. by C. Fairhurst (Univ. MN, Minneapolis, MN, June 8-10, 1988). Balkema, 1990, pp. 349-353.

Williams, T. J., C. J. Wideman, and D. F. Scott. Case History of a Slip-Type Rockburst. Pure and Appl. Geophys., v. 139, No. 3/4, 1992, pp. 627-637.

STRUCTURAL STRESS AND CONCENTRATION OF MINING-INDUCED SEISMICITY

By J. K. Whyatt,[1] B. G. White,[2] and W. Blake[3]

ABSTRACT

In situ stress on the scale of a tunnel or mine may be distorted by geologic structures. The resulting variations of in situ stress have a direct bearing on the potential for mining-induced seismicity. New evidence from the Lucky Friday Mine collected by U.S. Bureau of Mines researchers, as well as a review of case studies, demonstrates that in situ stress variations affect the spatial distribution of mining-induced seismicity. Although overcore stress measurements have been useful in these studies, they are too expensive and, depending on conditions, may be too difficult to use routinely in mapping stress variations. However, information from borehole and raisebore breakouts; deformation of mine openings; and patterns of seismicity, ground-control problems, and rock-burst damage can be used to build a stress database. This database can then be used in conjunction with maps of mine structure and geology and models of rock mass behavior to build a map of in situ stress variations. Such a map provides a means to anticipate patterns of mining-induced seismicity that are likely to be encountered and, hence, provide a means for planning appropriate measures to ameliorate rock-burst hazards.

INTRODUCTION

Rock bursts constitute a serious ground-control problem in many mines, particularly the deep mines of the Coeur d'Alene Mining District of northern Idaho. The research described here was undertaken by the U.S. Bureau of Mines (USBM) as part of its effort to protect miners from ground control hazards. Protecting miners while preserving the economic viability of seismically active mines requires efficient employment of rock-burst countermeasures, including enhanced ground-control systems, preconditioning, and use of alternative mining methods.

It is well known that mining-induced seismicity is affected by stress magnitude. The pattern of induced stress developed in the vicinity of mine openings has been studied extensively and has provided the basis for improvements in mining methods and sequences. However, mine seismicity often clusters in ways that cannot be explained by mining-induced stress alone.

Because stress is a key factor in determining the intensity of mining-induced seismicity, it appeared likely that some of this clustering was related to natural variations in stress associated with geologic structures. Structural redistribution of stress creates concentrations of stored elastic energy that may drive seismic rock mass failure. As mine excavations approach a structure where stress is concentrated, mining-induced magnification of stress levels hastens loading of intact rock, pillars, and faults to the point of failure.

In situ stress is generally considered to be a primary factor in determining rock mass response to mining and is normally thought of as a uniform rock mass condition. However, solid mechanisms require that, as William Pariseau noted (1994), "loading of a heterogeneous material leads to a heterogeneous stress field." For

[1]Mining engineer, Spokane Research Center, U.S. Bureau of Mines, Spokane, WA.
[2]Geologist, Spokane Research Center.
[3]Consultant, Hayden Lake, ID.

instance, Brady and others (1986) argue that the episodes of tectonic and gravitational loading, fracturing, unloading, heating, cooling, water infusion, drainage, and drying that have occurred in most rock masses preclude a homogeneous stress field. Each of these physicochemical processes is capable of generating a highly heterogeneous stress state in a rock mass. Brady and others also infer that stresses associated with current tectonic processes will dominate the current stress state.

Fairhurst (1986, p. 5) emphasizes the role of rock mass failure in the following argument for presuming variability in natural in situ stress:

> The existence throughout the earth's crust of faults, folds, and fractures in geological structures that have not totally disintegrated clearly indicates that stable redistribution of loads and stresses, and hence heterogeneity of stress distribution, is a pervasive feature in rock masses. Given the usual inhomogeneities, such as folded and faulted rock formations of differing compressibility, and discontinuities, such as faults, joints, bedding planes, it is clear that the in situ gradational and tectonic forces will be distributed more or less nonuniformly through the rock mass.

The critical element of Fairhurst's argument is the stiff or "nonfollowing" nature of the forces that drive disintegration or slip (in the case of rock masses, with joints or discontinuities) within rock masses at depth. That is, unlike many artificial structures, the "essentially infinite" outer boundary of a rock mass ensures the opportunity for the forces to be redistributed from disintegrating or slipping regions into other regions that can sustain these forces. In this case, the disintegrating or slipping rock unloads as it deforms and hence will not disintegrate fully but will stabilize with some residual strength.

Empirical evidence of stress variations associated with geologic structures has been widely reported. Regional, continental, and world-wide patterns of stress have been the subject of considerable study (e.g., world stress - Zoback, 1992; stress in North America - Zoback and Zoback, 1989; stress in Europe - Muller and others, 1992; stress in China - Zhorghuai and others, 1992). Moreover, a number of case studies have documented mine-scale and smaller structural stress variations, some of which have been associated with rock bursts. A selection of these case studies is reviewed in this paper.

Recent advances in rock mechanics and computing power have greatly increased the precision with which the evolution of mining-induced stress fields can be followed over the life of a mine. The ability of numerical models to track a rock mass through significant periods of geologic time, however, is primitive. The controlling variables, especially load history and long-term (geologic) rock mass properties, are difficult to estimate. This factor led Budavari (1983) to conclude that—

> Neither tectonic nor residual stresses lend themselves to analytical treatment. Consequently, their magnitudes are impossible to predict even to a fair degree of certainty without the measurement of in situ stress. In order to obtain a reasonable knowledge of the state of the virgin stress in a region, one must be familiar with its geology, collect and analyze the results of previous stress measurements, and observe the effects of natural stresses on existing structures in rock.

However, some insight into patterns of stress variation can be gained by studying the numerous instances of natural stress variation that have been reported in the literature. This USBM paper describes an investigation of natural stress variations associated with geological structures and the resulting spatial distribution of mining-induced seismicity. A case is made for using geologic information, mine observations, and simple mechanical models to recognize stress variations in operating mines and to apply this knowledge to the design of mine geometry, mining method, mining sequence, and ground-control systems.

INVESTIGATION OF STRUCTURAL STRESS

The greatest obstacle to mapping structural stress distributions in a mine is obtaining sufficient baseline information. As a practical matter, the expense of obtaining in situ stress measurements precludes building stress maps from measurements alone. In this study, direct measurements of in situ stress are supplemented with observations of rock mass conditions and structures indicative of the pattern of in situ stress variation. Various sources of in situ stress information are described in this section. Interpretation of stress patterns with simple mechanical models is described in the following section.

An investigation of in situ stress at the Lucky Friday Mine (Coeur d'Alene Mining District, Idaho) is used to illustrate this procedure. This investigation began with a

simple goal: improve in situ stress estimates to support a numerical model of an experimental stope. However, an overcore measurement collected to provide this improvement was at odds with all previous work involving stress field characteristics in this mine. Additional information was needed to confirm and bound this anomalous stress measurement and support investigations of the underlying structural stress mechanisms.

REGIONAL TECTONIC SETTING

Knowledge of regional geology and tectonic loading provides a foundation for studying local stress fields. Tectonic stresses extend over large areas (hundreds of square kilometers) and have been well mapped for the continental United States (figure 1). However, Cuisiat and Haimson (1993) note that local stresses can differ from regional stresses as a result of topographic relief, rock structure (faults, folds, or joints), or changes in rock properties. They estimate the extent of these stress perturbations to be as large as several square kilometers. Thus, while a region may be characterized by a well-documented state of stress, stress on the scale of a mine, or a part of a mine, may be quite different.

The Coeur d'Alene district lies within the Lewis and Clark line (figure 2), a major tectonic lineament that has undergone right-lateral slip, indicating a northwest orientation of maximum principal stress. This orientation has been generally confirmed by other indications of stress direction (Hobbs and others, 1965; Skinner and others, 1974). [On the other hand, Zoback and Zoback (1989) place a question mark in this area on their tectonic map of North America (figure 1).]

GEOLOGIC MAPPING AND ANALYSIS

A good understanding of rock structure and the relative mechanical properties of rock mass elements is essential to any study of structural stresses. Some geologic features relevant to rock bursts are only observable on a

Figure 1
Stress Provinces of United States.

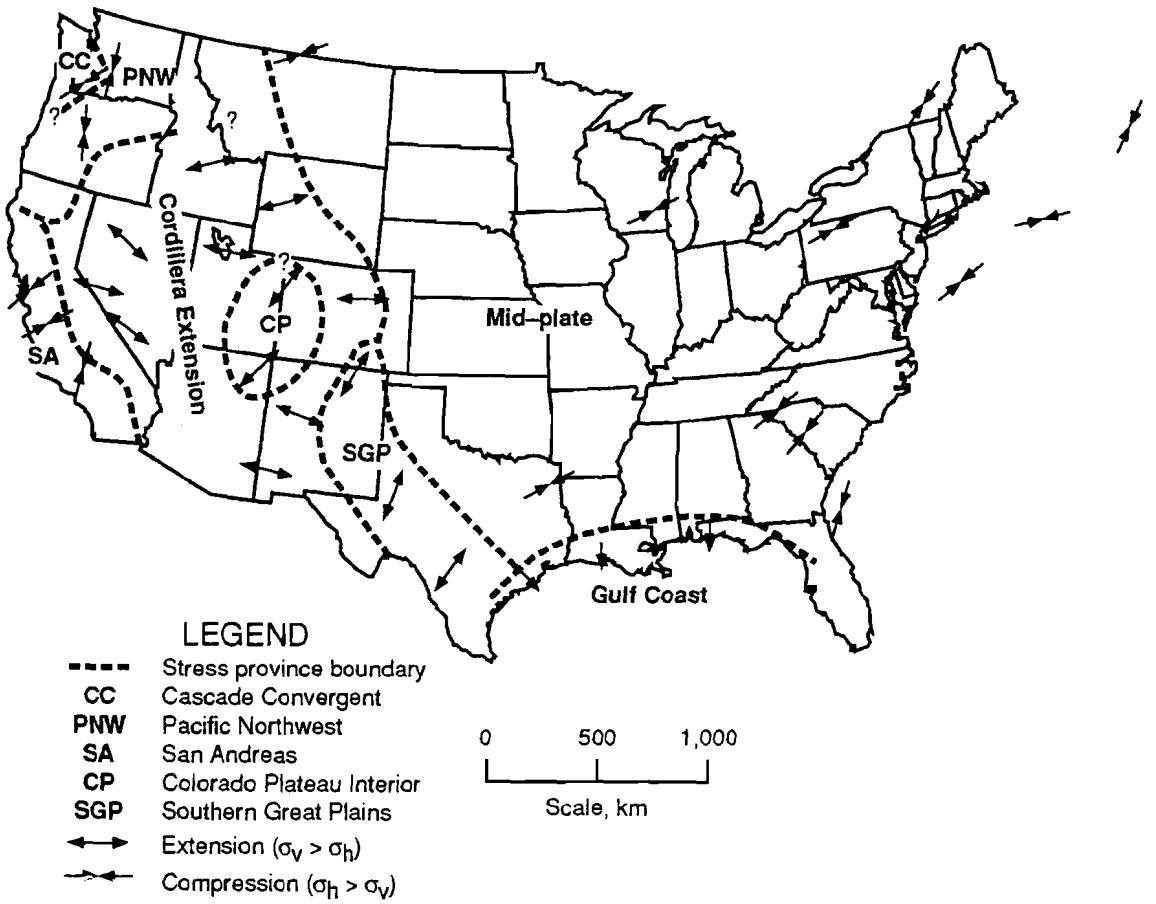

σ_v = Vertical stress. σ_h = Horizontal stress. (After Zoback and Zoback, 1989.)

Figure 2
Lucky Friday Mine and Regional Geology.

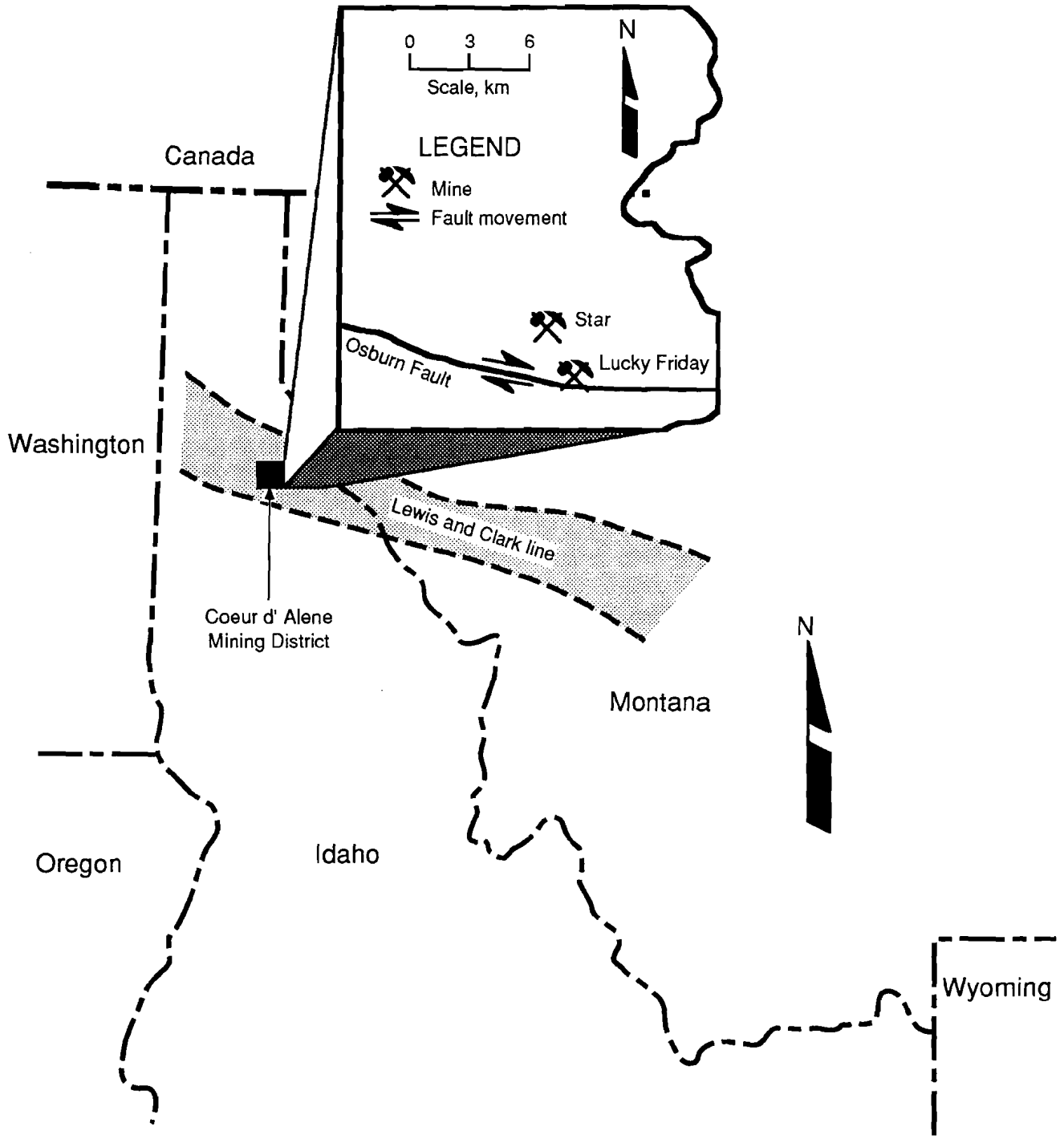

microscopic scale. Examination of these small-scale features often aids understanding of rock mass behavior. However, most geologic information can be acquired through careful mine mapping at standard mapping scales. Proper interpretation and clear presentation of these features are keys to recognizing significant structural stress patterns and mechanisms.

Geologic mapping was a significant part of the Lucky Friday Mine investigation, and a number of features were mapped, including faults, folds, and stratigraphy. Rocks are predominately composed of quartz and fine-grained white mica, generally known as sericite in this region, and are classified into three major rock types according to relative sericite content. From sericite-rich to sericite-poor, these types are defined as siltite-argillite, sericitic quartzite, and vitreous quartzite. The strength, stiffness, and brittleness of the rock increases greatly as sericite content is reduced. The argillite-siltite beds are very weak, have a soapy feel, and occur in laminations ranging from millimeters to several centimeters thick. Sericitic quartzite beds are considerably more competent. Vitreous quartzite beds are extremely strong, stiff, and brittle.

Direct mapping of these beds, few of which are greater than a meter in thickness, produced complex geologic maps that were difficult to relate to large-scale rock mass behavior (figure 3). However, soft sericitic quartzite beds occur in clusters and are associated with thin, very soft, argillite-siltite beds. Hard vitreous quartzite beds also occur in clusters and are often joined by a relatively strong, fused interface. These natural groups of relatively hard and soft beds were used to define subunits 20 to 50 m thick. The result (figure 4) provided a much clearer picture of mine-scale variations in lithology.

OVERCORE MEASUREMENTS

Overcore measurements provide a full three-dimensional measure of principal stress magnitudes and directions at a specific location. Hydraulic fracturing can also be used to measure some stress components. These techniques are covered in most rock mechanics texts (e.g., Goodman, 1989; Jaeger and Cook, 1979), and standard test procedures have been published by the International Society for Rock Mechanics (1987). While useful, these measurements are generally too expensive for routine use in mapping of structural stress patterns. Rock mass conditions, including core discing, may also preclude use of some overcore cells altogether. However, conducting one or two measurements provides a valuable anchor for establishing stress magnitudes.

The Lucky Friday Mine investigation benefitted from three overcore measurements,[4] two of which were conducted during early development of this method. While the original analyses of the early measurements were largely valid, a detailed reanalysis improved the solutions and provided a look at small-scale stress variability. One site, on the 4250 level of the mine, straddled vitreous and sericitic subunits and provided a direct view of structural stress differences between hard and soft subunits (figure 5). A similar measurement on the 5300 level, located in a hard subunit near a fault, presented a puzzling stress rotation that became the motivating factor for much of this work. An adequate explanation of this anomalous rotation required much more information than the single overcore measurement could provide. In order to avoid the costs associated with additional overcore measurements, other sources of information were sought.

BREAKOUT MAPPING

In many cases, stress characteristics can be observed in the deformation of mine openings. Breakouts in boreholes, bored raises, and relatively equidimensional drifts can provide essential information on stress direction (figure 6). The use of breakouts to deduce stress orientation has been widely reported (e.g., Zoback and others, 1985) and is used in well bores. Similar routinely observations of rock deformation and failure have also been used to deduce the orientation of stresses in coal mines (Mucho and Mark, 1994). Any evidence of spatial variations in the existence or severity of ground control problems can also be instructive.

At the Lucky Friday Mine, several vertical bored raises and ore passes experienced breakouts that indicated the orientation of horizontal secondary principal stresses (figure 7). Stress directions in sericitic and vitreous subunits (figures 8 and 9, respectively) were generally in agreement. A breakout in a vitreous quartzite subunit near the 5300-level site confirmed the overcore stress rotation and bounded it to vitreous subunits near the 38/Offset Fault, considerably clarifying the problem.

SEISMICITY

The distribution of mining-induced seismicity is also a good indicator of structural stress conditions because

[4]This research by Whyatt and others will be published in a forthcoming series of USBM Reports of Investigations, of which the first (Whyatt and Beus, 1995) is now available.

Figure 3
Geologic Map Showing Closely Spaced Features at Lucky Friday Mine.

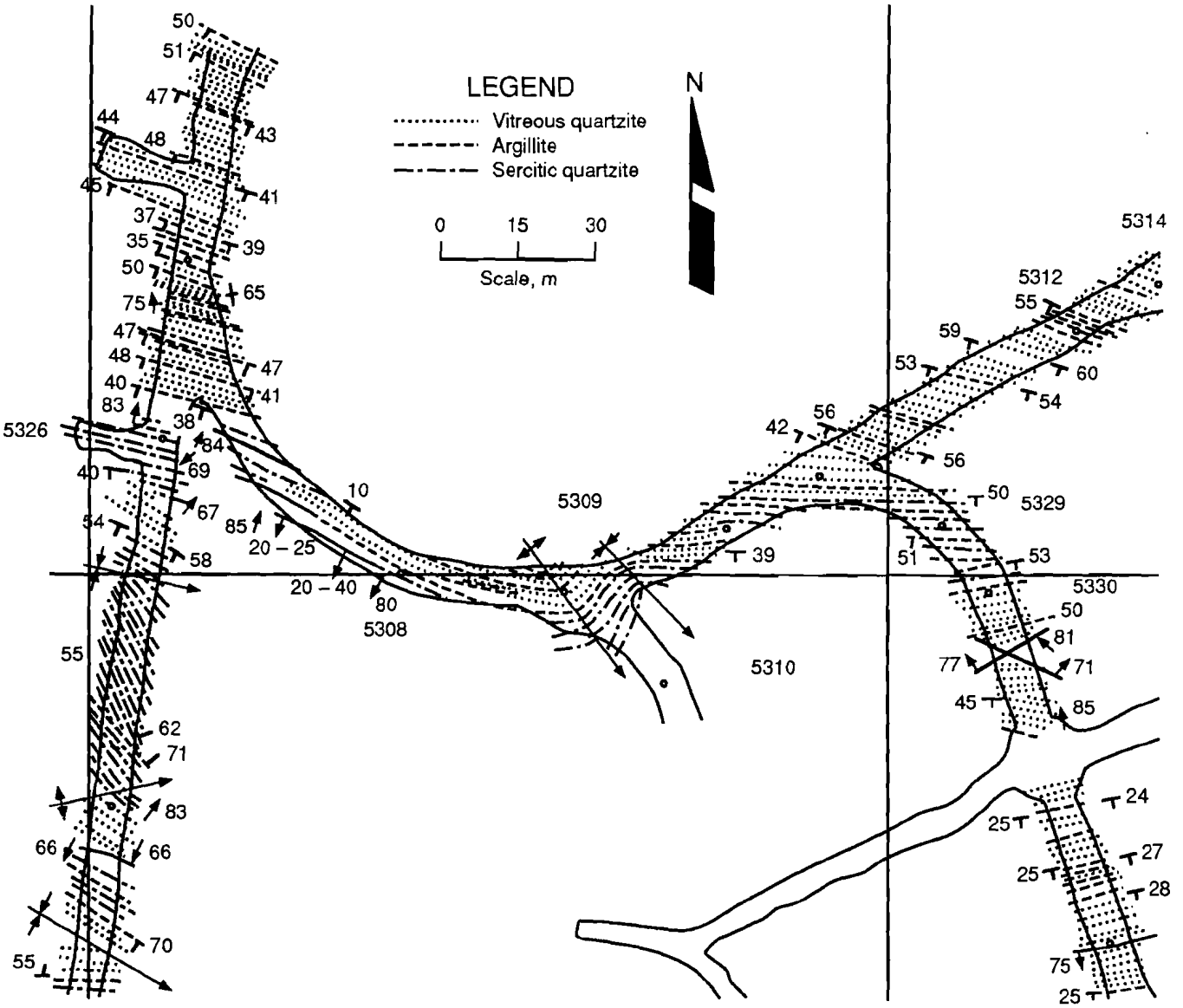

Figure 4
Geology of Lucky Friday Mine.

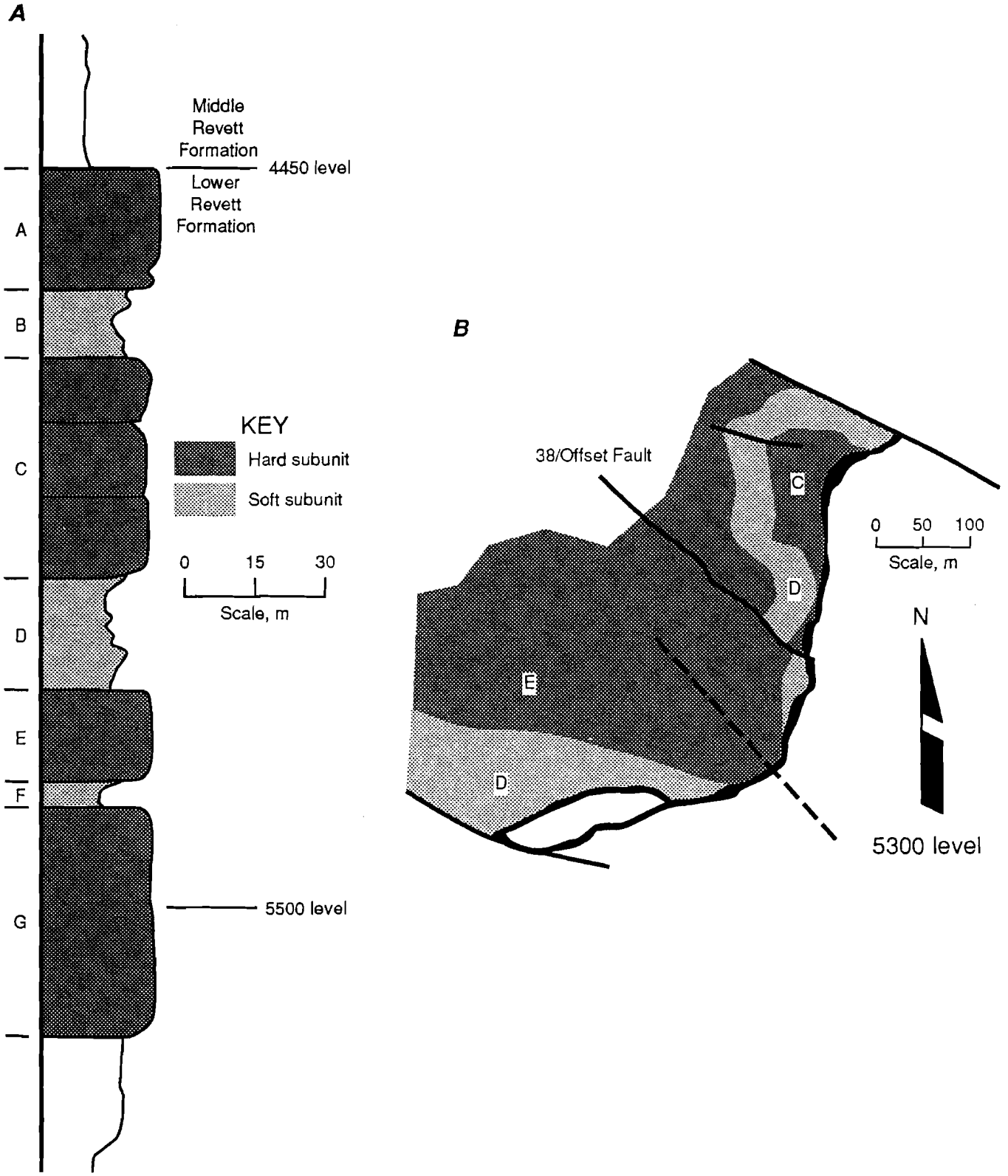

A, Simplified geologic column; *B*, 5300 level plan view. Dotted line indicates trace of axial plane of Hook anticline. The 38/Offset Fault splits into two faults, the 38 Fault and the Offset Fault, above the 5100 level.

Figure 5
Stress Change Across Subunit Boundary Measured at 4250-Level Site, Lucky Friday Mine.

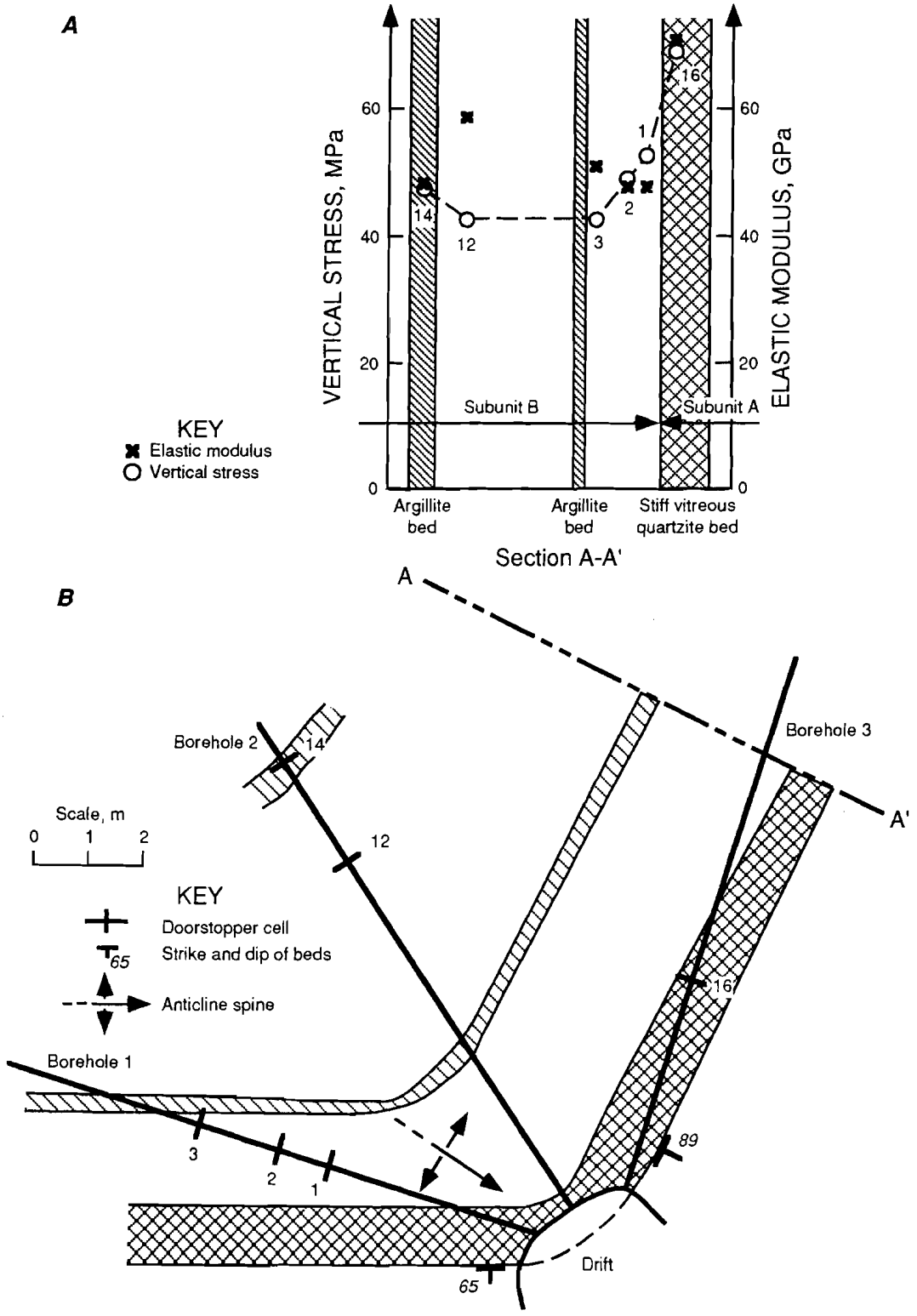

A, Vitreous quartzite is part of hard subunit A, while argillite and unmarked sericitic quartzite are part of soft subunit B. *B*, Vertical stress and elastic modulus plotted by stratigraphic location in an anticline at test site.

Figure 6
Typical Breakout Pattern and Orientation of Maximum Stress (o_1) in Plane Perpendicular to Opening.

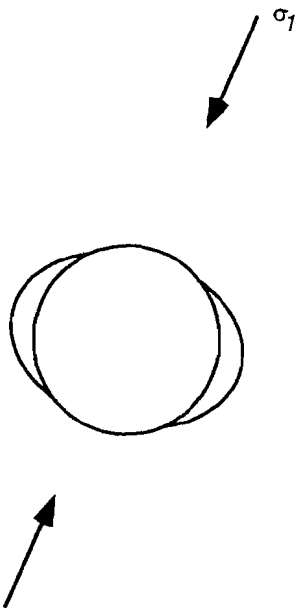

seismicity generally results when a geologic structure is stressed to its limits. Seismicity is generally preferred to rock-burst damage for tracing structural stresses because rock-burst damage depends on many other factors, including ground support measures and local geologic structures. In mines with digital seismic monitoring systems, first-motion patterns of seismic events can also be measured. For slip events, a double-couple, first-motion pattern shows directions of lengthening and shortening consistent with local stress conditions.

Geologic factors clearly influence the occurrence of bursting in development openings at the Lucky Friday Mine and the adjacent Star Mine. Beds of massive vitreous quartzite have proven, in general, to be more burst-prone than the thin-bedded sericitic quartzite (e.g., Blake, 1987). However, not all massive quartzites have proven to be burst-prone, and damaging rock bursts in thin-bedded sericitic quartzite do occur.

At the Lucky Friday Mine, clusters of large seismic events and damaging rock bursts are routinely reported. Some of these clusters are clearly controlled by mining-induced stress (in pillars, etc.). However, other clusters occur in development openings far enough away from mining that natural stress concentrations are suspect. One such cluster was noted by mine staff in development openings and immediately east of the axial plane of the Hook anticline (figure 10), from the 5150 to the 5400 levels.

One of these rock bursts, documented by Williams and others (1992), indicated a direction of strike-slip movement that was clearly impossible in the regionally predominant in situ stress field. Evidence of the direction of strike-slip movement, including direct observations of slip offset in a ramp and a first-motion analysis of digitally recorded waveforms, indicated a local rotation of the maximum principal stress from a north-west to a west-southwest direction.

STRESS PATTERN INTERPRETATION

Developing descriptions of stress patterns likely to exist in common geologic structures is the next step in this mapping procedure. These patterns are used to extrapolate stress conditions in unmeasured portions of the rock mass from the stress database. In this section, structural stresses resulting from simple models including (1) regions of different elastic properties and (2) discontinuities are examined. Model conditions have been selected to provide a sample of simple structural stress mechanisms, but are not meant to be all-inclusive. These simple models are compared to a number of published case studies and Lucky Friday Mine stress information.

CONTRASTING ROCK PROPERTIES

One of the simplest and most common set of assumptions in developing numerical models is that the rock mass is initially unstressed, elastic, homogeneous, and subject to simple displacement or stress boundary conditions. This set of assumptions disregards the complex load and deformation history of the rock and considers only the elastic response of the rock to present tectonic loading. The ideal, unfractured rock mass responds to changes in load as if it were a continuum, and the resulting stresses and strains can be calculated with the tools of continuum

Figure 7
Bored Raises and Ore Passes, Lucky Friday Mine.

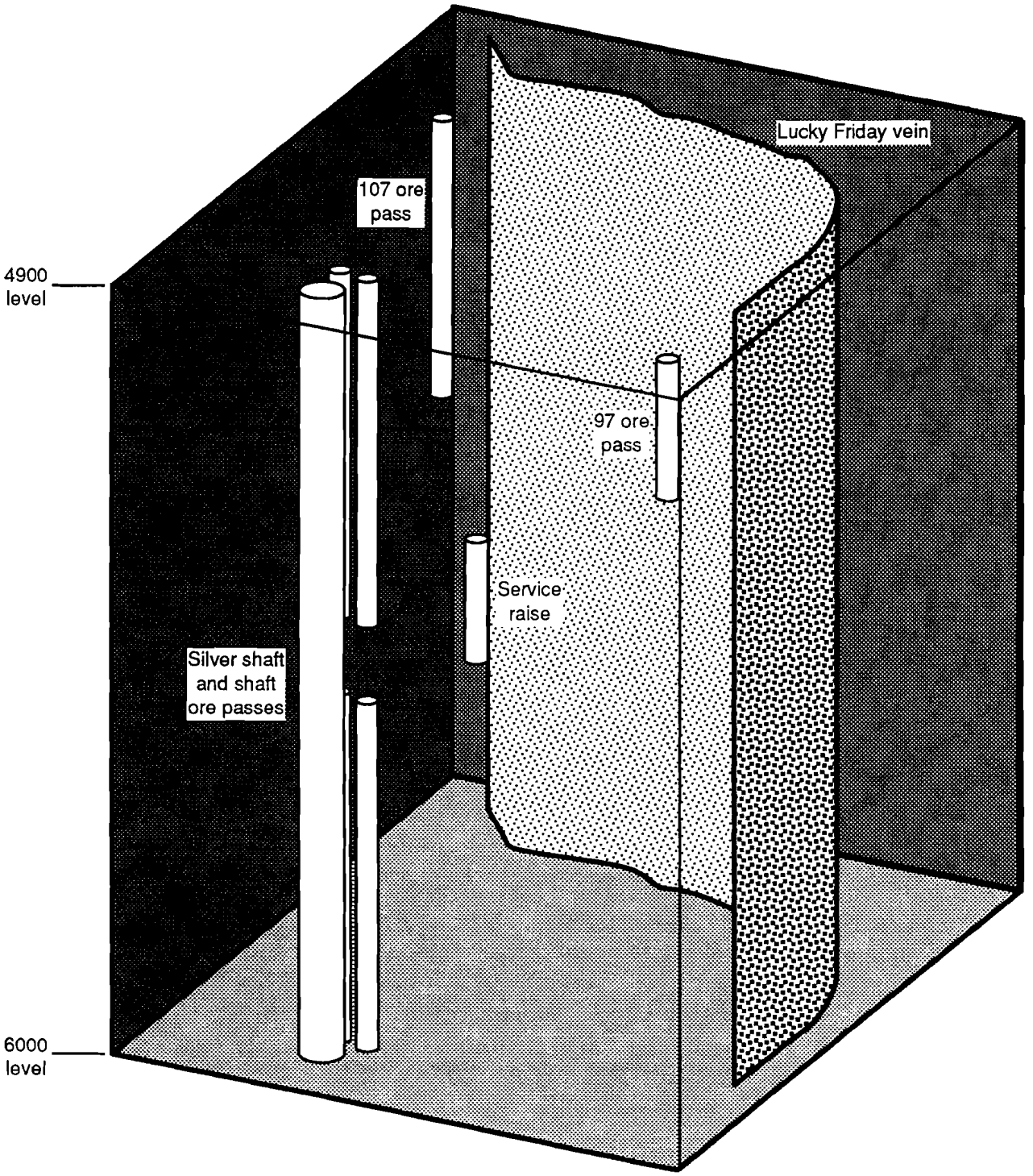

Figure 8
Horizontal Stress Orientation in Sericitic Quartzite Subunits On and Around 5300 Level, Lucky Friday Mine.

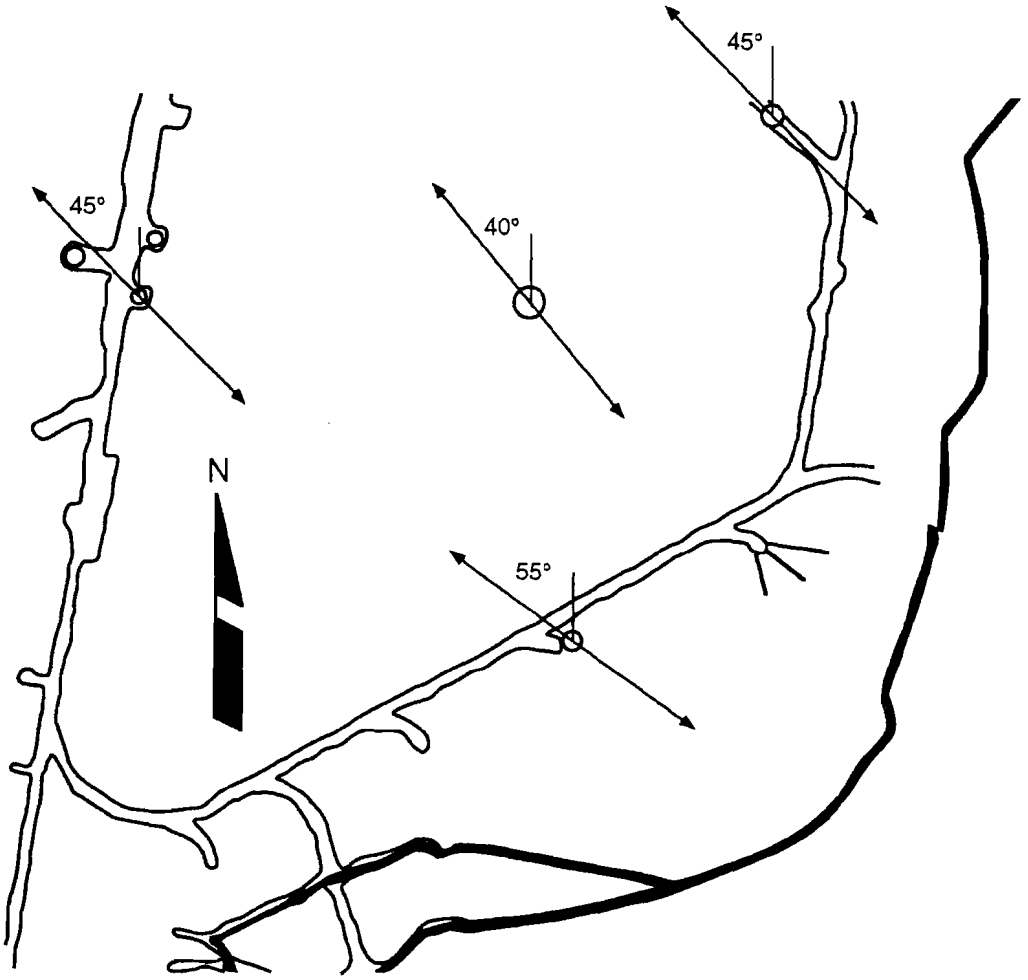

Figure 9
Horizontal Stress Orientation in Vitreous Quartzite Subunits On and Around 5300 Level, Lucky Friday Mine.

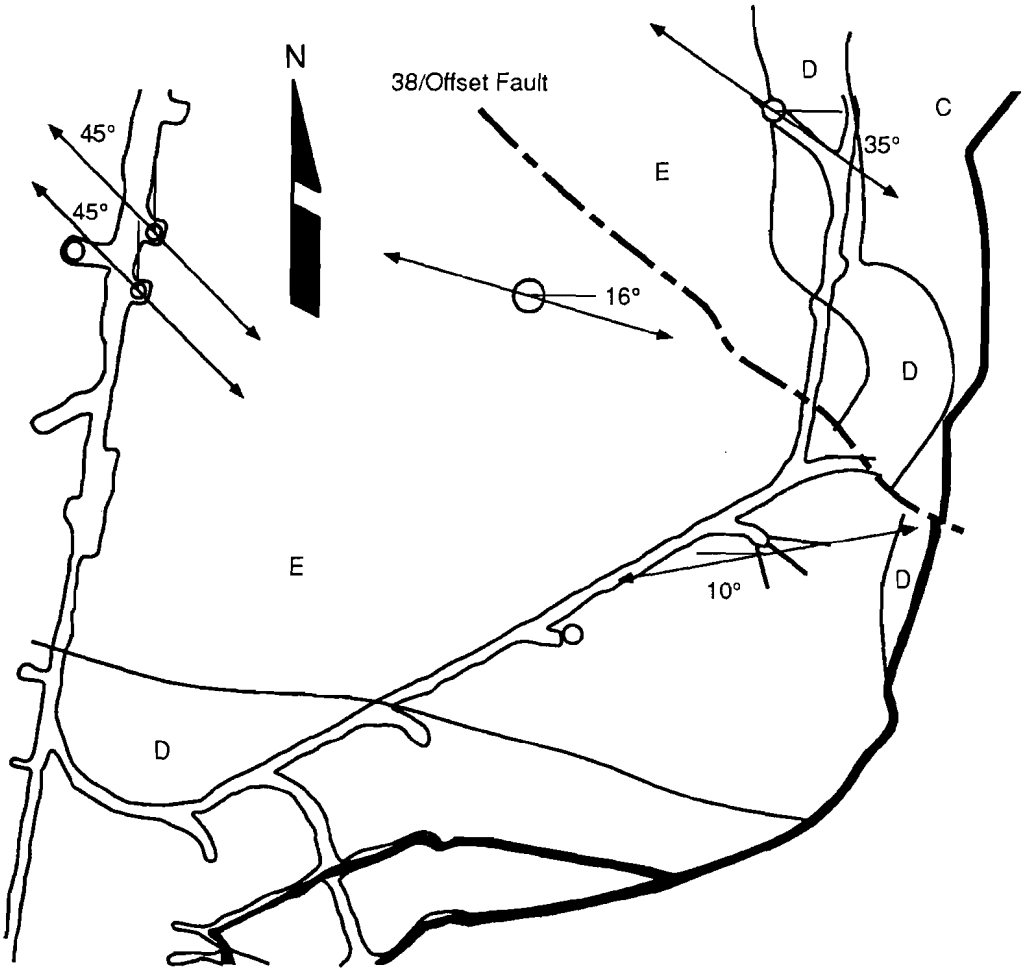

Figure 10
Concentration of Seismicity and Rock Bursts Near Axial Plane of Hook Anticline During Development.

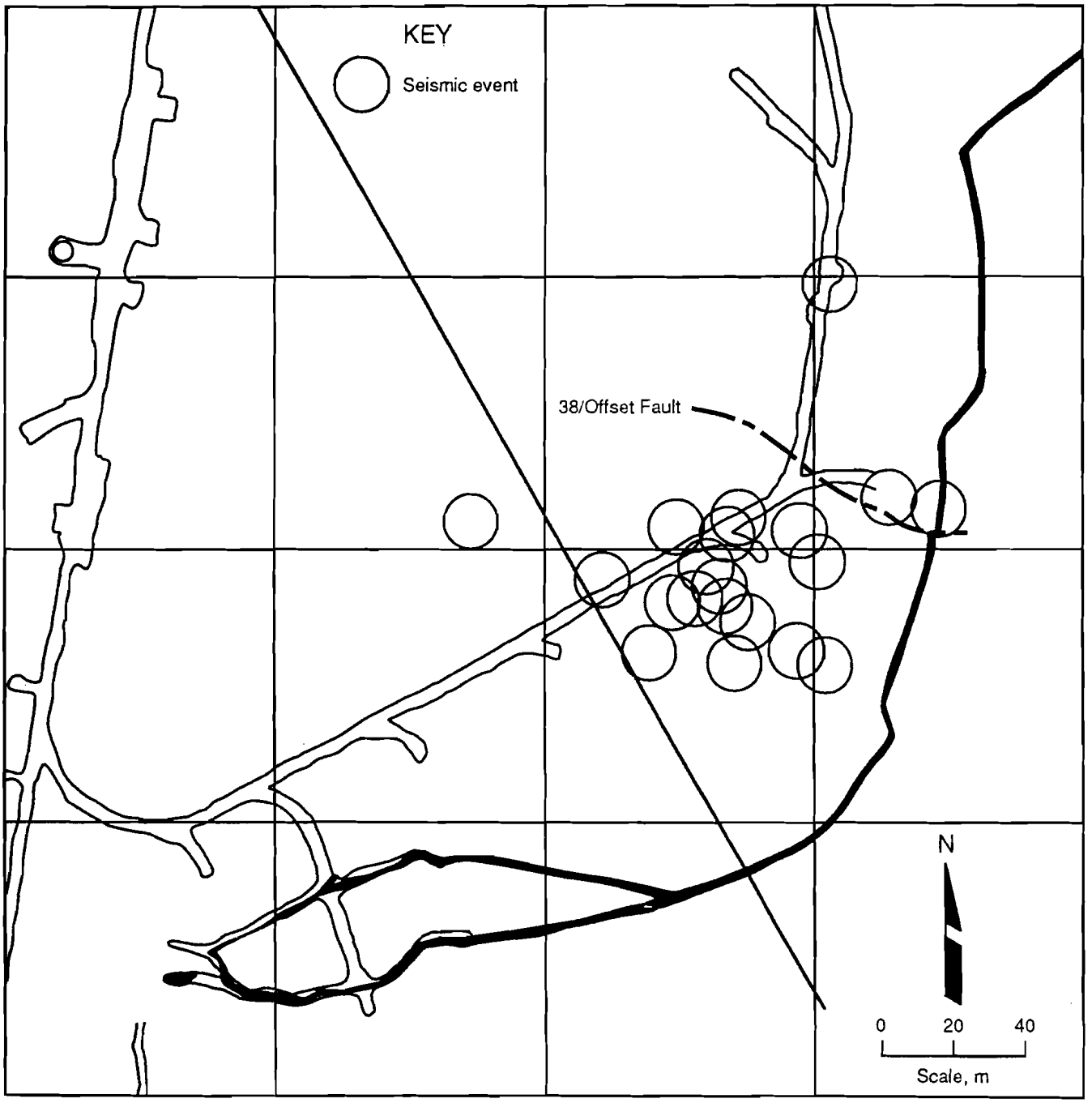

mechanics. This approach has proven to be both appropriate and valuable for studying stresses and deformations induced by mining.

Rock masses often contain a number of rock types with different elastic properties. The introduction of regions with different elastic properties is a simple extension of this approach that can generate significant structural stresses. For purposes of analysis, the shapes of these regions can be classified generally into inclusions and strata, depending on whether the region is locally bounded or extends indefinitely. Stresses and displacements induced in these complex geologic structures by mining can be readily estimated with any of a number of computer programs. The types of structural stress associated with each of these geometries can be explored through simple models and case studies.

Inclusions

The primary effect of hard and soft inclusions is that hard inclusions attract soft inclusions and shed stresses from the surrounding rock mass. One of the simplest cases to solve involves a cylindrical inclusion of rock that has either a stiffer or a softer elastic modulus than the surrounding rock mass. This problem has been solved exactly (see Jaeger and Cook, 1979, pp. 261-264). The stress pattern induced around a soft inclusion resembles the pattern that develops around a similarly shaped void (a void is obviously a very soft inclusion).

Irregular inclusions can be readily analyzed with most stress analysis programs. As an example, a rectangular soft inclusion with one-fourth the stiffness of the surrounding rock was analyzed using a ratio of principal stresses in a horizontal plane of 2:1. The greatest principal stress was oriented perpendicular to the long axis of the soft inclusion. The results show both concentration and reduction of stress (figure 11).

A soft inclusion encountered at Minnova, Inc.'s, Ansil deposit 500 km northwest of Montreal, PQ, in the Canadian shield has a similar rectangular geometry in plan section. Germain and Bawden (1989) measured highly unusual in situ stress tensors at depths between 1,200 and 1,500 m. The stresses were seemingly unrelated to normal regional field stresses. They concluded that the mine's massive sulfide ore body behaved as a soft inclusion relative to the host formations. Consequently, the natural concentration of stress around the soft inclusion resulted in zones of rock bursting and heavy ground in some development openings (figure 12). Zones of reduced stress, which resulted in sections of loose blocks in the stope wall, were also encountered.

Strata

The ability of parallel plates to develop in-plane stress in proportion to elastic modulus under constant strain conditions is well known. In geologic settings, stiffer strata tend to concentrate in-plane stress as well. Goodman (1989) provides a simple example of a tunnel encountering varying stresses as it passed through a fold (figure 13). This model is a simple, two-dimensional version of the saddle-shaped folding of vitreous quartzite strata in the vicinity of the Lucky Friday Mine (figure 14). Vertical stress jumps in hard strata can be seen in the generic example of figure 13 and stresses measured at the 4,250 level overcore site (figure 5). Similar results have been reported in coal mines (Maleki and others, 1992).

McGarr and others (1975) studied seismicity in East Rand Proprietary Mines and found activity concentrated in a stiff set of beds in the reef hanging wall. These beds were unusually thick and consisted of quartzite with a glassy texture. In contrast, the rocks in the footwall were thinly bedded and more argillaceous. McGarr and others also noted increased activity in an aplite sill (actually a dike cutting the strata at a low angle). They found that both stress and seismicity were concentrated in the quartz strata and aplite sill.

FAULTS, JOINTS, AND FRACTURES

An alternative set of simple models can be built from the same initial ideal rock mass by introducing discontinuities representing faults, fractures, and/or joints instead of regions containing different rock types. For this analysis, the discontinuities are treated as simple frictional interfaces with no cohesion, although the friction angle is allowed to vary. This model is available in most stress analysis programs for rock mechanics.

Slip

Slip on discontinuities disrupts the continuous variation of stress and concentrates shear strain, redistributes shear stress, and causes jumps in the stress component parallel to the discontinuity. The effects of discontinuity slip are illustrated in the case of steeply inclined faults near the surface (Crouch and Starfield, 1983). In this case, the faults are considered to be frictionless. Fault slip causes a rotation of principal stresses towards orientations either parallel or perpendicular to the fault (figure 15).

An example of the ability of discontinuities to create spatial variability in both stress and rock bursting was reported by Martna and Hansen (1986). They describe

Figure 11
Structural Stresses Developed by Rectangular (2.5:1) Soft Inclusion in Biaxial Stress Field (σ_x:σ_y = 2:1).

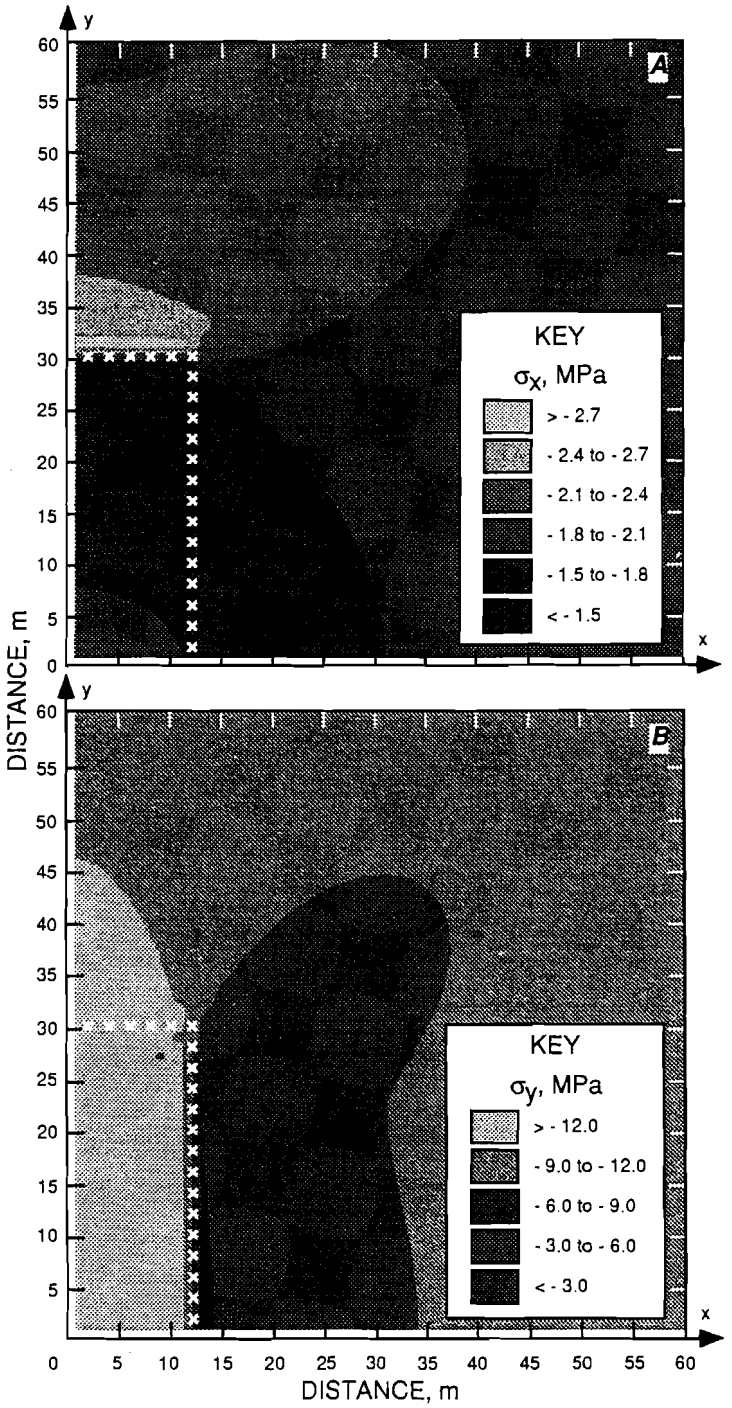

The soft inclusion has one-fourth the elastic modulus of the surrounding rock. Tangential stress in the surrounding rock on the boundary of the soft inclusion is (*A*) increased on the boundary parallel to the greatest principal stress (σ_x) and (*B*) reduced parallel to the least principal stress (σ_y). The stress analysis was conducted with the finite-difference program FLAC, version 3.22 (Itasca, 1993).

Figure 12
Ground Conditions and Assumed Stress Behavior.

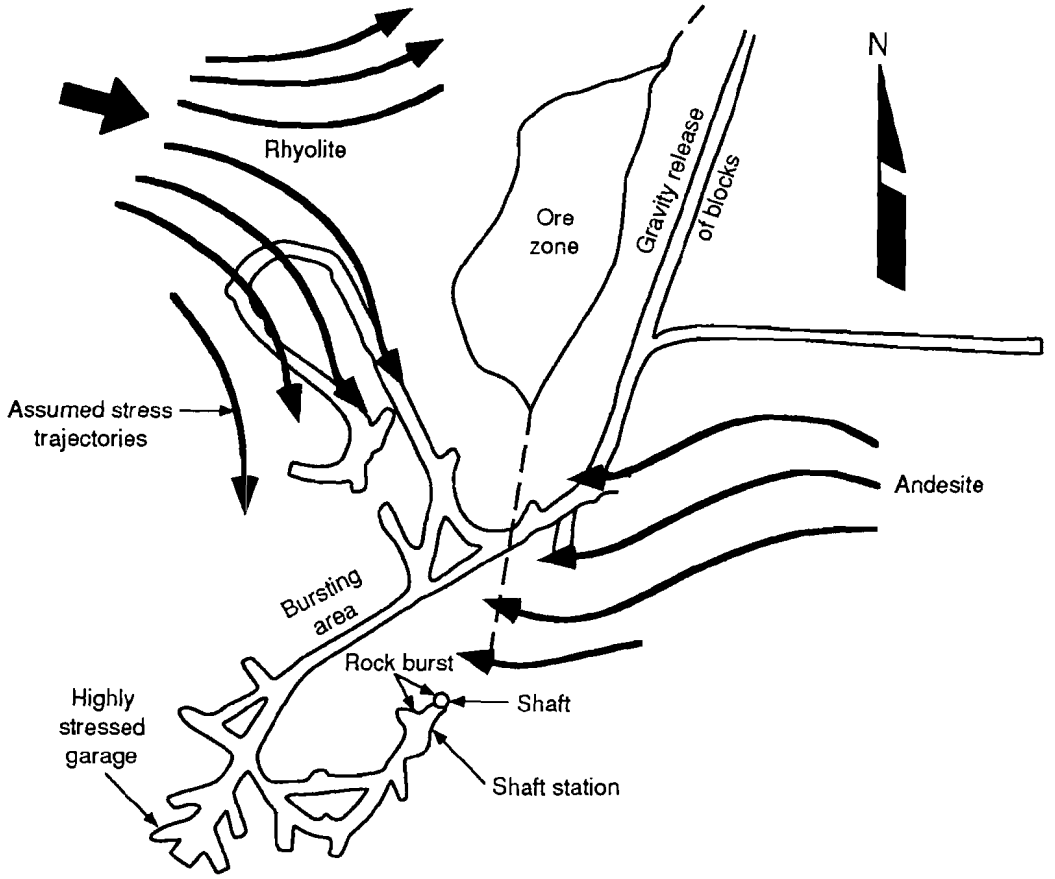

Plan view of 9th level, Ansil deposit (after Germain and Bawden, 1989).

Figure 13
Influence of Fold in Heterogeneous, Layered Rock on Vertical Stresses.

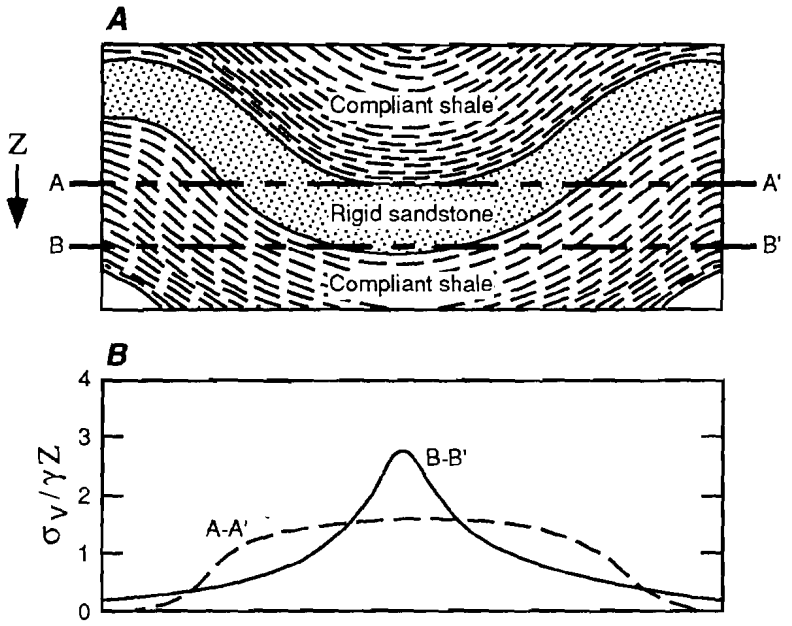

A, Vertical section cutting across typical fold; *B*, vertical stress sections A-A′ and B-B′ (after Goodman, 1989). Z = Depth. σ_v = Vertical stress. γ = Density.

Figure 14
Folds in Vicinity of Lucky Friday Mine.

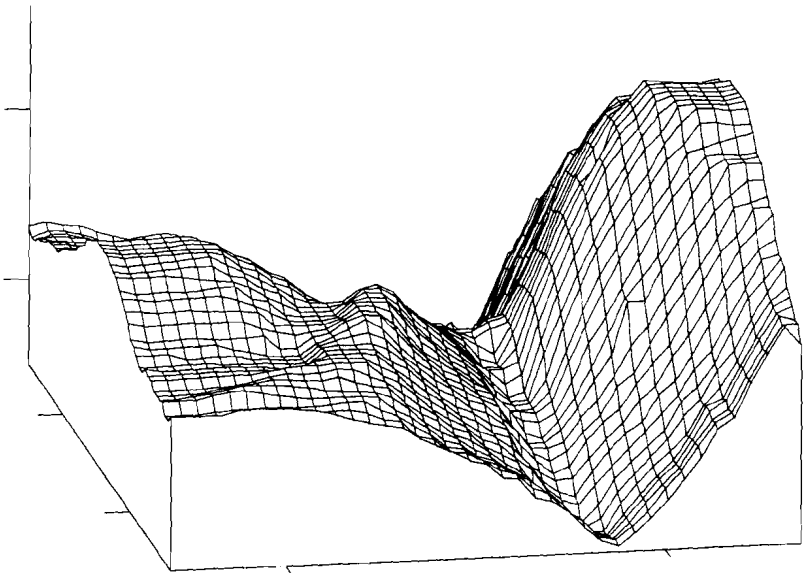

Intersecting west-northwest- and north-northeast-striking sets of folds create complex saddle-shaped geometry. Limbs of saddle concentrate stress as indicated by 4250 overcore measurement (see figure 5) and Goodman's model (see figure 13).

a set of 134 rock stress measurements and rock burst experiences during excavation of Vietas headrace tunnels No. 2 and 3 in Sweden. Very high stresses were measured in sections of the tunnel where rock bursts occurred, with the maximum stress four to five times overburden pressure. Other sections were relatively unstressed except for overburden pressure. The high-stress rock-burst zones appeared to be controlled by a series of faults that formed a graben. Stress measurements provided a clear picture of a significant stress discontinuity across a fault boundary of the graben (figure 16).

Asperities

The resistance to slip on a discontinuity depends on a number of factors, many of which vary along the discontinuity. For instance, surface roughness and material properties are important factors in determining the friction angle of sliding surfaces. Discontinuities that have experienced significant offset through geologic deformation are often slickensided in the direction of slip, although they often are corrugated in other directions.

Corrugations and variations in friction angle introduce spatial variations in the resistance to slip and result in structural redistribution of stress. Strong sections, commonly referred to as asperities, concentrate shear stress when weaker sections slip. The resulting stress field (figure 17) can be calculated with off-the-shelf software. In this case, the model shows local elevation of shear stress magnitudes and rotation of principal stress orientation. Slip at such an asperity has an increased potential for releasing a significant amount of seismic energy and damaging mine openings.

The localized stress rotation and rock bursting observed along the Offset/38 Fault at the Lucky Friday Mine (recall figures 9 and 10) correspond to the characteristics observed in the fault asperity model. The asperity appears to be located in a small area where vitreous quartzite is contained in both walls of the fault (figure 4). Adjacent regions of the fault have weaker sericitic quartzite in one or the other wall.

Figure 15
Stress Field Computed for Inclined Faults With Boundary-Element Method.

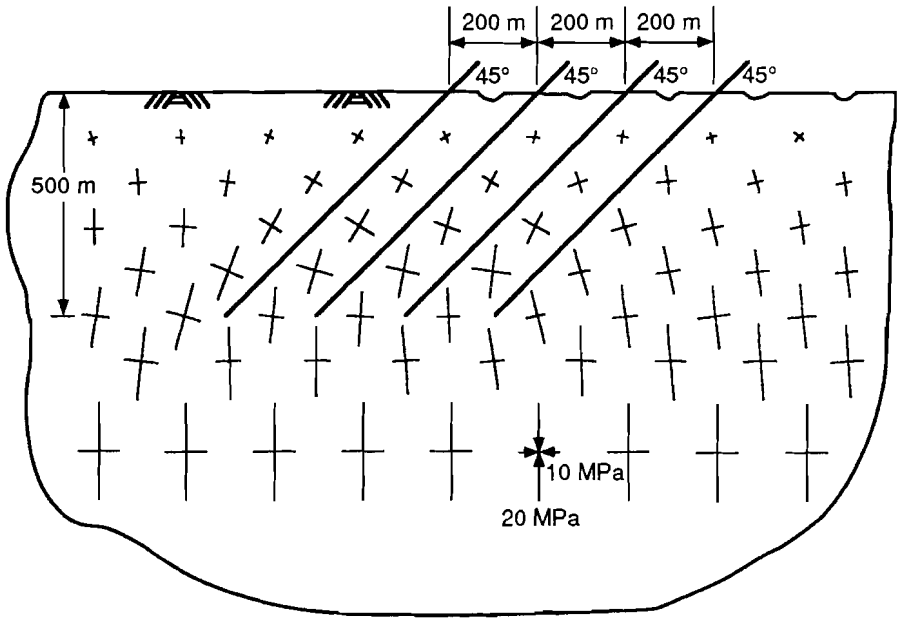

(After Crouch and Starfield, 1983.)

Figure 16
Rock Stresses Around Fault at Section 5 + 320 (Tunnel 3), Vietas Headrace, Sweden.

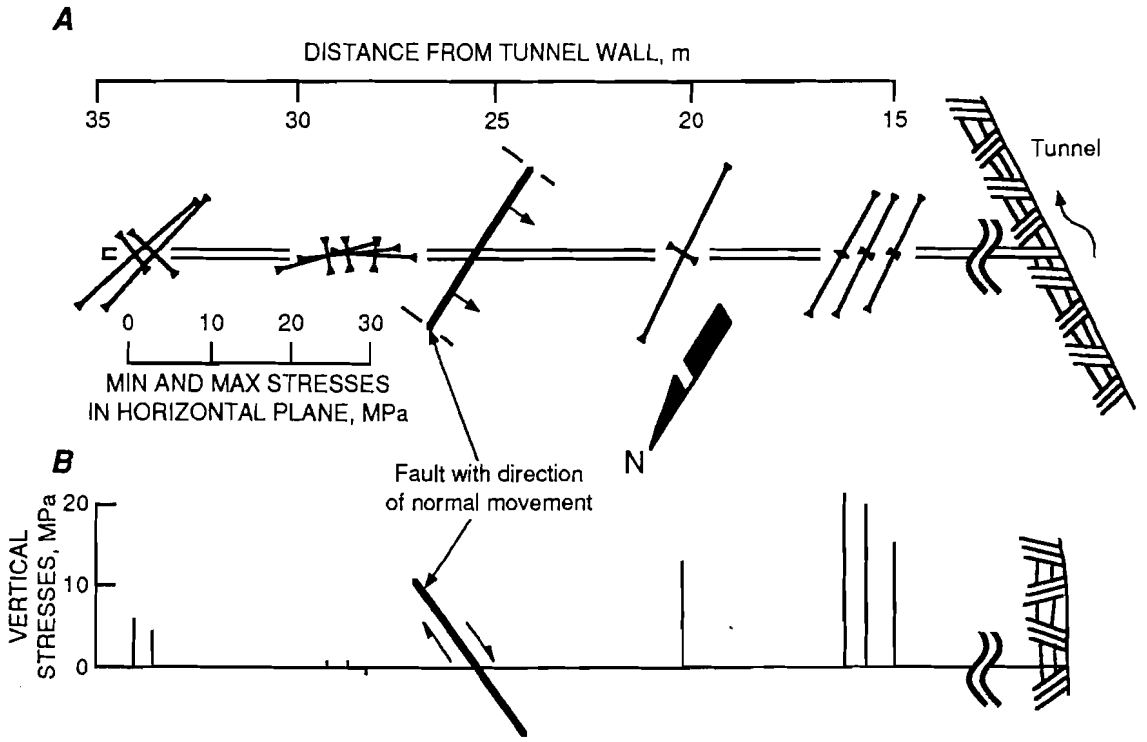

A, Horizontal principal stress; *B*, vertical stresses measured in borehole crossing normal fault. Note differences in stress direction and level between hanging wall and footwall on fault (after Martna and Hansen, 1986).

Figure 17
Idealized Model of Structural Stresses.

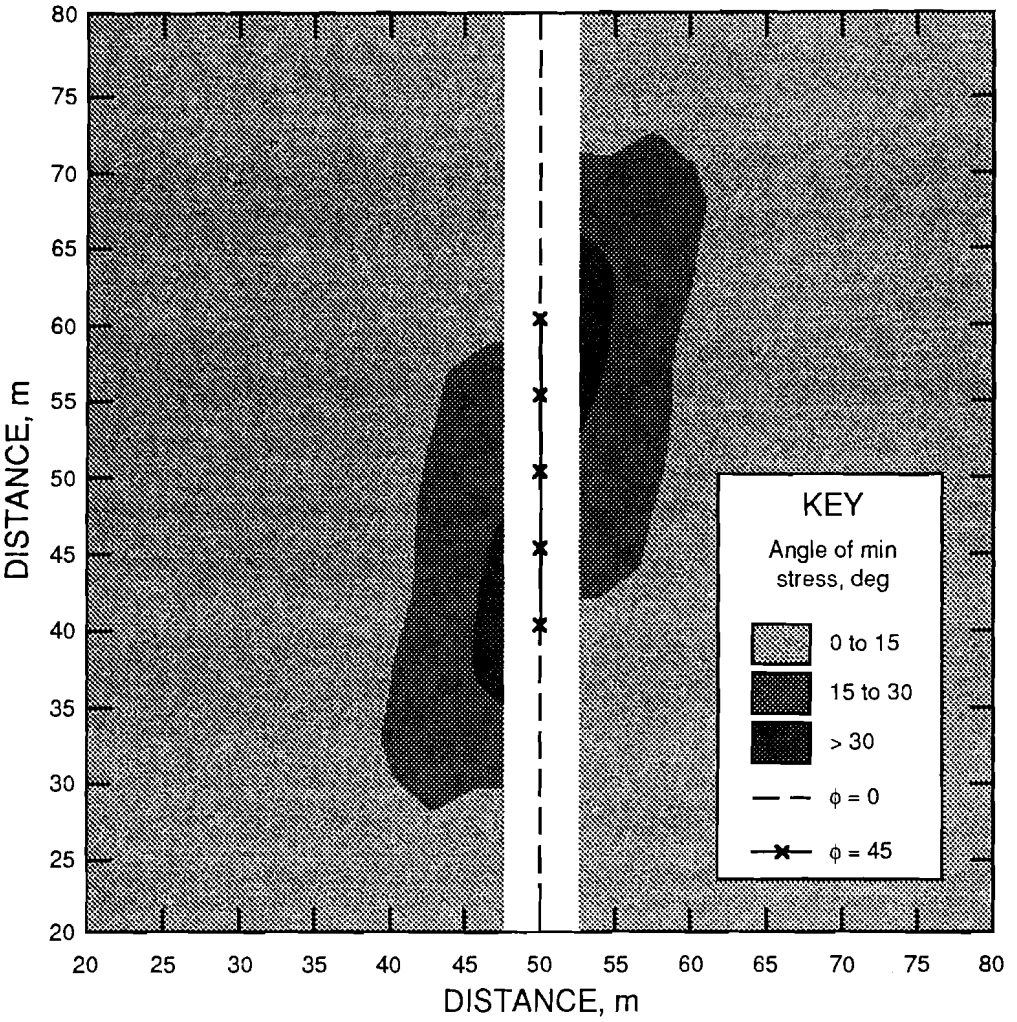

This model shows pattern of structural stresses resulting from strong asperity on weak fault. Weak sections of fault are modeled as having no strength, and asperity is modeled with friction angle (ϕ) of 45°. Stress analysis was conducted with finite-difference program FLAC, version 3.22 (Itasca, 1993).

DISCUSSION AND CONCLUSIONS

An understanding of the structural stress variations present in a seismically active mine can be used to optimize design criteria for support elements, preconditioning, and pillars. In the absence of any knowledge of stress field variation, a design must be sufficiently conservative so that localized stress variations, whatever they may be, will not exceed design strength, a potentially expensive provision. With adequate knowledge, barrier pillars can be positioned in zones of natural concentrations of stress while extraction ratios can be increased in other, naturally destressed, areas, providing a sufficient safety factor while freeing ore reserves.

The formation of rock occurs during a complex load and deformation history spanning geologic epochs, creating an intractable mechanical problem. However, the mechanical response of rock to short-term loading is well understood, and models constructed on this basis can produce stress patterns that are qualitatively comparable to those encountered in a number of case studies. Quantitative stress estimates can be developed by fitting the stress pattern to stress measurements and observations.

This process has been used successfully to develop an understanding of a number of structural stress mechanisms at the Lucky Friday Mine, including increased in-plane stresses in hard subunits and rotation of principal stress directions near a fault asperity, that have localized mining-induced seismicity. Ongoing work is aimed at identifying additional zones of localized seismic activity, analyzing stress patterns in three dimensions, and projecting structural stress patterns to anticipate future patterns of mining-induced seismicity.

ACKNOWLEDGMENTS

Dr. Charles Fairhurst, Department of Mining Engineering, University of Minnesota, Minneapolis, MN; Mark Board, Itasca Consulting Group, Minneapolis, MN; and Mel Poad, group supervisor, Spokane Research Center, USBM, Spokane, WA, provided invaluable support and guidance during this protracted study. The assistance provided by Ted Williams, Jeff Johnson, Mike Jenkins, and Robert McKibbin, mining engineers at the Spokane Research Center, in collecting information for the Lucky Friday Mine in situ stress database is also gratefully acknowledged.

REFERENCES

Blake, W. Rock Burst Occurrences in the Coeur d'Alene Mining District of Northern Idaho. Paper in 6th International Conference on Ground Control in Mining: Proceedings, ed. by S. S. Peng (WV Univ., Morgantown, WV, June 9-11, 1987). Dep. of Min. Eng., WV Univ., 1987, pp. 52-60.

Brady, B. H. G., J. V. Lemos, and P. A. Cundall. Stress Measurement Schemes for Jointed and Fractured Rock. Paper in Rock Stress and Rock Stress Measurements: Proceedings of the International Symposium on Rock Stress and Rock Stress Measurements, ed. by O. Stephansson (Stockholm, Sept. 1-3, 1986). Centek, Lulea, Sweden, 1986, pp. 3-17.

Budavari, S. Response of the Rock Mass to Excavations Underground. Paper in Rock Mechanics in Mining Practice, ed. by S. Budavari. S. Afr. Inst. of Min. and Metall., Johannesburg, S. Afr., 1983, pp. 55-76.

Crouch, S. L., and A. M. Starfield. Boundary Element Methods in Solid Mechanics. George Allen and Unwin, London, 1983, 321 pp.

Cuisiat, F. D., and B. C. Haimson. The Scale Dependency of In Situ Rock Stress Measurements. Paper in Scale Effects in Rock Masses 93, ed. by Pinto da Cunha. Balkema, 1993, pp. 15-25.

Fairhurst, C. In Situ Stress Determination—An Appraisal of Its Significance in Rock Mechanics. Paper in Rock Stress and Rock Stress Measurements: Proceedings of the International Symposium on Rock Stress Measurements, ed. by O. Stephansson (Stockholm, Sept. 1-3, 1986). Centek, Lulea, Sweden, 1986, pp. 3-17.

Germain, P., and W. F. Bawden. Interpretation of Abnormal In Situ Stress in Great Depth. Paper in Rock at Great Depth: Rock Mechanics and Rock Physics at Great Depth, ed. by V. Maury and D. Fourmaintraux (Proc., ISRM Symp., Paris, Aug. 28, 1989). V. 2, Balkema, 1989, pp. 999-1004.

Goodman, R. E. Introduction to Rock Mechanics. John Wiley and Sons, 2nd ed, 1989, 562 pp.

Hobbs, S. W., A. B. Griggs, R. E. Wallace, and A. B. Campbell. Geology of the Coeur d'Alene District, Shoshone County, Idaho. U.S. Geol. Surv. Prof. Paper 478, 1965, 139 pp.

International Society for Rock Mechanics. Suggested Methods for Rock Stress Determination. Int. J. Rock Mech. Min. Sci. & Geomech. Abstr., v. 24, No. 1, 1987, pp. 53-74.

Itasca Consulting Group, Minneapolis, MN. FLAC: *Fast Lagrangian Analysis of Continua*. User's Manual, Version 3.22. V. 1, 1993.

Jaeger, J. C., and N. G. W. Cook. Fundamentals of Rock Mechanics. 3rd ed., Chapman and Hall, 1979, 593 pp.

Maleki, H., W. Ibrahim, Y. Jung, and P. A. Edminster. Development of an Integrated Monitoring System for Evaluating Roof Stability. Paper in Proceedings, Fourth Conference on Ground Control for Midwestern U.S. Coal Mines, ed. by Y. P. Chugh and G. A. Beasley (Mt. Vernon, IL, Nov. 2-4, 1992). Dep. of Min. Eng., S. IL Univ., 1992, pp. 255-271.

Martna, J., and L. Hansen. Initial Rock Stresses Around the Vietas Headrace Tunnels Nos. 2 and 3, Sweden. Paper in Rock Stress and Rock Stress Measurements: Proceedings of the International Symposium on Rock Stress and Rock Stress Measurements, ed. O. Stephansson (Stockholm, Sept. 1-3, 1986). Centek, Lulea, Sweden, 1986, pp. 605-613.

McGarr, A., S. M. Spottiswoode, and N. C. Gay. Relationship of Mine Tremors to Induced Stresses and to Rock Properties in the Focal Region. Bull. Seism. Soc. Am., v. 65, No. 4, 1975, pp. 981-993.

Mucho, T. P., and C. Mark. Determining Horizontal Stress Direction Using the Stress Mapping Technique. Paper in Proceedings of 13th International Conference on Ground Control in Mining, ed. by S. S. Peng (WV Univ., Morgantown, WV, Aug. 2-4, 1994). Dep. of Min. Eng., WV. Univ., 1994, pp. 277-289.

Muller, B., M. L. Zoback, K. Fuchs, L. Mastin, G. Gergersen, N. Pavoni, O. Stephansson, and C. Ljunggren. Regional Patterns of Tectonic Stress in Europe. J. Geophys. Res., v. 97, No. B8, 1992, pp. 11,783-11,803.

Skinner, E. H., G. G. Waddell, and J. P. Conway. In Situ Determination of Rock Behavior by Overcore Stress Relief Method, Physical Property Measurements, and Initial Deformation Method. USBM RI 7962, 1974, 87 pp.

Whyatt, J. K., and M. J. Beus. In Situ Stress at the Lucky Friday Mine (In Four Parts): 1. Reanalysis of Overcore Measurement from 4250 Level. USBM RI 9532, 1995, 25 pp.

Williams, T. J., C. J. Wideman, and D. F. Scott. Case History of a Slip-Type Rockburst. PAGEOPH, v. 139, No. 3/4, 1992, pp. 627-637.

Zhonghuai, X., W. Suyun, H. Yurui, and G. Ajia. Tectonic Stress Field of China Inferred from a Large Number of Small Earthquakes. J. Geophys. Res., v. 97, No. B8, 1992, pp. 11,867-11,877.

Zoback, M. D., D. Moos, L. Mastin, and R. N. Anderson. Well Bore Breakouts and In Situ Stress. J. Geophys. Res., v. 90, No. B7, 1985, pp. 5523-5530.

Zoback, M. L. First- and Second-Order Patterns of Stress in the Lithosphere: The World Stress Map Project. J. Geophys. Res., v. 97, No. B8, 1992, pp. 11,703-11,728.

Zoback, M. L., and M. D. Zoback. Tectonic Stress Field of North America. Ch. in Geophysical Framework of the Continental United States. Geol. Soc. of Am. Mem. 172, 1989, pp. 339-366.

COMPARISON OF DATA FROM IN-MINE ROCK-BURST MONITORING SYSTEMS AND NORTH IDAHO SEISMIC NETWORK, LUCKY FRIDAY MINE, MULLAN, ID

By T. J. Williams,[1] C. J. Wideman,[2] K. F. Sprenke,[3] J. M. Girard,[4] and T. L. Nichols[1]

ABSTRACT

Rock bursts have been a problem in the Coeur d'Alene Mining District of northern Idaho for nearly a century. For over 20 years, acoustic monitoring systems installed at the Galena Mine, Lucky Friday Mine, Star Mine, and Sunshine Mine have gathered data on rock bursts and microseismic events. Currently, three separate systems monitor seismicity and rock bursts at the Lucky Friday Mine. A microseismic system run by the mine provides event locations, a macroseismic system operated by the U.S. Bureau of Mines estimates event locations and saves full waveform files for seismic studies, and the North Idaho Seismic Network monitors rock bursts in the mine as well as seismic activity near the mine not covered by the other two systems. This paper is a review of the data acquisition and analysis methods and presents an example showing how the systems complement each other.

INTRODUCTION

Rock bursts have been a problem in the Coeur d'Alene Mining District of northern Idaho from as early as 1914, when two miners were killed in an "air blast" in the Greenhill-Cleveland Mine (Bell, 1914). The first microseismic system used to study acoustic emissions associated with rock bursts was designed by the U.S. Bureau of Mines (USBM) Denver Research Center (DRC) (Obert, 1941). The theory behind the microseismic system is that arrival times for an acoustic wave front caused by failure in highly stressed rock can be recorded by an array of geophones (figure 1). The source of the wavefront can then be estimated using any of several mathematical algorithms (Blake and others, 1974). The precision of the location is determined by the density of the array; that is, the more geophones, the better the identification of the source location. The first of the modern generation of microseismic monitoring systems was installed at the Galena Mine in the late 1960's by DRC (Blake and others, 1974) and monitoring continued until the mine ceased operations in 1992 (Swanson and others, 1992; Boler and Swanson, 1990).

At the Lucky Friday Mine (figure 2), the first microseismic system became operational in December 1973 (Langstaff, 1974) and is still operating today with an upgraded computer system. This system provides data on wavefront arrival times from each of the geophones and a reading on the relative energy of the seismic event. From the arrival times at geophones with known coordinates and an estimated velocity structure, the location of the event is calculated. The goal of the microseismic studies was to develop historical patterns of microseismicity prior to large rock bursts to assist in predicting similar rock bursts in the future. There have been few successful predictions, but mine management routinely uses seismic frequency data from the system when deciding whether to keep miners out of an area.

The complex geology at the mine is one reason why predicting events is difficult; that is, wave paths and velocity structure cannot be determined because of the variation in rock type. Another reason is that while the

[1]Mining engineer, Spokane Research Center, U.S. Bureau of Mines, Spokane, WA.

[2]Professor of geophysical engineering, Montana College of Mining and Technology, Butte, MT.

[3]Professor of geophysics, University of Idaho, Moscow, ID.

[4]General engineer, Spokane Research Center.

Figure 1
Seismic Source Location Geometry.

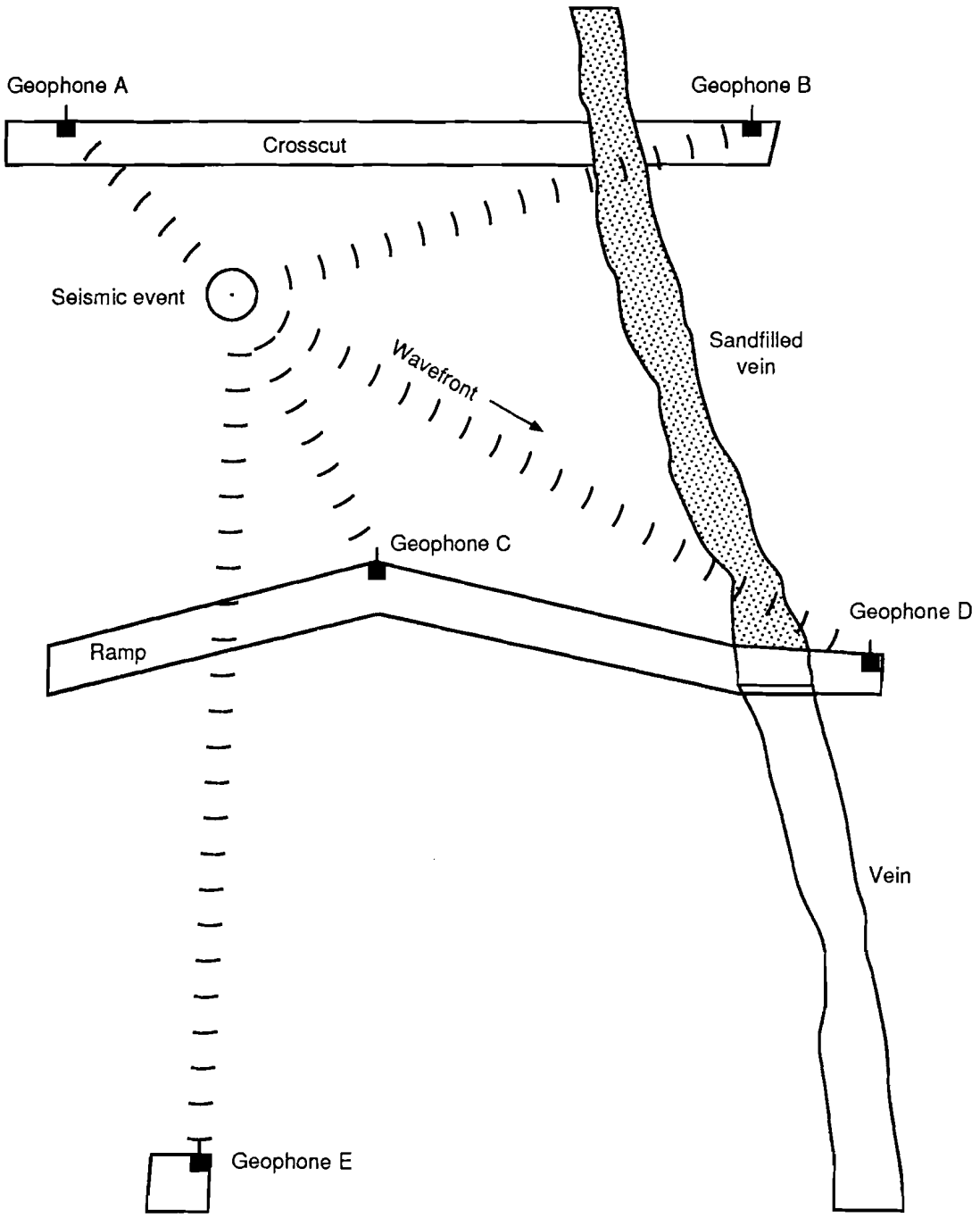

microseismic system provides location and timing information for a statistical analysis, no information is provided on the mechanism of failure. Information on the geologic setting of the Lucky Friday Mine and the interaction between mining-induced changes in the regional stress field and the actual failure mechanism are needed to understand the rock-burst problem.

Cost reductions brought about by advances in design of personal-computer-(PC) based seismic monitoring, particularly the International Association of Seismology and Physics of the Earth's Interior (IASPEI) system, by the U.S. Geological Survey (USGS) in the late 1980's (Lee and others, 1988) led to the USBM installing a macroseismic system for gathering full waveform data from rock bursts at the Lucky Friday Mine in 1989. Full waveform data can be used in many ways, but the goal of the USBM was to conduct first-motion studies to determine failure mechanisms and to relate these mechanisms to mining and local geology.

The theory behind first-motion analysis is that when two sides of a fault move relative to one another, the wavefront P-waves traveling from the center of the event will have compressional and dilatational phases. These phases are defined by the polarity of the first motion arriving at a recording station; in general, positive first arrivals are from compressional P-waves and negative first arrivals are from dilatational P-waves. Movement along a fault always generates two possible solutions when this method is used, so information about the geologic structure is needed to choose the right solution. Figure 3*A* illustrates this relationship for right-lateral movement along a vertical fault striking east-west or for left-lateral movement along a vertical fault striking north-south. Figure 3*B* shows first-motion output from a geophone as projected on a Schmidt net.

Full waveform recording of seismic events and the use of three-component seismometers were described by Jenkins and others (1990). The paper by Girard and others (1995) in this proceedings describes the hardware for this system in detail. The in-mine design of the macroseismic

Figure 2
Map of Lucky Friday Mine.

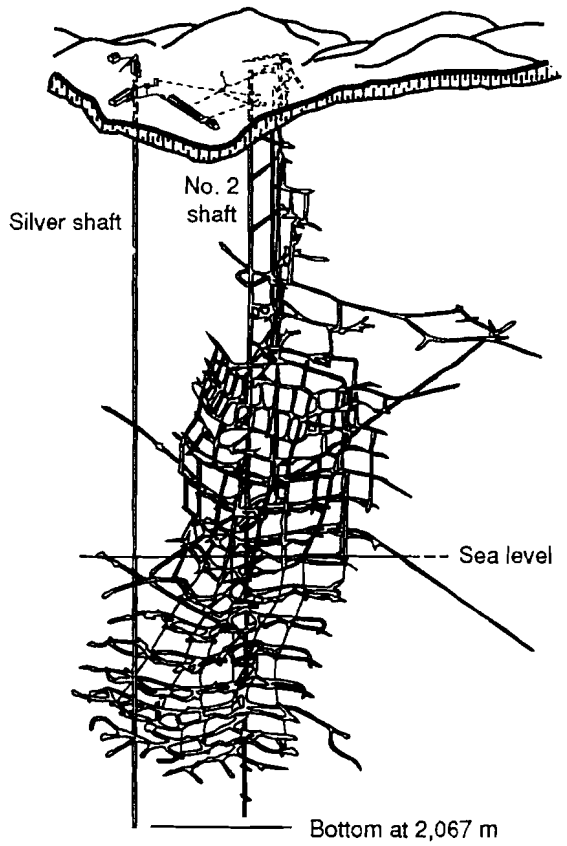

Figure 3
Representation of Fault-Slip First Motion.

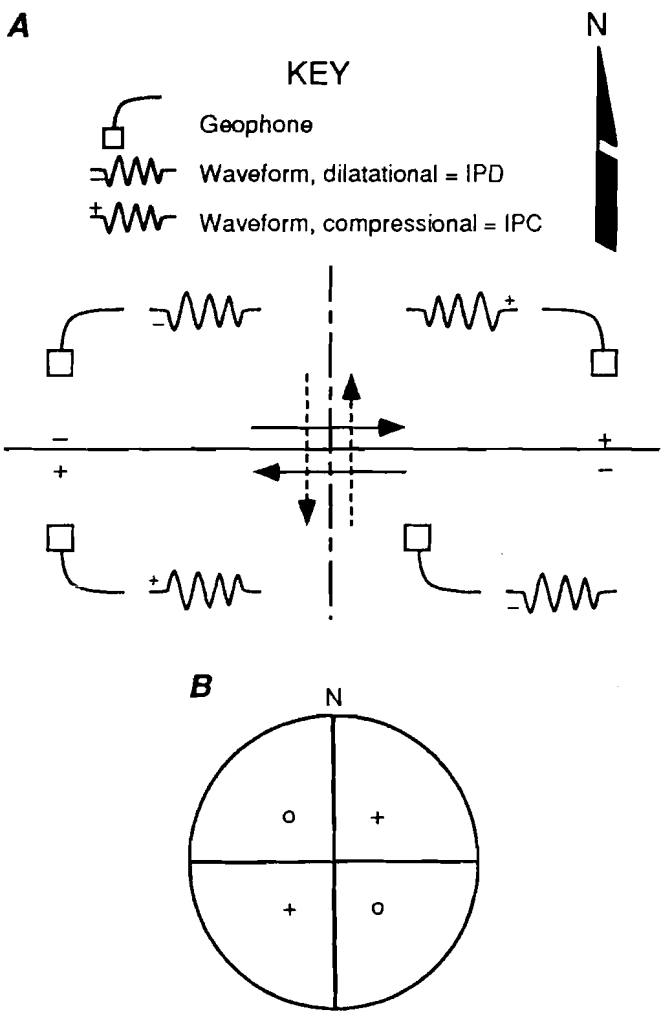

A, Sensing first motions on fault; *B*, Schmidt net representation.

system was considerably different than the design of the original IASPEI system. The geophone locations are approximately 350 m apart, whereas the IASPEI system was designed for geophone spacings on the order of tens of kilometers. Thus, arrival picks and location codes lacked sufficient numerical precision for the macroseismic array. The USBM developed several programs to adapt the macroseismic system for the IASPEI software. This paper briefly describes the software for the system and the data analysis procedures.

The regional nature of the problem suggested that a district-wide seismic monitoring network could be used to identify similarities and differences between rock bursts at various mines in the district, as well as to record any regional earthquakes. It could also record data from events near a mine but outside the areas covered by the in-mine array. The three-geophone surface array installed by the University of Idaho in 1983 was expanded to 16 geophones funded by the USBM in 1991.[5] The array, the North Idaho Seismic Network (NISN), consists of geophones positioned around the Coeur d'Alene Mining District and powered by solar panels and 12-V batteries (figure 4). Signals from the geophones are sent via radio telemetry to the Lucky Friday Mine. At the mine, an IBM-type PC running the IASPEI software records the events. Because this is a regional array, no modifications to the processing software were needed. Another advantage of the NISN is that geophone locations are not restricted to areas where there are accessible mine openings, which is the case with the macroseismic system, so there is better coverage of the mine.

This paper provides a discussion of the interaction among the three systems and data for a seismic event at the edge of the macroseismic array. Analysis of the data shows the source locations from the micro- and macroseismic systems were consistent and that the NISN data were consistent with the data gathered by the macroseismic system. With only the macroseismic data, the source mechanism was poorly constrained, but when combined with the NISN data, the source mechanism indicated an implosional event.

Figure 4
Installation of NISN Station.

GEOLOGIC SETTING

Figure 5 shows a plan view of the 5100 level of the Lucky Friday Mine and three major zones (A, B, and C) in the mine. In general, the trend of the mine workings is northeast-southwest; however, some mine workings trend north-south or east-west.

There are abrupt changes in the orientations of geologic formations throughout the mine. In the northeast portion of the mine, bedding trends north-south and dips steeply to the east. However, close to the North Control Fault, where the event described in this paper occurred, strikes and dips of the beds change rapidly. The North Control Fault is a major tectonic feature that strikes northwest and dips at a near-vertical angle. Offset on the fault is believed to be left-lateral,[6] and near the fault, the strike of the bedding can change by as much as 90°.

In the southwest portion of the mine (zone B in figure 5), the general strike of the bedding is approximately

[5]Funds for district-wide rock-burst monitoring and analysis were provided to the University of Idaho by the USBM's Generic Mineral Technology for Mines System Design and Ground Control, Virginia Polytechnic Institute, Blackburg, VA.

[6]Personal communication from W. Blake, mining consultant, Hayden Lake, ID, 1989.

Figure 5
Plan View of 5100 Level, Lucky Friday Mine.

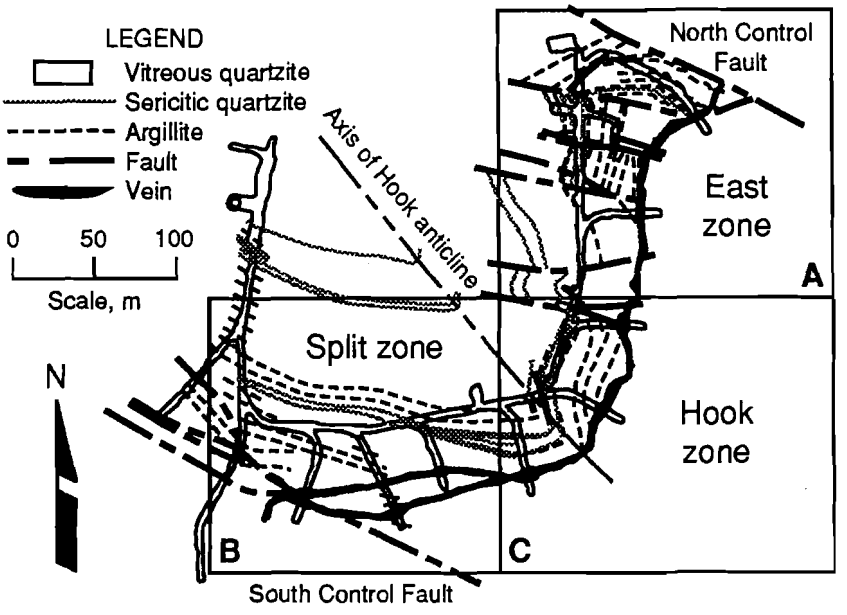

east-west and dips are to the south. Another major tectonic feature, the South Control Fault, is located in this area of the mine. The intersection between bedding and faults in zone B is not as complex as at the intersection in zone A. Because trends of bedding and faulting are similar and because some tectonic separation is thought to have occurred as a result of slip along bedding planes, the identification of faults in the southwest portion of the mine is somewhat difficult (Scott and others, 1993).

MICROSEISMIC SYSTEM

Figure 6 shows a plan view of the Lucky Friday microseismic array as it was in late 1993. The geophones are approximately 60 m apart. The signals received by the geophones are amplified and sent over a series of wires to an Electrolab MP250 system. The MP250 processes the incoming signals to determine if five or more with sufficient energy have arrived in a 100-ms time window. If the trigger criteria are met, the MP250 sends arrival times and channel numbers to a PC (table 1). The computer immediately processes the source location for the event, relates it to the nearest mining, and sends the information to a printer.

Example of source location output (in U.S. customary units)

Event time = 09:28:47
x = 498 ft
y = 632 ft
z = -1,911 ft
Energy = 6,656 V
Distance error = 46 ft
Location = 70 ft northeast, 60 ft below 510-07 #17W
Julian date = 295 days (day of year)
Channel(s) removed from solution = 44

The microseismic system is used in conjunction with a drum-type seismograph and a geophone located on the surface. When a large event is recorded by the drum seismograph (figure 7), the origin time is determined and the microseismic database is analyzed to determine where the event occurred. Teams are then sent to that portion of the mine to look for any possible problems.

Table 1. Example of arrival times file as data appear on screen

Geophone	Time, ms	Year	Julian date	Hour	Minute	Second
2	8	1993	215	9	29	32
17	12					
14	78					
6	122					
13	230					
23	369					
8	412					
32	511					
41	634					

Note: Information on year, Julian date, and time are shown only once for each event.

Figure 6
Plan View of Microseismic Array, 1993.

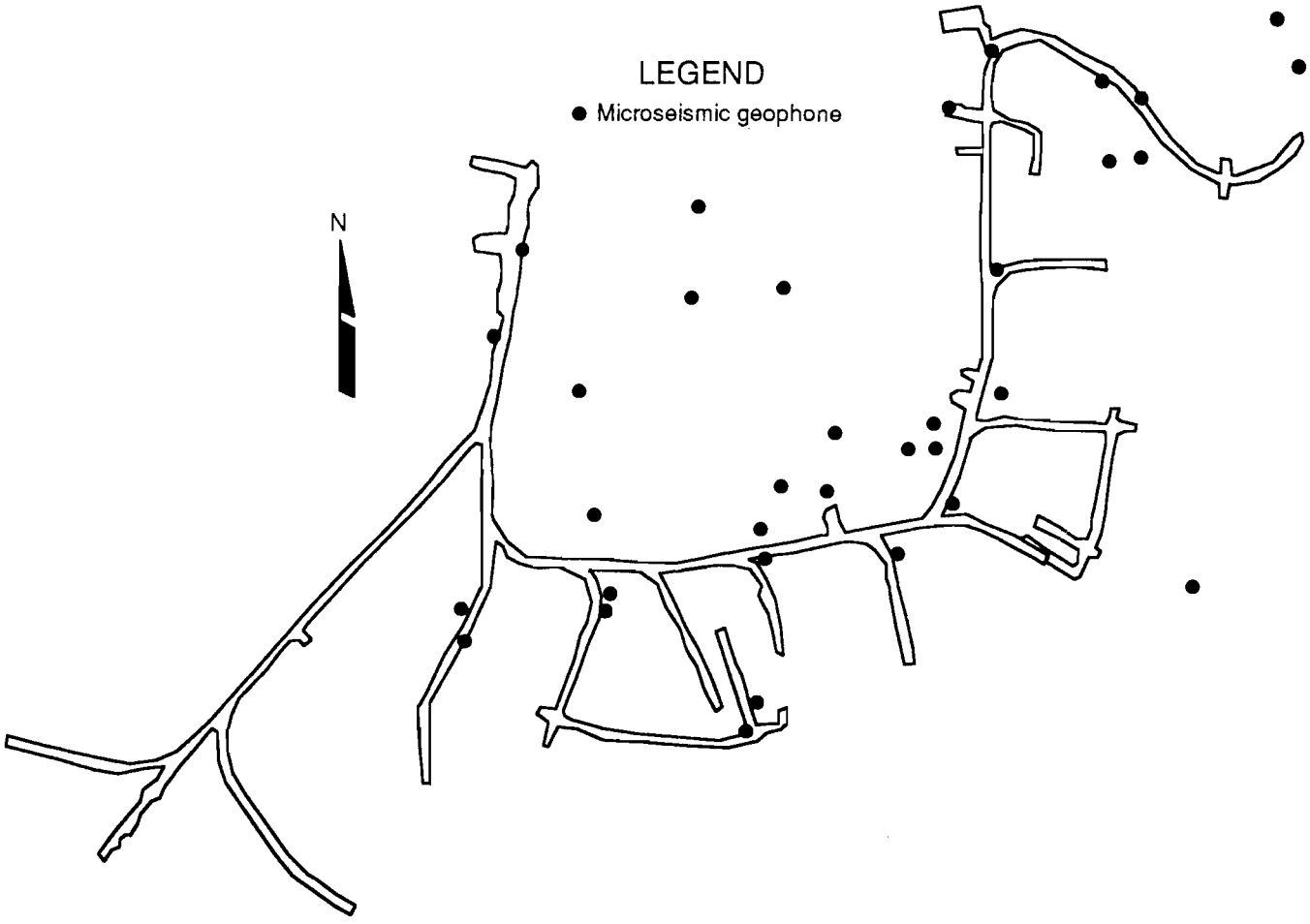

Figure 7
Rock Burst Recorded by Drum-Type Seismograph.

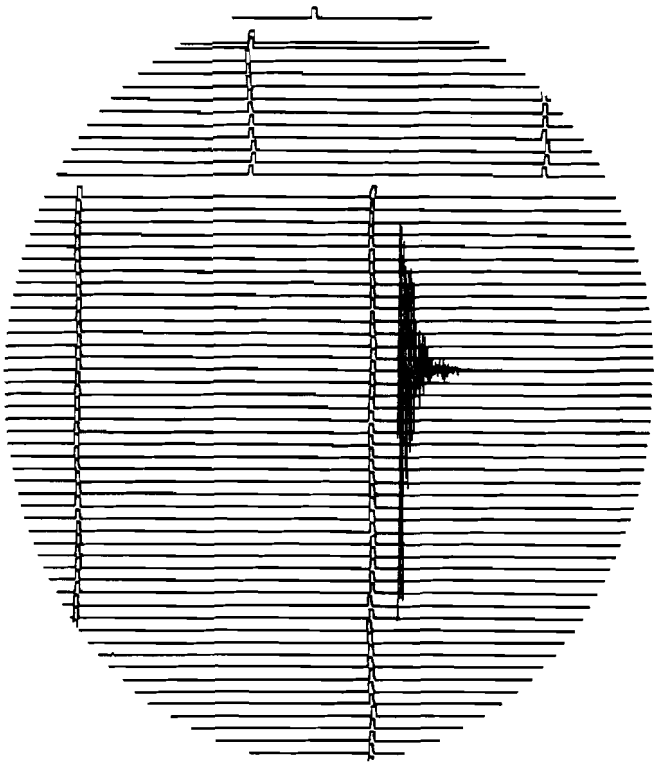

Sept. 7, 1987
81–mm burst

USBM MACROSEISMIC SYSTEM

The difference between the microseismic and macroseismic systems is the ability of the latter to record full waveform data that can be analyzed later, whereas the microseismic system saves only first arrival times and geophone numbers. The original waveform data were obtained by only five seismometers in the mine. The receiver array was modified in January 1991 and now includes a mixed array of three-component and single-component seismometers. The number of receivers was increased to 11, and this new array has operated successfully since it was installed. With the macroseismic array, the distance between event and detector can range from 50 m to as much as 2 km. The macroseismic system is used to locate rock bursts when the microseismic system misses the event or when its solution might be in error because of extraneous noise.

The USBM uses two programs developed by the USGS, FPFIT and FPPLOT*, for first-motion studies, also known as fault plane solutions. Several steps must be taken to go from the digitized waveform data to the final plane plot. First, the P-wave arrival times and wave polarity (whether the wave motion is up or down) must be picked for each channel that recorded the waveform. Figure 8 is an example of a typical recorded waveform from a triaxial geophone. The P-wave information must be stored in a file, such as the text file shown in figure 9. This file, which contains the P-wave arrival times along with the coordinates of the geophone, is used to determine the event location. Then the distance, azimuth, and inclination (vertical angle) between each geophone and the event is computed. This information is stored in a file that is used as input to the FPFIT program. The specific format details are available in Reasenberg and Oppenheimer (1985), but basically the file contains the station name, distance, azimuth, and inclination between the station and the event and information on the seismic wave, as shown in figure 10. The resulting output is a double-couple source mechanism solution that best fits the data (figure 11). These programs are used to generate fault plane solutions on projections on a lower hemisphere stereonet projection. Each solution is analyzed to see if the pattern of arrival times is unique or if the pattern can be incorporated into composite solutions.

If the fault plane solution is similar to several other solutions for events in the same area of the mine, a composite solution is made. Composite solution files are

obtaned by concatenating P-wave arrival time files for similar events. A new input file based on an average event location is computed for the concatenated data, and a composite fault plane solution is calculated with the FPFIT and FPPLOT programs.

As source solutions are obtained, they are inspected to determine the general patterns of first-motion arrivals. If, for instance, the geophones of the array all generate plots within the southwest quadrant of the focal sphere, and all the arrivals are dilatational, the focal mechanism solution is obviously poorly constrained. The event could also have been an implosional one where all first arrivals are dilatational and the program is actually looking for a slip plane that is not present. This was one of the problems encountered during the data analysis and probably represents a worst-case scenario. Usually the macroseismic receiver array, although constrained by mine geometry, is deployed so that arrivals are plotted in at least three quadrants, if not all four, of the focal sphere. Events from zone A that have similar allowable source solutions are grouped together as a single event, and the composite solution, as shown in figure 12*A*, is obtained.

As a result of grouping events into composite solutions, at least four distinct classes of events were determined. Figure 12*B* illustrates the types of source mechanism solutions obtained by combining the recordings for selected events with all dilatational arrivals. Each of the events selected originated in the northeast part of the mine. The actual events used for the composite source mechanisms are indicated on the figures. Because the major faults of the area trend northwest-southeast, the source mechanism classification was related to the sense of motion that could have occurred on these faults. However, these motions may also have indicated an implosional collapse in the area. In addition to all-dilatational events, some source mechanisms were right lateral, some were left lateral, and some were dip slip. This work is continuing, and large events are being analyzed and added to the current database.

Figure 8
Computer Display of RPEAK Program, File 92073000.WVA.

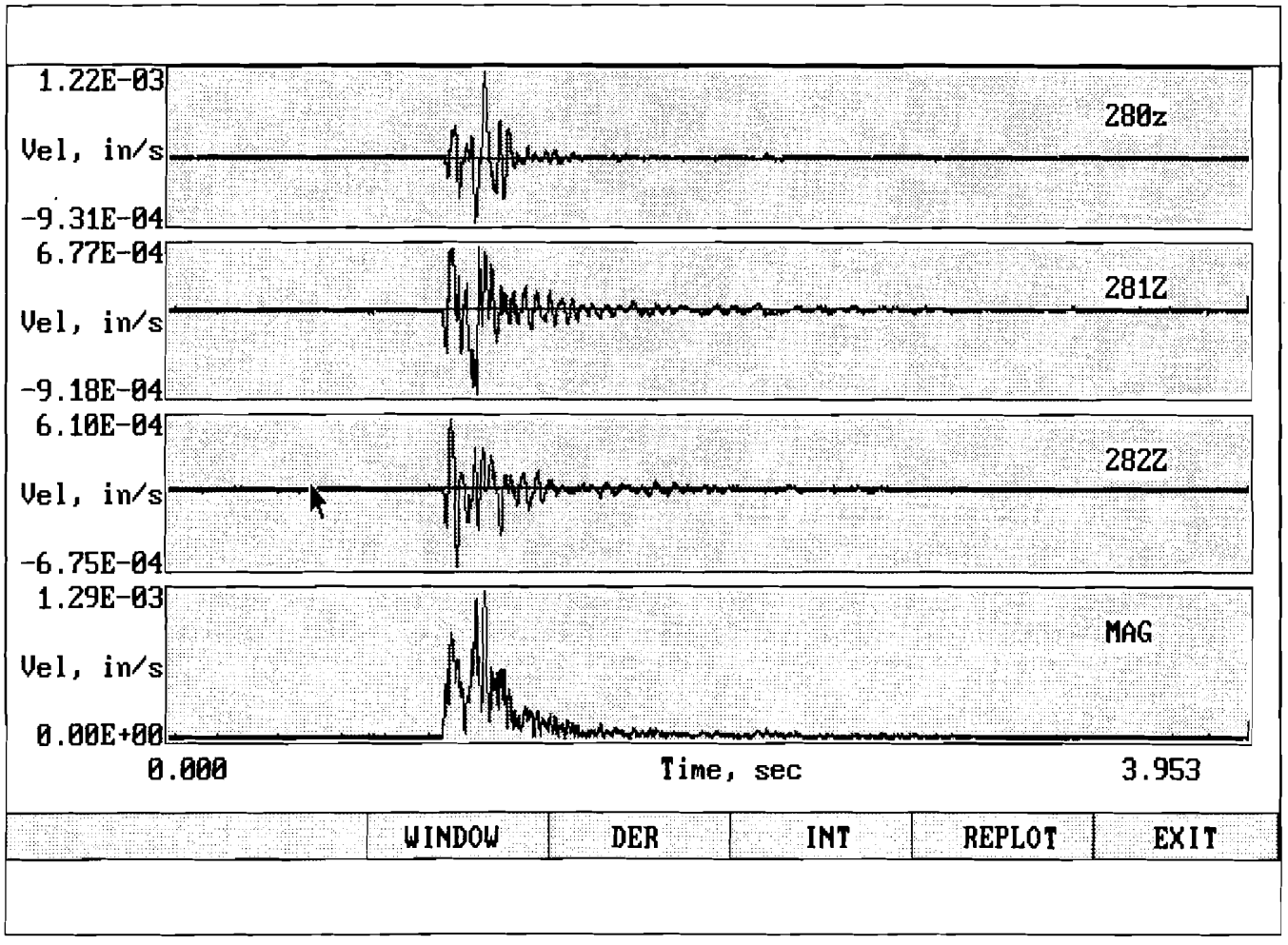

Figure 9
Example of P-Wave Arrival Time Data File.

400X	1252	23:38:22.5378	−9
400Y	1252	23:38:22.5378	1
400Z	1252	23:38:22.5378	-4
280Z	1300	23:38:22.5748	−5
280Z	1300	23:38:22.5748	-5
280Z	1300	23:38:22.5748	−5
281Y	1294	23:38:22.5702	−2
281Y	1294	23:38:22.5702	−2
281Z	1294	23:38:22.5702	-1
440Y	1217	23:38:22.5115	-35
440Z	1217	23:38:22.5115	−35
440Z	1217	23:38:22.5115	−2
282Z	1300	23:38:22.5748	−5
282Z	1300	23:38:22.5748	−5
282Z	1300	23:38:22.5748	-5
590X	1217	23:38:22.5108	1
590Y	1217	23:38:22.5108	0
590Z	1217	23:38:22.5108	2
510X	1253	23:38:22.5385	1
510Y	1253	23:38:22.5385	17
510Z	1253	23:38:22.5385	1
5150	1172	23:38:22.4760	1
5150	1172	23:38:22.4760	1
5150	1172	23:38:22.4760	1

Column 1 is geophone name and component. Column 2 is sample number corresponding to P-wave arrival time in column 3. Number in final column represents magnitude and polarity of first motion. Negative numbers indicate downward motion; positive numbers indicate upward motion.

Figure 10
Example of Input File to FPFIT.

DATE	ORIGIN	LAT N	LONG W	DEPTH	MAG
92073000	.00	47-26.10	115-43.09	-17.31	.30
STN	DIST	AZM	INC	PRMK	
280	2.4	249	161	IPD	
281	2.3	32	170	IPD	
510	1.8	227	89	IPD	
590	1.4	250	54	IPD	
440	1.4	157	118	IPD	
400	1.8	270	126	IPD	
282	2.3	370	169	IPD	
570	0.9	224	40	IPD	
400	1.8	313	132	IPD	

File 92073000.DAT. STN = Geophone locations. DIST = Distance. AZM = Azimuth. INC = Inclination. PRMK = P-wave remark. IPD = Impulsive P-wave with dilatational motion. IPC = Impulsive P-wave with compressional motion.

Figure 11
Source Solution for Single Event.

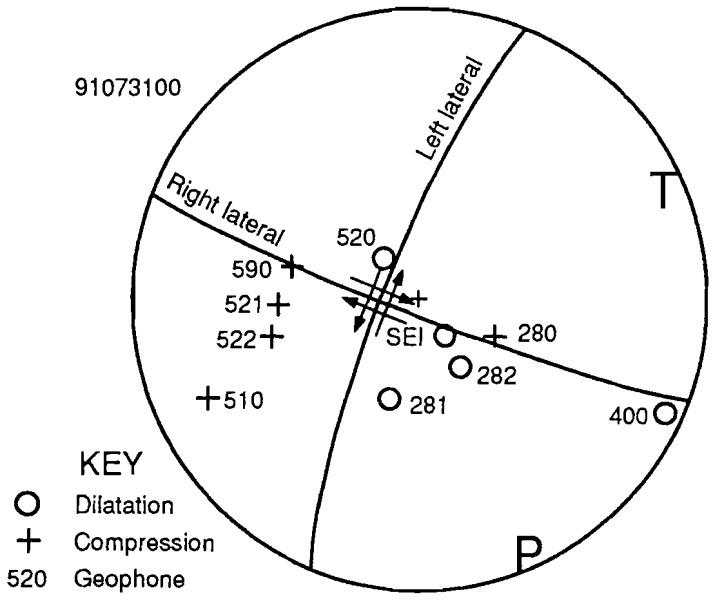

Solution shows possible right-lateral, strike-slip motion on northwest-trending fault or left-lateral strike-slip motion on northeast-trending fault. T = Least compressive stress. P = Most compressive stress.

Figure 12
Composite Source Solution.

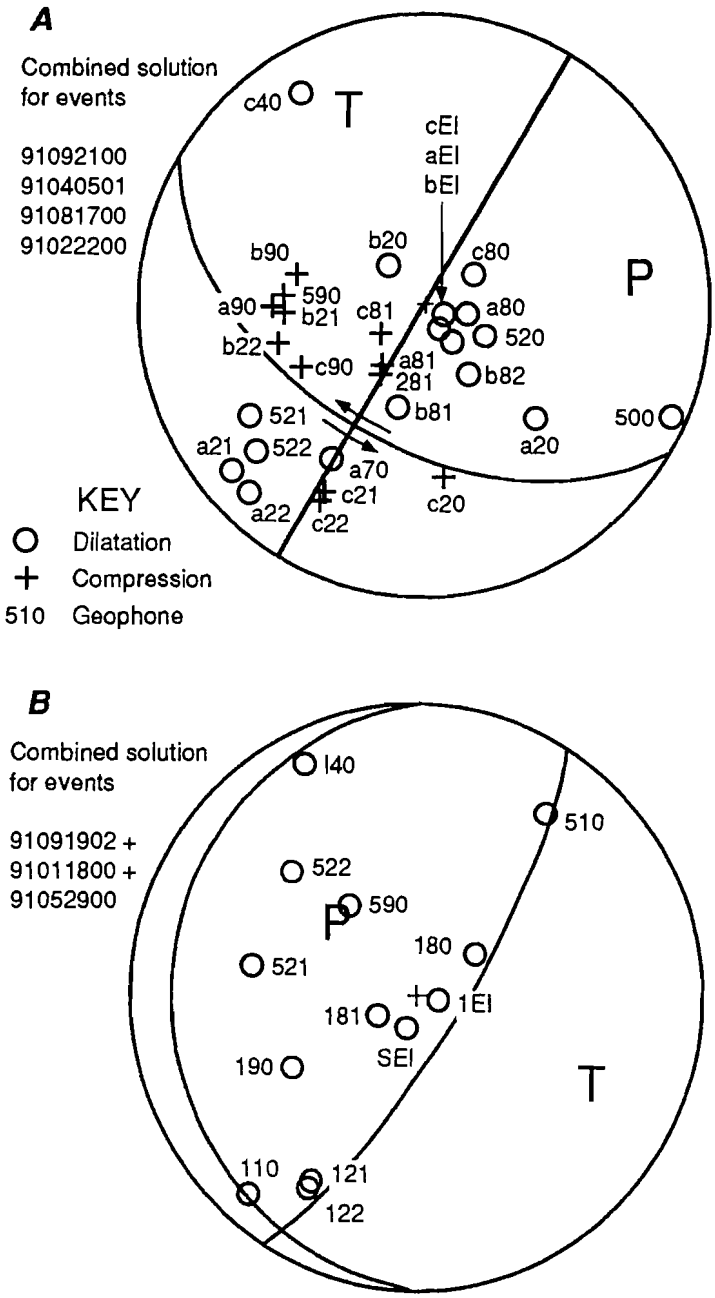

A, Solution shows possible left-lateral, strike-slip motion on northwest-trending fault; *B*, solution generated from events having all-dilatational first arrivals. T = Least compressive stress. P = Most compressive stress.

NORTH IDAHO SEISMIC NETWORK

The NISN was established to identify whether regional tectonism played an important role in rock-burst problems at the mine, to serve as a backup to the macroseismic system at the Lucky Friday Mine, and to collect data from all mines in the district to identify similarities and differences in rock-burst source mechanisms. The geometry for the network is shown in figure 13. The main difference in the operation of the NISN system is that most of the signals are sent to the Lucky Friday Mine via radio telemetry instead of over wires. The NISN is an entirely IASPEI-based system, so no special software had to be developed. The first-motion output from the NISN is identical in format to that from the macroseismic system.

The NISN has also shown that most of the seismic activity in northern Idaho is associated with the operating mines (Lourence and others, 1993). During the time the system has been in operation, no significant earthquake has occurred in the Coeur d'Alene Mining District.

Data from the NISN have shown the same general patterns for first motions as those recorded by the macroseismic system at the Lucky Friday Mine. These data have been useful in analyzing the events that occurred near the North Control Fault at the edge of the microseismic and macroseismic arrays. The following case history is of an event similar to the ones shown in figure 12*B*, where the source mechanism, as determined from first-motion studies, could have been slippage along a fault or an implosional collapse.

CASE HISTORY OF EVENT ON JULY 30, 1992

On July 30, 1992, at 12:38:21 a.m., a seismic event of 2.5 Richter magnitude occurred in the northeast part of

Figure 13
NISN Array, 1992.

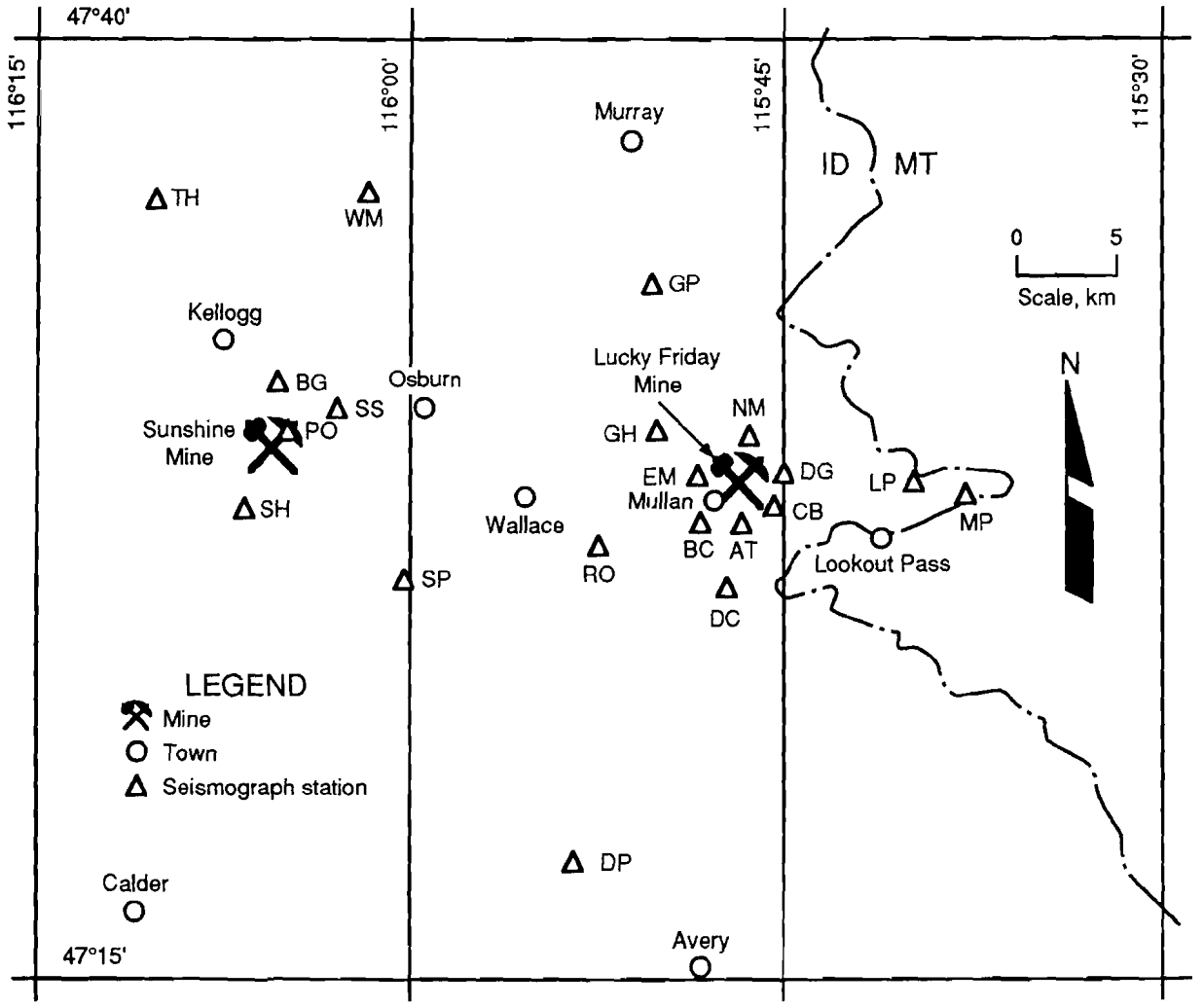

Capital letters (THI, DPI, MP, etc.) indicate station names.

the Lucky Friday Mine at the edge of the microseismic and macroseismic arrays. The event was recorded by all three seismic systems.

The microseismic system located the event at 20998, 20844, -1668 (x, y, z mine coordinates). The macroseismic system located the event at 20901, 20887, -1731. Figure 14 is a plan view of the locations and shows the event as being located just north of mining on the North Control Fault on the 5100 level at an elevation -1,730 ft. Figure 15 shows the locations in a section view along the North Control Fault. The macroseismic system located the event near an ore pillar left alongside the fault. Although the solutions were 32 m apart horizontally and 19 m apart vertically, they were close enough that an investigative team would have been sent to that stope if there had been miners in that area.

The first-motion analysis from the macroseismic system showed all the first arrivals were dilatational and could be plotted in two quadrants of a double-couple solution (figure 16). This solution was poorly constrained because the arrivals were plotted in only two quadrants; therefore, it was not possible to determine whether the event was a fault-slip event or an all-dilatational implosional event. One peculiarity of this event was that the P-wave first arrivals were also very large, which would not be expected if this were a fault-slip event.

The solution from the NISN showed this was an implosional event because all 13 geophones on the network had dilatational first arrivals. Figure 17 shows the first few seconds of full waveform data recorded by the NISN. Although amplitudes were clipped by the relatively strong ground motion of this 2.5 M_l event, the first motions are all easily visible and are all clearly dilatational. Stations LPID, NMID, MPID, BCIC, EMID, and ROID have reversed polarity, that is, the upward motion is dilatational, while the other stations have normal polarity. The top trace is an IRIG timing signal.

Figure 18 shows the Schmidt projection for these data; for this event, the NISN data were an improvement over the macroseismic data because all four quadrants were

Figure 14
Location of July 30, 1992, Event.

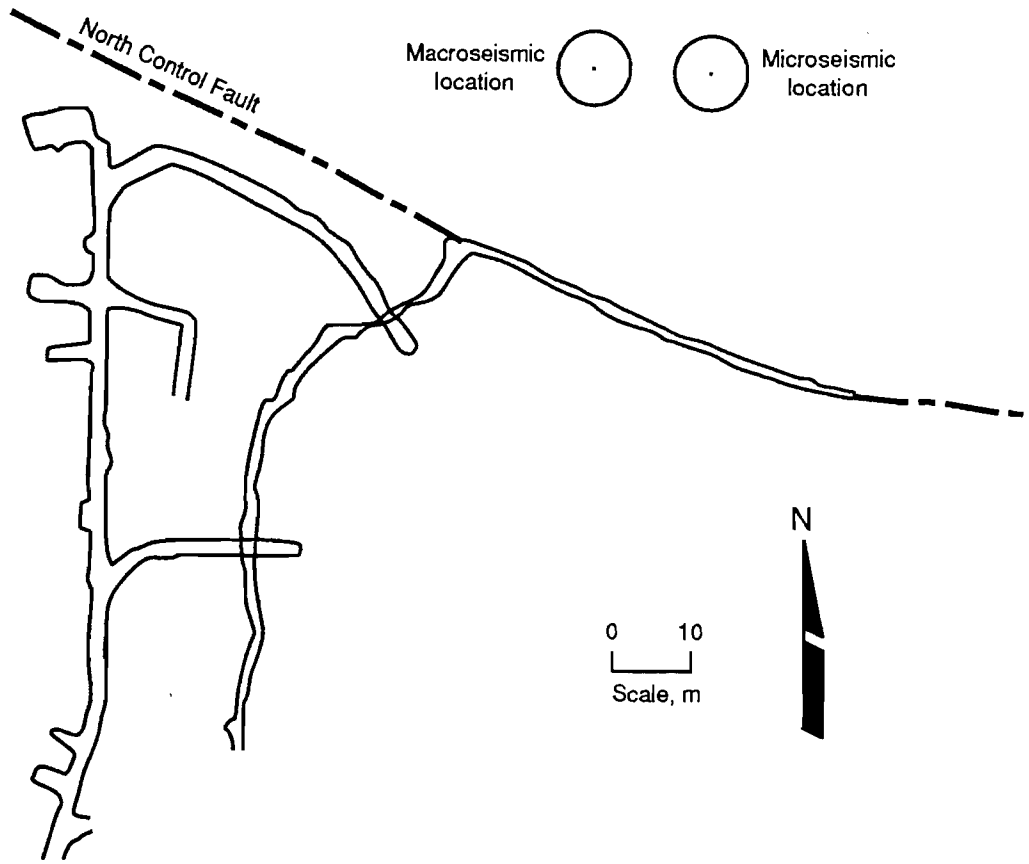

Plan view of northeast portion of Lucky Friday Mine showing location of 2.5-Richter-magnitude event as determined by microseismic and macroseismic systems (circles).

Figure 15
Section View Along North Control Fault Looking N 30° E.

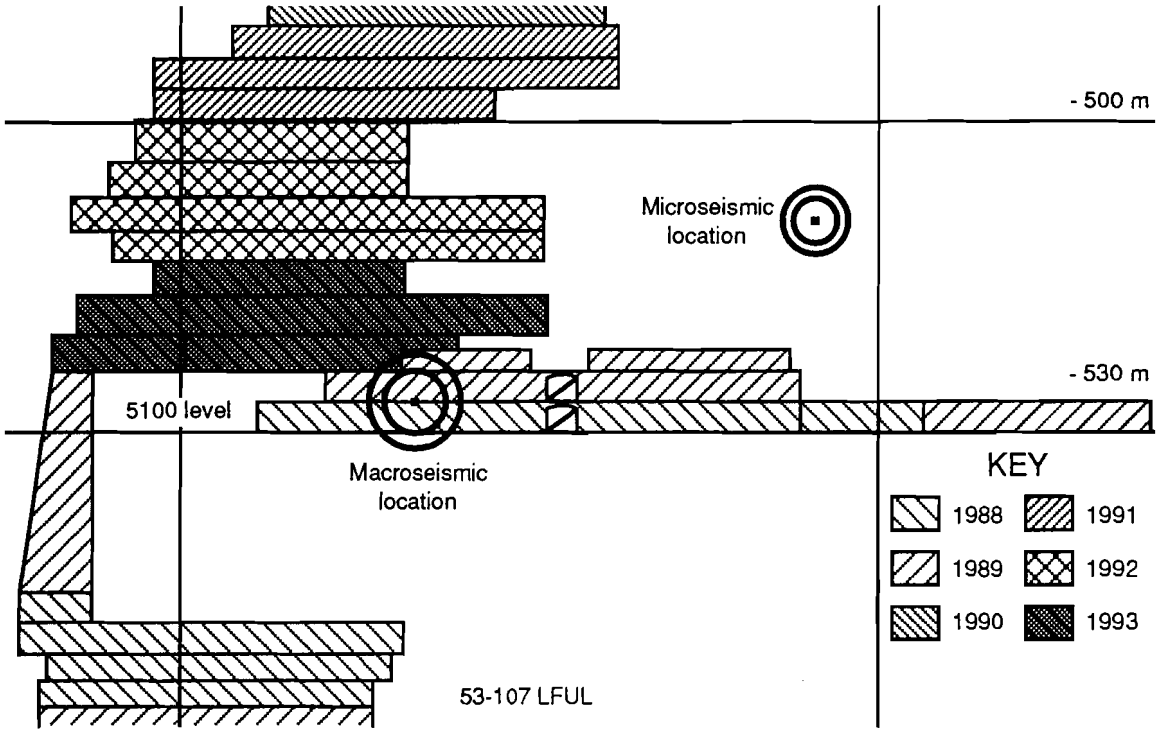

Location of July 30, 1992, event and its relation to mining.

Figure 16
First-Motion Data from Macroseismic System for July 30, 1992, Event.

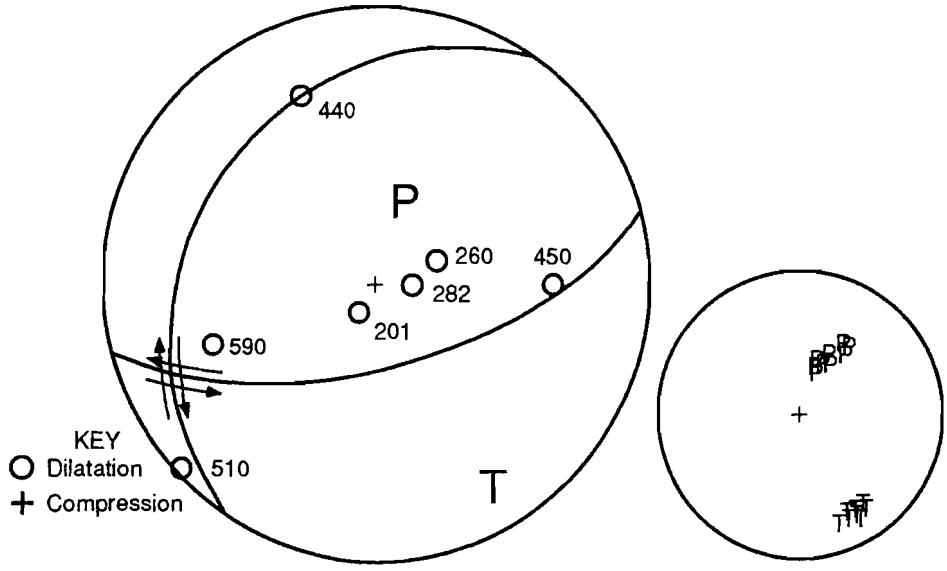

Data indicate all-dilatational arrivals. T = Least compressive stress. P = Most compressive stress.

Figure 17
Full Waveform Data Generated by NISN for July 30, 1992, Event.

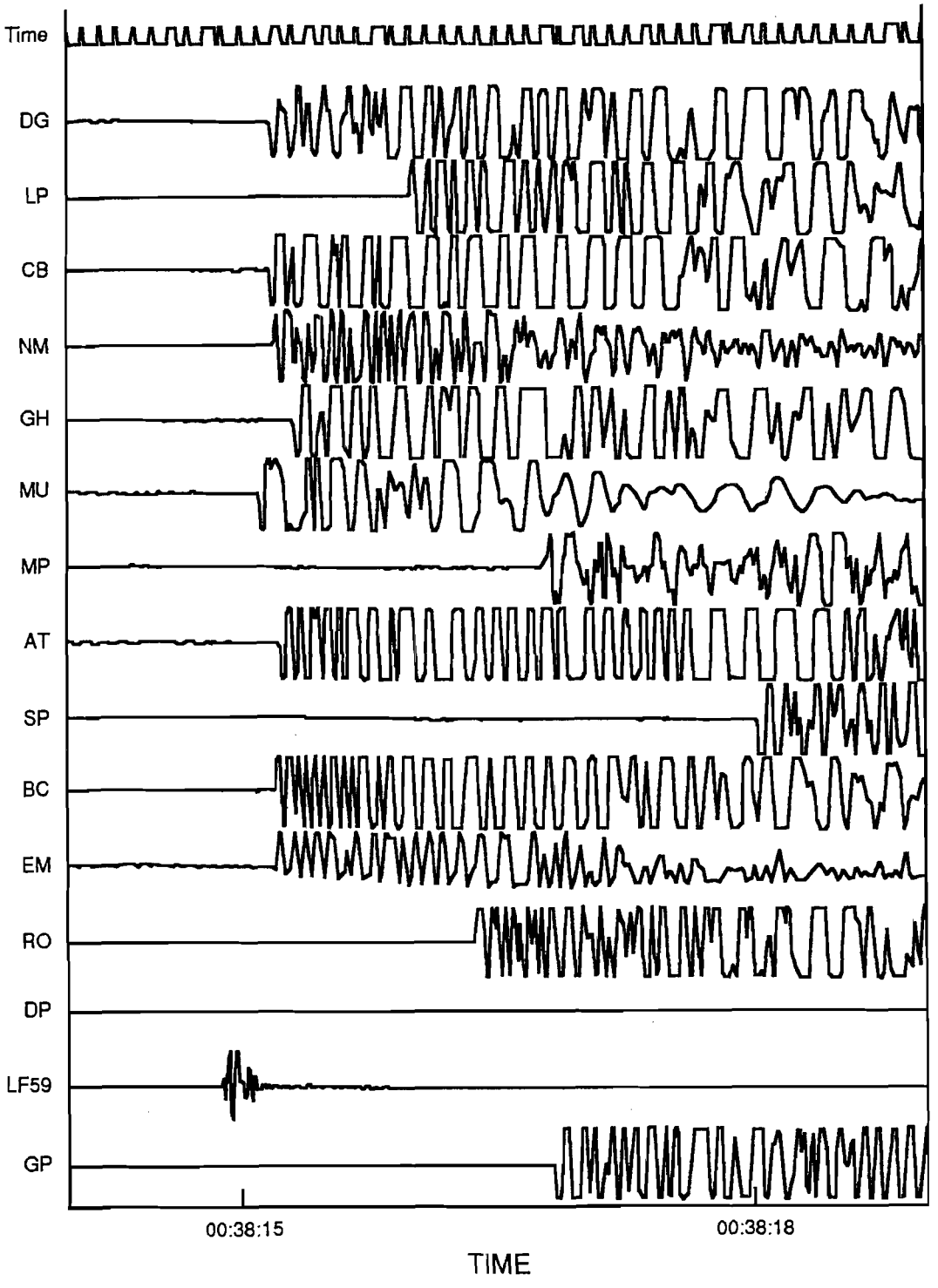

Figure 18
NISN Data for July 30, 1992, Event.

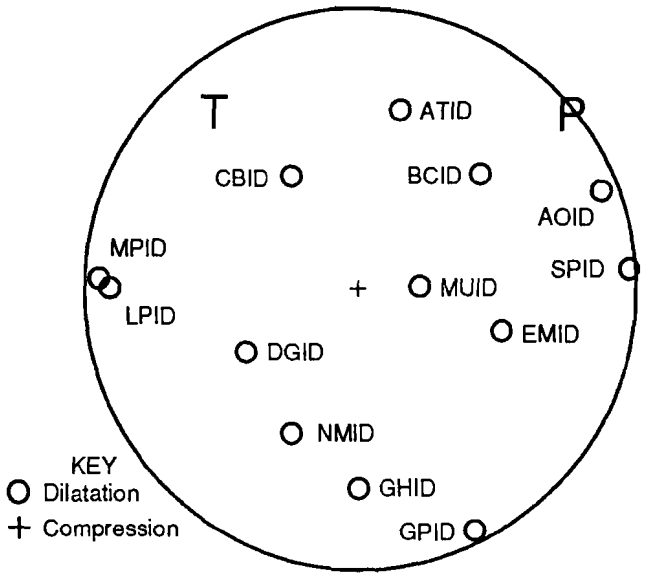

Data indicate 13 all-dilatational, first-motion arrivals. T = Least compressive stress. P = Most compressive stress.

covered. The two sets of focal data are consistent with one another, and when taken together, imply a non-double-couple, implosional failure mechanism consistent with collapse.

Analysis of the location of the event, first-motion source mechanism data, and mining along the North Control Fault indicated that the event could have been related to the collapse of a pillar along the fault (figure 15), or collapse of some unknown structure north of the fault. Because there was no longer access to this area of the mine, it was impossible to determine exactly what happened. However, this event received special attention because it was the largest all-dilatational event ever recorded at the mine.

CONCLUSIONS

Low-cost hardware and software are now available as research tools to study the failure mechanisms that result in rock bursts. The three seismic systems in use at the Lucky Friday Mines complement one another, and all three provide valuable information on rock bursts. Further studies will be conducted to document the interaction between mining geometry, local geology, and source mechanisms for rock bursts to improve mining layouts and rock support designs.

ACKNOWLEDGMENTS

The authors would like to thank the personnel of Hecla Mining Co. for access to the Lucky Friday Mine and for help in installing and troubleshooting the macroseismic system since the beginning of the project in 1989. Maps provided by mine staff were extremely valuable in analyzing rock bursts and were greatly appreciated by USBM staff. A special thanks goes to Wilson Blake, consultant, Hayden Lake, ID, for his assistance in the design, installation, and operation of the macroseismic system.

REFERENCES

Bell, R. N. Sixteenth Annual Report of the Mining Industry of Idaho for the Year 1914. State of Idaho, 1914, 55 pp.

Blake, W., F. Leighton, and W. Duvall. Microseismic Techniques for Monitoring the Behavior of Rock Structures. USBM Bull. 665, 1974, 65 pp.

Boler, F. M., and P. L. Swanson. Computer-Automated Measurement and Control-Based Workstation for Microseismic and Acoustic Emission Research. USBM IC 9262, 1990, 9 pp.

Gerard, J. M., T. J. McMahon, W. Blake, and T. J. Williams. Installation of PC-Based Seismic Monitoring Systems With Examples From the Homestake, Sunshine, and Lucky Friday Mines. Paper in Proceedings: Mechanics and Mitigation of Violent Failures in Coal and Hard-Rock Mines. USBM Spec. Publ. 01-95, 1995, pp. 303-312.

Jenkins, F. M., T. J. Williams, and C. J. Wideman. Rock Burst Mechanism Studies at the Lucky Friday Mine. Paper in Rock Mechanics Contributions and Challenges: Proceedings of the 31st U.S. Symposium, ed. by W. A. Hustrulid and G. A. Johnson (CO Sch. Mines, Golden, CO, June 18-20, 1990). Balkema, 1990, pp. 955-962.

Langstaff, J. Seismic Detection System at the Lucky Friday Mine. World Min., Oct. 1974, v. 27, No. 11, pp. 58-61.

Lee, W. H. K., D. M. Tottingham, and O. J. Ellis. A PC-Based Seismic Data Acquisition and Processing System. U.S. Geol. Surv. OFR 88-751, 1988, 31 pp.

Lourence, P. B., S. J. Jung, and K. F. Sprenke. Source Mechanisms at the Lucky Friday Mine: Initial Results from the North Idaho Seismic Network. Paper in Rockbursts and Seismicity in Mines 93. Proceedings of the 3rd International Symposium on Rockbursts and Seismicity in Mines, ed. by R. P. Young (Kingston, ON, Aug. 16-18, 1993). Balkema, 1993, pp. 217-222.

Reasenberg, P., and D. H. Oppenheimer. FPFIT, FPPLOT, and FPPAGE: Fortran Computer Programs for Calculating and Displaying Earthquake Fault-Plane Solutions. U.S. Geol. Surv. OFR 85-0739, 1986, 109 pp.

Obert, L. Use of Subaudible Noises for Prediction of Rock Bursts. USBM RI 3555, 1941, 4 pp.

Scott, D. F., B. G. White, and T. J. Williams. Host Structures for Slip-Induced Seismicity at the Lucky Friday Mine. Paper in Rockbursts and Seismicity in Mines 93. Proceedings of the 3rd International Symposium on Rockbursts and Seismicity in Mines, ed. by R. P. Young (Kingston, ON, Aug. 16-18, 1993). Balkema, 1993, pp. 245-248.

Swanson, P. L., L. H. Estey, F. M. Boler, and S. Billington. Accuracy and Precision of Microseismic Event Locations in Rock Burst Research Studies. USBM RI 9395, 1992, 40 pp.

OVERVIEW OF USBM MICROSEISMIC INSTRUMENTATION AND RESEARCH FOR ROCK-BURST MITIGATION AT THE GALENA MINE, 1987-1993

By Louis H. Estey[1]

ABSTRACT

Mining-related microseismic activity at the Galena Mine, Wallace, ID, was targeted by the U.S. Bureau of Mines for studies of possible indicators of imminent rock bursts. Two systems were developed and deployed for microseismicity studies: one involving routine monitoring of several rock-burst-prone stopes and the other using digitally recorded signals. Research included a complete analysis of microseismic location errors for both systems. P-wave polarity patterns and focal mechanisms were correlated with local geology and intrastope activity. Evidence for sympathetic interstope activity was found. In a tomographic study, the area of greatest velocity decrease in a pillar that had been acoustically scanned did not correlate with microseismicity. A correlation was found between seismicity and sudden offsets in stope closure gage and borehole pressure cell signals, though aseismic creep accounted for 20 to 70 pct of the closure signals. Clustering, fractality, and planarity analyses were done on the microseismic data. Research at the Galena Mine indicates there is not a reliable indicator of all rock bursts that can be identified at the present time. For rock-burst forecasting, it may be crucial to identify, characterize, and measure the mechanics of mine geologic structures in both seismic and aseismic areas of a mine.

INTRODUCTION

A rock burst can be considered to be a seismic event in a hard-rock mine that caused damage to mine structure or caused or could have caused personal injury or death (Swanson and Sines, 1991). Rock bursts at the Galena Mine, Wallace, ID, have been occurring since the mid-1950's, when mining began at the 2400 level at depths of almost 1 km and deeper. This onset roughly coincided with mining operations moving from the softer St. Regis Formation down into the harder and more competent Revett Quartzite (Hobbs and others, 1965), which continues down to at least the 5500 level.

An overhand cut-and-fill method of mining has been used at the Galena Mine to remove ore from the nearly vertical, narrow (1- to 2-m wide) veins. Horizontal drifts in these veins were opened on levels every 60 m down to the 3400 level and every 90 m below that. Rock-burst problems often started when about three-quarters of the vertical extent of certain veins had been removed between the drifts of two consecutive levels, presumably coinciding with a critical geometry and/or stress state.

The sizes of rock bursts at the Galena Mine have been characterized using a local-magnitude (M_L) scale (Swanson and Sines, 1991), which is a cousin of the Richter-magnitude scale. The largest rock bursts at the Galena Mine have probably been about M_L 3.5, equivalent to moments of about 200,000 to 300,000 GN•m. The largest rock burst occurring between 1987 and 1993 was about M_L 3.1 (about 70,000 GN•m). The smallest damaging rock burst during this time was about M_L 0.5 (about 8 GN•m), and the smallest rock burst that could have caused personal injury or death was about M_L -0.5 (about

[1]Geophysicist, Denver Research Center, U.S. Bureau of Mines, Denver, CO.

0.2 GN•m). During the last few years, the rate of rock burst occurrence has been about one event of M_L 1 or greater per month (Swanson and Sines, 1991).

By event count, most seismic activity at the Galena Mine occurs as "microseismic" events, where a microseismic event can be considered to be any event smaller than about a local magnitude of 3 and having a practical detection lower limit of local magnitude of about -5.[2] This definition is consistent with the conventional understanding that a "seismic" event is large enough to be recorded and located using some portion of a regional or world-wide, array, such as the World-Wide Standard Seismologic Network, and that a seismic event currently has a practical detection lower limit of local magnitude of about 2.5 to 4.5 for these types of arrays (Engdahl and Rinehart, 1991). The largest rock bursts in the Coeur d'Alene district qualify as seismic events. Obviously, by these seismological quantitative measures, there is some overlap in magnitude between what is considered a rock burst and what is considered a large microseismic event or a small seismic event. In reality, perhaps the only distinction is happenstance: Whether a large microseismic event or a small seismic event happens to be located or oriented in such a way that it does or does not cause damage to mine structures and/or cause enough rock to be expelled into a mine opening to be hazardous. Therefore, in this paper a microseismic event is considered to be an event that is not a seismic event (i.e., not large enough to be detected on a wide-area or world-wide array) and is not a rock burst (i.e., no damage is done to mine structures and it is not considered to be hazardous).

The number of detectable microseismic events at the Galena Mine when the mine was in production was truly astounding, well in excess of 1 million per year. Some of the more active stopes generated many hundreds of thousands of microseismic events per year, of which 100,000 per year could be located by a routine monitoring system (described in the section on "Instrumentation" in this paper).

The two primary tenets that had been argued that would help solve the rock-burst problem were that (1) there should be anomalous microseismic activity before a rock burst or (2) there should be an increase in seismic velocity in the region that gives rise to the rock burst (Blake and others, 1974) due to some increase in stress. By the mid-1970's, the second idea was abandoned, and research was redirected toward obtaining direct stress measurements, rather than velocity surveys, in a burst-prone area (Leighton, 1976). However, this approach also did not prove useful because the observed changes in stress were coseismic (i.e., occurring at the same time as a microseismic or seismic event).

Microseismic events were still targeted for study as possible indicators of subsequent—and less frequent—rock-burst activity, due in part to the occurrence of microseismic events in large numbers. Other reasons were that microseismic events can be easily detected by sensors approximately in the acoustic range (Hz to kHz), and they can be detected passively, i.e., no intentional sources are needed. Also, the approach of studying small events to learn more about the characteristics of large events is exactly analogous to studying so-called foreshocks and aftershocks to learn more about large and moderate earthquakes.

This paper is an overview of U.S. Bureau of Mines (USBM) research performed at the Galena Mine from 1987 through mid-1993, done in cooperation with ASARCO, Inc., in an effort to reduce hazards associated with rock bursts. Much work done by the USBM and ASARCO at the Galena Mine precedes 1987 (Blake, 1971; Blake and others, 1974; Leighton, 1976; Leighton, 1982; Rowell and Yoder, 1984; Coughlin and Sines, 1985).[3] However, in recent years, USBM research has had a more distinct seismological emphasis. In late June 1992, the Galena Mine was placed on standby mode, essentially terminating USBM rock-burst research at the mine, but further monitoring of the decay of microseismic events—and a few rock bursts—continued until mid-1993. The analysis of these data continues.

INSTRUMENTATION

Two types of passive monitoring systems were developed and deployed at the Galena Mine. The first system is referred to as the routine monitoring system and the second is called the digital research system.

ROUTINE MONITORING SYSTEM

The routine monitoring system was developed for continuous monitoring of both microseismic and rock-burst activity in rock-burst-prone stopes, though such a system

[2]This is equivalent to a moment of 10 N•m, about 13 orders of magnitude smaller than the largest rock bursts that occur at the Galena Mine.

[3]Additional information from W. Blake and F. Leighton, USBM, 1961 and 1969.

could be used anywhere in the mine where microseismic activity occurred. For each monitored stope, this system consists of the following hardware units: (1) an array of high-frequency accelerometers, (2) 12-V preamplifiers, (3) four-conductor cables to (4) a rock-burst monitoring unit built by Science Applications International Corp. (SAIC), of Las Vegas, NV, installed at or near the stope, (5) RS-232 cables to 6) an Apollo workstation located in an underground instrumentation room. The accelerometer stations were always uniaxial; the one component usually measured the near-horizontal component of ground acceleration at a rib-mounted sensor position (station).

The design of the SAIC unit was based on a portable microseismic recorder developed and tested earlier by the USBM (Coughlin and Sines, 1985). Each SAIC unit was designed to provide stable, 12-V power to the preamplifiers near each accelerometer, digitally analyze up to 16 incoming signals from the accelerometer array, decide when a transient event occurs on five or more channels, select relative arrival times for all channels possible via a floating-threshold, first-break algorithm to the nearest 0.1 ms, and provide a measure of the energy by time integration of the square of the voltage signal over a fixed time window on up to four preselected channels.

For each transient event that triggers the SAIC unit, the internal time of the SAIC unit, the relative arrival times for each channel, and the energy measures are transmitted via the RS-232 cables back to a dedicated workstation for the particular array. An array file in the workstation holds the coordinates of the accelerometers of the array; this file is updated manually when the actual sensor array is changed. As event information from the SAIC unit is read by the workstation, software screens arrival times, locates the event if possible, and displays the event location on the workstation monitor using three orthogonal views of the stope. In addition, the raw data from the SAIC unit are stored in one file on the workstation system (the times file) and the processed location is stored in another file (the location file). The total amount of time from detection of an event by the SAIC unit to display of the event location at the workstation and resetting the SAIC unit is about 0.3 s, thus providing near-real-time monitoring of stope microseismic activity.

The routine monitoring system was an outgrowth of earlier systems developed for and tested with a single stope array. The complete routine monitoring system, however, links several SAIC-Apollo systems together with a token ring local area network (LAN) at the underground instrumentation room, allowing data archiving and other system activities from any single workstation node on the LAN (Steblay and others, 1990a, 1990b).

This arrangement allowed the system at the Galena Mine to be expanded so that ultimately 8 arrays, composed of up to 128 accelerometers, were monitoring up to 11 rock-burst-prone veins in production throughout the mine. In addition, almost 3 km of six-conductor, fiber-optic cable was installed from the office-dry building on the surface, along the surface adit to the No. 3 shaft, down the No. 3 shaft to the 4600 level, and about half a kilometer along the 4600 level to the underground instrumentation room. Using optical transceivers and two of the fiber-optic lines allowed a separate workstation on the surface to be included in the token ring LAN, and thus data from any instrumented stope could be easily accessed at the surface in near real time. Data for all monitored stopes (array files, times files, and location files) were written to cartridge tape and mailed back to the Denver Research Center (DRC) for further processing. Monitoring and event detection continued in three to four stopes through at least September 1994, 27 months after the initiation of standby mode at the Galena Mine.

The near-real-time display (microseismic event location in relationship to stope geometry) possible with this type of system proved to be a valuable tool for mine personnel. However, from a geophysical research point of view, any analyses are limited in scope if they involve temporal and/or spatial characteristics of event locations or crude estimates of event energy. For example, some of the fundamental pieces of seismological data missing for each event are the identity of the first-break point, the polarity of each incoming wave at each sensor, estimates of later arrivals (such as any S-wave arrivals), and so on.

DIGITAL RESEARCH SYSTEM

To overcome some of these limitations, a second type of system, called the digital research system, was developed, primarily for geophysical research (Swanson and Boler, 1988a; Boler and Swanson, 1990). The first use of this system took advantage of hardware already in place for the routine monitoring system. The SAIC unit was still used to power the accelerometer preamplifiers. The analog signals from the sensors continued to be input to the routine monitoring system as before, but these analog signals were also input into the second system in which the signals from each event above a certain threshold were digitized and recorded.

Satisfying several simultaneous requirements led to the creation of a data acquisition system combining modular computer-automated measurement and control (CAMAC) instruments with a UNIX-based workstation. CAMAC modules for amplification, analog-to-digital (A/D) conversion, memory, and CAMAC crate control are manufactured by a number of companies. Furthermore, as the research needs of the system evolved, different CAMAC modules were added without the necessity of redesigning the basic hardware of the system, and software modifications to the workstation were minimal. It should be

recognized that the digital research system was not designed to replace the routine monitoring system, but to collect highly detailed "snapshots" of microseismic activity that would be amenable to detailed analysis of each recorded event (Swanson and Boler, 1988b). This system was used to collect microseismic data centered on the 4300 level during production in the 120 vein around the 115 stope for 4 months in 1988, during production and destressing in the nearby 104 vein around the 99 stope from August 1989 through March 1991, and finally to collect about a month's worth of data in each of five stopes from October 1992 through April 1993.

The flexible characteristics of the digital research system eventually allowed simultaneous monitoring of accelerator signals of kilohertz frequencies and quasistatic rock mechanics measurements in the 99 stope. The former requires monitoring and high-density digitizing of transient signals that can occur at any time, and the latter requires only periodic point sampling of each pertinent channel. A second system was added later for a lower frequency underground mine-wide array using velocity geophones of 3 to 250 Hz. Furthermore, for both systems, as many stations as possible were triaxial (three mutually perpendicular uniaxial sensors installed to measure all components of ground motion at a single station). Our goal by 1991 was to monitor large events throughout the mine with a mine-wide array of eight underground triaxial stations and a dedicated CAMAC-workstation system, and to continue to monitor microseismic activity with another CAMAC-workstation system in various stopes that were rock-burst prone.

The digital research system tends to be limited by the hard disk due to the large size of the binary data files of the digital waveforms. The data files for a single microseismic event are often on the order of 0.1 to 1 Mbyte in size (e.g., 32 channels with a sampling rate of 50 kHz, a time window of 0.1 s, and a dynamic range of 16 bits (2 bytes) per channel yields 0.32-Mbyte data files per event). During operation at the Galena Mine, limitations in technology, economy, and practicality allowed only about 200 to 300 Mbyte of free hard disk space for data. For some of the more active stopes, this disk-size limitation allowed only a few days of data collection before the hard disk would become full, requiring a tape dump and removal of files from the hard disk.

Finally, another set of optical transceivers were used with two more of the fiber-optic lines to the surface to establish a carrier-sense, multiple access with collision detection (CSMA/CD) LAN between the underground data acquisition workstation of the digital research system and another UNIX workstation at the surface. A pair of high-speed Telebit WorldBlazer modems allowed connection and high-speed data transfer over ordinary, nondedicated voice telephone lines. These modems have a built-in optimization for UNIX-to-UNIX copy (UUCP) protocol. Using a 19.2-kbaud RS-232 cable connection to the workstation and this protocol, transfer rates of almost 0.1 Mbyte of binary data per minute (1,600 bytes per second) are possible. Thus, data files for a few critical events could be copied from the underground digital research system to a workstation at DRC in a matter of minutes without stopping data acquisition.

SURFACE SEISMIC SYSTEM

By late 1990, we realized the scientific and practical utility of also establishing a surface array and decided to experiment with another type of digital research system. This second digital system is the PCQuake system of the International Association of Seismology and Physics of the Earth's Interior (IASPEI), which had just become widely available (Lee and others, 1988; Lee, 1989). Being based on a personal computer (PC), it is inexpensive compared to a CAMAC-workstation system.

The basic PCQuake system is a dedicated PC that monitors up to 16 A/D channels, each with 12-bit dynamic range. This allows monitoring of five triaxial stations with one free channel. In addition, the PC clock can be forced to Coordinated Universal Time (UTC) (plus or minus an integer number of hours) using the Inter-Range Instrumentation Group (IRIG) B time code input to a TrueTime Model PC-SG synchronized generator card, which is installed on the PC bus. The IRIG-B code was supplied by a TrueTime Model 468-DC clock, which has an accuracy of ±0.5 ms when it is locked on to one or more of the Geostationary Operational Environmental Satellites (GOES).[4] By the time the Galena Mine was placed in standby mode, two triaxial stations and a few uniaxial stations were in place and linked to the surface PCQuake system by cable, using largely the same type of velocity sensors being installed with the underground mine-wide digital array.

ROCK MECHANICS

At the end of July 1989, an array of borehole pressure cells (BPC's) was also installed at one corner of a pillar formed by the 104-vein drift and the crosscut intersection on the 4300 level (Boler and Swanson, 1993a; 1993b). The purpose of this array was to monitor stress changes associated with seismic events (whether rock bursts or not) and planned destress blasts in the vein below the drift.

Each BPC is essentially an oblong, flattened, stainless-steel bladder encased in grout and sized so that it can be inserted into a standard borehole. After insertion into a

[4]The GOES system transmits a time code referenced to UTC which, when fully corrected, usually has an accuracy of ±0.10 ms.

borehole, the BPC is hydraulically pressurized to a level approximating a local maximum principal stress, and thereafter the hydraulic fluid pressure is monitored (Haramy and Kneisley, 1991) for example, using a Bourns 35-MPa pressure transducer.

The installed array consisted of three mutually perpendicular boreholes and eight BPC's oriented so as to be at maximum sensitivity to the three suspected principal directions of the local stress field. Two of the BPC's provided some redundancy. Logging of the pressure readings by CAMAC digital voltmeter on the digital research system began in February 1990. Readings were taken on every cell every 10 min and continued through March 1991.

In the 99 stope beneath the 104-vein drift on the 4300 level, a small array of three stope convergence gages was installed by June 1990 and was monitored through March 1991 (Boler and Swanson, 1992). These gages were designed to be inexpensive and expendable, but they had to be watertight and robust enough to withstand both the water-sand slurry used to backfill stopes and the production blasts as the stope was excavated upward in the ore vein. Internally, each gage consisted of a constant-tension spring motor that turned the wiper of a potentiometer. The voltage across this potentiometer in each gage was amplified and cabled back to the digital research system, which took a voltage reading on every gage every 10 min. The bidirectional gages were designed to measure only on-axis displacements and had a total range of 0.6 m. The limiting component for repeatable accuracy was the internal spacing of potentiometer windings, which limited the convergence steps and bidirectional reproducibility of the gage to 0.2 mm.

SOFTWARE

TIME-SYNCING

The final goal in seismological data collection at the Galena Mine was to coordinate digital waveform acquisition from a stope-level CAMAC-workstation system, the underground mine-wide CAMAC-workstation system, the surface PCQuake system, and two regional arrays [the North Idaho Seismic Network (NISN) (Lourence and others, 1993) and the Montana seismograph network (Stickney, 1993)] for monitoring rock-burst events and large microseismic events in the near and far fields. Although this final goal was not realized, it is noteworthy to understand why we were concerned with obtaining a common time base for all these arrays.

The P-wave velocity for the quartzites in the Silver Valley is roughly 5 km/s. Thus, if the NISN, the Montana network, and the local PCQuake system are each tied to a common time base (e.g., UTC) that has an accuracy of ±0.5 ms, this time uncertainty equates to an equivalent spatial drift and jitter of up to ±10 m in array coordinates when tying the data sets together, which is about equivalent to the accuracy of an inexpensive GPS survey of array coordinates. In other words, no significant additional errors would be introduced into a seismological inversion, such as event location, because of clock errors in the separate systems.

However, in tying a surface system to an underground system separated by 1.5 to 2 km, for example, this same ±10 m could be significant, because this would be equivalent to about ±10 m of random errors in array coordinates between the two systems for different events. We felt that if any local time base uncertainty between any surface system and any underground system could be reduced by an order of magnitude (i.e., an equivalent spatial jitter of about ±1 m), the result would be acceptable. Software experiments performed at DRC on a CSMA/CD LAN showed that probably the best that two UNIX workstation system clocks could be synchronized would be about ±1 ms owing to the nondeterministic nature of CSMA/CD packet traffic. Also, because of clock stabilities of only a few parts in a million, even if the two workstation clocks could be synchronized exactly at some instant, the clocks could drift apart in time by as much as a millisecond in only a few minutes.

Through further software experiments on the LAN at DRC, we determined that the clock drift of two separate workstations probably could be monitored to a precision of a few tens of microseconds, which is well within the synchronization target of 0.1 ms. Although the same experiments were never performed on the fiber-optic LAN at the Galena Mine, this precision probably could have been achieved there as well.

DATA ACQUISITION

The data acquisition and display software for the routine monitoring system is very tightly bound to the Domain-Aegis operating system and display manager of Apollo workstations. This attribute alone would make it very difficult to port to another type of computer. However, all the source code is written in C, and it should be possible to extract the functionality of many algorithms for use elsewhere.

Data acquisition by any CAMAC-based system will necessarily be tied to the type of bus selected for communication between the CAMAC crate and the controlling

computer. For the digital research system, a general-purpose interface bus (GPIB) crate controller was selected. Also, the Hewlett-Packard (HP) UNIX workstations selected as the controlling computer had a compatible HP interface bus (HPIB), HPIB being the forerunner of the GPIB standard. The data acquisition software developed for the research system is written in C and uses a small number of low-level HPIB function calls to communicate with the CAMAC crate.

Two different A/D systems were developed using CAMAC technology. One system involved use of modules built by DSP Technology, Inc., of Fremont, CA, resulting in a system with up to 100-kHz sampling and 12-bit dynamic range (Boler and Swanson, 1990). Because of the 12-bit resolution of the A/D modules, analog data for each channel were sometimes digitally recorded twice, once at high gain to capture the smallest events and simultaneously at low gain to avoid digital clipping of the larger microseismic events. This C software eventually evolved into the USBM's current in-house *TraqAcq* code.

The other system involved the use of modules built by KineticSystems Corp., of Lockport, IL, resulting in a system with up to 85-kHz sampling (with 16 channels) and 16-bit dynamic range. The KineticSystem A/D modules can be easily linked to provide a system that simultaneously captures up to 64 channels. We were able modify and test the original *TraqAcq* code to handle the KineticSystems modules with DSP amplifier modules in just 4 days, an accomplishment that demonstrates the flexibility of the data acquisition software design. This code is called *KS16Acq*.

For both sets of modules and their associated software, a standard HPIB interface is used between the CAMAC crate and the workstation. The total amount of time from triggering the digitizers on the CAMAC, to data transfer to the workstation, to setting up for the next triggering of the digitizers is proportional to the total amount of digital data saved for an event. This delay is about 16 s/Mbyte for both.

Both *TraqAcq* and *KS16Acq* are designed to work in a UNIX operating system and communicate with the CAMAC crate with GPIB commands. Both functions can also access a set of other UNIX commands that, for example, can be a sequence of event-processing filters to be applied to each event file recorded. This set of commands could pass the file on for first-arrival picking, event location, and archiving of the event location. A log of data acquisition startup, stoppage, warnings, and errors can be dumped to a log file or dumped to a printer. For field use, a simplified, menu-driven interface called *CamAcq* was written to start and stop either *TraqAcq* or *KS16Acq*, copy files from hard disk to tape, remove files from hard disk, plot event files, and do a variety of other tasks.

WAVEFORM MANIPULATION

Two graphical user interface (GUI) C programs were developed to manipulate the collected waveform files. One of these programs, *plot*, was based on HP's Starbase graphics functions and was simplified for field use to allow a minimum of functionality, which currently includes arbitrary record selection, waveform magnification, arrival picking, and event location with display of calculated arrivals. The other program, *sgp* (seismic graphics program), was modified after a version supplied by Lamont-Doherty Geological Observatory of Columbia University, New York, NY. This second GUI is for use in an X11 Window System environment. It currently includes all the functionality of *plot*, plus the capability of display or manipulation of waveforms in time domain or frequency domain, time-domain hodogram display for biaxial or triaxial sensor stations, focal-sphere first-motion display with interactive or software-search solutions, and other functionalities.

Another important set of C software adapted from Lamont-Doherty was that of UNIX filters for the waveform files. These filters currently include methods of forward and inverse fast-Fourier transforms, time-series signal inversion, detrending, demeaning, windowing, Butterworth filtering, P-wave arrival picking, attenuation correction, fast-Fourier transform integration and differentiation, event location in homogeneous or plane-layered media, source parameter fitting, and other functionalities. These filters, along with the two GUI waveform display programs, provide the backbone for analyzing the bulk of the digital waveform data collected by the digital research system.

THREE-DIMENSIONAL SOLIDS RENDERING

Another software tool was developed to display graphically the varied and complex three-dimensional assortment of data needed for tracking microseismicity in a mine. This assortment includes the microseismic locations themselves, mine openings, local geology, and calculated quantities such as three-dimensional stress or strain fields. Many of these items can vary as a function of time. An interactive graphics package, *4d_render*, which also uses HP's Starbase graphics functions, was developed to meet these needs. The additional use of HP's graphics hardware accelerators allows the calculation and display of realistic three-dimensional images (i.e., solids rendering) in near real time. Limited only by the amount of computer

memory, *4d_render* stores and links together in memory the data for an arbitrary number of graphics primitives, which are then accessed in an optimized fashion during the rendering. Taking advantage of many of the advanced features of Starbase, *4d_render* includes functionalities such as the specification of an arbitrary set of lighting conditions, solid or wire-frame surfaces, partial transparency of surfaces, arbitrary positioning of the viewer and image reference points, forward or reverse time-sequence display, and, when used in an X11 environment, a stereographic image pair. These and numerous other features of *4d_render* have made it an invaluable tool for combining and visualizing the diverse data sets and results used in research.

TEMPORAL AND SPATIAL STATISTICAL ANALYSES

Several new and innovative methods of statistical analysis were applied to the data collected by the routine monitoring system to discern temporal and spatial patterns of microseismicity (Coughlin and Kranz, 1991; Kranz and others, 1994).[5] These methods include fractal analyses of time of occurrence and locations of microseismicity, event attribute clustering, and planarity searches of spatial distributions of microseismicity. In addition, the decay of microseismicity following production blasts and rock bursts around the 99 stope was analyzed using the maximum-likelihood method of Ogata (1983) to determine modified-Omori decay fits.

RESEARCH RESULTS

EVENT LOCATION ERRORS

One of the first areas of research was an evaluation of event location errors that could be reliably associated with the locations produced by the routine monitoring system and by the digital research system (Swanson and others, 1992a, 1992b). The two systems must be examined separately because there are several major differences in the sources of error in the two systems.

The first source of error is the uncertainty in the coordinates of the sensor stations. For the routine monitoring system, station coordinates were estimated from using tape measures and mine maps. For the digital research system, in the worst cases, coordinates were obtained in the same way, and in the best cases, coordinates were surveyed. Using an electronic distance-measuring device on a theodolite, such a survey produced coordinates with uncertainties we estimated to be about ±5 cm. Performing a least squares fit between coordinates obtained with these two methods showed that the tape measure and mine map method results in an average error of about 1 m, and that an individual error for a single station, even in the horizontal direction, can be 2 m or more. Some portion of this error was probably attributable to changes in actual mine geometry due to large-scale deformation of the mine occurring between the time when the mine was originally surveyed and mapped and the time of the microseismic array installation, about 25 years for the 4300 level. From various surveys performed to obtain station coordinates, the magnitude of this deformation is estimated to be 0.2 to 0.4 m over distances of 100 m in crosscuts between veins and about 1 m or more in drifts on the levels.

The second source of error is the uncertainty in arrival time picks of the seismic ground motion at each sensor. For the routine monitoring system, the picks are accomplished in near real time by a hardware algorithm in the SAIC units. For the digital research system, the picks are done manually using one of the GUI's. In comparing differences in arrival time picks between the two systems of the same event, it was noticed that a hardware pick tended to be either coincident with or later than the corresponding manual pick. Differences in a suite of arrivals for different events showed that this delay of the hardware picking had a distribution that approximated an exponential function with a 140-μs time constant, and delays in excess of 1 ms are possible. With a P-wave velocity of about 5 km/s, this distribution is equivalent to distance errors from a few tenths of a meter up to at least 5 m on occasion.

The third source of error is in essence the same for both systems, i.e., the uncertainty in the velocity model used. The velocity structure in the vicinity of a stope is quite complex, owing to the volume of fractured rock and sand- and air-filled openings, as well as preexisting variations in local geologic structure. The velocity structure is in fact so complex and varies as a function of time in such a way that the only reasonable assumption that can be made is that some mean P- and S-wave velocities apply, though this assumption is obviously incorrect in detail. For the routine monitoring system, a mean P-wave velocity of 5.64 km/s had been previously determined on the basis of a set of test blasts involving sensors installed underground over a wide portion of the mine. In January 1990, another set of test blasts was done using the digital research system around the 115 stope; a mean P-wave velocity of 5.02 km/s was found with extremes of 3.26 and 5.70 km/s. For this test area, the slowest path was entirely near the stope, and the fastest path was through largely

[5]Kranz, R. L., J. Coughlin, and S. Billington. Characterization of Blasting and Rock Burst Aftershock Sequences in a Hard Rock Mine. Abstract in Workshop on Induced Seismicity (33rd U.S. Symp. Rock Mech., Santa Fe, NM, June 8-10, 1992). 1992, p. 11.

undisturbed country rock (Estey and others, 1990). It was also found that the country rock may be weakly anisotropic, but this finding was not explored further.

The fourth source of error involves the choice of location algorithm. The location algorithm used with the routine monitoring system was that of Blake and others (1974). For the digital research system, a variety of location algorithms were investigated, which included examining different basis functions (Swanson and others, 1992a) and solving the resulting system of equations using different L2-norm minimization (least squares) algorithms and an L1-norm minimization simplex method (Riefenberg, 1989a, 1989b). As a result of this investigation, it was discovered that the accuracy of a particular algorithm is strongly dependent on the types of errors in the total solution model, i.e., arrival times, station coordinates, and velocity model (Estey, 1990). In short, if all the sources of error are random, algorithms involving iterative gradient solutions tend to yield locations with the smallest spatial errors. These algorithms also tend to minimize the travel-time residuals of the location solutions. However, in the presence of a systematic error in the velocity, the algebraic algorithm and exact choice of basis functions used by Godson and others (1980) yield the smallest spatial errors, even though the gradient algorithms continue to produce location solutions with the lowest travel-time residuals. The algebraic algorithm of Blake and others (1974) tends to give poor results in either case. Because it was noted that the method described by Godson and others also does fairly well with the random error cases, and because the uncertainty in velocity seems to be one of the major contributors to final location errors, this location method was selected as the primary one for the digital research system.

The total amounts of spatial location errors were estimated by using synthetic numerical models incorporating the above errors and by locating actual test blasts in the 115 stope with a sensor array about 150 m in dimension. Average random location errors of ±0.7 m for the digital research system and ±3.6 m for the routine monitoring system occurred over large areas of the array, these average random location errors being dominated by the errors in arrival-time picking for both cases. An additional average location error component of ±1.2 m for the digital research system and ±7.0 m for the routine monitoring system occurs because of the choice of mean velocity and location algorithm. All of these errors are well modeled. However, based on the test blasts, an additional systematic location error of up to 10 m for locations within the array can occur for both systems, apparently resulting from additional uncertainty and variation in the velocity structure. Put another way, the random location errors for the routine monitoring system were found to be about five times larger than the best that can be achieved with the digital research system, but a velocity-based systematic error is about the same for both systems.

P-WAVE POLARITY PATTERNS

When the digital research system was first installed, one of the first areas of investigation was to see if information about the change of stress in a stope could be inferred from first-motion P-wave polarity data. Digital data from a 1-week production period in April 1988 were collected for about 250 locatable events using the 115 stope array of 11 uniaxial sensors. P-wave polarities were manually picked for these events. Various unknowns at the time precluded the use of traditional focal sphere methods for analyzing the P-wave polarities. Therefore, a pattern recognition search was performed to identify groups of events with consistent patterns of P-wave first motions as they had been recorded at the sensors. Six groups (a total of 54 events) were identified on the basis of the pattern recognition search, spatial relationships, and elimination of ambiguous polarities at one station.

This study (Boler and others, 1988; Billington and others, 1990a) clearly indicated that groups of microseismic events with similar P-wave polarity patterns existed and were identifiable. Also, it was found that there was a progression from one group of events to another in the rock mass surrounding the stope during the hours following routine production blasting. This observation of the migration of microseismic activity and its associated change in polarity pattern with event location is consistent with a transfer of stress around a stope following blasting and can be identified at the scale of only a few meters.

P-WAVE FOCAL MECHANISMS

A focal mechanism is a standard seismological method of projecting information received at an array of sensors back to a small imaginary sphere surrounding the source, or focal, region. The simplest focal mechanism to construct is that of the P-wave first motion, because P-waves are the fastest waves in a solid medium and are less likely to be contaminated by the coda of later waves received at a sensor. It is best to have triaxial sensor stations, especially when the P-wave energy will be arriving from an arbitrary direction, such as occurs when the stations are underground. However, with the routine monitoring system arrays, the data sets are dominated by uniaxial stations. These sensors are often mounted (for convenience) such that motion in the horizontal (or near horizontal) direction is best detected. This sometimes precludes use of polarity data from certain uniaxial stations, depending on the orientations of the ray paths from the source to the sensors and the uniaxial orientation of those sensors, because the sensors are insensitive to P-wave motion arriving in a direction normal to the axis of the sensor.

Seismic sources can usually be represented by slip on a fault surface (i.e., a shear dislocation), which gives rise to a quadrupole radiation pattern for both P- and S-waves

(Aki and Richards, 1980). For an elastically uniform, isotropic source site, the quadrupole has a symmetry center such that any point on the focal sphere can be projected through the center to the other side. Thus, only one hemisphere of the focal sphere needs to be considered. Also, nodal planes of zero P-wave motion occur in the plane of slip and on an auxiliary plane normal to the direction of slip.

Focal mechanisms were computed for several rock bursts and the microseismicity around them using the data collected by the digital research system (Boler and Swanson, 1993a, 1993b). Several important findings are that (1) focal mechanisms are found that are consistent with a quadrupole radiation pattern, implying slip on a locally planar surface, (2) the quadrupole quadrants are consistent with an elastically uniform isotropic or near-isotropic source region, (3) the orientation of one of the nodal planes of the focal mechanisms is in agreement with the local orientation of bedding plane faults in the mine, which strike about N. 45° W. and have near-vertical dips, and (4) composite focal mechanisms (i.e., superposition of data from more than one event on a single focal sphere) show that groups of events can have essentially the same source mechanism. The latter finding agrees with the earlier finding from the P-wave polarity pattern study.

However, an ongoing study of focal mechanisms of large events (M_L 0 to M_L 3, including rock bursts and nondamaging events) in the 99 stope at the Galena Mine shows that the standard, symmetric quadrupole model does not fit the observed data in all cases. For some large events, a quadrupole model is quite consistent with the data (figure 1*A*). Other large events appeared to yield a large distribution of dilatational arrivals on the focal sphere (figure 1*B*), which is more consistent with an implosional source mechanism. Still other large events appeared to yield a large distribution of compressional arrivals on the focal sphere (figure 1*C*) more consistent with an explosional source mechanism. Nearby (in time and space) microseismic events associated with a main event appeared to have the same type of focal sphere pattern as the main event in the few cases examined.

There are some possible explanations for the latter two sets of cases of deviation from a standard, symmetric quadrupole model. (1) The ray paths from the source region to at least some of the stations are highly contorted from the assumed straight path, (2) the source region deviates in a significant way from the assumed uniform isotropic model, and/or (3) the kinematics of the source is such that the assumption of slip on a planar surface is wrong. The first explanation is not favored because most microseismic events examined to date are largely consistent with the standard quadrupole model. If either (2) or (3) are correct, they may lead to a better understanding of certain kinds of large seismic events that result in rock bursts.

ENERGY RELEASE

Even though most of the seismic activity (in terms of number of events) in the mine occurs as microseismicity, most stored strain energy is released through infrequent rock bursts and other large events. For the smallest events detected (about M_L -5), the volume of rock that undergoes strain energy release is about 5×10^{-3} m^3 or a sphere about 0.2 m in diameter, which yields a few times 10^{-5} J of seismic energy. In contrast, for an M_L 3.0 event, the volume of strain energy release is about 2.5×10^7 to 4.5×10^7 m^3, or a sphere about 300 to 440 m in diameter (Swanson, 1992; Boler and Swanson, 1993a). Such a volume at the Galena Mine would encompass a number of

Figure 1
Equal-Area Focal-Sphere Plots of Selected Rock Bursts.

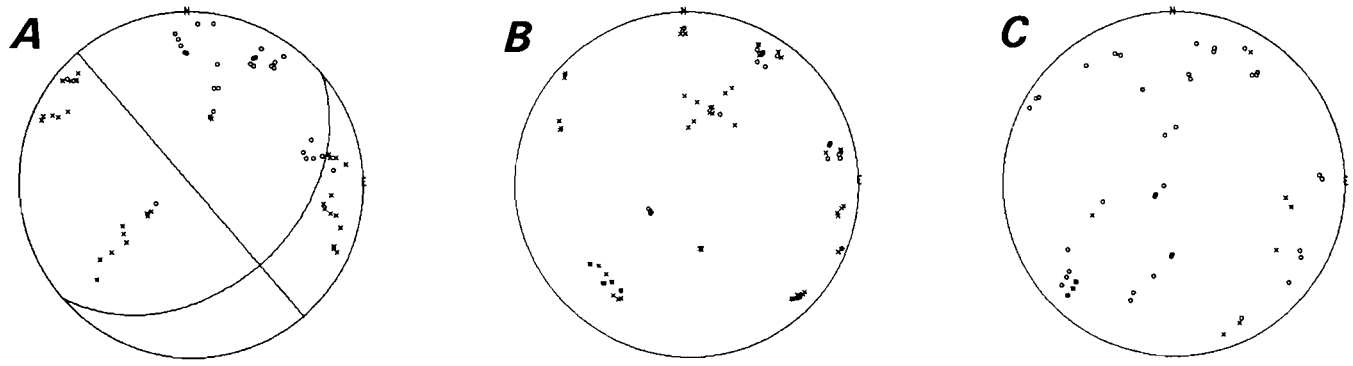

Composite upper hemisphere, equal-area focal-sphere plots of selected rock burst events in the 99 stope. Compressional arrivals at sensors are indicated by an "o," dilatational arrivals at sensors are indicated by an "x." *A*, M_L 0.9 event of February 7, 1990, as well as two foreshock and three aftershock microseismic events with P-wave quadrupole analysis; *B*, event of November 18, 1990, as well as one foreshock and two aftershock microseismic events with mainly dilatational arrivals; *C*, event of October 10, 1990, of two main events plus one aftershock with mainly compressional arrivals.

different working stopes on different levels. The energy release of the large events completely dominates the total; for a period of 18 months, 80 pct of the energy released along the main trend of the Galena Mine was released in just four events totaling over 2.8 GJ (Swanson, 1992). Using typical values of seismic efficiency of no greater than 0.1 down to 0.01, the total energy in these four rock bursts would have been roughly equivalent to the chemical energy in 10 to 100 t of TNT.

The occurrence of a large event significantly alters the state of stress in a volume of rock comparable to the volume involved in strain energy release. For example, at the Galena Mine, in the 10.5 h following one M_L 2.9 rock burst and using four stope arrays, over 4,000 microseismic events were detected and located by the routine monitoring system within about 200 m of the hypocenter of the main event (Swanson, 1992). The actual number of microseismic events within this volume of strain release was probably much larger because these four arrays only partially covered the volume.

MICROSEISMIC DECAY SEQUENCES

The decay of aftershocks following a large seismic event can be modeled as a modified-Omori decay:

$$n'(t) = k(t + c)^{-p},$$

where t is the elapsed time after the main event; $n'(t)$ is the number of aftershock events occurring per unit time; and k, c, and p are constants to be determined. An iterative approach using a maximum likelihood method can be used to determine the value of the constants (Ogata, 1983).

The idea of whether the microseismicity following a production blast or large seismic event in a mine follows a modified-Omori decay was tested by Satoh of the Geological Survey of Japan during a 3-month visit to DRC in 1991.[6] Satoh looked at data concerning events that were detected and located by the routine monitoring system around the 99 stope and collected over 11 months. Sixty-nine blasts and large events within this 11-month window were selected. Each had an uninterrupted sequence of microseismicity long enough to analyze. Satoh found that the microseismic decay following these events can, in fact, be fit by a modified-Omori decay model; figure 2 shows one of these fits following a routine production blast. Note that the routine monitoring system saturates at 12,000 events per hour because of the lower limit of 0.3 s/cycle of the SAIC unit, so that the calculated values of k and c have a much higher degree of uncertainty than is indicated by the fit.

[6]Satoh, T. Report of the Stay in Denver Research Center, U.S. Bureau of Mines, February to April 1991. USBM internal memorandum, 1991, 8 pp.

Figure 2

Example of Microseismicity Decay Following Production Blasting.

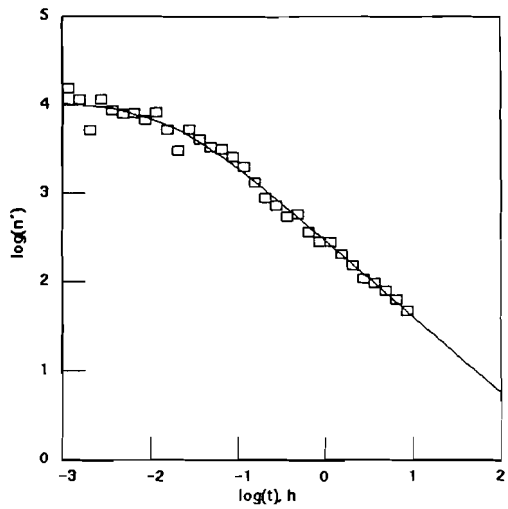

Modified-Omori decay fit (solid line) to typical post-production blasting microseismic event rate (n′ = events per hour) from data collected by routine monitoring system for the 99 stope. Data histogram is represented by rectangles. Saturation at 12,000 events per hour occurs owing to cycle time of the SAIC rock-burst monitoring unit. Three small rock bursts followed the blast, which was on April 30, 1990, at the end of day shift. The parameters of decay fit (with 1 σ uncertainty) are p = 0.860 (±0.021), k = 290.7 (±8.3), and c = 0.015 (±0.003).

It was found that the value of p (which indicates decay rate) of production blasts is indistinguishable from that of the larger seismic events at the mine (so-called bumps, including rock bursts). Satoh also noted that p for these decays (figure 3*A*) tended to yield a more tightly clustered distribution with a smaller mode (p of 0.8 to 0.9) than decays following large earthquakes (p of 1.3) (Utsu, 1969), meaning that microseismicity in this mining environment dies out more slowly than natural aftershocks.

Later analyses of these same microseismicity decays following production blasts indicate that a larger mode of p can be found if the modified-Omori fits are cut off at 2 or 1 h after the time of the blasts, yielding p modes of 0.9 and 1.0, respectively (figure 3*B* and *3C*, respectively). An anomalous rise in activity following many of the routine production blasts is observed to start about 1 to 8 h after the blasts. Two examples of this behavior are shown in figure 4.

The main motivation for this study was a recent finding that the foreshocks of the Loma Prieta earthquake had a smaller p than the aftershocks and that p changed from

Figure 3
Example of Time History of p Following Blasts and Bursts.

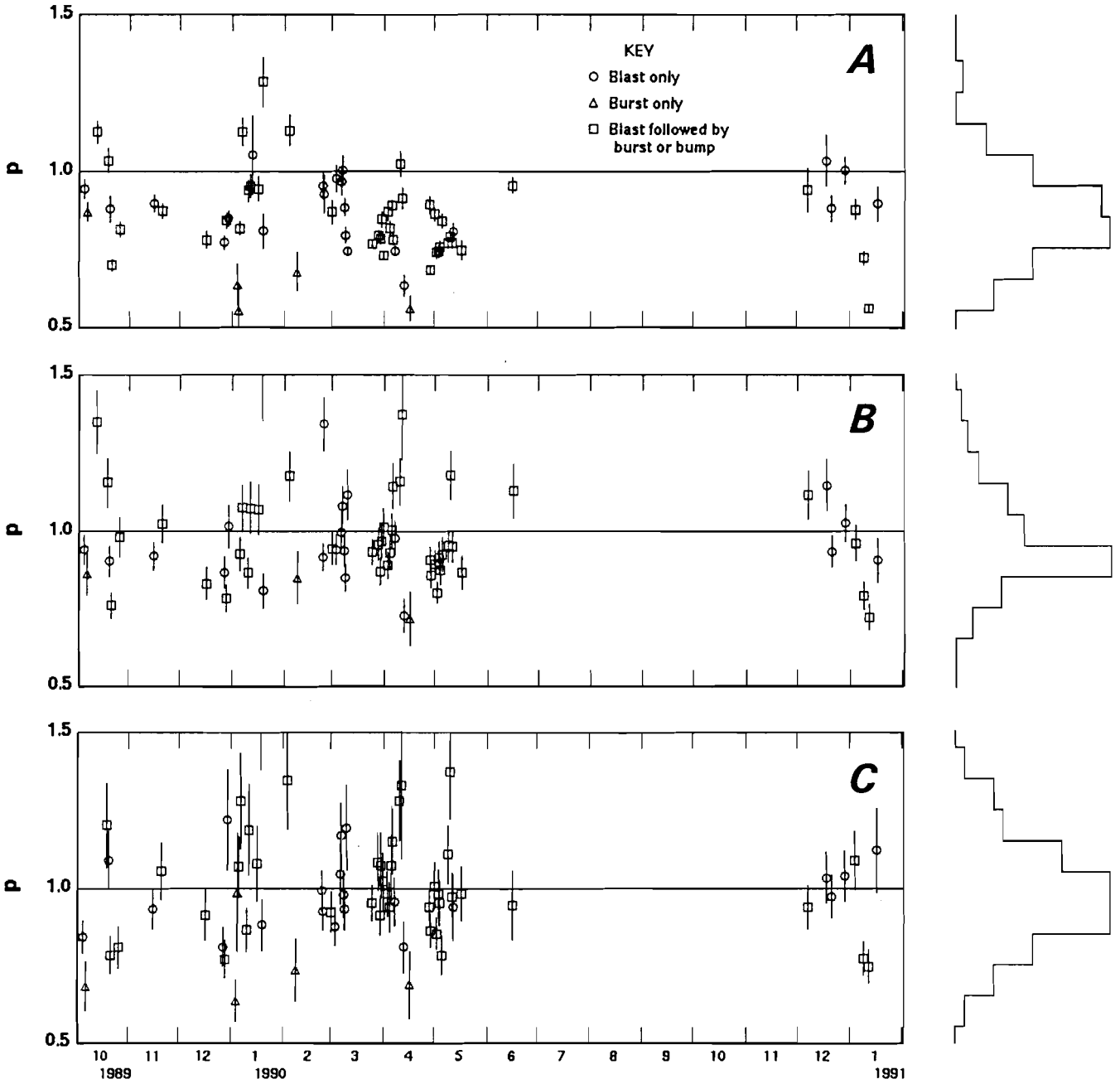

p of modified-Omori decays fit to blast and rock-burst sequences from October 1989 through January 1991 in the 99 stope. Vertical line at each p shows the 1 σ uncertainty. A relative histogram of the p-value distribution is shown at the left. *A*, Analysis of all data until next blast or burst, sometimes for sequences of 100 hours; *B*, termination of fit to events within 2 hours after main event; *C*, termination of fit to events within 1 hour after main event.

Figure 4
Example of Microseismic Decay Following Blasts With Increases in Rate.

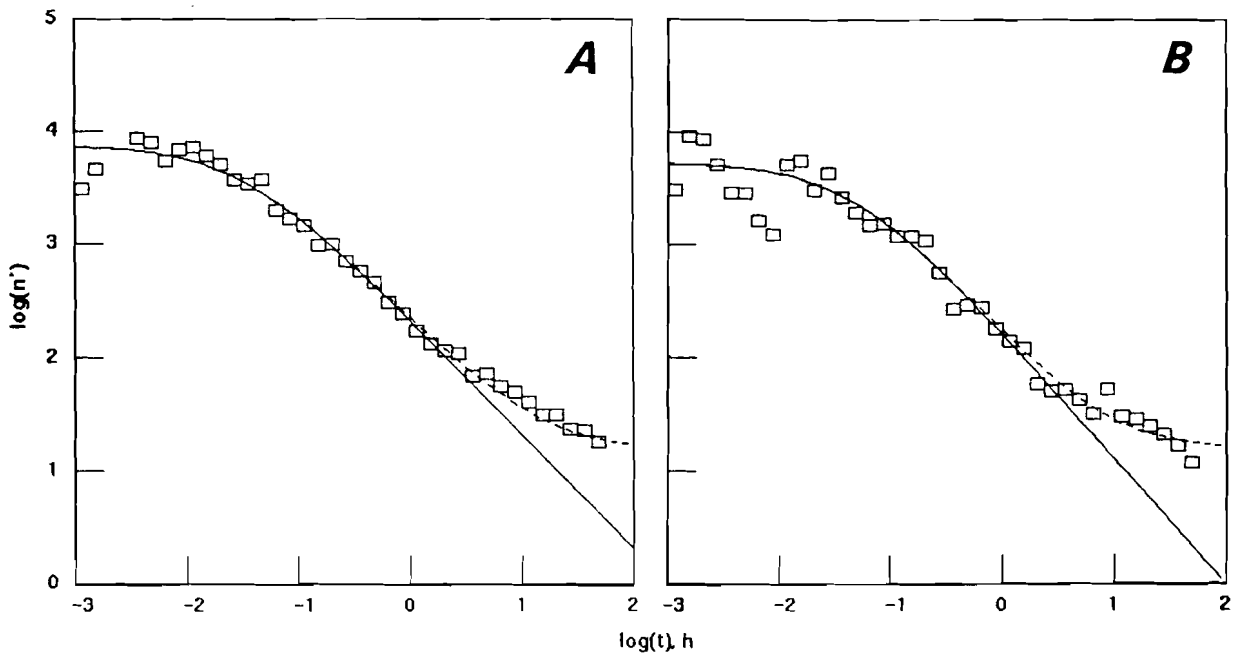

Same as figure 2, but for two other blasting events. Decay shows a break in slope at about 1-2 hours after the blasts. Dashed line is modified-Omori fit plus hypothetical constant rate of 15 events per hour. *A*, events following production blast on March 30, 1990, with a parameter fit of p = 1.011 (±0.060), k = 215.7 (±11.0), and c = 0.030 (±0.009); *B*, events following production blast on March 9, 1990, with a parameter fit of p = 1.116 (±0.080), k = 161.9 (±9.5), and c = 0.044 (±0.013).

about 0.6 to 1.1 at the time of the main event (Reasenberg, 1990). However, in the 99 stope area, there was no statistically significant temporal variation of p in the blast microseismic sequences before and after a burst.

TWO-DIMENSIONAL TOMOGRAPHY EXPERIMENT

Although the digital research system was designed for monitoring passively, the software was slightly modified to allow it to be used for one active source study (Billington and others, 1990b).[7] This study was designed to gauge the success of one or more planned destressing blasts in a vertical sill pillar above the 99 stope. This stope at the time of the planned destressing would be nearing the critical geometry for large rock bursts (outlined in "Introduction"), i.e., it would be about 25 to 30 m below the drift that would form one side of the horizontal pillar to be examined. The objective was to collect data both before and after the destress blast so that velocity tomograms of the horizontal pillar could be calculated. The difference tomogram would show where velocities changed: Increases in velocity might be due to increases of normal stress - thereby closing microcracks - and decreases in velocity might be due to an increase in microcrack population, showing internal damage to the pillar. An expected result was that if destressing the vertical sill pillar above the stope were successful, then an increase in stress somewhere in the horizontal pillar might be observed afterward.

To prepare sites for the tomographic sources and receivers, 30 jackleg holes were drilled from 0.6 to 1.2 m into the ribs of two drifts and one crosscut making up three sides of the horizontal pillar. The two drifts were the 104-vein drift in the vein under production (located above the planned destress blasts) and the 120-vein drift on the same level in a previously mined vein. The jackleg holes allowed the sources and receivers to be placed somewhat away from the highly fractured rind of rock that immediately surrounds mine openings in hard-rock mines. Magnetic stainless-steel plugs were affixed at the ends of the jackleg holes to provide the base for the active source (a tamping rod hit against the plug) and the receivers (Wilcoxon Research 793M-40 accelerometers) attached by magnets.

[7]Billington, S., F. M. Boler, P. L. Swanson, and L. H. Estey. A 2-D P-Wave Velocity Tomographic Experiment in a Deep Mine. Also presented at the Workshop on Induced Seismicity, 33rd U.S. Symp. Rock Mech., Santa Fe., NM, June 8-10, 1992.

To gain partial acoustic access to the fourth side of the pillar, two NX boreholes (7.49 cm in diameter) were drilled, one from the end of both drifts toward the end of the opposite drift. Into each borehole was placed one triaxial station made up of three mutually perpendicular 2 Hz to 25 kHz accelerometers.

The total pillar dimension that was scanned was about 60 by 90 m. The coordinates of all source and receiver sites were surveyed, and in most cases, the uncertainties of these coordinates were about ±0.05 m in all three directions. The majority of stations were clustered within ±0.3 m of a horizontal plane, though the total z-coordinate variation of the coordinates was about 2.7 m. The sampling frequency of the recorded waveforms was selected to be 50 kHz (equivalent to a spatial resolution in each waveform of about 0.1 m).

With the above array, 30 sites could be occupied as a source site, yielding 31 independent travel-time paths at each source site. For each tomographic image attempted, at least five separate impacts of the tamping rod were recorded at each source site. This amounts to about 5,000 waveforms per tomographic image. In all, data for three tomographic images were obtained, each data set being collected in less than two consecutive mining shifts on August 3, 1989, November 30, 1989, and February 13, 1990. The tomographic inversion was done with software developed by researchers at the USBM's Twin Cities Research Center (Jackson and others, 1992; Friedel and others, 1992), which allows for linear velocity gradients of an isotropic velocity within specified rectangular pixels on a plane.

These three tomographic data sets spanned four rock bursts in or near the 99 stope area, as well as two destressing blasts. The rock bursts occurred on October 5, 1989 (M_L 2.1), February 4, 1990 (M_L 1.2), and February 7, 1990 (M_L 2.9 followed 8.4 h later by an M_L 0.9 event). The destress blasts were done on December 15, 1989, and February 2, 1990, and caused immediate releases of seismic energy no greater than about M_L -0.5 and M_L 0.0, respectively. The first rock burst (M_L 2.1) had a source hypocenter near the corner of the pillar formed by the 120-vein drift and the crosscut and caused damage to the ribs in that area; the burst on February 4 (M_L 1.2) occurred off the end of the 104-vein drift; the first burst on February 7 (M_L 2.9) was about 60 m higher in the mine above one end of 120-vein drift; and the second burst on February 7th (M_L 0.9) was between the destress area of the vein and the 104-vein drift (Boler and Swanson, 1993a; 1993b).

The tomogram results can be summarized as follows. Each of the three tomograms have a low P-velocity region around most of both the drift and crosscut openings, a finding that is consistent with a fractured rind. The lowest P-velocities are near two raises in the 104 vein and at the corner formed by the 104-vein sill drift and the crosscut. There is also a high P-velocity core to the pillar. These results are very similar to those of a cruder P-velocity survey of a vertical sill pillar by Blake and others (1974) elsewhere in the mine. In the August 1989 tomogram, there is no indication of a high P-velocity area at or near the region where the future M_L 2.1 event was to occur in October. The main feature of the difference tomograms is a P-velocity decrease in the corner of the pillar damaged by the M_L 2.1 event, consistent with the damage on the ribs that had been observed immediately following the event.

Microseismic event activity, as determined by the routine monitoring system for the 99 stope in a ±3-m horizontal slice centered on the imaged pillar, was concentrated around the 104-vein drift. There was no concentration of microseismic activity in the area of the source of the M_L 2.1 event, neither before nor after the event occurred. Conversely, there was a concentration of microseismic activity in the area of the raise going down to the stope where the first difference tomogram (August 1989 to November 1989) shows a P-velocity increase. The second difference tomogram (November 1989 to February 1990), which brackets both destressing attempts in the sill pillar, shows only a slight increase in P-velocity in certain areas of the interior of the horizontal pillar. This increase also has no obvious correlation with microseismic activity at the time.

BPC MONITORING

The BPC array was fully operational during the time of the two rock bursts near the tomographic array on February 7, 1990. In addition, both microseismic systems were operational. Unfortunately, the first event (M_L 2.9) was not captured by the digital research system, as it was triggered 4 s earlier by a microseismic event near the 99 stope. This event was, however, captured by the routine monitoring system and was later located by using the arrival times recorded by that system and the location method used by the digital research system. A foreshock of the M_L 2.9 event, which was located in the same place as the main event, occurred about 40 min earlier and was captured by the digital research system. Using the P-wave polarity information from this foreshock of the M_L 2.9 event, and the M_L 0.9 event and its two foreshocks and three aftershocks, a focal mechanism was constructed for each large event. The strike of one of the nodal planes of each mechanism approximately matched the strike of the locally mapped, near-vertical faults in that part of the mine (Boler and others, 1990; Boler and Swanson, 1993a, 1993b).

For both the M_L 2.9 and M_L 0.9 events, a linear, three-dimensional dislocation model was used to compute expected coseismic pressure changes on each cell of the BPC array. The dislocation plane selected for each event

coincided with one focal mechanism nodal plane. The area of each dislocation plane was determined using an empirical magnitude-size relationship (Swanson, 1992). Then, a least squares fit was performed to find a scaling factor for the dislocation slip (and, for the M_L 2.9 event, to also find an orientation for the slip vector of the dislocation) that matched the coseismic pressure changes recorded on the BPC array. The final results show that the M_L 2.9 event can be modeled as 1.9 mm of combined left-lateral strike-slip and dip-slip over 88,000 m^2 of fault surface, and the M_L 0.9 event can be modeled as 0.5 mm of combined left-lateral strike-slip and dip-slip over 780 m^2 of fault surface (Boler and Swanson, 1993b).

Another important result of these dislocation models is that the M_L 2.9 event may have enhanced the likelihood that the later M_L 0.9 event would occur. This might have been caused by the dislocation motion of first event, which modified the stress across the future fault surface of the future M_L 0.9 event, lowering by 0.1 to 0.2 MPa the normal stress and also increasing by 0.4 MPa the particular shear stress component that led to the observed sense of dip-slip fault motion. However, the dislocation model of the M_L 2.9 event also yields a decrease of 0.3 MPa in the shear stress leading to left-lateral strike-slip motion on the plane of the M_L 0.9 event, which would have inhibited the fault-plane motion observed in the M_L 0.9 event.

STOPE CLOSURE MONITORING

A strong time correlation was found between stope closure as monitored with the convergence gages and the largest events occurring around the 99 stope (Boler and Swanson, 1992). In particular, the largest coseismic closure was 1.25 mm associated with an M_L -1 event located less than 10 m away from one of the gages. Closures of 0.2 mm were observed for an M_L 2 event located in another stope 190 m away. Coseismic convergence was observed for events down to about M_L -2. Also noted was that the convergence rates of the gages correlate with the position of the production face. However, aseismic creep (i.e., creep with no detected or associated seismicity) accounted for 18 pct of the total closure of one gage and 65 to 70 pct of the closure of the other two gages.

LARGE DOUBLET EVENTS

A doublet is defined here as two large events of significant magnitude and rock-burst potential occurring in about the same place in the mine and separated in time by a few minutes to a few days. Large doublet events (and in some cases, multiplet events) occurred in many areas in the Galena Mine. Figure 5 shows the occurrence of large doublets over a 20-month period in a stope that was not being monitored for microseismicity. About half the large

Figure 5
Example of Doublet Sequence for One Stope.

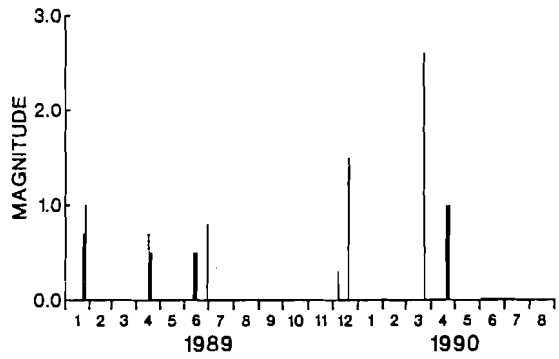

Sequence of rock bursts for the 49-133 stope area for a 20-month period. Local magnitudes were determined from surface seismograph records. Four sets of closely spaced bursts are identified as "doublets" (see text). Time interval between the two events of each doublet is actually less than 24 h.

events of M_L greater than 1 throughout the mine over this same time period were doublets that occurred within 24 h of one another (Swanson and Sines, 1990, 1991).

Two models were considered for explaining these large doublet events. One model relies on the modification of the local stress field on an existing fault surface resulting from the motion of the first event (Swanson, 1992; Boler and Swanson, 1993a, 1993b), as discussed above for the M_L 2.9 and M_L 0.9 events in the 99 stope. The other model relies on two facts: (1) Many of the veins in the Galena Mine are roughly perpendicular to bedding plane faults, and (2) many of stopes in these veins are roughly normal to direction of the large horizontal principal stress in the mine. In this model, the compliance of the stope results in a stress concentration around the end of the stope that favors dislocation slip on a plane approximately perpendicular to the main trend of the stope. Thus, at the Galena Mine, when a stope face would advance to the vicinity of a critically stressed bedding fault, the fault on one side of the stope may have been activated, followed shortly by activation of the fault on the other side. The probability of activation of the second half of the fault increases in both models discussed here. Given the ubiquitous presence of faults in the Galena Mine, it is difficult to determine which of these two models is correct (if either).

EVIDENCE OF STATE OF CRITICALITY

This section describes several examples showing that the rock surrounding recently mined openings has faults and fractures in a state of criticality, so that minor perturbations in stress or strain appear to induce seismic activity on some of these faults and fractures. Taken

together, these examples suggest that minor or distant (and seemingly insignificant) changes or activities in the mine environment can have a profound impact on inducing local seismic activity—even though the induced stress from these changes or activities is very small. It is important to realize that we are conjecturing real increases in seismic activity apparently resulting from increases in cultural activity in the mine (including both mining activity such as barring down, drilling, rock bolting, etc., and other activity such as movement of motors and ore cars, opening and closing of air doors, etc.), i.e., the increases in seismic activity are not a result of mistaking the noise of cultural activity for real seismic activity associated with rock fracture or slip.

(1) Prior to the resumption of mining in the 99 stope after a hiatus of over 2-1/2 years, a miner was sent into the stope to bar down loose rock. The miner reported a sharp increase in rock noise—or acoustic microseismicity—in the stope as the barring down took place. The stope had been quiet prior to this time.

(2) An increase in microseismicity in one stope has been observed to coincide with a production blast in another, nearby stope. For example, four adjacent stopes being simultaneously monitored by the routine monitoring system were selected for study. We noted that even when there had been no production blast in a certain stope, a flurry of microseismic activity in that stope would often occur at the time of production blasting (at the end of shift) when there was blasting in one or more of the other three stopes. The located events are deemed not to be a numerical artifact of a stope system mislocating events around another stope, as the detection times for these events do not correlate with the detection time for events in any of the other stopes.

(3) A statistical observation of the effect noted in (2) can be achieved by using a modified-Omori decay model. As discussed in the section on "Microseismic Decay Sequences," decay cutoffs of 1 to 2 h were used to fit microseismicity after routine production blasts. This was because, in many cases, a kink in the decay curve can be seen in which the data deviate from a modified-Omori decay fit about 1 to 8 h after the blast in the stope (figure 4). This 1- to 8-h period brackets the onset of increased cultural activity throughout the mine at the beginning of the next shift (1 h) and the time of blasting at the end of the next shift (8 h). Although a constant background of 15 to 20 events per hour could account for this kink in the modified-Omori curves (figure 4), a constant background is not deemed to be a reasonable explanation owing to the occasional lack of this kink following some blasts (e.g., figure 2). In fact, as seen in figure 4*B*, the data after the point of the kink resemble a small, new, modified-Omori curve, suggesting activation of a small, new source region.

(4) The occurrence of sympathetic activity suggested by (2) and (3) above may not be limited to small microseismic events. At the other end of the spectrum, as discussed in the section "BPC Monitoring" (M_L 0.9 event in the 99 stope following a nearby M_L 2.9 event) and in Swanson and Sines (1990) and Swanson (1992), there is evidence to support an increase in the probability of occurrence of large events from the occurrence of other nearby large events. The data compiled by Swanson (1992) show that between January 1989 and May 1992, there were several other occurrences of bursts within a short window of time in the same or different stopes of the mine where the subsequent event occurred at a time of enhanced cultural activity in the mine (but not at blast time). The question then arises: Why does the second event in the doublet occur when it does? Do minor stress perturbations due to the cultural activity sometimes trigger the subsequent event, or is the occurrence of this event at these times of cultural activity just a random happening? We do not yet have an answer to these questions.

FRACTALITY, CLUSTERING, AND PLANARITY OF MICROSEISMIC EVENTS

To better understand the response of the damaged rock mass in the neighborhood of active stopes, microseismicity was examined using various statistical methods to characterize spatial and temporal activity after blasts and rock bursts in the vicinity of these stopes (Coughlin and Kranz, 1991; Kranz and others, 1994). These methods attempt to characterize a sequence of events following a progenitor (blast or burst) as a whole and do not rely on details of individual microseismic events. The data archived by the routine monitoring system are ideal for these methods because waveform analysis is not required.

One finding using these methods is that microseismic activity around stopes has a fractal or self-similar nature in time and space. In time, the fractality extends over scales at least from minutes to days, where these temporal scales are currently limited by the inability to capture and detect all seismic activity immediately after a blast or burst at the smallest scale and the interference of effects from subsequent blasts or bursts at the largest scale. In space, fractality extends over scales from 1 to 100 m, where these spatial scales are currently limited by event location precision at the smallest scale and the array size at the largest scale. There appears to be no statistical difference in the distributions of fractal dimensions in comparisons of microseismic sequences following blasts and seismic events (including those involved in rock bursts) and no differences in the distributions of fractal dimensions in

comparisons of data from different stope arrays. This result suggests that the physical processes responsible for rock mass relaxation following a sudden stress change in the mine are the same, regardless of the stress change progenitor or the stope location.

An ongoing study, however, is revealing that different attributes of this relaxation response may vary depending on whether the progenitor is a rock burst or a blast and may also vary from stope to stope. Differences in attributes that measure spatial extent, event decay rate, accumulative event counts, and the energy of these sequences are found. On the other hand, the attributes of fractal dimension are indistinguishable. This suggests that there are methods to characterize the rock mass in a mining environment by characterizing microseismicity and that any such characterization will be independent of the progenitor of the microseismicity.

Billington and others (1990a) showed that it was possible to identify and map active faults within the country rock (within the coverage of an array) by identifying concentrations of microseismic events outside of normal stope activity. The locations of these active faults can be found to the same degree of accuracy as the locations of microseismic events, i.e., a few meters. The more rigorous methods of Kranz and others (1994)[8] show that microseismicity in different stopes usually has a primary planarity that approximates that of the vein being mined, which agrees with the work of Billington and others (1990a), and that the microseismic planarity is the same regardless of the progenitor. Routine identification of bedding plane faults by this method is rare. Several interpretations of why the bulk of the microseismicity in a stope approximates the vein are currently being investigated.

BEHAVIOR SINCE JULY 1992

The initiation of standby mode at the Galena Mine in mid-1992 afforded an opportunity to continue monitoring microseismicity at the mine in the absence of development and production blasting. Microseismicity continued even in the absence of large events. Also, microseismicity decays continued to follow a modified-Omori decay law, lending support to the premise that the kinks at 1 to 8 h in the decays of stope activity during production were in fact due to activation of microseismic slip from blasting and cultural activities elsewhere in the mine and were not due to background activity.

Data from the 99 stope array are used to illustrate these points. The 99 stope array is selected because there were no changes in station number or station position during the period of time shown (figures 6 and 7), and there were relatively few large data gaps resulting from power outages and other hardware problems. The few main data gaps are in mid-September 1992 (100.3-h gap), mid-November 1992 (49.5-h gap), early May 1993 (75.1-h gap), mid-May 1993 (160.2-h gap), and late June 1993 (31.6-h gap).

Microseismic activity decays smoothly in the 99 stope following the last blast in the afternoon of June 3, 1992. A near-constant rate of activity occurs for about the next 100 h or so, probably corresponding to sympathetic activity induced by blasting in nearby areas. This activity finally ceases by mid-June 1992, and the activity steadily decays following a power-law decrease ($p \sim 0.76$) until the occurrence of an M_L 3.0 rock burst in the afternoon of March 18, 1993.

The decay of microseismic activity following the March 18 event is shown in figure 8. The decay is a near-perfect power law also with a p of about 0.76, because the two low points of the decay are due to the data gaps in May and June 1993.

A second M_L 3.0 rock burst occurred about 280 m from the 99 stope on July 1, 1993, a year after the cessation of routine blasting at the mine. The decay of microseismic activity following this event is shown in figure 9. Here there seems to be two different rates of decay. The first has a p about equal to that following the March 18 event, ending about 30 h after the main event; the second has a p of about 0.45.

Three other small rock bursts (M_L 0.0 $\pm$0.5) occurred elsewhere in the mine on September 6, 1992, September 10, 1992, and January 20, 1994. These events did not affect the event rate in the 99 stope.

These results, combined with the earlier microseismic decays during production, suggest that the mine has two or possibly three different inherent damage structures. The interpretation of the various values of p (1.0, 0.76, and possibly 0.45) is still being investigated.

PRECURSOR ACTIVITY BEFORE ROCK BURSTS AND OTHER LARGE EVENTS

The main underlying assumption that led to the intense microseismic monitoring effort at the Galena Mine was the belief that some type of microseismic precursor activity would occur and would be detectable prior to large seismic events, allowing for an acceptable amount of time to relocate mine personnel to avoid or reduce the possibility of injury. For example, models of source preparation and laboratory experiments indicate that there should be an acceleration of small events prior to a main event. In fact, at the Galena Mine on at least one occasion, an increase in activity did occur. On January 3, 1990, a sharp increase in microseismic activity occurred 2 to 3 h prior to the first of two small rock bursts (M_L -0.5 or less) at the face of

[8]See also footnote 5.

Figure 6
Microseismic Event Decay During Standby at Galena Mine in One Stope.

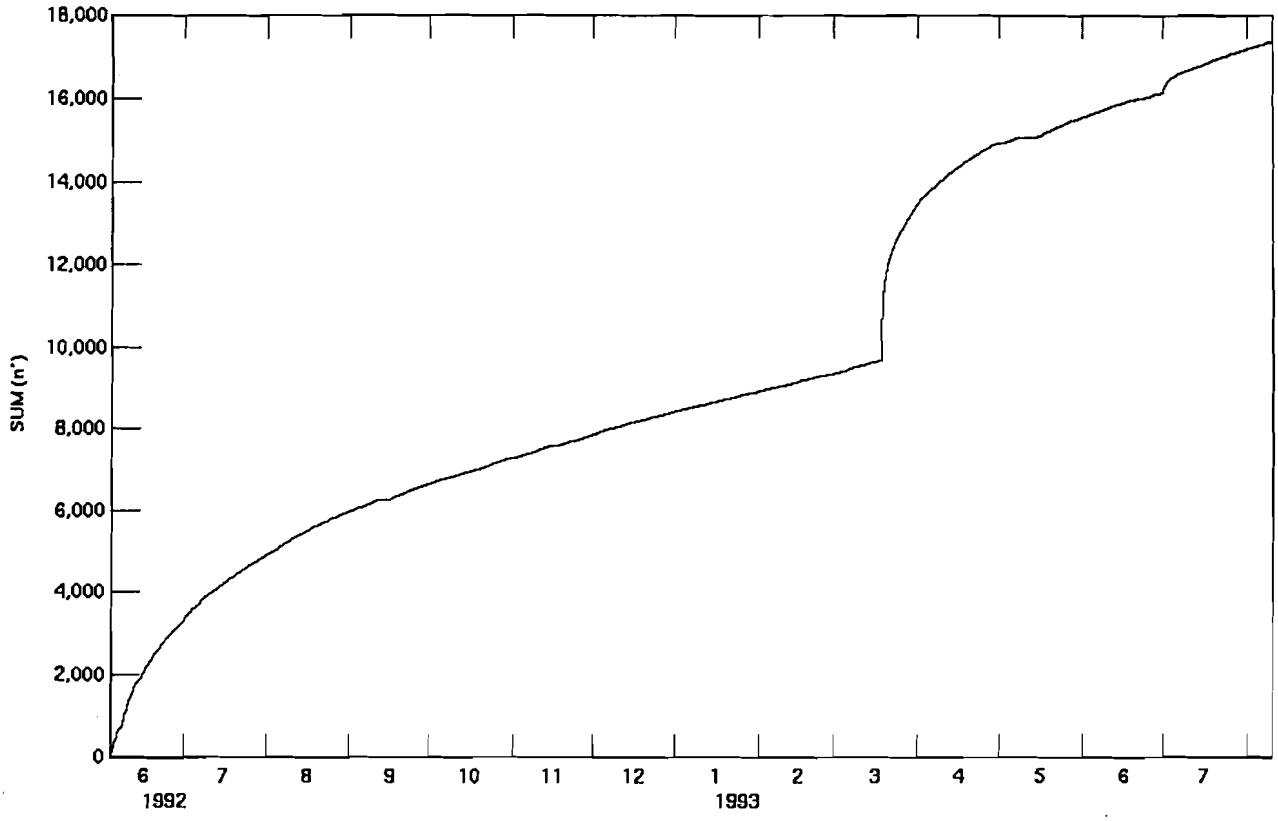

Accumulative number of located microseismic events in 99 stope area following the last blast in the stope, following day shift on June 3, 1992. A few periods of zero accumulation are due to data gaps (see text). The increases in March and July 1993, coincide with a M_L 3.0 event on March 18 in stope area and another M_L 3.0 event about 280 m away on July 1.

the 99 stope. This stope was being monitored by the routine monitoring system at the time. The increase in activity alerted personnel in the instrumentation room, so there was time to contact the miners in this stope and suggest they take an early lunch. Thus, no one was working at the face at the time when the first burst occurred, and work in the stope was suspended for the rest of the day. However, the microseismic activity of the stope had dropped almost to the normal background rate by the time of the first burst, i.e., there was no continuing buildup in activity leading up to the main event.

An attempt was made to identify in a consistent fashion any change, whether an increase or a decrease, in microseismic activity that may have occurred prior to 35 large seismic events in the mine having an M_L from about 1 to 3 (Swanson, 1993). This study included the two M_L 3.0 events that occurred after the Galena Mine went into standby mode, but excluded the two small events of January 3, 1990. Microseismic activity was found to increase in the days and weeks prior to some of these large events, probably because of increases in local stress concentrations as a result of mining. However, no obvious increase in activity was found to occur in the seconds to 2 h preceding these large events. In fact, microseismic activity before these events was completely consistent with the activity expected from a modified-Omori decay following the last mining blast or large event in the area. If the accumulative number of microseismic events occurring during the 2 h before these 35 large events are stacked, a near-linear increase in accumulative microseismic events is found, which indicates a near-zero rate of change in average activity prior to these events. Thus, contrary to predictions of failure models, results of laboratory experiments, and our predilections, there is not a consistent acceleration of small events before large events at the Galena Mine. If there is accelerating creep-like deformation in the moments before a large main event in the mine, this acceleration is accompanied by microseismic events that are no larger than 7 to 9 orders of magnitude smaller in energy than the main event.

Figure 7
Microseismic Event Decay From June 3, 1992 Through March 18, 1993.

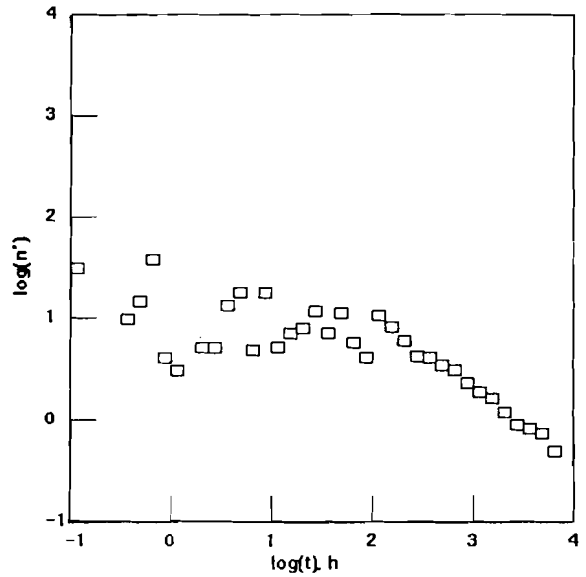

Histogram of microseismic decay rate for located events in 99 stope area following the last blast. The decay starting at about 100 h after the last blast probably signifies end of sympathetic activity resulting from blasting in nearby areas and has a p of about 0.76.

CONSIDERATION OF LARGE ASEISMIC DEFORMATIONS

The studies of Swanson (1992) and Boler and Swanson (1993a, 1993b) show the significant changes in slip potential that can result in different areas of the mine as compliant mine openings deform and dislocation motion takes place in other parts of the mine. It is vital to note that although these studies are attempts to model the changes in slip potential resulting from large seismic events in the mine, there is nothing to limit the overall conclusions as resulting from only seismic events. In fact, at the Galena Mine, a large amount of aseismic deformation (up to several centimeters per year) would routinely take place in certain areas. These areas tended to be in the soft St. Regis Formation and thus tended not be rock-burst prone and transmitted only a small amount of rock noise. Therefore, none of these areas were instrumented to monitor microseismicity. But to understand the driving mechanisms that affect rock-burst-prone areas, these aseismic areas are just as relevant as seismic areas and require an understanding of the overall deformation of the mine. In short, monitoring and understanding the seismic component of deformation represents only part of the overall problem of monitoring and understanding rock bursts.

Figure 8
Microseismic Event Decay From March 18 Through July 1, 1993.

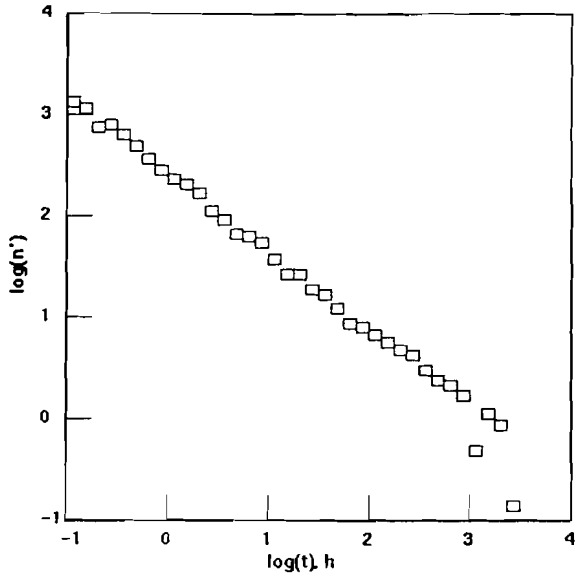

Histogram of microseismic decay rate for located events in 99 stope area following the March 18, 1993, M_L 3.0 rock burst. This decay also has a p of about 0.76.

Figure 9
Microseismic Event Decay Following July 1, 1993.

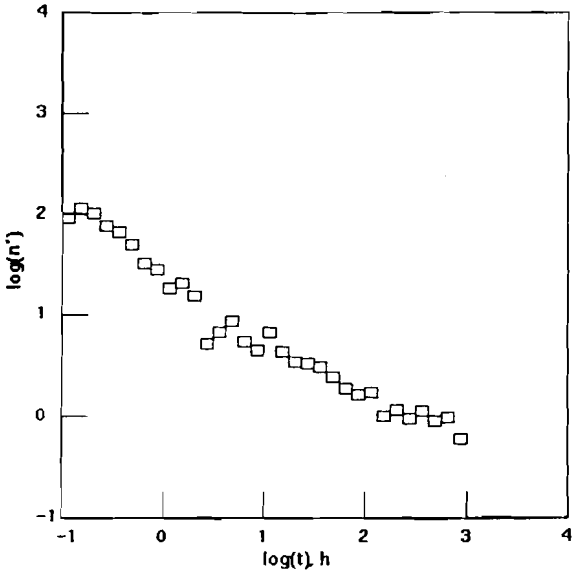

Histogram of microseismic decay rate for located events in 99 stope area following the July 1, 1993, M_L 3.0 rock burst 280 m distant. This decay appears to have two power-law segments; first has a p of about 0.76; second starting about 30 h after the main event, has a p of about 0.45.

SUMMARY AND FUTURE DIRECTIONS

Two types of microseismic monitoring systems were designed, tested, and used to monitor a number of rock-burst-prone stopes at the Galena Mine. Much of the data collected with these systems has been archived and continues to be a valuable resource for study to elucidate aspects of the rock-burst problem. One of the systems uses an array of receivers to detect and locate events automatically and then archives the data, as well as some statistical information about each event. The other system collects digital waveform data from the array, which allows for a more complete analysis of each event, and can be used to collect and analyze other dynamic and quasistatic measurements at the same time microseismic activity is being monitored. The data collected by each system are complementary and are amenable to a suite of different analysis methods.

The idea that there might be some type of anomalous microseismic activity before a rock burst has been tested in a variety of ways. Whereas isolated cases have been identified in which there was a sudden increase in activity before a burst, there appears to be no unique, reliable, easily detectable, or statistically significant occurrence of anomalous microseismic activity before rock bursts at the Galena Mine. Thus, a reliable short-time indicator of an impending rock burst that would allow for the safe relocation of personnel in the area does not yet exist.

However, several methods of analysis suggest that there are ways to forecast changes in the likelihood of the occurrence of rock bursts. One such method is the characterization of the rock mass around a stope through the use of microseismic events; moreover, this characterization seems to be statistically independent of the progenitor of the microseismic events. Nearly all microseismic events and many rock bursts appear to occur by slip on a plane, whether on preexisting faults or bedding planes, or on surfaces resulting from new fracture. Changes in slip potential on preexisting fault or bedding surfaces resulting from either seismic or aseismic deformation in other regions of the mine can be calculated. The seismic component is readily amenable to study by analysis methods already developed for full waveform data, but the aseismic component will be very difficult to measure and characterize for an entire mine. Our understanding of the problem at this time leads us to think that a simultaneous monitoring of both the seismic and the aseismic deformations in a mine such as the Galena (where significant amounts of both types of deformation occur) will be required in order to estimate accurately any changes in slip potential in the rock-burst-prone areas of the mine and then to correlate these predicted changes with the actual occurrence of large seismic events. Also, the source mechanisms of some rock bursts and associated microseismic events are not understood at this time; an active part of ongoing research is focused toward gaining an understanding of these different types of mechanisms. The problem remains to fully identify, characterize, and measure the mechanics of the geologic and mining-induced structures using both seismic and aseismic components of mine deformation.

REFERENCES

Aki, K., and P. G. Richards. Quantitative Seismology: Theory and Methods. V. 1, W. H. Freeman, 1980, 557 pp.

Billington, S., F. M. Boler, P. L. Swanson, and L. H. Estey. P-Wave Polarity Patterns from Mining-Induced Microseismicity in a Hard-Rock Mine. Paper in Rock Mechanics Contributions and Challenges: Proceedings of the 31st U.S. Symposium, ed. by W. A. Hustrulid and G. A. Johnson (CO Sch. Mines, Golden, CO, June 18-20, 1990). Balkema, 1990a, pp. 931-938.

____. 2-D P-Wave Velocity Tomographic Experiment in an Idaho Silver Mine. Abstract in Trans. Am. Geophys. Union, EOS, v. 71, 1990b, p. 1454.

Blake, W. Rock Burst Research at the Galena Mine, Wallace, Idaho. USBM TPR 39, 1971, 22 pp.

Blake, W., F. Leighton, and W. I. Duvall. Microseismic Techniques for Monitoring the Behavior of Rock Structures. USBM Bull. 665, 1974, 65 pp.

Boler, F. M., and P. L. Swanson. A CAMAC-Based Workstation for Microseismic and Acoustic Emission Research. USBM IC 9262, 1990, 9 pp.

____. Observations of Heterogeneous Stope Convergence Behavior and Implications for Induced Seismicity. Pure and Appl. Geophys., v. 139, No. 3/4, 1992, pp. 639-656.

Boler, F. M., and P. L. Swanson. Seismicity and Stress Changes Subsequent to Destress Blasting at the Galena Mine and Implications for Stress Control Strategies. USBM RI 9448, 1993a, 21 pp.

____. Modeling of a Destress Blast and Subsequent Seismicity and Stress Changes. Paper in Rockbursts and Seismicity in Mines 93. Proceedings of the 3rd International Symposium on Rockbursts and Seismicity in Mines, ed. by R. P. Young (Kingston, ON, Aug. 16-18, 1993). Balkema, 1993b, pp. 35-40.

Boler, F. M., P. L. Swanson, and S. Billington. Patterns of Microseismicity in an Idaho Silver Mine. Abstract in Trans. Am. Geophys. Union, EOS, v. 69, 1988, p. 1050.

Boler, F. M., P. L. Swanson, S. Billington, and L. H. Estey. Seismicity and Stress Changes Associated With an ML 2.9 Rock Burst in an Idaho Silver Mine. Abstract in Trans. Am. Geophys. Union, EOS, v. 71, 1990, pp. 1453-1454.

Coughlin, J., and R. Kranz. New Approaches to Studying Rock Burst-Associated Seismicity in Mines. Paper in Rock Mechanics as a Multidisciplinary Science: Proceedings of the 32nd U.S. Symposium, ed. by J. C. Roegiers, (Univ. OK, Norman, July 10-12, 1991). Balkema, 1991, pp. 491-500.

Coughlin, J., and C. D. Sines. Field Trials of a Portable Microseismic Processor Recorder. USBM IC 9022, 1985, 8 pp.

Engdahl, E. R., and W. A. Rinehard. Seismicity Map of North America Project. Ch. 2., Neotectonics of North America. Geol. Soc. Am., 1991, pp. 21-28.

Estey, L. H. Seismic Source Locations: The Fallacy of the Assumption of Minimum Travel-Time Residuals. Abstract in Trans. Am. Geophys. Union, EOS, v. 71, 1990, pp. 1479-1480.

Estey, L. H., P. L. Swanson, F. M. Boler, and S. Billington. Microseismic Source Locations: A Test of Faith. Paper in Rock Mechanics Contributions and Challenges: Proceedings of the 31st U.S. Symposium, ed. by W. A. Hustrulid and G. A. Johnson (CO Sch. Mines, Golden, CO, June 18-20, 1990). Balkema, 1990, pp. 939-946.

Friedel, M. J., D. R. Tweeton, M. J. Jackson, J. A. Jessop, and S. Billington. Mining Applications of Seismic Tomography. (Pres. at Ann. Meet., Soc. Explor. Geophys., New Orleans, LA, 1992). Extended Abstr., Soc. Explor. Geophys., 1992, pp. 58-62.

Godson, R. A., M. C. Bridges, and B. M. McKavanagh. A 32-Channel Rock Noise Location System. Paper in Proceedings, Second Conference on Acoustic Emission/Microseismic Activity in Geologic Structures and Materials, ed. H. R. Hardy, Jr., and F. W. Leighton (PA State Univ., University Park, PA, Nov. 13-15, 1978). Ser. on Rock and Soil Mech., v. 5., Trans Tech Pub., 1980, pp. 117-161.

Haramy, K. Y., and R. O. Kneisley. Hydraulic Borehole Pressure Cells: Equipment, Technique, and Theories. USBM IC 9294, 1991, 26 pp.

Hobbs, S. W., A. B. Griggs, R. E. Wallace, and A. B. Campbell. Geology of the Coeur d'Alene District, Shoshone County, Idaho. U. S. Geol. Surv. Prof. Paper 478, 1965, 139 pp.

Jackson, M. J., D. R. Tweeton, and S. Billington. Seismic Crosshole Tomography using Wavefront Migration and Fuzzy Constraints: Application to Fracture Detection and Characterization. Paper in Proceedings of the 6th National Outdoor Action Conference on Aquifer Restoration, Ground Water Monitoring, and Geophysical Methods. Nat. Groundwater Assoc., 1992, pp. 741-754.

Kranz, R. L., J. Coughlin, and S. Billington. Studies of Stope-Scale Seismicity in a Hard Rock Mine, Part I: Methods and Factors. USBM RI 9525, 1994, 27 pp.

Lee, W. H. K. (ed.) IASPEI Software Library Volume 1: Toolbox for Seismic Data Acquisition, Processing, and Analysis. Int. Assoc. Seismo. Phys. Earth's Interior, 1989, 283 pp.

Lee, W. H. K., D. M. Tottingham, and J. O. Ellis. A PC-Based Seismic Data Acquisition and Processing System. U.S. Geol. Surv. OFR 88-751, 1988, 31 pp.

Leighton, F. W. A Case History of a Major Rock Burst. USBM RI 8701, 1982, 14 pp.

____. Rock Burst Research at the Galena Mine--1976. USBM TPR 10020, 1976, 29 pp.

Lourence, P. B., S. J. Jung, and K. F. Sprenke. Source Mechanisms at the Lucky Friday Mine: Initial Results from the North Idaho Seismic Network. Paper in Rockbursts and Seismicity in Mines 93. Proceedings of the 3rd International Symposium on Rockbursts and Seismicity in Mines, ed. by R. P. Young (Kingston, ON, Aug. 16-18, 1993). Balkema, 1993, pp. 217-222.

Ogata, Y. Estimation of the Parameters in the Modified Omori's Formula for Aftershock Frequencies by the Maximum Likelihood Procedure. J. Phys. Earth, v. 31, 1983, pp. 115-124.

Reasenberg, P. A., Microclusters and Compound Clusters. Abstract in Trans. Am. Geophys. Union, EOS, v. 71, 1990, p. 1457.

Riefenberg, J. A Simplex Method-based Algorithm for Source Location of Microseismic Events Associated with Underground Mining. Paper in Rock Mechanics as a Guide for Efficient Utilization of Natural Resources: Proceedings of the 30th U.S. Symposium, ed. by A. W. Khair (WV Univ., Morgantown, WV, June 19-22, 1989). Balkema, 1989a, pp. 655-662.

____. A Simplex-Method-Based Algorithm for Determining the Source Location of Microseismic Events. USBM RI 9393, 1989b, 12 pp.

Rowell, G. A., and L. P. Yoder. The Effect of Geophone Emplacement on the Observed Frequency Content of Microseismic Signals. Paper in Acoustic Emission/Microseismic Activity in Geologic Structures and Materials: Proceedings of the Third Conference, ed. by H. R. Hardy, Jr., and F. W. Leighton (PA State Univ., University Park, PA, Oct. 5-7, 1981). Ser. on Rock and Soil Mech., v. 8, Trans Tech Publ., 1984, pp. 707-727.

Steblay, B. J, B. T. Brady, and E. E. Hollop. A Networked Minewide Microseismic Rock Burst Monitoring System. Paper in Mining for the Future: Trends and Expectations. (Proc. 14th World Min. Congr., Beijing, China, May 14-18, 1990). Pergamon, 1990a, pp. 861-868.

Steblay, B. J, B. T. Brady, and T. J. Swendseid. Innovative Microseismic Rockburst Monitoring System. Paper in Rockbursts and Seismicity in Mines, Proceedings of the 2nd International Symposium on Rockbursts and Seismicity in Mines, ed. by C. Fairhurst (Univ. MN, Minneapolis, MN, June 9-10, 1988). Balkema, 1990b, pp. 259-262.

Stickney, M. C. Montana Seismicity 1989. MT Bur. Mines and Geol. OFR-263, 1993, 46 pp.

Swanson, P. L. Mining-Induced Seismicity in Faulted Geologic Structures: An Analysis of Seismicity-Induced Slip Potential. Pure and Appl. Geophys., v. 139, No. 3/4, 1992, pp. 657-676.

____. Search for Accelerating Deformation in the Seconds Prior to Mining-Induced Seismic Events. Abstract in Trans. Am. Geophys. Union, EOS, v. 74, 1993, p. 411.

Swanson, P. L., and F. M. Boler. Application of AE/MS Waveform Analysis to Hazard Detection, Evaluation, and Control in Underground Mines. Paper in Process in Acoustic Emission IV (Proc. 9th Int. Acous. Emiss. Symp., Kobe, Japan, Nov. 14-17, 1988). 1988a, pp. 303-310.

____. Opportunities for Observation of Fault Activation in an Underground Mine. Abstract in Trans. Am. Geophys. Union, EOS, v. 69, 1988b, p. 1050.

Swanson, P. L., L. H. Estey, F. M. Boler, and S. Billington. Accuracy and Precision of Microseismic Event Locations in Rock Burst Research Studies. USBM RI 9393, 1992a, 40 pp.

____. Mining-Induced Microseismic Event Location Errors: Accuracy and Precision of Two Location Systems. Pure and Appl. Geophys., v. 139, No. 3/4, 1992b, pp. 375-404.

Swanson, P. L., and C. D. Sines. Repetitive Seismicity (M – 2-3) and Rock Bursting along a Plane Parallel to Known Faulting in the Coeur d'Alene District, ID. Abstract in Trans. Am. Geophys. Union, EOS, v. 71, 1990, p. 1453.

____. Characteristics of Mining-Induced Seismicity and Rock Bursting in a Deep Hard-Rock Mine. USBM RI 9393, 1991, 12 pp.

Utsu, T. Aftershocks and Earthquake Statistics, Part I: Some Parameters which Characterize an Aftershock Sequence and Their Interpretations. J. Fac. Sci. Hokkaido Univ., v. 3, 1969, pp. 129-195.

INSTALLATION OF PC-BASED SEISMIC MONITORING SYSTEMS WITH EXAMPLES FROM THE HOMESTAKE, SUNSHINE, AND LUCKY FRIDAY MINES

By J. M. Girard,[1] T. J. McMahon,[2] W. Blake,[3] and T. J. Williams[2]

ABSTRACT

Researchers from the U.S. Bureau of Mines have installed low-cost, personal-computer-based data acquisition systems to monitor mining-induced seismicity and rock mass deformation at three underground hard-rock mines: the Homestake Mine, Lead, SD; the Sunshine Mine, Osburn, ID; and the Lucky Friday Mine, Mullan, ID. The basic components of the systems include geophones, amplifiers, signal-conditioning equipment, and data acquisition hardware and software. Each system is capable of automatically recording and storing full-waveform information from seismic events in the mine. By combining data from these systems with rock mechanics information from the mine, a modified excavation plan may minimize rock burst occurrences and may allow recovery of more resources from highly stressed ground.

The process of selecting recording devices, designing system layout, and installing the equipment are described in detail. Examples from the systems at the three mines are included.

INTRODUCTION

The seismic monitoring systems described in this paper were developed as an integral part of the U.S. Bureau of Mines' (USBM) rock-burst research program. These systems, which are referred to as macroseismic systems, are capable of digitally recording the full waveform of a seismic event. The system control is provided by a program running on a personal computer (PC), which is also used to store the waveform information from the seismic events. The digital waveform records can be used to study the characteristics of rock bursts and provide valuable information regarding the location, amount of energy release, frequency response, and probable first-motion planes. When this information is combined with operating data and information on geologic structure, development plans can be changed to reduce the incidence of rock bursts. The components of the monitoring system and basic installation procedures are discussed in this paper. Williams and others (1995)[4] describe the applications of macroseismic systems.

[1]General engineer, Spokane Research Center, U.S. Bureau of Mines, Spokane, WA.

[2]Mining engineer, Spokane, Research Center.

[3]Consultant, Hayden Lake, ID.

[4]Williams, T. J., C. J. Wideman, K. F. Sprenke, J. M. Girard, and T. L. Nichols. Comparison of Data from In-Mine Rock-Burst Monitoring Systems and the North Idaho Seismic Network for the Lucky Friday Mine. Paper in Proceedings: Mechanics and Mitigation of Violent Failure in Coal and Hard-Rock Mines. USBM Spec. Publ. 01, 1995, pp. 265-281.

PC-BASED SEISMIC MONITORING EQUIPMENT

The equipment making up a PC-based seismic monitoring system can be divided into three components: geophones, wiring network, and data acquisition equipment. Appendix A gives examples of seismic monitoring systems installed by the USBM.

GEOPHONES

Geophones are transducers sensitive to seismic energy traveling through rock. As energy radiates from a seismic source, it causes motion in the rock mass. Geophones produce a signal voltage proportional to this movement when the seismic energy is sufficient to cause displacement of the mass within the geophone.

Geophones are either single axis or triaxial. Single-axis geophones are sensitive to seismic motion in one direction only, usually in the direction of the geophone's longitudinal axis. Triaxial geophones are sensitive to seismic motion on three mutually orthogonal axes. While a single-axis geophone produces one signal, a triaxial geophone produces three independent signals.

Velocity Geophones

Geophones that produce an output voltage proportional to the velocity of a rock particle are called velocity geophones. These typically consist of a coil of fine wire wound around a core, which in turn surrounds a permanent magnet suspended from a spring (figure 1*A*). Relative motion of the magnetic mass in the coil windings induces a voltage linearly proportional to rock particle velocity. The frequency response for velocity geophones is typically in the range of 1 to 2,500 Hz, with a resonant frequency for the mass and spring of about 10 Hz.

Accelerometer Geophones

Geophones that produce a voltage proportional to the acceleration of a rock particle are called accelerometer geophones or accelerometers. Accelerometers are often smaller than velocity geophones and typically employ a mass acting on a piezoelectric device to produce a signal (figure 1*B*). When these transducers are displaced by an incident seismic wave, the pressure exerted by the spring-loaded mass on the piezoelectric crystal produces a signal voltage proportional to particle acceleration. Accelerometers are typically dampened to have flat frequency responses in the range of 100 Hz to 10 kHz and pronounced rolloff outside this range.

Preamplifiers

The signals produced by most geophones are generally very weak and often must be transmitted long distances to a data acquisition and monitoring system. Preamplifiers

Figure 1
Inner Workings of *A*, Velocity Geophone and *B*, Accelerometer Geophone.

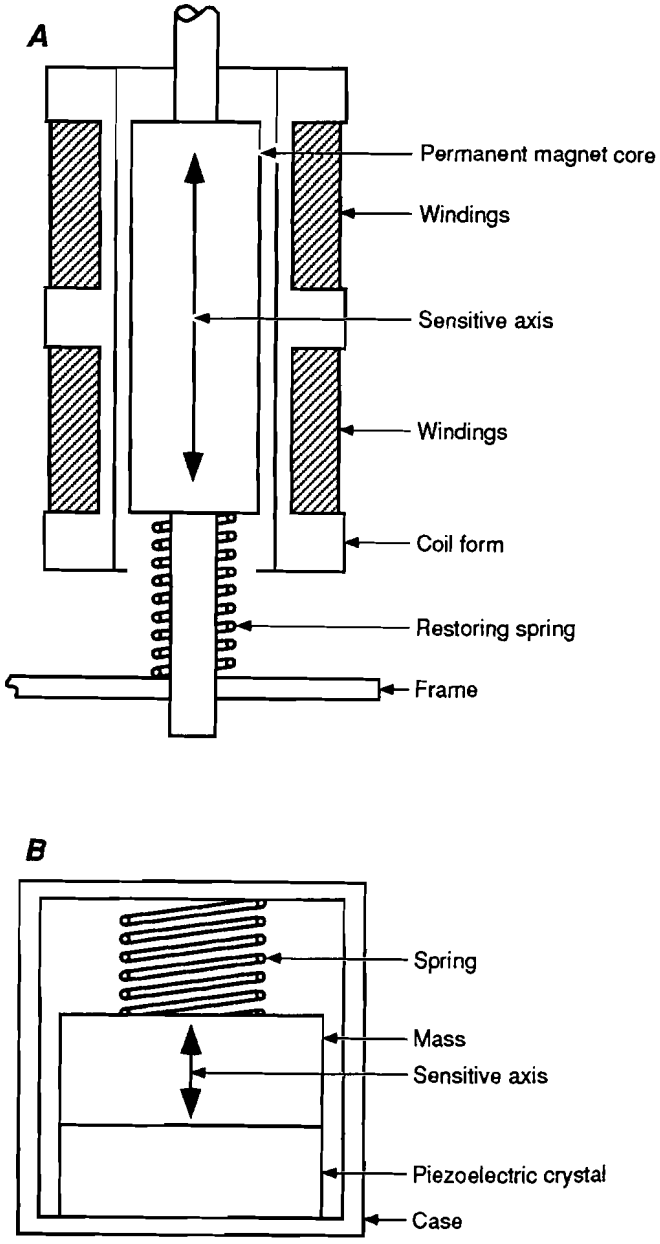

near the geophones are therefore required to amplify the signal to a level well above the level of any noise that may enter the transmission path. Figure 2 shows a geophone and a preamplifier.

Power Supplies

The location of power supplies should be as close to the geophones and preamplifiers as practical to avoid an excessive voltage drop for signals being transmitted over long distances. Different brands of geophones have different voltage requirements. This should be taken into consideration when designing a system. Voltages not falling within the allowable range for the equipment selected may cause malfunctions, such as data loss or the generation of erroneous data.

WIRING NETWORK

Transmission of the seismic signal from the geophone or geophone-preamplifier to the data acquisition system is the function of the system's wiring network. The network consists of multipair cables and junction boxes where all connections are made. Experience has shown that whenever possible, the data acquisition system should be located on the surface. However, depending on the depth of the mine, a surface monitoring room may require an impractical amount of cable. In such cases, the monitoring system will have to be located underground.

Figure 2
Geophone With Preamplifier.

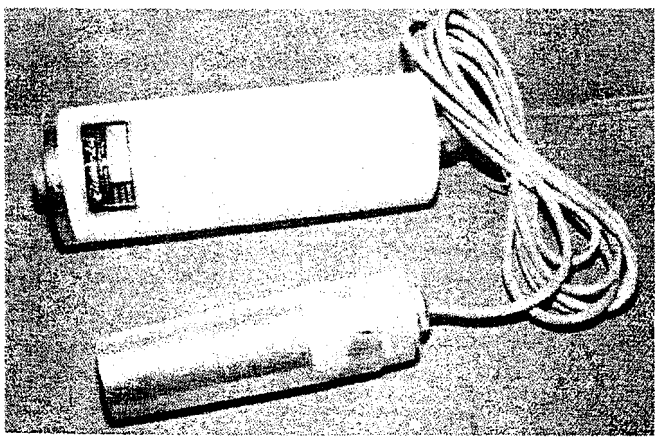

Multipair Cables

The greatest threat to the operation of an underground seismic system is water seeping into the cables, which will cause intermittent short circuits and ground loops and will allow various degrees of noise to be induced into the lines, and, in an extreme case, will cause system failure. The most common ways that water enters a cable are through nicks and cuts in the outer sheath or improperly or inadequately sealed junctions.

Use of direct-burial-type cable solves most water infiltration problems. This type of cable has been used exclusively for all new cable installed in USBM seismic systems in recent years. The cable features a tough polyethylene outer sheath, a flexible aluminum foil shield, and color-coded copper wires that are completely surrounded by waterproof gel. Even if the sheath and shield were to become nicked, the gel surrounding the wires resists the intrusion of water.

Direct-burial cable is available with various numbers of pairs and in various gauges. Care must be taken to match the requirements of the geophones and the type of wire. The wrong gauge may not be capable of carrying the current. The wires from individual geophones are usually connected to multipair feeder cables at junction boxes installed on specific mine levels, and the feeder cables are connected to a larger multipair cable in a shaft that connects the levels with the monitoring room.

Junction Boxes

The selection and preparation of junction boxes is as important as the selection of cable to prevent problems with water in underground seismic systems. Junction boxes must have waterproof door seals and watertight cable grips for all cables entering the box. The size of the box should be large enough to accommodate the terminal blocks, power supplies, and ac power receptacles. Terminal blocks and other insulating parts should not be made of materials such as bakelite because these materials absorb moisture and swell. Crimp spade connectors with screwdown barrier terminal blocks or direct clamp terminal blocks provide the most reliable wire connections. The box should also be large enough to permit easy access when installing the cable initially and when making wiring changes later.

DATA ACQUISITION EQUIPMENT

The data acquisition system consists of components for conditioning, processing, and recording the seismic signals. These components are filters, special connector boards, an analog-to-digital (A/D) board, and a PC to run the software and store the data.

Antialiasing Filters

The purpose of the antialiasing filter is to prevent the data acquisition system from producing false signals. A problem can occur when the data acquisition system's rate of sampling is less than about three times the highest frequency component in the analog signal. If insufficient samples are taken (i.e., the sampling rate is too low), a false or alias signal component with a frequency much lower than that of the original will be reproduced. The filter prevents aliasing by functioning as a low-pass filter and cutting off high-frequency components of the signal and then amplifying them before they are digitized.

Hardware

Data Acquisition Card and Screw Terminal Panel

The A/D board is a circuit board installed in the computer of the data acquisition system that converts analog signals to digital codes for computer processing and storage. Wire pairs from each geophone are connected to a general-purpose screw terminal panel that permits all input signals to be transferred via a ribbon cable from the wire pairs to the A/D board in the PC. The ribbon cable plugs into the connector on the data board, allowing the signals from each channel to be monitored continuously by the computer. The number of input channels on the A/D board should be greater than or equal to the number of geophones in the system and should be capable of monitoring all channels simultaneously.

Computer

High speed and ample memory are the two most important features of the PC monitoring system. Sampling rates of the digitized data are influenced by both the A/D board and the computer speed. Sampling rates that are too low allow the wave to travel large distances between sample data, which increases the likelihood of error in the measurements. For example, a rock-burst wave traveling at 5,100 m/s will travel 10.2 m between sampling points on a system with a digitizing rate of 500 samples per second, whereas the same wave would only travel 2.04 m between samples on a system capable of digitizing 2,500 samples per second. As the sampling rate increases, however, the size of the waveform file also increases, and more data must be stored in random access memory (RAM). Depending on the application of the system, the accuracy desired, the amount of hard disk storage capacity available, and the level of seismic activity, a tradeoff may have to be made between file size and sampling density.

As an example, a 16-channel array recorded for 5 s with a sample density of 1,500 samples per second will produce a file approximately 200 kbyte in size. To overcome space limitations, a removable mass storage device (such as a magneto-optical drive) can be installed. The magneto-optical platters can be written to as events are recorded, and each platter can be removed and replaced when full. Currently, magneto-optical platters can store up to 1.7 Gbyte.

Another option is to back up data files periodically on a tape, then erase the files from the computer's hard drive. (Note: A tape backup unit would be unsuitable for recording events because the read-write access time for tapes is much too slow.) In addition to sufficient hard disk space, a computer must have enough RAM to store the digitized data while the software determines whether a rock burst is occurring. While high sampling rates are more accurate, the increased number of digitized points may cause buffer overflow errors if the PC has insufficient RAM. The minimum computer requirements for USBM systems are given in appendix A.

Software

To detect seismic events, data from all channels must be monitored continuously and evaluated simultaneously. A typical detection algorithm first checks for an abrupt change in the incoming signal and sets a flag if one is encountered. Another parameter is used to confirm the number of geophones that experienced the abrupt signal change. In addition, a short-term average (STA) is computed for a window of data and compared with the long-term average (LTA). When a critical number of flags are set and the STA/LTA ratio exceeds user-specified criteria, the data are recorded on the PC.

INSTALLATION OF PC-BASED SEISMIC MONITORING SYSTEM

The successful installation of any underground seismic monitoring equipment requires careful planning and attention to detail. One of the most important steps in designing a system is choosing locations for the geophones. The geophones should surround the area of interest in all three dimensions, and the distance from each geophone to the area of interest should be roughly equal. While this may appear to be a simple task, the irregularities and complexities of mine openings do not always allow geophones to be placed in an optimum location.

Once sites have been chosen, a second important step is to make a reconnaissance of the site to ensure that the geophone will not be damaged by mining equipment and is not near any source of constant vibration, such as a pump house. In addition, the geophone should be in an area that is easy to access and where the rock is competent, so as to provide good seismic coupling with the rock mass.

While doing a reconnaissance, plans for positioning the junction boxes and laying the cable should be made. It may be necessary to change or expand the geophone array as new areas are developed. If the wiring network is designed with such possible future changes in mind, expanding or moving the array will be much simpler.

Modern seismic equipment is generally rugged and well sealed to resist hostile underground mine environments. Most problems with seismic systems come from faulty electrical connections or moisture in the wiring. Physical damage to underground equipment can be minimized by careful planning and installation. Figure 3 is a schematic of all components of an installed system. An explanation of each phase of the installation follows.

GEOPHONES AND PREAMPLIFIERS

Geophones must be mounted in a location that will provide a solid coupling with the surrounding rock mass and must be in an area reasonably safe from physical damage. In addition, some geophones require an installation in an exact vertical or horizontal orientation.

Mounting

The rock surrounding underground openings is often fractured from the blasting that formed the opening. When choosing a location, the geophone must be mounted in rock that is solidly a part of the surrounding rock mass. If the geophone is mounted in fractured rock, the fractures will tend to insulate the geophone from the seismic energy traveling through the rock and the strength of the induced signals will be reduced. In locations where solid rock cannot be found, it may be necessary to drill a hole through the fractured zone into solid rock and mount the geophone at the end of the hole. Geophones with a threaded stud can be mounted by first installing a mounting plate with a tapped hole for the stud. This plate can be secured to the rock with a cement such as an epoxy or a quick-setting plaster such as hydrostone. In some cases, existing rock bolt plates may be drilled and tapped. Tapered geophones are easily mounted by machining an aluminum tube with a matching taper. The outer tube is positioned and mounted with cement, and when the cement is set, the geophone is inserted in the tube.

Because many of the geophones used in underground seismic systems are long and slender and are mounted by a stud at the end, they are readily damaged if bumped. When a protected location cannot be found, the geophone can be mounted in a drill hole. The geophones should not be installed near any machinery that generates vibrations in the surrounding rock, such as a pump station, because these machine vibrations will appear as background noise in any seismic signals from the geophone.

Orientation

The orientation of the longitudinal axis of an installed velocity geophone is critical for proper operation, while accelerometers will function properly installed in any position. In general, single-axis velocity geophones must have their longitudinal axis within a few degrees of vertical if designed for vertical mounting, or within a few degrees of horizontal when made for mounting in the horizontal position. The frequency response of the geophone will not be correct if improperly mounted.

Each geophone must be precisely surveyed to locate seismic events accurately. The orientation of the axis or axes of the mounted velocity geophones must also be determined with respect to the mine coordinate system.

WIRING NETWORK

The wiring network consists of (1) all the cable connecting the underground geophone array with the data acquisition system and (2) the junction boxes where connections are made. The wiring should be laid out in a network that branches out from a multipair trunk line cable in the shaft through junction boxes to the geophones on each level.

Figure 3
Components of Installed Seismic Monitoring System.

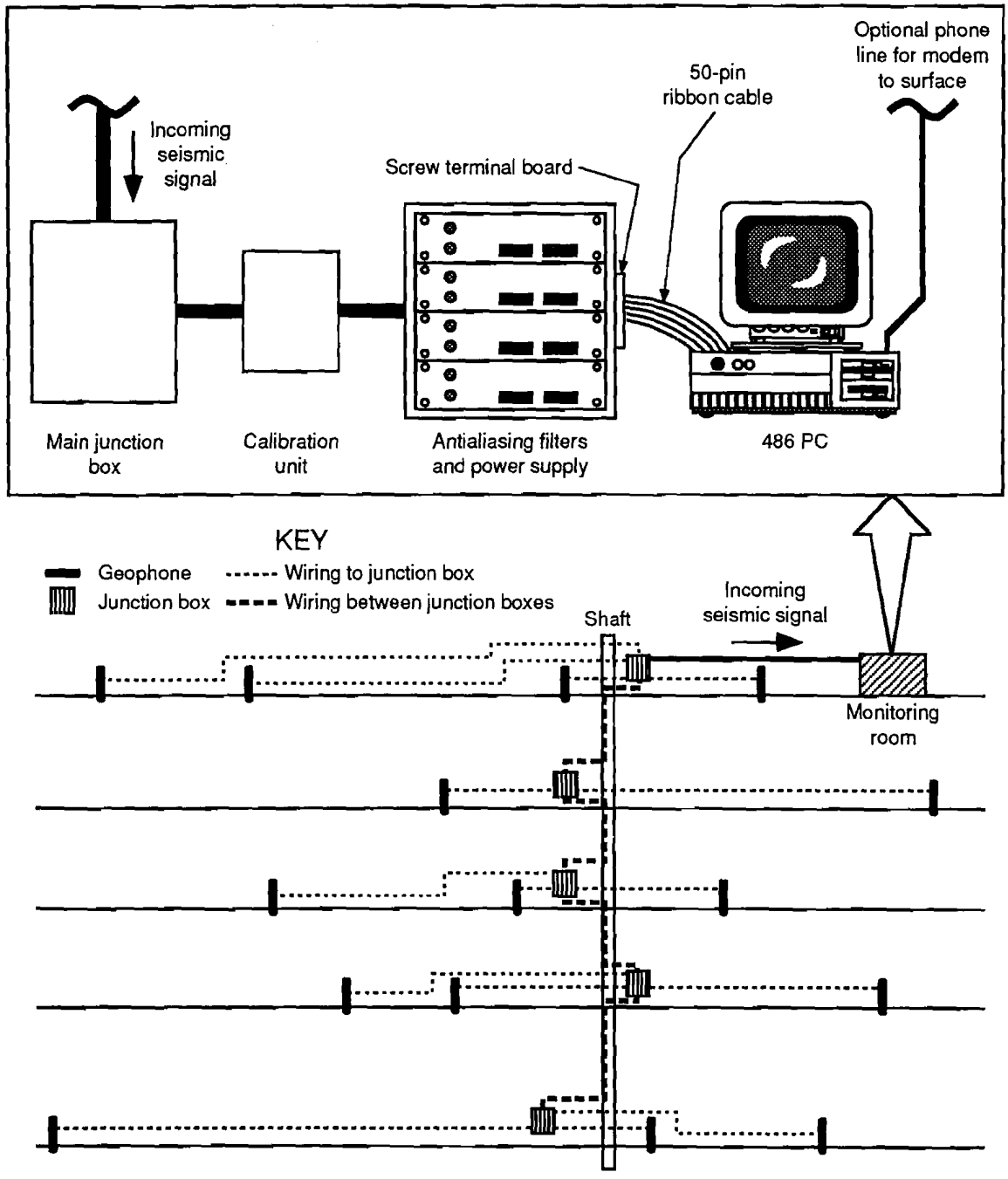

Installation of the wiring network requires special care because a system that is properly installed will be relatively trouble free, while a system that is poorly installed will be a constant source of problems.

Cable Routing and Mounting

The routing of cable in underground mines is often difficult because space, which is at a minimum, must be shared with other signal and communication cables, power cables, compressed air and water lines, and ventilation lines. On underground levels, cable is often subject to damage by mining equipment, and in shafts, it is subject to damage from falling rock.

Whenever possible, it is good practice to route seismic system cable by itself, away from other cables. Shielding the cable is crucial when the seismic transmission lines are near power lines. The shields on the cables coming from the geophones must be connected to the shield of the cable leading toward the data acquisition equipment. The shield must only be grounded at one point on the network to prevent noise from induced ground loop currents. A ground rod or some other positive grounding point located at the data acquisition equipment can then be used to ground the system. On underground levels, the cable can be suspended from cable ties with plastic chain-link mesh, rock bolts and plates, and other hangers found in drift openings. In shafts, the cable will probably have to be routed through the utility compartment and can be hung from the shaft lining with cable grips. The grips must be placed close enough together so that no part of the cable will be subjected to excessive tension, which would stretch the cable.

Junction Boxes

The installation of seismic system junction boxes is greatly simplified if they are planned and preassembled prior to taking them underground. Preassembly can include installing the terminal strips, marking individual or groups of terminals, and installing geophone power supplies and ac power receptacles. Holes should not be drilled in the boxes for cables until the box has been installed.

Junction boxes should be protected from water in wet locations and possible damage by mining equipment, yet convenient to access. Junction boxes with power supplies for the geophones must be located near 110-V ac power. This is seldom a problem on shaft stations, but ac power is not always available at convenient places away from the shaft. In very humid locations, condensate may form on everything inside the box and cause problems, such as corrosion and electrical short circuits. One method of preventing condensation is to place a heat source in the box, such as a 75-W light bulb.

Calibration

A means of testing and verifying the operation of the geophones and preamplifiers, wiring network, and data acquisition components of a seismic monitoring system is provided by a calibration signal generator. By sending a known signal through the wiring network to all the preamplifiers and geophones, the instruments will return a proper response if installed correctly. The polarity of the wiring can be checked by comparing the first motion of the calibration signal with the first motion of the instrument response.

DATA ACQUISITION EQUIPMENT

The most convenient location for the data acquisition equipment is in a building on the surface. When this is not practical, such as in a large mine where the geophone array is a long distance from a convenient surface location, the monitoring system can be located in an underground room. The system computer can then be accessed from the surface by modem to retrieve files if a telephone line is installed between the surface and the underground room.

Monitoring Rooms

The monitoring room must be clean and dry. Air conditioners, dehumidifiers, and air filters can be used to maintain the environment for computers and electronic equipment. The room should be large enough to provide space to operate and maintain the equipment, store data processing and office supplies, and contain a workbench to test equipment and make minor repairs.

CONCLUSION

Attention to detail and preplanning will minimize problems associated with installation of a microseismic monitoring system and data collection. The systems described here are easy to install and have been used successfully by the USBM for several years. The system can be designed to fit the particular needs of each mine. While equipment brands other than those listed in appendix A can be used when designing a system, components should be carefully chosen for compatibility. By recording and analyzing rockburst data collected by the system, ground-control engineers may be able to devise alternate mining plans to minimize the occurrence of rock bursts and optimize resource recovery.

APPENDIX A.—EXAMPLES FROM ACTUAL INSTALLATIONS

DATA ACQUISITION SYSTEM

Software

The USBM's seismic monitoring system was adapted from earthquake monitoring software developed by the U.S. Geological Survey (USGS).[1,2] The USGS software is published and maintained by the International Association of Seismology and Physics of the Earth's Interior (IASPEI).

For information on becoming a registered user of the IASPEI software write to

International Association of Seismology
and Physics of the Earth's Interior
P.O. Box I
Menlo Park, CA 94026

This system is capable of recording full waveforms from up to 16 receivers. Some modifications to the system were necessary to adapt the software to monitoring mine seismicity instead of earthquakes. However, the hardware is essentially the same for either type of system.

Computer

The absolute *minimum* requirements for a computer to run this type of seismic data acquisition system are

- 80286 IBM-compatible PC with math coprocessor.
- CPU speed of at least 8 MHz.
- 2 Mbyte of RAM (120 nanoseconds or faster), first 640 kbyte of RAM as base memory and the remaining kbyte of RAM as extended memory.
- Hard disk with at least 30 Mbyte of free space and access time <40 m/s.
- DT2821 A/D input-output board with a DT707 screw terminal connecting a panel and a 50-pin ribbon cable.
- EGA monitor.
- Stable ac power source with surge protection.

All computers used for seismic data acquisition by the USBM are 486/33 MHz machines with 200 Mbyte hard drives, 8 Mbyte RAM, 9600 baud send-receive modems, and VGA monitors.

Analog-to-Digital Boards

The A/D boards used in the USBM's systems are 2821 Series boards made by Data Translation, Inc., Marlboro, MA. These boards have 16 channels and a sampling rate of 50 kHz. Each channel then has a sampling rate of 3.13 kHz. These boards have 12-bit resolution, which is a measure of the accuracy with which the digitized signal matches the analog signal. A resolution of 12 bits means that the maximum amplitude of the analog signal may be divided or resolved into 4,096 parts or counts. This is 0.024 pct of the analog signal's range. While other A/D boards may work in this type of system, neither IASPEI nor the USBM have tested other brands.

SEISMIC MONITORING EQUIPMENT

Geophones

The geophones used by the USBM in the three mines discussed in this report are manufactured by Electro-Lab in Spokane, WA. Some of the geophones in use at the Lucky Friday Mine and the Sunshine Mine are 1131-series triaxial velocity geophones, but most of the geophones at the Sunshine Mine are model 11SB velocity geophones. The Lucky Friday Mine also has 1130-series velocity geophones installed in the macroseismic system. All of the geophones in use at the Homestake Mine are 272 accelerometer geophones. The types of geophones used in the USBM systems are summarized in table A-1.

[1]Lee, W. H. K., and S. W. Stewart. Principles and Applications of Microearthquake Networks. Advances in Geophysics, Supplement 2, Academic Press, 1981, 293 pp.

[2]Lee, W. H. K., D. M. Tottingham, and J. O. Ellis. A PC-Based Seismic Data Acquisition and Processing System. U.S. Geol. Surv. OFR 88-751, 1988, 31 pp.

Table A-1.—Geophones used in USBM microseismic systems

Geophone series number	Axis	Type		Mine		
		Velocity	Accelerometer	Homestake	Lucky Friday	Sunshine
11SB	Single	X		No	No	Yes
1130	Single	X		No	Yes	No
1131	Triaxial	X		No	Yes	Yes
272	Single		X	Yes	No	No

Triaxial velocity geophones such as the series 1131 have the y-axis parallel to the longitudinal axis of the geophone. The x, y, and z axes are mutually orthogonal and form a right-handed coordinate system. The z-axis is normally the vertical coordinate, and in the USBM systems, positive in the up direction. A flat, milled end on the geophone provides a reference surface to orient the axes properly.

Wiring Network and Junction Boxes

The cable used in the wiring networks is 22-gauge, direct-burial, shielded cable and includes 6-pair, 25-pair, and 50-pair cables. The junction boxes accommodate 25- and 50-pair cables and are made of fiberglass. The junction boxes have watertight seals and measure 76.2 cm high by 61.0 cm wide by 20.3 cm deep. Smaller steel boxes with watertight door seals have been used for the junctions of the smaller geophone cables with the feeder cables.

Antialiasing Filter

The antialiasing filter used in the USBM data acquisition systems is an Electro-Lab type 405 AA filter. This unit provides a separate channel for each geophone and can accommodate up to 64 channels. Each channel contains an amplifier with the gain adjustable in 10 db steps from 0 to 50 db. The filter is actually a band-pass filter in that both high-frequency signal components and those below 10 Hz are cut off. The 10-Hz cutoff is fixed while the high frequency cutoff may be set between 1 kHz and 9.9 kHz in 100-Hz increments by means of a switch.

Calibration Unit

The USBM systems also include an automatic calibration unit. The calibration pulse generator developed by Electro-Lab generates a 7.5-cycle pulse of 60-Hz ac at an amplitude of 24-V RMS. When the calibrator is triggered, this signal burst is transmitted on a separate pair of wires in the wiring network to all the preamplifiers. Properly installed preamplifiers respond to the calibration pulse by producing a 1-V peak-to-peak square wave. The calibration signal always starts with a positive wave so that the polarity of the wiring can also be checked.

Monitoring Rooms

The monitoring rooms at the Lucky Friday and Sunshine mines are located on the surface. However, since the seismic monitoring system at the Homestake spans levels between 2,043 and 2,384 m below the surface, the monitoring room was located underground (figure A-1).

Seismic Equipment Specifications

For specific information about the seismic equipment in use by the USBM at these three mines, contact the authors at

Spokane Research Center
315 E. Montgomery Ave.
Spokane, WA 99207-2291
(509) 484-1610

Figure A-1
Underground Monitoring Room at Homestake Mine.

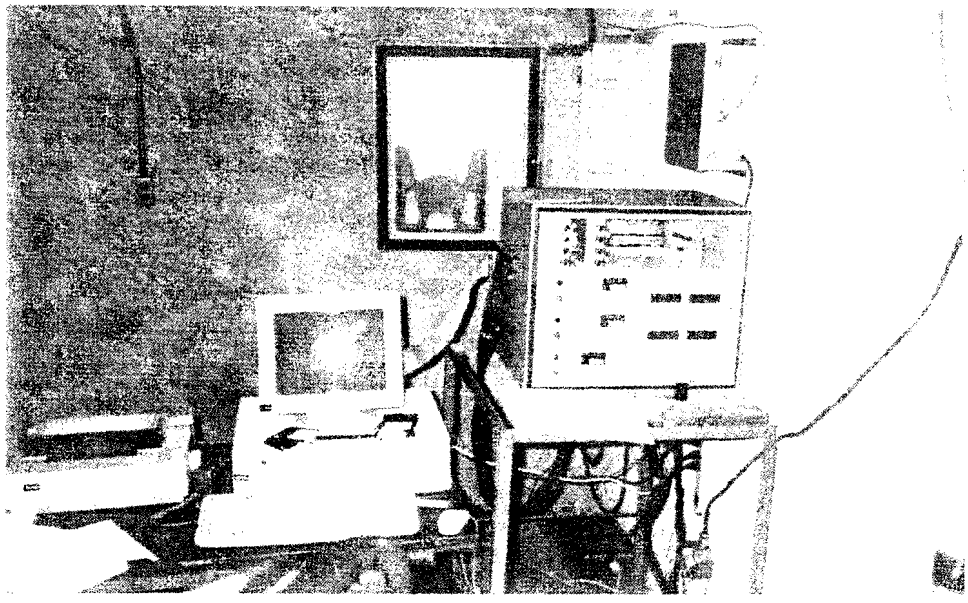

APPLICATION OF TOMOGRAPHIC METHODS FOR STUDY OF STRUCTURAL FAILURE

By H. Maleki[1]

ABSTRACT

U.S. Bureau of Mines researchers investigated the principles, limitations, and application of tomographic measurements for monitoring the history of strata fracturing and failure. These measurements were complemented by static measurements, core testing, fracture mapping, and underground observations to relate measured changes in velocity patterns to the formation of fracture zones, changes in stress, structural stability, and secondary support requirements.

These measurements provided new insight into the mechanism of time-dependent failure and excavation-induced rock damage. It was shown that rock damage occurred at the development stage and was influenced by floor and pillar behavior. Tomographic methods clearly identified the development of damaged zones in the mine roof even though there was no visual indication of fracturing at the excavation surface. Fractures initially formed on one side of the roof but later propagated to the other sides, forming a block. In addition, significant changes in velocity in the pillar were measured and related to load transfer from mined-out areas to the pillar.

INTRODUCTION

Mining results in a redistribution of stresses around mine openings and the formation of fractures. These fractures are not of great concern unless they grow to intersect other potential failure zones and fail suddenly. However, gradual failure of rocks and ore is easily controlled by timely scaling, cleaning, and bolting.

On the other hand, sudden failure of rocks and coal involving over 100 t of material influences access to mine openings, compromises safety, and increases mining costs. Measurements in underground mines (Maleki, 1988) have shown that these failures are not instantaneous and generally take between 1 day to several years before the material actually collapses. These time-dependent failures are influenced by limited deformation of geologic material, changes in geologic conditions, effectiveness of support systems, and groundwater conditions, among other causes.

Sudden and violent failure of material around mine excavations are called bumps or bursts. These failures are common in both deep coal mines and hard-rock mines and require large-scale remedial actions.

The U.S. Bureau of Mines (USBM) has long been involved in the development of measurement techniques for assessing ground conditions and guidelines for detecting "sudden failures" in U.S. mines (Maleki, 1994). Recently, the author studied violent failures in U.S. coal mines and proposed an engineering approach for assessing bump-prone conditions (Maleki, 1995). In this approach, potential bump-prone areas may be identified using measurements of stress, considerations of the stiffness of surrounding rocks, and energy release from breakage of strata. Once an area is identified as bump prone, both static and geophysical measurements are recommended as a means of predicting where coal bumps will occur.

Among monitoring techniques, geophysical measurement methods are widely used in the study of coal bumps

[1]Mining engineer, Spokane Research Center, U.S. Bureau of Mines, Spokane, WA.

and rock bursts because they can be used to monitor large areas. These methods use either an active source, such as a blasting cap, to generate a signal or involve listening to rock noise. An active source is generally used in tomography to construct velocity and/or amplitude patterns in the area of interest. Microseismic methods, on the other hand, simply monitor seismic emissions, evaluate the energy involved, and locate rock noises.

Tomography provides some new capabilities for predicting violent failure. By conducting periodic surveys, one can identify abnormal geologic conditions during the early stages of mining; this finding would enable an operator to focus on remedial actions where changes in geologic conditions occur. Also, by repeating measurements at the location of interest, one can monitor changes in wave properties and infer the development of fractures (Maleki and others, 1993), yield zones (Maleki, 1995), and areas of high stress during later mining, which would permit timely assessment of the likelihood of violent failures.

The focus of this paper is on applying tomography to the study of rock fracturing, stress change, and failure. To achieve this goal, an extensive measurement program, consisting of both geophysical and static measurements, was implemented in an underground mine. Static measurements and borehole observations were used to relate changes in seismic velocity to strata fracturing and the failure process; these measurements resulted in a better understanding of the initiation and growth of failure zones around mine openings.

TOMOGRAPHIC METHODS

Tomography is an inversion technique that provides an image of a physical property of a solid material on a plane of interest. The word tomography is derived from the Greek word "tomos", meaning "a slice." Three-dimensional images can be obtained by repeating measurements along multiple planes (slices) and combining the two-dimensional images to create a three-dimensional image. Physical property measurements are obtained remotely.

Tomography was first applied in the medical industry as computer-assisted tomography (CAT) or computed tomography (CT) scans. There is extensive literature on the physics, mathematics, and design of CT scanners (Brooks and DiChiro, 1976). Briefly, CT rotates an X-ray source at least 180° around the object of study (human brain, etc.), causing the X-rays to intersect the object with numerous waves and create an image at several positions along the object. A three-dimensional image can be reconstructed from these sequential images as the object is moved through the scanner. CT scanners use X-ray attenuation and create images through computer manipulation of data. Contrast resolution is excellent. The scans are then viewed by trained personnel who identify abnormal conditions within the object.

During the last decade, tomography has also been widely used in studies of the physics of the earth and has advanced rapidly as a result of significant improvements in data acquisition methods, imaging theory, and computation speeds. Recently, the USBM applied this technology to ground control problems (Maleki and others, 1992, 1993; Maleki, 1994; Westman, 1993) and environmental research (Jessop and others, 1992).

Figure 1 presents the lithology of a typical mine roof and the location of sources and receivers around an area of interest. At such a mine, both variations in roof lithology near a sandstone channel and time-dependent strata separation contribute to roof falls. To conduct a tomographic survey, a number of sources and receivers are attached around the boundaries of the area of interest. Each source is excited, and the full waveform is recorded at all receivers. By then exciting other sources, the area of interest is intersected by a number of waves, resulting in a pattern of spatial variations of rock properties within the image zone. For example, by picking first-arrival times and using inverse methods, one can construct a wave velocity image of the mine roof. Similarly, an attenuation image may be constructed using wave amplitude.

Tomographic surveys have limitations influenced by (1) physical access to the area of interest and (2) nonlinear travel paths. Lack of access to all sides of an area (figure 2*A*) results in poor ray coverage in the upper portion of the roof. In contrast, figure 2*B* presents good ray coverage for a pillar survey where there is sufficient access from all four sides of the pillar. Nonlinear travel paths for elastic waves are influenced by contrasts in material properties. X-rays travel along straight lines, without the spreading and diffraction characteristics associated with elastic waves.

INSTRUMENTATION PROGRAM

Velocity tomographic surveys were conducted at high resolutions in a Western U.S. trona mine to study velocity patterns in the mine roof, pillar, and floor. Figures 3 and 4 illustrate instrument layout and the location of impact

sources and receivers for the roof and floor surveys, as well as the positions of multipoint extensometers in the mine roof. Both a bolt-impulse source and seismic caps were used in this study.

These measurements were complemented by detailed deformation measurements, stress measurements, fracture mapping, and photographic records to relate changes in the velocity pattern to strata fracturing, stress build-up, structural stability, and supplementary support requirements. Static measurements were taken with 13 multipoint roof extensometers, 5 vibrating wire stressmeters, 5 rib dilation pins, 5 floor dilation pins, and 2 pillar convergence pins and provided a detailed history of strata deformation toward the entry. In addition, borehole shear tests, plate-bearing tests, and overcore stress measurements were obtained to measure the in situ strength properties of the rock strata. The instruments were installed in a four-entry panel access using 5-m (17-ft) wide entries and pillars at depths of 426 m (1,400 ft).

The tomographic surveys were completed on a biweekly to bimonthly schedule, depending on face position and rate of change in strata fracturing. Some static measurements were obtained either at the beginning or the end of the monitoring program. Other measurements were obtained on a daily to weekly basis. Systematic fracture mapping was also completed during each tomographic survey. Monitoring was continued until the retreat face approached the instrumented area.

TOMOGRAPHIC IMAGES AND GROUND CONDITIONS

The application of tomographic imaging to the study of strata fracturing and failure is demonstrated by using selected images from several time windows during the measurement program. Static measurements, numerical modeling, fracture mapping, and underground observations were used to develop schematics of roof and floor deformation and failure history. Selected pillar images were included to show how the method was used for monitoring stress changes in mine structures.

Wave velocity images for the mine roof and floor at the development face position (figure 5) have provided new insights into the mechanics of rock fracturing and damage, e.g., roof velocity was significantly lower near the pillar side than the solid block side. This significant change over a distance of 4 m (14 ft) was influenced by the composite behavior of the pillar and floor and associated shear fracturing (Maleki and others, 1993). This is an important finding because it confirms that damage to the rock mass is initiated during the development phase, while "sudden" failures may occur several months to years after mining. These measurements also identified the shortcomings of observational techniques for assessing ground conditions, because there was no sign of fracturing on the skin of the roof (figure 5*B*).

Wave velocity patterns in the mine floor showed a similar trend, but the magnitude of deformation, fracturing, and rock damage was higher than wave magnitudes in the mine roof. This pattern was based on observations of floor heave, fracturing, borehole inspection, and the velocity images. The large difference between roof and floor velocities was also influenced by lithologic differences between the roof and the floor material. Laboratory velocity measurements on intact core samples from both roof and floor, however, confirmed that excavation-induced rock damage was significantly greater for floor rocks. In fact, the premature failure of floor rocks contributed to the fracturing of the mine roof (Maleki and others, 1993).

Wave velocity in the mine roof changed significantly (25 pct) during this 6-month monitoring period as damage to the rock mass increased because of the growth of fractures and increases in bed separations. Figure 6 illustrates the velocity pattern and ground conditions when the retreating face approached within 15 m (50 ft) of the instruments. Initially, the roof behaved like a cantilever beam as rock fracturing developed toward the pillar side. In time, other fractures formed in the upper portion of the roof (near the solid block), forming a block of rock that was suspended from the upper strata by additional roof bolts. The operator installed sets of secondary support [wire mesh and 2.4-m (8-ft) long bolts] and tertiary support [3.6-m (12-ft) long bolts] to control block movements.

Wave velocity pattern was generally uniform, as measured in a 5.5- by 8.5-m (17- by 30-ft) portion of a mine pillar prior to the retreat of the mechanized face equipment (figure 7*A*). Velocities increased across the pillar as the face retreated toward the pillar, transferring stresses from the mined-out areas toward the pillar (figure 7*B*). At the time of the last measurement, the face-pillar distance was 15 m (50 ft). These measurements are in general agreement with the stress measurements and confirm that tomographic measurements are suitable for monitoring changes in stress conditions in mine structures.

Figure 1
Considerations in Tomographic Surveys.

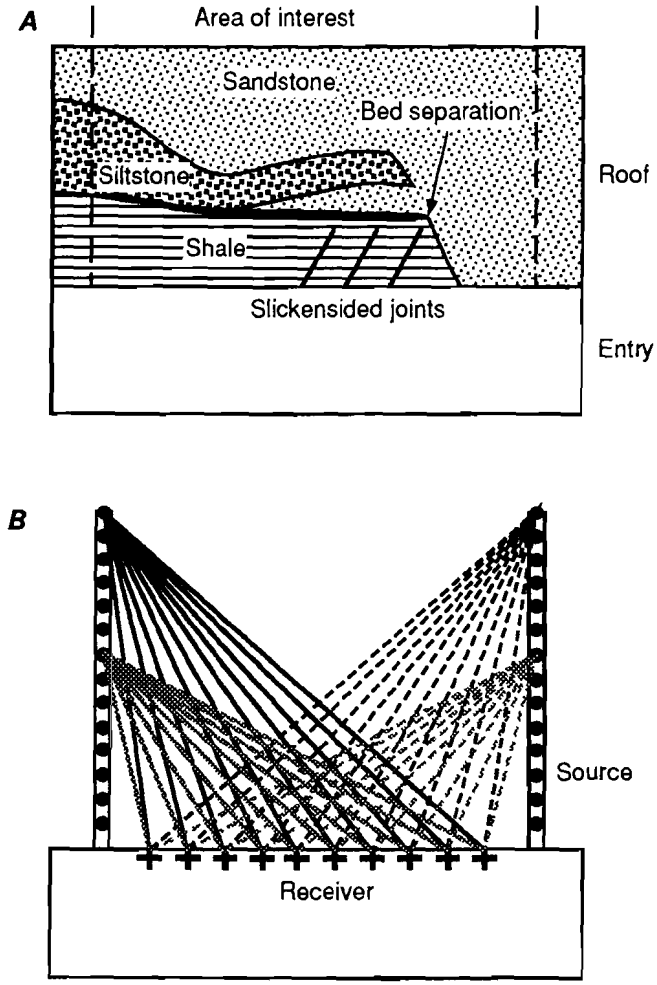

***A*, Types of typical geologic variations; *B*, location of sources and receivers.**

Figure 2
Ray Coverage as Influenced by Position of Instruments and Ray Bending.

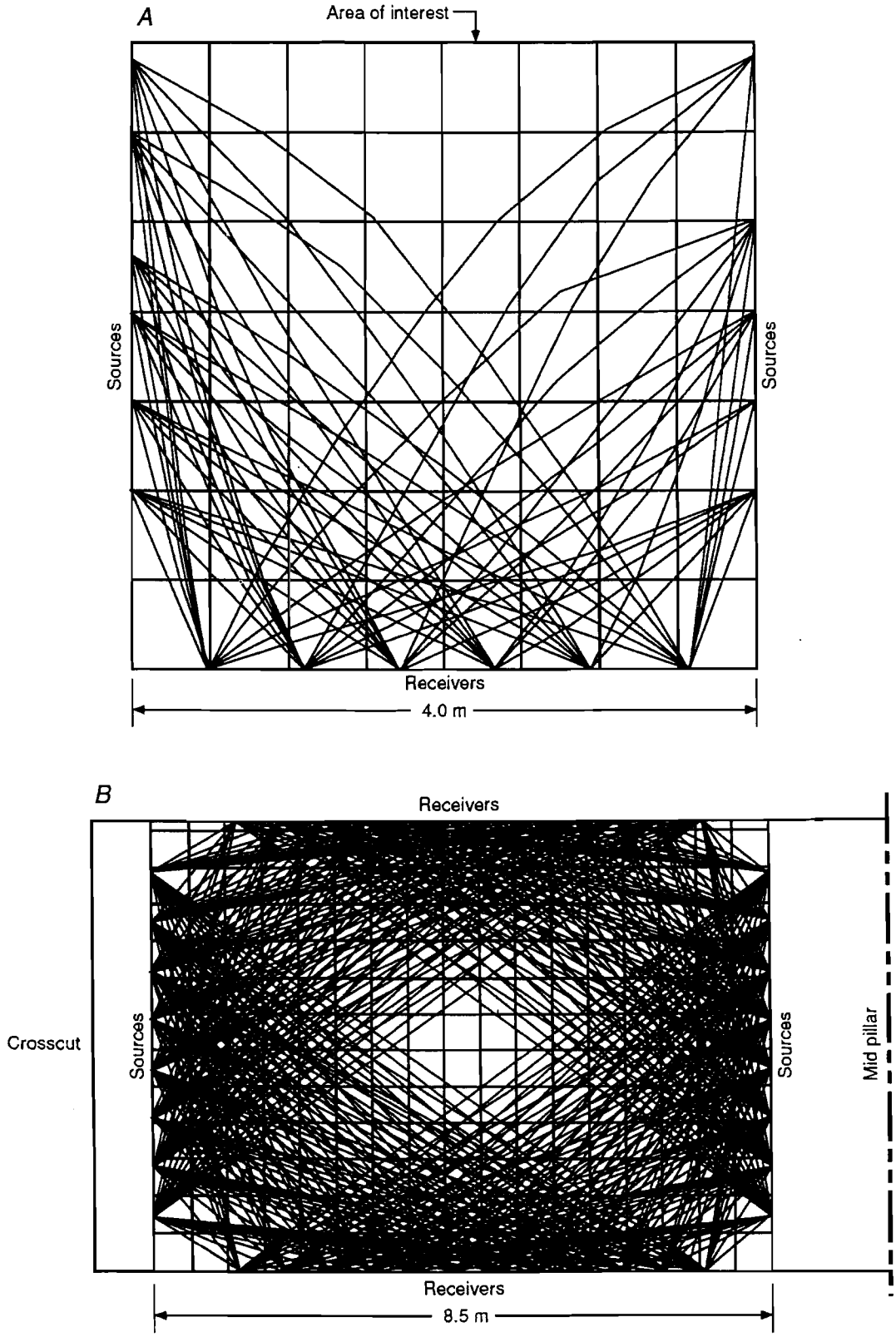

A, Three-sided roof survey; *B*, four-sided pillar survey.

Figure 3
Instrument Position and Mining Geometry.

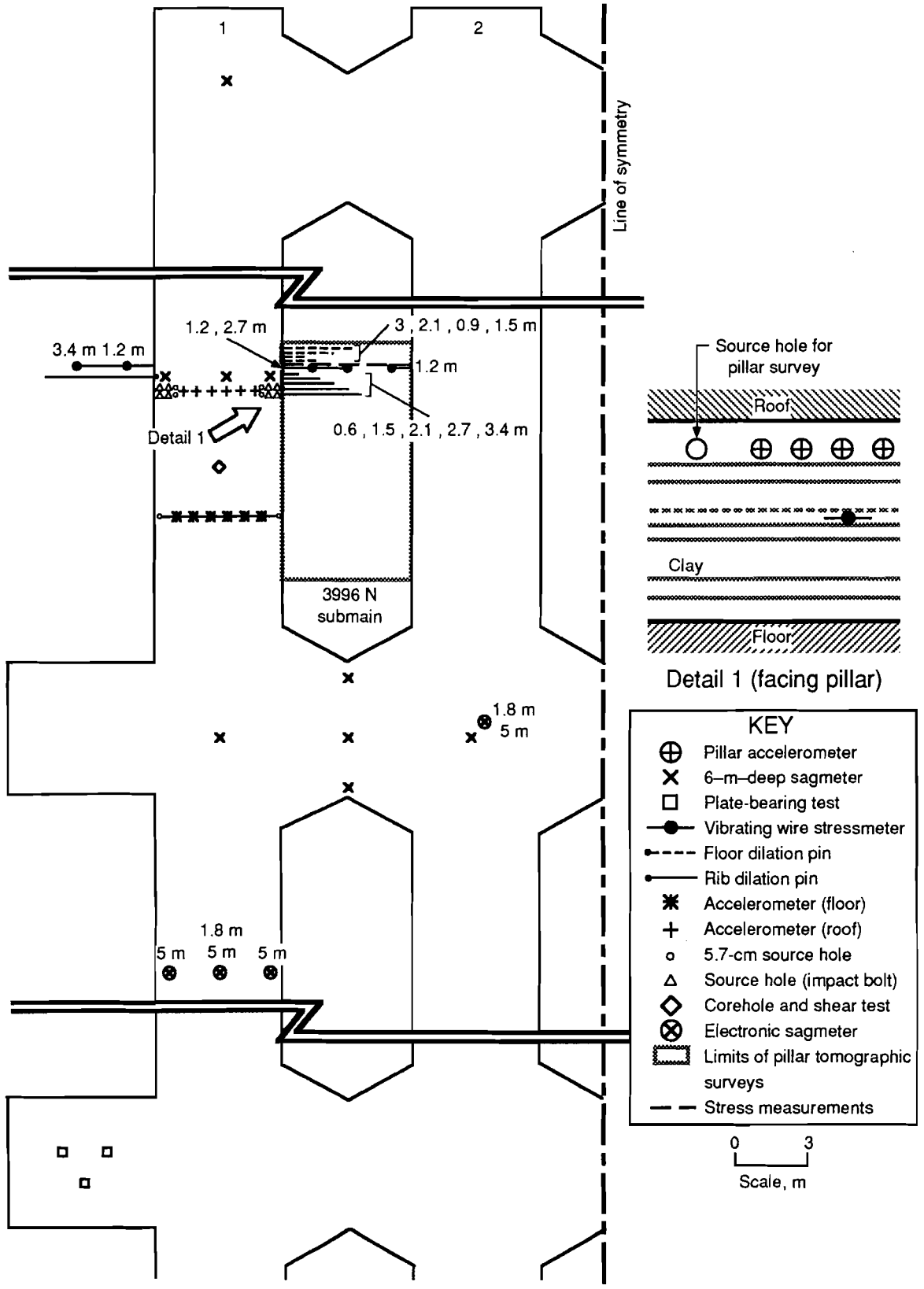

Figure 4
Details of Instrument Location.

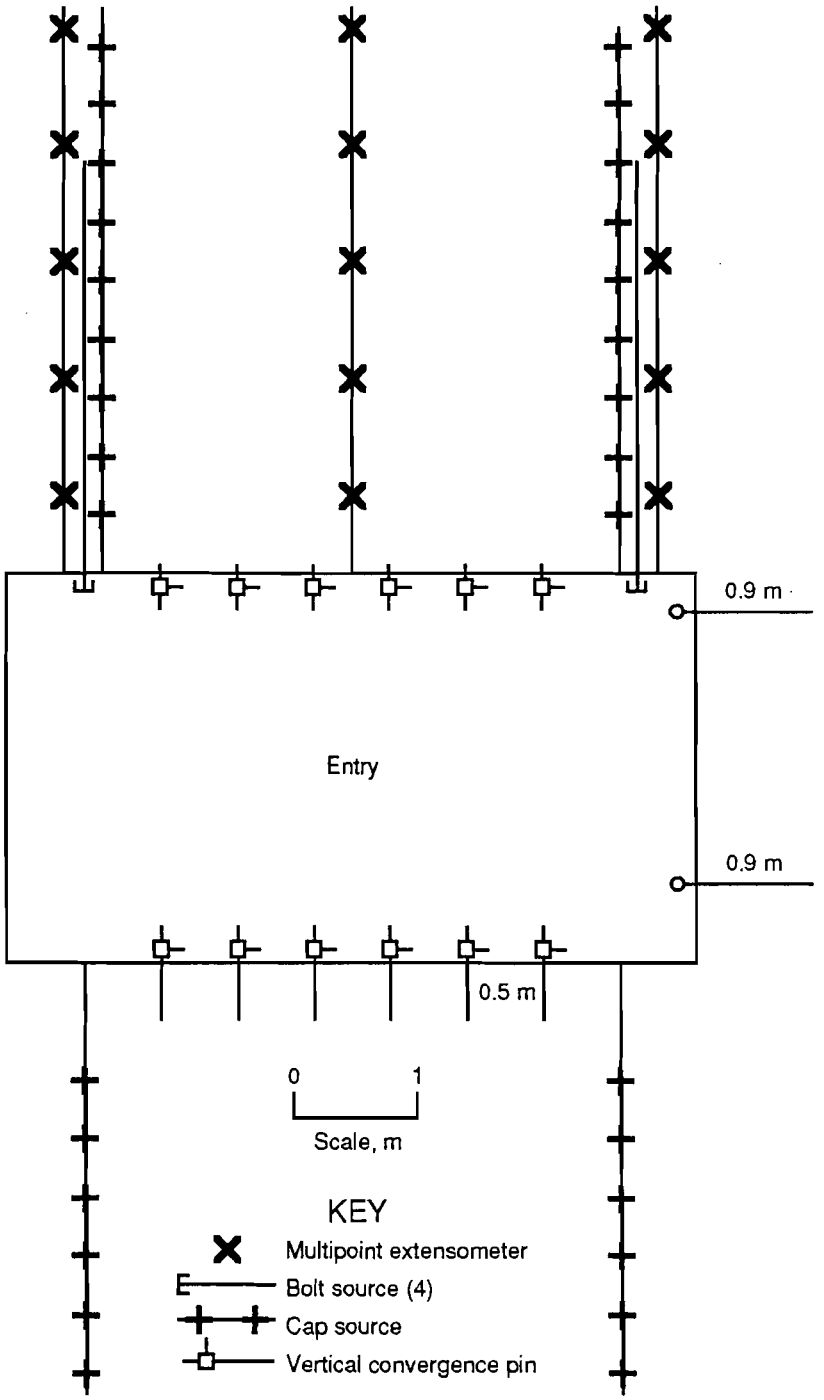

Figure 5
Velocity Contours and Ground Conditions at Development Face Position.

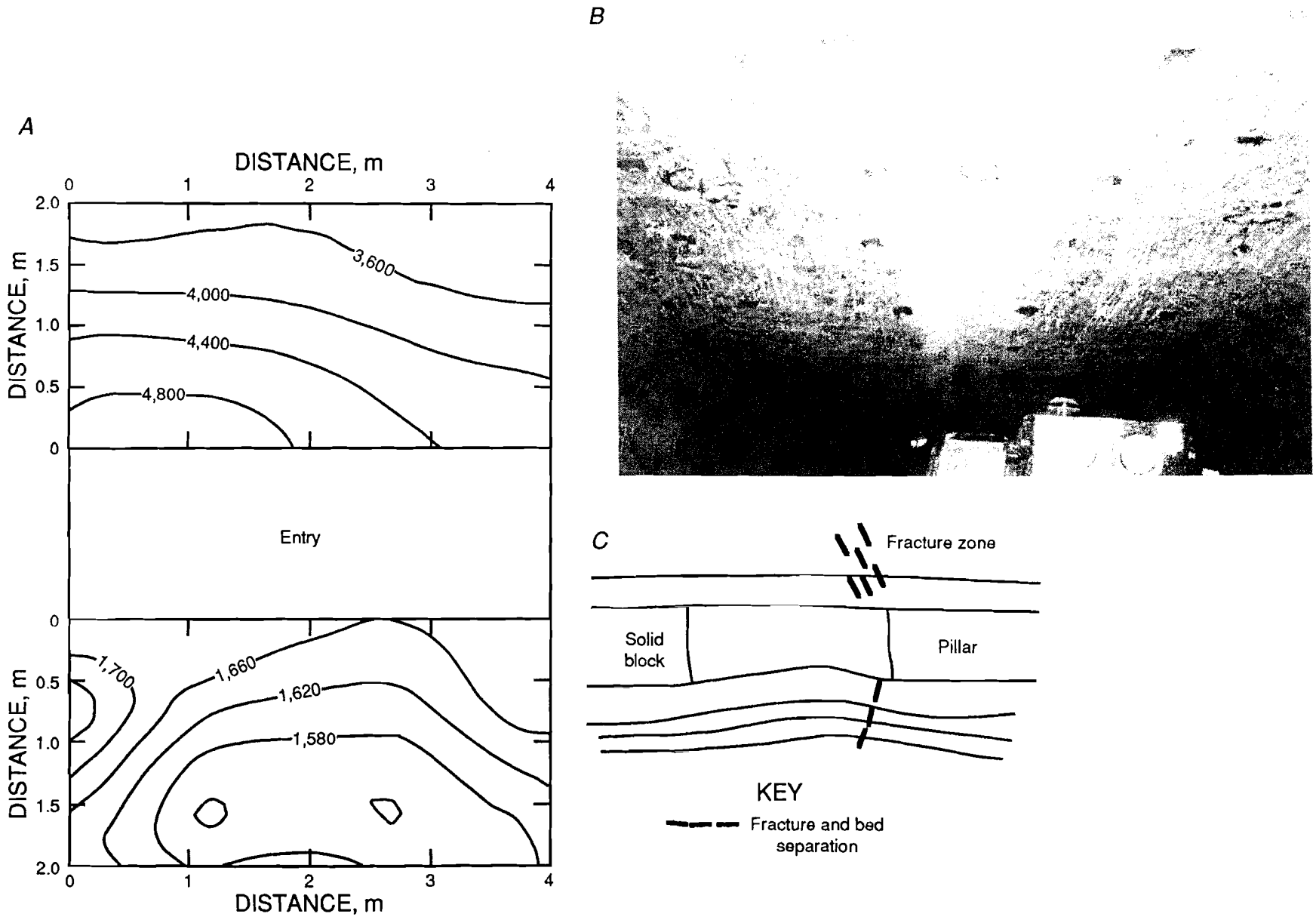

***A*, Velocity image, m/s; *B*, actual roof conditions; *C*, schematic of strata movements.**

Figure 6
Velocity Pattern and Ground Conditions at Retreating Face Position.

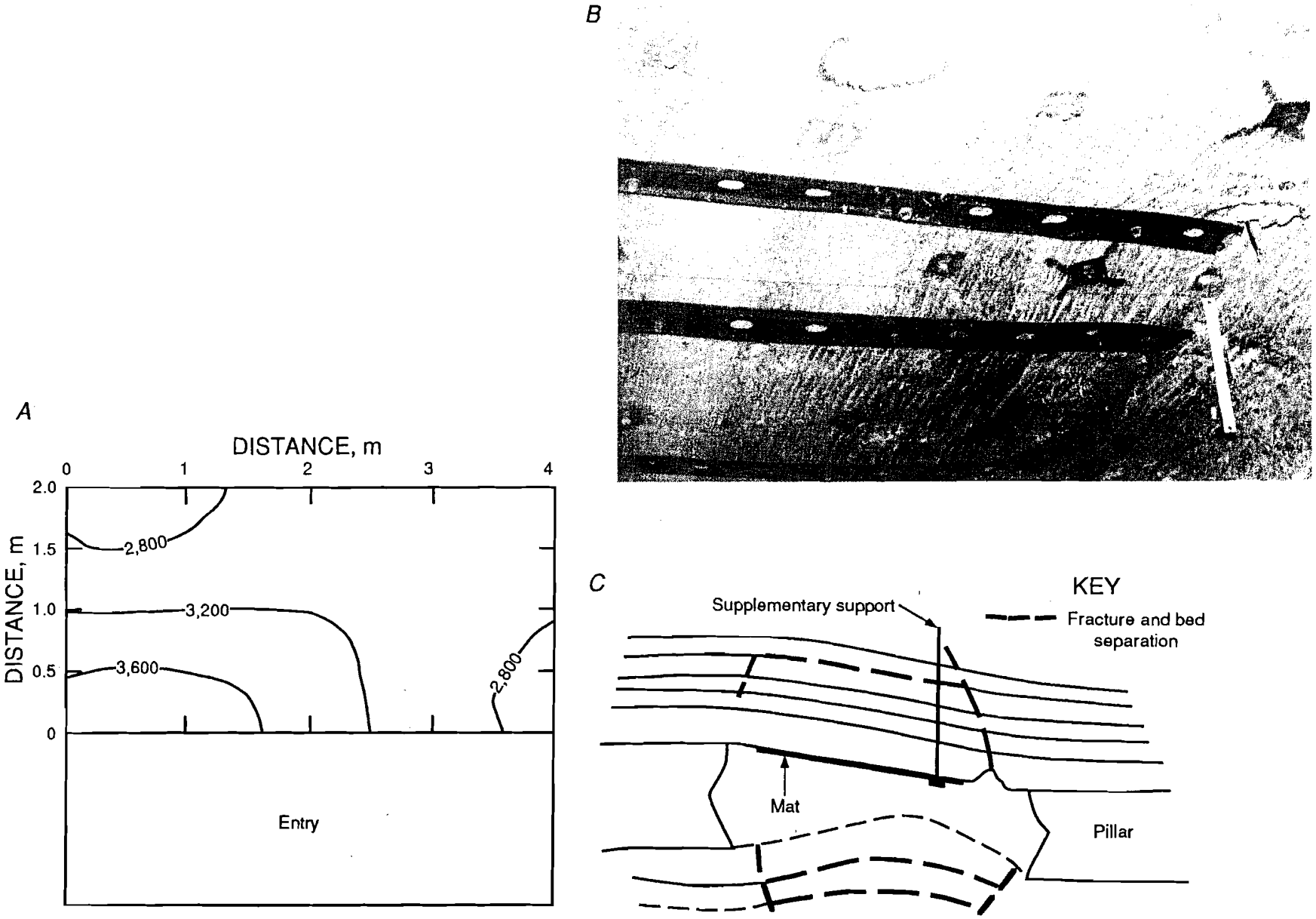

***A*, Velocity image, m/s; *B*, actual roof conditions; *C*, schematic of strata fracturing.**

Figure 7
Velocity Pattern in Mine Pillar, Meters Per Second.

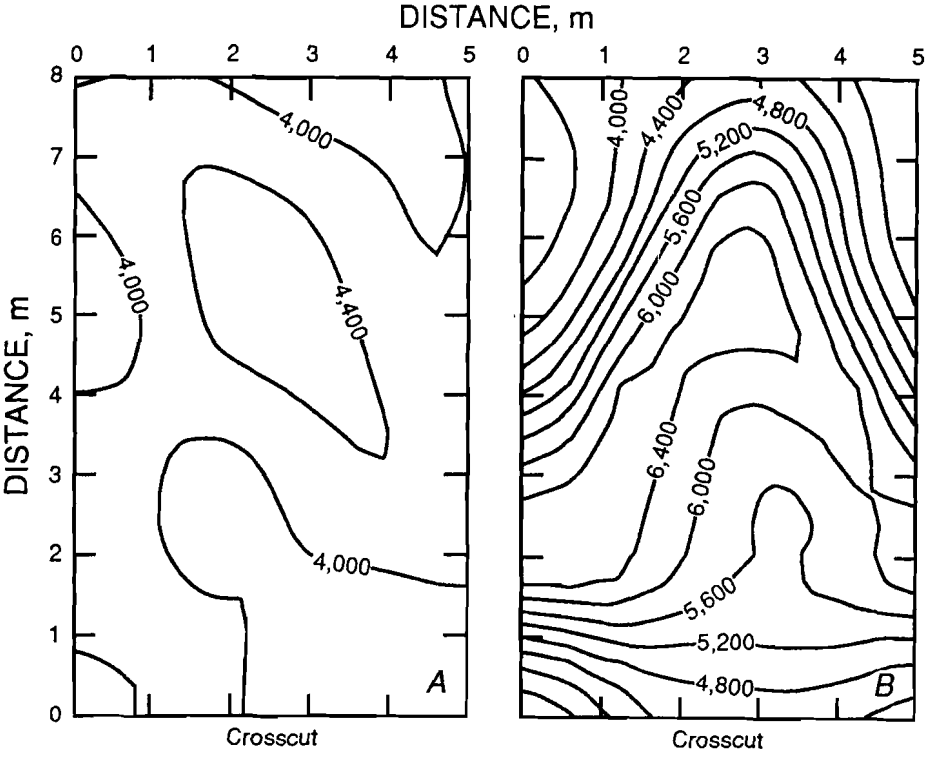

A, Prior to retreat; *B*, at retreating face position.

CONCLUSIONS

The application of tomographic methods to the study of time-dependent strata fracturing and stress changes was demonstrated using field measurements of the roof, floor, and pillar in a Western U.S. mine. The measurements were successful in identifying the location and timing of mining-induced fractures in the mine roof and floor. Pillar measurements revealed changes in velocity as the retreating face approached the instrumented pillar. This confirms laboratory investigations and a relationship between velocity and stress levels (Wepper and Christensen, 1991).

REFERENCES

Brooks, R. A., and G. DiChiro. Principles of Computer-Assisted Tomography in Radiographic and Radioisotopic Imaging. Phys. Med. Biol. 21, 1976, pp. 689-732.

Jessop, J. A., M. J. Friedel, D. R. Tweeton, and M. J. Jackson. Fracture Detection with Seismic Crosshole Tomography for Solution Control in a Stope. Paper in Application of Geophysics to Engineering and Environmental Problems, 5th Symposium (SAGEEP), ed. by R. S. Bell. Soc. Eng. & Miner. Explor. Geophy., 1992, pp. 487-508.

Maleki, H. An Analysis of Violent Failure in U.S. Coal Mines. Paper in Proceedings: Mechanics and Mitigation of Violent Failure in Coal and Hard Rock Mines. USBM Spec. Publ. 01-95, 1995, pp. 5-25.

Maleki, H. Effective Monitoring Techniques for Assessing Structural Stability. Paper in New Technology for Longwall Ground Control: Proceedings, U.S. Bureau of Mines Longwall Technology Transfer Seminar, compiled by C. Mark, R. J. Tuchman, R. C. Repsher, and C. L. Simon. USBM Spec. Publ. 01-94, 1994, pp. 117-129.

Maleki, H. Ground Response to Longwall Mining. CO Sch. Mines Q, v. 83, No. 3, 1988, 14 pp.

Maleki, H., W. Ibrahim, Y. Jung, and P. A. Edminster. Development of an Integrated Monitoring System for Evaluating Roof Stability. Paper in Proceedings, Fourth Conference on Ground Control for Midwestern U.S. Coal Mines, ed. by Y. P. Chugh and G. A. Beasley (Mt. Vernon, IL, Nov. 2-4, 1992). Dep. Min. Eng., S. IL Univ., 1992, pp. 255-271.

Maleki, H., Y. Jung, and K. Hollberg. Case Study of Monitoring Changes in Roof Stability. Int. J. Rock Mech. Min. Sci. & Geomech. Abstr., v. 30, No. 7, 1993, pp. 1395-1401.

Wepper, W. W., and N. I. Christensen. A Seismic Velocity-Confining Pressure Relation, with Applications. Int. J. Rock Mech. Min. Sci. & Geomech. Abstr., v. 28, No. 5, 1991, pp. 451-462.

Westman, E. C. Characterization of Structural Integrity and Stress State via Seismic Methods: A Case Study. Paper in Proceedings of 12th International Conference on Ground Control in Mining, ed. by S. S. Peng (Morgantown, WV, Aug. 3-5, 1993). Dep. Min. Eng., WV Univ. 1993, pp. 327-329.

USE OF TOMOGRAPHIC IMAGING AS A TOOL TO IDENTIFY AREAS OF HIGH STRESS IN REMNANT ORE PILLARS IN DEEP UNDERGROUND MINES

By D. F. Scott,[1] M. J. Friedel,[2] M. J. Jackson,[2] and T. J. Williams[3]

ABSTRACT

Rock masses in deep mines are subject to high stress, which can result in unexpected, violent failure of rock into mined-out openings. One method to evaluate relative stress is tomographic imaging, a technique based on the principle that highly stressed rock will demonstrate relatively higher velocities than rock under less stress (load). The success of tomography depends on subsequent surveys in which increases, decreases, or changes in locations and magnitude of stress are compared.

Researchers at two U.S. Bureau of Mines centers, the Spokane Research Center and the Twin Cities Research Center, have been investigating tomographic imaging as a tool for identifying stress in remnant ore pillars in deep mines. Work has proceeded at two mines, the Lucky Friday Mine, Mullan, ID, and the Homestake Mine, Lead, SD, and two successive tomographic surveys have been completed at each mine.

Software has been developed to produce three-dimensional tomograms showing areas of high and low velocities (stress) in pillars at both mines. Mined-out openings, haulageways, ramps, and crosscuts are areas of low velocity that correlate well to fractured rock and indicate low stress. Areas of higher velocity (therefore higher stress) are well delineated above backfilled stopes.

INTRODUCTION

Stress in deep underground mine pillars is difficult to detect and quantify. If undetected, the result can be unexpected and catastrophic failure of large volumes of rock into mined-out openings. Current methods of stress determination are expensive, time consuming, and confined to determinations at a single point.

Using an impact source to send seismic waves through a rock mass and recording the velocities of these waves at receivers positioned around the area of interest enables the construction of a tomogram. A tomogram is a snapshot of the velocities and can be used along with information about the geology and seismicity of a pillar to assign relative stress to the pillar.

To evaluate the usefulness of the technique, U.S. Bureau of Mines (USBM) researchers conducted tomographic surveys in pillars at two deep underground mines, the Lucky Friday Mine, Mullan, ID (March and November

[1]Geologist, Spokane Research Center, U.S. Bureau of Mines, Spokane, WA.

[2]Geophysicist, Twin Cities Research Center, U.S. Bureau of Mines, Minneapolis, MN.

[3]Mining engineer, Spokane Research Center.

1993) and the Homestake Mine, Lead SD (July and October 1993). This paper describes work during the first survey in the Lucky Friday Mine. The objectives of the research were to enhance existing three-dimensional software to simulate stress based on observed velocities; utilize existing mine conditions for a tomographic survey without requiring additional mine development; determine if velocities could be used to identify areas of high and low stress in a rock mass; and use geologic information, seismic activity, and tomography as tools to determine the state of stress of a deep underground pillar.

The Lucky Friday Mine (figure 1) is accessed primarily by the Silver shaft, which extends to a depth of about 1,859 m below the surface. Levels are about 61 m apart; current mining is mechanized underhand cut-and-fill along a nearly vertical vein. Stopes average about 122 m long, 3 m wide, and 61 m high, with sublevels about 30 m apart. Load-haul-dump units are used for ore and waste removal. The pillar, which is approximately 152 m long, 91 m thick, and 61 m high, was mined by overhand cut-and-fill methods from the 5100 level upward about 21 m. This pillar was chosen for the survey because it is in an area known to have elevated stress levels; part of the pillar had already been mined and backfilled; access above, below, and around the pillar was sufficient for a survey; and seismicity was associated with the pillar.

Figure 1
Location of Lucky Friday Mine.

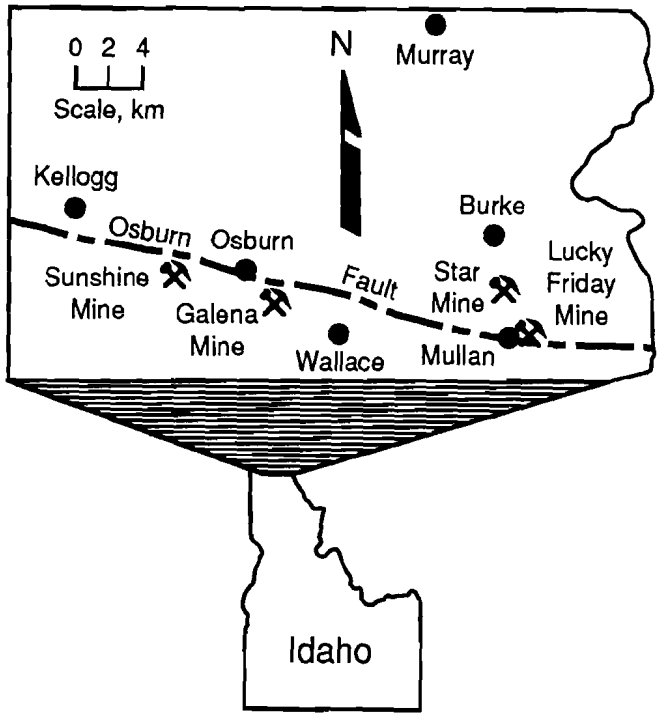

GEOLOGIC SETTING

The Lucky Friday Mine is developed primarily along a single, tabular, nearly vertical vein (the Lucky Friday). The vein occurs mainly in the Revett Formation, which is composed of Precambrian quartzite, sericite, and argillite. The vein ranges from several centimeters to about 4.3 m thick and contains massive galena, sphalerite, and tetrahedrite, which are the ore minerals for lead, zinc, and silver, respectively. Gangue materials are quartz and siderite. The vein is sigmoidal in shape and is bounded on the north by the North Control Fault and on the south by the South Control Fault. The vein generally coincides with a large anticline and dips 70° to 90° to the south, with a southeast rake. Because the vein dips more steeply than the anticline, it contacts increasingly older rocks with depth and intersects the Upper Revett about 549 m below the surface.

The pillar investigated at the Lucky Friday Mine is composed of mainly fine-grained vitreous quartzite, which occurs in flat, laminated-to-cross-bedded, 46- to 91-cm-thick beds that contain abundant quartz veins. Sericitic quartzite, next in abundance, is softer than vitreous quartzite and occurs in flat, laminated, 30- to 91-cm-thick beds. It appears randomly along bedding planes in the vitreous quartzite and is commonly associated with thin beds of argillite. Argillite is pale green to light brown. The argillite becomes clay-like when wet, similar to fault gouge. The argillite occurs in flat, laminated beds ranging from about 0.4 to 7.6 cm thick and is interbedded with both the vitreous and sericitic quartzites. Bedding can be defined by the argillite.

TOMOGRAPHIC METHODS

PRINCIPLES

Inducing a seismic wave through a rock mass and recording the velocities of the first arrivals of the wave at various geophones provides a base for tomographic imaging of a rock mass (figure 2). The velocities are statistically tested for validity, and average velocity is calculated on the basis of the principle that the more compact the rock mass (that is, the more loading or stress a rock mass contains), the higher the velocities. Low velocities would be associated with fractured rock masses or rock under less stress.

EQUIPMENT

The geophones used were 100 and 60 Hz (figure 3). The cables were 137 m in length, with 20 takeouts spaced 6 m apart. A Bison Digital Instantaneous Floating Point Signal Stacking Seismograph, Model 9024, Series 9000 (figure 4), was used for data collection. The seismograph was powered with a heavy-duty 12-V marine battery. A two-pair shielded cable was also used to communicate to the seismograph operator and send sledgehammer trigger signals to the seismograph. A distinct advantage of the field equipment was its compactness, which enabled it to be easily set up on a flatcar (figure 5).

SOFTWARE AND HARDWARE

Underground, data from the seismograph was downloaded to a 486 computer (figure 6). The first-arrival waves to reach the geophones were picked and stored. All geophone coordinate data were input into a spreadsheet along with the first-arrival times. MIGRATOM,[4] a USBM-developed software package, was used to process data from the spreadsheets, and two- and three-dimensional tomograms were generated. Final contouring of the tomograms was done with a commercial software contouring package.

DATA COLLECTION

Access to nearly all sides of a pillar is critical to ensuring that ray paths cross all parts of a pillar. The first step was to establish suitable geophone locations. Most mines use mechanical rock bolts with metal plates. Because the geophones used were mounted with bolts, it was decided to mount the geophones on the end of a rock bolt or the metal plate. At about 6-m intervals, the ends of the rock bolts were drilled and tapped (figure 7). If the bolt could not be drilled, the rock bolt plate was drilled and tapped instead. Figure 8 shows geophone locations on the 4900 and 5100 levels. Using the mine coordinate system, project personnel surveyed each bolt from the existing spads in the roof of the drifts, crosscuts, or haulageways. Sixty-two geophones were installed on the 4900 level and 66 were installed on the 5100 level. The source used for generating a signal to the seismograph was a 5.4 kg sledgehammer (figure 9). Twenty to thirty impacts per bolt were needed to stack signals on the seismograph.

A two-dimensional survey was completed for each level. To complete a three-dimensional survey, geophones were positioned on one level and the signals were generated on the other. One complete survey, using three workers, took four 8-h shifts. Because drilling, blasting, and noise from equipment during the day shifts interfered with signal recording, work was done during the 11:00 p.m. to 7:00 a.m. shift. This time worked well because the survey then resulted in a minimum amount of interference with other mining activities.

[4]Jackson, M. J., and D. R. Tweeton. MIGRATOM—Geophysical Tomography Using Wavefront Migration and Fuzzy Constraints. USBM RI 9497, 1994, 35 pp.

Figure 2
Location of Receivers Around Pillar in Lucky Friday Mine, 4900 Level.

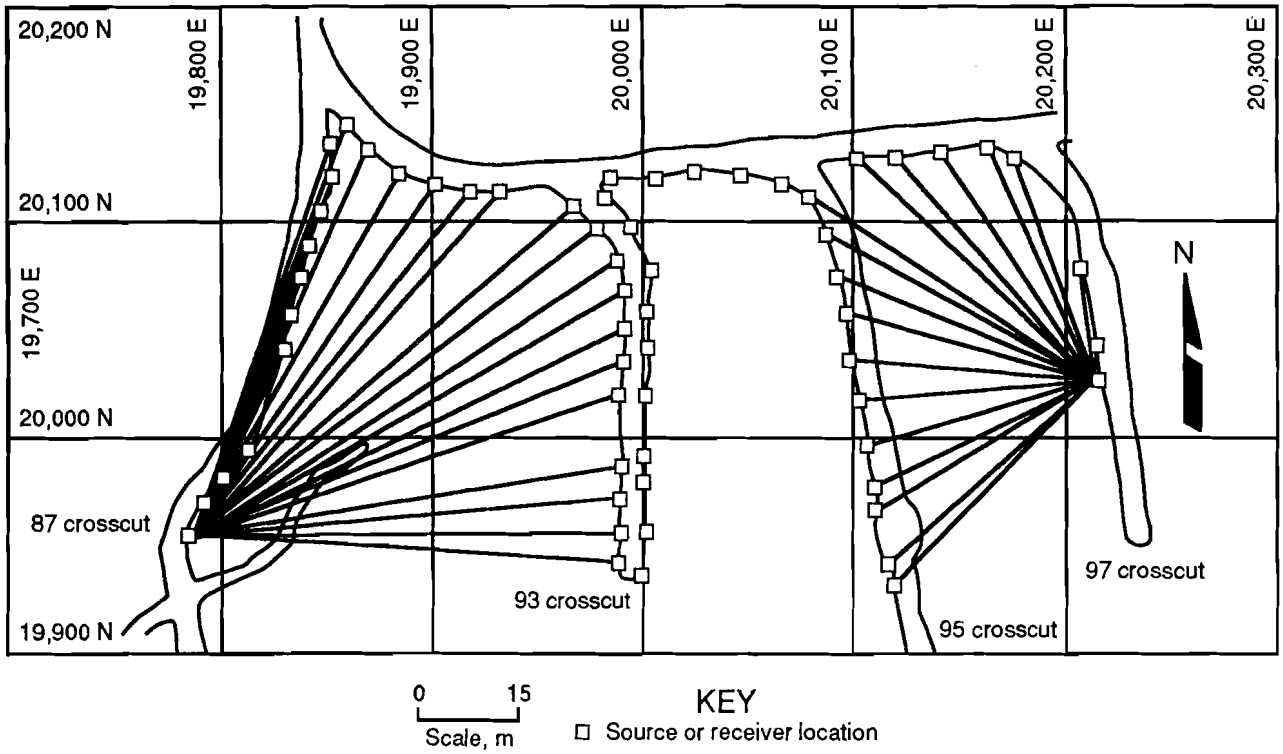

Figure 3
Geophones Attached to Cable Along Wall.

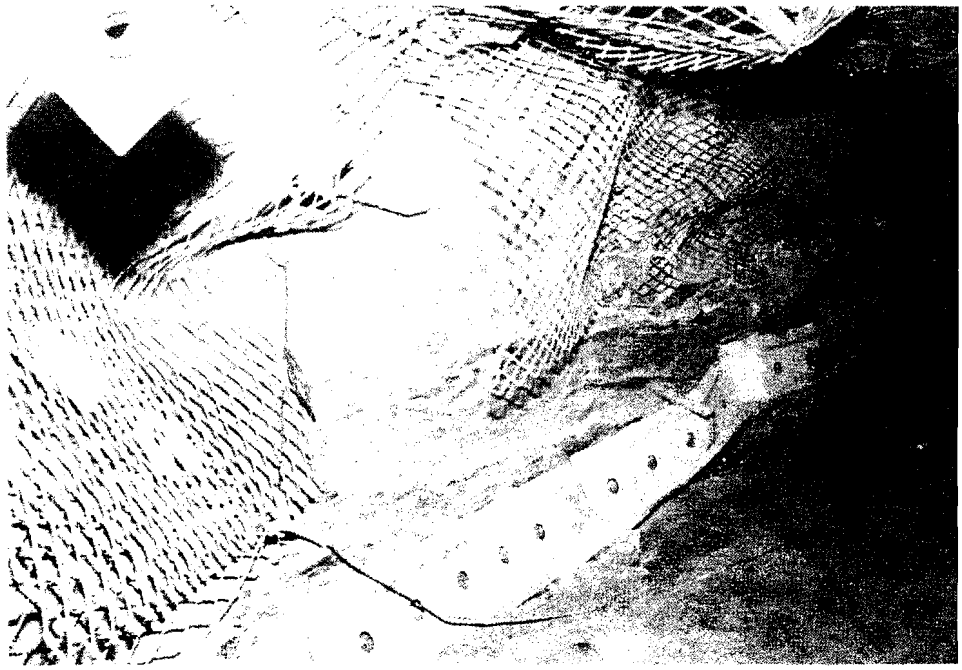

Figure 4
Seismograph.

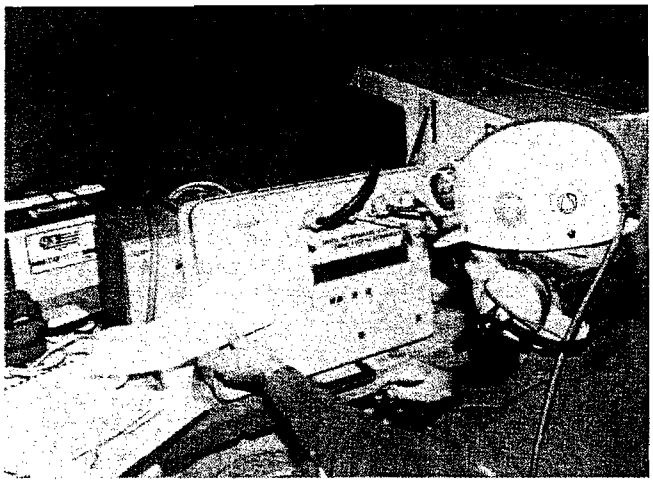

Figure 5
Data Collection Equipment on Flatcar.

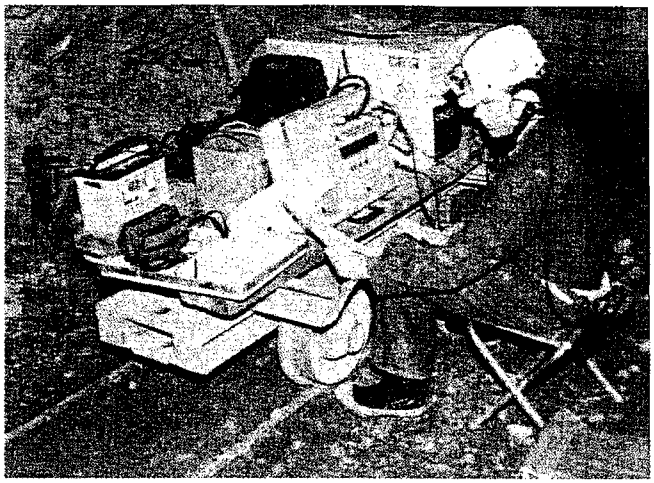

Figure 6
Downloading Data From Seismograph to 486 Computer.

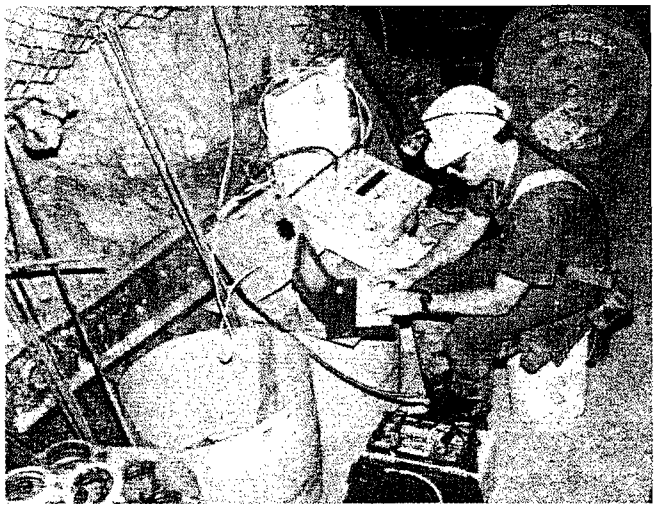

Figure 7
Drilling Rock Bolt Plate.

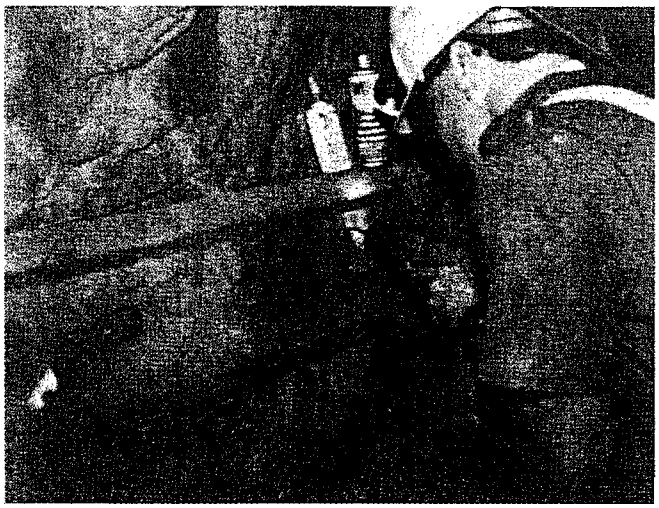

Figure 8
Location of Geophones.

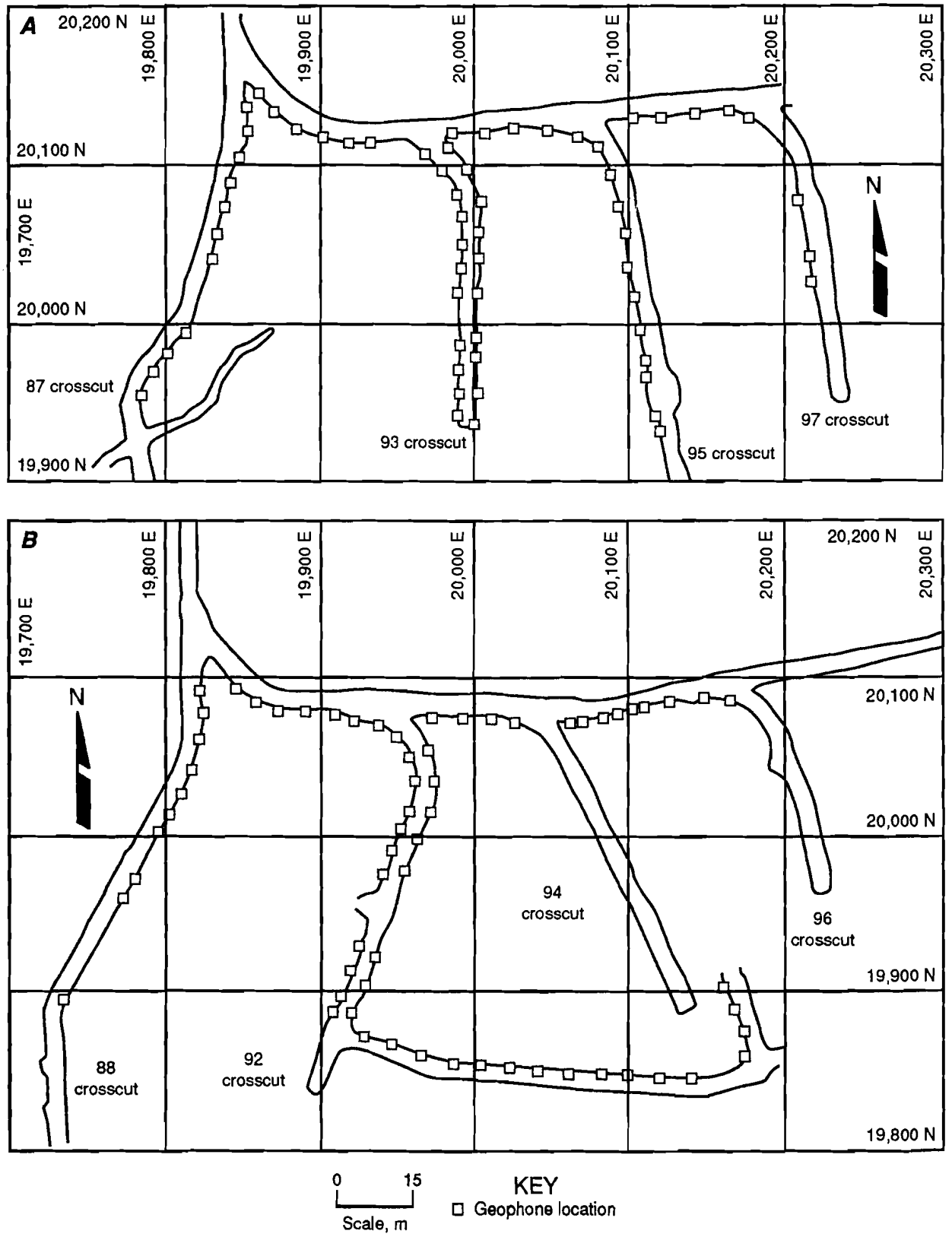

A, 4900 level; *B*, 5100 level.

Figure 9
Using Sledgehammer To Create Seismic Energy.

INTERPRETATION OF TOMOGRAMS

Figures 10 and 11 are plan-view tomograms of the 4900 and 5100 levels, respectively, and figure 12 shows cross sections of the pillar looking east from the mine's east-west coordinate system at 20,000 and 20,050. Based on the tomograms, figures 10 and 11 clearly show regions of low velocity around mine openings and regions of high velocity near the center of the pillars created by the crosscuts (between crosscuts 87 and 93 and between 93 and 95) (figure 8*A*). This pattern reflects a reasonable stress scenario that a finite-element model would predict for mining the pillar. Areas of very high stress (figure 11) also appear in the pillar east of the 92 crosscut. Figure 12 shows several areas of high stress between levels. Most conspicuous are the areas of high stress above the mined-out vein. These areas of the pillar were abandoned several years ago because high stress in the area forced mining to halt. Directly below the upper backfilled vein on the 4900 level (figure 12*B*) is another large area of high stress. Based on the tomograms, there is a considerable portion of the pillar that is under high stress and that may require destressing prior to mining. Low velocities are mainly associated with development openings, which would coincide with a fractured skin along the openings.

The seismic data shown in figures 10, 11, and 12 were collected 90 days before, during, and 90 days after the survey. Figures 11 and 12*A* show increased seismicity in the area of the ramp from the 5100 level down. Physical inspection of the ramp verified that the ramp had indeed been hit by numerous seismic events, as evidenced by the shattered condition of the back and walls. Figure 12*B* also shows increased seismicity associated with high stress just above the 5100 level between the backfilled veins.

Figure 10
P-Wave Velocity, 4900 Level.

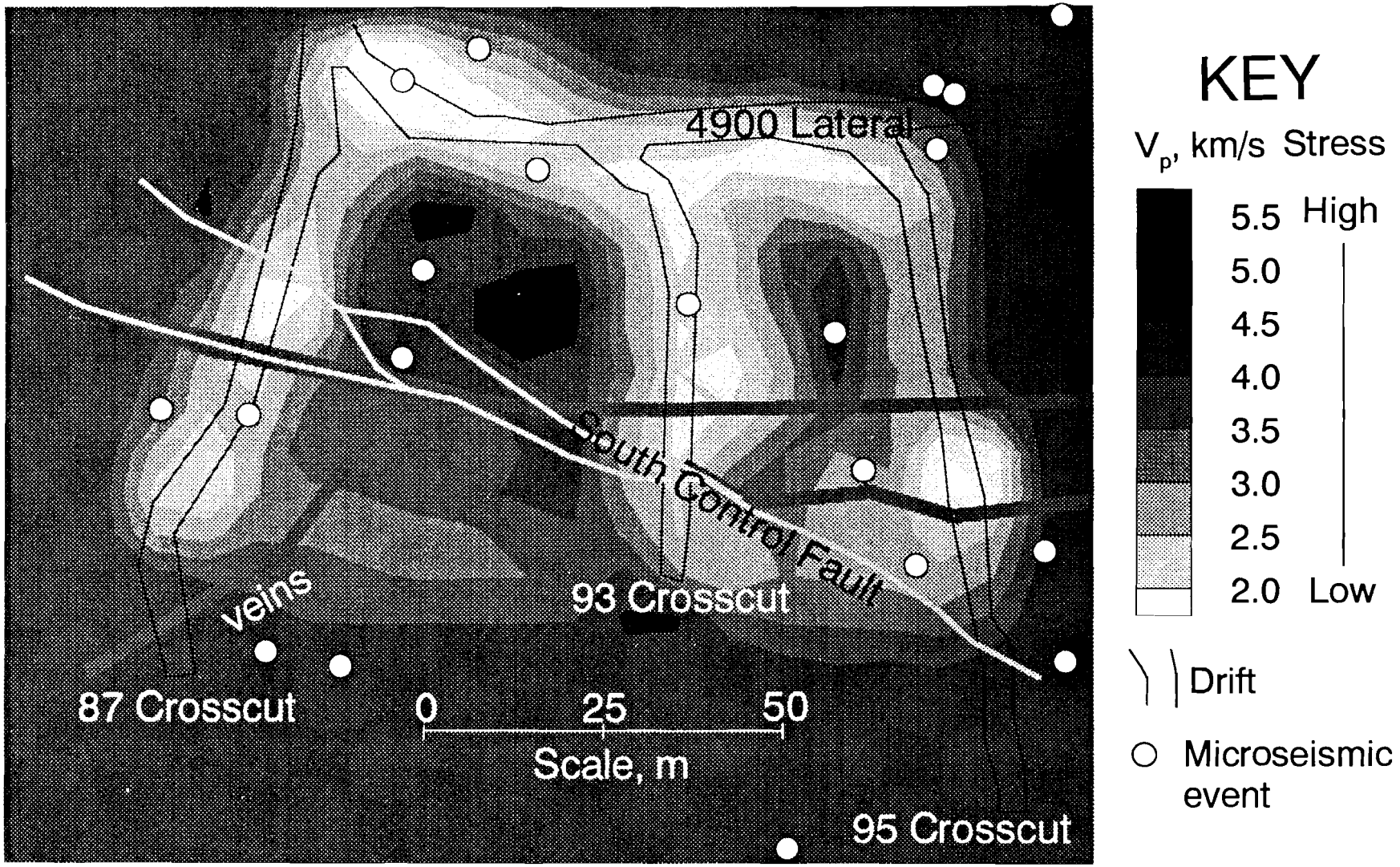

Figure 11
P-Wave Tomograms, 5100 Level, March 1993.

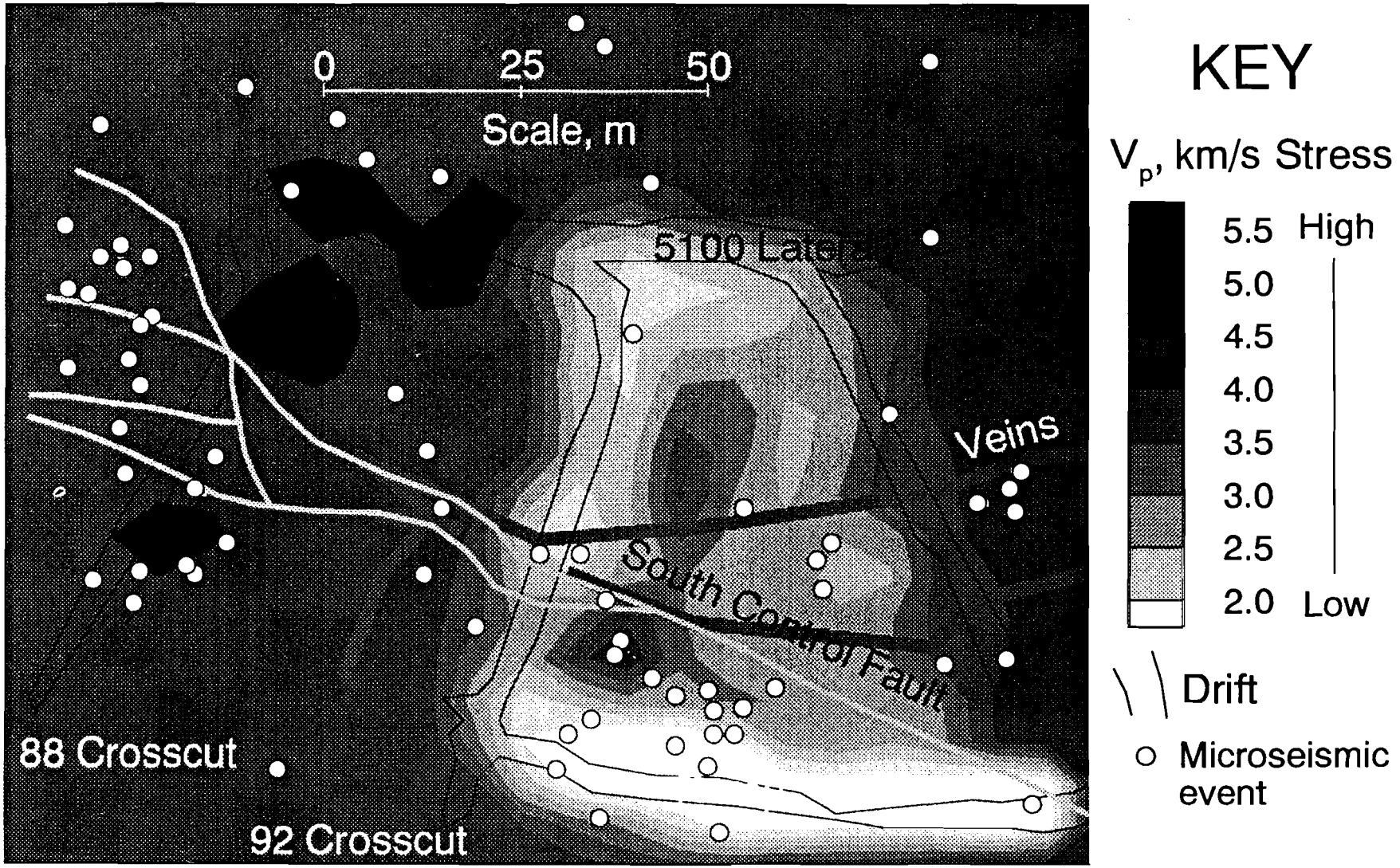

Figure 12
P-Wave Tomograms, March 1993.

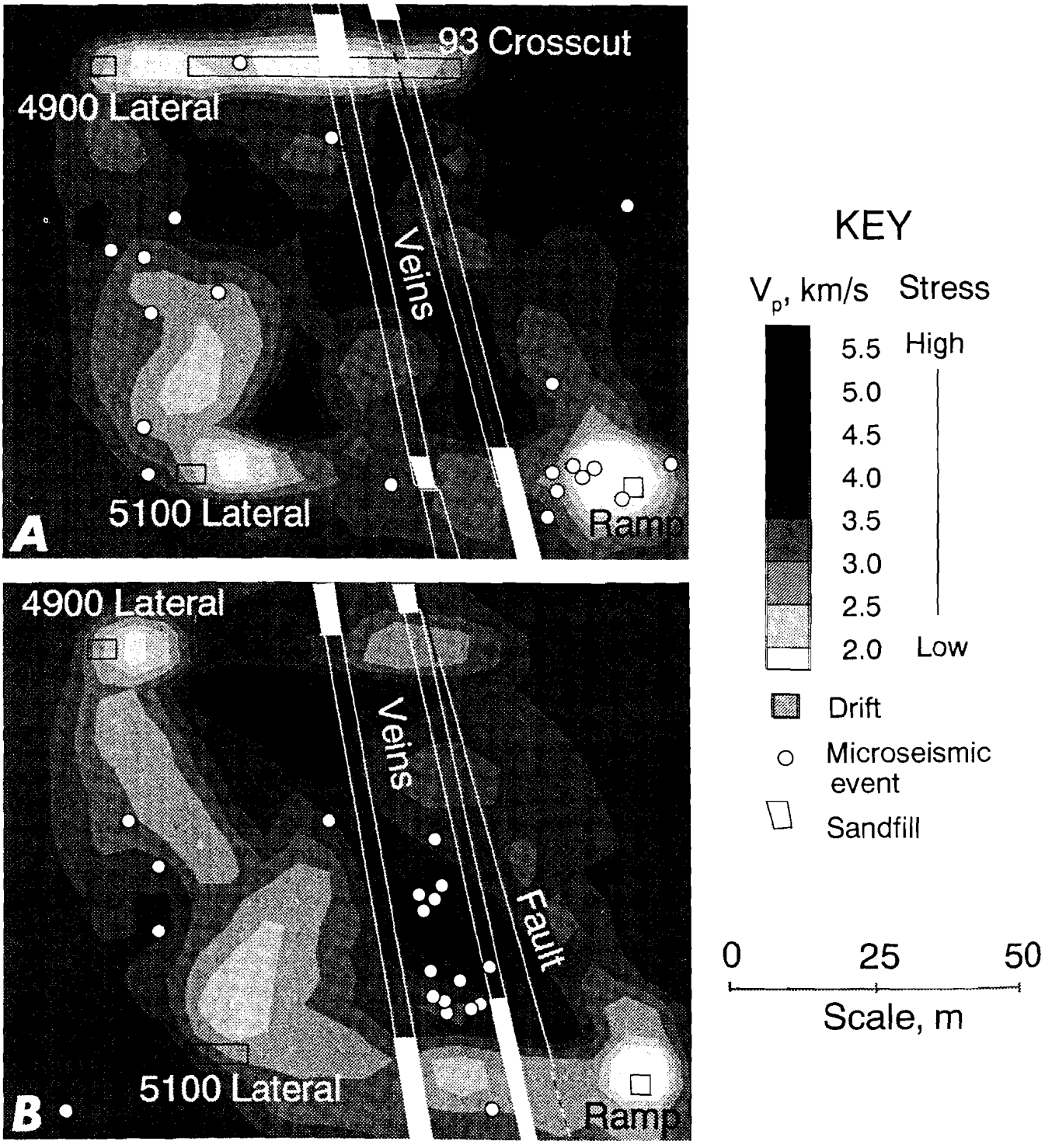

View to the east. Mine coordinate system: *A*, 20,000 Easting; *B*, 20,050 Easting.

CONCLUSIONS

Three-dimensional tomograms were produced using updated versions of MIGRATOM. Existing mine support components (rock bolts, rock bolt plates, and spads) proved satisfactory for conducting the survey. Wave velocities from an impact source identified areas of high and low stress and correlated well with finite-element models of stress distribution.

Tomographic surveys to delineate areas of high and low stress in a deep underground pillar have proven to be useful. The advantages of tomographic surveys as compared to conventional methods of stress determination, such as overcoring, are that the cost of a tomographic survey is considerably less than costs of overcoring; the time needed to conduct a tomographic survey is less; repeating a tomographic survey is very easy; and stress analyses can be done for an entire pillar rather than just one point.

Tomographic surveys can be conducted by engineers, mine planners, and geologists to analyze stress conditions before and after blasting, identify damaged areas or bad ground associated with areas of low stress in fractured ground, and plan mine development on the basis of stress conditions. Mining companies will benefit by having a snapshot of pillar stress conditions prior to development. Knowing the location of areas of high and low stress in a pillar will result in increased safety for miners.

Future work will involve another deep underground mine in which stress in a pillar resulted in a burst that killed a miner.

ACKNOWLEDGMENTS

The authors appreciate the logistical support, mine maps, and geologic information provided by Mr. Clyde Peppin, engineering supervisor, and Mr. Douglas Wollant, mine manager, Lucky Friday Mine, Mullan, ID.

UNDERHAND LONGWALL PROGRAM AT LUCKY FRIDAY MINE, MULLAN, ID

By M. E. Poad,[1] G. Johnson,[2] J. K. Whyatt,[3] and J. R. Hoskins[3]

ABSTRACT

Researchers from the U.S. Bureau of Mines (USBM) have been investigating alternative mining methods to reduce the number and severity of mining-induced seismic events in the deep mines of the Coeur d'Alene Mining District of northern Idaho. In 1984, USBM entered into a three-way memorandum of agreement with Hecla Mining Co., Mullan, ID, and the University of Idaho, Moscow, ID, to design, implement, and evaluate a mining system that could be used safely and productively for vein mining in a rock-burst-prone mine. A mechanized underhand longwall cut-and-fill method using a ramp system for access was chosen for study at the Lucky Friday Mine, Mullan, ID. A 122-m (400-ft) long test stope was developed between the 5100 and 5300 levels. In the underhand method, a block of ground is mined from the top down in a single advancing face, always toward virgin ground; this procedure eliminates the development of a highly stressed sill pillar. Because an engineered fill is placed after each cut, a more competent back is created for the next cycle. Success of the test stope led to adoption of the underhand longwall as the primary mining method throughout the mine.

INTRODUCTION

The U.S. Bureau of Mines (USBM) has been involved in rock-burst research in the Coeur d'Alene Mining District of northern Idaho since the 1970's. As mines go deeper, the number of seismic events, and, correspondingly, the number of damaging rock bursts has increased. (A rock burst is defined here as a mining-induced seismic event that damages mine openings.) The potential for catastrophic injury and loss of life is of ongoing concern.

Control of rock bursts has been pursued in a number of ways. This paper describes a research program directed at improving deep mine safety and productivity through modification of mining methods. In 1979, the USBM conducted a study to examine the potential of the underhand cut-and-fill stoping method as a means of improving ground control in Coeur d'Alene district mines. A subsequent demonstration conducted at Hecla Mining Co.'s Star Mine was limited to pillar recovery but indicated the practicality of the method. The USBM's involvement in the Lucky Friday underhand longwall (LFUL) began in April of 1984 when a three-way memorandum of agreement was entered into with the Hecla Mining Co., Mullan, ID, and the University of Idaho, Moscow, ID.

The LFUL program was not limited to mining methods but included research into backfill, equipment, safety assessment, ground control, seismic response, and productivity. It is not the objective of this paper to report on everything that has been done within the program. A bibliography of related research is included.

[1]Supervisory mining engineer, Spokane Research Center, U.S. Bureau of Mines, Spokane, WA.

[2]Manager of mines/metal, Hecla Mining Co., Coeur d'Alene, ID.

[3]Mining engineer, Spokane Research Center, U.S. Bureau of Mines, Spokane, WA.

LUCKY FRIDAY MINE[4]

DESCRIPTION

The Lucky Friday Mine is located on the eastern edge of the Coeur d'Alene Mining District of northern Idaho (figure 1). The first claims were filed in 1889; however, it wasn't until 1941 that the first commercial ore was found. In 1958, Hecla Mining Co. purchased a 38 pct interest in the mine, and in 1964, the mine was merged into Hecla. The mine has operated continuously since that time, except when low metal prices and a worsening rock-burst problem forced a partial shutdown between April of 1986 and June of 1987.

Between 1980 and 1983, the Silver shaft was sunk to a depth of 1,890 m (6,200 ft) and is the only circular, concrete-lined shaft in the district (figure 2). The present mining horizon is near the 5500 level. Since the first commercial shipments in 1942, more than 5,715,000 t (6,300,000 st) of ore have been mined, yielding 2,863,300 kg (101,000,000 oz) of silver, 614,200 t (677,000 st) of lead, and 76,200 t (84,000 st) of zinc. Production during 1993 was—

Gold	972 troy oz
Silver	60,180 kg (2,122,738 oz)
Lead	17,960 t (19,795 st)
Zinc	3,980 t (4,385 st)
Copper	310 t (339 st)
Ore milled	162,910 t (179,579 st)

GEOLOGY

The Lucky Friday vein at 1,600 m (1 mile) below the surface forms an S-shape in plan view extending horizontally about 490 m (1,600 ft). Splits off the main vein extend the potential stope length to over 610 m (2,000 ft) along strike. Mineralogically, the vein is composed of galena, sphalerite, and tetrahedrite in a quartz and siderite gangue. The vein is 0.6 to 9 m (2 to 30 ft) wide and averages about 1.5 m (5 ft) wide. The vein is in the Precambrian Revett Formation, which hosts most of the silver- and lead-producing mines in the Coeur d'Alene district.

Because the vein itself dips steeply (70° to 90°) to the south and east, it comes into contact with progressively older rocks with depth (figure 3). Presently, mining is encountering Precambrian Superbelt rocks of the upper submember of the lower member of the Revett Formation.

Numerous faults and secondary folds are apparent, and some of these intersect the vein structure. The most pronounced faults are the North and South Control Faults that delineate the ends of the 460-m (1,500-ft) long Lucky Friday vein. The rock mass surrounding the vein is made up of vitreous quartzite and sericitic quartzite beds from 30 to 91 cm (12 to 36 in) thick with soft interbeds of argillite generally less than 2.5 cm (1 in) thick. These beds have been grouped into 15- to 46-m (50- to 150-ft) thick subunits of predominantly hard, brittle, vitreous quartzite and relatively soft, plastic argillite and sericitic quartzite (figure 4).

Figure 1
Location of Lucky Friday Mine, Mullan, ID.

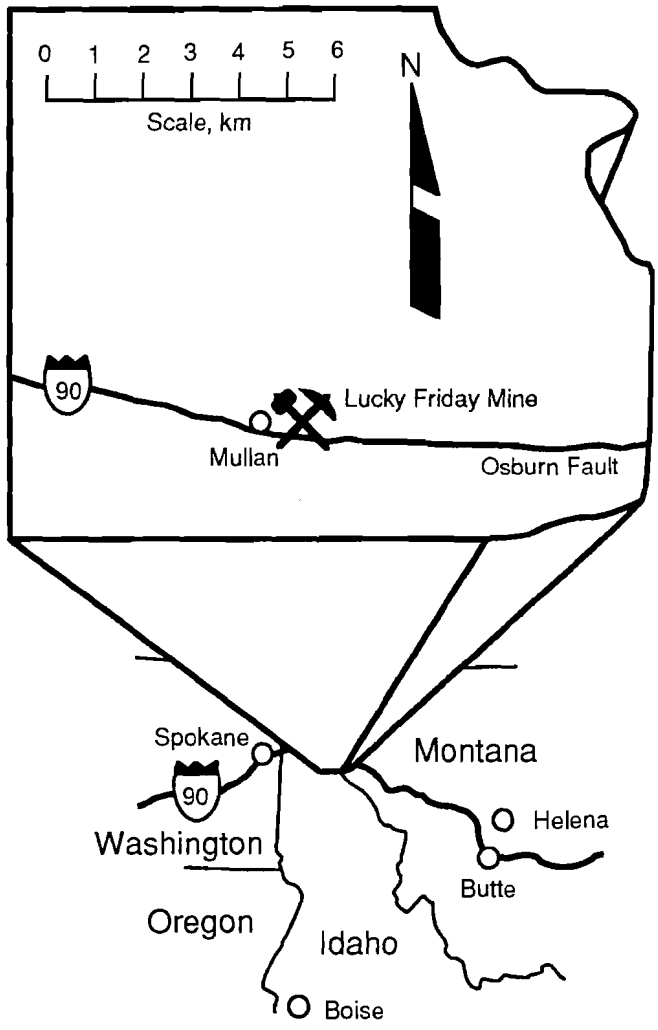

[4]Mine information was provided by D. G. Wollant, unit manager, Lucky Friday Unit, in a report on the history of the Lucky Friday Mine, January 1993.

Figure 2
Map of Lucky Friday Mine.

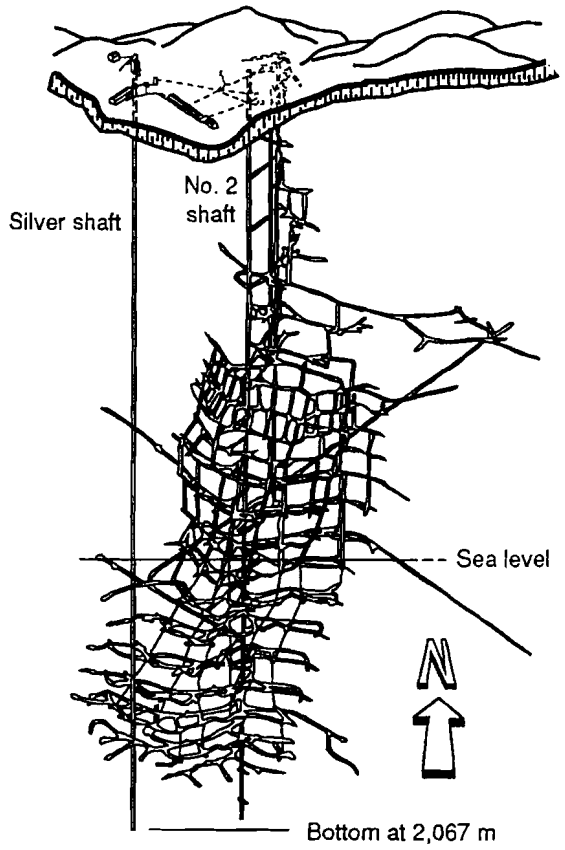

Figure 3
Major Geologic Structures of Lucky Friday Mine, Plan View.

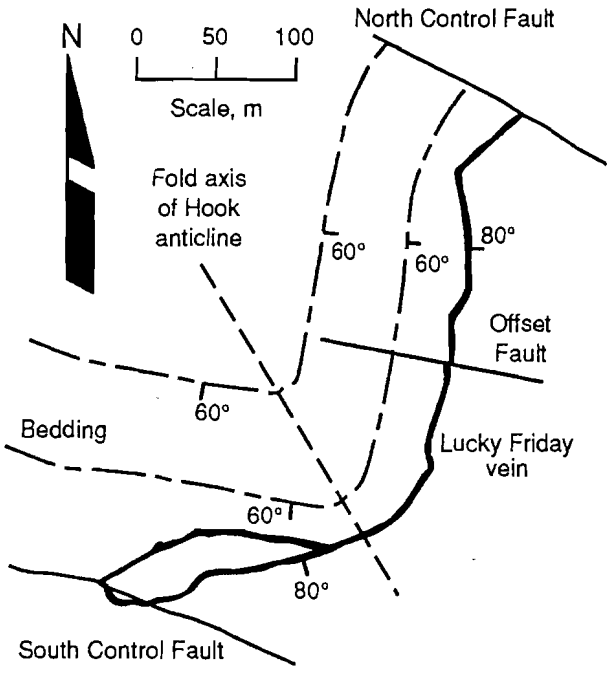

Figure 4
Geology Around Lucky Friday Mine.

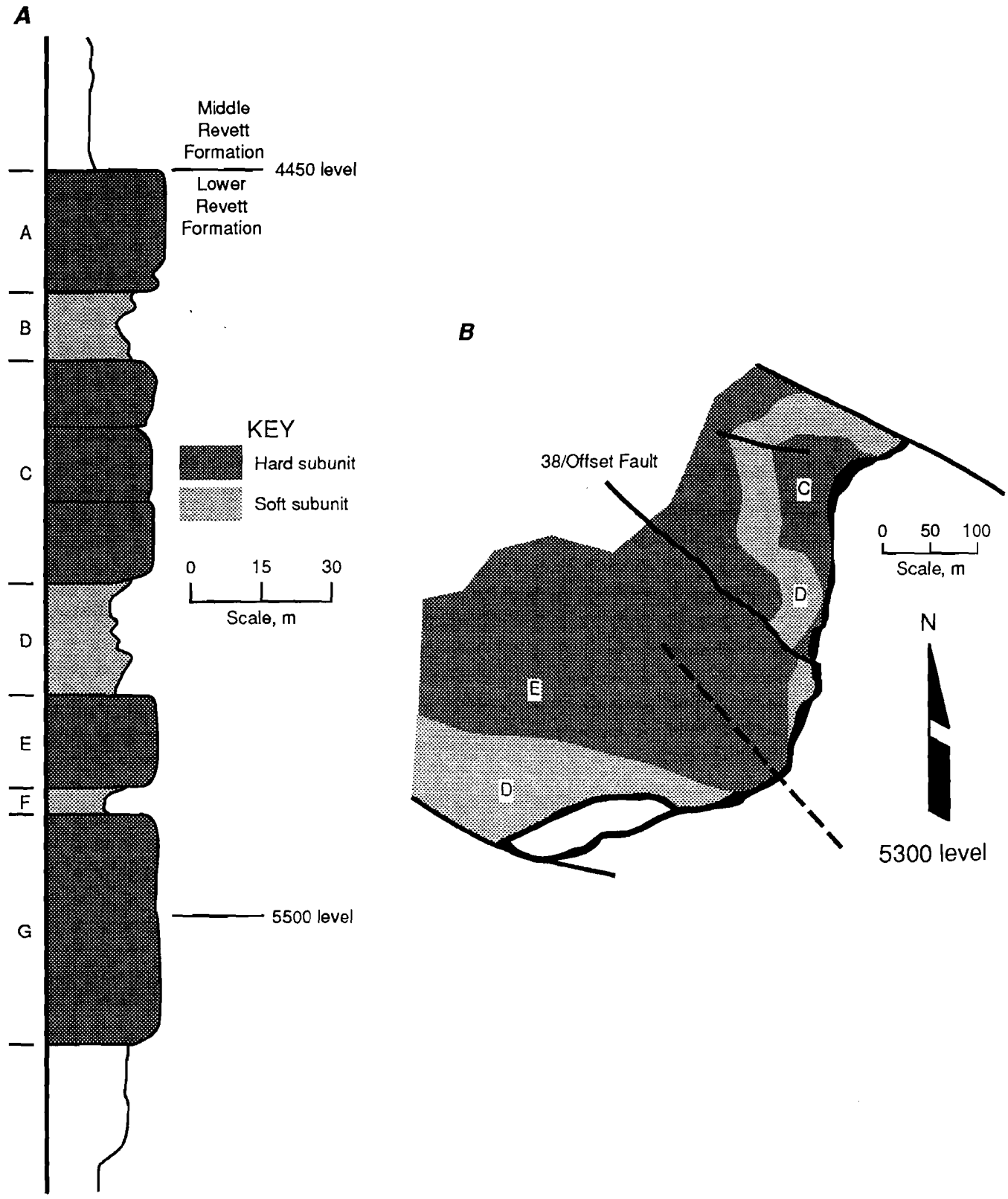

A, Simplified geologic column; *B*, geology and faults near Hook anticline (dotted line), 5300 level.

MINING METHODS

TRADITIONAL MINING METHOD—OVERHAND CUT-AND-FILL

The Lucky Friday vein was mined by a traditional overhand cut-and-fill method until 1986. The vein was developed vertically on 61-m (200-ft) intervals with track haulage levels driven parallel to the vein and extending between the Silver and No. 2 shafts. Crosscuts from the main haulage levels were driven horizontally at approximately 76-m (250-ft) intervals.

Large, heavily timbered raises were constructed at vein-crosscut intersections, with eight stopes generally developed per level. At 6 m (20 ft) above the track elevation, a sublevel was mined for approximately 76 m (250 ft) along strike. Overhand stoping and breasting down on an unconsolidated mill tailings backfill using jackleg drills and electric slushers advanced the stope upward in a series of 2.4-m (8-ft) high lifts toward the next working level. Timbers were placed in at least 15 m (50 ft) of the stope length, and at times along the entire length of the stope. Productivity in these overhand stopes ranged from 11 to 18 t (12 to 20 st) per crew member per shift over a cut-and-fill cycle. Approximately 24 developed stopes were needed to ensure a production rate of 900 t/d (1,000 st/d), which required a minimum of three developed levels to be operating at once. Because of rock-burst damage, the need to replace timbers, and sandfilling, only 50 pct of the stopes were generally producing ore on any given day. Broken ore was slushed from the stope into ore chutes, loaded into 2.7-t (3-st) cars, and transported to the skip loading systems at either shaft. Figure 5 illustrates a typical overhand stope with its raise, ore chute, backfill operation, and active stoping area.

One characteristic of the overhand stoping method is that it produces a pillar of vein rock as mining proceeds upward toward previously mined areas. This pillar is steadily reduced in size until it is completely removed. As the pillar becomes smaller, stress concentrates in the remaining portion until it eventually fails. Failure may be violent or nonviolent, depending upon the relative stiffness of the pillar and the wall rock. A nonviolent failure is characterized by gradual fracturing and yielding, while violent failure is characterized by the release of seismic energy. When sufficient seismic energy is produced to damage mine openings, the failure is called a rock burst.

Ground control, including the necessity of preventing or reducing the magnitude of rock bursts, is the single largest factor influencing mining method, safety, and costs at the Lucky Friday Mine. Argillaceous beds nearly parallel to the vein dry out and lose cohesion after exposure to air, requiring vigilance to spot loose ground in the stope after every blast. The heavy lead ore itself is very brittle and prone to spalling. Once an opening is made, the rock will not support itself long without timber or rock bolts. Wall rocks experience significant squeeze and over 0.6 m (2 ft) of closure is common in raise areas. These factors make the mine prone to large-scale, unpredictable rock bursts.

DEVELOPMENT OF THE LUCKY FRIDAY UNDERHAND LONGWALL MINING SYSTEM

Increasingly difficult economic conditions prompted Hecla Mining Co. to form a Mining Research Department in 1983 to identify and test alternative technologies and techniques that would improve the safety and profitability of its overhand cut-and-fill operations.[5] The research department quickly determined that its primary objective would be to find a solution to the rock-burst problem. The department also forged a close working relationship with the USBM and students and staff of the Department of Mining and Metallurgy at the University of Idaho. University of Idaho participation was funded largely by the USBM's Generic Minerals Institute program.

Promising results from a USBM study at Hecla's Star Mine encouraged Hecla's research group to begin investigating variations of the underhand cut-and-fill method. Underhand cut-and-fill operations at Magma Copper's Superior Mine, Superior, AZ, and Homestake Mining Co.'s Bulldog Mine, Creed, CO, were reviewed (Cummings and Given, 1973; Murray, 1982). Canadian research and practice, primarily in Inco, Ltd.'s, large nickel mines in northern Canada (Hustrilid, 1982), were also studied.

Underhand cut-and-fill stoping is a method in which a block of ore is mined by cutting and filling in sequence from the top of the block to the bottom (rather than from the bottom to the top as in the overhand cut-and-fill method), so the intact vein forms the stope floor instead of the stope back. As in the overhand cut-and-fill method, the vein is accessed through crosscuts from laterals, and mining is conducted with a conventional drill, blast, and muck cycle. Figure 6 shows a typical underhand cut-and-fill stope with ore chutes and a filled area above the stope.

Design and Evaluation

As a result of this review, Hecla determined that a successful mining method must include the following design factors:

1. It must reduce rock-burst activity by removing remnant pillars.

[5]Company information supplied by S. Lautenschlaeger, unit manager, Lucky Friday Unit, in a report on the Lucky Friday Mine, Jan. 1990.

Figure 5
Overhand Cut-and-Fill Stope.

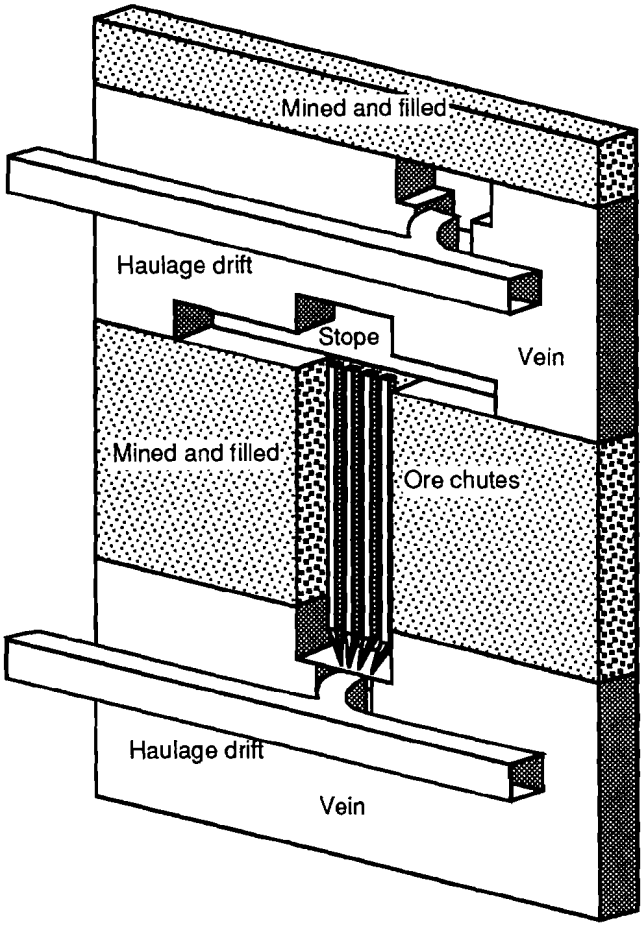

Figure 6
Underhand Cut-and-Fill Stope.

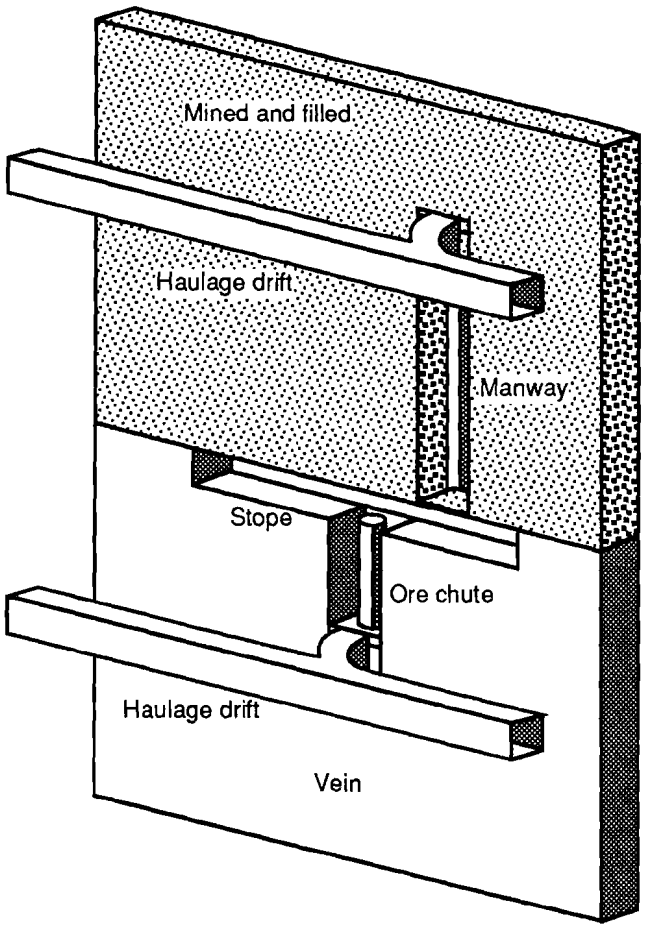

2. It must be mechanized to reduce the direct cost of mining.

3. It must include a competent, reinforced fill back resistant to shock loading and able to support high regional in situ stresses.

The company proposed an underhand longwall method that uses the principle of a single advancing face in conjunction with the underhand cut-and-fill method to reduce rock-burst hazards. This method had been recommended by the South African High-Level Committee on Rock Bursts and Rock Falls (1977) as a means of reducing rock-burst hazards associated with mining remnants (or sill pillars) as early as 1924 and is now standard practice in South Africa.

Two ground control conditions were identified as crucial to successful implementation of the underhand longwall mining method. These were that—

1. The ramp system must remain stable and operational throughout the life of the stope, and

2. The rock mass response to changing the mining method should not make conditions worse, and should reduce, rock-burst hazards, especially for rock bursts originating at the mining face.

The Hecla research department developed a proposal for evaluating the LFUL test stope. Hecla committed funding for the study and entered into a joint research agreement with the University of Idaho and the USBM for a cooperative project involving stope instrumentation and analysis. The research program concentrated on ground control, mechanization, and fill technology. The University of Idaho worked primarily in mechanization and fill technology while the USBM examined the state of in situ stress, numerical modeling of deep mines, mechanized mining equipment, and backfill technology.

An instrumentation plan was developed for the LFUL stope with the goal of monitoring conditions during mining the first half of the stope block [about 30 vertical m (100 vertical ft)].

Test Stope

The first rock was broken in development for the LFUL test stope in January of 1985. The stope is located on the east end of the Lucky Friday vein between the 5100 and the 5300 levels in the 5300-107 block, approximately 1,555 m (5,100 ft) below the surface and 520 m (1,700 ft) below sea level. Scott (1990) provides an in-depth description of stope geology. This block of ore lies in the upper submember of the lower member of the Revett Formation.

The LFUL test stope uses conventional underhand cut-and-fill methods and a ramp system to provide access for mechanized mining equipment.[6] Slushers were replaced with load-haul-dump equipment (LHD's), which increased mucking efficiency sufficiently to allow stope lengths to be increased from 61 to 275 m (200 to 500 ft), thereby reducing the number of development ramps required.

Each cut is about 3 m (10 ft) high and extends approximately 76 m (250 ft) along the vein to each side of the ramp. The declination of the ramp provides one "turn" adjacent to the ore body every 9 vertical meters (30 vertical feet). Crosscuts are driven from the turning point of the ramp to provide access for services and LHD's. Once a cut is completed, the stope and crosscut are filled with cemented fill. After the fill sets up, a new crosscut is driven from the ramp to the next stope level. Noyes, Johnson, and Lautenschlaeger[7] described the method in detail as it emerged during the development of the experimental LFUL stope. Figure 7 shows the resulting mining plan as implemented in the experimental LFUL stope.

Ground control and backfill data gathered from instruments in the LFUL stope and ramp system provided sufficient basis for confirming the geomechanical soundness of the underhand longwall stope design (Williams and Cuvelier, 1988). Approximately midway through the test stope demonstration in June of 1987, Hecla's executive staff felt that sufficient safety and economic benefits were being shown to justify full implementation of an underhand longwall mining system throughout the mine.

Current LFUL Mining System[8]

The vein is excavated in 24-m (88-ft) intervals vertically by sublevels accessed from a main ramp in the footwall of the vein. Crosscuts from each sublevel are driven to divide the vein into four stopes between 122 and 198 m (400 and 650 ft) long. Development openings 3.4 m (11 ft) wide and 3 m (10 ft) high are advanced by crews utilizing a hydraulic drill jumbo and a 1.5-m^3 (2-yd^3) LHD.

An 3.4-m (11-ft) high cut is drilled and blasted horizontally along strike. Broken muck is removed by either 0.8- or 1.5-m^3 (1- or 2-yd^3) LHD's and hauled to the shaft in a 14.5-t (16-st) truck. After the entire cut is mined, a high-quality cemented backfill is hydraulically placed in the stope to provide safe cover overhead during the next cut. Mining crews then reaccess the vein for a new cut by blasting the floor at a grade of -20 pct to reach the vein at proper elevation. A sublevel plan for the 5400 through 5930 levels is shown in figure 8.

[6]See footnote 5.

[7]Presentation at the 94th annual meeting of the Northwest Mining Association, Spokane, WA, Dec. 2, 1988.

[8]See footnote 4.

Figure 7
Lucky Friday Underhand Longwall (LFUL) Test Stope.

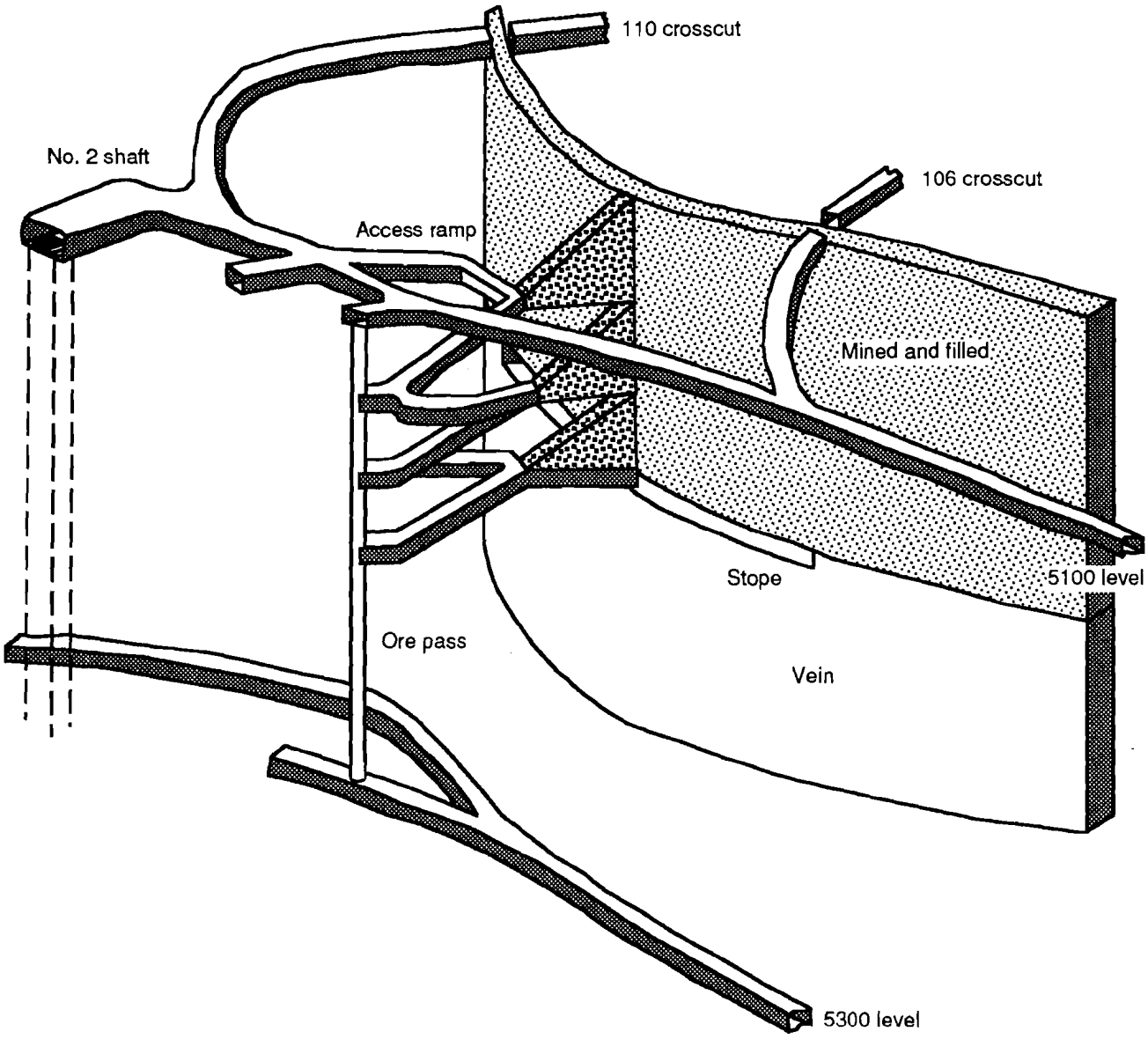

Figure 8
Sublevel Plan at Lucky Friday Mine.

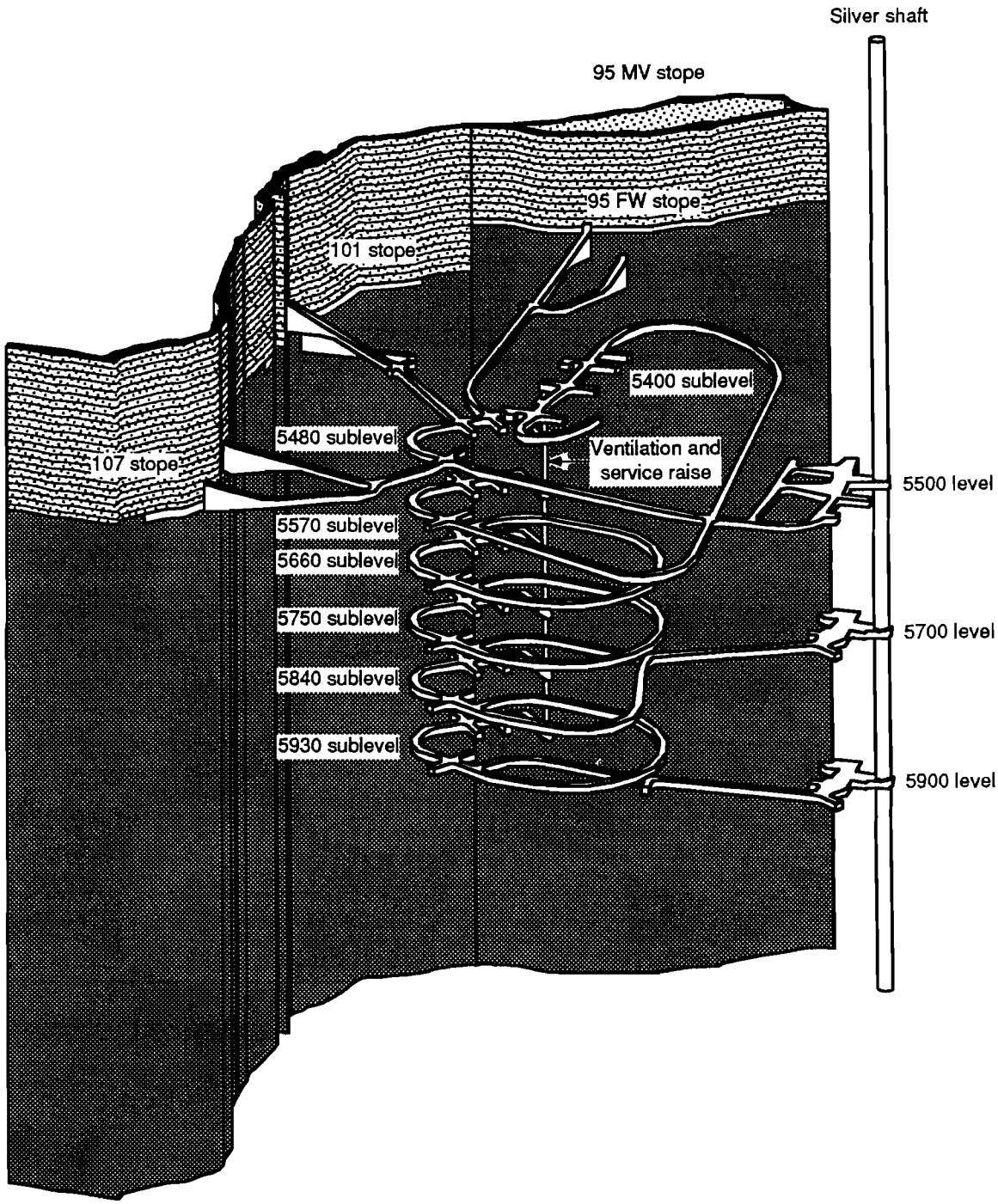

MV = Main vein. FW = Footwall.

DISCUSSION

The Lucky Friday Mine is considered to be the most seismically active mine in the Coeur d'Alene district and among the most seismically active mines in North America (Jenkins and others, 1990). Sprenke and others (1991) estimate that the Lucky Friday Mine experiences a rock burst of local magnitude (M_L) of 2.5 or greater on the average of once every 15 weeks.

Design studies of the LFUL projected an increase in *overall* seismicity but a decrease in the *magnitude* of the largest events. Demonstrating that this has indeed happened is important for evaluating and improving the underhand longwall method.

A plot of annual rock burst activity normalized to metric tons of ore mined for the 10-year period between 1983 and 1993 was prepared (figure 9). An initial increase in seismic activity (1983 to 1987) reflected the progress of mining from the relatively soft Middle Revett Formation to the harder (and more rock-burst-prone) Lower Revett. This number dropped as pillar recovery operations were reduced and the longwall stopes initiated. As the stopes approached a full longwall configuration (1993), the number of rock bursts is again increasing. Lucky Friday Mine personnel have determined that seismic events registering 300 mm or more on the mine's seismograph have the potential to cause damage.

The most dangerous rock bursts, those with M_L greater than 1.5, are plotted in figure 10 for the 8-year period between 1985 and 1993 (without normalization to production): This plot shows that while large bursts occurred at a rate roughly proportional to the entire class of bursts, there was a decoupling after 1990. Initiation of pillar mining increased the relative propensity for large bursts in 1991. This trend reversed in 1992 and 1993 as the mining pattern finally began to resemble a longwall with a single advancing face, and the frequency of large rock bursts fell dramatically, even as the number of small rock bursts increased.

The underhand cut-and-fill method is proving to be a much safer way to mine in rock-burst-prone ground. Many of the large rock bursts that were caused by pillar recovery are being eliminated as the primary stopes progress away from previously mined areas. The cemented backfill has proven to be a reliable and competent roof above the worker.

This is not to say that rock bursts are not a problem in the mine, however, because they are also caused by unfavorable geologic conditions and high stress levels, which are expected to remain.

The underhand cut-and-fill method is also proving to be a more efficient way to mine, and production now averages 33 t (36 st) per crew member per shift. This includes the time spent in a typical 8-week cut cycle to mine the vein, backfill, and reaccess the following cut. Overall mine production is limited to four primary stopes, one or two secondary stopes working on remnant pillars left over from the overhand method, and one Silver vein stope. The number of stopes mined still must be limited because of the danger of rock bursts, and the full implications of the new LFUL mining method are still being evaluated.

Figure 9
Rock Burst Activity Related to Production.

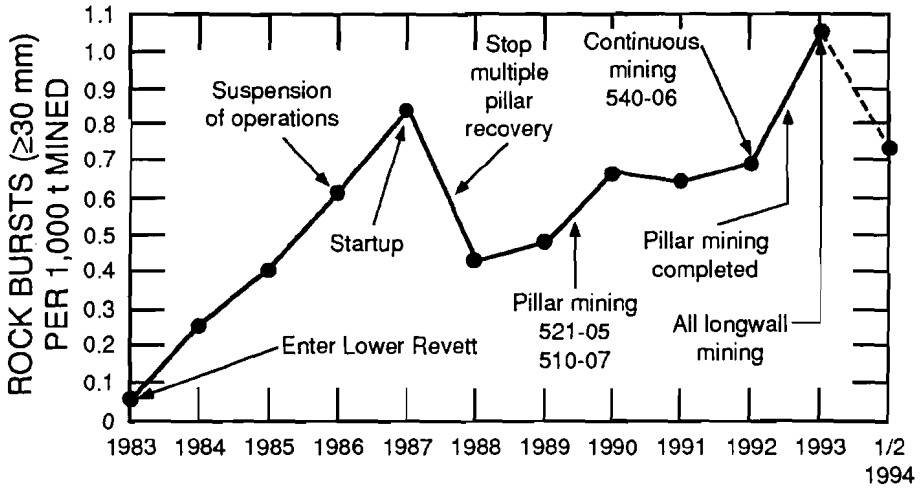

Figure 10
Rock Burst Activity Greater Than Local Magnitude of 1.5.

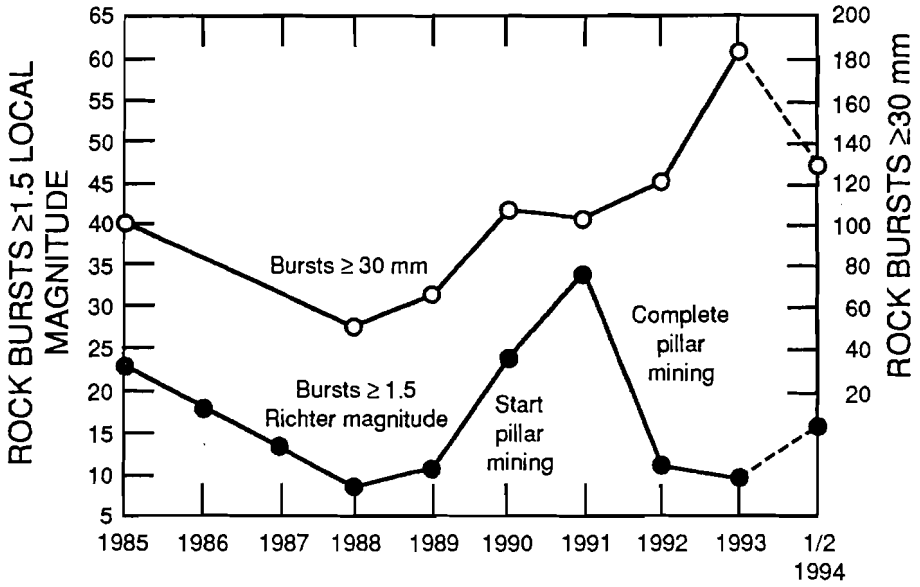

ACKNOWLEDGMENTS

As the extensive list of references demonstrates, this research was the product of a community of people from the USBM, University of Idaho, and Hecla Mining Co. Among the people who made key contributions to this program are Fred Brackebusch, manager of Mining Research for Hecla (now president of Mine Systems Design, Kellogg, ID) and Wally Crandall, vice-president of Research for Hecla (now retired), who were responsible for organizing research efforts. Dave Cuvelier, mining engineer with Hecla, and Mike Werner, mining engineer (now with TUX, Toronto, ON), coordinated mine access. The Department of Mining and Metallurgy of the University of Idaho committed graduate students and expertise. Mark Board, a mining engineer formerly with the USBM and now at Itasca Consulting Service, Minneapolis, MN, planned the monitoring and instrumentation phase. Wilson Blake, mining consultant, Hayden Lake, ID, deserves thanks for providing his expertise in seismicity and rock-burst analysis. Mike Jenkins, Terry McMahon, and Ted Williams, mining engineers, and Doug Scott, geologist, from the USBM, James Vickery, mining engineer for Kennecott Mining Co., Salt Lake City, UT, and William Pariseau, professor of Mining Engineering, University of Utah, Salt Lake City, UT, assisted with mapping, instrument installation, and monitoring and analysis. Most significantly, the employees at the Lucky Friday Mine are acknowledged for their commitment and ingenuity in successfully implementing the underhand cut-and-fill mining method.

REFERENCES

Cummings, A. B., and I. A. Given. UC-SME Mining Engineering Handbook. V. 1, Am. Inst. Min. Metall. Pet. Eng., 1973, 243 pp.

High-Level Committee on Rockbursts and Rockfalls. An Industry Guide to the Amelioration of the Hazards of Rockbursts and Rockfalls. Chamber of Mines of S. Afr., Johannesburg, S. Afr., 1977, 123 pp.

Hustrilid, W. A., ed. Underground Mining Methods Handbook. Am. Inst. Min. Metall. Pet. Eng., 1982, 1754 pp.

Jenkins, F. M., T. J. Williams, and C. J. Wideman. Analysis of Four Rockbursts in the Lucky Friday Mine, Mullan, Idaho, USA. Paper in International Deep Mining Conference: Technical Challenges in Deep Level Mining, ed. by D. A. J. Ross-Watt and P. D. K. Robinson (Johannesburg, Sept. 17-21, 1990). S. Afr. Inst. of Min. and Metall., Johannesburg, S. Afr., 1990, pp. 1201-1212.

Murray, J. W. Undercut and Fill Mining. Ch. in Underground Mining Methods Handbook, ed. by W. A. Hustrilid. Am. Inst. Min. Metall. Pet. Eng., 1982, pp. 631-638.

Scott, D. F. Relationship of Geologic Features to Seismic Events, Lucky Friday Mine, Mullan, Idaho. Paper in Rockbursts and Seismicity in Mines, Proceedings of the 2nd International Symposium on Rockbursts and Seismicity in Mines, ed. by C. Fairhurst (Univ. of MN, Minneapolis, MN, June 8-10, 1988). Balkema, 1990, pp. 401-406.

Sprenke, K. F., M. C. Stickney, D. A. Dodge, and W. R. Hammond. Seismicity and Tectonic Stress in the Coeur d'Alene Mining District. Bull. Seismo. Soc. Am., v. 81, No. 4, Aug. 1991, pp. 1145-1156.

Werner, M. The Lucky Friday Underhand Longwall Mining Method. Ph. D. Dissertation, Univ. ID, Moscow, ID, 1990, 132 pp.

Williams, T. J., and D. J. Cuvelier. Report on a Field Trial of an Underhand Longwall Mining Method to Alleviate Rock Burst Hazards. Paper in Rockbursts and Seismicity in Mines, Proceedings of the 2nd International Symposium on Rockbursts and Seismicity in Mines, ed. by C. Fairhurst (Univ. of MN, Minneapolis, MN, June 8-10, 1988). Balkema, 1990, pp. 513-522.

BIBLIOGRAPHY

Board, M. P., and S. L. Crouch. Mine Planning to Control Rock Bursts in Cut and Fill Excavations. Paper in Design Methods in Rock Mechanics, Proceedings of the 16th U.S. Symposium on Rock Mechanics (Univ. MN, Sept. 22-24, 1975). Am. Soc. Civil Eng., 1977, pp. 249-255.

Board, M. P., and M. D. Voegele. Examination and Demonstration of Undercut and Fill Stoping for Ground Control in Deep Vein Mining. Paper in Application of Rock Mechanics to Cut-and-Fill Mining, Proceedings of the Conference on the Application of Rock Mechanics to Cut-and-Fill Mining, ed. by O. Stephansson and M. J. Jones (Univ. Lulea, Lulea, Sweden, 1-3 June, 1980). Inst. Min. Metall., London, England, 1981, pp. 300-306.

Bush, D. D., W. Blake, and M. P. Board. Evaluation and Demonstration of Underhand Stoping to Control Rock Bursts. USBM OFR 62-85, 1982, 191 pp.

Chan, S. S. M. Problems of Prediction of Ground Stability in Cut and Fill Operation in Deep Vein Mines with Finite-Element Method. Paper in Application of Rock Mechanics to Cut-and-Fill Mining, Proceedings of the Conference on the Application of Rock Mechanics to Cut-and-Fill Mining, ed. by O. Stephansson and M. J. Jones (Univ. Lulea, Lulea, Sweden, 1-3 June, 1980). Inst. Min. Metall., London, England, 1981, pp. 293-299.

Corp, E. L. Rock Mechanics Research in the Coeur d'Alene Mining District. Paper in Application of Rock Mechanics to Cut-and-Fill Mining, Proceedings of the Conference on the Application of Rock Mechanics to Cut-and-Fill Mining, ed. by O. Stephansson and M. J. Jones (Univ. Lulea, Lulea, Sweden, 1-3 June, 1980). Inst. Min. Metall., London, England, 1981, pp. 40-48.

Gooch, A. E. Cut and Fill Mining as Practiced in the U.S.A.—An Overview. Paper in Application of Rock Mechanics to Cut-and-Fill Mining, Proceedings of the Conference on the Application of Rock Mechanics to Cut-and-Fill Mining, ed. by O. Stephansson and M. J. Jones (Univ. Lulea, Lulea, Sweden, 1-3 June, 1980). Inst. Min. Metall., London, England, 1981, pp. 25-27.

Hedley, D. G .F., and R. J. Wetmiller. Rockbursts in Ontario Mines During 1984. MRL Report SP85-5, CANMET, July 1985, 36 pp.

Leighton, F. A Case History of a Major Rock Burst. USBM RI 8701, 1982, 14 pp.

McMahon, T. Rock Burst Research and the Coeur d'Alene District. USBM IC 9186, 1988, 49 pp.

Murray, J. W. Undercut and Fill Mining. Ch. in Underground Mining Methods Handbook, ed. by W. A. Hustrilid. Am. Inst. Min. Metall. Pet. Eng., 1982, pp. 631-638.

Pariseau, W.G. Finite-Element Method Applied to Cut and Fill Mining. Paper in Application of Rock Mechanics to Cut-and-Fill Mining, Proceedings of the Conference on the Application of Rock Mechanics to Cut-and-Fill Mining, ed. by O. Stephansson and M. J. Jones (Univ. Lulea, Lulea, Sweden, 1-3 June, 1980). Inst. Min. Metall., London, England, 1981, pp. 284-292.

Pariseau, W. G., J. K. Whyatt and T. J. McMahon. Rock Mechanics Investigations at the Lucky Friday Mine (In Three Parts): 3. Calibration and Validation of a Stope-Scale Finite Element Model. USBM RI 9434, 1992, 16 pp.

Whyatt, J. K. Geomechanics of the Caladay Shaft. M. S. Thesis, Univ. ID, Moscow, ID, 1986, 195 pp.

Whyatt, J. K., and M. P. Board. Numerical Exploration of Shear-Fracture-Related Rock Bursts Using a Strain-Softening Constitutive Law. USBM RI 9350, 1991, 16 pp.

Whyatt, J. K., T. J. Williams, and M. P. Board. Rock Mechanics Investigations at the Lucky Friday Mine (In Three Parts): 2. Evaluation of Underhand Backfill Practice for Rock Burst Control. USBM RI 9433, 1992, 10 pp.

Whyatt, J. K., T. J. Williams, and W. G. Pariseau. Trial Underhand Longwall Stope Instrumentation and Model Calibration at the Lucky Friday Mine, Mullan, Idaho, USA. Paper in Rock Mechanics Proceedings of the 33rd Symposium, ed. by J.R. Tillerson and W. R. Wawersik (Santa Fe, NM, June 3-5, 1992). Balkema, 1992, pp. 511-519.

Williams, T. J., J. K. Whyatt, and M. E. Poad. Rock Mechanics Investigations at the Lucky Friday Mine (In Three Parts): 1. Instrumentation of an Experimental Underhand Longwall Stope. USBM RI 9432, 1992, 26 pp.

SEISMIC STUDIES AND NUMERICAL MODELING AT THE HOMESTAKE MINE, LEAD SD

By M. T. Filigenzi[1] and J. M. Girard[2]

ABSTRACT

Stresses around mine openings at depth can cause the surrounding rock to fail, releasing stored strain energy. When this happens, the rock may literally explode or "burst" into the opening without warning. As mining progresses deeper into the earth, the possibility of seismic events and rock bursts increases.

Researchers at the U.S. Bureau of Mines are currently studying seismic activity in three underground hard-rock mines in the United States: the Homestake Mine, Lead, SD; the Lucky Friday Mine, Mullan, ID; and the Sunshine Mine, Kellogg, ID. Waveforms from seismic events are recorded by personal-computer-based hardware and software. In addition, researchers are modeling the deep levels of the Homestake Mine using a finite-element code. These models generate stress and displacement values for a given loading condition. By studying in situ stresses and seismic activity along with actual stope sequencing, researchers can make correlations between stresses induced by mining and the frequency and magnitude of seismic events.

Information on seismic events coupled with results from finite-element analyses have increased understanding of rock mass behavior and the mechanisms that may lead to rock bursts. Optimization of stope sequencing designs as a result of these studies could reduce rock burst hazards.

INTRODUCTION

The Homestake Mine in Lead, SD (figure 1), is the oldest continuously operating gold mine in the United States. Opened in 1876, the Homestake Mine has produced over 37 million troy ounces of gold. However, as development of the ore body progresses, mining extends to greater depths. Because of greater stress in the deep levels of the mine, the potential for rock bursts increases, which emphasizes the need for thorough mine design. Nonetheless, even with careful planning and extensive support systems, the increased stress in the deeper levels may cause seismic events.

A seismic event is defined as a transient earth motion caused by a sudden release of potential or stored strain

Figure 1
Location of Homestake Mine, Lead, SD.

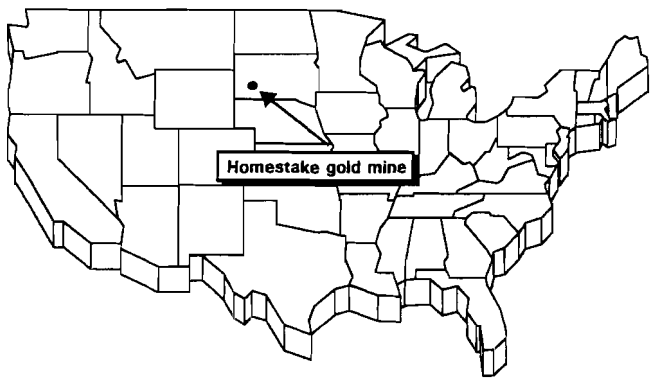

[1]Mechanical engineer.
[2]General engineer.
Spokane Research Center, U.S. Bureua of Mines, Spokane, WA.

energy in the rock. When a seismic event is sudden and violent and causes injury to people or damage to underground workings or equipment, it is referred to as a rock burst.

Between April 1990 and November 1991, the Homestake Mine experienced several seismic events that resulted in ground failures. Many of the events were large enough to be recorded by seismographs 145 km away near Gillette, WY. Following a Mine Health and Safety Administration (MSHA) investigation, a recommendation was made to Homestake personnel to install a system that would continuously record data on mine seismicity. In September 1992, the U.S. Bureau of Mines (USBM) entered into an agreement with the mine to install a seismic data collection system that would monitor the source of seismic activity in the deep levels of the mine.

SEISMIC MONITORING SYSTEM

HARDWARE

The seismic data collection system consists of an array of 16 accelerometers mounted vertically in the back on the 6950, 7100, 7250, 7400, and 7700 levels of the mine. Each accelerometer is wired to a junction box, which in turn is wired to a main junction box in the computer room on the 6950 level (figure 2). A 486 personal computer (PC) is used to record all data, which can be transferred to the surface via modem links. Girard and others (1995)[3] describe seismic monitoring systems in detail.

[3]Girard, J. M., T. J. McMahon, W. Blake, and T. J. Williams. Installation of PC-Based Seismic Monitoring Systems With Examples From the Homestake, Sunshine, and Lucky Friday Mines. USBM Spec. Publ. 01-95, 1995, pp. 303-312.

Figure 2
Underground Seismic Monitoring System.

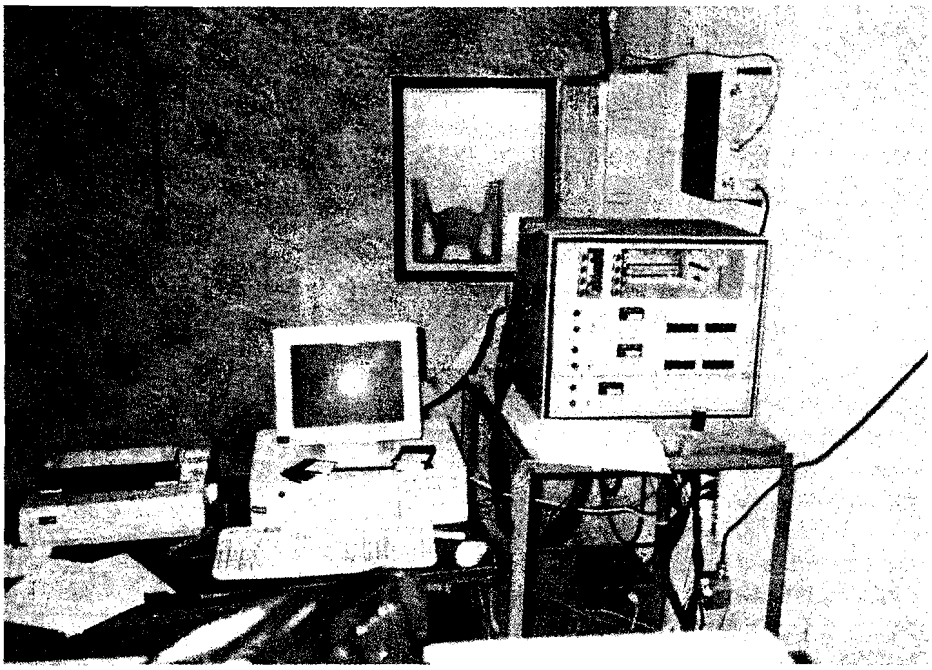

Figure 3
Computer Printout of Rock Burst Waveform.

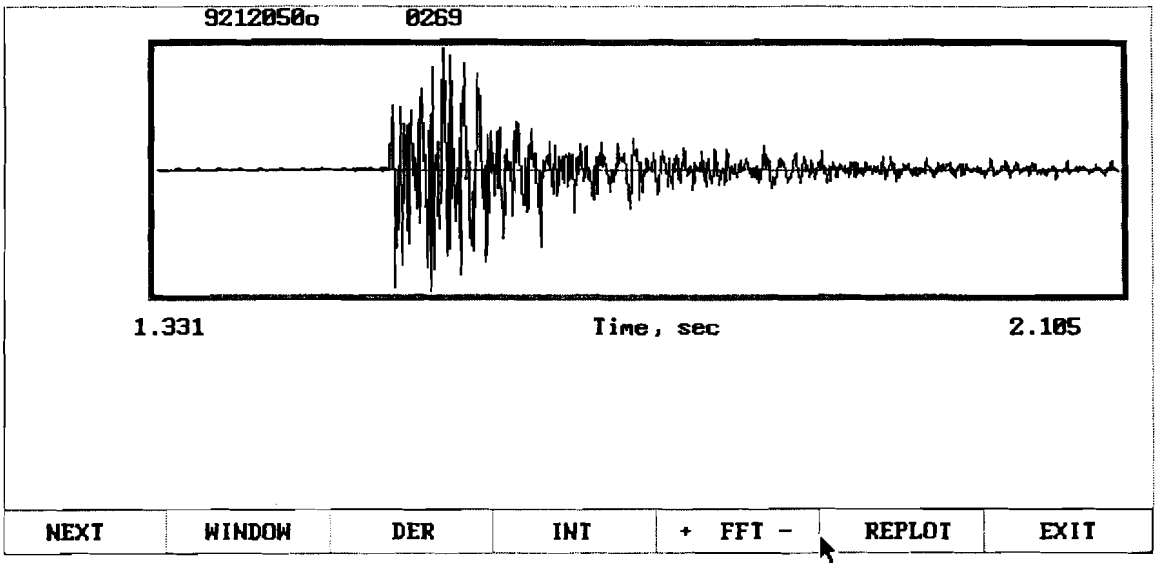

SOFTWARE

A software program continuously monitors the information from each of the 16 accelerometers. If an event has sufficient energy, the recording system is triggered, and the waveform is stored on the hard drive of the PC. Figure 3 shows the typical waveform of an event.

By examining the digital waveform record, the arrival times of P-waves (compressional and dilatational first-wave motion) at each accelerometer can be picked. This arrival time information is used as input to a software program[4] that will compute the coordinates of the event location. Because solution accuracy is dictated by the solution method, the arrival time picks, and the mine's velocity structure,[5] an error residual on origin times for each event is also calculated and taken into account when performing data analysis. In addition, a measure of relative magnitude for each event is computed by averaging the maximum geophysical count of the waveform at each accelerometer. (This method for computing the magnitude is used because the mine does not have a seismograph installed.) A database is used to store event name, coordinates, relative magnitude, and time and date for all data recorded. The original waveform files are archived and stored on a magneto-optical platter.

SEISMIC DATA

Since system operation began, approximately 1,100 seismic events have been recorded. Each event is located on mine maps, and a relative magnitude is calculated. By studying this information, areas of higher activity are targeted for detailed numerical analysis by the USBM. Figure 4 depicts several events plotted using the computer software program AutoCAD. The clustering of events represented by a circle in the figure was chosen as the focus of the finite-element analysis described in this paper.

[4]Blake, W. BBLOCK.FOR computer program, June 1985. Adapted from an original program CBLOCK.FOR by G. Swan and P. Rochon, CANMET, Feb. 1985.

[5]P. L. Swanson, L. H. Estey, F. M. Boler, and S. Billington. Accuracy and Precision of Microseismic Event Location in Rock Burst Research Studies. USBM RI 9395, 1993, 40 pp.

Figure 4
Computer Printout of Cross-Sectional View of Seismic Event Locations.

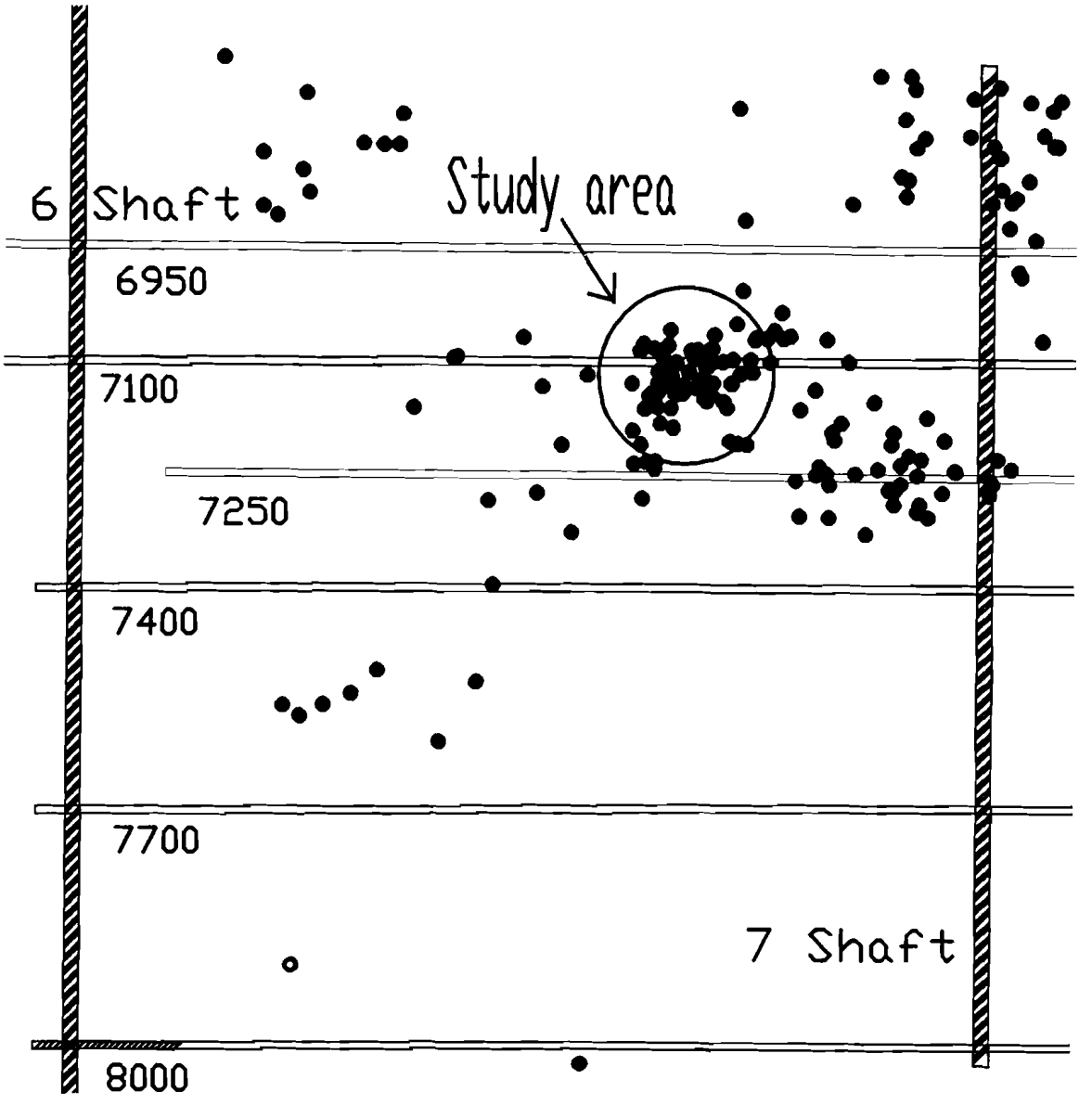

FINITE-ELEMENT ANALYSIS

Finite-element analysis is one of the many numerical modeling techniques chosen for predicting the behavior of a particular system subjected to a given loading condition. By performing a finite-element analysis of proposed mine designs, areas of high stress and potential mining-induced seismic activity can be located. Using stress analysis techniques allows researchers to vary stope size and sequences in an effort to reduce the occurrence of seismic events.

To perform a finite-element analysis, a model of the system under study must be created on a computer. A mesh is then created with a number of discrete elements. These elements are given numerical values equivalent to the material properties of the system under study. The appropriate loading and boundary conditions are applied, and the resulting stresses and displacements are calculated. Finite-element analyses generally require a large number of calculations. In the past, such analyses were carried out primarily on large mainframe computers or supercomputers. With advances in microprocessors and modeling software, engineers can now approximate complex systems

using a PC. For this project, USBM researchers used a Pentium PC and a suite of software, including a finite-element analysis program, AutoCAD; DXF2ANSYS, a screen capture program; and a picture-editing program.

The first step in creating a finite-element model usually involves defining the geometry of the model. For this project, the Homestake Mine provided plans that included stope geometry, mining sequence, and mine geology. Three formations compose most of the rock mass: the Poorman Formation, the Ellison Formation, and the Homestake Formation. The exact formation geometry was simplified for analysis (figure 5*A*). The upper stope of the area under study is 2,043 m below the surface, and the lowest stope is 2,384 m below the surface. Figure 5*B* depicts the stope geometry predicted for 1994. This particular analysis focused on the mine's 44 pillar area. The mine plans were digitized and converted to an appropriate format for the finite-element model. This provided the finite-element program with line segments defining the stope geometry and boundaries of the three geologic formations.

With the model geometry defined, physical properties of the host rock must be specified. For this analysis, researchers relied on the material properties described by Pariseau (1985).[6] Next, an element type for the specific model was defined. A two-dimensional linear elastic anisotropic element with midside nodes was selected. This element type is desirable because the analysis performed is linear elastic and because elements with midside nodes are more accurate than elements without midside nodes.

With the geometry and material properties defined, the finite-element mesh can be created. One of the difficulties that must be overcome when using finite-element analysis is determining mesh density. A very dense mesh will provide very accurate solutions but will also require greater computer resources. A very coarse mesh will obtain a solution using a minimum of resources but may not provide an accurate solution. Experience has shown that the mesh should be fine (at least five nodes) around mine openings. Away from a mine opening, the accuracy of the solution is not as critical, and a coarse mesh density is usually sufficient. The model must be large enough to avoid any boundary effects. Any initial mode size is estimated and an analysis run. If boundary effects become apparent, the size of the model is increased and the analysis re-run. Once the mesh parameters are defined, the program will automatically generate the finite elements (figure 6).

The next step in performing the analysis is to define all constraints and loads. This model is constrained along the bottom to anchor the model in space. Loading is applied to the sides to simulate the horizontal stresses that increase with depth and to the top to simulate overburden. These in situ stresses are described by Pariseau (1985).[7] Gravity loading is applied to simulate increased vertical stresses with increased depth.

[6]Pariseau, W. G. Research Study on Pillar Design for Vertical Crater Retreat (VCR) Mining (Contract JO215043, Univ. of UT). USBM OFR 44-86, Oct. 1985, 233 pp.; NTIS: PB 86-210960.

[7]See footnote 6.

Figure 5
Mine Plans.

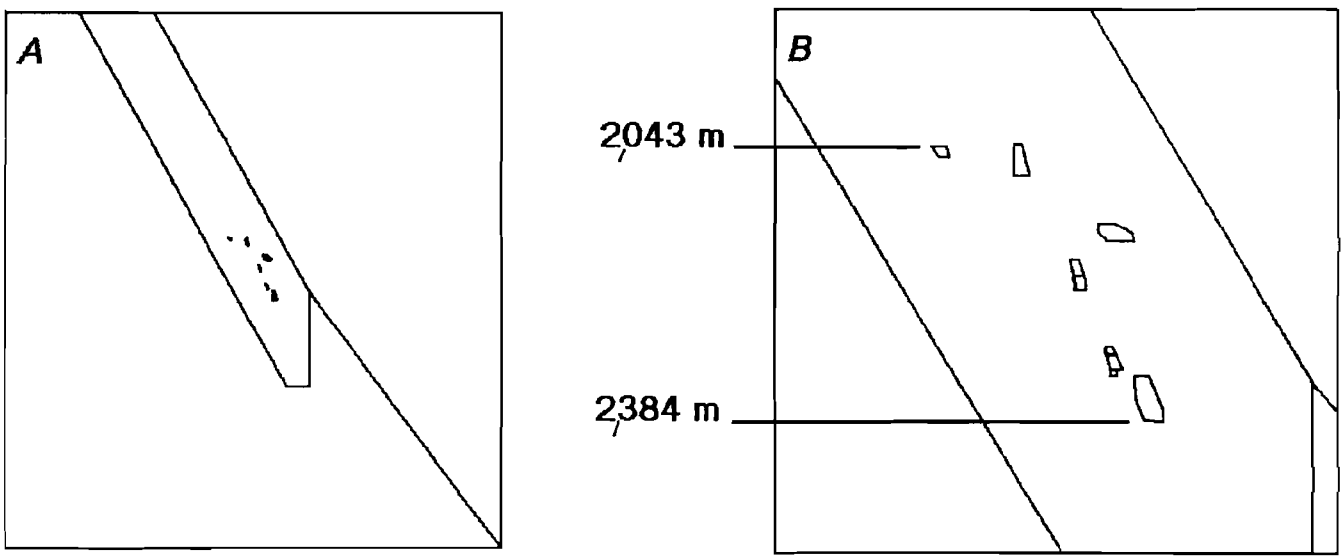

***A*, Overall mine geometry and geology; *B*, detailed mine area under study.**

The analysis type was defined as plane-strain. This type prohibits the elements from deforming into or out of the plane of the model. To simulate stope sequencing between 1992 and 1994, the analysis was performed using multiple load steps. The first load step determined the in situ stress state before mining. The stresses and displacements obtained in this premining condition were then used as initial conditions for the second load step. This load step turned off, or "killed," the elements that represented the stope sections that had been excavated as of 1992. This provided the state of stress in the mine at the end of 1992. These stresses and displacements were used as initial conditions for the third load step. This third load step then modeled the excavations proposed for 1993. Again, the proper elements were killed, providing the stress state at the end of 1993. Finally, the stresses and displacements obtained from the third load step were used as initial conditions for the fourth load step, which computed the stresses and displacements in the mine at the end of 1994.

With the calculations complete, results were available for review. Figures 7*A* through 7*H* illustrate changes in safety factors around the mine openings. The safety-factor values were contained using the calculations as described in Pariseau (1985).[8]

In addition to safety factor calculations, the finite-element program will allow the user to plot principal stresses, vertical stresses, horizontal stresses, displacements, and a host of other solution parameters.

[8]See footnote 6.

Figure 6
Finite-Element Mesh.

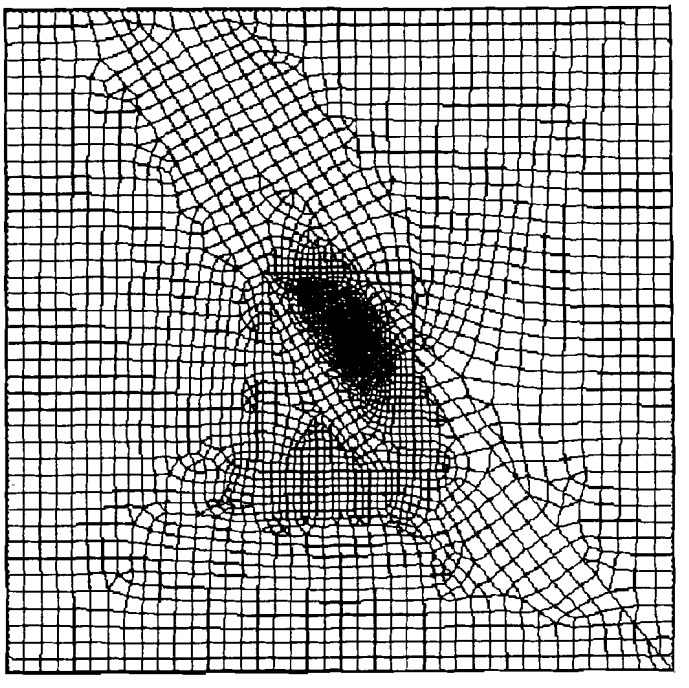

Figure 7
Safety Factor Calculations.

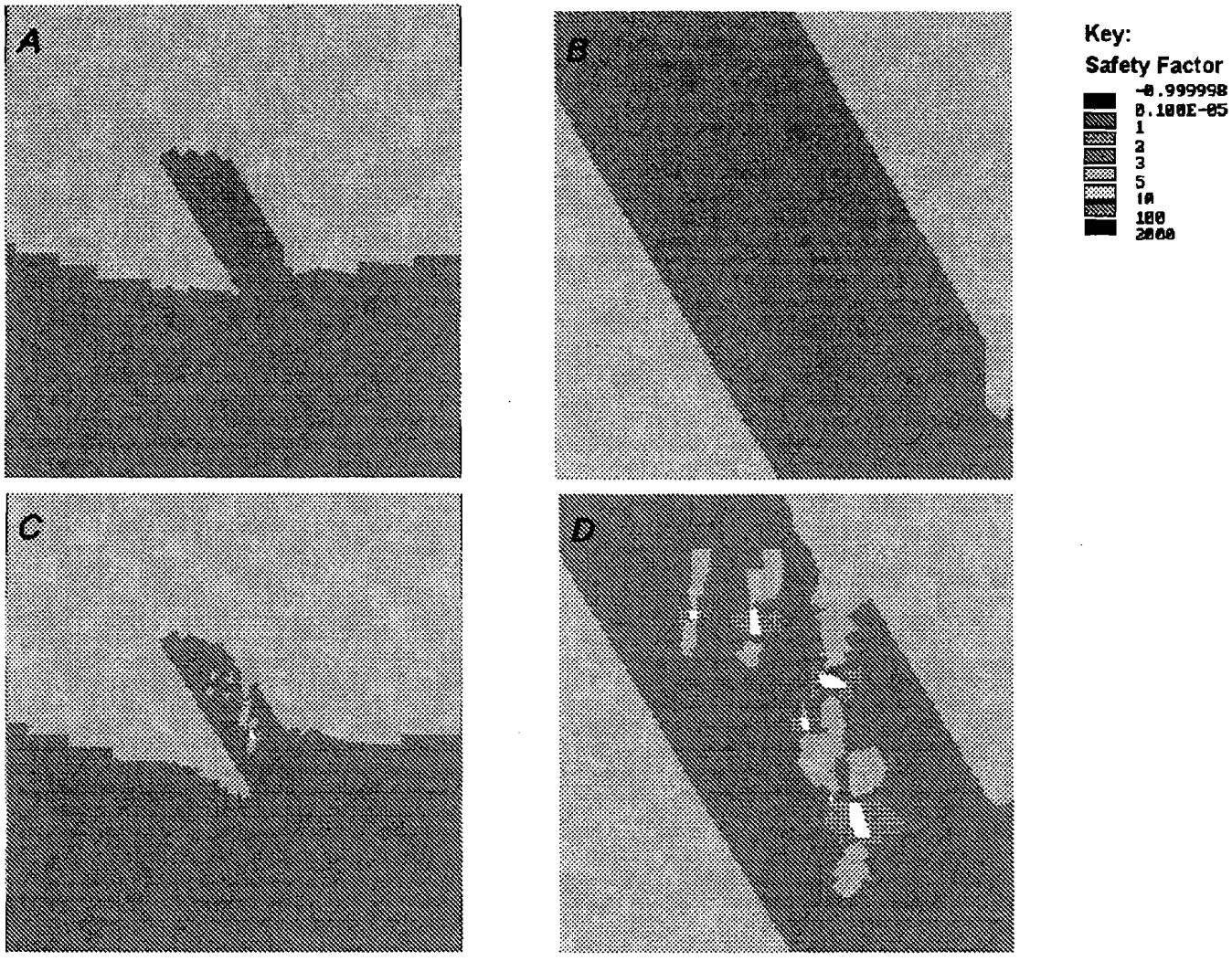

A, Load step 1; *B*, load step 1 closeup; *C*, load step 2; *D*, load step 2 closeup.

Figure 7
Safety Factor Calculations—Continued.

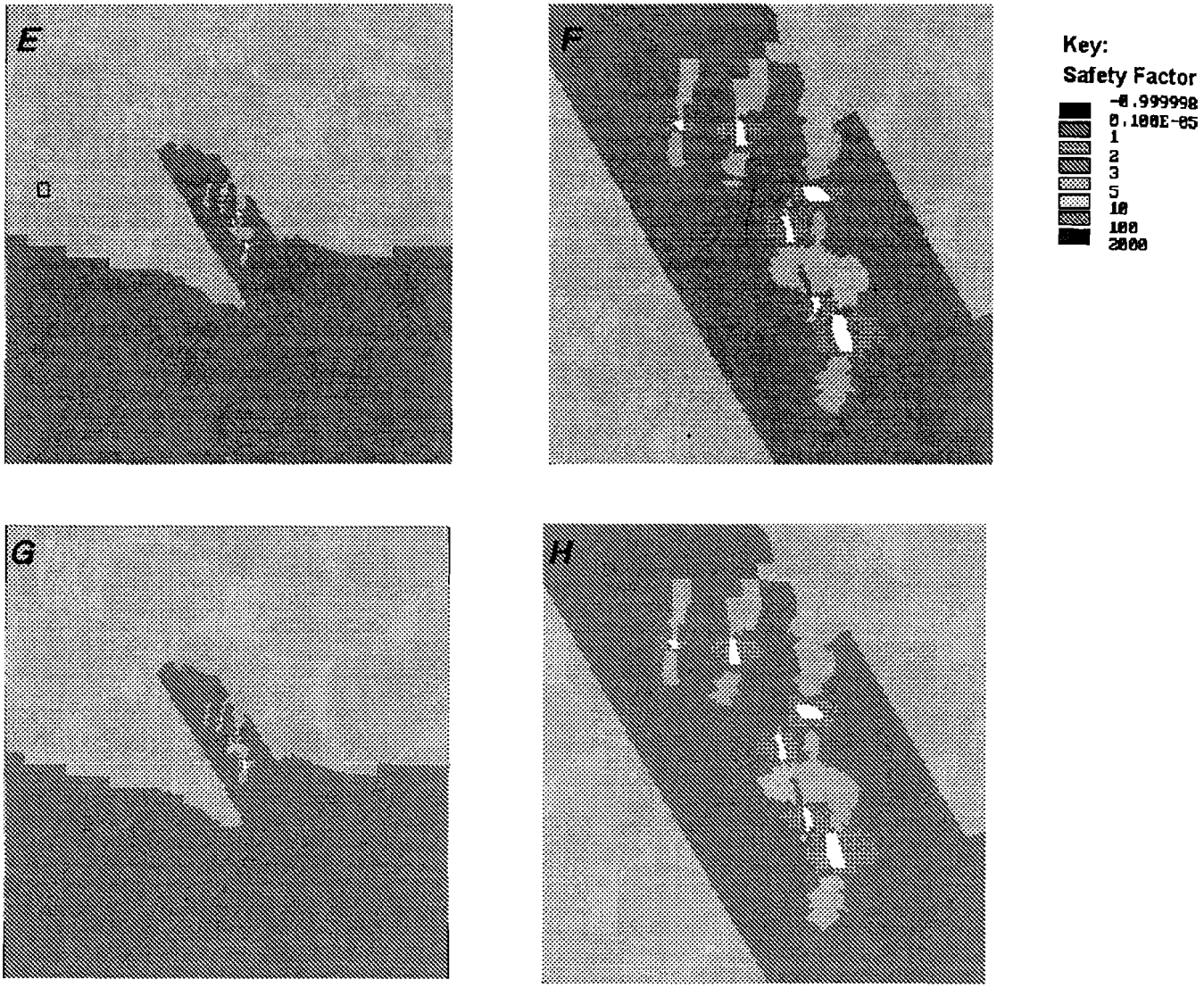

E, load step 3; *F*, load step 3 closeup; *G*, load step 4; *H*, load step 4 closeup.

ANALYSIS AND CONCLUSIONS

Figure 8 overlays all the seismic data from the 44 pillar that were recorded between September 1992 and October 1993. Regions of increased seismicity correspond to regions of lower safety factors as determined using the finite-element program. This finding may indicate a causal link between mining-induced stresses and seismic activity. However, while these preliminary results appear promising, the model was developed as a two-dimensional, linear-elastic analysis. A more rigorous analysis would require a three-dimensional model that incorporates failure criteria and more detailed information on actual mining sequences.

Combining data from seismic recording systems with stope sequencing information and numerical modeling results can be a powerful tool for mine design. Designers may use this tool to avoid mine layouts that could result in the creation of seismically active regions.

Figure 8
Seismic Events at 44 Pillar.

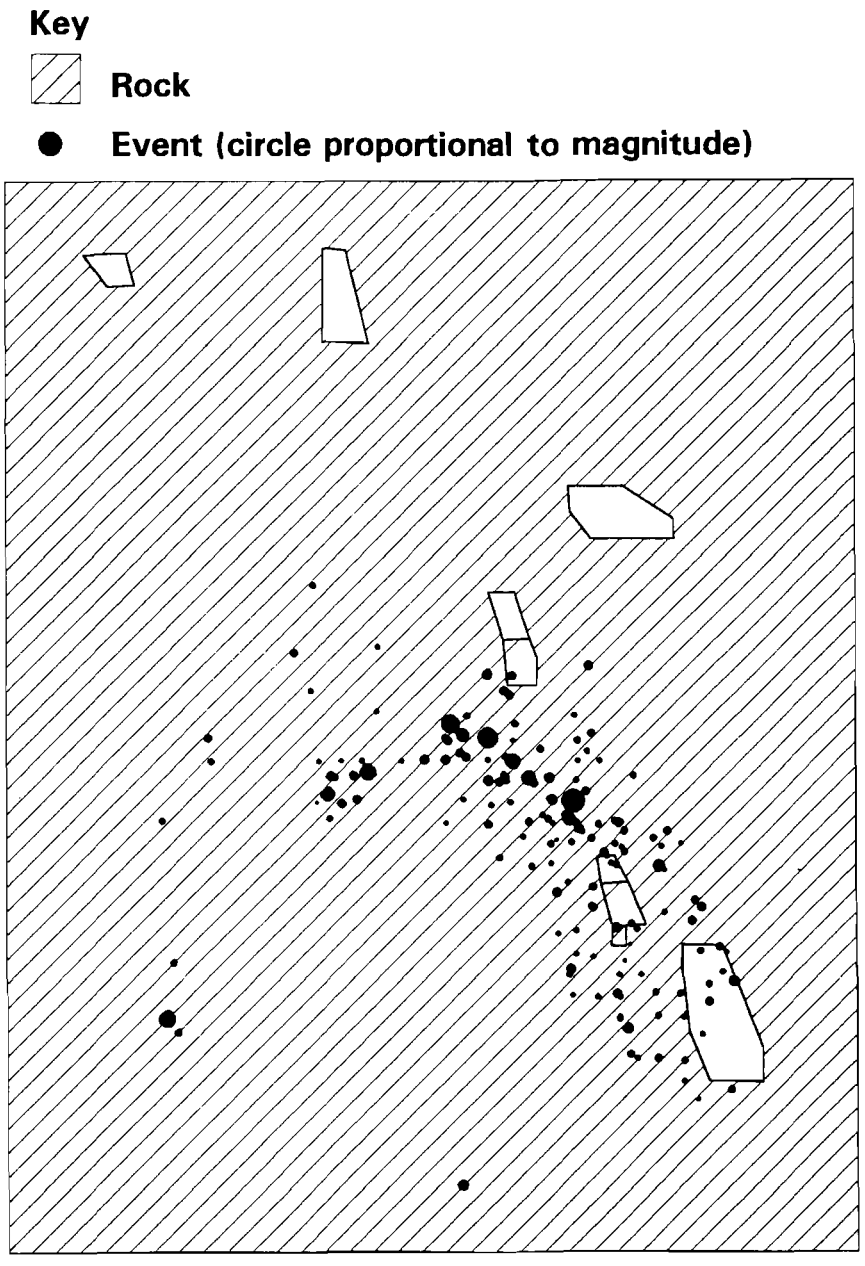

☆ U.S. GOVERNMENT PRINTING OFFICE: 1995—609-377